# 2008 Condensed Phase and Interfacial Molecular Science Research Meeting

**Airlie Conference Center Warrenton Virginia October 19-22, 2008**

Office of Basic Energy Sciences

**Chemical Sciences, Geosciences & Biosciences Division**

## Foreword

This volume summarizes the scientific content of the 2008 Research Meeting on Condensed Phase and Interfacial Molecular Science (CPIMS) sponsored by the U. S. Department of Energy (DOE), Office of Basic Energy Sciences (BES). This marks the fifth meeting of CPIMS.

Since its founding, the CPIMS Contractors' Meeting has fostered connections across BES research programs based on common topical interests. In keeping with that notion, we have invited two investigators who are funded under the BES Separations and Analysis Program to speak about their research: Jan Miller (University of Utah) and Frank Bright (University at Buffalo, The State University of New York). We have also invited an investigator from the Atomic, Molecular, and Optical Sciences (AMOS) Program: Kelly Gaffney (Stanford Linear Accelerator Center). We hope that the blending of these external experts with the CPIMS principal investigators will provide an interesting and useful cross-fertilization of ideas and concepts that benefits both groups.

This year's speakers are most gratefully acknowledged for their investment of time and for their willingness to share their ideas with the meeting participants. Thanks go to William Millman for consultations regarding the Separations and Analysis Program and to Jeffrey Krauss and Michael Casassa for consultations regarding the AMOS Program. Finally, this meeting would not be possible without the excellent logistical support it receives from Diane Marceau from our Division, Margaret Lyday and Camella Mitchell from the Oak Ridge Institute of Science and Education, and the staff of the Airlie Conference Center. Finally, we thank Larry Rahn for his expert help in assembling this volume.

Gregory J. Fiechtner and Mark R. Pederson
Fundamental Interactions Team
Chemical Sciences, Geosciences and Biosciences Division
Office of Basic Energy Sciences
October 2008

Cover art courtesy of Diane Marceau, Office of Basic Energy Sciences, Chemical Sciences, Geosciences, and Biosciences Division.

This document was produced under contract number DE-AC05-06OR23100 between the U.S. Department of Energy and Oak Ridge Associated Universities.

The research grants and contracts described in this document are supported by the U.S. DOE Office of Science, Office of Basic Energy Sciences, Chemical Sciences, Geosciences and Biosciences Division.

# U. S. Department of Energy
# Office of Basic Energy Sciences
# 2008 Meeting on Condensed Phase and Interfacial Molecular Sciences

## Sunday, October 19

| | |
|---|---|
| 3:00-6:00 pm | **** Registration **** |
| 6:00 pm | **** Reception (Whistling Swan Pub, No Host) **** |
| 7:00 pm | **** Dinner (Airlie Room) **** |

## Monday, October 20

| | |
|---|---|
| 7:00 am | **** Breakfast (Airlie Room) **** |
| 8:30 am | *Introductory Remarks*<br>**Gregory J. Fiechtner**, DOE Basic Energy Sciences |
| **Session I** | *Chair:* **Michael D. Morse,** University of Utah |
| 8:45 am | *Catalysis at Metal Surfaces Studied by Non-Equilibrium and STM Methods*<br>**Ian Harrison,** University of Virginia |
| 9:15 am | *Pump-Probe Studies of Photodesorption and Reaction on TiO2(110)*<br>**Mike G. White,** Brookhaven National Laboratory |
| 9:45 am | *Ultrafast Reaction Dynamics in a Bimolecular Adlayer: Carbon Monoxide and Oxygen on Palladium*<br>**Nicholas Camillone III,** Brookhaven National Laboratory |
| 10:15 am | **** Break **** |
| 10:45 am | *Probing Catalytic Activity in Defect Sites in Transition Metal Oxides and Sulfides Using Cluster Models: A Combined Experimental and Theoretical Approach*<br>**Caroline Chick Jarrold,** Indiana University |
| 11:15 am | *Thermochemistry and Reactivity of Transition Metal Clusters and Their Oxides*<br>**Peter B. Armentrout,** University of Utah |
| 11:45 am | *Gas Phase Investigation of Condensed Phase Phenomena*<br>**Lai-Sheng Wang,** Pacific Northwest National Laboratory |
| 12:15 pm | **** Lunch (Airlie Room) **** |
| **Session II** | Chair: **Shawn Kathmann,** Pacific Northwest National Laboratory |
| 4:00 pm | *Interfacial Surfactant Structures and their Significance in Particle Separation by Froth Flotation*<br>**Jan D. Miller,** University of Utah |
| 4:30 pm | *Interfacial Solvation under Aggressive Conditions*<br>**Frank V. Bright,** University at Buffalo - The State University of New York |
| 5:15 pm | **** Reception (No Host, Jefferson Room) **** |

6:00 pm **** Dinner (Airlie Room) ****

**Session III** Chair: **Robert A. Crowell,** Brookhaven National Laboratory

7:00 pm *Computational Studies of Liquid Interfaces, $CO_2$ Capture, and Ionic Liquids*
**Liem X. Dang,** Pacific Northwest National Laboratory

7:30 pm *Understanding Nanoscale Confinement Effects in Solvent-Driven Chemical Reactions*
**Ward H. Thompson,** University of Kansas

8:00 pm *Statistical Mechanical and Multiscale Modeling of Surface Reaction Processes*
**Jim Evans,** Ames Laboratory

## Tuesday, October 21

7:00 am **** Breakfast (Airlie Room) ****

**Session IV** Chair: **Bret E. Jackson,** University of Massachusetts

8:30 am *Probing Catalytic Activity in Defect Sites in Transition Metal Oxides and Sulfides Using Cluster Models: A Combined Experimental and Theoretical Approach*
**Krishnan Raghavachari,** Indiana University

9:00 am *The Role of Electronic Excitations on Chemical Reaction Dynamics at Metal, Semiconductor and Nanoparticle Surfaces*
**John Tully,** Yale University

9:30 am *Structures and Dielectric Properties of Atomic Clusters*
**Koblar Jackson,** Central Michigan University

10:00 am **** Break ****

10:30 am *Laser Dynamic Studies of Photoreactions on Single-Crystal & Nanostructured Surfaces*
**Richard Osgood,** Columbia University

11:00 am *Laser Induced Reactions in Solids and at Surfaces*
**Wayne P. Hess,** Pacific Northwest National Laboratory

11:30 am *Structural Dynamics in Chemical Systems*
**Kelly J. Gaffney,** Stanford Linear Accelerator Center

12:00 pm **** Lunch (Airlie Room) ****

**Session V** Chair: **Daniel M. Chipman,** Notre Dame Radiation Laboratory

4:30 pm *Influence of Medium on Radical Reactions*
**David M. Bartels,** Notre Dame Radiation Laboratory

5:00 pm *Ionic Liquids: Radiation Chemistry, Solvation Dynamics and Reactivity Patterns*
**James F. Wishart,** Brookhaven National Laboratory

5:30 pm *X-ray Spectroscopy of Volatile Liquids and their Surfaces*
**Richard J. Saykally,** Lawrence Berkeley National Laboratory

| | |
|---|---|
| 6:15 pm | **** Reception (No Host, Jefferson Room) **** |
| 7:00 pm | **** Banquet Dinner (Airlie Room) **** |

## Wednesday, October 22

| | |
|---|---|
| 7:00 am | **** Breakfast (Airlie Room) **** |
| **Session VI** | Chair: **Greg A. Kimmel,** Pacific Northwest National Laboratory |
| 9:00 am | *Photochemistry at Interfaces*<br>**Kenneth B. Eisenthal,** Columbia University |
| 9:30 am | *Solvation/Fluidity on the Nanoscale, and in the Environment*<br>**James P. Cowin,** Pacific Northwest National Laboratory |
| 10:00 am | *Fundamentals of Solvation under Extreme Conditions*<br>**John L. Fulton,** Pacific Northwest National Laboratory |
| 10:30 am | *Model Catalysis by Size-Selected Cluster Deposition*<br>**Scott Anderson,** University of Utah |
| 11:00 am | *Closing Remarks*<br>**Greg Fiechtner**, DOE Basic Energy Sciences |
| 11:30 am | **** Lunch (Airlie Room) **** |

# *Table of Contents*

# Table of Contents

**Foreword** ..... i

**Agenda** ..... ii

**Table of Contents** ..... v

**Guest Speaker Abstracts** ..... 1

**Jan D. Miller –** Interfacial Surfactant Structures and their Significance in Particle Separation by Froth Flotation ..... 1
**Frank V. Bright –** Interfacial Solvation under Aggressive Conditions ..... 3
**Kelly J. Gaffney –** Structural Dynamics in Chemical Systems ..... 5

**CPIMS Principle Investigator Abstracts** ..... 7

**Musahid Ahmed –** Investigating Atoms to Aerosols with Vacuum Ultraviolet Radiation ..... 7
**Scott Anderson –** Model Catalysis by Size-Selected Cluster Deposition ..... 11
**P. B. Armentrout –** Thermochemistry and Reactivity of Transition Metal Clusters and Their Oxides ..... 15
**K. Balasubramanian –** Electronic Structure of Transition Metal Clusters and Actinide Complexes and Their Reactivity ..... 19
**David M. Bartels –** Influence of Medium on Radical Reactions ..... 23
**Ian Carmichael –** Electron-Driven Processes in Condensed Phases ..... 27
**A. W. Castleman, Jr. –** Elucidating the Molecular–Level Details of Heterogeneous Catalytic Oxidation Reactions ..... 31
**Sylvia T. Ceyer –** An Exploration of Catalytic Chemistry on Au/Ni(111) ..... 35
**David Chandler –** Theory of Dynamics of Complex Systems ..... 39
**Andrew R. Cook –** Center for Radiation Chemistry Research: Electron Capture by Extended Polymer Molecules in Solution, and Excited States of Quinine Radical Anions ..... 43
**James P. Cowin –** Chemical Kinetics and Dynamics at Interfaces; Solvation / Fluidity on the Nanoscale and in the Environment ..... 47
**Liem X. Dang –** Computational Studies of Liquid Interfaces, $CO_2$ Capture, and Ionic Liquids ..... 51
**Michael A. Duncan –** Infrared Spectroscopy of Transition Metal-Molecular Interactions in the Gas Phase ..... 55
**Michel Dupuis –** Electronic Structure and Reactivity Studies for Aqueous Phase Chemistry ..... 59
**Kenneth B. Eisenthal –** Photochemistry at Interfaces ..... 63
**G. Barney Ellison –** Interfacial Oxidation of Complex Organic Molecules ..... 67
**Mostafa A. El-Sayed –** The Proton Pump in Bacteriorhodopsin, the other Photosynthetic System ..... 73
**Jim Evans –** Statistical Mechanical and Multiscale Modeling of Surface Reaction Processes 77
**Michael D. Fayer –** Liquid and Chemical Dynamics in Nanoscopic Environments ..... 81
**John L. Fulton –** Chemical Kinetics and Dynamics at Interfaces ..... 85

**Bruce C. Garrett –** Reactions of Ions and Radicals in Aqueous Systems ..... **89**
**Phillip L. Geissler –** Ion Solvation in Nonuniform Aqueous Environments ..... **93**
**Mark S. Gordon –** Theoretical Studies of Surface Science and Intermolecular Interactions .. **95**
**Stephen K. Gray –** Computational Nanophotonics: Modeling Optical Interactions and Transport in Tailored Nanosystem Architectures ..... **99**
**Charles B. Harris –** Dynamics of Electrons at Interfaces on Ultrafast Timescales ..... **107**
**Ian Harrison –** Catalysis at Metal Surfaces Studied by Non-Equilibrium and STM Methods ..... **111**
**Carl Hayden –** Fluctuations in Macromolecules Studied Using Time-Resolved, Multi-Spectral Single Molecule Imaging ..... **115**
**Martin Head-Gordon –** Electronic Structure and Optical Response of Nanostructures ..... **119**
**Teresa Head-Gordon –** Experimental and Simulation Studies of Bulk Water and Hydration Water at Interfaces ..... **123**
**Wayne P. Hess –** Chemical Kinetics and Dynamics at Interfaces: Laser Induced Reactions in Solids and at Surfaces ..... **127**
**So Hirata –** Breakthrough Design and Implementation of Electronic and Vibrational Many-Body Theories ..... **131**
**Wilson Ho –** Optical Spectroscopy at the Spatial Limit ..... **135**
**Bret E. Jackson –** Theory of the Reaction Dynamics of Small Molecules on Metal Surfaces ..... **139**
**Caroline Chick Jarrold –** Probing Catalytic Activity in Defect Sites in Transition Metal Oxides and Sulfides Using Cluster Models: A Combined Experimental and Theoretical Approach ..... **143**
**Ken D. Jordan and Mark A. Johnson –** Understanding the Electron-water Interaction at the Molecular Level: Integrating Theory and Experiment in the Cluster Regime . **147**
**Shawn M. Kathmann –** Nucleation: From Vapor Phase Clusters to Crystals in Solution ..... **151**
**Bruce D. Kay –** Chemical Kinetics and Dynamics at Interfaces: Structure and Reactivity of Ices, Oxides, and Amorphous Materials ..... **155**
**Greg A. Kimmel –** Chemical Kinetics and Dynamics at Interfaces: Non-Thermal Reactions at Surfaces and Interfaces ..... **159**
**Jay A. LaVerne –** Radiation Effects in Heterogeneous Systems and at Interfaces ..... **163**
**Marsha I. Lester –** Intermolecular Interactions of Hydroxyl Radicals on Reactive Potential Energy Surfaces ..... **167**
**H. Peter Lu –** Single-Molecule Chemical Imaging Studies of Interfacial Electron Transfer . **171**
**Michael D. Morse –** Spectroscopy of Organometallic Radicals ..... **175**
**Christopher J. Mundy –** *Ab initio* Approach to Interfacial Processes in Hydrogen Bonded Fluids ..... **179**
**Richard Osgood –** Laser Dynamic Studies of Photoreactions on Single-Crystal & Nanostructured Surfaces ..... **183**
**Richard J. Saykally –** X-Ray Spectroscopy of Volatile Liquids and their Surfaces ..... **189**
**Gregory K. Schenter –** Molecular Theory & Modeling: Development of Statistical Mechanical Techniques for Complex Condensed-Phase Systems ..... **193**
**Timothy C. Steimle –** Generation, Detection and Characterization of Gas-Phase Transition Metal Containing Molecules ..... **197**
**Ward H. Thompson –** Understanding Nanoscale Confinement Effects in Solvent-Driven Chemical Reactions ..... **201**

**Andrei Tokmakoff –** Structural Dynamics in Complex Liquids Studied with Multidimensional Vibrational Spectroscopy ..... **205**
**John C. Tully –** The Role of Electronic Excitations on Chemical Reaction Dynamics at Metal, Semiconductor and Nanoparticle Surfaces ..... **209**
**Lai-Sheng Wang –** Chemical Kinetics and Dynamics at Interfaces: Gas Phase Investigation of Condensed Phase Phenomena ..... **213**
**Michael G. White –** Surface Chemical Dynamics ..... **217**
**James F. Wishart –** Ionic Liquids: Radiation Chemistry, Solvation Dynamics and Reactivity Patterns ..... **221**
**Alec M. Wodtke –** Electronically Non-adiabatic Interactions in Molecule Metal-surface Scattering: Can We Trust the Born-Oppenheimer Approximation in Surface Chemistry? ..... **225**
**Sotiris S. Xantheas –** Development of Interaction Potentials for the Modeling of the Vibrational Spectra of Aqueous Environments ..... **229**

**Author Index** ..... **233**

**List of Participants** ..... **235**

# *Guest Speaker Abstracts*

# Interfacial Surfactant Structures and their Significance in Particle Separation by Froth Flotation

J. D. Miller
Department of Metallurgical Engineering
College of Mines and Earth Sciences
University of Utah

Froth flotation is a physico-chemical process that is used to separate particles in an aqueous suspension via differences in hydrophobicity as established by the interaction of various reagents at the solid/water, solid/gas and water/gas interfaces. The use of this technology is perhaps most significant in the mineral industry where in the U.S. alone over 500,000 tons/day of nonsulfide minerals are processed by flotation. Flotation technology is of critical importance to the energy and mineral industries which contribute substantially to our nation's economy. The estimated value of all nonfuel mineral materials processed in the United States during 2006 totaled $542 billion.

Research is in progress to examine nonsulfide flotation phenomena such as interfacial water structure, surfactants at surfaces, and the hydrophobic surface state. All of these matters provide a fundamental foundation for a better understanding of the flotation chemistry of nonsulfide minerals with the intent to improve flotation technology for the recovery and utilization of energy and mineral resources. Techniques such as In-situ FTIR Internal Reflection Spectroscopy and Sum Frequency Vibrational Spectroscopy (SFVS), Molecular Dynamics Simulations (MDS), and Atomic Force Microscopy (AFM), in addition to more traditional surface chemistry techniques, have been used to examine interfacial characteristics. Topics discussed include interfacial water structure/nanobubble stability, and surfactant organization at hydrophobic and hydrophilic surfaces. The attractive hydrophobic force such as that which occurs in the attachment of an air bubble to a hydrophobic particle during the flotation separation is examined at short range (~1nm) and at long range (~100nm) considering the results from SFVS, MDS, and in-situ AFM force and imaging measurements. The organization of surfactant hemimicelles at hydrophobic carbon surfaces seems to have little dependence on surfactant charge as revealed from in-situ AFM imaging taking into consideration the effect of crystallinity. These AFM results for hydrophobic surfaces are compared to the results from MDS. Finally, surfactant organization (alkylamines) at hydrophilic silica surfaces from monolayer to micelle structures is dependent on charge and these structures are discussed based on results from in-situ AFM images, MDS, and SFVS. Of particular interest is a pH dependent interfacial dehydration reaction which occurs during amine adsorption under certain conditions creating a strong hydrophobic character.

Condensed Phase and Interfacial Molecular Science (CPIMS 2008)
Sponsored by DOE Office of Basic Energy Science
Airlie Conference Center
Warrenton, VA
19-22 October 2008

# Interfacial Solvation under Aggressive Conditions

Frank V. Bright

Department of Chemistry, University at Buffalo, The State University of New York, Buffalo, New York 14260-3000, 716-645-6800 x 2162 (voice), 716-645-6963 (FAX), chefvb@buffalo.edu (e-mail)

Solvation plays an important role in the outcome of chemical reactions and modern separations. Over the past several years we have been studying solute solvation at silica surfaces that are in contact with supercritical fluids (e.g., $CO_2$, $CO_2$/alcohol mixtures) or ionic liquids (e.g., $[BMIM]^+[Tf_2N]^-$, $[C_4mpy]^+[Tf_2N]^-$, and $[P(C_6)_3C_{14}]^+[Tf_2N]^-$). These particular solvent classes are considered by many to be "environmentally friendly"; silica remains the most common support matrix.

Production of pure $H_2$ is one piece to an "$H_2$ economy" that could provide $H_2$ as a clean, renewable source of energy. A key step in obtaining pure $H_2$ is its separation from other gaseous molecules, mainly $CO_2$, that often accompany $H_2$ in industrial-scale reactions. Polymeric membranes are amongst the most studied $H_2$ purification platforms; however, $H_2$ production at economically viable levels requires membranes to operate under conditions where the gas stream mixture is above its critical point. Under these conditions, dilation and/or plasticization become major issues. Recently, we set out to elucidate the phenomena that occur within polymeric membranes when they are operated under viable $H_2$ purification conditions. Toward this end, we began by creating and studying the solvation of relevant monolayer structures formed on the surface of silica when they are contacted with pure $CO_2$ over the gas, liquid and supercritical range.

This presentation will describe our motivation; summarize some of our previous efforts on solute solvation at silica surfaces (capped and end-capped) in alcohol-modified supercritical $CO_2$, and present preliminary results on the local dynamics within silica-bonded monolayers when they are subjected to pure $CO_2$ over the gas, liquid and supercritical range. Our primary measurement tools are steady-state and time-resolved fluorescence spectroscopy.

# Structural Dynamics in Chemical Systems

**Kelly J. Gaffney**, PULSE Institute, Photon Science, SLAC,
Stanford University, Menlo Park, CA 94025
Telephone: (650) 926-2382
Fax: (650) 926-4100
Email: kgaffney@slac.stanford.edu

**I. Scientific Progress**: The successful achievement of the scientific objectives of the 'Structural Dynamics in Chemical Systems' grant requires the development of experimental techniques and tools applicable to a wide range of ultrafast x-ray science. The LCLS will produce intense femtosecond x-ray pulses with a first harmonic upper energy range up to 8 keV, a narrow spectral width of ~20 eV FWHM, and limited frequency tuning capability in the beginning. All of these attributes make x-ray emission spectroscopy (XES), x-ray absorption near edge spectroscopy (XANES), and resonant inelastic x-ray scattering (RIXS) the preferred spectroscopic techniques for the LCLS. These techniques are ideally suited to studying electron transfer in organometallic compounds because they provide easily interpretable information about the oxidation state, spin multiplicity, and the local coordination of the metal centers in these complexes.

**I.A. *X-ray spectroscopy studies of electron dynamics in organometallic chemistry*:** A key component of our research will be utilizing x-ray spectroscopy to probe the charge, spin, and covalency dynamics in photoexcited organometallic complexes. Organometallic structures catalyze a wide range of chemical reactions, most prominently in metallo-enzymes, but the time evolution of the electronic structure during photochemical reactions cannot be robustly determined with standard UV/visible spectroscopy. We have decided to emphasize manganese and iron based complexes given their prominence and diversity in metallo-enzymatic systems, as well as the compatibility of their x-ray absorption K-edges with the energy range of the LCLS.

This project has been focusing on two key developments. Firstly, the construction of an ultrafast laser system for probing photochemical dynamics with time resolved electronic and vibrational spectroscopy. We are finalizing the commissioning of the UV/visible pump-probe set-up with our first test experiment, and we have already begun collecting data with our ultrafast vibrational spectroscopy set-up. Secondly, developing the ability to perform and interpret x-ray emission and resonant inelastic x-ray scattering (RIXS) experiments. We have made significant progress in this area as well, having submitted our first x-ray spectroscopy manuscript in 2008.

**I.B. *Vibrational spectroscopy studies of dynamics in ionic solutions*:** Aqueous ionic solutions lubricate the chemical machinery of natural and biological systems and electrical energy storage devices currently rely on organic solvents with high concentrations of dissolved salts. We utilize time resolved vibrational spectroscopy to study the dynamics on these ionic solutions.

We initiated our investigations with aqueous sodium perchlorate solutions. In these studies we have utilized multidimensional vibrational correlation spectroscopy (MVCS) to study the exchange between water-water hydrogen bonds and water-ion hydrogen bonds. Aqueous perchlorate solutions have a hydroxyl stretch absorption spectrum that has a peak that originates from hydroxyl groups that donate a hydrogen bond to a perchlorate ion and a peak that originates from hydroxyl groups that donate a hydrogen bond to another water molecule. With MVCS we can characterize the dynamics of each of these sub-ensembles separately, as well as determine how quickly these sub-ensembles interconvert. These studies have demonstrated that water molecules equilibrate within there local hydrogen bond structure before exchanging hydrogen bond environments. We have established a collaboration with Micheal Odelius of Stocklholm University to conduct ab initio molecular dynamics simulations of the system aqueous sodium perchlorate. We have submitted our first manuscript describing data collected with this system.

# *CPIMS*
# *Principle Investigator Abstracts*

***(Alphabetical by last name)***

***"Investigating atoms to aerosols with vacuum ultraviolet radiation"***

Musahid Ahmed, Kevin R. Wilson and Stephen R. Leone
Chemical Dynamics Beamline, MS 6R-2100, 1 Cyclotron road
Lawrence Berkeley National Laboratory, University of California, Berkeley, CA 94720
mahmed@lbl.gov

The Chemical Dynamics Beamline at the Advanced Light Source (ALS) is a synchrotron user facility dedicated to state-of-the-art investigations in combustion dynamics, aerosol chemistry, nanoparticle physics, biomolecule energetics, spectroscopy, kinetics, and chemical dynamics processes using tunable vacuum ultraviolet light for excitation or detection. The broad goals of the Chemical Dynamics Beamline are to perform high quality investigations in chemical physics and dynamics utilizing vacuum ultraviolet (VUV) light, while providing the user community with efficient access to the synchrotron and its sophisticated equipment, and at the same time fulfilling the missions and interests of the Department of Energy.

**Aerosol Chemistry** - Heightened concern over global climate change has led to increased scrutiny of the direct and indirect effects of aerosols on radiative forcing, and particle size and chemical composition are important factors in determining the magnitude of such effects. Heterogeneous reactions of organic aerosols (OA) with gas-phase oxidants can alter both composition and size, in some cases activating the particles for cloud formation. Furthermore, as a result of volatilization of OA, oxidative aging may also liberate a host of volatile organic compounds (VOCs) that are potentially important intermediates in photochemical cycles such as smog formation. Here we report recent experiments on the oxidative aging of OA with OH radicals using a photoionization aerosol mass spectrometry experimental setup at the ALS/LBNL.[10,19] We have determined that OH reactions with simple particle phase alkanes, such as squalane (Sq) proceeds via a sequential oxidation mechanism. Furthermore we find that there is an average of 1 oxygen atom added for every squalane molecule consumed in the reaction. Depending on OH concentration and exposure time, these simple oxidation products, i.e. SqO, $SqO_2$, $SqO_3$, etc (products consisting of the Sq hydrocarbon chain with progressively added oxygen atoms) account for 50-80% of the particle by mass. The formation mechanisms of these particular products can be well understood by some analogous gas phase reactions between OH and small alkanes. In addition to these mechanistic details, a relative rates technique is used to determine the heterogeneous reaction rates of OH with squalane. The reactive uptake coefficient depends upon OH concentration and is observed to increase as OH concentrations approach atmospheric levels. One explanation for an increase in reactive uptake coefficient with decreasing OH concentration is the role of heterogeneous secondary chemistry occurring in the particle phase. These results could have important implications for understanding the loss mechanism of organic molecules in ambient aerosols in the troposphere.

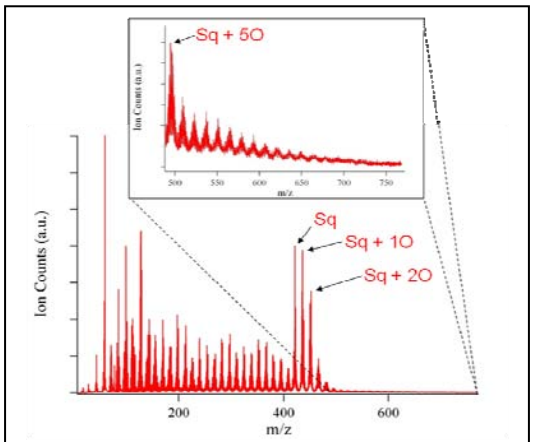

VUV Mass Spectra of reacted squalane

**Molecular nano-imaging-** Advancements in imaging techniques have been instrumental in recent progress in the fields of biology and material science. However, techniques for imaging samples with both chemical specificity at the molecular level and nanoscale spatial resolution remains a challenge. Our group is developing a novel technique utilizing tunable vacuum ultraviolet (VUV) synchrotron radiation to probe localized chemistry of heterogeneous systems. The basic principle is built upon secondary ion/neutral mass spectrometry (SIMS/SNMS) microscopy, where a focused beam of primary ions desorb charged and neutral molecules from the surface of interest. In the present setup, an Ion-Tof TOF.SIMS 5 mass spectrometer coupled to a VUV synchrotron light terminal is used to desorb and post-ionize sputtered neutral surface

species. So far, we have applied the post-ionization (PI) method to obtain mass spectra and photo-ionization efficiency curves for several systems such as Au, Cu, Pt, Si, Zn, Ge, Ga, as well as GaAs and a copper grid embedded in indium to characterize its capabilities.

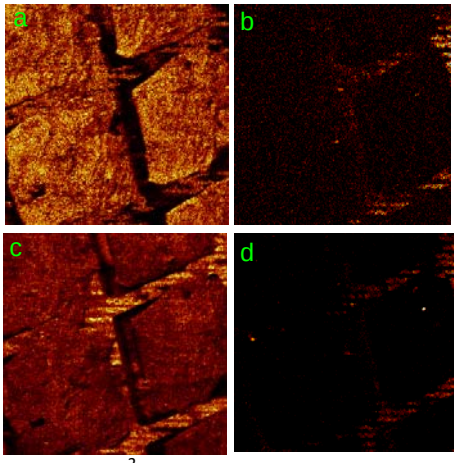

100x100µm$^2$ (256x256 pixels) Images of Cu grid embedded in In. (a) and (b) are PI images of In and Cu, respectively. (c) and (d) are SIMS images.

With SIMS, where the desorbed *ions* are detected, signals can fluctuate dramatically from spot to spot on the sample due to sensitivity of the ionization mechanisms on the local chemical environment. This can sometimes result in artifactual mass spectra that are more reflective of the trace chemical contaminants on the surface instead of the sample itself. We have demonstrated that these so-called matrix effects are less prominent in SNMS, allowing for cleaner, and more chemically reflective mass spectra that are easier to interpret (see mass spectra below). Furthermore, single photon ionization (SPI) bypasses intermediate dissociative states that might be accessed in multi-photon ionization techniques, and our group has shown that it holds promise as an efficient method of ionizing fragile molecules.[11]

The mass-to-charge ratio and photon energy dependence of the molecular signals are unique fingerprints of each molecule, reducing the ambiguity of molecular assignments to each observed mass peak. This enhanced molecular specificity is essential to probe complex, chemically heterogeneous systems such as biological cells where thousands of different chemical compounds may be present. An additional advantage of imaging by chemical species mass is that labeling is not required due to the high molecular specificity of the mass spectrometry method. Thus, coupled with sub-micron resolution (theoretical lateral limit ~5-10 nm, with depth profiling at the monolayer level) and enhanced sensitivity to the chemicals present at the surface, SNMS-PI shows great promise in tackling the yet unsolved problems in biology and material science.

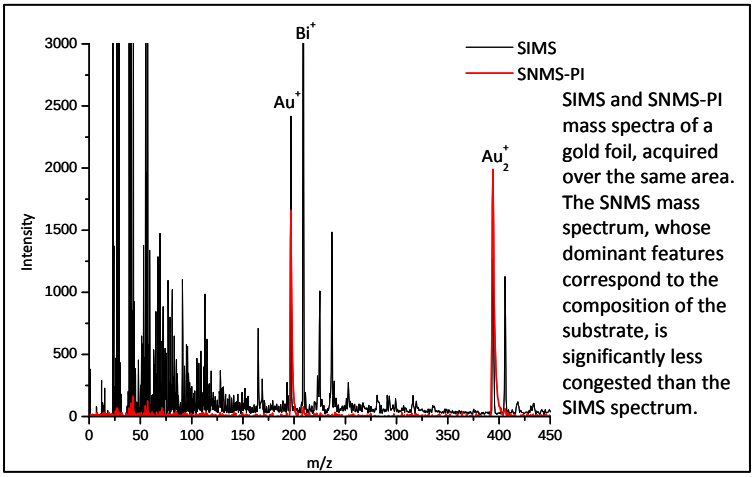

SIMS and SNMS-PI mass spectra of a gold foil, acquired over the same area. The SNMS mass spectrum, whose dominant features correspond to the composition of the substrate, is significantly less congested than the SIMS spectrum.

**Laser ablation and cluster chemistry-** Our vigorous program in using VUV light to study laser ablated[16,17] species and hydrogen bonded clusters continues. In collaboration with Ricardo Metz (U Mass), we measured the thermodynamic properties of PtC, PtO and $PtO_2$.[1] The molecules are prepared by laser ablation of a platinum tube, followed by reaction with $CH_4$ or $N_2O$ and supersonic expansion. These measurements provide the first directly measured ionization energy for PtC. The direct measurement also gives greatly improved ionization energies for the platinum oxides. The ionization energy connects the dissociation energies of the neutral and cation, leading to greatly improved 0 K bond strengths for the neutrals. Much of the error in previous Knudsen cell measurements of platinum oxide bond strengths is due to the use of thermodynamic second law extrapolations. Third law values calculated using statistical mechanical thermodynamic functions are in much better agreement with values obtained from ionization energies and ion energetics. This work has been extended to study the thermodynamic properties of H-Pt-H, Pt-$CH_2$ and H-Pt-$CH_3$ and $TaO_x$ (up to x=6) generated using the ablation apparatus.

Extending our carbon cluster work,[4,6,15] in collaboration with Ralf Kaiser (U Hawaii), we are studying the reactions of small carbon clusters with $N_2O$ which gives rise to a series of $C_nO$ and $C_nN$ clusters, and reactions with diacetylene and acetylene which produce a series of carbon rich hydrocarbon species. The thermodynamic properties of organo silicon molecules are of paramount importance in understanding the formation of silicon-bearing nanostructures together with their precursors from the 'bottom up' in the interstellar medium, in our Solar System, and in chemical vapor deposition processes. Towards this end we have started performing reactivity studies of Si clusters generated by laser ablation with a variety of hydrocarbons and oxidizing molecules. Reactions with acetylene generated a large number of long chain organo silicon molecules and radicals, while reaction with $CO_2$ gave rise to gaseous SiO and $SiO_2$. $SiO_2$ is incredibly difficult to detect in the gas phase, however using our laser ablation technique coupled to VUV photoionization allowed for a direct determination of its ionization energy.

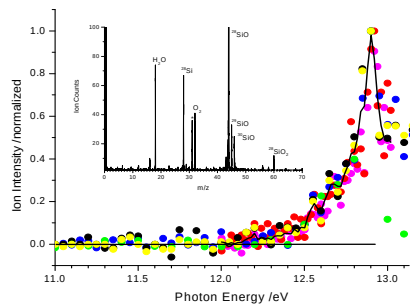


Photoionization efficiency curve for $SiO_2$ generated via laser ablation of Si in an expansion of $CO_2$. (Inset) Mass Spectra of resulting beam at 13.0 eV.

In continuation of our studies on photoionization of hydrogen bonded systems,[3,6] we performed a systematic study of the VUV photoionization mechanisms of clusters of methanol and methanol with water. Protonated methanol clusters of the form $(CH_3OH)_nH^+$ (n=1-12) dominate the mass spectrum below the ionization threshold of the methanol monomer. With an increase in water concentration, small amounts of mixed clusters of the form $(CH_3OH)_n(H_2O)H^+$ (n=2-11) are detected. There is also some contribution to the mixed cluster signal from ion-molecule reactions within ionized pure methanol clusters. The only unprotonated species observed in this work are the methanol monomer and dimer. Appearance energies are obtained by evaluating photoionization efficiency curves for $CH_3OH^+$, $(CH_3OH)_2^+$, $(CH_3OH)_nH^+$ (n=1-9) and $(CH_3OH)_n(H_2O)H^+$ (n=2-9 ) as a function of photon energy. With an increase in the water content in the molecular beam, there is substantial enhancement of photoionization intensity for protonated methanol monomer and unprotonated methanol dimer at threshold. This may be explained by enhanced formation of a cyclic structure containing two methanol molecules and a water monomer connected via three hydrogen bonds.[2]

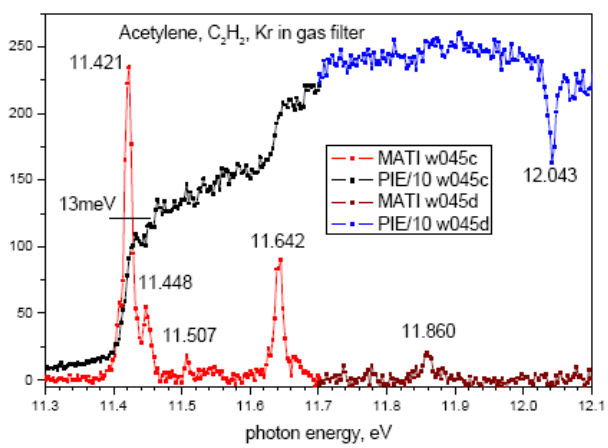


MATI spectrum of $C_2H_2$. Upper trace is PIE

In recent work we have adapted the ablation apparatus to perform mass analyzed threshold ionization (MATI) at the synchrotron. This opens up a novel way to perform spectroscopy at the beamline and improve resolution in ionization onset measurements. The idea is to have access to spectroscopy that is typically available in photoelectron spectroscopy but with mass resolution. This would be invaluable in studying mixtures of molecules, conformers and isomers, and clusters. MATI spectrum was recorded for Ar,$O_2$, $N_2$, $H_2O$, $N_2O$ and $C_2H_2$. In future experiments, we plan to incorporate our aerosol VUV mass spectrometer to MATI to be able to record vibrationally resolved photoionization spectra of fragile biomolecules.[13]

With an eye to increasing sensitivity in photoionization experiments we developed a high pressure photoionization source at the beamline. Photoionization is performed a few mm in front of an atmospheric pressure sampling nozzle and the resulting ion beam is guided into the detector chamber where they are

pulse field extracted into a reflectron mass spectrometer. Initially we are focussing our efforts in probing ion-molecule reactions in methanol cluster beams. Photoionization is performed at different nozzle to VUV light distances and the resulting mass spectra provide some evidence that could be interpreted as ion induced nucleation.

**References (DOE funded work 2005-present)**


1. M. Citir, R. B. Metz, L. Belau and M. Ahmed, *"Direct Determination of the Ionization Energies of PtC, PtO and $PtO_2$ with VUV Radiation"*, J. Phys. Chem. A (**in press**)
2. O. Kostko, L. Belau, K. R. Wilson, and M. Ahmed, *"Vacuum-ultraviolet (VUV) photoionization of small methanol and methanol-water clusters",* J. Phys. Chem. A (**in press**)
3. L. Belau, K. R. Wilson, S. R. Leone and M. Ahmed, *"Vacuum Ultraviolet (VUV) photoionization of small water clusters"* J. Phys. Chem A. **111**, 10075 (2007)
4. L. Belau, S. E. Wheeler, B. W. Ticknor, M. Ahmed, S. R. Leone, W. D. Allen, H. F. Schaefer III, and M. A. Duncan, *"Ionization Thresholds of Small Carbon Clusters: Tunable VUV Experiments and Theory."* J. Am. Chem. Soc. **129** 10229 (2007)
5. K. R. Wilson, S. Zou, J. Shu, E. Rühl, S. R. Leone, G. C. Schatz and M. Ahmed, *"Size-Dependent Angular Distributions of Low Energy Photoelectrons emitted from NaCl Nanoparticles"* Nano Letters **7**, 2014 (2007) 195.
6. L. Belau, K. R. Wilson, S. R. Leone, and M. Ahmed, *"Vacuum-Ultraviolet photoionization studies of the micro-hydration of DNA bases (Guanine, Cytosine, Adenine and Thymine),"* J. Phys. Chem. A. **111,** 7562 (2007)
7. R. I. Kaiser, L. Belau, S. R. Leone, M. Ahmed, Y. Wang, B. J. Braams, and J. M. Bowman, *"A combined experimental and computational study on the ionization energies of the cyclic and linear $C_3H$ isomers,"* ChemPhysChem **8**, 1236 (2007)
8. M.J. Northway, J.T. Jayne, D.W. Toohey, M.R. Canagaratna, A. Trimborn, K-I. Akiyama, A. Shimono, J.L. Jimenez, P.F. DeCarlo, K.R. Wilson, and D.R. Worsnop. *"Demonstration of a VUV lamp photoionization source for improved organic speciation in an aerosol mass spectrometer."* Aerosol Science & Technology **41**, 828 (2007)
9. M. Ahmed, *"Photoionization of desorbed neutrals from surfaces."* Encyclopedia of Mass Spectrometry, Vol. 6, p264 Elseiver (2007).
10. E. Gloaguen, E. R. Mysak, S. R. Leone, M. Ahmed, and K. R. Wilson *"Investigating the chemical composition of mixed organic-inorganic particles by "soft" VUV photoionization: the reaction of ozone with anthracene on sodium chloride particles,"* Int. J. Mass Spectrom. **258**, 74 (2006).
11. J. Shu, K. R. Wilson, M. Ahmed, and S. R. Leone, *"Coupling a versatile aerosol apparatus to a synchrotron: vacuum ultraviolet light scattering, photoelectron imaging, and fragment free mass spectrometry,"* Rev. Sci. Instrum. **77**, 043106 (2006)
12. K. R. Wilson, D. S. Peterka, M. Jimenez-Cruz, S.R. Leone, and M. Ahmed. *"VUV Photoelectron Imaging of Biological Nanoparticles – Ionization energy determination of nano-phase glycine and phenylalanine-glycine-glycine".* Phys. Chem. Chem. Phys. **8**, 1884 (2006).
13. K. R. Wilson, L. Belau, C. Nicolas, M. Jimenez-Cruz, S. R. Leone, and M. Ahmed, *"Direct determination of the ionization energy of histidine with VUV synchrotron radiation"* Int. J. Mass Spectrom. **249-250**, 155, (2006)
14. K. R. Wilson, M. Jimenez-Cruz, C. Nicolas, L. Belau, S. R. Leone, and M. Ahmed, *"Thermal Vaporization of Biological Nanoparticles: Fragment-Free VUV Photoionization Mass Spectra of Tryptophan, Phenylalanine-Glycine-Glycine and β-carotene***,"** J. Phys. Chem. A **110**, 2106 (2006)
15. J. Shu, K. R. Wilson, M. Ahmed, S. R. Leone, C. E. Graf, and E. Ruhl*, "Elastic light scattering from nanoparticles by monochromatic vacuum-ultraviolet radiation,"* J. Chem. Phys. **124**, 034707 (2006)
16. C. Nicolas, J. Shu, D. S. Peterka, M. Hochlaf, L. Poisson, S. R. Leone, and M. Ahmed, *"Vacuum ultraviolet photoionization of $C_3$,"* J. Am. Chem. Soc. **128**, 220 (2006)
17. R. B. Metz, C. Nicolas, M. Ahmed, and S. R. Leone, *"Direct determination of the ionization energies of FeO and CuO with VUV radiation."* J. Chem. Phys. **123,** 114313 (2005).
18 . J. Shu, K. R. Wilson, A. N. Arrowsmith, M. Ahmed, and S. R. Leone, *"Light scattering of ultrafine silica particles by VUV synchrotron radiation."* Nano Lett. **6,** 1009 (2005)
19. E. R. Mysak, K. R. Wilson, M. Jimenez-Cruz, M. Ahmed, and T. Baer. *"Synchrotron Radiation Based Aerosol Time-of-Flight Mass Spectrometry for Organic Constituents"* Anal. Chem. **77**, 5953 (2005)

**Model Catalysis by Size-Selected Cluster Deposition**

Scott Anderson, Chemistry Department, University of Utah, 315 S. 1400 E. Rm. 2020, Salt Lake City, UT 84112. anderson@chem.utah.edu

**Program scope:** We are interested in understanding the effects of cluster size on physical and chemical properties of planar model catalysts prepared to depositing size-selected cluster ions on well defined substrates in ultra-high vacuum. Tools available include a variety of pulsed and temperature-programmed mass spectrometric techniques, x-ray photoelectron spectroscopy (XPS), Auger electron spectroscopy (AES), ion scattering (ISS), and infrared reflection absorption spectroscopy (IRAS). The goal is produce model catalysts that are well characterized, and where properties such as metal loading, substrate defect density, and metal cluster size can be varied independently, allowing us new insights into these very complex systems.

**Recent Progress**

In the past couple years we have worked in two areas. Current work is focused on oxidation of size-selected Pd clusters on alumina, and Pd-catalyzed redox chemistry on alumina supports.

**1. $Au/TiO_2$: Effects of oxygen vacancies and water adsorption on agglomeration.**

In past work,[1,2] we found that $Au_n$ deposited on vacuum-annealed $TiO_2$ did not sinter significantly on the time scale of our experiments. STM experiments agreed with this conclusion,[3] except for Au atoms, where substantial sintering was observed in STM after deposition of both $Au^+$ and Au under similar conditions.[3,4] Our XPS work suggested that Au atoms diffuse to and bind at oxygen vacancy sites, where they are stable with respect to further diffusion at room temperature. We speculated that the difference from the STM work was due to the longer STM experimental time scale, which might result in some adventitious adsorbate blocking vacancy sites, and preventing them from binding Au. STM work by several groups[5,6] pointed to water as a likely culprit, and since this is an important issue in our of use of ISS for morphological probing, we felt the need to get a definitive answer.

We used temperature-programmed desorption (TPD) to monitor water dissociation, recombination, and desorption on $TiO_2$ and $Au/TiO_2$, and ion-scattering (ISS) to look at morphology changes in the gold induced by water adsorption and heating either before or after gold deposition. It was found that water does indeed enhance thermally activated Au agglomeration, as monitored by ISS. We also gained considerable insight into the effects of ion-induced damage in water layers on $TiO_2$ and $Au/TiO_2$ . This work has been published in Journal of Physical Chemistry.[7]

**2. Oxidation of $Pd_n/Al_2O_3$ and CO oxidation catalyzed by $Pd_n/Al_2O_3$.**

Supported $Pd/Al_2O_3$ catalysts are widely used in catalytic methane combustion, and also in a number of other reactions. For catalytic oxidation, the general mechanism involves oxidation of the nanoparticulate Pd by oxygen or other oxygen-containing species in the reaction mix. The oxidized Pd subsequently interacts with methane or other fuel molecules, oxidizing them and becoming reduced to complete the cycle. As discussed in a recent review,[8] the system is complicated because the oxidation state of the Pd varies with temperature and reaction conditions, and it is likely that the surface properties of the catalyst change when it is taken out of operating conditions for study. Our expectation was that both oxidation chemistry of the Pd and ability of the oxidized Pd to react with hydrocarbons is likely to be strongly dependent on Pd cluster size.

The deposition substrate is a two layer thick $Al_2O_3$ film grown on NiAl(110), using procedures developed by Freund and co-workers,[9] and used by them in studies of CO adsorption and reaction on $Pd/Al_2O_3$.[10-12] Pd clusters of controlled size are deposited at impact energies of a few electron volts – below both the lattice displacement energy and expected Pd-Pd bond energies. XPS is used to monitor oxidation, which is found to be strongly dependent on both cluster size and oxidation temperature. Oxidation was examined for $O_2$ exposures at 100K, 300K, 400K, and 500K, and stability of oxides formed at lower temperatures was probed for surface temperatures up to 600 K. For clusters smaller than $Pd_5$, no oxidation was observed for moderate $O_2$ exposures (180 L) at any temperature. For larger clusters, partial oxidation by $O_2$ is observed at cryogenic temperatures, as a shift to higher binding energy of the Pd 3d XPS peaks. The magnitude of the shift is only ~0.4 eV, indicating that the Pd is only

partially oxidized (PdO shift ≅ 1 eV, $PdO_2$ shift ≅ 2.5 eV). If the oxidized sample is annealed in vacuum the oxidation state is reasonably stable, with only partial shift back to the initial peak position for annealing up to 600 K. Somewhat surprisingly, if the clusters are exposed to $O_2$ at 300K or above, no XPS shift, i.e., no oxidation, is observed. This result suggests that oxidation is mediated by a weakly bound precursor, and that the precursor lifetime becomes too short for efficient mediation as the temperature is raised. Presumably under higher pressure conditions the oxidizer flux onto the surface is high enough to enable oxidation at high temperatures.

CO oxidation was chosen as our initial target system because it is (nominally) simple, and has been studied on both real and planar model $Pd/Al_2O_3$ catalysts by many groups. CO TPD from $Al_2O_3$/NiAl and $Pd_n/Al_2O_3$/NiAl surfaces was studied to see how stable CO is on the Pd sites. CO desorbs from terrace sites on $Al_2O_3$/NiAl at ~100 K,[13] but there is a small component attributed to CO at defects in the film, that desorbs in the temperature range from 300 – 400 K. This defect component is eliminated if the sample is first exposed to $O_2$ at low temperatures, presumably because $O_2$ binds at and blocks CO adsorption at these sites. Even after heating to desorb any molecularly adsorbed $O_2$, the sites remain blocked, presumably because the defects have been healed. On $Pd_n/Al_2O_3$/NiAl samples, the CO TPD shows a weak feature between 200 and 350K that is attributed to CO bound to Pd.

CO oxidation has been studied with several protocols. The $Al_2O_3$ films are grown with $^{18}O_2$, and we have done experiments with various combinations of Pd oxidation by $^{18}O_2$, followed by reaction with both $C^{18}O$ and $C^{16}O$, and also including varying doses of $H_2{}^{16}O$, which is also observed to supply oxygen for CO oxidation. If CO and $O_2$ are both dosed at low temperature, then the sample is heated, little $CO_2$ is produced, and from the isotope distribution it is clear that both $O_2$ and water are active in the reaction. If the Pd oxidation is carried out at low temperatures, then CO is dosed at 300K, followed by TPD, CO is observed to desorb in two features, with $CO_2$ desorbing together with only the higher temperature of the two CO features. From this pattern it appears that some CO is molecularly adsorbed to the surface, probably from adsorption of residual CO during sample cool-down after the room temperature CO dose. The higher temperature feature indicates that some species, e.g. carbonate, is present on the surface, that decomposes to generate both CO and $CO_2$ at high temperatures.

We also are using a pulsed-dosing mass spectrometry approach. For these experiments, the sample is cooled and exposed to $^{18}O_2$, with and without co-adsorption of $H_2{}^{16}O$. The sample temperature is then raised to various values of interest, and while the temperature is held constant, the sample is exposed to millisecond pulses of CO, each corresponding to a fraction of a Langmuir exposure. The pulses of CO and all $CO_2$ isotopologs evolving from the surface are monitored as a function of time with a differentially pumped mass spectrometer. No $CO_2$ production is observed for $T_{surface}$ of 100 or 200 K, but at 300K we start to observe $CO_2$ pulses tracking the CO reactant pulse. If the sample is heated after a sequence of these CO pulses, additional $CO_2$ desorbs, suggesting formation of some stable species that can decompose to $CO_2$ at elevated temperatures.

**Future plans**

The chemistry of Pd-catalyzed CO oxidation has proven to be surprisingly complicated, and I anticipate that several months of additional experiments will be required to sort out the effects of cluster size, oxidation temperature, reaction temperature, and water on the reaction. After that, we will begin to look at hydrocarbon catalytic combustion reactions, and probably will also look at catalytic oxidation of $H_2$

**Citations:**


(1) Lee, S.; Fan, C.; Wu, T.; Anderson, S. L. *J. Am. Chem. Soc.* **2004**, *126*, 5682-5683.

(2) Lee, S.; Fan, C.; Wu, T.; Anderson, S. L. *Surface Science* **2005**, *578*, 5-19.

(3) Tong, X.; Benz, L.; Kemper, P.; Metiu, H.; Bowers, M. T.; Buratto, S. K. *J. Am. Chem. Soc.* **2005**, *127*, 13516-18.

(4) Wahlstrom, E.; Lopez, N.; Schaub, R.; Thostrup, P.; Ronnau, A.; Africh, C.; Laegsgaard, E.; Norskov, J. K.; Besenbacher, F. *Phys. Rev. Lett.* **2003**, *90*, 026101/1-026101/4.

(5) Wendt, S.; Schaub, R.; Matthiesen, J.; Vestergaard, E. K.; Wahlstrom, E.; Rasmussen, M. D.; Thostrup, P.; Molina, L. M.; Lægsgaard, E.; I. Stensgaard; Hammer, B.; Besenbacher, F. *Surf. Sci.* **2005**, *598*, 226–245.

(6) Zhang, Z.; Bondarchuk, O.; Kay, B. D.; White, J. M.; Dohnálek, Z. *J.Phys.Chem.B* **2006**, *110*, 21840.

(7) Wu, T.; Kaden, W. E.; Anderson, S. L. *J. Phys. Chem. C* **2008**, *112*, 9006-15.

(8) Ciuparu, D.; Lyubovsky, M. R.; Altman, E.; Pfefferle, L. D.; Datye, A. *Catalysis Reviews - Science and Engineering* **2002**, *44*, 593-649.

(9) Libuda, J.; Meusel, I.; Hoffmann, J.; Hartmann, J.; Freund, H. J. *Journal of Vacuum Science & Technology, A: Vacuum, Surfaces, and Films* **2001**, *19*, 1516-1523.

(10) Meusel, I.; Hoffmann, J.; Hartmann, J.; Heemeier, M.; Bäumer, M.; Libuda, J.; Freund, H.-J. *Catal. Lett.* **2001**, *71*, 5-13.

(11) Sandell, A.; Libuda, J.; Bruehwiler, P. A.; Andersson, S.; Maxwell, A. J.; Baeumer, M.; Maertensson, N.; Freund, H. J. *J. Vac. Sci. Technol. A* **1996**, *14*, 1546-1551.

(12) Wolter, K.; Seiferth, O.; Libuda, J.; Kuhlenbeck, H.; Bäumer, M.; Freund, H.-J. *Surf. Sci.* **1998**, *402-404*, 428-432.

(13) Bäumer, M.; Freund, H.-J. *Prog. Surf. Sci.* **1999**, *61*, 127-198.

**DOE-Funded Publications Since 2005**

"Agglomeration, Support Effects, and CO Adsorption on Au/$TiO_2$ (110) Prepared by Ion Beam Deposition" Sungsik Lee, Chaoyang Fan, Tianpin Wu, and Scott L. Anderson, Surf. Sci. 578 (2005) 5-19

"Agglomeration, Sputtering, and Carbon Monoxide Adsorption Behavior for Au/$Al_2O_3$ Prepared by $Au_n^+$ Deposition on $Al_2O_3$/NiAl(110)", Sungsik Lee, Chaoyang Fan, Tianpin Wu, and Scott L. Anderson, J. Phys. Chem. B109 (2005) 11340-11347

"Cluster size effects on CO oxidation activity, adsorbate affinity, and temporal behavior of model $Au_n$/$TiO_2$ catalysts", Sungsik Lee, Chaoyang Fan, Tianpin Wu, and Scott L. Anderson, J. Chem. Phys. 123 (2005) 124710 13 pages.

"Water on rutile $TiO_2$(110) and Au/$TiO_2$(110): Effects on Au mobility and the isotope exchange reaction", Tianpin Wu, William E. Kaden and Scott L. Anderson, J. Phys. Chem C; **2008**; 112(24); 9006-9015. DOI: 10.1021/jp800521q

# THERMOCHEMISTRY AND REACTIVITY OF TRANSITION METAL CLUSTERS AND THEIR OXIDES

P. B. Armentrout
315 S. 1400 E. Rm 2020, Department of Chemistry, University of Utah,
Salt Lake City, UT 84112; armentrout@chem.utah.edu

## Program Scope

The objectives of this project are to obtain quantitative information regarding the thermodynamic properties of transition metal clusters, their binding energies to various ligands, and their reactivities. This is achieved using a metal cluster guided ion beam tandem mass spectrometer (GIBMS) to measure absolute cross sections as a function of kinetic energy for reactions of size-specific transition metal cluster ions with simple molecules. Analysis of the kinetic energy dependent cross sections reveals quantitative thermodynamic information as well as kinetic and dynamic information regarding the reactions under study.

Since 2004, our DOE sponsored work has included studies of the kinetic energy dependences of the size-specific chemistry of $Co_n^+$ ($n$ = 2 - 16) cluster ions reacting with $D_2$,[1] of $Co_n^+$ ($n$ = 2 - 20) reacting with $O_2$,[2] of $Fe_n^+$ ($n$ = 1 - 19) cluster ions reacting with $N_2$,[3] of $Ni_n^+$ ($n$ = 2 - 16) with methane ($CD_4$),[4] and of $Co_n^+$ ($n$ = 1 - 18) reacting with $N_2$.[5] Data has been obtained and analyzed for reactions of $Co_n^+$ ($n$ = 2 - 16) cluster ions reacting with $CD_4$,[6] and these results are presently being written up. This work can be directly compared with our previous studies of the $Fe_n^+$ and $Ni_n^+ + CD_4$ systems.[4,7] Finally, we have quantitatively examined the collision-induced dissociation of small iron oxide cluster cations with Xe to ascertain their stabilities. These results, the first of which are being written up,[8] are discussed further below.

An invited review of our recent work that emphasizes the relationship to bulk phase properties is presently being considered for publication.[9]

## Recent Progress

**Reactions of Clusters with $CD_4$.** We have studied the kinetic energy dependences of reactions of $Fe_n^+$ ($n$ = 2 - 16)[7] and $Ni_n^+$ ($n$ = 2 - 16)[4] with $CD_4$, and that for $Co_n^+$ ($n$ = 2 - 16) is undergoing final analysis.[6] Figure 1 shows results typical of most clusters. All observed reactions are endothermic. The lowest energy process for iron and cobalt clusters is generally dehydrogenation, whereas for nickel, double dehydrogenation is efficient enough that the $Ni_nCD_2^+$ species is not observed except for the smallest and largest clusters. These results are qualitatively consistent with observations that carbide formation is an activated process for reactions of hydrocarbons on Fe, Co, and Ni surfaces. Indeed, formation of $Co_nCD_4^+$ (observed for larger clusters, e.g., Figure 1) has a threshold that directly corresponds to the activation energy for dissociative chemisorption.

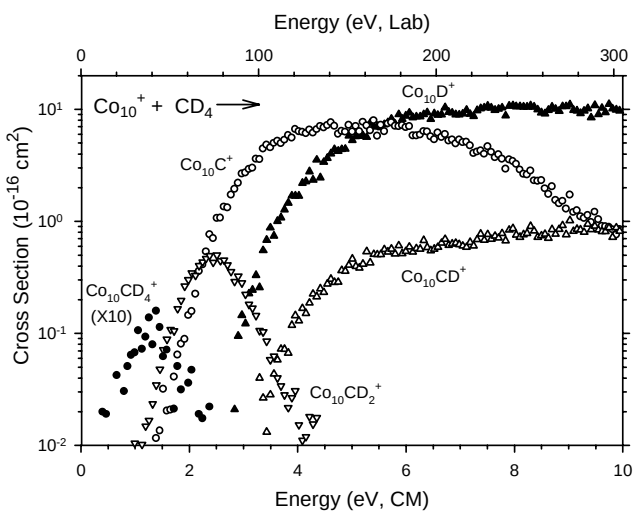


Figure 1. Reaction of $Co_{10}^+$ with $CD_4$ to form primary products.

Thresholds for the various primary and secondary reactions are analyzed and bond dissociation energies (BDEs) for cluster bonds to C, CD, and $CD_2$ are determined. Importantly, the accuracy of these BDEs can be assessed because there are usually two independent routes to measure BDEs for each cluster to D, C, CD, and $CD_2$, e.g., $D_0(Co_{10}^+\text{-D})$ can be measured in the primary reaction of $Co_{10}^+$ or the secondary reaction of $Co_{11}^+$ (to form $Co_{10}D^+ + Co + D$). Values obtained from the primary and secondary processes are in good agreement for D (which also agree with the results from $D_2$ studies),[10-12] C, and CD. For the $CD_2$ ligand, BDEs obtained from primary reactions are generally low compared to those from secondary reactions, which demonstrates that the initial dehydrogenation reactions have barriers in excess of the endothermicity. For larger clusters, this barrier often corresponds to the initial dissociative chemisorption step.

Figure 2 shows the final BDEs determined in the cobalt study,[6] which vary for small clusters but rapidly reach a relatively constant value at larger cluster sizes. The magnitudes of these bonds are consistent with simple bond order considerations, namely, D (and $CD_3$) form one covalent bond, $CD_2$ forms two, and CD and C form three. Previous results indicate that for D and O,[10-15] bond energies for larger clusters ($n > 10$) closely approach bulk phase values. Therefore, it seems reasonable to conclude that our experimental BDEs for larger clusters should provide reasonable estimates for heats of adsorption to surfaces for these molecular species. As little experimental information is available for *molecular* species binding to surfaces, the thermochemistry derived here for clusters bound to C, CD, and $CD_2$ provides some of the first experimental thermodynamic information on such species.

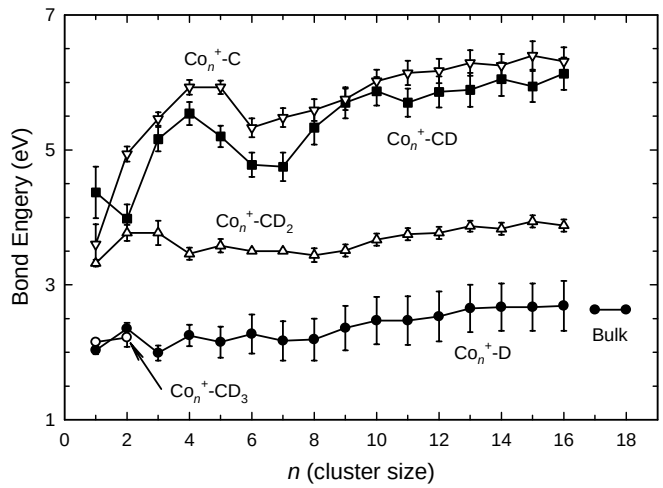


Figure 2. BDEs of D, C, CD, $CD_2$, and $CD_3$ to $Co_n^+$ vs. cluster size.

**Reactions of Clusters with $N_2$.** Our studies of the reactions of $N_2$ with $Fe_n^+$ ($n$ = 1 - 19)[3] and $Co_n^+$ ($n$ = 1 – 18)[5] are designed to provide insight into the rate-limiting step in the Haber process, which uses a promoted iron catalyst to manufacture ammonia from $N_2$ and $H_2$ at high pressures and temperatures. Despite the very strong $N_2$ bond energy of 9.76 eV, activation of this molecule on iron and cobalt cluster cations is observed, as

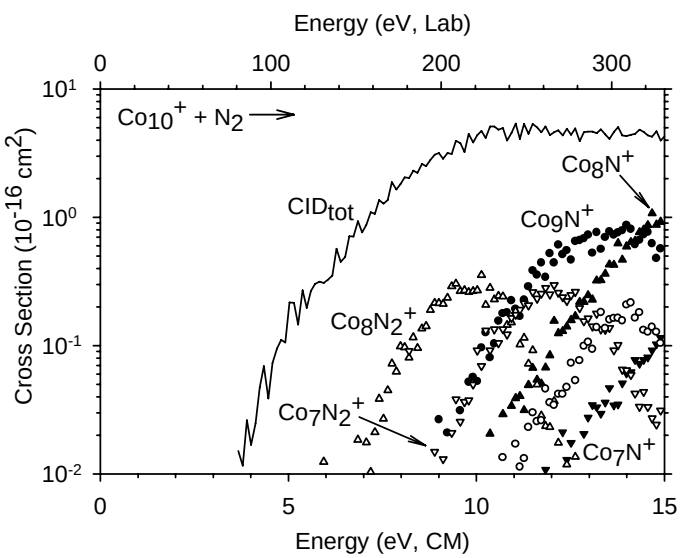


Figure 3. Reaction of $Co_{10}^+$ with $N_2$ showing cross sections for dinitride (open symbols), mononitride (closed symbols), and the total CID products (solid line).

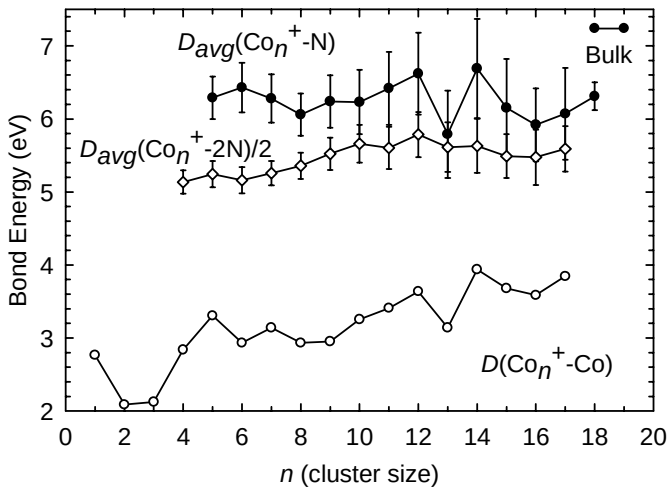


Figure 4. Comparison of the average cluster dinitride bond energies, $D_0(Co_n^+–2N)/2$ (open diamonds) with the average cluster nitride bond energies, $D_0(Co_n^+–N)$ (closed circles). The estimated bulk-phase value for N binding from Benziger (Ref. 10) to cobalt surfaces is shown to the right. $D_0(Co_n^+–Co)$ bond energies (Refs. 11 and 12) are indicated by open circles.

illustrated in Figure 3. Both $Co_mN_2^+$ and $Co_mN^+$ product ions, where $m \leq n$, are observed and the former can be identified as dinitride species. On iron clusters, an energetic barrier for $N_2$ activation of 0.48 ± 0.03 eV is obtained for the largest clusters, whereas this barrier is 0.78 ± 0.12 eV on larger cobalt clusters. This difference reflects the efficacy of iron as the preferred catalyst for the Haber process as nitrogen activation is the rate limiting step in the catalytic reaction. $Fe_n^+$-N, $Fe_n^+$-2N, $Co_n^+$-N, and $Co_n^+$-2N bond energies as a function of cluster size are derived from threshold analysis of the kinetic-energy dependences of the endothermic reactions, as shown in Figure 4. These experimental values are somewhat smaller than bulk phase estimates, although this is potentially because the activation barriers for $N_2$ activation have been underestimated in the surface work, as previously suggested by Benziger.[16] In the cobalt case, the bulk phase estimate does not follow periodic trends and may therefore be too high. Comparison to the $D_0(Co_n^+–Co)$ bond energies[17,18] demonstrates that nitrided cobalt surfaces should desorb cobalt atoms more readily than nitrogen, in agreement with observations.[19,20]

**Iron oxide cluster cations.** We have also initiated studies of oxygenated iron clusters, $Fe_nO_m^+$, which might mimic the chemistry of metal oxide surfaces. A broad range of stoichiometries have been produced although larger clusters tend to form clusters containing nearly equal numbers of iron and oxygen atoms. Initially, our studies are focusing on characterizing the thermodynamic stabilities of these clusters by examining their dissociation behavior in collisions with Xe. Some 30 different iron oxide cluster cations (with $n$ = 1 - 10) have been examined, including $FeO_m^+$ ($m$ = 1 - 5), $Fe_2O_m^+$ ($m$ = 1 - 6), $Fe_3O_m^+$ ($m$ = 2 - 4, 8), $Fe_4O_m^+$ ($m$ = 1 - 6), $Fe_5O_m^+$ ($m$ = 4 - 6),

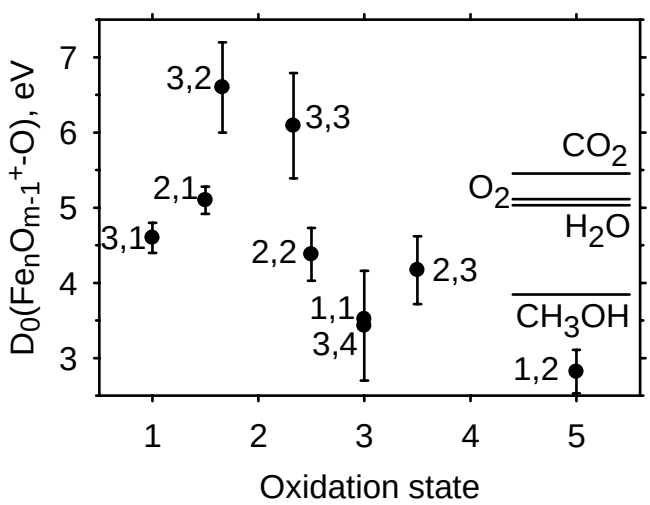


Figure 5. Oxygen atom bond energies to $Fe_nO_{m-1}^+$ clusters indicated by ($n$,$m$) versus the average oxidation state of the iron atoms. Similar bond energies for the species on the right are indicated for comparison.

$Fe_6O_m^+$ ($m$ = 5 - 8), $Fe_7O_m^+$ ($m$ = 6 - 8), $Fe_8O_m^+$ ($m$ = 7 - 9), $Fe_9O_m^+$ ($m$ = 8 - 10), and $Fe_{10}O_x^+$ ($x$ = 9 - 11). Not surprisingly, oxygen rich clusters tend to dissociate by losing O, $O_2$, or $FeO_2$, whereas iron rich clusters dissociate by losing Fe or FeO, in agreement with the qualitative CID study of Castleman and coworkers.[21] Particularly stable clusters include $Fe_2O_2^+$, $Fe_3O_3^+$, and $Fe_6O_6^+$. For larger clusters, fission is not uncommon, e.g., $Fe_6O_6^+$ dissociates to $Fe_3O_3^+$ + $Fe_3O_3$ at relatively low energies. The kinetic energy dependent collision-induced dissociation cross sections for the smaller clusters have been analyzed to obtain both oxygen and iron bond energies for these clusters and these results are being prepared for publication.[8] Preliminary results are shown in Figure 5. As can be seen, the oxygen atom bond energies can be tuned over a broad range by altering the stoichiometry and oxidation state of the cluster, such that specific clusters may prove useful as efficient catalysts for oxidation of species like methane and CO, as previously examined by Castleman and coworkers.[21] Future studies will examine the energetics and kinetics of such oxidation reactions.

**Publications resulting from DOE sponsored research in 2004 – present (1 – 6, 8, 9) and References**


1. F. Liu and P. B. Armentrout, J. Chem. Phys. **122**, 194320 (2005).
2. F. Liu, F.-X. Li, P. B. Armentrout, J. Chem. Phys. **123**, 064304 (2005).
3. L. Tan, F. Liu, P. B. Armentrout, J. Chem. Phys. **124**, 084302 (2006).
4. F. Liu, X.-G. Zhang, R. Liyanage, and P. B. Armentrout, J. Chem. Phys. **121**, 10976 (2004).
5. F. Liu, M. Li, L. Tan, P. B. Armentrout, J. Chem. Phys. **128**, 194313 (2008).
6. F. Liu, M. Citir, P. B. Armentrout, work in progress.
7. R. Liyanage, X.-G. Zhang, and P. B. Armentrout, J. Chem. Phys. **115**, 9747 (2001).
8. S. Liu, M. Li, P. B. Armentrout, work in progress.
9. P. B. Armentrout; W. C. Castleman and P. Jena, editors; submitted for publication.
10. J. Conceição, S. K. Loh, L. Lian, P. B. Armentrout, J. Chem. Phys. **104**, 3976 (1996).
11. F. Liu, R. Liyanage, P. B. Armentrout, J. Chem. Phys. **117**, 132 (2002).
12. F. Liu, P. B. Armentrout, J. Chem. Phys. **122**, 194320 (2005).
13. J. B. Griffin, P. B. Armentrout, J. Chem. Phys. **106**, 4448 (1997).
14. D. Vardhan, R. Liyanage, P. B. Armentrout, J. Chem. Phys. **119**, 4166 (2003).
15. F. Liu, F.-X. Li, P. B. Armentrout, P. B. J. Chem. Phys. **123**, 064304 (2005).
16. J. B. Benziger, in *Metal-Surface Reaction Energetics*, edited by E. Shustorovich (VCH, New York, 1991), pp. 53–107.
17. D. A. Hales, C. X. Su, L. Lian, P. B. Armentrout, J. Chem. Phys. **100**, 1049 (1994).
18. P. B. Armentrout, B. L. Kickel, *Organometallic Ion Chemistry*, B. S. Freiser, ed. Kluwer, Dordrecht, 1996, pp. 1–45.
19. L. Maya, M. Paranthaman, J. R. Thompson, T. Thundat, R. J. Stevenson, J. Appl. Phys. **79**, 7905 (1996).
20. J.-S. Fang, L.-C. Yang, C.-S. Hsu, G.-S. Chena, Y.-W. Lin, G.-S. Chen, J. Vac. Sci. Technol. A **22**, 698 (2004).
21. N. M. Reilly, J. U. Reveles, G. E. Johnson, J. M. del Campo, S. N. Khanna, A. M. Köster, A. W. Castleman, Jr. J. Phys. Chem. C **111**, 19086 (2007).

**"Electronic Structure of Transition Metal Clusters and Actinide Complexes and Their Reactivity" DEFG2-05ER15657**

**K. Balasubramanian, California State University East Bay, Hayward CA 94542**

Our research in this area since October 2007 has resulted in seven completed publications[1-7] and more papers of the completed work are in progress. Our work during this period principally focused on actinide complexes with secondary emphasis on spectroscopic properties and electronic structure of metal complexes. As the publications are available online with all of the details of the results, tables and figures, we are providing here only a brief summary of major highlights, in each of the categories.

**Electronic Structure of Actinide Complexes.**

We have carried out a number of actinide complexes in aqueous solution; as such complexes are of considerable importance in our understanding of behavior of actinide species in the environment and high level nuclear wastes. A major highlight of our work during this period is experimental-theoretical collaboration on curium (III) complexes with mutli-dentate ligands with Professor Nitsche and coworkers at LBNL. Our focus was on Cu(III) complexes with ligands that have both carboxylic and phosphoric acid groups so that relative binding strengths of the two ligands can be assessed as a with varying pH. Experimental studies have revealed intriguing trends that could not be explained. We have also studied aqueous complexes of U(VI), NP(VI) and Pu(VI) with $OH^-$.

Extensive *ab inito* computations have been carried out to study the equilibrium structure, infrared spectra, and bonding characteristics of a variety of hydrated $NpO_2(CO_3)_m^{q-}$ complexes by considering the solvent as a polarizable dielectric continuum as well as the corresponding anhydrate complexes in the gas-phase.[3] The computed structural parameters and vibrational results at the MP2 level in aqueous solution are in good agreement with Clark et al.'s experiments and provide realistic pictures of the neptunyl complexes in an aqueous environment. Our computed hydration energies reveal that the complex with water molecules directly bound to it yields the best results. Our analysis of the nature of the bonding of neptunyl complexes provides insight into the nature of 6d and 5f-bonding in actinide complexes.We have studied the electronic and spectroscopic properties of plutonyl di and tri carbonate complexes of the types $PuO_2[CO_3]_2$ and $PuO_2[CO_3]_3Ca_3$ using coupled cluster (CC) and other techniques.[4] In particular the structures, and select vibrational spectra, electron density and molecular orbital contour plots of plutonium(VI) complexes of environmental importance such as $[PuO_2(CO_3)_2]^{2-}$ and $[PuO_2(CO_3)_3]^{4-}$ were computed. We have shown that $Ca^{2+}$ is efficacious in gas-phase modeling of electronic and spectroscopic properties of multiply charged plutonyl di and tricarbonate anions through complexes such as $PuO_2(CO_3)_2Ca$ and $[PuO_2(CO_3)_3Ca_3]^{2+}$. Our computed equilibrium geometries and vibrational spectra of these species agree quite well with the EXAFS and Raman data available on related complexes. We have obtained the electron density plots and molecular orbital plots. The results of our computations at the DFT, MP2 and CCSD levels show that the computed geometries and vibrational frequencies are in reasonable agreement among these theoretical levels. We have also compared our computed properties with the available experimental data on the plutonyl carbonate complexes in solutions and solid phases. Our computed geometries for the various interatomic distances at both MP2 and DFT levels agree quite well with the experimental EXAFS results of Clark et al..

A joint experimental-theoretical study[6] was carried out on curium (III) complexes with multidentate ligands such as phosphonic acid (PPA) which has both carboxylic and phosphoric acid groups to explain the observed dramatic variations in the nature of the observed complexes as a function of pH. Theoretical studies of $CmH_2PPA^{2+}$ and $CmHPPA^+$ complees were carried out in aqueous solution. All possible isomers in the gas phase and aqueous solution have been calculated. The effects of the aqueous solvent in the configuration preferences of $CmH_2PPA^{2+}$ and $CmHPPA^+$ have been investigated. The free energies of solvation were predicted using a self-

consistent reaction-field model and a combined discrete-continuum model. Results provided by the different methods were compared and discussed.

Spectroscopic studies on Cm(III) aquoion were carried out by a fluorescence emission spectroscopy at Berkeley, which revealed a band maximum at 593.8 nm. There is a pronounced red-shift of the emission as a result of the complex formation with the PPA molecule, accompanied by an increase in the fluorescence emission lifetime from 65 μs for the Cm(III) aquoion. The TRLFS (time-resolved laser-induced fluorescence spectroscopy) spectra have also been obtained for Cm(III) and PPA species. The PPA molecule can interact with metal ions via the oxygen atoms from the phosphate group and the carboxylate group, thus relative competition of the two groups and their binding propensities with Cm(III) were the central objectives.

Geometries and energy differences of $CmH_2PPA^{2+}$ in aqueous solution were computed using the IEFPCM continuum solvation model and the combined discrete-continuum model at the DFT/B3LYP level. The theoretical results by inclusion of the continuum solvent models produce a relative stabilization of $CmH_2PPA^{2+}$ in aqueous solution. The equilibrium geometries are presented in Fig. 1 and the corresponding geometries of $HPPA^{2-}$ with Cm(III) were also optimized. The conformational free energy difference ($\Delta G_{conf}$) in solution was estimated by adding solvation free energy $\Delta\Delta G_{sol}$ to the gas-phase energy . $\Delta G_{conf} \approx \Delta E + \Delta\Delta G_{sol}$. The calculation with the SCRF model, surprisingly, indicates that the most stable structure is the monodentate phosphate complexation (Cm-P, Fig. 1a) which is the least stable structure in the gas phase. The second stable structure is the bidentate carboxylate complexation (Cm-C2, Fig. 1b), followed by bidentate complexation (Cm-CP2, Fig. 1e). The monodentate carboxylate complexation is even higher in energy in aqueous solution, which is not a stable structure in the gas phase. The tridentate complexation which is the most stable structure in the gas phase is 35.3 kcal/mol higher in energy than the monodentate phosphate complexation. We have also optimized geometries of (a) $Cm[H_2PPA]_2^+$ and (b) $Cm[HPPA]_2^-$ in aqueous solution.

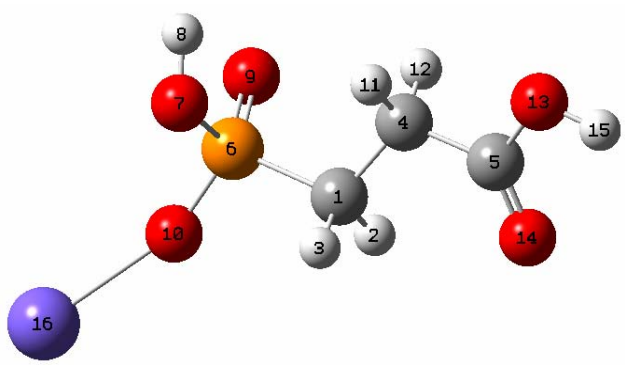


(a) Cm-P ($\Delta\Delta G_{conf}$ = 0.00 kcal/mol)

$P_6$-$O_7$: 1.626
$P_6$-$O_9$: 1.493
$P_6$-$O_{10}$: 1.534
$Cm_{16}$-$O_{10}$: 2.331
$P_6$-$C_1$: 1.826
$C_5$-$O_{13}$: 1.347
$C_5$-$O_{14}$: 1.216
$C_1$-$C_4$: 1.533
$C_4$-$C_5$: 1.518

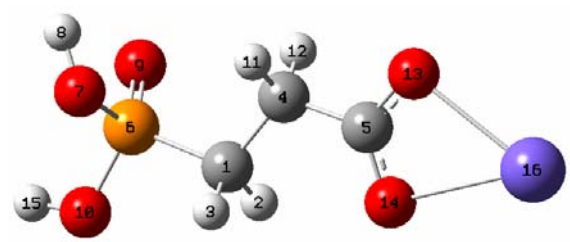


(b) Cm-C2

$P_6$-$O_7$: 1.604
$P_6$-$O_9$: 1.482
$P_6$-$O_{10}$: 1.596
$P_6$-$C_1$: 1.809
$C_5$-$O_{13}$: 1.277
$C_5$-$O_{14}$: 1.263
$C_1$-$C_4$: 1.535
$C_4$-$C_5$: 1.525
$Cm_{16}$-$O_{13}$: 2.498
$Cm_{16}$-$O_{14}$: 2.637

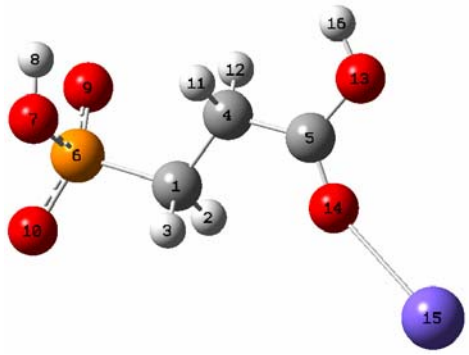

(c) Cm-C ($\Delta\Delta G_{conf}$ = 17.17 kcal/mol)

$P_6$-$O_7$: 1.646
$P_6$-$O_9$: 1.505
$P_6$-$O_{10}$: 1.501
$P_6$-$C_1$: 1.842
$C_5$-$O_{13}$: 1.331
$C_5$-$O_{14}$: 1.229
$C_1$-$C_4$: 1.530
$C_4$-$C_5$: 1.512
$Cm_{15}$-$O_{14}$: 2.582

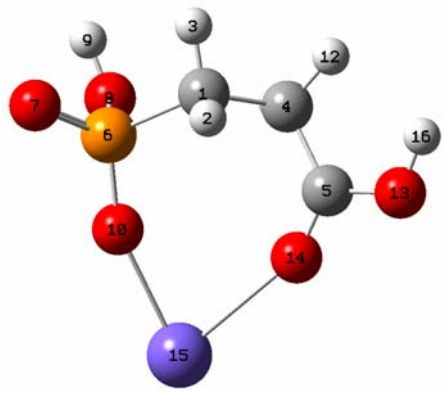

(d) Cm-CP ($\Delta\Delta G_{conf}$ = 7.09 kcal/mol)

$P_6$-$O_7$: 1.490
$P_6$-$O_8$: 1.621
$P_6$-$O_{10}$: 1.529
$P_6$-$C_1$: 1.830
$C_5$-$O_{13}$: 1.331
$C_5$-$O_{14}$: 1.227
$C_1$-$C_4$: 1.553
$C_4$-$C_5$: 1.517
$Cm_{15}$-$O_{10}$: 2.340
$Cm_{15}$-$O_{14}$: 2.572

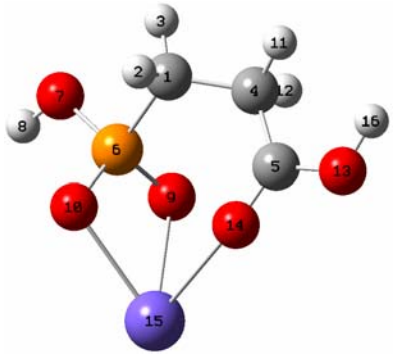

$P_6$-$O_7$: 1.598
$P_6$-$O_9$: 1.527
$P_6$-$O_{10}$: 1.526
$P_6$-$C_1$: 1.826
$C_5$-$O_{13}$: 1.328
$C_5$-$O_{14}$: 1.227
$C_1$-$C_4$: 1.538
$C_4$-$C_5$: 1.516
$Cm_{15}$-$O_9$: 2.499
$Cm_{15}$-$O_{10}$: 2.480
$Cm_{15}$-$O_{14}$: 2.598

(e) Cm-CP2 ($\Delta\Delta G_{conf}$ = 18.74 kcal/mol)

We find that the ordering of the calculated conformational Gibbs energies in solution is different from the ordering of energies from the pure continuum model. The tridentate complex Cm-CP2 is the most stable structure in aqueous solution. The next are Cm-P and Cm-C2. Cm-P and Cm-C are not stable structures in the gas phase. Aqueous solution geometries were used in the calculations of gas phase energies. There are significant changes on geometries after solvation in aqueous solution. The conformational Gibbs energy of Cm-P2 is only ca. 6 kcal/mol larger than that of Cm-C2. The carboxylate complexation is capable of displacing the phosphate binding in aqueous solution. Cm-CP is even more unstable. The most stable structure is the tridentate complex Cm-CP2. This might explain the experimental observation that the lifetime of $CmHPPA^+$ is 160 μs while the lifetime of $CmH_2PPA^{2+}$ is 112 μs. $CmHPPA^+$ binds less coordinated water molecules than $CmH_2PPA^{2+}$ in solution.

Extensive *ab initio* calculations have been carried out to study equilibrium structures, vibrational frequencies, and bond characters of hydrated $UO_2(OH)^+$, $UO_2(OH)_2$, $NpO_2(OH)$, and $PuO_2(OH)^+$ complexes in aqueous solution and the gas phase.[7] The structures have been further optimized by considering long-range solvent effects as a polarizable continuum dielectric model. The hydrolysis reaction Gibbs energy of $UO_2(H_2O)_5^{2+}$ is computed to be 8.11 kcal/mol at the MP2 level in good agreement with experiments. Our results reveal that it is necessary to include water molecules bound to the complex for proper treatment of the hydrated complex and the dielectric cavity. Structural reoptimization of the complex in a dielectric cavity seems inevitable to seek subtle structural variations in the solvent and to correlate with the observed spectra and thermodynamic properties in the aqueous environment.

The optimized structure of some of these complexes is not the same in the gaps phase and aqueous solution illustrating the importance of carrying out these computations in solution. Our results also show that the bulk effects are important on the vibrational frequencies of hydrated actinyl hydroxide complexes, especially the $UO_2(OH)_2(H_2O)_3$ and $NpO_2(OH)(H_2O)_4$. They were found to be four-coordinated in the first coordination shell and one water molecule in the second shell in the gas phase, whereas their solvation structures are five-coordinated in the first coordination shell in the continuum PCM model. Moreover, with the equilibrium geometries reoptimized in aqueous solution, the computed Gibbs energy of hydrolysis reaction of $UO_2(H_2O)_5^{2+}$ in solution is 7.27 kcal/mol, which is in good agreement with the experimental value. It is also necessary to include water molecules bound to the complex in the first hydration sphere for proper treatment of the hydrated complex and the dielectric cavity.
phase (left) and aqueous solution (right).

**Proposed Plan.**

We plan to continue our works on environmental actinide complexes and transition metal species. We are investigating Cm(III) complexes with other ligands such as $OH^-$ and $CO_3^{2-}$ in collaboration with Professor Nitsche and his coworkers who are carrying out EXAFS and time-resolved xray fluorescence studies of such curium(III) complexes in solution. Likewise structures and properties of Bk(III) complexes remain unknown at this time and one often has to rely on analogous lanthanide complexes, which often results in erroneous deductions, as transplutonium complexes tend to behave quite differently from the lanthanide analogs due to relativistic effects. The observed behavior of these complexes as a function of pH is far from understood. Moreover there is a scarcity of thermodynamic solvation energy data on Bk(III) and Am(III) species which occur not only in high level nuclear wastes but also in nuclear reactor reactions during fission process. There have been some exciting experimental findings concerning proton transfers in actinide water complexes. At present there are no theoretical studies to provide insight into these species. We also propose to continue our work on transition metal species and these actinide with specific focus on spectroscopic properties, geometries, Gibbs Free energies in solutions and potential energy curves.

**Publications from the DOE BES Grant Oct 2007-Present**


1. Balasubramanian, K.; Felter, T. E.; Anklam, T.; Trelenberg, T. W.; McLean II, W., Atomistic level relativistic quantum modelling of plutonium hydrogen reaction. *Journal of Alloys and Compounds* **2007,** 444, p.447-452, [PDF]

2. Suo, B.; Balasubramanian, K., Spectroscopic constants and potential energy curves of yttrium carbide (YC). *Journal of Chemical Physics* **126**, 224305 (2007) [PDF]

3. Balasubramanian, K and Z. Cao, "Theoretical Studies on Structures of Neptunyl Carbonates: $NpO_2(CO_3)_m(H_2O)_n^q$ (m =1-3, n = 0-3) in Aqueous Solution**",** *Inorganic Chemistry***,** 46, 10510-10519 (2007)

4. Balasubramanian, K. and D. Chaudhuri, "Computational modeling of environmental plutonyl mono-, di- andtricarbonate complexes with Ca counterions: Structures and spectra: $PuO_2(CO_3)_2^{2-}$ , $PuO_2(CO_3)_2Ca$, and $PuO_2(CO_3)_3Ca_3$, Chemical Physics Letters, *450, Issues 4-6, Pages 196-202, 2008.*

5. Balasubramanian, K., and Cao, Z., "Geometries and energy separations of electronic states of $In_3N$, $InN_3$, and their ions", J. Theoretical and Computational Chemistry, 2008.

6. Cao, Z., Balasubramanian, K., Calvert, M., Nitsche, H., "Solvation effects on the isomeric preference of binding of Curium$^{3+}$ with phosphocarboxylic acid multidentate ligands: $mH_2PPA^{2+}$ and $CmHPPA^+$", Manuscript to be submitted

7. Cao, Z., Balasubramanian, K., "Unusual Structures and Energetics of U(VI), NP(VI) and Pu(VI) complexes with $OH^-$ in aqueous solution: $UO_2(OH)(H_2O)_4^+$, $UO_2(OH)_2(H_2O)_3$, $NpO_2(OH)(H_2O)_4$, and $PuO_2(OH)(H_2O)_4^+$ complexes", in prep.

# Influence of medium on radical reactions

David M. Bartels, John Bentley and Daniel M. Chipman
Notre Dame Radiation Laboratory, Notre Dame, IN 46556
e-mail: bartels.5@nd.edu; Bentley.1@nd.edu ; chipman.1@nd.edu

**Program definition**

This project pursues the use of radiolysis as a tool in the investigation of solvent effects in chemical reactions, particularly the free radicals derived from solvent which are copiously generated in the radiolysis excitation process. Most recently we have focused on radical reactions in high-temperature water, and some of these results are described below. The project has now evolved toward the particular study of solvent effects on reaction rates in supercritical (sc-)fluids where the fluid density becomes a primary variable. One proposed thrust will be the study of solvated electrons under these conditions. Others will focus on small radicals in supercritical water and $CO_2$. A theoretical component has also recently been joined with this project, which will be directed to support the analysis and interpretation of experimental results.

An anthropomorphic way to think about near-critical phenomena, is that the fluid is trying to decide whether it is a liquid or a gas. The cohesive forces between molecules that tend to form a liquid are just being balanced by the thermal entropic forces that cause vaporization. The result, on a microscopic scale, is the highly dynamic formation and dissipation of clusters and larger aggregates. The fluid is extremely heterogeneous on the microscopic scale. A solute in a supercritical fluid can be classified as either attractive or repulsive, depending on the potential between the solute and solvent. If the solute-solvent potential is more attractive than the solvent-solvent potential, the solute will tend to form the nucleus of a cluster. When the solute-solvent potential is repulsive, one might expect the solute to remain in a void in the fluid as the solvent molecules cluster together. Extremely large partial molal volumes are known for hydrophobic molecules in near-critical water, indicating an effective phase separation. Such variations in local density around the solute will have implications for various spectroscopies and for reaction rates.

The ultimate goal of our study is the development of a predictive capability for free radical reaction rates, even in the complex microheterogeneous critical regime. Our immediate goal is to determine representative free radical reaction rates in sc-fluid and develop an understanding of the important variables to guide development and use of predictive tools. Electron beam radiolysis of water (and other fluids) is an excellent experimental tool with which to address these questions. The primary free radicals generated by radiolysis of water, $(e^-)_{aq}$, OH, and H, are respectively ionic, dipolar, and hydrophobic in nature. Their recombination and scavenging reactions can be expected to highlight the effects of clustering (i.e. local density enhancements) and solvent microheterogeneity both in terms of relative diffusion and in terms of static or dynamic solvent effects on the reaction rates. We already have transient absorption data for several of these species that highlights interesting and unexpected reaction rate behavior. A major thrust of the next several years will be to push time-resolved EPR detection of H atoms in sc-water. The Chemically Induced Dynamic Electron Polarization (CIDEP) generated in H atom recombination reactions provides another unique probe of the cage dynamics and potential of mean force. How different will be the potential of mean force between H atoms and between $(e^-)_{aq}$ and H? How easily will H atoms penetrate into water clusters?

**Recent Progress**

Accurate knowledge of the rates of second order recombination reactions of small free radicals derived from water radiolysis, and of their temperature dependence up to and beyond the supercritical point, continues to be of the utmost importance in nuclear reactor chemistry.

The temperature dependence of the OH radical self termination:

$$\mathrm{OH} + \mathrm{OH} \rightarrow \mathrm{H_2O_2} \tag{1}$$

has been previously reported. For radical combination rates involving the hydrated electron:

$$e^-_{aq} + e^-_{aq} \rightarrow \mathrm{H_2} + 2\,\mathrm{OH}^-_{aq} \tag{2}$$

$$e^-_{aq} + \mathrm{H} \rightarrow \mathrm{H_2} + \mathrm{OH}^-_{aq} \tag{3}$$

an extinction coefficient for the hydrated electron must be used to convert transient absorption data into rate constant information for these reactions, because the parameters actually extracted by fitting the data are $k/\varepsilon_{e^-}$. At any given wavelength these numbers are temperature sensitive, because the entire hydrated electron spectrum shifts to the red with higher temperature. In our opinion the values of $\varepsilon_{e^-}$ previously reported for elevated temperature (to 200 °C) were not very reliable, so we assumed conservation of oscillator strength vs. temperature in our paper to derive values of $\varepsilon_{e^-}$. This year extensive direct measurements of the extinction coefficient have been made.

The method adopted is intended to be valid in supercritical water where no measurements have been reported to date, and where radiolysis yields are not well established. Essentially the transient absorption of the solvated electron is recorded in the presence of a scavenger, S, to accomplish the reaction

$$e^-_{aq} + \mathrm{S} \rightarrow \mathrm{P} \tag{3}$$

The product, P, corresponding to a given number of radiolysis shots is then measured to deduce the total number of electrons present. A simple formula can be derived

$$\varepsilon\ell[\mathrm{P}]_\infty = k_S[\mathrm{S}]A_{\mathrm{int}} \tag{4}$$

relating the product concentration [P], the extinction coefficient, ε, the scavenging rate $k_s$[S] and the time-integrated transient absorption, $A_{\mathrm{int}}$. Two scavengers have been used, $N_2O$ and $SF_6$. Preliminary data, in contrast to previous reports, reveal very little temperature effect on the extinction coefficient at the maximum absorption. A similar lack of temperature dependence was previously assumed in evaluating the rates in reactions (2) and (3).

Surprisingly the room temperature value returned by this experiment is higher by some 10-20% over all other literature reports. To confirm this new measurement a simple experiment was carried out comparing transient absorption of $e^-_{aq}$ and methyl viologen in the reaction

$$e^-_{aq} + \mathrm{MV}^{2+}_{aq} \rightarrow \mathrm{MV}^{+}_{aq} \tag{5}$$

The $MV^+_{aq}$ radical cation extinction coefficient at 605 nm has been carefully measured in the past. Using the ratio of signals from $MV^+_{aq}$ and $e^-_{aq}$ we can deduce a $e^-_{aq}$ extinction coefficient in excellent agreement with our other scavenging experiment. The reaction rates for reactions (2) and (3) measured in our earlier experiment need to be corrected upwards by about 20%.

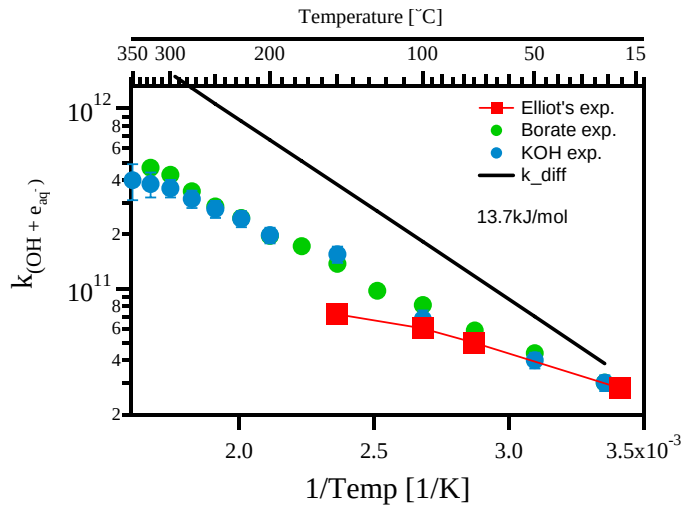


**Figure 1** – *Arrhenius plot for reaction of $e^-_{aq}$ with OH. New results are compared with literature values of Elliot and an estimate of the diffusion limit k_diff.*

Given reliable values for reaction (1) and for reactions (2) and (3), it is now possible to fit data collected on the cross-reaction

$$e^-_{aq} + OH \rightarrow OH^-_{aq} \qquad (6)$$

Results are shown in Figure 1. This is the most important reaction in nuclear reactor cooling loops, leading to recombination of the dominant reducing radical and the dominant oxidizing radical. As a result in the coming year we should be able to compile and evaluate a much more accurate model of high temperature radiolysis chemistry up to about 350 ˚C.

Work has progressed on the very old, yet still unsolved, problem of carbonate radical, $CO_3^-$, recombination. The long-lived $CO_3^-$ absorbs at 600 nm, but there are no easily measured properties of the products. A dimeric intermediate, $(C_2O_6)^{2-}$, with lifetime of less than a microsecond, is postulated to explain the observed non-Arrhenius and temperature insensitive second-order reaction rate. The initial products are believed to be $HCO_3^-$ and $HOOCO_2^-$, based on conductivity experiments which rule out virtually all other possibilities. In neutral, as opposed to basic, solution, the decay kinetics are apparently not second-order. One explanation is protonation of the short-lived intermediate, leading to a potentially more stable form as in (7).

$$(C_2O_6)^{2-}_{aq} + H_2O \rightleftharpoons (HC_2O_6)^-_{aq} + OH^-_{aq} \qquad (7)$$

Thermodynamics of hydration for free radicals are of great practical importance to calculate relatively slow reaction rates at high temperature. Computer simulations have become a very valuable approach for estimating these energies. In the past year the hydration of hydroxyl radical has been analyzed in terms of a many-body decomposition of quantum chemical calculations on the interaction energy between OH and water molecules in a wide variety of cluster structures. Works in the literature on water clusters have shown that two-body interactions are of primary importance, three-body effects are smaller but significant, and higher order effects are very small. We find that OH radicals involved in single-donor single-acceptor hydrogen bonding arrangements follow a very similar pattern to the analogous parent water clusters. But surprisingly, OH radicals involved in single-donor double-acceptor hydrogen bonding arrangements display substantial higher order effects, with up to six-body interactions

being significant. These results will be used in the future to guide development of a force field suitable for molecular dynamics simulation on the properties of hydroxyl radical in liquid water over a wide range of temperatures and pressures.

**Future Plans**

Immediate plans are to continue the optical transient absorption measurements of OH radical and hydrated electron reaction rates. A most important target for experimental measurement is the reaction $H_2$ + OH in supercritical water. Mechanisms of prototypical radiolytic reactions in aqueous solution such as H + OH → $H_2O$, $H_2$ + OH → H + $H_2O$, $H_2$ + O- → H + OH-, OH + OH → $H_2O_2$ and OH + OH- → O- + $H_2O$ , as well as the OH/O- equilibrium, will be characterized by ab initio methods as initial steps toward the ultimate goal of understanding their unusual temperature dependences. Work on understanding of solvated electron reaction rates is to be continued by measuring reaction rates in supercritical alcohols for comparison with unusual behavior in supercritical water.

**Publications**, 2006-2008


Hare, P. M., Price, E. A., Bartels, D. M., (2008). *J. Phys. Chem. A 112*(30): 6800-6802. Hydrated electron extinction coefficient revisited.

Bonin, J.; Janik, I.; Janik, D.; Bartels, D. M. (2007). *J. Phys. Chem. A 111*(10): 1869-1878. Reaction of the Hydroxyl Radical with Phenol up to Supercritical Conditions.

Du, Y.; Price, E.; Bartels, D. M. (2007). *Chem. Phys. Lett. 438*: 234-237. Solvated electron spectrum in supercooled water and ice.

Janik, I.; Bartels, D. M.; Jonah, C. D. (2007). *J. Phys. Chem. A 111*: 1835-1843. Hydroxyl Radical Self-Recombination Reaction and Absorption Spectrum in Water up to 350$^o$C.

Janik, I.; Marin, T.; Jonah, C. D.; Bartels, D. M. (2007). *J. Phys. Chem. A 111*(1): 79-88. Reaction of $O_2$ with the Hydrogen Atom in Water up to 350$^o$C.

Marin, T. W.; Takahashi, K.; Jonah, C. D.; Chemerisov, S.; Bartels, D. M. (2007) *J. Phys. Chem. A* 111(45): 11540-11551. Recombination of the Hydrated Electron at High Temperature and Pressure in Hydrogenated Alkaline Water.

Chipman D.M. (2006). *J. Chem. Phys. 124*, 224111/1-10. New formulation and implementation for volume polarization in dielectric continuum theory.

Chipman D.M.; Chen F. (2006). *J. Chem. Phys. 124*, 144507/1-5. Cation electric field is related to hydration energy.

Shao Y.; Molnar L.F.; Jung Y.; Kussmann J.; Ochsenfeld C.; Brown S.T.; Gilbert A.T.B.; Slipchenko L.V.; Levchenko S. V.; O'Neill D. P.; DiStasio Jr. R.A.; Lochan R. C.; Wang T.; Beran G.J.O.; Besley N.A.; Herbert J.M.; Lin C.Y.; Van Voorhis T.; Chien S.H.; Sodt A.; Steele R. P.; Rassolov V.A.; Maslen P.E.; Korambath P.P.; Adamson R.D.; Austin B.; Baker J.; Byrd E.F.C.; Dachsel H.; Doerksen R.J.; Dreuw A.; Dunietz B.D.; Dutoi A.D.; Furlani T.R.; Gwaltney S.R.; Heyden A.; Hirata S.; Hsu C.-P.; Kedziora G.; Khalliulin R.Z.; Klunzinger P.; Lee A.M.; Lee M.S.; Liang W.Z.; Lotan I.; Nair N.; Peters B.; Proynov E.I.; Pieniazek P.A.; Rhee Y.M.; Ritchie J.; Rosta E.; Sherrill C.D.; Simmonett A.C.; Subotnik J.E.; Woodcock III H.E.; Zhang W.; Bell A.T.; Chakraborty A.K.; Chipman D.M.; Keil F.J.; Warshel A.; Hehre W.J.; Schaefer III H.F.; Kong J.; Krylov A.I.; Gil P.M.W.; Head-Gordon M. (2006). *Phys. Chem. Chem. Phys. 8*, 3172-3191. Advances in methods and algorithms in a modern quantum chemistry program package.

## ELECTRON-DRIVEN PROCESSES IN CONDENSED PHASES

### PRINCIPAL INVESTIGATORS

I Carmichael (*carmichael.1@nd.edu*), DM Bartels, DM Chipman, JA LaVerne
*Notre Dame Radiation Laboratory, University of Notre Dame, Notre Dame, IN 46556*

### SCOPE

Fundamental physicochemical processes in water radiolysis are probed in an experimental program measuring spur kinetics of key radiolytic transients at elevated temperatures and pressures using a novel laser-based detection system with interpretation supported by computer simulations. Related experimental and computational studies focus on the electronic excitation of liquid water, important aqueous radiolytic species, and the significance and mechanism of dissociative electron attachment in the liquid. Radiolytic decay channels in nonaqueous media are investigated, both experimentally, with product analysis under γ and heavy-ion irradiation and transient identification under pulse radiolysis, and theoretically, via kinetic track modeling and electronic structure calculations.

### PROGRESS AND PLANS

An apparatus has been constructed to satisfactorily record the vacuum UV absorption spectra of supercritical water. To measure the first absorption maximum, which has an extinction coefficient of about 1500 $M^{-1}$ $cm^{-1}$ at 8 eV, required a sapphire-windowed cell with a 1 micron pathlength, in addition to a very large dynamic detection range of about 6 orders of magnitude. The constructed flow cell is shown in Figure 1. Gold spacers of about 1 micron width are deposited directly onto the sapphire prior to assembly. Experiments have begun this summer at the LAMPF synchrotron facility at the University of Wisconsin, Madison. Once this apparatus is operational, deep UV spectra of many solutes will become accessible in supercritical water.

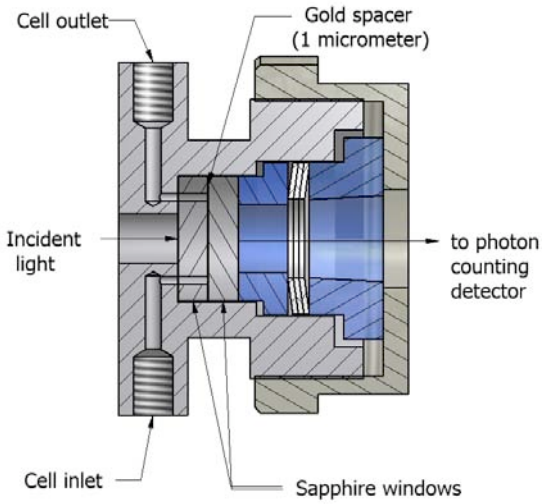


**Figure 1** – *Flow cell designed for optical absorption measurements in supercritical fluids.*

Room temperature ionic liquids (RTILs) composed of organic anions and cations have recently been proposed as "green" alternative solvents for many industrial processes, due to their inherently low vapor pressures. Preliminary radiation stability assessment studies suggest RTILs as possible solvents within the nuclear fuel cycle. The unique properties of ionic liquids, e.g. exceptionally large distribution coefficients in systems for extraction of metallic cations, make them especially attractive for solvent extraction of actinides from the spent nuclear fuel. To begin investigating the radiation stability of ionic liquids at a fundamental level we have measured radiation yields of gaseous hydrogen formed during radiolysis of room temperature ionic liquids representing the five most popular classes of ionic liquids – imidazolium, quaternary ammonium, pyridinium, phosphonium and pyrrolidinium associated with the bis(trifluoromethylsulfonyl)imide ($Tf_2N^-$) anion. RTILs comprising this anion are

characterized by having the lowest melting points, lowest viscosities and highest conductivities of currently available ionic liquids. The $Tf_2N^-$ anion also produces ionic liquids with excellent thermal, electrochemical, water and air stability. These properties might be particularly important for the application of ionic liquids within the nuclear fuel cycle.

Small samples of the purified ionic liquids were degassed and sealed, then irradiated with 3 MeV electrons to a dose of less than 200 Gray, so that Fricke dosimeter solutions could be used. The evolved hydrogen was measured using a mass spectroscopy technique. $H_2$ yields proved linear with accumulated dose up to 1.6 kGy (Figure 2). As in earlier work, aromatic compounds are more stable with respect to $H_2$ evolution than are aliphatic compounds. Imidazolium and pyridinium ILs had the lowest yields, while the phosphonium liquid, with its long aliphatic chains, had large yields. Other gaseous products are also measured, the most abundant being $C_2F_6$ from recombination of $CF_3$ radicals. Further investigation of the degradation pathways in these liquids is underway using EPR spin trapping techniques as well as pulse radiolysis/transient absorption.

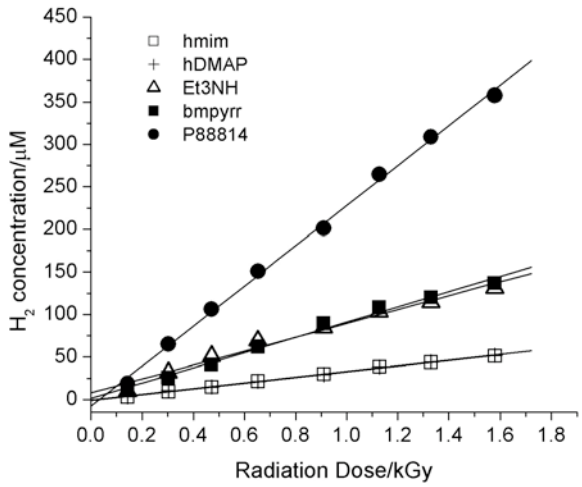


**Figure 2** – *Comparative plot of H2 yields depending on radiation dose applied to five different RTILs*

The hydroxyl (OH) radical, being the primary oxidizing species produced in water radiolysis, is fundamental to aqueous radiation chemistry and its chemical reactions are also of great importance in many biological systems. Measurements of rate constants involving the OH radical reacting with various substrates in aqueous solution are often based on monitoring the characteristic UV absorption band of OH, which peaks at about 235 nm. We have investigated this question with high level electronic structure calculations on OH interacting in various ways with a water molecule, together with a dielectric continuum representation of remaining bulk effects. The main aqueous absorption band is found to be due primarily to hemibonded arrangements, wherein a novel "charge transfer *from* solvent" transition contributes near the peak and on its blue side, and the valence transition localized on OH contributes on the red side. Such hemibonded arrangements are attractive between the two partners, but are not usually local minimum energy structures and so occur only transiently. They contribute to the spectrum far out of proportion to their population due to having large associated oscillator strengths. The more common hydrogen bonded arrangements contribute instead mainly to the weak broad shoulder that is observed in the 300-400 nm region. Further work on this problem will couple molecular dynamics simulations of local structures with quantum chemical calculations of excitation energies to obtain statistically representative samples. The goal is to interpret experimental results that are currently being obtained in this laboratory on the temperature and pressure dependence of the aqueous OH spectrum, and thereby to achieve a quantitative molecular level understanding of OH radical hydration under varying conditions.

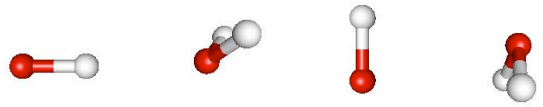

*Hydrogen bonded OH* *Hemibonded OH*

Benchmarks have been established for the quantum mechanical treatment of delocalization and charge transfer effects on excited states of water clusters. These will be used to develop more facile methods that can be applied to simulation of the UV absorption spectrum of liquid water. This work will be coupled to an experimental program in this laboratory that explores the temperature and pressure dependence of the water absorption spectrum.

H atom yields determined by subtraction of total molecular hydrogen production in neat water from that observed in formate solutions are found to agree well with the more direct measurement of HD using deuterated formate as a scavenger. H atoms yields are found to decrease with the evolution of the radiation track and decrease with increasing LET. Variation of the H atom yield with increasing concentration of nitrate anion as an electron scavenger has shown that the H atom and molecular hydrogen probably have the same precursor. The most likely candidate for this precursor is the excited water molecule formed by neutralization of the water cation and not the water anion.

Efforts are underway to elucidate the mechanism of radiation damage induced during macromolecular X-ray crystallography at synchrotrons, a phenomenon now known to sharply curtail the reliable use of such high flux sources. In collaboration with the Laboratory of Molecular Biophysics, Department of Biochemistry, University of Oxford, room temperature experiments have revealed surprising inverse dose-rate effects on crystal lifetimes with much less intense sources and scavenger studies have uncovered dramatic alterations in kinetics, suggesting possible strategies for devising effective room temperature data collection conditions.

### BES supported publications (2005-2008)


Enomoto K.; LaVerne J.A.; Tandon L.; Enriquez A.E.; Matonic J.H. *J. Nuclear Materials* **2008**, *373*, 103-11. The radiolysis of poly(4-vinylpyridine) quaternary salt ion exchange resins.

Hare P.M.; Price E.A.; Bartels D.M. *J. Phys. Chem. A* **2008**, *112*, 6800-2. Hydrated electron extinction coefficient revisited.

Hull K.L.; Carmichael I.; Noll B.C.; Henderson K.W. *Chem. Eur. J.* **2008**, *14*, 3939 – 53. Homo- and heterodimetallic geminal dianions derived from the bisphosphinimine $\{Ph_2P(Me_3Si)N\}_2CH_2$ and the alkali metals Li, Na and K.

Klepach T.; Zhang W.; Carmichael I.; Serianni A.S. *J. Org. Chem.* **2008**, *73*, 4376-87. $^{13}C$-$^{1}H$ and $^{13}C$-$^{13}C$ NMR *J*-couplings in $^{13}C$-labeled *N*-acetyl-neuraminic acid: Correlations with molecular structure.

LaVerne J.A.; Carrasco-Flores E.A.; Araos M.S.; Pimblott S.M. *J. Phys. Chem. A* **2008**, *112*, 3345-51. Gas production in the radiolysis of poly(vinyl chloride).

Zhao H.; Carmichael I.; Serianni A.S. *J. Org. Chem.* **2008**, *73*, 3255-7. Oligosaccharide trans-glycoside $^{3}J_{COCC}$ Karplus curves are not equivalent: Effects of internal electronegative substituents.

Chipman D.M. *J. Chem. Phys.* **2007**, *127*, 194309/1-8. Dissociative electron attachment to the hydrogen-bound OH in water dimer through the lowest anionic Feshbach resonance.

Du Y.; Price E.; Bartels D.M. *Chem. Phys. Lett.* **2007**, *438*, 234-7. Solvated electron spectrum in supercooled water and ice.

Enomoto K.; LaVerne J.A.; Araos M.S. *J. Phys. Chem. A* **2007**, *111*, 9-15. Heavy ion radiolysis of liquid pyridine.

Janik I.; Bartels D.M.; Jonah C.D. *J. Phys. Chem. A* **2007**, *111*, 1835-43. Hydroxyl radical self-recombination reaction and absorption spectrum in water up to 350 $^{0}C$.

LaVerne J.A.; Enomoto K.; Araos M.S. *Radiat. Phys. Chem.* **2007**, *76*, 1272-4. Radical yields in the radiolysis of cyclic compounds.

Pimblott S.M.; LaVerne J.A. *Radiat. Phys. Chem.* **2007**, *76*, 1244-7. Production of low energy electrons by ionizing radiation.

Rajesh P.; LaVerne J.A.; Pimblott S.M. *J. Nuclear Material* **2007**, *361*, 10-7. High dose radiolysis of aqueous solutions of chloromethanes: Importance in the storage of radioactive organic wastes.

Southworth-Davies R.J.; Medina M.A.; Carmichael I.; Garman E.F. *Structure* **2007**, *15*, 1531-41. Observation of decreased radiation damage at higher dose rates in room temperature protein crystallography.

Chipman D.M. *J. Chem. Phys.* **2006**, *124*, 044305/1-9. Stretching of hydrogen-bonded OH in the lowest singlet excited electronic state of water dimer.

Enomoto K.; LaVerne J.A.; Pimblott S.M. *J. Phys. Chem. A* **2006**, *110*, 4124-30. Products of the triplet excited state produced in the radiolysis of liquid benzene.

Enomoto K.; LaVerne J.A.; Seki S.; Tagawa S. *J. Phys. Chem. A* **2006**, *110*, 9874-9. Formation and decay of the triplet excited state of pyridine.

Filipiak P.; Camaioni D.M.; Fessenden R.W.; Carmichael I.; Hug G.L. *J. Phys. Chem. A* **2006**, *110*, 11046-52. Reactions of 1-hydroxy-1-methylethyl radicals with $NO_2^-$: Time-resolved electron spin resonance.

Juliarena M.P.; Lezna R.O.; Feliz M.R.; Ruiz G.T.; Thomas S.; Ferraudi G.; Carmichael I. *J. Org. Chem.* **2006**, *71*, 2870-3. On the association and structure of radicals derived from dipyridil[3,2-*a* : 2 ' 3 '-*c*]–phenazine. Contrast between the electrochemical, radiolytic, and photochemical reduction processes.

Maiti N.C.; Zhu Y.P.; Carmichael I.; Serianni A.S.; Anderson V.E. *J. Org. Chem.* **2006**, *71*, 2878-80. $^1J_{CH}$ correlates with alcohol hydrogen bond strength.

Marin T.W.; Takahashi K.; Bartels D.M. *J. Chem. Phys.* **2006**, *125*, 104314/1-11. Temperature and density dependence of the light and heavy water ultraviolet absorption edge.

Päch M.; Macrae R.M.; Carmichael I. *J. Am. Chem. Soc.* **2006**, *128*, 6111-25. Hydrogen and deuterium atoms in octasilsesquioxanes: Experimental and computational studies.

Thomas S.L.; Carmichael I. *Physica B* **2006**, *374-375*, 290-4. Hyperfine interactions in muonium-containing radicals.

Bartels D.M.; Takahashi K.; Cline J.A.; Marin T.W.; Jonah C.D. *J. Phys. Chem. A* **2005**, *109*, 1299-307. Pulse radiolysis of supercritical water III. Spectrum and thermodynamics of the hydrated electron.

Chipman D.M. *J. Chem. Phys.* **2005**, *122*, 044111/1-10. Excited electronic states of small water clusters.

Chipman D.M.; Bentley J. *J. Phys. Chem. A* **2005**, *109*, 7418-28. Structures and energetics of hydrated oxygen anion clusters.

Garrett B.C.; Dixon D.A.; Camaioni D.M.; Chipman D.M.; Johnson M.A.; Jonah C.D.; Kimmel G.A.; Miller J.H.; Rescigno T.N.; Rossky P.J.; Xantheas S.S.; Colson S.D.; Laufer A.H.; Ray D.; Barbara P.F.; Bartels D.M.; Becker K.H.; Bowen H.; Bradforth S.E.; Carmichael I.; Coe J.V.; Corrales L.R.; Cowin J.P.; Dupuis M.; Eisenthal K.B.; Franz J.A.; Gutowski M.S.; Jordan K.D.; Kay B.D.; LaVerne J.A.; Lymar S.V.; Madey T.E.; McCurdy C.W.; Meisel D.; Mukamel S.; Nilsson A.R.; Orlando T.M.; Petrik N.G.; Pimblott S.M.; Rustad J.R.; Schenter G.K.; Singer S.J.; Tokmakoff A.; Wang L.S.; Wittig C.; Zwier T.S. *Chem. Rev.* **2005**, *105*, 355-89. Role of water in electron-initiated processes and radical chemistry: Issues and scientific advances.

LaVerne J.A.; Carmichael I.; Araos M.S. *J. Phys. Chem. A* **2005**, *109*, 461-5. Radical production in the radiolysis of liquid pyridine.

LaVerne J.A.; Stefanic I.; Pimblott S.M. *J. Japan. Soc. Rad. Chem.* **2005**, *79*, 9-12. Hydrated electron yields in the proton radiolysis of water.

LaVerne J.A.; Stefanic I.; Pimblott S.M. *J. Phys. Chem. A* **2005**, *109*, 9393-401. Hydrated electron yields in the heavy ion radiolysis of water.

LaVerne J.A.; Tandon L.; Knippel B.; Montoya V.M. *Radiat. Phys. Chem.* **2005**, *72*, 143-7. Heavy ion radiolysis of methylene blue.

Mahoney J.M.; Stucker K.A.; Jiang H.; Carmichael I.; Brinkmann N.R.; Beatty A.M.; Noll B.; Smith B.D. *J. Am. Chem. Soc.* **2005**, *127*, 2922-8. Molecular recognition of trigonal oxyanions using a ditopic salt receptor: Evidence for anisotropic shielding surface around nitrate anion.

Pan Q.; Klepach T.; Carmichael I.; Serianni A.S. *J. Org. Chem.* **2005**, *70*, 7542-9. $^4J_{COCCH}$ and $^4J_{CCCCH}$ as probes of exocyclic hydroxymethyl group conformation in saccharides.

Pimblott S.M.; Milosavljevic B.H.; LaVerne J.A. *J. Phys. Chem. A* **2005**, *109*, 10294-301. Radiolysis of aqueous solutions of 1,1- and 1,2-dichloroethane.

*Elucidating the Molecular–Level Details of Heterogeneous Catalytic Oxidation Reactions*

**A. W. Castleman, Jr.**
The Pennsylvania State University
Departments of Chemistry and Physics
104 Chemistry Building
University Park, PA 16802
awc@psu.edu

**Program Scope:**

Conventional supplies of energy are limited and consumption continues to rise worldwide. This situation has led to major expansions in research efforts directed toward developing novel energy sources and less energy intensive processes. Catalysts significantly lower the energy requirements of chemical reactions and, in addition, aid in pollution abatement by degrading atmospheric contaminants. Furthermore, catalysts increase the selectivity of reactions by promoting the creation of desired products. Catalysts are also widely employed in the production and conversion of both conventional as well as alternative forms of energy. Improvement of existing catalysts and development of new ones rely on gaining an elementary molecular level understanding of catalytic processes. The current approach to the large scale design of heterogeneous catalysts involves primarily the combinatorial preparation and testing of different catalytic materials. Unfortunately, this method provides little understanding about the structure-reactivity relationships responsible for enhanced catalytic activity. Surface science has provided substantial insight into the atomic-level structure of heterogeneous catalysts. However, an active site specific understanding of catalysts, in which the reactivity of each surface site is examined, is at times difficult to obtain.

Gas-phase cluster reactivity experiments, in combination with high-level theoretical calculations, provide a method to investigate the reaction mechanisms occurring over transition metal oxides which are used as industrial oxidation catalysts. Employing a multistage mass spectrometry technique we investigate, with atomic level precision, the influence that the chemical and physical characteristics of different materials have on catalytic oxidation reactions.

The properties of catalytically active bulk materials have been effectively modeled and investigated using gas-phase metal oxide clusters. Muetterties has proposed that metal clusters have an extraordinary potential for providing models of surfaces in chemisorption and catalytic processes. Additionally, Somorjai has established that the binding of absorbed molecules on a surface takes a “clusterlike” form. Moreover, reactions of gas-phase clusters have been found to generate comparable products to those created by reaction on a corresponding bulk-phase catalyst. The investigation of clusters provides a method to examine the reactivity of individual surface sites in the absence of solvent effects and surface inhomogeneities that often complicate bulk-phase research. Charging effects caused by specific catalyst-support interactions can also be modeled by investigating the reactivity of ionic clusters. Furthermore, the effect of size on catalytic activity can be examined on an atom-by-atom basis. This is significant as the reactivity of small clusters has been shown to be unique in comparison with larger metal oxides due to the exceedingly reduced dimensions which influence their structure and properties. Indeed, the activity of such nanoscale species can change drastically with the addition or removal of a single atom. Lastly, due to their small size, high level theoretical calculations can be performed on cluster systems which provide complimentary information enabling a more complete understanding of experimentally observed processes. Through gas-phase cluster studies, we are uniquely capable of determining the influence of size, stoichiometry, elemental composition and ionic charge state on the reactivity of metal oxides that are used as catalyst materials. The knowledge gained through these investigations may aid in the directed design of future catalysts with improved activity and selectivity.

**Recent Progress:**

Throughout the recent grant period, we investigated zirconium oxide to determine the molecular-level details of its role as a heterogeneous oxidation catalyst. In one series of experiments a range of cationic zirconium oxide

clusters were reacted with carbon monoxide (CO), acetylene ($C_2H_2$), and ethylene ($C_2H_4$) to determine the influence that size and stoichiometry have on the oxidation of these chemicals. To acquire more detailed insight into the mechanisms and energetics of these reactions we collaborated with the theoretical chemistry group of Professor Vlasta Bonačić-Koutecký at the Institut für Chemie, Humboldt Universität zu Berlin.

Zirconium oxide has been utilized as a catalyst and catalyst-support material for a variety of industrially relevant processes due to its exceptional stability over a wide temperature range and resistance to poisoning. For example, bulk-phase studies have revealed zirconia ($ZrO_2$) to be an effective catalytic material for the oxidation of methane ($CH_4$) and CO and the epoxidation of propylene ($C_3H_6$). Through guided-ion-beam mass spectrometry experiments, a distribution of zirconium oxide clusters was created of varying stoichiometry and size. The series of stoichiometric $(ZrO_2)_x^+$ (x = 1-4) clusters were determined to exhibit enhanced activity and selectivity for the strongly exothermic oxidation of CO to carbon dioxide ($CO_2$), $C_2H_4$ to acetaldehyde ($C_2H_4O$), and $C_2H_2$ to ethenone ($C_2H_2O$). These reactions represent one half of a catalytic oxidation cycle. Regeneration of the active stoichiometric clusters is easily accomplished by reaction of $N_2O$ with oxygen deficient $(Zr_xO_{2x-1})^+$ species, thus completing the catalytic cycle. Therefore, through experimentation it has been demonstrated that the series of stoichiometric zirconium oxide clusters possess exceptional activity in comparison to other zirconium oxides which make them potential candidates for incorporation into a cluster assembled catalyst.

In addition to stoichiometry effects, zirconium oxide cations $(ZrO_2)_x^+$ (x = 2-5) of different size were found to exhibit varying reactivity. For instance the $Zr_2O_4^+$ cluster was found to have the most intense oxygen transfer product accounting for approximately 50% of the total ion intensity at the maximum pressure of CO. The oxygen transfer products for the remaining clusters were found to be approximately equivalent accounting for 25-30% of the total ion intensity at the corresponding maximum pressure. These results reveal size dependence for the reactivity of CO with zirconium oxide clusters in which smaller clusters have a higher activity. Phenomenological rate constants were calculated from experimental data to enable a better qualitative comparison of the relative reactivity of the different clusters than can be obtained from the normalized ion intensities. For the oxidation of CO, the rate constants were determined to be on the order of $2.4 \times 10^{-12}$ $cm^3s^{-1}$ for $Zr_2O_4^+$, $1.6 \times 10^{-12}$ $cm^3s^{-1}$ for $Zr_3O_6^+$, $1.2 \times 10^{-12}$ $cm^3s^{-1}$ for $Zr_4O_8^+$ and $6.3 \times 10^{-13}$ $cm^3s^{-1}$ for $Zr_5O_{10}^+$. The kinetic analysis confirms that $Zr_2O_4^+$ is the most reactive species, and that the relative reactivity of the clusters decreases with increasing size from $Zr_2O_4^+$ to $Zr_5O_{10}^+$. The knowledge gained in this investigation shows that small stoichiometric zirconium oxide cations are efficient promoters of CO oxidation.

The oxidation of $C_2H_4$ and $C_2H_2$ are processes of widespread industrial relevance. In particular, acetaldehyde is of the most widely produced chemicals. Experiments revealed that the stoichiometric series $(ZrO_2)_x^+$ (x = 1-4) of zirconium oxide clusters exhibited pronounced oxygen transfer products when reacted with $C_2H_4$. The $ZrO_2^+$, $Zr_2O_4^+$ and $Zr_4O_8^+$ clusters were found to have oxygen transfer products accounting for approximately 25% of the total ion intensity. In contrast, the oxygen transfer product of the $Zr_3O_6^+$ cluster was only 8% of the total ion intensity and a product channel corresponding to the association of $C_2H_4$ onto the cluster was more pronounced. To enable a proper qualitative comparison of the reactivity of different size clusters, the phenomenological rate constants were determined to be on the order of $1.3 \times 10^{-12}$ $cm^3s^{-1}$ for $ZrO_2^+$ and $Zr_2O_4^+$, $3.1 \times 10^{-13}$ $cm^3s^{-1}$ for $Zr_3O_6^+$ and $9.6 \times 10^{-13}$ $cm^3s^{-1}$ for $Zr_4O_8^+$. As expected, the $Zr_3O_6^+$ cluster is relatively less reactive towards the oxidation of $C_2H_4$ while the other clusters have comparable reactivity. Theoretical calculations determined that the most energetically favorable oxidation product is indeed acetaldehyde and not an alternative isomer of $C_2H_4O$.

The oxygen transfer products from stoichiometric zirconium oxide clusters toward $C_2H_2$ were very pronounced for each cluster in the series. The $Zr_4O_8^+$ cluster exhibited the largest oxygen transfer product accounting for around 70% of the total ion intensity. The $Zr_2O_4^+$ and $Zr_3O_6^+$ clusters were observed to have comparable oxygen transfer products while that for $ZrO_2^+$ was found to be relatively less intense. The phenomenological rate constants for the oxidation of $C_2H_2$ were determined to be approximately $1.5 \times 10^{-12}$ $cm^3s^{-1}$ for $ZrO_2^+$, $5.9 \times 10^{-12}$ $cm^3s^{-1}$ for $Zr_2O_4^+$, $2.8 \times 10^{-12}$ $cm^3s^{-1}$ for $Zr_3O_6^+$ and $4.0 \times 10^{-12}$ $cm^3s^{-1}$ for $Zr_4O_8^+$. The rate constants indicate an odd-even oscillation in $C_2H_2$ oxidation reactivity with increasing cluster size.

As mentioned above, the oxygen deficient product clusters $Zr_xO_{2x-1}^+$ (x = 1-4) generated through the oxidation of CO, $C_2H_4$ or $C_2H_2$, may be oxidized back to the original active stoichiometry through reaction with $N_2O$ which has a particularly weak $N_2$-O bond. A strong oxygen addition product is observed for each cluster indicating regeneration of the series of stoichiometric zirconium oxide clusters. Again, the phenomenological rate constants

were calculated for the oxidation of each cluster and were determined to be approximately 2.4 x $10^{-12}$ $cm^3s^{-1}$ for $ZrO^+$, 1.2 x $10^{-12}$ $cm^3s^{-1}$ for $Zr_2O_3^+$, 1.3 x $10^{-12}$ $cm^3s^{-1}$ for $Zr_3O_5^+$, and 4.3 x $10^{-13}$ $cm^3s^{-1}$ for $Zr_4O_7^+$. The rate constants for regeneration of the active stoichiometric clusters are comparable to the rate constants for the oxidation reactions, indicating the absence of a severely rate limiting step in the full catalytic cycle.

Our experimental findings, therefore, provide atomic level insight into the influence of size and stoichiometry on the oxidation of CO, $C_2H_4$ and $C_2H_2$ by zirconium oxides. To gain a more complete understanding of the oxidation mechanisms for each reaction, theoretical calculations were conducted by our collaborators in Berlin. The enhanced reactivity of the stoichiometric clusters is attributed, on the basis of theory, to the presence of a radical oxygen center with an elongated zirconium-oxygen bond. The radical is manifest, on the cationic cluster, as a spin unpaired electron localized at a terminal oxygen atom. The electron deficient oxygen radical is an electrophilic site at which CO and unsaturated hydrocarbons will preferentially bond. The calculated energy profiles for all three reactions demonstrate that the overall processes are exothermic and that the barriers to oxidation are significantly lower in energy than the reactants. Consequently, our findings suggest that radical oxygen centers may be responsible for oxidation over bulk zirconia and, furthermore, indicate that a material assembled to contain such sites may result in a greatly enhanced oxidation catalyst.

**Future Studies:**

Charge transfer interactions between support materials and catalyst particles may create regions of charge accumulation that will alter the catalytic activity of a surface. Therefore, to build on our recent findings with cationic zirconium oxides, a systematic study of the anionic species will be undertaken. We intend to investigate the reactivity of the distribution of anionic zirconium oxides with CO, $C_2H_2$, and $C_2H_4$ to give the most appropriate comparison with the cationic stoichiometric species studied thus far. It is possible that a different ratio of zirconium to oxygen may result in the formation of a radical oxygen center in the anionic clusters which may lead to increased activity. This study will also provide insight into whether oxygen radical centers alone are sufficient to promote oxidation reactions or whether an interplay between radical centers and a specific charge state is required. As was important for the cationic clusters, the anions will be reacted with $N_2O$ to examine whether reactive species may be regenerated.

Another transition metal of particular interest for future study due to its widespread application as a catalyst and support material is titanium. The extensive use of titanium oxide is due to its high durability, resistance to corrosion, and the high oxidation potential of its valence band. These properties are important for titanium oxide to be used in the degradation of organic pollutants or in performing useful transformations of hydrocarbon compounds. One of the early studies applying titanium oxide as a catalyst provided insight into the photosplitting of water on a single-crystal $TiO_2$ electrode, prompting further study of the species. Many studies have also shown the use of $TiO_2$ in the degradation of organic pollutants such as phenol. Gas-phase reactivity studies will be performed to identify how size and stoichiometry affect the activity of titanium oxide as an oxidation catalyst. In particular, the oxidation of CO by titanium oxide clusters will be studied due to the importance of this process in pollution abatement. Additionally, reactions with $SO_2$ will aid in determining if titanium oxides may provide an energetically favorable route for the production of $SO_3$, an intermediate in the large scale industrial production of sulfuric acid. The influence of charge state will be examined by interacting the chemicals of interest with the full spectrum of cationic and anionic clusters. These studies should provide molecular level understanding of the oxidation reactions occurring on catalytic surfaces and may aid in the future directed design of catalysts.

**Publications Resulting from this Grant (2004 to Present):**

570. "Elucidating Mechanistic Details of Catalytic Reactions Utilizing Gas Phase Clusters," M. L. Kimble, D. R. Justes, N. A. Moore, and A. W. Castleman, Jr., Clusters and Nano-Assemblies: Physical and Biological Systems (P. Jena, S. N. Khanna, B. K. Rao, Eds.) World Scientific: Singapore, New Jersey, London, 127-134 (2005).

573. "A Kinetic Analysis of the Reaction between $(V_2O_5)^+_{n=1,2}$ and Ethylene," N. A. Moore, R. Mitrić, D. R. Justes, V. Bonačić-Koutecký, and A. W. Castleman, Jr., J. Phys. Chem. B. 110, 3015 (2006)

584. "Influence of Charge State on the Mechanism of CO Oxidation on Gold Cluster," N. M. Reilly, G. E. Johnson, M. L. Kimble, A. W. Castleman, Jr., C. Bürgel, R. Mitrić, and V. Bonačić-Koutecký, J. Am. Chem. Soc. 130, 1694 (2008)

586. "Clusters: A bridge between disciplines," A. W. Castleman, Jr., Puru Jena, Proc. Nat. Acad. Sci. 103, 10552 (2006)

588. "Interactions of CO with $Au_nO_m^-$ ($n \geq 4$)", M. L. Kimble, A. W. Castleman, Jr., C. Bürgel, R. Mitrić, and V. Bonačić-Koutecký, Int. J. Mass. Spec. 254, 163 (2006).

592. "Clusters: A bridge across the disciplines of physics and chemistry," Puru Jena, A. W. Castleman, Jr., Proc. Nat. Acad. Sci. 103, 10560 (2006)

593. "Clusters: A bridge across the disciplines of environment, materials science, and biology," A. W. Castleman, Jr., Puru Jena, Proc. Nat. Acad. Sci. 103, 10554 (2006)

595. "Joint Experimental and Theoretical Investigations of the Reactivity of $Au_2O_n^-$ and $Au_3O_n^-$ (n=1-5) with Carbon Monoxide," M. L. Kimble, N. A. Moore, G. E. Johnson, A. W. Castleman, Jr., C. Bürgel, R. Mitrić, and V. Bonačić-Koutecký, J. Chem. Phys. 125, 204311 (2006)

599. "Reactivity of Anionic Gold Oxide Clusters Towards CO: Experiment and Theory," M. L. Kimble, N. A. Moore, A. W. Castleman, Jr., C. Bürgel, R. Mitrić, and V. Bonačić-Koutecký, Eur. Phys. J. D 43, 205 (2007)

600. "Influence of Charge State on the Reaction of $FeO_3^{+/-}$ with Carbon Monoxide," N. M. Reilly, J. U. Reveles, G. E. Johnson, S. N. Khanna, and A. W. Castleman, Jr., Chem. Phys. Lett. 435, 295 (2007)

601. "Recent Advances in Cluster Science," A. W. Castleman, Jr., Proceedings for the Advances in Mass Spectrometry for the 17th Eur. J. Mass Spectrom., 13, 7-11 (2007)

603. "Femtochemistry VII: Fundamental Ultrafast Processes in Chemistry, Physics, and Biology," A. W. Castleman, Jr., and M. L. Kimble, Elsevier, ISBN 0 444 52821 0

606. "Multi-component fitting of cluster dynamics," K. L. Knappenberger, Jr., and A. W. Castleman, Jr., Femtochemistry VII: Fundamental Ultrafast Processes in Chemistry, Physics, and Biology, Elsevier, ISNB 0 444 52821 0

610. "Experimental and Theoretical Study of the Structure and Reactivity of $Fe_{1-2}O_{\leq 6}^-$ Clusters with CO," N. M. Reilly, J. U. Reveles, G. E. Johnson, S. N. Khanna, and A. W. Castleman, Jr., J. Phys. Chem. A. 111, 4158 (2007)

613. "Experimental and Theoretical Study of the Structure and Reactivity of $Fe_{1-2}O_{1-5}^+$ with CO," N. M. Reilly, J. U. Reveles, G. E. Johnson, J. M. del Campo, S. N. Khanna, A. M. Köster, and A. W. Castleman, Jr., J. Phys. Chem. C, 111, 19097 (2007)

617. "The Reactivity of Gas Phase Metal Oxide Clusters: Systems for Understanding the Mechanisms of Heterogeneous Catalysts," N. M. Reilly, G. E. Johnson, and A. W. Castleman, Jr., book chapter to be published in, "Model Systems in Catalysis: From Single Crystals and Size-Selected Clusters to Supported Enzyme Mimics"

621. "Oxidation of CO by Aluminum Oxide Cluster Ions in the Gas Phase," G. E. Johnson, E. C. Tyo, and A. W. Castleman, Jr., J. Phys. Chem. A, 112, 4732 (2008)

623. "Cluster Reactivity Experiments: Employing Mass Spectrometry to Investigate the Molecular Level Details of Catalytic Oxidation Reactions," G E. Johnson, E. C. Tyo, and A W. Castleman, Jr., Proc. Natl. Acad. Sci. (in press)

624. "Gas-Phase Reactivity of Gold Oxide Cluster Cations with CO," G. E. Johnson, E. C. Tyo, A. W. Castleman, Jr., J. Phys. Chem. C, 112, 9730 (2008)

627. "Stoichiometric Zirconium Oxide Cations as Potential Building Blocks for Cluster Assembled Catalysts," G. E. Johnson, E. C. Tyo, A. W. Castleman, Jr., R. Mitrić and V. Bonačić-Koutecký, J. Am. Chem. Soc. (in press)

628. "Effect of Charged State and Stoichiometry on the Structure and Reactivity of Nickel Oxide Clusters with CO," G. E. Johnson, N. M. Reilly and A. W. Castleman, Jr., Int. J. Mass Spectrom. (in press)

630. "Influence of Stoichiometry and Charge State on the Structure and Reactivity of Cobalt Oxide Clusters with CO," G. E. Johnson, J. U. Reveles N. M. Reilly, E. C. Tyo, S. N. Khanna and A. W. Castleman, Jr., J. Phys. Chem. (accepted)

**An Exploration of Catalytic Chemistry on Au/Ni(111)**

Professor S. T. Ceyer
Department of Chemistry
Massachusetts Institute of Technology, Cambridge, MA 02139
stceyer@mit.edu

**Project Scope**

This project explores the breadth of catalytic chemistry that can be effected on a Au/Ni(111) surface alloy. A Au/Ni(111) surface alloy is a Ni(111) surface on which less than 50% of the Ni atoms are replaced at random positions by Au atoms. The alloy is produced by vapor deposition of a small amount of Au onto Ni single crystals. The Au atoms do not result in an epitaxial Au overlayer or in the condensation of the Au into droplets. Instead, the Au atoms displace and then replace Ni atoms on a Ni(111) surface, even though Au is immiscible in bulk Ni. The two dimensional structure of the clean Ni surface is preserved. This alloy is found to stabilize an adsorbed peroxo-like $O_2$ species that is shown to be the critical reactant in the low temperature catalytic oxidation of CO and that is suspected to be the critical reactant in other oxidation reactions. These investigations may reveal a new, practically important catalyst for catalytic converters and production of some widely used chemicals.

**Recent Progress**

We discovered that the Au/Ni(111) surface alloy efficiently catalyzes the oxidation of CO at 70 K. Saturation coverage of molecular $O_2$ is adsorbed on the 0.44 ML Au/Ni surface alloy at 77 K. The dominant feature, at 865 $cm^{-1}$, of the vibrational spectrum of the oxygen layer, as measured by high resolution electron energy loss spectroscopy, is assigned to the vibration of the O=O bond of molecular oxygen adsorbed on the alloy with its bond axis largely parallel to the surface. Molecular oxygen so adsorbed is characterized as a peroxo ($O_2^{-2}$) or superoxo ($O_2^{-1}$) species. Shoulders at about 950 $cm^{-1}$ and 790 $cm^{-1}$ indicate the presence of both peroxo or superoxo species at multiple sites.

The feature at 865 $cm^{-1}$ and its shoulders disappear after heating this layer to 150 K while two features at 580 and 435 $cm^{-1}$, attributed to atomically adsorbed O, grow in. The feature at 580 $cm^{-1}$ is the same frequency as observed for O atoms bound to Ni(111) while a lower frequency feature, at 435 $cm^{-1}$, is attributed to O atoms bound to Ni atoms that are adjacent to the Au atoms. Note that there is no evidence for atomically bound O at 77 K. Therefore, $O_2$ adsorption on the Au/Ni(111) surface alloy at 77 K is solely molecular. In contrast, $O_2$ dissociatively adsorbs on Ni(111) at 8 K, while it adsorbs neither molecularly nor dissociatively on Au(111) at or above 100 K.

When a beam of thermal energy CO is directed at the $O_2$ covered Au/Ni(111) surface alloy held at 70 K, gas phase $CO_2$ is immediately produced. A control experiment demonstrates that no $CO_2$ is produced when the CO beam impinges on the crystal mount. Clearly, CO reacts with molecularly adsorbed $O_2$ on this alloy at 70 K.

After exposure of the $O_2$-covered surface alloy at 70 K to CO, two C=O stretch vibrational modes are observed at 2170 and 2110 $cm^{-1}$, along with the Au/Ni-CO stretch mode at 435 $cm^{-1}$. The O=O mode at 865 $cm^{-1}$ is much reduced in intensity, while the shoulder at 790 $cm^{-1}$ has maintained its intensity. The decrease in intensity of the 865 $cm^{-1}$ feature is interpreted to mean that some of the molecularly adsorbed $O_2$ has reacted with CO to form gas phase $CO_2$. The product remaining from this reaction is an O atom adsorbed to Au, as evidenced by the appearance of a new feature at 660 $cm^{-1}$. The molecularly adsorbed $O_2$ that gives rise to the feature at 790 $cm^{-1}$ does not react with CO.

This alloy surface covered with CO and some adsorbed $O_2$ is heated at 2 K/s while the partial pressures at masses 44 and 28 are monitored. Rapid production and desorption of $CO_2$ is clearly observed between 105-120 K, along with CO desorption. Production of $CO_2$ in this temperature range occurs at the same temperature at which $O_2$ dissociates. This observation suggests that $CO_2$ formation occurs between a CO and a "hot" O atom that has not yet equilibrated with the surface after bond dissociation. From 120 K to about 250 K, $CO_2$ is slowly produced by reaction of the adsorbed O atoms represented by 660 $cm^{-1}$ mode and by the adsorbed O atoms that did not react immediately as a hot O atom upon $O_2$ dissociation.

These results demonstrate that Au/Ni(111) catalyzes the oxidation of CO at low temperature. Clearly, substitution of a small number of Ni atoms on the Ni(111) surface by Au atoms has dramatically changed the Ni chemistry. The oxidation of CO on Ni has never been observed under UHV laboratory conditions, presumably because both the oxygen atom and CO are too strongly bound, and hence the barrier to their reaction is too large. Introduction of Au into the Ni lattice serves to weaken the bonds between oxygen and CO so as to allow the reaction to proceed. These results also imply that nanosize Au clusters are not a necessary requirement for low temperature CO oxidation in general. Rather, interaction of the Au atoms around the perimeter of the Au nanocluster with the transition metal of the oxide support likely provides the active sites that stabilize the adsorption of molecular $O_2$ that is necessary for the oxidation of CO.

**Current Status**

We temporarily ceased experimentation in 2006 in order to renovate the laboratory space housing our apparatus. About a year ago, we were able to start bringing the vacuum chamber and equipment up to its operating condition and our initial goal was

to reproduce the CO oxidation experiments carried out on the Au/Ni(111) surface alloy prior to the move. With our new Au source coupled with a quartz crystal microbalance that we developed and fabricated during the lab renovation, we determined that the Au coverage needed to be recalibrated by a factor of 1.8 larger than our previous calibration. Additional measurements of the $CO_2$ production at 77 K as a function of Au coverage show that $CO_2$ production correlates with molecular $O_2$ coverage (as measured by the intensity of the adsorbed peroxo species at 950 and 856 $cm^{-1}$), where the maximum $CO_2$ production and molecular $O_2$ coverage occurs at 0.4 ML Au. A Monte Carlo simulation of the molecular $O_2$ coverage as a function of Au coverage was carried out to probe the site requirements for $O_2$ adsorption. The best agreement between the simulated and experimental $O_2$ coverage is observed when $O_2$ sits in a Ni atom bridge site of an ensemble of 6 Ni and 4 Au atoms of any hexagonal configuration. Molecular adsorption is blocked when an adsorbed O atom is within 5 Å of the bridge site. Finally, we recently observed a negative ion resonance at about 2 eV in the high resolution electron energy loss spectra of the adsorbed molecular $O_2$. The resonance scattering resulted in increased intensity of the vibrational spectra that allows the observation of additional adsorbed $O_2$ vibrational modes not observed at more typical excitation energies (5 eV). These high resolution vibrational spectra of molecularly adsorbed $O_2$ on the Au/Ni(111) surface alloy will serve as important benchmarks for the continued development of density functional theory for surface adsorbates.

**Future Plans**

A major thrust of this project is to explore the range of reactivity of the $O_2$ species molecularly adsorbed on the Au/Ni(111) surface alloy. The hypothesis is that our newly observed molecular $O_2$ adsorbate is the crucial reactant in two oxidation reactions to be studied: the direct synthesis of $H_2O_2$ from $H_2$ and $O_2$ and the epoxidation of propylene to form propylene oxide. In addition, it is planned to investigate whether the Au/Ni surface alloy is also active for the reduction of NO by CO. It is possible that a molecularly adsorbed NO species with a bond order approaching one is the active species in the NO reduction reaction at low temperature on the Au/Ni(111) surface alloy.

**Publication**

Catalyzed CO Oxidation at 70 K on an Extended Au/Ni Surface Alloy
D. L. Lahr and S. T. Ceyer, *J. Am. Chem. Soc.* **128**, 1800 (2006)

**Ph.D. Thesis**

Molecular Oxygen Adsorbates at a Au/Ni(111) Surface Alloy and Their Role in Catalytic CO Oxidation at 70 – 250 K. D. L. Lahr - June, 2006 – MIT

**Patent Application**

U.S. Pat. Apl. Ser. No.: 11/335,865. S. T. Ceyer and D. L. Lahr

**Theory of Dynamics of Complex Systems**

David Chandler

*Chemical Sciences Division, Lawrence Berkeley National Laboratory*
and
*Department of Chemistry, University of California, Berkeley CA 94720*

DOE funded research in our group concerns the theory of dynamics in systems involving large numbers of correlated particles. Glassy dynamics is a quintessential example. Here, dense molecular packing severely constrains the allowed pathways by which a system can rearrange and relax. The majority of molecular motions that exist in a structural glass former are trivial small amplitude vibrations that couple only weakly to surrounding degrees of freedom. In contrast, motions that produce significant structural relaxation take place in concerted steps involving many particles. In our recent work, we have provided a theory and simulation results for the spatial scaling of dynamical heterogeneity [4],[1] and demonstrated in atomistic simulations the essential features of our theory – the decoupling of exchange and persistence [8]. An interesting consequence of this decoupling is negative response. For example, the drift velocity in response to a pulling force can on average *decrease* with increasing pulling force [10]. We have also shown that dynamic heterogeneity manifests a first-order phase transition in trajectory space [3]. This first-order transition is the glass transition. It is a non-equilibrium phenomenon that is distinct from traditional equilibrium phase transitions.

The kinetics or nucleation of equilibrium phase transitions is another example of correlated many-particle dynamics. On this topic, we have carried out trajectory studies and compared theory to experiments [1]. In addition, we have studied the dynamics of hydrophobic assembly [6,9]. This process is closely related to nucleation of vapor in water and the formation of a water-vapor interface, and it the nature of this interface that controls the likelihood of solvent fluctuations [12] and free energies of solvation [7]. We have also studied self-assembly as it occurs in formation of virus-capsids [10]. In this case, the requisite conditions for successful assembly are not only thermodynamic meta-stability, but also the ability to self-anneal. Clusters that gather too quickly cannot self-anneal, and clusters that cannot self-anneal are malformed with frozen defects.

For the future, we plan DOE funded research on electron transfer, chemical dynamics and inhomogeneous fluids. Our first efforts in this direction have produced three papers [5,11,13]. We aim to develop techniques and concepts that will ultimately prove useful in the specific context of combining sunlight and renewable resources to produce transportation fuels. That specific effort will be part of the LBNL Helios SERC. To reach the point where we can contribute to Helios, we plan to use our DOE support in this program to address basic underlying issues. Applications can then be done with Helios

[1] Numbers in square brackets refer to papers cited in **Recent DOE Supported Research Publications**

support. The first of these basic issues is the nature of ionic solutions at metal and semiconductor surfaces. In our first paper on the topic, we have demonstrated the dominant effect of fluctuations from mean ionic densities [11]. The second is the development of ways to carry out numerical simulations of electronically non-adiabatic transitions. For this topic, we have been developing new path sampling methods [5], and we have explored a way to reliably mimic aspects of quantum dynamics with classical computation and used the method to treat the behavior of an electron in a fluid [13].

**Recent DOE Supported Research Publications**


1. Pan, A.C, T.J. Rappl, D. Chandler, and N.P. Balsara, "Neutron scattering and Monte Carlo determination of the variation of the critical nucleus size with quench depth," *J. Phys. Chem. B* **110**, 3692-96 (2006).

2. Hagan, M.F. and D. Chandler, "Dynamic pathways for viral capsid assembly," *Biophys. J.* **91**, 42-54 (2006).

3. Jack, R.L., J.P. Garrahan and D. Chandler, "Spacetime thermodynamics and subsystem observables in a kinetically constrained model of glassy systems," *J. Chem. Phys.* **125**, 184509.1-11 (2006).

4. Chandler, D., J.P. Garrahan, R.L. Jack, L. Maibaum and A.C. Pan, "Lengthscale dependence of dynamic four-point susceptibilities in glass formers," *Phys. Rev. E* **74**, 051501.1-9 (2006).

5. Miller, T.F. and C. Predescu, "Sampling diffusive transition paths," *J. Chem. Phys.* **126**, 144102.1-12 (2007) .

6. Miller, T.F., E. Vanden-Eijnden and D. Chandler, "Solvent coarse-graining and the string method applied to the hydrophobic collapse of a hydrated chain," *Proc. Natl Acad. Sci. USA* **104**, 14559-64, (2007).

7. Maibaum, L. and D. Chandler, "Segue between favorable and unfavorable solvation," *J. Phys. Chem. B* **111**, 9025-9030 (2007).

8. Hedges, L.O., L. Maibaum, D. Chandler and J.P.Garrahan "De-coupling of Exchange and Persistence Times in Atomistic Models of Glass Formers," *J. Chem. Phys.* **127**, 211101.1-4 (2007).

9. Willard, A. P., D. Chandler "The Role of Solvent Fluctuations in Hydrophobic Assembly," *J. Phys. Chem. B* **112**, 6187-6192 (2007).

10. Jack, R.L., D. Kelsey, J.P. Garrahan and D. Chandler, "Negative differential mobility of weakly driven particles in models of glass formers," *Phys. Rev. E* **78**, 011506.1-9 (2008)

11. Willard, A.P., S.K. Reed, P.A. Madden, and D. Chandler, "Water at an electrochemical interface - a simulation study," arXiv:0804.2891 (2008).

12. Willard, A.P., and D. Chandler, "Coarse Grained Modeling of The Interface Between Water and Heterogeneous Surfaces," arXiv:0804.1134 (2008).

13. Miller, T.F., “Isomorphic classical molecular dynamics model for an excess electron in a supercritical fluid,” arXiv: 0809.4522 (2008).

**Center for Radiation Chemistry Research: Electron capture by extended polymer molecules in solution, and excited states of quinine radical anions.**

**Principle Investigators**: Andrew R. Cook & John R. Miller
Chemistry Department, Brookhaven National Laboratory
Bldg. 555, Upton NY 11973
acook@bnl.gov, jrmiller@bnl.gov

**Program Definition**: Our group examines charged and radical species in solution and develops tools to create and probe such species. Principal among these tools is the Laser Electron Accelerator Facility (LEAF) at Brookhaven that produces 7 ps electron pulses and associated detection systems. Pulse radiolysis is often the most convenient and sometimes the only method to rapidly produce and study isolated radical species. Discussed below are recent advances in studies of diffusional and "dry" electron capture by a series of different length polymer molecules, and comparison to theoretical models for such process involving very extended, non-spherical species. Also provided are updated results for charge capture by excited states of quinone radical anions. Additional efforts in our lab are separately described in a summary by Jim Wishart.

**Recent Progress**:

**1. Length and Time Dependent Rates in Diffusion-Controlled Reactions with Conjugated Polymers.** This work examines diffusion-controlled reactions, specifically electron capture, by long conjugated molecules having lengths from 1 to over 100 nm. An ultimate goal of this work is to study charge transport along such molecules. Before this can be done very well, it is important to understand the complex kinetics of initial charge capture, as it likely occurs on, or overlaps with the timescales for charge transport. In addition to providing the basis for charge transport studies, these experiments provide a unique opportunity to explore diffusion reactions with non-spherical molecules and to provide a test of theoretical descriptions of such processes. Classically, rate constants for diffusion-controlled reactions depend only on the diffusion coefficient and reaction radius, with little dependence on specific reactivities of the reacting species. The theory of Smoluchowski produced an equation, the simple form of which has proved to be remarkably durable:

$$k(t) = 4\pi R_{eff} D N_A (1 + R_{eff}/(\pi D t)^{1/2}) \quad (1)$$

$$k_{inf} = 4\pi R_{eff} D N_A \quad (2)$$

This rather simple equation gives the rate constant for a bimolecular, diffusion-controlled reaction in terms of just two parameters: a mutual diffusion coefficient D and the effective reaction radius, $R_{eff}$. For this work, D was taken as an average of published values, $1.30 \times 10^{-4}$ $cm^2/s$. For small spherical molecules, $R_{eff}$ is approximated as the sum of the physical radii of the two reactants. Recent theoretical models for reactions with non-spherical molecules use the same equation, but compute $R_{eff}$ using functional forms for diffusion of point particles (or spheres) to the surfaces of shapes including ellipsoids, lines, planes and cubes of spherical reactants. These important changes to eq 1 by many theoreticians greatly extend the utility of the Smoluchowski equation. The experiments described below test the validity of these models and provide a quantitative test of the second or "transient" term of eq 1, which predicts the observed rate to change with time, leading to non-exponential capture kinetics. This last effect is seldom seen for small molecules, as its effect is typically only important on picosecond time scales.

The reaction of solvated electrons ($e_s^-$), formed in pulse radiolysis, to 1-10 unit long oligofluorenes (oF) and 23-133 unit long polyfluorenes (pF) was investigated in THF solvent. The data seen in the graph to the right were collected not only by direct observation of either $e_s^-$ decay or oF or pF growth kintecs, but also by competition with other molecules, AX. Over an increase in length of the polymers by a factor of 133, the rate of capture increases about 16 times. The experimental results enable determination of how $k_{inf}$ for attachment of electrons to oF or pF and therefore $R_{eff}$ depend on length. This in turn allows evaluation of theoretical models in the literature for diffusive reactions with non-spherical molecules, shown schematically in the figure to the right. The data were well described by the model describing the polymer molecule as a prolate spheroid:

$$R_{eff} = L*z/(\ln((1+z)/(1-z)))$$

$$z = (1-(2\, r_x/L)^2)^{1/2}$$

The fit shown above was obtained by substituting $R_{eff}$ computed by the expression above into eq 2, giving a reaction distance $r_x$ = 0.58 nm. It was found that models using touching spheres in a line or large open polygon could also give a good fit to the data. An advantage of the prolate spheroid model is that it does not require approximations.

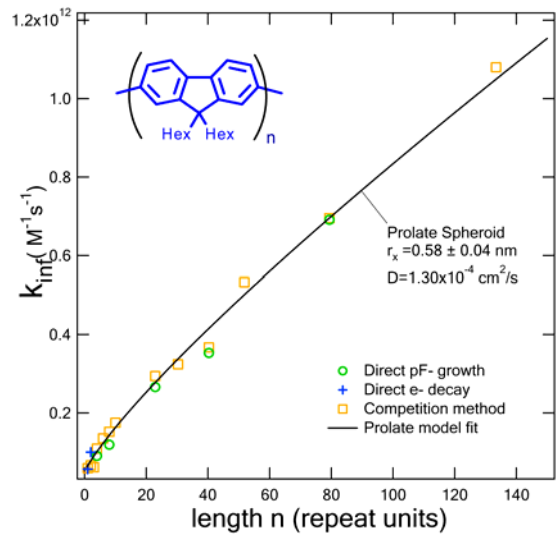


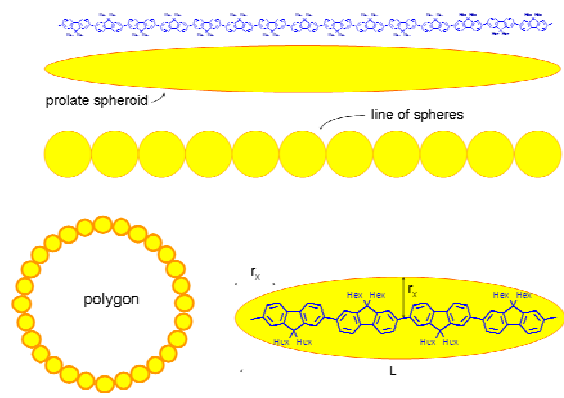


Once $R_{eff}$ is determined it is possible to test the ability of eq 1, augmented by models for long extended molecules, to quantitatively predict the time dependence of the electron capture rate. Using the competition method and a given concentration of AX, the median time over which electrons are captured by pF is given by the first half life, $t_{1/2}$, of $e_s^-$. The figure below shows the time dependence of $k_1^{att}(t)$ for electron capture by a 133 unit long pF. The solid line is a fit using eq 1 to only the lowest concentration points where the effects of the approximations using this method are the smallest, showing an apparent discrepancy at short times. Eq 1 predicts $k_1^{att}(t)$ to increase by more than a factor of ten from its $k_{inf}$ value at times as short as 0.1 ns, but the measurements find a larger increase. This larger increase was shown in a more exact treatment of this data to be accounted for largely by correcting the approximation used that the rate was constant over the $e_s^-$ half life. An additional small correction can be made by allowing for a small amount of fast capture by presolvated or "dry" electrons. The excellent agreement over all concentrations used supports the conclusion that eq 1 extended by the prolate spheroid model or one-dimensional arrays of spheres provides a

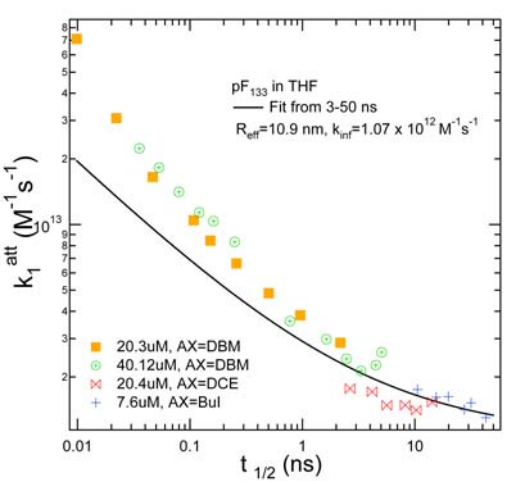

good description of diffusion-controlled reactions of these long molecules. Large transient effects were observed in which k(t) increases by more than a decade at early times, supporting those predicted by theory. The size of the transient terms and the quantitative confirmation of eq 1 is unprecedented.

**2. Ultrafast single-shot (UFSS) detection system.** This novel detection system utilizes a bundle of 100 optical fibers, each providing a different probe delay time, allowing for collection of ps timescale transient data in very few shots, which is critical for samples of limited availability. The fiber based UFSS detection system was upgraded in many ways to improve ease of use and signal to noise. Further improvement came from installation of a remote sample changer, which allows collection of necessary calibration factors before the electron beam drifts, which is the major source of noise in UFSS experiments. This apparatus has tremendous potential to enable new science in our lab, and is currently being employed for studies of Ionic Liquids, described by Jim Wishart, and in both studies of charge capture and transport by conjugated polymers.

**3. "Step" electron capture by Conjugated Polymers.** As noted to above, at higher concentrations of polymer, very rapid, non-diffusional capture of electrons can be observed. The upgraded UFSS experiment provided very high quality data on electron capture rates by a 79-monomer unit pF in THF (left). An exciting observation is the large, sub-20 ps "step" formation of $pF^{-\bullet}$ anion absorption at 580 nm. After determining and removing small contributions due to absorption from pF excited states, cations, and solvated electrons, a large step remains. Comparison of the step height to the number of electrons available at 20 ps in THF leads to the startling observation that at the highest concentration, 30% of the available electrons are captured in less than 20 ps. If electrons are localized on or near (within $r_x$) of a pF molecule, they are expected to be captured promptly. Using the 0.58 nm reaction distance found above, it is possible to estimate that only ~10% of the step comes from such electrons, with the conclusion that the majority of the step is due to capture of pre-solvated ("dry") electrons. The step furthermore corresponds to ~50% of the total number of electrons captured at longer times, which is a huge advantage for measuring fast electron mobility on the wires by transport to attached end caps.

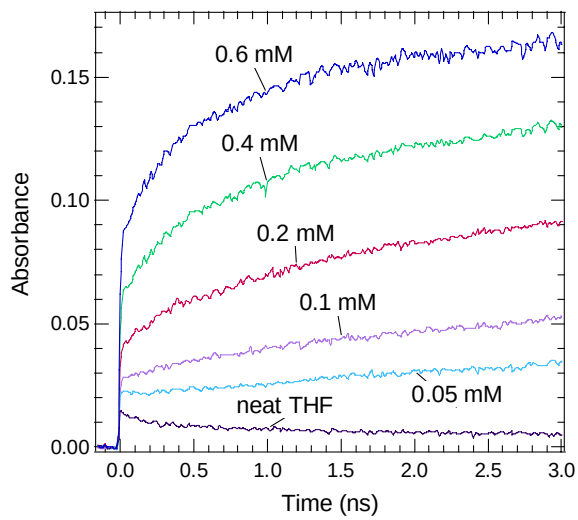


**4. Excited Radical Ions.** Inhibitions of electron transfer with the lowest excited state of benzoquinone (BQ) radical anion were further confirmed in experiments that attach electrons in mixtures of solvents to vary the electron energy, and hence the driving force for charge capture into the different excited states of $BQ^{-\bullet}$. The experiments utilized conductivity detection in collaboration with R. Holroyd. The attachment rate slowed when the energy of the solvated electron was below the second excited state. The results confirm that: 1) Electron transfer is very slow into the first excited state due probably to the need for a two-electron transition, 2) Variation of free energy change by blending fluids of different ground state energy levels ($V_0$) or by alteration of pressure in tetramethylsilane affected rate vs. free energy curves, although only

over small ranges of free energy. These segments may represent windows showing portions of the free energy curve. This second finding is remarkable because the reactions of electrons in these nonpolar fluids have not been understood in terms of Marcus-Jortner electron transfer theories; their rates presented a complex pattern that has defied quantitative description. The new results present an important opportunity in electron transfer. The significant inhibitions of ET into the long-lived lowest excited state of $BQ^{-\bullet}$ probably means that this state is of little use in driving electron transfer chemistry contrary to previous ideas.

**Future Plans**:

- Work will be done to better understand recombination of $pF^-$ and solvent holes, which appears to be slower than expected. At high concentration, "step" or "dry" electron capture will be examined in different length polymers to understand how it scales with length and concentration. Studies of charge capture will be expanded to compare to molecules with less rigid structures or those that are know to aggregate for comparison. Rates of hole capture by long molecules will be studied.
- Apply the description of capture kinetics to systems with endcapped wires. Can we observe charge transfer rates to the ends of these molecules, and what factors effect them?
- The free energy change for electron capture into $BQ^{-\bullet **}$, the second excited state of $BQ^{-\bullet}$, will be varied by changing pressure over a larger range to enlarge the "windows" into the rate vs. free energy curves. Then by changing the solvent or solute to overlap these windows we hope to get a sense of the entire curve describing rate as a function of electron energy, and hence the driving force for charge capture.
- Continued enhancement to the fiber-UFSS experiments is planned to further improve noise, extended time range bundles and simplified wavelength tuning. These will be important to ongoing experiments with conjugated polymers and ionic liquids, as well as other new directions.

**Recent DOE Supported Publications**:


1. Increased yields of radical cations by arene addition to irradiated 1,2-dichloroethane, Funston, A. M.; Miller, J. R. *Radiation Physics and Chemistry* **2005**, *72*, 601-611.
2. One-electron reduction of an "extended viologen" p-phenylene-bis-4,4 '-(1-aryl-2,6-diphenylpyridinium) dication, Funston, A.; Kirby, J. P.; Miller, J. R.; Pospisil, L.; Fiedler, J.; Hromadova, M.; Gal, M.; Pecka, J.; Valasek, M.; Zawada, Z.; Rempala, P.; Michl, J. *Journal of Physical Chemistry A* **2005**, *109*, 10862-10869.
3. Superexchange and sequential mechanisms in charge transfer with a mediating state between the donor and acceptor, Paulson, B. P.; Miller, J. R.; Gan, W. X.; Closs, G. *Journal of the American Chemical Society* **2005**, *127*, 4860-4868.
4. Nature and energies of electrons and holes in a conjugated polymer, polyfluorene, Takeda, N.; Asaoka, S.; Miller, J. R. *Journal of the American Chemical Society* **2006**, *128*, 16073-16082.
5. Spectroscopy and transport of the triplet exciton in a terthiophene end-capped poly(phenylene ethynylene), Funston, A. M.; Silverman, E. E.; Schanze, K. S.; Miller, J. R. *Journal of Physical Chemistry B* **2006**, *110*, 17736-17742.
6. Radical ion states of platinum acetylide oligomers, Cardolaccia, T.; Funston, A. M.; Kose, M. E.; Keller, J. M.; Miller, J. R.; Schanze, K. S. *Journal of Physical Chemistry B* **2007**, *111*, 10871-10880.
7. Rate and driving force for protonation of aryl radical anions in ethanol, Funston, A. M.; Lymar, S. V.; Saunders-Price, B.; Czapski, G.; Miller, J. R. *Journal of Physical Chemistry B* **2007**, *111*, 6895-6902.
8. Electron and Hole Transport To Trap Groups at the Ends of Conjugated Polyfluorenes, Asaoka, S.; Takeda, N.; Iyoda, T.; Cook, A.R.; Miller, J.R. *J. Am. Chem. Soc.*, Accepted.

# Chemical Kinetics and Dynamics at Interfaces

## *Solvation/Fluidity on the Nanoscale, and in the Environment*

James P. Cowin
Fundamental and Computational Sciences Directorate. Pacific Northwest National Laboratory
P.O. Box 999, Mail Stop K8-88, Richland, Washington 99352. jp.cowin@pnl.gov

### Program Scope

Interfaces, solid or liquid, have a unique chemistry, unlike that of any bulk phase. Ice interfaces also tend to have adherent liquid brine films in nature. This program explores interfacial effects including changes in fluidity, transport, and solvation. The knowledge gained relates to reactions and transport across two-phase systems (like microemulsions), electrochemical systems, and where a fluid is present in molecular-scale amounts. The latter includes cell membranes, enzymes and ion channels, and environmental interfaces at normal humidities, such as the surfaces of atmospheric or soil particles. We explore these systems via re-creating liquid-liquid interfaces using molecular beam epitaxy, and use of a molecular soft landing ion source. We also explore fundamental properties of bulk ice, related to proton transport, amorphous ice properties, unique electrical properties and even the effect of ice in formation of planets.

## Recent Progress (2005-2008)

### *Mapping the Oil-Water Interface's Solvation Potential [1]*

(Richard C. Bell, Kai Wu, Martin J. Iedema, Gregory K. Schenter, James P. Cowin)

Any ion that traverses the junction of water and low dielectric constant materials (air, oil, cell membranes, proteins, etc.) will experience a solvation energy that varies strongly according to its location with respect the interface. Recently much progress in understanding these interfaces was made via computational methods. This study adds important new measurements to the field. Directly measured is the solvation potential for $Cs^+$ as it approaches the oil-water interface ("oil" = 3-methylpentane), from 0.4 to 4 nm away. The oil-water interfaces with pre-placed ions are created at 40K using molecular beam epitaxy and a soft-landing ion beam. The solvation potential slope was determined at each distance by balancing it against an increasing electrostatic potential made by increasing the number of imbedded ions at that distance, and monitoring the resulting ion motion.

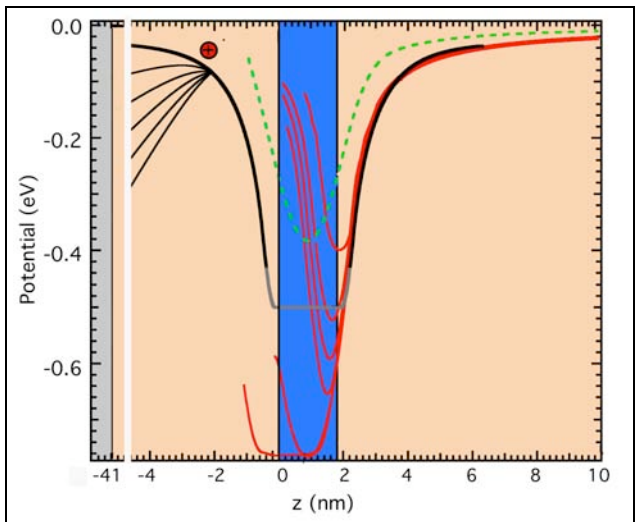


**Figure 1** The blue shaded region shows 1.8 nm water film, within a 3-methylpentane film (salmon). The measured solvation chemical potential for a single ion approaching the water film is the heavy black solid line. The red curves are Born calculations for 5Å = $r_b$ , $\varepsilon_1$=1.9, $\varepsilon_2$=100, and water films 0.15, 0.3, 0.45. 0.6, 1.8, and 3.0 nm (7.1 ML) thick. Green curve is Born model for a 1.8 nm water film with $\varepsilon_2$=5.

Figure 1 shows what the solvation chemical potential (in heavy black lines) for a single ion approaching a 4 monolayer (ML) film of water (shaded blue), immersed in 3-methylpentane (3MP) (salmon). To the far left is a metallic substrate. In a previous work [2], we roughly estimated the well depth of the solvation potential. In more recent work we determine the potential shape. When ions are placed several monolayers away from the oil water interface (left of Figure 1) they add to the solvation potential a collective electric potential. For increasing number of ions, the net potential begins to bend down, eventually reaching (and exceeding) zero slope at the initial ion position. When the number of ions is sufficient to bend the potential to locally have zero slope, this profoundly alters the ion motion. Simulations show that there should be a maximum amount of charge that can be trapped, and this corresponds closely to that charge needed to bend the solvation potential to have zero slope. What this implies is that the maximum amount of trapped charge/voltage is a direct measure of the slope of the solvation potential at that distance.

As predicted, we found for small numbers of ions nearly all the ions are trapped, while for increasing numbers of ions the amount trapped reaches an asymptotic limit. This gives the slope of the solvation potential at that distance away from the oil-water interface. Experiments were done for ions placed from 1 to 10 ML away from the water layer, and for water layers ranging from 2 to 30 ML thick. We integrated these slopes to give the solvation potential, which was then compared to various simple Born solvation models. The measured solvation potential is the thick black line in Figure 1. The results show the need for a "k-dependent" dielectric constant Born model. These measurements are a unique, direct bridging of molecular to semi-macroscopic distances.

## *Dissociation of Water on Pt(111), Buried Under Ice [2]*

(Yigal Lilach, Martin J. Iedema, James P. Cowin)

Adsorbed water, well studied on metallic surfaces, is largely thought to <u>not</u> dissociate on Pt(111). If $\Delta H_{ads}$ is several kT's smaller than the activation energy required for dissociation $E_a$, the molecules will desorb rather than dissociate. How could one manipulate this, to induce water to dissociate on Pt? Either by: 1) Increasing the kinetic barrier to desorption till it is bigger than $E_a$ 2) Changing in the energy levels of the reactants or products. We showed that growing thick layers of ice on Pt(111) does both, and leads to extensive dissociation in the first layer of water. Careful, 3-step temperature programmed desorption (TPD) and work function measurements show that water dissociates on Pt(111) for T as low as 151K [3][4].

## *Proton Segregation at Ice Interfaces [4]*

(Yigal Lilach, Martin J. Iedema, James P. Cowin)

Hydronium segregates to the surface of $H_2O$ ($D_2O$) ice films grown on Pt(111) above 151K (158K). This is observed as a voltage that develops across the films, utilizing work function measurements. For example 3500 ML $D_2O$ ice films, grown via the tube doser at $T_{growth}$ above 155 to 178K at about 400 ML/s form with a <u>positive</u> voltage (as much as 8V), due to the presence of trapped hydronium ions at the vacuum-ice interface. The $H_2O$ films have a slightly lower threshold temperature, 153K.

The coverage dependence of film voltages show that it is initially linear with coverage, then it reaches a saturation value at a coverage of several thousands of monolayers. This, and other evidence indicate that this voltage originates from charges on top of and within the ice films, that originally came from the Pt-ice interface. We found that a simple model fits the data well: Hydronium from the dissociation of water at the Pt-ice interface, at an initial ~0.1 ML concentration had a small probability (~1 % ) of being found at the ice-vacuum interface, in some sort of equilibrium. This was true only for the very first part of the ice growth (~30 ML ?). As the films get thicker, these hydroniums (~ 0.01 ML) at the ice-vacuum interface become trapped at the ice-vacuum interface in a local minimum. As the film grows, most of these ions will stay on top of the ice film. But a small fraction ( ≈ 0.02%) are lost for each new monolayer of ice, to become trapped in the bulk ice. Since $\Delta G = -RT\ln(K_{equil})$, the free energy for the charge segregation to the vacuum ice interface, compared to being stranded in the bulk ice was estimated. With some additional assumptions we extracted the free energy of moving a hydronium from the Pt-ice interface to the ice-vacuum interface.

## *Pyroelectricity of Water Ice [5]*

(Richard C. Bell, Kai Wu, Martin J. Iedema, Gregory K. Schenter, James P. Cowin)

Water ice usually is thought to have zero pyroelectricity by symmetry. However, biasing it with ions breaks the symmetry because of the induced partial dipole alignment. This unmasks a large pyroelectricity. Ions were soft-landed upon 1 $\mu$m films of water ice at temperatures greater than 160 K. When cooled below 140-150 K, the dipole alignment locks in. Work function measurements of these films then show high and reversible pyroelectric activity from 30 to 150 K. For an initial ~10V induced by the deposited ions at 160 K, the observed bias below T=150K varies roughly as $(10V)*(T/150K)^2$. This implies that water has pyroelectric coefficients as large as that of many commercial pyroelectrics, such as lead zirconate titanate (PZT). The pyroelectricity of water ice, not previously reported, is in reasonable agreement with that predicted using harmonic analysis of a model system of SPC ice. The pyroelectricity is observed in crystalline and compact amorphous ice, deuterated or not. This implies that for water ice between 0 and 150 K (such as

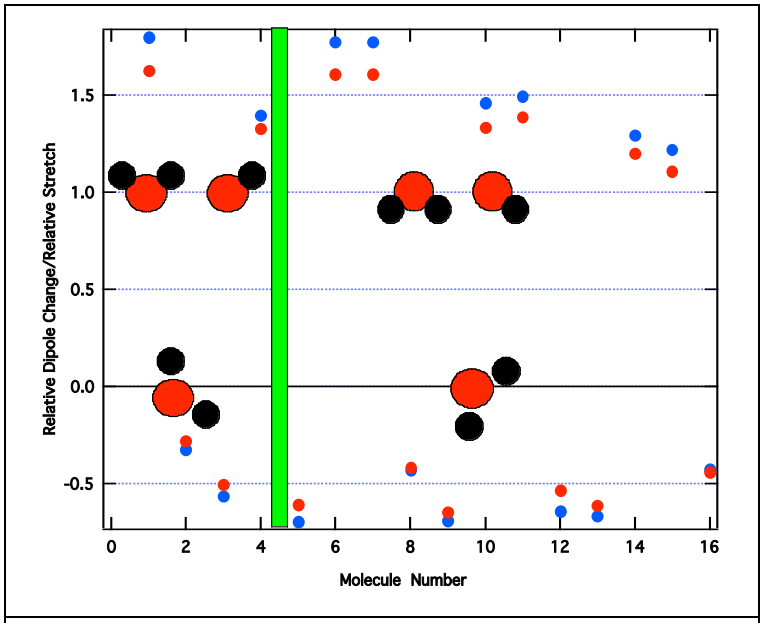


Figure 2. Two classes of piezoelectric water molecules, for all 16 molecules in the unit-cell used. Red/blue points are determined via squeezing/expanding the lattice. The first 4 molecules are up-dipole oriented, the rest down. Water molecules are shown that straddle the z-axis (top) or lay along it (bottom).

astrophysical ices), temperature changes can induce strong electric fields (~10 MV/m) that can influence their chemistry, ion trajectories, or binding.

One interesting new result is that when the source of the piezoelectricity is examined with the SPC ice model, it is clear that the contributions to the total piezoelectricity, when analyzed on a molecule-by-molecule basis (Figure 2), falls in to two very classes. The piezoelectric contributions are very different, depending upon if one of hydrogen-oxygen bond of the water molecule is lined up with the crystal axis under consideration, or straddles it. If lined up, a negative piezo coefficient results. If it straddles it, a positive and 3 times larger magnitude coefficient results. Yet in both cases the magnitude of the dipole aligned up with the z-axis is identical. This leads to the interesting possibility that the piezoelectric properties of ice, or even its sign, may vary substantially upon the preparation or history of the ice.

This work was cited by a Nature highlight [6]

## Future Plans

We recently added FTIR, to probe the surface and bulk species in our films. We have already added low energy secondary ion mass spectrometry (15 to 150 eV Cs ions). Together these will tell us a great deal about the identity and location of ions on and within the films. It will also answer many questions we have about the nature of the dissociated water created for the thick ice films. We will be able to understand the solvation effects on ion dissociation and transport much better, because of these new measurements. We also hope to better understand in bulk ice the motion of hydronium and L and D defects. We are working to expand our studies of liquids, via In-Situ/Liquid TOF-SIMS for Environmental Interfaces.

**References** (Papers under BES support from 2005-present, in **Bold**)


**[1] R. C. Bell, Kai Wu, M. J. Iedema, G. K. Schenter, J. P. Cowin Mapping the Oil-Water Interface's Solvation Potential [submitted to JACS, June 2008}**

[2] K. Wu, M.J. Iedema, J.P. Cowin, "Ion Penetration of the Oil-Water Interface", *Science* 286 (1999) 2482

**[3] Y Lilach, MJ Iedema, JP Cowin, "Dissociation of Water on Pt(111), Buried Under Ice", *Phys. Rev. Lett.* 98 (2006) 016105**

**[4] Y. Lilach, M.J. Iedema, J.P. Cowin, "Proton Segregation on a Growing Ice Interface" Surface Science, 602, (2008) 2886**

**[5] H. Wang, RC Bell, MJ Iedema, GK Schenter, K Wu, and JP Cowin. 2008. "Pyroelectricity of Water Ice." *J. of Physical Chemistry B* 112 (2008) 6379**

**[6] Slicing the ice, Nature, 453 (2008)**

**Garrett BC, et al. "Role of water in electron-initiated processes and radical chemistry: Issues and scientific advances", Chem. Rev. 105: 355-389 (2005)**

**Wang, HF, RC Bell, MJ Iedema, AA Tsekouras, JP Cowin, "Sticky Ice Grains Aid Planet Formation", Astrophys. J. 620, 1027 (2005).**

**Lilach, Y. MJ Iedema, JP Cowin, "Reply to Comment on 'Dissociation of Water on Pt(111), Buried Under Ice'", *Phys. Rev. Lett.* 99, 109602 (2007)**

**Bell RC, K. Wu, MJ Iedema, JP Cowin, "Hydronium ion motion in nanometer 3-methyl-pentane films" *J. Chem. Phys.* 127 024704 (2007)**

**Computational studies of liquid interfaces, $CO_2$ capture, and ionic liquids**

Liem X. Dang
Chemical and Materials Sciences Division
Pacific Northwest National Laboratory
Richland, WA 93352
liem.dang@pnl.gov

**Background and significance**

Molecular processes at interfaces of hydrogen-bonded liquids are of fundamental importance in a number of areas. For example, transport and chemical reactivity at liquid interfaces play crucial roles in a wide variety of problems important to the U.S. Department of Energy (DOE). Past practices at DOE production sites resulted in the discharge of chemical and radioactive material and extensive contamination of soils and ground water at these sites. A fundamental need in understanding the fate and transport of environmental contaminants is a detailed understanding of the factors that control the partitioning of ions and molecules between carrier solvents, minerals, and groundwater as well as the concomitant chemistry. Partitioning is dependent on interfacial structures, transport, and chemical reactivity. Underlying chemical and physical processes that govern transport across and chemical reactions at interfaces is the manner in which water molecules solvate ions. In addition, the structure and stability of large molecules and membranes are strongly dependent on the distribution of ions and counter-ions. The interface, including the adsorption and distribution of solute molecules such as hydroxyl radical or ozone and ions at interfaces, is a fundamental process encountered in a wide range of chemical, environmental, and biological systems.

The absorption selectivity for inclusion compounds of a molecular solid is an important criterion in identifying potential systems for separation of $CO_2$ from other components in gas streams. One important target for such a system is $CO_2$ capture in the production of gas and liquid hydrocarbon products from coal. The molecular solid of calixarene p-tert-butylcalix[4]arene (TBC4) is a prototypical example of a compound that might be used in such a system with gas stream temperatures in the 400–600K range. The TBC4 molecule is a fairly rigid polyphenolic molecule with a hemispherical cage-like structure. It crystallizes in a bilayer arrangement with the open end of the cages opposed and offset, forming a cavity. The crystal structure depends on temperature, growth conditions, and guest occupancy. The dynamics of guest motion in an open framework crystalline structure has primarily been of interest in trying to understand the glass-like thermal conductivity observed in many of these systems, including semiconducting clathrates.

Room temperature ionic liquids (ILs) have attracted significant attention in recent years. The term of room temperature ionic liquids refers to molten salts that are liquids near room temperature and generally consist of large organic cations and inorganic anions. The interest in this class of materials stems from their unusual chemical and physical properties. Typically, ionic liquids are nonflammable, have low vapor pressure, high ionic conductivity, and high thermal stability. Because of the broad selection of anion-cation combination, ionic liquids have great potential to be tailor-made for specific applications and have been widely used in many fields, including synthesis and catalysis, electrochemistry, and liquid-liquid extraction. Due to their nonvolatile nature, ionic liquids are regarded environmentally-friendly “green solvents”, and can be used as designer solvents for a broad range of chemical processes. An understanding of ionic liquids at the molecular level will aid in designing new ILs for specific applications.

**Progress Report**

*Understanding transfer of ions across aqueous interfaces*. Ion transport across aqueous interfaces is of fundamental importance for many processes, including phase transfer catalysis, ion extraction, biological processes, and drug delivers. These processes often depend on the properties at interfaces of water with an immiscible electrolyte solvent (IES). To understand ion transport across interfaces of water with an IES, a variety of factors need to be considered. For example, the interactions of water with the IES and the effect on interfacial tension and capillary waves need to be understood. In addition, the ion solvation environment at the interface and the interactions of the ion with the IES molecules need to be incorporated in any understanding of interfacial ion behavior. Density profiles provide a straightforward way to understand the propensity of various ions for an interface. Figure 1 gives the density profiles for $Cl^-$, $Br^-$, and $I^-$ for $H_2O$-vapor, $H_2O$-$CCl_4$, and the $H_2O$-DCE systems. These density profiles were all taken from 1M NaX

simulations with X being the anion. $I^-$ has the greatest propensity for all interfaces and has a clear trend of being greatest in $H_2O$-vapor > $H_2O$-$CCl_4$ > $H_2O$-DCE. $Br^-$ also has a greater propensity for the $H_2O$-vapor interface than $H_2O$-$CCl_4$. On the other hand, $Cl^-$ does not follow the same trend. The $Cl^-$ interfacial concentration is nearly identical for the $H_2O$-vapor and $H_2O$-$CCl_4$ systems. This shows that the presence of $CCl_4$ affects the $I^-$ and $Br^-$ interfacial concentrations, but not the $Cl^-$ concentration. Interfacial anions can then interact with $CCl_4$, which are generally unfavorable in relation to $H_2O$ interactions. The $Cl^-$ free energy profile shows no minimum at the interface, which is expected, because in the 1M NaCl solutions, $Cl^-$ was repelled from the $H_2O$-DCE interface. The $Cs^+$ ion has a free energy minimum around -6 Å from the Gibbs dividing surface (GDS). The effect of this is to repel anions from the $H_2O$-DCE interface, but for cations, this will increase their propensity for the interface. Unlike anions, cations are generally repelled from aqueous interfaces because they have low polarizability and prefer a fully solvated environment. This factor shows that DCE will likely improve the extraction of $Cs^+$, because cations have a propensity for the region near the interface that is not present for the $CCl_4$ phase.

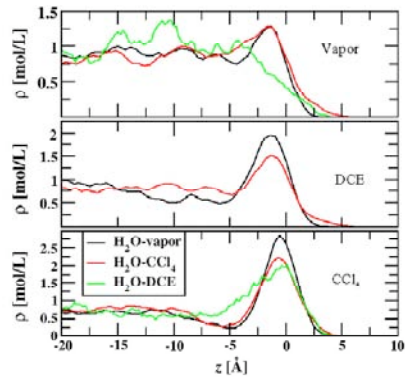

**Figure 1.** Computed density profiles

*Dynamics and free energies of $CH_4$ and $CO_2$ in the molecular solid of p-tert-butylcalix[4]arene*. In this work we study the absorption of $CO_2$ and $CH_4$ in a periodic crystalline solid using thermodynamic integration. In addition the temperature dependent guest molecule dynamics are studied using analysis of the velocity autocorrelation. The temperature dependence of the rattling motion is significant for $CH_4$ but less so for the heavier $CO_2$, although the mass differences are much smaller than between Xe and $N_2$ or $O_2$ in similar behavior found in clathrate hydrate systems. The presence of anharmonic coupling between the lattice acoustic modes and a guest atom or molecule in clathrate materials is often accompanied by glasslike thermal conductivity, although it is evident that this is not a uniquely causal effect. Owing to the importance of absorption free energies and thermal conductivity in potential applications of these materials, we recently reported our investigations of both the thermodynamics and dynamics of a single guest molecule in TBC4 (reference 20). The calculated Gibbs free energies of absorption are shown in Figure 2. We find that absorption of both $CO_2$ and $CH_4$ is favorable but more so for $CO_2$. The results for $CO_2$ are consistent with earlier gas phase cluster calculations.

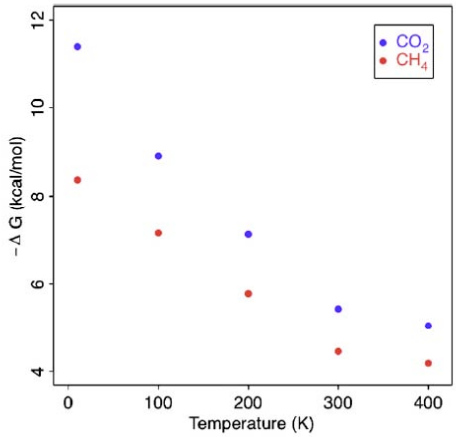

**Figure 2.** Gibbs free energy of inclusion for a single $CO_2$ or $CH_4$ molecule in TBC4 at various temperatures.

**Future Work**

*Ionic liquids and their interfaces*. We have recently carried out studies of the structure and dynamics of 1,3-dimethylimidazolim $[dmim]^+$-halide ILs. The radial distribution functions (RDF) between $[dmim]^+$ and anions ($I^-$, $Br^-$ and $Cl^-$) showed well-defined oscillations in the cation-anion RDFs, which clearly indicated that the ILs exhibit long-range, charge-ordered structure. All three anions show a well-defined structural correlation at short cation-anion separations due to strong electrostatic interactions, followed by a much broader second coordination shell. In Figure 3, we plot the running average of the surface tensions as a function of simulated time. Note that the computed surface tensions of $[dmim]^+$-$Br^-$ and $Cl^-$ are very close together at long times, as is the case of the enthalpy of vaporization of these bulk ILs. The surface tensions of the various ILs had been measured recently by Law and Watson. The results indicated that the surface tension decreases with increasing alkyl chain length for the ILs containing the same anion. Similarly, for a fixed cation, the compound with the larger anion usually has the higher surface tension, but the surface tensions exhibit a narrow range. For instance, the measured surface tensions for the $[omim]^+$-$Br^-$ and $Cl^-$

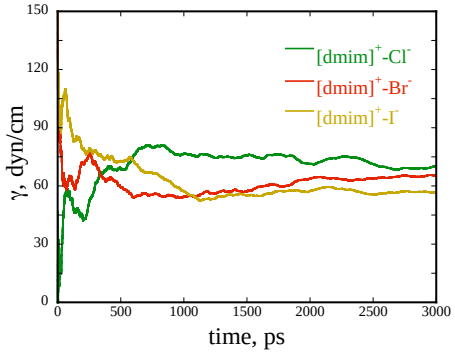


**Figure 3.** Computed surface tensions for ILs.

compounds are 32 and 30 dyn/cm, respectively. These values are significant smaller than our computed surface tensions due to a larger alkyl chain length in the experiments, but their difference is quite small and our simulation results have captured this trend. In addition, our computed surface tension for the $[dmim]^+$-$Cl^-$ compound is much smaller than the corresponding surface tension report by Lynden-Bell that employed a non-polarizable potential model (~100 dyn/cm). Voth and co-workers have demonstrated recently that simulations employing polarizable models give a surface tension in better agreement with the experimental surface tension and that are also smaller than the corresponding non-polarizable model.

Our research using MD techniques on ILs can readily be extended into other ILs such as the 1-alkyl-3 methyl imidazolium $[amim]^+$-$Cl^-$/$Br^-$/$I^-$ and to other complex molecular systems such as the molecular mechanism of cellulose dissolution in these ILs. The role of water at various concentrations in water-ionic mixtures will also be explored to see how they can affect the dynamic and mechanism of molecular process. In summary, our proposed research using molecular dynamics simulation approaches will provide detailed molecular-level understanding of the relation between the structure of solvated species and the solvent, the pathway of dissolution of complex molecular systems, and the effect of modifying anions/cations of ILs as well the roles of acids and bases on these processes.

*Nature of hydroxide ions at the aqueous liquid-vapor interface*. Simulating the molecular properties of the surface of aqueous solutions is essential to understanding a wide range of important in physical and environmental processes. The factor that gives rise to the thermodynamics properties (i.e., the free energy) of ions at interfaces is an area of research at the frontiers of basic chemical physics. From the point of view of molecular simulation, there are many possible ways to model hydroxide anions at an air-water interface. The first and foremost is classical empirical interaction potentials, which are only able to describe non-covalent bond interactions. A relevant quantity to discern the propensity of ions at interfaces is the free-energy profile of an ion as a function of interfacial depth. The classical potential was refined to reproduce the experimental hydration enthalpy, and the structural properties were found to be quite similar to the results that have been reported in the literature. Figure 4 summarizes the results of our study on the transport property of an $OH^-$ across the water/air interface using the constraint mean force approach. It is clear that the computed potential of mean force (PMF) shows a flat minimum near the GDS, which indicates that $OH^-$ can be found at the interface, but its free energy is about 1 kcal/mol above the PMF in the bulk liquid. We have also carried out simulations of a 1M CsOH salt solution and closely examining the results, we can make the preliminary conclusion that classical simulations show very few hydroxide ions at the aqueous interface, with the majority residing in the bulk liquid. Secondly, we are performing similar studies using the polarizable multi-state empirical valence bond (MS-EVB) approach, which contains dissociation and allows multiple waters to share protons with the hydroxide anion, but in a computationally efficient way. Lastly, it will be interesting to compare with *ab initio* approaches based on Kohn-Sham density functional theory (DFT), which contains the proper physics to describe charge transfer and chemistry, but are limited to short simulations even on leadership class computers.

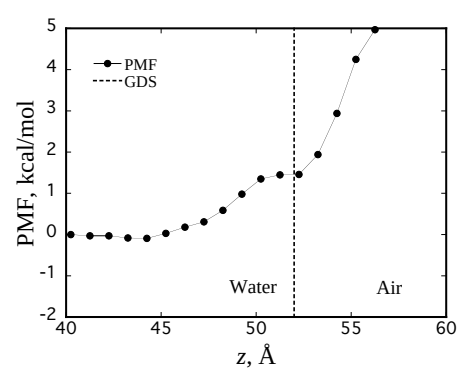


**Figure 4.** Computed potential of mean force

*Simulation studies of ions and solutes at the vapor-liquid interface.* In recent years, it has become clear that the air-water interface plays a more significant role in gas adsorption and reaction kinetics of many atmospheric processes than had previously been anticipated. Recently, surface complexes have been invoked to explain the initial step in a number of surface reaction mechanisms, including the reaction of gas-phase $SO_2$ with water. Understanding $SO_2$ interaction at aqueous surfaces is essential because of the central role of

sulfur in many atmospheric aerosols. Richmond and co-workers carried out an experimental study on the solvation of $SO_2$ molecules at the vapor-liquid interface using vibrational sum frequency spectroscopy. Among other results discussed in this work, their work demonstrated the presence of a weak $SO_2$:$H_2O$ complex at the water surface prior to reaction and dissolution. Richmond el al. proposed a structure of the complex $SO_2$-air-water interface. The focus of our work on solvation of the solute at the vapor-liquid interface aligns with previous work on the hydroxyl solvation at the water vapor-liquid interface. We begin this work by developing a polarizable model for the $SO_2$:$H_2O$ complex. To our knowledge, no such potential model has been described in the literature. We will make use of *ab initio* quantum chemical calculations on the $SO_2$:$H_2O$ complex, and we will use this information as well as the observed data to construct the potential model. We will carry out the PMF calculations and also molecular dynamics simulations on the solvation of $SO_2$ molecules to characterize the distribution and solvation property of the $SO_2$ molecules at the water surface and to compare to the result reported by Richmond et al.

**References to publications of DOE sponsored research (2005-present)**


1. T.-M. Chang and **LXD**, "Liquid/Vapor Interface of Methanol-Water Mixtures: A Molecular Dynamics Study" *J. Phys. Chem.* B 109, 5759 (**2005**).
2. M. Mucha, T. Frigato, L. Levering, H. C. Allen, D. J. Tobias, **LXD** and P. Jungwirth, "A unified molecular picture of the surfaces of aqueous acid, base, and salt solutions" *J. Phys. Chem.* B 109, 7617 (**2005).**
3. V.-A. Glezakou, Y. C. Chen, J. L. Fulton, G. K. Schenter and **LXD** "Electronic Structure, Statistical Mechanical Simulations, and EXAFS Spectroscopy of Aqueous Potassium" *Theoretical Chemistry Accounts* 115, 86 (**2006**).
4. **LXD** and T. M. Chang, "Recent Advances in Molecular Simulations of Ion Solvation at Liquid Interfaces" *Chemical Reviews* 106, 1305 (**2006**).
5. C. D. Wick, **LXD** and P. Jungwirth, "Simulated Surface Potentials at the Vapor-Water Interface for the KCl Aqueous Electrolyte Solution" *J. Chem. Phys*. 125, 024706 (**2006).**
6. C. D. Wick and **LXD**, "Computational Observation of Enhanced Solvation of the Hydroxyl Radical with Increased NaCl Concentration" *J. Phys. Chem.* B 110, 8917 (**2006**).
7. O. Höfft, A. Borodin, U. Kahnert, V. Kempter, **LXD** and P. Jungwirth, "Surface Segregation of Dissolved Salt Ions" *J. Phys. Chem.* B 110, 11971 **(2006).**
8. C. D. Wick and **LXD**, "Distribution, Structure, and Dynamics of Cesium and Iodide Ions at the $H_2O$-$CCl_4$ and $H_2O$-Vapor Interfaces" *J. Phys. Chem.* B 110, 6824 **(2006)**.
9. **LXD**, T. M. Chang, M. Roeselova, B. C. Garrett, D. J. Tobias, "On $NO_3^-$-$H_2O$ Interactions in Aqueous Solutions and at Interfaces" *J. Chem. Phys*. 124, 066101 **(2006).**
10. **LXD**, G. K. Schenter, J. L. Fulton, V.-A. Glezakou, "Molecular Simulation Analysis and X-ray Absorption Measurement of $Ca^{2+}$, $K^+$ and $C1^-$ Ions in Solution" *J. Phys. Chem*. B 110, 23644 **(2006).**
11. J. L. Daschbach, T.-M. Chang, L. R. Corrales, **LXD**, B. P. McGrail "Molecular Mechanisms of Hydrogen Loaded Beta-Hydroquinone Clathrate". *J. Phys. Chem. B* 110, 17291 **(2006)**.
12. L. Cwiklik, G. Andersson, **LXD**, and P. Jungwirth, *Chemphyschem* 8, 1457 (**2007).**
13. J. Thomas, J., M. Roeselova, **LXD** and D. J. Tobias, "Molecular dynamics simulations of the solution-air interface of aqueous sodium nitrate" *J. Phys. Chem.* A 111, 3091 **(2007).**
14. J. L. Daschbach and P. K. Thallapally, J. L. Atwood, B. P. McGrail and **LXD**, "Free energies of $CO_2$/$H_2$ capture by p-tert-butylcalix[4]arene: A molecular dynamics study. *J. Chem. Phys*. 127, 104703 **(2007).**
15. O. Hoefft, U. Kahnert, S. Bahr, V. Kempter, P. Jungwirth, and **LXD**, "Segregation of salt ions at amorphous solid and liquid surfaces. in Physics and Chemistry of Ice, ed. W. Kuhs, RSC Publishing, London, 217-223 **(2007).**
16. C. Wick and **LXD**, "Molecular Mechanism Of Transporting A Polarizable Iodide Anion Across The Water-Ccl4 Liquid/Liquid Interface" *J. Chem. Phys*. 126, 134702 **(2007).**
17. C. D. Wick, I-F. W. Kuo, C. J. Mundy, and **LXD**, "The Effect of Polarizability for Understanding the Molecular Structure of Aqueous Interfaces" J. *Chem. Theo. and Comp.* 3, 2002 **(2007).**
18. C. D. Wick and **LXD**, "Molecular Dynamics Study of Ion Transfer and Distribution at the Interface of Water and 1,2-Dichloroethane" *J. Phys. Chem.* C 112, 647 (**2008)**.
19. T.-M. Chang and **LXD**, "Computational Studies Of Liquid Water And Diluted Water In Carbon Tetrachloride" *J. Phys. Chem.* A 112, 1694 **(2008).**
20. J. L. Daschbach, P. K. Thallapally, B. P. McGrail and **LXD**, "Dynamics And Free Energies Of $CH_4$ And $CO_2$ In The Molecular Solid Of The P-Tert-Butylcalix[4] Arene" *Chem. Phys. Lett.* 453, 123 **(2008).**
21. C. D. Wick and **LXD**, "Recent Advances In Understanding Transfer Ions Across Aqueous Interfaces" *Chem. Phys. Lett.* 458, 1 **(2008).**

# Infrared Spectroscopy of Transition Metal-Molecular Interactions in the Gas Phase

DE-FG02-96ER14658

Michael A. Duncan

Department of Chemistry, University of Georgia, Athens, GA 30602-2556

maduncan@uga.edu

## Program Scope

Our research program investigates gas phase metal clusters and metal ion-molecular complexes as models for heterogeneous catalysis, metal-ligand bonding and cation solvation. The clusters studied are molecular sized aggregates of metal or metal compounds (oxides, carbides). We focus on the bonding exhibited by "physisorption" versus "chemisorption" on cluster surfaces, on metal-ligand interactions with benzene or carbon monoxide, and on solvation interactions exemplified by complexes with water, acetonitrile, etc. These studies investigate the nature of the metal-molecular interactions and how they vary with metal composition and cluster size. To obtain size-specific information, we focus on ionized complexes that can be mass-selected. Infrared photodissociation spectroscopy is employed to measure the vibrational spectroscopy of these ionized complexes. The vibrational frequencies measured are compared to those for the corresponding free-molecular resonances and with the predictions of theory to reveal the electronic state and geometric structure of the system. Experimental measurements are supplemented with calculations using density functional theory (DFT) with standard functionals such as B3LYP.

## Recent Progress

The main focus of our recent work has been infrared spectroscopy of mass-selected cation-molecular complexes of transition metal ions interacting with carbon monoxide, water or benzene, e.g., $M^+(H_2O)_n$, $M^+(bz)_n$ and $M^+(CO)_n$. These species are produced by laser vaporization in a pulsed-nozzle cluster source, size-selected with a specially designed reflectron time-of-flight mass spectrometer and studied with infrared photodissociation spectroscopy using an IR optical parametric oscillator laser system (OPO). We have studied the infrared spectroscopy of various transition metal ions in complexes with the ligands indicated. In each system, we examine the shift in the frequency for selected vibrational modes in the adsorbate molecule that occur upon binding to the metal. The number and frequencies of IR-active modes in multi-ligand complexes reveal the structures of these systems, while sudden changes in vibrational spectra or IR dissociation yields are used to determine the coordination number for the metal ion in these complexes. In some systems, new vibrational bands are found at a certain complex size that correspond to intra-cluster reaction products. In small complexes with strong bonding, we use the method of “rare gas tagging” with argon or neon to enhance dissociation yields. In all of these systems, we employ a close interaction with theory to investigate the details of the metal-molecular interactions that best explain the spectroscopy data obtained. We perform our own density functional theory (DFT) or MP2 calculations (using Gaussian 03W or GAMESS) and when higher level methods are required (e.g.,

CCSD), we collaborate with local theorists (Profs. P.v.R. Schleyer, H.F. Schaefer) or those at other universities (Prof. Mark Gordon, Iowa State). Our infrared data on these transition metal ion-molecule complexes provide many examples of unanticipated structural and dynamical information.

One technical improvement implemented recently has been the extension of our IR lasers to longer wavelengths. With the original configuration of our OPO system, the wavelength coverage was 2000-4500 $cm^{-1}$. Now we have added $AgGaSe_2$ and $LiInS_2$ crystals to this system, extending the coverage to the region of 550-2000 $cm^{-1}$. In particular, this allows investigation of the carbonyl stretching region, the bending mode of water, the carbon skeletal modes of benzene, etc. New spectra have been obtained in the longer wavelength region for several cation-molecular complexes.

$M^+(H_2O)_n$ complexes and those tagged with argon have been studied previously in our lab for the metals iron, nickel, cobalt and vanadium. We have recently extended these studies to titanium, manganese, chromium, scandium, copper, silver, gold and zinc complexes. We have studied the noble metal ions copper, silver and gold with one and two water molecules. The gold system prefers a coordination of two ligands, and red-shifts its O-H stretches much more than those of copper and silver. In the vanadium system, we have studied multiple water complexes. Hydrogen bonding bands appear for the first time for the complex with five water molecules, establishing that four water molecules is the coordination for $V^+$. Copper and zinc complexes with a single attached water have unexpected vibrational bands at high frequency above the normal region of the symmetric and asymmetric O-H stretches. With the help of theory by Prof. Anne McKoy (Ohio State), we are able to assign these features to combination bands involving the twisting motion of the water. Silver and chromium complexes were rotationally resolved, providing the H-O-H bond angle in these systems. In very new work, we have been able for the first time to produce multiply charged transition metal cation-water complexes for chromium, manganese and scandium systems tagged with multiple argons. IR spectra of these systems have very different intensity patterns and O-H shifts than those for the singly charged systems, and we are able to study the charge dependence of the cation-water interaction.

$M^+(CO)_n$ complexes are analogous to well-known species in conventional inorganic chemistry. However, we are able to make these systems without the complicating influences of solvent or counter ions. The C-O stretch in most stable neutral transition metal complexes shifts strongly to the red from free CO, and this vibration often falls below 2000 $cm^{-1}$. However, we have found that *cation* transition metal complexes have smaller red shifts, and the carbonyl stretches lie in the 2000-2200 $cm^{-1}$ region. We have examined vanadium and cobalt systems as a function of the number of carbonyl ligands attached. $Co^+(CO)_5$ has 18 electrons and is isoelectronic to the well-known neutral complex $Fe(CO)_5$, and we wanted to investigate the coordination number and the electronic state of this species. The stable coordination is found for the n=5 species, as expected, and the carbonyl stretch is hardly shifted from the free-CO value. In $V^+(CO)_n$ complexes, the n=7 species has 18 electrons and had been predicted to be stable by theory. However, we found that the stable coordination is not at n=7, but is at the 16 electron species $V^+(CO)_6$. The CO band shifts for the n=1-8 complexes reveal how this system gradually changes from a triplet for the mono-ligand species to a singlet for the n=6 species. We have also examined so-called non-classical carbonyl complexes of gold and platinum. $M^+(CO)_n$ complexes for these systems have been studied, and they exhibit the expected blue-shift of the carbonyl stretch relative to free CO. The size dependence of these resonances provides insight into the structures of these complexes. We collaborated on the gold system with Prof. Mark Gordon (Iowa State) who was able to do relativistic calculations to compare to our spectra.

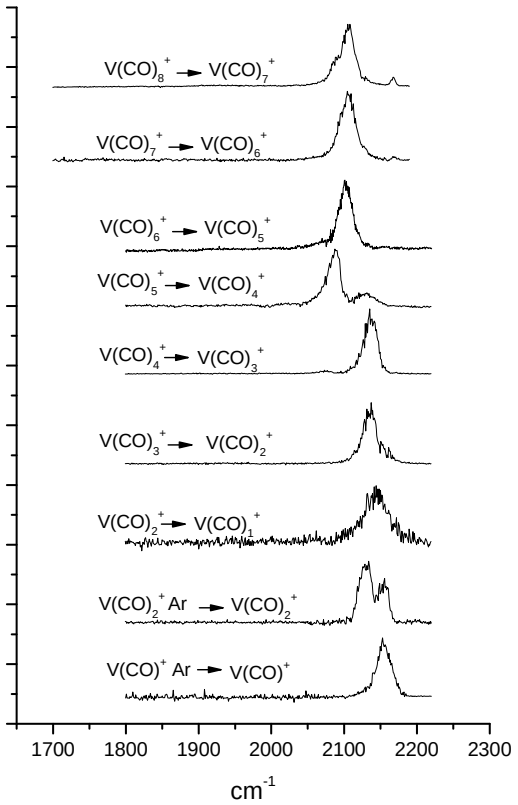


Figure 1. The IR spectra of $V^+(CO)_n$ complexes measured with mass-selected photodissociation.

Taking advantage of the longer wavelength IR laser coverage, we have also been able to study M=O stretching modes of metal oxides and their complexes near 900-1000 $cm^{-1}$. In the vanadium system, we have studied both the atomic cation and its oxides with $CO_2$ or CO ligands. An intracluster reaction takes place in larger $CO_2$ complexes that apparently produces a metal-carbonate species.

**Future Plans**

Future plans for this work include the extension of these IR spectroscopy studies to more ligands and to complexes with multiple metal atoms. Studies with more reactive metals and hydrocarbons such as ethylene or methane might produce carbenes, vinylidene or ethylidyne species. These systems should exhibit characteristic IR spectra, and allow us to make better connections with IR spectroscopy on metal surfaces. We have realized that larger metal clusters or their oxides are quite difficult to produce and cool simply by supersonic expansions. We are therefore exploring different designs of cryogenically cooled cluster sources to make these systems and tag them effectively.

In all of these studies, we have focused on the qualitative effects of metal-adsorbate interactions and trends for different transition metals interacting with the same ligand. Our theoretical work has revealed that density functional theory has some serious limitations for small metal systems that were not previously recognized. This is particularly evident in metals such as vanadium and iron, where two spin states of the metal lie at low energy. DFT has difficulty identifying the correct relative energies of these spin states. Further examinations of this issue are planned, as it has significant consequences for the applications of DFT.

**Publications (2005-2008) for this Project**


1. R.S. Walters, P.v.R. Schleyer, C. Corminboeuf and M.A. Duncan, "Structural Trends in Transition Metal Cation-Acetylene Complexes Revealed Through the C-H Stretch Fundamentals," *J. Am. Chem. Soc.* **127**, 1100 (2005).

2. T.D. Jaeger and M.A. Duncan, "Infrared Photodissociation Spectroscopy of $Ni^+$(benzene)$_x$ Complexes," *J. Phys. Chem. A* **109**, 3311 (2005).

3. E.D. Pillai, T.D. Jaeger and M.A. Duncan, "Infrared spectroscopy and density functional theory of small $V^+(N_2)_n$ clusters," *J. Phys. Chem. A* **109**, 3521 (2005).

4. R.S. Walters, E.D. Pillai and M.A. Duncan, "Solvation Processes in $Ni^+(H_2O)_n$ Complexes Revealed by Infrared Photodissociation Spectroscopy," *J. Am. Chem. Soc.* **127**, 16599 (2005).

5. R.S. Walters, E.D. Pillai, P.v.R. Schleyer and M.A. Duncan, "Vibrational spectroscopy of $Ni^+(C_2H_2)_n$ (n=1-4) complexes," *J. Am. Chem. Soc.* **127**, 17030 (2005).

6. N.R. Walker, R.S. Walters and M.A. Duncan, "Frontiers in the Infrared Spectroscopy of Gas Phase Metal Ion Complexes," *New J. Chem.* **29**, 1495 (2005).

7. E.D. Pillai, T.D. Jaeger and M.A. Duncan, "Infrared Spectroscopy of $Nb^+(N_2)_n$ Complexes: Coordination, Structures and Spin States," *J. Am. Chem. Soc.* **129**, 2297 (2007).

8. A.C. Scott, N.R. Foster, G.A. Grieves and M.A. Duncan, "Photodissociation of lanthanide metal cation complexes with cyclooctatetraene," *Int. J. Mass Spectrom.* **263**, 171 (2007).

9. V. Kasalova, W.D. Allen, H.F. Schaefer, E.D. Pillai and M.A. Duncan, "Model systems for probing metal cation hydration: The $V^+(H_2O)$ and $V^+(H_2O)$Ar complexes," *J. Phys. Chem. A* **111**, 7599 (2007).

10. L. Belau, S.E. Wheeler, B.W. Ticknor, M. Ahmed, S.R. Leone, W.D. Allen, H.F. Schaefer, and M.A. Duncan, "Ionization Thresholds of Small Carbon Clusters: Tunable VUV Experiments and Theory," *J. Am. Chem. Soc.* **129**, 10229 (2007).

11. J. Velasquez, III, B. Njegic, M. S. Gordon and M. A. Duncan, "IR Photodissociation Spectroscopy and Theory of $Au^+(CO)_n$ Complexes: Nonclassical Carbonyls in the Gas Phase," *J. Phys. Chem. A* **112**, 1907 (2008).

12. M.A. Duncan, "Structures, energetics and spectroscopy of gas phase transition metal ion-benzene complexes," *Int. J. Mass Spectrom.* **272**, 99 (2008).

13. P. D. Carnegie, B. Bandyopadhyay and M.A. Duncan, "Infrared spectroscopy of $Cr^+(H_2O)$ and $Cr^{2+}(H_2O)$: The role of charge in cation hydration," *J. Phys. Chem. A* **112**, 6237 (2008).

14. J. Velasquez, III and M. A. Duncan, "IR Photodissociation Spectroscopy of $Pt^+(CO)_n$ Complexes," *Chem. Phys. Lett.* **461**, 28 (2008).

Electronic Structure and Reactivity Studies for Aqueous Phase Chemistry

Michel Dupuis
Chemical and Materials Sciences Division
Pacific Northwest National Laboratory
902 Battelle Blvd.
Mail Stop K1-83
Richland, WA 99352
michel.dupuis@pnl.gov

**Program scope:**[#] We are interested in the theoretical characterization of thermochemical, spectroscopic, and reactive properties of molecules and clusters in the aqueous phase and at interfaces for chemistries relevant to DOE missions. Specifically, solvation data for many relevant, yet chemically challenging organic radical ions are needed for the development of reliable thermo-chemical kinetic models of solution reactivity, but often they are not easily measured. Methods to compute these properties are invaluable. Recently we have been interested in improving continuum models of solvation and proposed a very significant development that brings them to chemical accuracy, in particular for anions.

**Recent progress: "***Charge-Dependent Dielectric Continuum Model of Solvation (CD-COSMO) with Emphasis on Ions: Aqueous Solutes with Oxo, Hydroxo, Amino, Methyl, Chloro, Bromo, and Fluoro Functionalities"* (Dupuis with Camaioni, Ginovska, PNNL, *J. Phys. Chem. A 000, 0000 (2008)*)

*Motivation:* Current solvation models based on a dielectric continuum representation of the solvent still do not afford the needed accuracy for many species of interest (e.g. radical ions). The limitations can be traced to failure to capture strong solute-solvent interactions. Dielectric continuum solvation models are widely used because they are a computationally efficacious way to simulate equilibrium properties of solutes. With advances that allow for molecular-shaped cavities, they have reached a high level of accuracy, in particular for neutral solutes. However, benchmark tests show that existing schemes for defining cavities are unable to consistently predict accurately the effects of solvation on ions, especially anions.

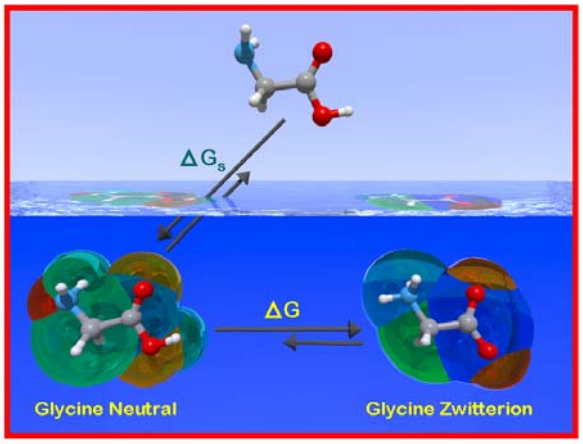


*Approach:* We have extended the Conductor-Screening-Model of solvation (COSMO) model into a novel Charge-Dependent COSMO (CD-COSMO) model in a highly accurate approach to capturing strong solute-solvent interactions. The work involved the further development of a protocol put forth earlier for defining the cavities of aqueous solutes, with resulting advances that are most striking for anions. Molecular cavities are defined as interlocked spheres around atoms or groups of atoms in the solute, but the sphere radii are determined by simple empirically-based expressions involving the effective atomic charges of the solute atoms (derived from molecular electrostatic potential) and base radii. Both of these terms are optimized for the different types of atoms or functional groups in a training set of neutral and charged solutes. Parameters in these expressions for radii were fitted by minimizing

residuals between calculated and measured standard free energies of solvation ($\Delta G_s$*), weighted by the uncertainty in the measured value. The calculations were performed using density functional theory with the B3LYP functional and the 6-311+G** basis set. The optimized radii definitions reproduce $\Delta G_s$* of neutral solutes and singly-charged ions in the training set to within experimental uncertainty and, more importantly, accurately predict $\Delta G_s$* of compounds outside the training set, in particular anions. Inherent to this approach, the cavity definitions reflect the strength of specific solute-water interactions. We surmise that this feature underlies the success of the model, referred to as the CD-COSMO model for Charge-Dependent (also Camaioni-Dupuis) COSMO model. These findings offer encouragement that we can keep extending this scheme to other functional groups and obtain better accuracy in using continuum solvation models to predict equilibrium properties of aqueous ionic solutes.

Mean Unsigned Error (kcal/mol) for Various solvation models

| | |
|---|---|
| **UAHF** | **2.5** |
| **UAKS** | **3.0** |
| **MST** | **4.1** |
| **SM6** | **4.4** |
| **CD-COSMO (this work)** | **0.4** |
| **Expt.** | **0.5** |

*Results:* The approach is illustrated for a number of test cases, including the determination of acidities of an amine base, a study of the tautomerization equilibrium of a zwitterionic molecule (glycine), and calculating solvation energies of transition states toward a full characterization of reaction pathways in aqueous phase, here in $S_N2$ exchange reactions. The calculated reactions barriers in aqueous solution are in excellent agreement with experimental values.

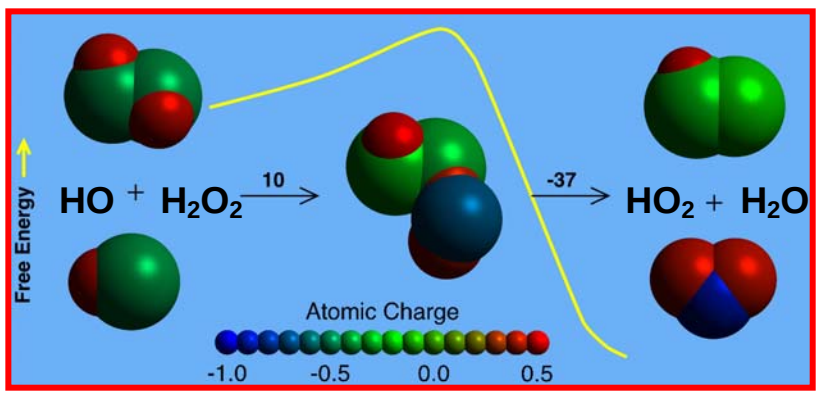


**The picture illustrates for the reaction OH + $H_2O_2$ → $H_2O$ + $HO_2$ how the cavity radii change with atomic charges: the stronger the charge, the smaller the radius.**

**Future Plans:** Experience and insights have led us to propose this novel protocol for the definition of molecular cavities. The protocol yields solvation energies within experimental uncertainty for a large number of functional groups. It is most strikingly accurate for anions where all other models fail. The protocol provides a well-founded framework for extensions to transition states and reaction pathways ($S_N2$ and others) and to other functionalities (S, SH, arenes, …)

References to publications of DOE Chemical Physics sponsored research (2005-present)


1. M.Aida and **M.Dupuis**, "Fundamental Absorption Frequency from Quasi-classical Direct ab initio Molecular Dynamics: Diatomic Molecule", Chem. Phys. Lett. 401, 170 (2005).
2. B.C.Garrett, D.A.Dixon, D.M.Camaioni, D.M.Chipman, M.A.Johnson, C.D.Jonah, G.A.Kimmel, J.H.Miller, T.N.Rescigno, P.J.Rossky, S.S.Xantheas, S.D.Colson, A.H.Laufer, D.Ray, P.F.Barbara, D.M.Bartels, K.H.Becker, K.H.Bowen, Jr., S.E.Bradforth, I.Carmichael, J.V.Coe, L.R.Corrales, J.P.Cowin, **M.Dupuis**, K.B.Eisenthal, J.A.Franz, M.S.Gutowski, K.D.Jordan, B.D.Kay, J.A.LaVerne, S.V.Lymar, T.E.Madey, C.W.McCurdy, D.Meisel, S.Mukamel, A.R.Nilsson, T.M.Orlando,

N.G.Petrik, S.M.Pimblott, J.R.Rustad, G.K.Schenter, S.J.Singer, A.Tokmakoff, L.S.Wang, C.Wittig, and T.S.Zwier, "The Role of Water on Electron-Initiated Processes and Radical Chemistry: Issues and Scientific Advances", Chem. Rev. 105, 355 (2005).

3. J.D. Watts and **M. Dupuis**, "A Coupled-Cluster Analysis of the Photoelectron Spectrum of $FeCl_3^-$ ", Molec. Phys. 103, 2223 (2005).
4. S. Hirata, M. Valiev, **M. Dupuis**, S.S. Xantheas, S. Sugiki, and H. Sekino, "Fast electron correlation methods for molecular clusters in the ground and excited states". Molec. Phys. 103 2255 (2005).
5. M. Kolaski, H.M. Lee, C. Pak, **M. Dupuis**, and K.S. Kim, "Ab Initio Molecular Dynamics Simulations of an Excited State of $X^-(H_2O)_3$ (X=Cl, I) Complex", J. Phys. Chem. A 109, 9419 (2005).
6. S. Du and J.S. Francisco,G.K. Schenter, T.D. Iordanov, B.C. Garrett, **M. Dupuis**, and J. Li, "The OH Radical-H2O Molecular Interaction Potential", J. Chem. Phys. 124, 224318 (2006).
7. A. Furuhama, **M. Dupuis**, and K. Hirao, "Reactions associated with ionization in water: a direct ab initio dynamics study of ionization in $(H_2O)_{17}$ ", J. Chem. Phys. 124, 164310 (2006).
8. M. Valiev, B.C. Garrett, M.K. Tsai, K. Kowalski, S. M. Kathman, G. K. Schenter, and **M. Dupuis**, "Hybrid Coupled Cluster Approach for Free Energy Calculations: Application to the Reaction of $CHCl_3$ and $OH^-$ in water", J. Chem. Phys. 127, 051102 (2007).
9. B. Gonovska, D. M. Camaioni, and **M. Dupuis**, "Reaction pathways and excited states in $H_2O_2$ + OH → $HO_2$ + $H_2O$: a New ab initio Investigation", J. Chem. Phys. 127, 084389 (2007).
10. M.K. Tsai, K. Kowalski, M. Valiev, **M. Dupuis**, "Signature OH Absorption Spectrum from Cluster Models of Solvation: A Solvent-to-Solute Charge Transfer State", J. Phys. Chem. A 000, 0000 (2007).
11. M. Ohisa, H. Yamataka, **M. Dupuis**, and M. Aida, "Two-Dimensional Free Energy Surface on Exchange Reaction of Alkyl Chloride/Chloride Using QM/MM-MC Method", Phys. Chem. Chem. Phys. 10, 844 (2008)
12. E. Bylaska, **M. Dupuis**, P. Tratnyek, "One-Electron Transfer Reactions of Polychlorinated Ethylenes: Concerted and Stepwise Cleavages", J. Phys. Chem. C 112, 3712 (2008)
13. M. Valiev, E. Bylaska, **M. Dupuis**, P. Tratnyek, "Combined Quantum Mechanical and Molecular Mechanics Studies of the Electron Transfer Reactions Involving Carbon Tetrachloride in Solution", J. Phys. Chem. A 12, 2713 (2008)
14. A. Furuhama, **M. Dupuis**, and K. Hirao, "Application of a kinetic energy partitioning scheme for ab initio molecular dynamics to reactions associated with ionization in water tetramers $(H_2O)_4^+$", Phys.Chem.Chem.Phys. 10, 2033 (2008).
15. B. Ginovska, D. M. Camaioni, and **M. Dupuis**, "The $H_2O_2$+OH → $HO_2$+$H_2O$ reaction in aqueous solution from a charge-dependent continuum model of solvation", J. Chem. Phys. 129, 014506 (2008).
16. B. Ginovska, D. M. Camaioni, **M. Dupuis**, C. Schwerdtfeger, and Q. Gilcrease, "Charge-Dependent Cavity Radii for an Accurate Dielectric Continuum Model of Solvation with Emphasis on Ions: Aqueous Solutes with Oxo, Hydroxo, Amino, Methyl, Chloro, Bromo and Fluoro Functionalities", J. Phys. Chem. A 000, 0000 (2008).

[#] This research was performed in part using the Molecular Science Computing Facility in the William R. Wiley Environmental Molecular Sciences Laboratory (EMSL) at the Pacific Northwest National Laboratory (PNNL). The EMSL is funded by DOE's Office of Biological and Environmental Research. PNNL is operated by Battelle for DOE.

**Photochemistry at Interfaces**

Kenneth B.Eisenthal
Department of Chemistry
Columbia University, MC 3107
New York, NY 10027
kbe1@columbia.edu

**Interfaces** are of fundamental scientific interest because of their unique chemical and physical properties, as manifested both in equilibria and time dependent phenomena. The interface selective methods characteristic of second harmonic generation (SHG) and sum frequency generation (SFG) spectroscopies, for interfaces bound by centrosymmetric or isotropic media, are used in our laboratory to investigate liquid interfaces, primarily aqueous interfaces, which include air/liquid, organic liquid/aqueous, liquid/solid, and nano-microparticles in aqueous media.

**Ultrafast Dynamics -- Femtosecond pump – probe experiments**

**A. Sum frequency Probe**

We have carried out the first time resolved experiments in which interfacial molecules are pumped to excited electronic states and probed by vibrational sum frequency generation. In this way the analytical and structural capability of a vibrational spectroscopy to probe time dependent changes via selected chromophores in interfacial molecules has been used in these initial experiments to study orientational and solvation dynamics at air/aqueous interfaces.

**Molecular Rotations**

The method that we have used to investigate rotational motions, both at interfaces and in bulk liquids, is to use a femtosecond polarized pulse of light to perturb the equilibrium orientational distribution of molecules by the preferential excitation of those molecules whose transition moments are more closely aligned with the polarization of the pump pulse. The simultaneously incident infrared and visible probe pulses, which are time delayed with respect to the pump pulse, generate an SFG signal, which is then used to monitor the return of the molecules to their equilibrium orientational distribution. By selecting the frequency of the IR to be in resonance with the carbonyl frequency, which we determine using SFG, various properties of the carbonyl group can be investigated. In the experiments reported here it was the time dependent changes in the orientation of the carbonyl group, the -C=O axis, with respect to the interfacial normal, for coumarin 314, C314, at the air/aqueous interface. The carbonyl chromophore was selected in these first experiments because of its ubiquity in a wide range of organic, inorganic, and biological molecules. Similarly a coumarin was selected because of the extensive information available and because it has electronic transitions in a convenient frequency range. The out of plane orientational relaxation time of the –C=O axis obtained from the SFG measurements was 220 ± 20 ps, which is considerably faster than the orientational relaxation time of 343 ± 13 ps obtained from SHG measurements. In order to determine the orientational relaxation time of C314 in bulk aqueous solutions we performed pump – linearly polarized absorption measurements that yielded a relaxation time of 262 ± 10 ps. How these different results for SHG and SFG are related and how in turn are they related to bulk measurementsis currently being investigated.

In addition to these ultrafast dynamics measurements we have combined SHG measurements that yielded the equilibrium orientation of the C314 permanent dipole moment axis with SFG measurements that yielded the orientation of the –C=O axis, which together yields the orientation of the C314 molecular plane with respect to the interfacial normal, and thereby determines the absolute orientation of the interfacial molecule.

**Solvation Dynamics** As a complement to our aforementioned investigations of the motions of interfacial solute molecules we have studied the motions of the solvent molecules surrounding interfacial solute molecules. The time dependent rearrangement of solvent molecules in response to a sudden charge redistribution in solute molecules is commonly referred to as solvation

dynamics. This sudden change was achieved in our experiments by the femtosecond photoexcitation of C314 molecules at the air/aqueous interface. In the SFG probe experiments two solvation time scales were observed, one at 230 ± 40 fs and the other at 2.17 ± 0.3 ps. Unlike the marked differences obtained in the SFG vs. SHG measurements of orientational relaxation the SFG solvation results are very close to the those obtained in the solvation SHG measurements. This close agreement in the solvation findings is interpreted to indicate that it is the time dependent change in the Raman part of the carbonyl SFG hyperpolarizabity due to the solvent reorganization that is responsible for the observed dynamics in the SFG experiments, and not due to solvation effects on the carbonyl vibrational frequency or transition strength

**B. Second Harmonic Probe**

**Solvent Isotope Effect on Molecular Rotations --- Air//$H_2O$ vs. Air/$D_2O$**

Because the zero point energy of $D_2O$ is smaller than that of $H_2O$ its hydrogen bonding strength and intermolecular interactions are stronger. One way that this can be manifested is in the resulting effects of larger barriers to rotation, i.e. larger rotational friction in $D_2O$ relative to $H_2O$. In linearly polarized pump- probe studies of the orientational relaxation of 314 in the bulk isotopic water liquids we found that the rotation time in $D_2O$ was 50 ps longer than in $H_2O$. To examine interfacial solute rotations we used the pump – SHG probe method and found that the out of plane orientational relaxation of C314 at the air/$D_2O$ interface was 100 ps longer than at the air/$H_2O$ interface. It was of interest to find that the effects of deuteration on orientational relaxation times was greater at the air/water interfaces than in the bulk water. Various explanations for this effect are being pursued.

**Structure of Water Under Air/Nitrile Interfaces**

The high surface tension of the air/water interface favors the strong adsorption of most solute molecules to the interface. In SFG studies of acetonitrile, $CH_3CN$, at the air/water-acetonitrile interface we found that the C≡N chromophore is hydrogen bonded to water up until the mole fraction of acetonitrile in the bulk solution exceeds 0.1. At this concentration the hydrogen bonds of the interfacial acetonitrile molecules are broken as evidenced by a spectral shift of 15 $cm^{-1}$ in the SFG spectrum of the C≡N vibration to its non- hydrogen bonded state. It is at this density that the surface approaches a full monolayer coverage as seen by the surface tension approaching that of neat acetonitrile. Similar behavior was observed for the long chain nitrile surfactant, $CH_3(CH_2)_{19}CN$, at a surface density of 27 $Å^2$, which is the coexistence to liquid state transition density in the surfactant phase diagram.

We now seek to investigate the structure of water beneath the acetonitrile monolayer. Research on the structure of water beneath a surfactant layer has been studied in a number of laboratories, but not its structure when the organic molecules that form the monolayer are also present in the bulk solution. In this case there is a competition between the bulk organic molecules and the bulk water molecules for contact with the air phase and also in the region below the top surface layer. In the SFG experiments reported here the water that was used was $D_2O$, selected for experimental reasons. It was found that as the bulk acetonitrile mole fraction increased the SFG water signal decreased both in the more weakly hydrogen bonding region, ~ 2500 $cm^{-1}$ region, and in the more strongly hydrogen bonding region, ~ 2350 $cm^{-1}$. At mole fractions greater than 0.07, no vibrational resonances were observed in the spectral regions associated with hydrogen bonding. The story is different in the free OD spectral region,~ 2700 $cm^{-1}$, where one of the two OD bonds is not hydrogen bonded to another $D_2O$. As the acetonitrile concentration increases a decrease in the magnitude of the SFG signal in this free OD spectral region was observed. However at coverages where no resonances were observed in the hydrogen bonding regions, it was found that resonance in the region of the free OD was still observed. This finding indicates that there are oriented $D_2O$ molecules having free OD bonds. The location of these oriented $D_2O$ molecules is not known at this time. We are currently pursuing various possibilities.

In order to determine the effects of having acetonitrile molecules not only competing with water molecules at the top surface layer but in the region below, we extended our studies to include the

long chain insoluble nitrile surfactant, $CH_3(CH_2)17CN$, at the air/$D_2O$ interface. In this case the water molecules beneath the surfactant remained oriented as expected , there being no solution molecules, acetonitrile or others, competing with $D_2O$ molecules in the space immediately below the nitrile surfactant. At surfactant densities in the coexistence region of the surface tension – surfactant density phase diagram the SFG signal from the more highly ordered hydrogen bonding spectral region was significantly decreased whereas in the less strongly hydrogen bonding region the SFG signal did not decrease appreciably relative to the neat air/$D_2O$ interface. We therefore note that in the coexistence region the effect of the nitrile surfactant on the water structure is to diminish the more strongly hydrogen bonding(more highly ordered) $D_2O$ interfacial structures. However very different behavior is observed at a surfactant density of $24(Å)^2$, which exceeds the coexistence to liquid transition density of $27(Å)^2$. At $24(Å)^2$ a very large increase in the SFG signal in the spectral region corresponding to the more strongly hydrogen bonding(more highly ordered) $D_2O$ structures was obtained. The SFG signal in this spectral region greatly exceeds the strength of the SFG for the neat air/$D_2O$ and exceeds that of the less strongly hydrogen bonding region both at both the air/$D_2O$ and the surfactant/$D_2O$ in the coexistence part of the phase diagram. This finding indicates that a significant change in the nitrile surfactant structure has taken place. Two different structural changes are being considered, one of which involves a change in the orientation of the -C≡N group with respect to the surface normal.

**Ions at Aqueous Interfaces**

The well known increase in the surface tension of water observed on addition of NaI to bulk water indicates, using the Gibbs Adsorption Isotherm, that there is a deficiency of NaI at the interface. However it has been concluded that there is a depletion of both $Na^+$ and $I^-$ ions at the interface. The physical explanation has been that charged species would be repelled at the air/water interface based on electrostatic image predictions. Recently computer simulations and spectroscopic measurements indicate that there is a significant population of $I^-$ ions at the interface. This does not contradict the surface tension measurements in that it is the sum of the $Na^+$ and $I^-$ ions that must be depleted. These results have prompted interest in more complex ions at the air/water interface. Measurements in several laboratories have shown that the interfacial population of phenolate ion, $C_6H_5O^-$, which is the simplest aromatic base, is enhanced relative to the bulk phenolate population based on the decrease in surface tension as sodium phenolate is added to bulk water. The difficulty with this conclusion is that it may be the population of the neutral acid form, $C_6H_5OH$, that is responsible for the decrease in surface tension, i.e. the acid-base equilibrium is not the same at the interface as in the bulk solution, and it is the neutral form that is favored. To address this question we have used SFG to differentiate phenol from phenolate at the air/water interface, recognizing that their vibrational spectra are different. In particular the carbon – oxygen bond is the most sensitive vibrational probe of the neutral -C-OH form versus the charged $-C-O^-$ form. In this way we have identified the interfacial spectra of the phenol and phenolate moieties at the interface. We find that even at a bulk pH of 13.2 there is a small but detectable population of the neutral form, i.e. phenol, at the air/water interface. This result indicates that the $pK_a$ of phenol at the interface is significantly higher than its bulk $pK_a$ value of 9.94. This is consistent with our measurements that yielded a $pK_a$ value of 11.7 for a long chain phenol at the air/water interface, while acknowledging the possibility that a free phenol and phenolate that is not constrained by a long chain in both its orientation and depth of location, could have a different interfacial $pK_a$ value. This issue will be resolved when we complete our SFG measurements of the populations of the neutral phenol and charged phenolates, which will be used to calculate the interfacial $pK_a$ value.

**Future Plans**

--Pathways and dynamics of bond breaking and bond formation using SFG of reactive vibration, e.g. simultaneous(single step , concerted) vs sequential bond breaking at liquid interfaces.

-- SFG vibrational spectroscopy of excited state molecules, e.g. $n,\pi^*$ vs. $\pi,\pi^*$ singlet and triplet states at different polarity interfaces

-- Dynamics of barrier crossing at liquid interfaces; coupling of reactive coordinate with the interfacial bath,e.g. unimolecuar photoisomeriztion.monitored by SFG of vibrations sensitive to reactant and product structures.

-- Dynamics of hydrogen atom transfer between donor and acceptor molecules as the sequence of electron transfer followed by proton transfer, e.g. donor amine molecules and excited state aromatic ketones. The carbonyl group is the site of reaction to be monitored by SFG of –C=O vibration.

-- Enhancement of SFG and SHG signals by coupling to noble metal plasmon resonances, e.g. proximity of molecule attached to nanogold and nanosilver particles.

**Publications**

Liu, Jian; Shang, Xiaoming; Pompano, Rebecca; Eisenthal, Kenneth B.. **Antibiotic assisted molecular ion transport across a membrane in real time.** Faraday Discussions (2005), 129 291-299.

Garrett, Bruce C.; Dixon, David A.; Camaioni, Donald M.; Chipman, Daniel M.; Johnson, Mark A.; Jonah, Charles D.; Kimmel, Gregory A.; Miller, John H.; Rescigno, Thomas N.; Rossky, Peter J.; Xantheas, Sotiris S.; Colson, Steven D.; Laufer, Allan H.; Ray, Douglas; Barbara, Paul F.; Bartels, David M.; Becker, Kurt H.; Bowen, Kit H., Jr.; Bradforth, Stephen E.; Carmichael, Ian; Coe, James V.; Corrales, L. Rene; Cowin, James P.; Dupuis, Michel; Eisenthal, Kenneth B.; Franz, James A.; Gutowski, Maciej S.; Jordan, Kenneth D.; Kay, Bruce D.; LaVerne, Jay A.; Lymar, Sergei V.; Madey, Theodore E.; McCurdy, C. William; Meisel, Dan; Mukamel, Shaul; Nilsson, Anders R.; Orlando, Thomas M.; Petrik, Nikolay G.; Pimblott, Simon M.; Rustad, James R.; Schenter, Gregory K.; Singer, Sherwin J.; Tokmakoff, Andrei; Wang, Lai-Sheng; Wittig, Curt; Zwier, Timothy S. **Role of water in electron-initiated processes and radical chemistry: issues and scientific advances.** Chemical Reviews (Washington, DC, United States) (2005), 105(1), 355-389.

Fitts, Jeffrey P.; Shang, Xiaoming; Flynn, George W.; Heinz, Tony F.; Eisenthal, Kenneth B.. **Electrostatic Surface Charge at Aqueous/α -Al2O3 Single-Crystal Interfaces as Probed by Optical Second-Harmonic Generation.** Journal of Physical Chemistry B (2005), 109(16), 7981-7986.

Fitts, Jeffrey P.; Machesky, Michael L.; Wesolowski, David J.; Shang, Xiaoming; Kubicki, James D.; Flynn, George W.; Heinz, Tony F.; Eisenthal, Kenneth B.. **Second-harmonic generation and theoretical studies of protonation at the water/α -TiO2 (110) interface.** Chemical Physics Letters (2005), 411(4-6), 399-403.

Rao, Yi; Comstock, Matthew; Eisenthal, Kenneth B.. **Absolute Orientation of Molecules at Interfaces.** Journal of Physical Chemistry B (2006), 110(4), 1727-1732.

McArthur, Eric A.; Eisenthal, Kenneth B.. **Ultrafast Excited-State Electron Transfer at an Organic Liquid/Aqueous Interface.** Journal of the American Chemical Society (2006), 128(4), 1068-1069Eisenthal, Kenneth B.. **Second harmonic spectroscopy of aqueous nano- and microparticle interfaces.** Chemical Reviews (Washington, DC, United States) (2006), 106(4), 1462-1477

Nguyen, Kim T.; Shang, Xiaoming; Eisenthal, Kenneth B.. **Molecular Rotation at Negatively Charged Surfactant/Aqueous Interfaces.** Journal of Physical Chemistry B (2006), 110(40), 19788-19792

Eisenthal, Kenneth B.. **Laser method to measure the effects of organic and inorganic species on direct and ion channel transport of ions and other species across lipid bilayers and other interface structures.** PCT Int. Appl. (2006), 38pp.

Subir,M.; Liu,J.; Eisenthal,K.B.. **Protonation at the aqueous interface of polymer nanoparticles with second harmonic generation.** Journal of Physical Chemistry B (2008) accepted for publication

Rao,Y.; Song.;D.; Turro,N.; Eisenthal,K.B.. **Orientational motions of vibrational chromophores in molecules at the air/water interface with time resolved sum frequency generation** Journal of Physical Chemistry B (2008) - accepted for publication

# Interfacial Oxidation of Complex Organic Molecules

G. Barney Ellison — (Grant DE-FG02-93ER14364)

We are studying the interfacial oxidation of organic films that coat water droplets. During the last year we have concentrated our efforts on two projects. a) We have finished a study of oxidation dynamics of beams of OH radicals impinging on films of alkanes mounted as self-assembled monolayers.[1] This device produces intense beams of OH radicals which are reactively scattered off hydrocarbon films mounted as self-assembled mononlayers on a gold surface. b) We are continuing to develop a new apparatus to study the oxidation of actual water droplets.[2] This instrument is designed to produce a stream of saline-water droplets that are coated with organics, to size-select them, and to inject them into an atmospheric flow tube where they will be dosed with OH radicals. The resulting oxidized particles will be analyzed with a novel mass spectrometer.

a) We have studied the reactions of OH with an organic film mounted as a self assembled monolayer (SAM) on a gold surface. The aim of this experiment is to understand the elementary steps of the heterogeneous oxidation chemistry surfactant films. We dose simple hydrocarbon films with OH radical beams under conditions where can monitor the interfacial region by infrared (IR) absorption spectroscopy. The hydrocarbon films are mounted as organic thiolate/gold SAMs because these samples are dense, stable structures. Reflection/absorption infrared spectroscopy (RAIRS) is a general technique to monitor the chemical nature of the surface of the SAM. We have used a corona discharge to produce clean beams of OH radicals with a Flux(OH) = $4(\pm 1) \times 10^{11}$

[1] Timothy D'Andrea, Xu Zhang, Evan B. Jochnowitz, Theodore G. Lindeman, C. J. S. M. Simpson, Donald E. David, Thomas J. Curtiss, and G. Barney Ellison, "Oxidation of Hydrocarbon Films by OH Radical Beams", J. Phys. Chem. B., **112**, 535-544 (2008).

[2] Luis A. Cuadra-Rodriguez, Donald E. David, Stephen E. Barlow, Alla Zelenyuk, and G. Barney Ellison, "Mass spectroscopy of saline-water droplets", J. Chem. Phys. (in preparation, 2009).

radicals $cm^{-2}$ $sec^{-1}$. LIF and 2 + 1 REMPI spectroscopy[3] of the OH radicals impinging on the SAM surface find that all are rotationally ($J'' \leq 5/2$) cold but about ¾ of the OH radicals are vibrationally ($v = 0$) relaxed while the other ¼ are in $v = 1$.

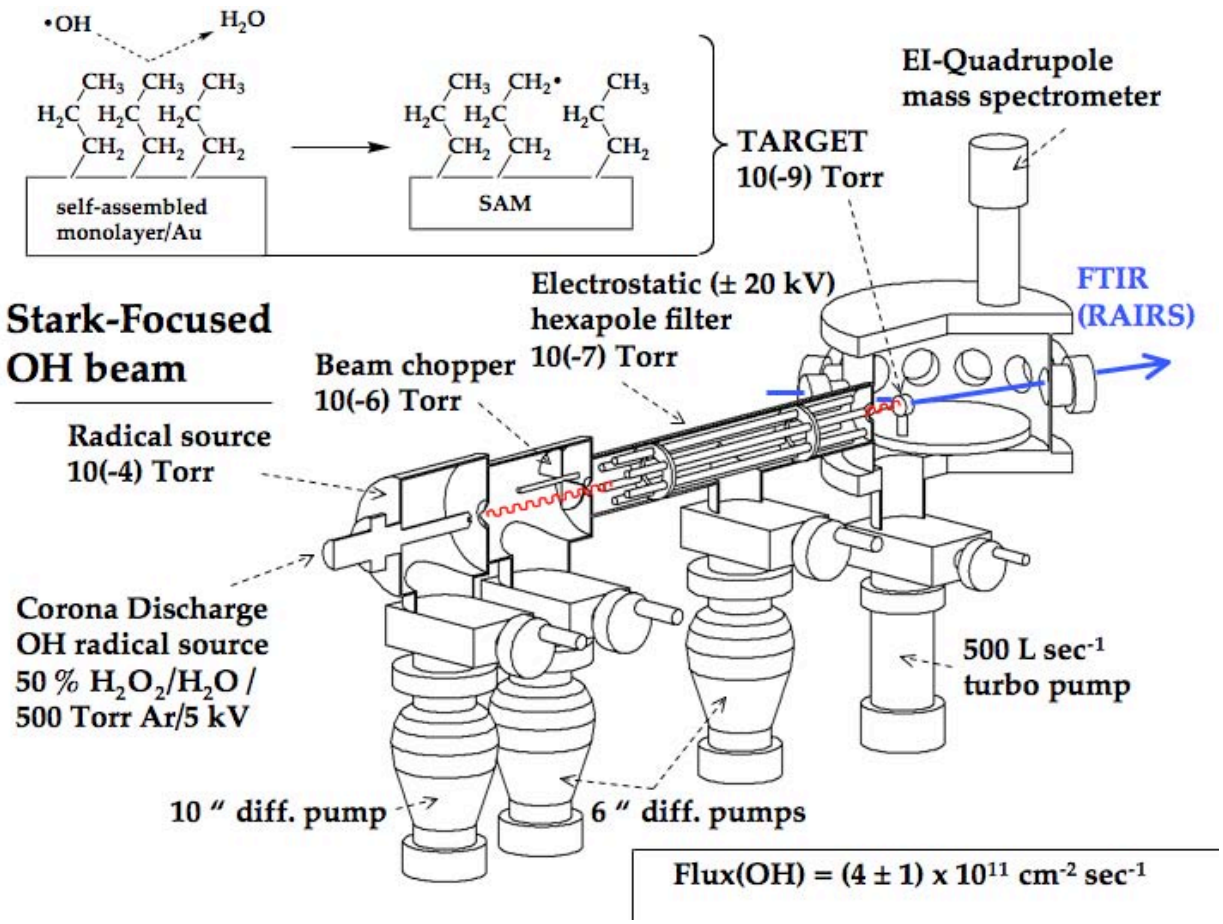


Dosing of the film with OH for 1 min. results in degradation of both $\nu_a(CH_3)$ and $\nu_s(CH_3)$ signals; by 10 min. both signals are largely destroyed while the $CH_2$ signals are still intact. The RAIRS spectra are shown in the Fig. below. During a 10 min. interval the alkyl SAM which is mounted on a 1 $cm^2$ target is dosed with 10 x 60 x (4 x $10^{11}$) or 2 x $10^{14}$ OH radicals. This is roughly 50% of a

[3] A. T. Droege; P. C. Engelking, "Supersonic Expansion Cooling of Electronically Excited OH Radicals", *Chem. Phys. Lett.*, 1983, **96**, 316-318; M. E. Greenslade; M. I. Lester; D. C. Radenovic; A. J. A. van Roij; D. H. Parker, "(2+1) resonance-enhanced ionization spectroscopy of a state-selected beam of OH radicals", *J. Chem. Phys.*, 2005, **123**, 074309.

monolayer. Other studies of the OH radical oxidation of a SAM of an alkene, undec-1-enethiol ($HS(CH_2)_9HC{=}CH_2$)/Au SAM, are reported in ref. 1.

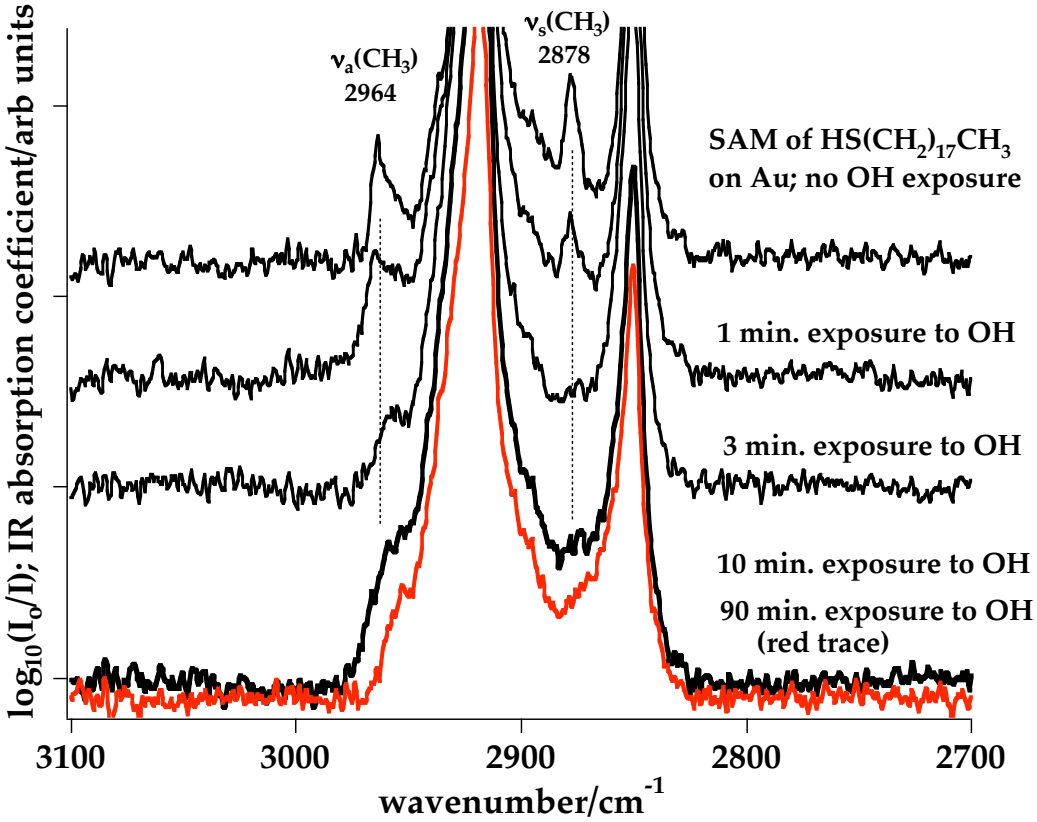


b) We have built is a novel mass spectrometer that can analyze a stream of $\mu$m-sized saline-water droplets that are coated with a film of surfactants.[2] Droplets are entrained in a flow tube in a stream of dry air (20% $O_2$/80% $N_2$) at 1 atm pressure. We plan to oxidize these surfactant-coated droplets with OH/$O_2$ radicals. Micron-sized saline-water droplets are coated with the salt of an organic acid such as SDS or lauric acid, $CH_3(CH_2)_{10}CO_2^-Na^+$.

In collaboration with PNNL's Dr. Alla Zelenyuk, we have used an atomizer to produce a stream of particles that are dried and size-selected with a differential mobility analyzer (DMA). The nucleation dynamics of sodium nitrate droplets has been carefully studied.[4] The DMA was selected to pass particles with $d_{dry}$ = 0.62 nm. The stream of mondisperse particles emerging from the

[4] I. N. Tang, H. R. Munkelwitz, *J Geophys. Res-Atmos* **99**, 18801-18808 (1994); I. N. Tang, A. C. Tridico, and K. H. Fung, *J Geophys. Res-Atmos*, **102**, 23269-23275 (1994).

DMA is re-humidified and the dried $Na^+NO_3^-$/surfactant particles will grow to 1 $\mu$m at 80% relative humidity (RH) because of the measured[4] growth factor of 1.6. Our device generates about $10^4$ droplets $cm^{-3}$. The resulting saline-water droplets are entrained in a stream of air ($V_{stream} \cong 10$ cm $sec^{-1}$) in a flow tube with the RH carefully regulated at 80%.

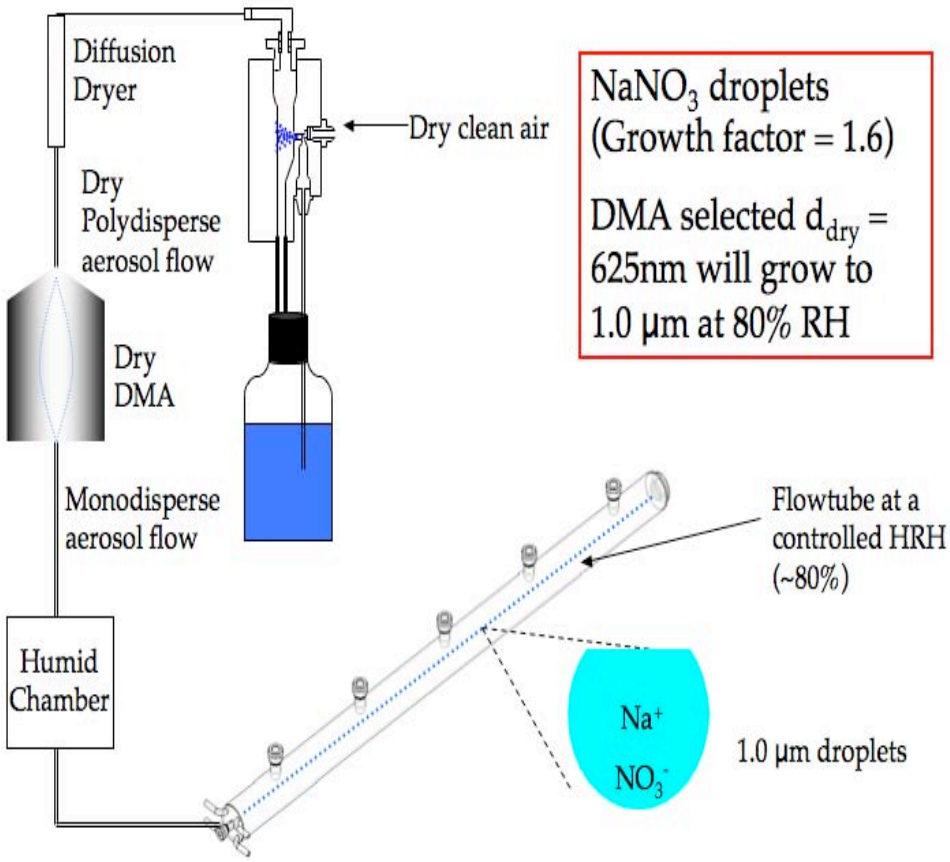


Currently we are experimenting with a vibrating orifice aerosol generator as a simple means to produce size-selected water droplets. My student Luis Cuadra-Rodriguez continues to visit EMSL at the Pacific Northwest National Laboratories where he works in Dr. A. Zelenyuk's laboratory. Some of the results from Cuadra-Rodriguez's visits to PNNL are described[5] [6] by two papers; other results were reported[7] [8] [9] [10] at several national meetings.

---

[5] Alla Zelenyuk, Dan Imre, and Luis A. Cuadra-Rodriguez, "Evaporation of Water from Particles in the Aerodynamic Lens Inlet: An Experimental Study",

Anal. Chem. **78**, 6942-6947 (2006).

[6] Alla Zelenyuk, Dan Imre, Luis A. Cuadra-Rodriguez, and Barney Ellison, "Measurements and interpretation of the effect of a soluble organic surfactant on the density, shape and water uptake of hygroscopic particles", *J. Aerosol Sci.*, **38**, 903-923 (2007).

[7] Cuadra-Rodriguez, L. A., Zelenyuk, A., Imre, D., and Ellison B. (2006). The Effect Of Organic Surfactants On The Properties Of Common Hygroscopic Particles: Effective Densities, Reactivity And Water Evaporation Of Surfactant Coated Particles, Eos Trans. AGU, 87(52), Fall Meet. Suppl., Abstract A33A-0951.

[8] Zelenyuk, A., L. Cuadra-Rodriguez, D. Imre, S. Shimpi, and A. Warey. Comprehensive Characterization of Ultrafine Particulate Emission From 2007 Diesel Engines: PM Size Distribution, Loading And Individual Particle Size And Composition. Eos Trans. AGU, 87(52), Fall Meet. Suppl., Abstract A43A-0121.

[9] Zelenyuk, A., D. Imre, L. Cuadra-Rodriguez, S. Shimpi, A. Warey. The Size And Composition Of Individual Ultrafine Diesel Emission Particulate From 2007 Diesel Engines With And Without After treatment. The 12th Annual Diesel Engine Emission Reduction (DEER) Conference, Detroit, MI, August 2006.

[10] Zelenyuk, A., Imre, D., Cuadra-Rodriguez, L. A., and Ellison B. Measurements and Interpretation of the Effect of Soluble Organic Surfactants on the Density, Shape and Water Uptake of Hygroscopic Particles. The 26th Annual American Association for Aerosol Research (AAAR) Conference, September 24-28, 2007, Reno, NV.

**Title:** The Proton Pump of Bacteriorhodopsin, the other Photosynthetic System.

**P.I.** : M. A. El-Sayed, School of chemistry and Biochemistry.Georgia Institute of Technology 770 State Street, Atlanta Georgia 30332-0400. **: :melsayed@gatech.edu**

**Report: Gold Nanoparticls Plasmonic Field Effects on the Primary Step in the Photosynthesis of Bacteriorhodopsin**

The aim of our research is to examine the coupling and the effect of gold nanoparticles on the functions of important biological systems such as Baceriorhodopsin. So much of our efforts was directed towards the study of the binding of these nanoparticles to different cells and understanding their photo-thermal and plasmonic field effects on Biological Functions.The binding of gold nanoparticles to bacterio-rhodopsin membrane patches proved to be very difficult and took great amout of time. We had to learn and develop different conjugation metods to different kinds of cells.Finally we were able to bind them to bR membrane to study :

**Gold Nanoparticles Plasmonic Field Effects on the Primary Step in the Photosynthesis of Bacteriorhodopsin**.

Gold nanoparticles have three important properties: 1)they absorp and scatter light strongly used in sensing , imaging and diagnostics; 2) the absorped light is rapidly converted into heat which is useful in many photo-thermal applications, and 3) when their localized surface plasmon oscillations are excited, the induced surface plasmon fields decay with distance which is used as a nanometer ruler in biological systems and can affect many processes, This is what our group has recently been developping. The present report describes the results of some experiments that suggest that plasmonic fields of gold nanorods slow down the rate of retinal photo-isomerizaion, the primary step in the photo synthesis fubction of Bacterio-rhodopsin (bR).

We have reported last year preliminary results*[1]* suggesting the observation of plasmonic field effects on the photo-isomerisation rate of retinal in bR. Since then we have carried out a series of different femtosecond time resolved transient absorption experiments on aqueous solution of bR mixed with gold nanorods.The aim of these experiments is to systematically investigate the effect of the localized surface plasmon (LSP) field generated by optical excitation of gold nanorods on subpicosecond photoisomerization processes of the retinal chromophore in bR. The transient absorption life time determination experiement, the kinetic traces were recorded with pump laser wavelength at 560 nm and probed at 490 nm, which are in the resonance with the absorption maximum of bR in the ground and in the $I_{460}$ excited state of its retinal, respectively. The retinal photo-isomerisatiom decay was determed in the presence and in the absence of of the plasmonic field induced by exciting the longtitudinal LSR with our 800 nm femtosecond pulses. The experimental results below clearly demonstrate the apparent effect of LSP field on the decay of the ultrafast retinal photoisomerization processes (A). In (B) the results show the dependence of photoisomerization decay on the pump fluence of the femtosecond laser with wavelength centered at 800 nm for exciting LSP. In (C), the results show the dependence of photoisomerization decay on the Au nanorod concentration. It is obvious that as we increase either the pump fluence or the Au nanorod concentration, the photoisomerization lifetime increases. The results in(D) convincingly show that the effect can only be observed under resonance situation, i.e. when the wavelength of excitation laser coincides with the absorption maximum of the longitudinal surface plasmon mode

of Au nanorod. In order to do this experiment, three nanorods having different longitudinal absorption maxima( i.e. have different aspect ratios) are used. Only the nanorod whose surface plasmon field can be induced,( i.e. the one whose absorption coincides with our 800 nm laser wavelength) showed the effect.

The model explaining the ultrafast photoisomerization dynamics in retinal has evolved from one dimensional barrierless two state model*[2]* to three state model*[3, 4]* and to currently two dimensional model for accommodating conical intersection*[5, 6]*. For the retinal in the bR, two factors determine the ultrafast isomerization processes *[3, 5-8]*(REF). One is the conical intersection connecting excited state potential energy surface of all-trans and ground state potential energy surface of 13-cis state*[5, 6]*. The slope of the potential energy surface in the vicinity of the conical intersection determines the speed and efficiency of internal conversion from all-trans to the 13-cis*[5, 6]*. The other*[3, 7, 8]* is that the rigid protein structure immobilized the retinal which provides a unique environment for the ultrafast photoisomerization of retinal through selectively exciting asymmetric vibrational mode along the reaction coordinate, which induces fast wavepacket motion through the conical intersection. It is well known that the rates of photoisomerisation of retinals in solution is much slower.. Therefore, the rigid protein structure provides an optimized catalytic environment for the ultrafast isomerization of retinal. Both the property of conical intersection and the immobilization of retinal by protein structure depend on the electrostatic interactions between positive charged protonated Schiff base and the negative charged amino acid side chains*[9]*. One should also realize that in the excited state retinal has a very large dipole moment. Thus, the observed change in the photoisomerization lifetime by the field could be due to the perturbation of the electrostatic interaction within retinal binding pocket by intense plasmonic field generated by gold nanorods. This perturbation could affect the charge distribution around the retinal slightly and the geometry of the conical intersection. Both could cause the change of the photoisomerization rate.

The reason why the rapidly oscillating electric field of localized surface plasmon at optical frequencies can have net effect on the electrostatic interactions could result from nonlinear optical rectification. Optical rectification is a second order nonlinear difference frequency mixing. DC generation via optical rectification has been observed as early as 1960s*[10, 11]* by passing intense laser beam through crystals. For ultrashort laser pulses that have large bandwidth, the generated frequency components via optical rectification has bandwidth from 0 to several THz*[12]*. These very low frequency electromagnetic waves could interact and disturb intra-protein electrostatic interaction and thus induce the observed change in the photoisomerization processes. The observed dependence of the effect on the laser fluence (Fig 1B) could support this proposal.

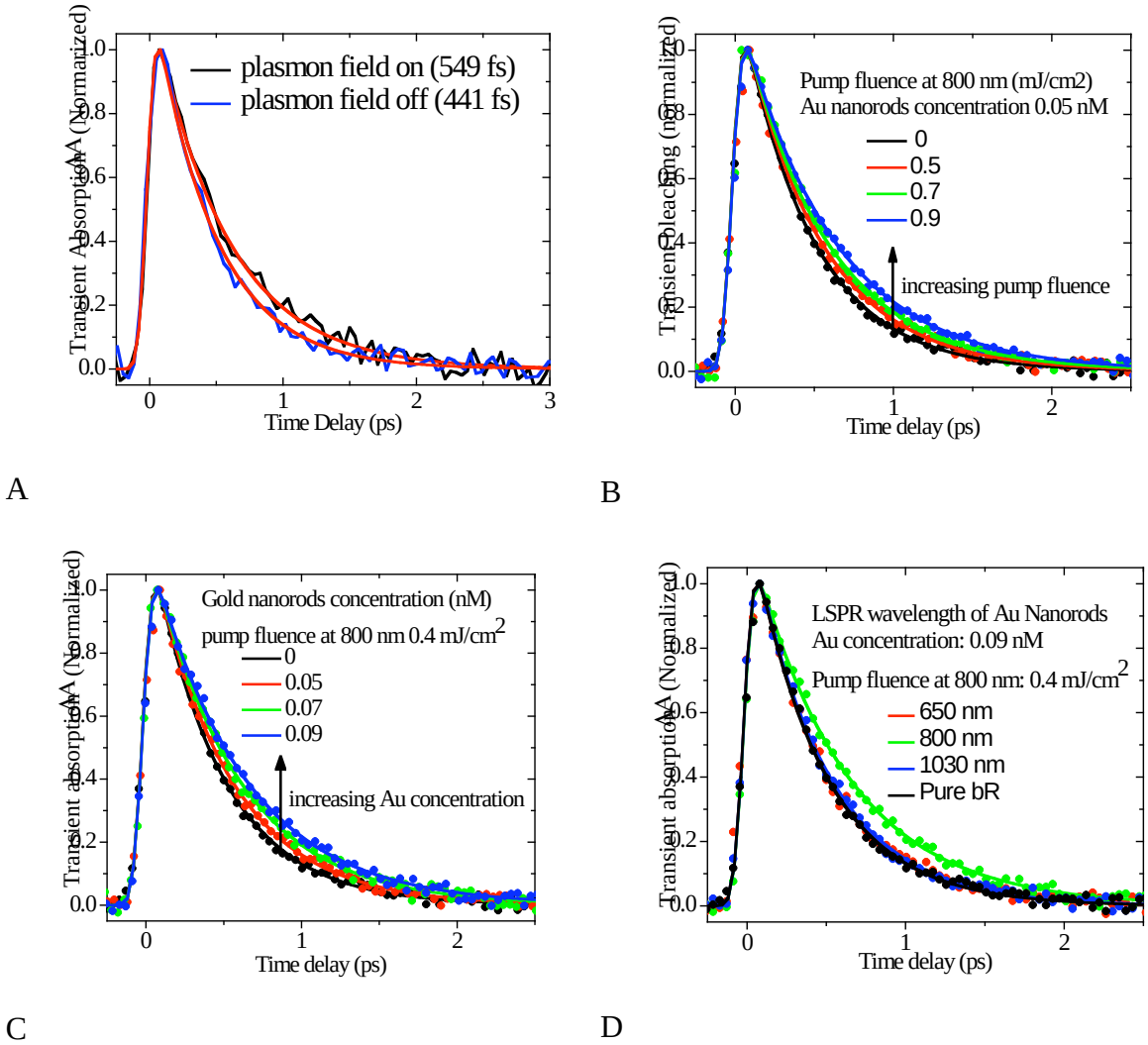


Figure 1. The effect of localized surface plasmon field generated by optical excitation of gold nanorods on photoisomerization of retinal chromophore in Bacteriorhodopsin. In the femtosecond transient absorption experiement, the aqueous solution of bR mixed with gold nanorods are pumped at 560 nm and probed at 490 nm, which are in the resonance with the absorption maxima of bR ground and $I_{460}$ intermediate state, respectively. (A) shows that in the presence of femtosecond laser with wavelength centered at 800 nm for exciting localized surface plasmon (LSP) field of gold nanorods (maximum absorption of longitudinal mode at 800 nm) with pump fluence of 0.4 mJ/cm$^2$, the lifetime of photoisomerization of retinal is elongated from original 441 fs without exciting LSP field to 549 fs.(Ref to our comm. In JACS) (B) demonstrates the dependence of the photoisomerization lifetime on pump fluence of the femtosecond laser exciting LSP field without change in the concentration of gold nanorods. It is obvious that as pump fluence increases, the photoisomerization lifetime becomes longer. (C) illustrates the dependence of the photoisomerization lifetime on gold nanorod concentration under the same pump fluence. It is also apparent that the lifetime increases by increasing the gold nanorod concentration. (D) explains how does the plasmonic field effect depend on localized longitudinal surface plasmon mode of gold nanorods. by changing the aspect ratio of rod, the longitudinal surface plasmon mode could be tuned. Here, it is very clear that the plasmonic field effect could only be observed when using

nanorods whose LSR can be excited with the femtosecond laser we use (i.e. at a wavelength of 800 nm).

[1] A. Biesso, W. Qian, M. A. El-Sayed, *Journal of the American Chemical Society* **2008**, *130*, 3258.
[2] R. A. Mathies, C. H. B. Cruz, W. T. Pollard, C. V. Shank, *Science* **1988**, *240*, 777.
[3] K. C. Hasson, F. Gai, P. A. Anfinrud, *Proceedings of the National Academy of Sciences of the United States of America* **1996**, *93*, 15124.
[4] T. Kobayashi, T. Saito, H. Ohtani, *Nature* **2001**, *414*, 531.
[5] S. Hahn, G. Stock, *Journal of Physical Chemistry B* **2000**, *104*, 1146.
[6] B. G. Levine, T. J. Martinez, *Annual Review of Physical Chemistry* **2007**, *58*, 613.
[7] J. T. M. Kennis, D. S. Larsen, K. Ohta, M. T. Facciotti, R. M. Glaeser, G. R. Fleming, *Journal of Physical Chemistry B* **2002**, *106*, 6067.
[8] H. Chosrowjan, N. Mataga, Y. Shibata, Y. Imamoto, F. Tokunaga, *Journal of Physical Chemistry B* **1998**, *102*, 7695.
[9] L. Song, M. A. Elsayed, J. K. Lanyi, *Science* **1993**, *261*, 891.
[10] M. Bass, P. A. Franken, J. F. Ward, *Physical Review* **1965**, *138*, A534.
[11] M. Bass, J. F. Ward, G. Weinreich, P. A. Franken, *Physical Review Letters* **1962**, *9*, 446.
[12] A. Nahata, A. S. Weling, T. F. Heinz, *Applied Physics Letters* **1996**, *69*, 2321.

**Plans for the comming year:** We plan to extend the study of the effect of the plasmon fields on the other steps of the Bacterio-Rhodopsin photo-cycle as well as studies of the binding of gold nanoparticles to the cells of different kinds of biological cells.

**References of published work since 2005:**

1. Dickerson, Erin B.; Dreaden, Erik C.; Huang, Xiaohua; El-Sayed, Ivan H.; Chu, Hunghao; Pushpanketh, Sujatha; McDonald, John F.; El-Sayed, Mostafa A.. Gold nanorod assisted near-infrared plasmonic photothermal therapy (PPTT) of squamous cell carcinoma in mice. Cancer Letters (Shannon, Ireland) (2008), 269(1), 57-66.
2. Jain, Prashant K.; Huang, Xiaohua; El-Sayed, Ivan H.; El-Sayed, Mostafa A.. Noble Metals on the Nanoscale: Optical and Photothermal Properties and Some Applications in Imaging, Sensing, Biology, and Medicine. Accounts of Chemical Research ACS ASAP.
3. Biesso, Arianna; Qian, Wei; El-Sayed, Mostafa A.. Gold Nanoparticle Plasmonic Field Effect on the Primary Step of the Other Photosynthetic System in Nature, Bacteriorhodopsin. Journal of the American Chemical Society (2008), 130(11), 3258-3259.
4. Jain, Prashant K.; Huang, Xiaohua; El-Sayed, Ivan H.; El-Sayed, Mostafa A.. Review of some interesting surface plasmon resonance-enhanced properties of noble metal nanoparticles and their applications to biosystems. Plasmonics (2007), 2(3), 107-118.
5. Huang, Xiaohua; El-Sayed, Ivan H.; Qian, Wei; El-Sayed, Mostafa A.. Cancer Cells Assemble and Align Gold Nanorods Conjugated to Antibodies to Produce Highly Enhanced, Sharp, and Polarized Surface Raman Spectra: A Potential Cancer Diagnostic Marker. Nano Letters (2007), 7(6), 1591-1597.
6. Sanii, Laurie S.; El-Sayed, Mostafa A.. Partial dehydration of the retinal binding pocket and proof for photochemical deprotonation of the retinal Schiff base in bicelle bacteriorhodopsin crystals. Photochemistry and Photobiology (2005), 81(Nov./Dec.), 1356-1360.
7. Sanii, Laurie S.; Schill, Alex W.; Moran, Cristin E.; El-Sayed, Mostafa A.. The protonation-deprotonation kinetics of the protonated Schiff base in bicelle bacteriorhodopsin crystals. Biophysical Journal (2005), 89(1), 444-451.
8. El-Sayed, Ivan H.; Huang, Xiaohua; El-Sayed, Mostafa A.. Surface plasmon resonance scattering and absorption of anti-EGFR antibody conjugated gold nanoparticles in cancer diagnostics: Applications in oral cancer. Nano Letters (2005), 5(5), 829-834

# Statistical Mechanical and Multiscale Modeling of Surface Reaction Processes

Jim Evans (PI) and Da-Jiang Liu
Ames Laboratory – USDOE and Department of Mathematics,
Iowa State University, Ames, IA 50011
evans@ameslab.gov

## PROGRAM SCOPE:

A major component of the Chemical Physics Program at Ames Laboratory focuses on the modeling of **heterogeneous catalysis and other complex reaction phenomena** at surfaces. This effort integrates ***electronic structure analysis, non-equilibrium statistical mechanics, and multi-scale modeling***. The *electronic structure* component includes DFT-VASP analysis of chemisorption and reaction energetics on metal surfaces, as well as application of QM/MM methods in collaboration with **Mark S. Gordon (PI)** to treat adsorption and reaction phenomena on semiconductor and oxide surfaces. The *non-equilibrium statistical mechanics and multi-scale modeling studies* of surface phenomena include Kinetic Monte Carlo (KMC) simulation of atomistic models, coarse-grained, and heterogeneous multiscale formulations. One aspect of this effort relates to heterogeneous catalysis on metal surfaces, where we consider both reactions on extended single crystal surfaces (including connecting atomistic to mesoscale behavior) as well as nanoscale catalyst systems (exploring the role of fluctuations). Another aspect focuses on reaction processes on semiconductor surfaces and in mesoporous oxides. In addition, we are exploring cooperative behavior in general statistical mechanical models for chemical reactions which exhibit non-equilibrium phase transitions and critical phenomena.

## RECENT PROGRESS:

CHEMISORPTION AND HETEROGENEOUS CATALYSIS ON METAL SURFACES

**(i) Interaction of sulfur with metal surfaces**. Metal catalysts are often sensitive to sulfur (S) poisoning. In addition, sulfide formation can occur potentially either reducing or enhancing catalytic activity. We have analyzed the interaction of S with the Ag(111) surface [17]. STM studies by our experimental collaborators reveal a novel self-organized "dot-row" structure below 300K. DFT analysis indicates that the "dots" are $Ag_3S_3$ clusters or complexes in the form of triangular $Ag_3$ trimers decorated by three S on the outer (100) microfacets. These decorated trimers might be viewed as incorporating three linear $AgS_2$ clusters, and their stability seems to derive from that of the $AgS_2$ cluster on the Ag(111) surface. Formation of stable Ag-S complexes is also a key ingredient in greatly enhanced metal mass-transport which we observe on Ag(111) surfaces exposed to S. Indeed, motivation for this study derives in part from the observation that formation of metal-chalcogen complexes could promote sintering of metal nanoclusters.

**(ii) Guided self-assembly of metal nanostructures on surfaces: quantum size effects**. A fundamental and general goal in catalysis is to tune the structure of metal surfaces or nanostructures to enhance catalytic activity and selectivity. One strategy is to exploit "quantum size effects (QSE)" of electrons confined in metal overlayers. QSE can lead to selection of preferred film heights and also a strong dependence of surface electronic properties on film thickness. We have explored QSE in the Ag/NiAl(110) system which is ideally suited to high-level modeling: a perfect lattice-match between Ag(110) and NiAl(110) facilitates formation of lateral strain-free Ag(110) films with a simple film-interface structure. DFT analysis [15,18]

elucidates the initial bilayer-by-bilayer growth model observed in STM studies of film growth for a broad range of temperatures (130-300 K), even film heights being preferred due to QSE.

**(iii) Multi-site lattice-gas modeling of reactions on metal(100) surfaces**. A basic goal for theoretical surface science since the early 1980's has been to develop realistic atomistic models for "complete" catalytic reaction processes on metal surfaces (rather than just treating adsorption or desorption or ordering of individual reactants). We have continued [19] development of realistic multi-site lattice-gas models and efficient KMC simulation algorithms to describe CO-oxidation on unreconstructed metal(100) surfaces [7,9-11,14,19]. We emphasize that the incorporation of multiple adsorption sites with distinct binding for CO is key to realistically describing the relevant "reaction configurations" for $CO_2$ production in mixed reactant adlayers. Recent work has focused on modeling Temperature Programmed Reaction (TPR) spectra for Pd(100) and Rh(100) surfaces where different site preferences for CO result in different configurations contributing to $CO_2$ production [19]. Success of these models also requires incorporating accurate adspecies interactions which control ordering in the mixed adlayer (selection of interactions is guided by DFT, but refined to describe key experimental observations for constituent single-adspecies systems); rapid surface mobility of CO and lower mobility of O; and a realistic description of adsorption-desorption and LH reaction kinetics.

## FUNDAMENTAL PHENOMENA IN FAR-FROM-EQUILIBRIUM REACTION SYSTEMS

Our general statistical mechanical studies of non-linear reaction systems focus on non-equilibrium phase transitions and associated metastability and critical phenomena. The goal is to develop understanding of these phenomena to a level comparable to that for equilibrium systems. Such problems are targeted in the ***BESAC Science Grand Challenges*** report under the heading ***Cardinal Principles of Behavior beyond Equilibrium,*** and require advancing from traditional mean-field kinetics models of reactions to atomistic statistical mechanical modeling.

We have thus analyzed a statistical mechanical version of Schloegl's second model for autocatalysis (aka the quadratic contact process) and various generalizations of this model [12,13,16]. These models display a discontinuous non-equilibrium transition between reactive and unreactive (extinct or poisoned) states. Metastability occurs upon sweeping through this transition akin to equilibrium systems. However, in dramatic contrast to equilibrium systems, we find a remarkable "generic two-phase coexistence" (i.e., both reactive and extinct states are stable) for a finite range of control parameter! We have explained this feature in terms of dependence of equistability on the orientation of the interface between the coexisting phases.

Recent work for various generalizations of Schloegl's model has focused on elucidating: generic two-phase stability by analyzing the disappearance of droplets of one phase embedded in the other; propagation of interfaces between reactive and unreactive phases; poisoning kinetics in the metastable regime quantifying the nucleation of unreactive droplets within the reactive phase; and development of approximate analytic tools to elucidate these various phenomena [16].

## REACTION AND SELF-ASSEMBLY PROCESSES IN OTHER COMPLEX SYSTEMS

*Morphological evolution during etching and growth on stepped surfaces.* Exposure of vicinal Si(100) to oxygen at ~600° C produces step recession due to etching [Si + O(ads) $\rightarrow$ SiO(gas) + vacancy] in competition with surface oxide formation [Si + 2O(ads) $\rightarrow$ $SiO_2$]. Oxide islands mask etching of the underlying Si and pin receding steps [3,5]. Based on new STM data, we have refined our previous atomistic model to include a more realistic treatment of oxide island nucleation (for which QM/MM analysis can determine the energetics). Work continues on

coarse-graining of the atomistic model to obtain reliable and efficient step-dynamics and phase-field models for evolution of surface morphologies coupled with appropriate reaction kinetics.

*Self-organization during deposition.* We continue analysis of the formation of single-atom thick atomic rows or "wires" during deposition of Group III metals on Si(100) [4,8] both using Gordon's QM/MM analysis of adatom binding and diffusion, and via KMC simulation of atomistic lattice-gas models accounting for recently quantified reversibility in row formation.

## FUTURE PLANS:

CHEMISORPTION AND HETEROGENEOUS CATALYSIS ON METAL SURFACES

**(i) CO-oxidation and NO-reduction reactions on Rh, Pd,… surfaces**. We will develop further realistic atomistic models for KMC simulation of catalytic reactions on various metal (111) and (100) surfaces. Such models can elucidate reaction behavior in nanoscale systems (e.g., FET's and supported clusters) [10,11]. New efforts will explore higher-pressure catalysis and associated oxide formation processes. Our models will incorporate input from electronic structure studies.

**(ii) Heterogeneous Coupled Lattice-Gas (HCLG) multiscale modeling of surface reactions**. Our HCLG approach [1] uses continuous-time parallel KMC simulation to provide a realistic atomistic-level description of the reaction process at distinct macroscopic points distributed across a surface. Suitably coupling these simulations accounting for the chemical diffusion fluxes of mobile reactants, we can describe mesoscale reaction-diffusion behavior. Some heterogeneous multiscale simulation methods take large time-steps tracking just macro-variables (coverages). This requires assuming local equilibrium so that micro-states can be regenerated from macro-variables ("lifting"). Local equilibrium is often not satisfied in reaction systems, so we are developing more sophisticated "lifting" procedures accounting for local correlations.

**(iii) Chemisorbed adlayer structure and dynamics and the role of steps in reactions.** We plan to explore ordering and dynamics in chemisorbed layers on metal surfaces probed by in-situ STM: the dynamics of CO clusters in CO + H on Pd (Salmeron - LBL), and interaction of chalcogens with coinage metals (Thiel - Ames Lab). We will also explore the role of steps in reactions involving NO dissociation. We plan to develop models which couple reaction kinetics to step dynamics, allowing description of behavior observed with in-situ LEEM (Imbihl).

FUNDAMENTAL PHENOMENA IN FAR-FROM-EQUILIBRIUM REACTION SYSTEMS

Analysis will continue of non-equilibrium phase transitions in a variety of statistical mechanical reaction models. Issues of metastability and nucleation, and well as critical phenomena, are of fundamental interest for these non-equilibrium systems where the standard thermodynamic framework (e.g., involving a free energy) cannot be applied. The ramifications of anomalous behavior such as "generic two-phase coexistence" will be explored. We are extending these analyses to various ZGB-type surface reaction models, which although too simplistic to describe standard low-pressure reaction behavior, may provide a valuable paradigm for higher-pressure low-surface-mobility fluctuation-dominated reaction systems.

REACTION AND SELF-ASSEMBLY PROCESSES IN OTHER COMPLEX SYSTEMS

Our modeling of etching, oxidation, and other *reactions on stepped Si(100)* will focus on development of coarse-grained phase-field type formulations describing evolution of surface morphology. This approach is versatile, allowing efficient integration of various models for the surface chemistry with a computationally efficient framework to describe complex surface morphologies. DFT and QM/MM will be utilized to provide reliable energetic input. Additional investigations related to *catalysis in mesoporous systems* will explore both the catalyst formation

process (e.g., template-driven growth), and well as the kinetics of specific reactions. For the latter, we will continue to analyze stochastic atomistic models for polymerization kinetics. We aim to describe entropic and other driving forces for extrusion, and the control of reactant input via "gatekeepers" at the pore openings which induce diffusion offsets for different reactants.

**PUBLICATIONS SUPPORTED BY USDOE FOR 2005-PRESENT**: (*partial SciDAC support)


**[1]** *Connecting-the-Length-Scales from Atomistic Ordering to Mesoscale Spatial Patterns in Surface Reactions: HCLG Algorithm*, D.-J. Liu, J.W. Evans, SIAM Multiscale Modeling **4**, 424-446 (2005)*

**[2]** *Kinetic Monte Carlo Simulation of Non-Equilibrium Lattice-Gas Models… Surface Adsorption Processes*, J.W. Evans, Handbook Materials Modeling A, S. Yip, Ed. (Springer, Berlin, 2005), Ch.5.12.*

**[3]** *Competitive Etching and Oxidation of Vicinal Si(100) Surfaces*, M.A. Albao, D.-J. Liu, C.H. Choi, M.S. Gordon, J.W. Evans, MRS Proc. **859E**, JJ3.6 (2005).*

**[4]** *Monotonically Decreasing Size Distributions for One-Dimensional Ga Rows on Si(100)*, M.A. Albao, M.M.R Evans, J. Nogami, D. Zorn, M.S. Gordon, J.W. Evans, Phys. Rev. B **71**, 071523 (2005).*

**[5]** *Simultaneous Etching and Oxidation of Vicinal Si(100) Surfaces: …Modeling of Morphological Evolution*, M.A. Albao, D.-J. Liu, M.S. Gordon, J.W. Evans, Phys. Rev. B. **72**, 195420 (2005).

**[6]** *Morphological Evolution during Epitaxial Thin Film Growth: Formation of 2D Islands and 3D Mounds*, J.W. Evans, P.A. Thiel, M.C. Bartelt, Surface Science Reports, **61**, 1-128 (2006).

**[7]** *Atomistic Lattice-Gas Modeling of CO-oxidation on Pd(100): Temperature-Programmed Spectroscopy & Steady-State Behavior*, D.-J. Liu, J.W. Evans, J. Chem. Phys. **124**, 154705 (2006).

**[8]** *Reply to Comment: Monotonically Decreasing Size Distributions for Ga Rows on Si(100)*, M.A. Albao, M. Evans, J. Nogami, D. Zorn, M.S. Gordon, J.W. Evans, Phys. Rev. B **74**, 037402 (2006).*

**[9]** *Chemical Diffusion in Mixed CO+O Adlayers and Reaction Front Propagation in CO-oxidation on Pd(100)*, D.-J. Liu, J.W. Evans, J. Chem. Phys. **125**, 054709 (2006).*

**[10]** *Fronts and Fluctuations in a Tailored Model for CO-oxidation on Unreconstructed Metal(100) Surfaces*, D.-J. Liu, J.W. Evans, J. Phys.: Cond. Matt., **19**, 065129 (2007).

**[11]** *Fluctuations and Patterns in Nanoscale Surface Reaction Systems: Influence of Reactant Phase Separation during CO-oxidation*, D.-J. Liu, J.W. Evans, Phys. Rev. B **75**, 073401 (2007).*

**[12]** *Quadratic Contact Process (Schoegl's Model for Autocatalysis): Phase Separation with Interface-Orientation-Dependent Equistability*, D.-J. Liu, X. Guo, J.W. Evans, Phys. Rev. Lett., **98**, 050601 (2007).

**[13]** *Generic Two-Phase Coexistence, Relaxation, Kinetics, and Interface Propagation in the Quadratic Contact Process*: *Simulation Studies*, X. Guo, D.-J. Liu, J.W. Evans, Phys. Rev. E., **75**, 061129 (2007).

**[14]** *CO-oxidation on Rh(100): Multi-site LG Modeling*, D.-J. Liu, J. Phys. Chem. C **111**, 14698 (2007).

**[15]** *Scanning Tunneling Microscopy and Density Functional Theory Study of Initial Bilayer Growth of Ag Films on NiAl(110)*, B. Unal, F. Qin, Y. Han, D.-J. Liu, et al., Phys. Rev. B, **76**, 195410 (2007).

**[16]** *Generic Two-Phase Coexistence, Relaxation, Kinetics, and Interface Propagation in the Quadratic Contact Process*: *Analytic Studies*, X. Guo, J.W. Evans, D.-J. Liu, Physica A, **387**, 177-201 (2008).

**[17]** *Novel Self-Organized Structure of a Ag-S Complex on the Ag(111) Surface below Room Temperature*, M. Shen, D.-J. Liu, C.J. Jenks, P.A. Thiel, J. Phys. Chem. C **112**, 4281-4290 (2008).

**[18]** *Quantum Stabilities and Growth Modes of Thin Metal Films: Unsupported and NiAl-supported Ag Films*, Y. Han, J.W. Evans, D.-J. Liu, Surface Science, **602**, 2532-2540 (2008).

**[19]** *Atomistic and multiscale modeling of CO-oxidation on Pd(100) and Rh(100): From nanoscale fluctuations to mesoscale reaction fronts*, D.-J. Liu, J.W. Evans, Surf. Sci. (Ertl Issue), in press (2008).

**Liquid and Chemical Dynamics in Nanoscopic Environments (DE-FG03-84ER13251)**

Michael D. Fayer
Department of Chemistry, Stanford University, Stanford, CA 94305
fayer@stanford.edu

The research group of Michael D. Fayer is investigating topics directed toward understanding how nanoscopic size, interfaces, and nanoconfinement influence the dynamics of water and processes that occur in nanoconfined water, for example, proton transport dynamics. The research is focused on nanoscopic water and water at interfaces because of water's importance in a wide range of chemical, materials, biological processes and technological devices relevant to energy applications. In many systems, water is not found in its bulk form. Our recent work was the first to use ultrafast infrared methods to directly examine the dynamics of nanoscopic water, that is, water confine on a length scale of a few nanometers.[1-4]

Water can make up to four hydrogen bonds and forms an extended hydrogen bonding network. The network structure is constantly undergoing changes on timescales ranging from tens of femtoseconds to picoseconds.[11,12] Water's ability to reorganize its hydrogen bonding network and thereby solvate charges and other chemical species gives it its unique importance. When water is confined on nanoscopic distance scales, its hydrogen bond network dynamics change, and these changes influence processes, such as proton transport, that occur in nanoscopic water. To understand the role of nanoconfinement and interfaces on the dynamics and properties of water, a variety of materials are being investigated. These include ionic and non-ionic reverse micelles,[1-6,18] Nafion a polyelectrolyte fuel cell membrane,[7-8] phospholipid multibilayer,[9] lamellar structures, and concentrated salt solutions.[6,10,13] The research addresses how such physical constraints on systems influence chemical and physical processes. Proton transport is an important focus[15,16,19-21] particularly in fuel cell membranes.[17,18] Photoinduced electron transfer has also been investigated.[22-24]

The experimental methods that are being employed are able to focus directly on the dynamics of water and proton (hydronium ion) dynamics. The IR experiments include ultrafast 2D-IR vibrational echo spectroscopy and polarization selective IR pump-probe experiments. These experiments make measurements on the hydroxyl stretching mode of water. The 2D-IR vibrational echo experiments measure spectral diffusion through the time dependence of the 2D-IR lineshapes. Spectral diffusion measures the time evolution of the hydroxyl stretch frequencies that evolve as the hydrogen bond network structure changes with time. The polarization selective pump-probe experiments measure the orientational relaxation of water and the vibrational population relaxation.[14] The orientational relaxation provides information on the concerted rearrangement of hydrogen bonds, and the population relaxation provides information on different local water environments. UV/Vis experiments including ultrafast pump – broadband probe transient absorption and stimulated emission spectroscopy, and time dependent fluorescence using time correlated single photon counting, are used to study proton dynamics. In these experiments, a photoacid is electronically excited and injects a proton into the systems. Proton transfer, solvation, solvent separation of contact ion pairs, and proton transport are then followed by the associated spectroscopic changes.

Because of lack of space, only a few highlights will be given of recent results. Many interfaces involve ionic group. To understand the influence of ions on water dynamics, we have begun studies of water in salt solutions. Hydrogen bond dynamics of water in NaBr solutions were studied using ultrafast two-dimensional infrared (2D-IR) vibrational echo spectroscopy and polarization-selective infrared (IR) pump-probe experiments.[6,10,13] The hydrogen bond structural dynamics are observed by measuring spectral diffusion of the OD stretching mode of dilute HOD in $H_2O$ in a series of high concentration aqueous NaBr solutions with 2D-IR vibrational echo spectroscopy. The time evolution of the 2D-IR spectra yields the frequency-frequency

correlation functions, which permits quantitative comparisons of the influence of NaBr concentration on the hydrogen bond dynamics. The results show that the global rearrangement of the hydrogen bond structure, which is represented by the slowest component of the spectral diffusion, slows, and its time constant increases from 1.7 ps to 4.8 ps as the NaBr concentration increases from pure water to ~6 M NaBr. Orientational relaxation is analyzed with a wobbling-in-a-cone model describing restricted orientational diffusion that is followed by complete orientational randomization described as jump reorientation. The slowest component of the orientational relaxation increases from 2.6 ps (pure water) to 6.7 ps (~6 M NaBr). An important comparison of the vibrational echo results and the orientational relaxation results showed that the slowest time component of the two observables have the same concentration dependence, confirming that both are controlled by the same global hydrogen bond rearrangement dynamics. Vibrational population relaxation of the OD stretch also slows significantly as the NaBr concentration increases.

Water dynamics, particularly the global hydrogen bond structural rearrangement that is necessary for processes such as proton transport is controlled by the hydrogen bonding potential. It is difficult to obtain direct experimental information on the potential. The short time orientational relaxation of water was studied by ultrafast infrared pump-probe spectroscopy of the hydroxyl stretching mode (OD of dilute HOD in $H_2O$).[12] The anisotropy decay displays a sharp drop at very short times caused by inertial orientational motion, followed by a much slower decay that fully randomizes the orientation. Investigation of temperatures from 1 °C to 65 °C shows that the amplitude of the inertial component (extent of inertial angular displacement) depends strongly on the stretching frequency of the OD oscillator (hydrogen bond strength) at higher temperatures, although the slow component is frequency independent. The inertial component becomes frequency independent at low temperatures. At high temperatures, there is a correlation between the amplitude of the inertial decay and the strength of the O-D---O hydrogen bond, but at low temperatures the correlation disappears, showing that a single hydrogen bond (OD---O) is no longer a significant determinant of the inertial angular motion. It is suggested that the loss of correlation at lower temperatures is caused by the increased importance of collective effects of the extended hydrogen bonding network. Using a new harmonic cone model, the experimentally measured amplitudes of the inertial decays yield the characteristic frequencies of the intermolecular angular potential for various strengths of hydrogen bonds. The frequencies are in the range of ~400 $cm^{-1}$. A comparison with recent MD simulations employing SPC/E water at room temperature shows that the simulations qualitatively reflect the correlation between the inertial decay and the OD stretching frequency.

We are using photoacids as probes of proton transfer in nanoconfined systems, particularly, Nafion fuel cell membranes. We have conducted a study to gain an improved understanding of the photoinduced proton transfer process. The photoacid 8-hydroxy-N,N,N',N',N",N"-hexamethylpyrene-1,3,6-trisulfonamide (HPTA) and related compounds were used to investigate the steps involved in excited-state deprotonation in polar solvents using UV/Vis pump-probe spectroscopy and time correlated single photon counting fluorescence spectroscopy. The dynamics show a clear two-step process leading to excited state proton transfer. The first step after electronic excitation is charge redistribution occurring on a tens of picoseconds time scale followed by proton transfer on a nanosecond time scale. The three states observed in the experiments (initial excited state, charge redistributed state, proton transfer state) are recognized by distinct features in the time dependence of the pump-probe spectrum and fluorescence spectra. In the charge redistributed state, charge density has transferred from the hydroxyl oxygen to the pyrene ring, but the OH sigma bond is still intact. The experiments indicate that the charge redistribution step is controlled by a specific hydrogen bond donation from HPTA to the accepting base molecule. The second step is the full deprotonation of the photoacid. The full deprotonation is clearly marked by the growth of

stimulated emission spectral band in the pump-probe spectrum that is identical to the fluorescence spectrum of the anion.

Our current and future work is moving in a number of directions. Previously we have studied proton transfer in Nafion fuel cell membranes in which $Na^+$ is the counter ion for the sulfonate head groups. In fuel cells, the membranes are protonated, and considered to be superacids. We have been able to put the photoacid HPTA into Nafion. HPTA will photodissociate even under extreme acid conditions (concentrated sulfuric acid). Initial results are showing that protonated Nafion is not as acidic as has been believed. We will obtain proton transfer dynamics in the protonated Nafion membranes as a function of hydration and compare the results to Nafion with $Na^+$ counter ions. We are investigating the dynamics of water in a variety of nanoconfined systems with different topologies, for example lamellar structures made with AOT surfactant and phospholipid multibilayers by directly examining the water with IR experiments. To date we have initial studies of vibrational relaxation and orientational relaxation. We will extend these initial studies to full wavelength dependences, which can identify the dynamics of water in distinct environments. We will also perform the first really detailed ultrafast 2D IR vibrational echo experiments. We have spent most of the last year in developing the next generation 2D IR spectrometer. The 2D IR vibrational echo is an exceedingly complex experiment that yields a great deal of information that is not obtainable by other means. Like the early days of NMR, the state-of-the-art instrumentation is home built and requires a good deal of nursing. The experiment involves five femtosecond IR pulses with times that are critical. Knowledge of the timing to better than 1 fs is required and drifts of even a femtosecond over a day cause serious problems with the data. We have now automated the measurement and maintenance of the times between pulses 1, 2, and 3, which generate the vibrational echo and the timing between the vibrational echo and the local oscillator that gives the signal with full phase information. This is a major advance. We have also recently developed new theoretical methods for more rapidly and accurately extracting the important information from the data. With the new spectrometer and theoretical methods, we will examine in great detail the dynamics in nanoscopic water systems. The new methodology will allow us to take apart the 2D IR spectra to separate data for water at interfaces vs. water farther from interfaces. We will conduct experiments on ionic and non-ionic surfactant head group reverse micelles, water in nominally hydrophobic environments, Nafion fuel cell membranes, lamellar structures, salt solution, etc. Combining the 2D IR vibrational echo experiments with IR pump-probe experiments and linear spectroscopy will provide a very detailed view of water as well as other liquids at interfaces, in nanoconfinement and interacting with ions.

**Publication from DOE Sponsored Research 2005 – present**

**Nanoconfined, Interfacial, Salt Solutions, and Bulk Water**


(1) "Dynamics of Water Confined on a Nanometer Length Scale in Reverse Micelles: Ultrafast Infrared Vibrational Echo Spectroscopy," Howe-Siang Tan, Ivan R. Piletic, Ruth E. Riter, Nancy E. Levinger and M. D. Fayer, Phys. Rev. Lett. 94, 057405(4) (2005).

(2) "Orientational Dynamics of Water Confined on a Nanometer Length Scale in Reverse Micelles," Howe-Siang Tan, Ivan R. Piletic, and M. D. Fayer, J. Chem. Phys. 122, 174501 (2005).

(3) "The Dynamics of Nanoscopic Water: Vibrational Echo and IR Pump-probe Studies of Reverse Micelles," Ivan R. Piletic, Howe-Siang Tan, and M. D. Fayer, J. Phys. Chem. B 109, 21273-21284 (2005).

(4) "Testing the Core/Shell Model of Nanoconfined Water in Reverse Micelles Using Linear and Nonlinear IR Spectroscopy," Ivan R. Piletic, David E. Moilanen, D. B. Spry, and Nancy E. Levinger, M. D. Fayer, J. Phys. Chem. A 110, 4985-4999 (2006).

(5) "Confinement or Properties of the Interface? Dynamics of Nanoscopic Water in Reverse Micelles," David E. Moilanen, David B. Spry, Nancy E. Levinger, and M. D. Fayer, J. Am. Chem. Soc. 129, 14311-14318 (2007).

(6) "Water Dynamics – The Effects of Ions and Nanoconfinement," Sungnam Park, David E. Moilanen, and M. D. Fayer J. Phys. Chem. B 112, 5279-5290 (2008).

(7) "Tracking Water's Response to Structural Changes in Nafion Membranes," David E. Moilanen, Ivan R. Piletic, and M. D. Fayer, J. Phys. Chem. A 110, 9084-9088 (2006).

(8) "Water Dynamics in Nafion Fuel Cell Membranes: the Effects of Confinement and Structural Changes on the Hydrogen Bonding Network," David E. Moilanen, Ivan R. Piletic, Michael D. Fayer J. Phys. Chem. C 111, 8884-8891, (2007).

(9) "Water at the Surfaces of Aligned Phospholipid Multi-Bilayer Model Membranes Probed with Ultrafast Vibrational Spectroscopy," Wei Zhao, David E. Moilanen, Emily E. Fenn, and M. D. Fayer J. Am. Chem. Soc. accepted (2008).

(10) "Hydrogen Bond Dynamics in Aqueous NaBr Solutions," Sungnam Park and M. D. Fayer, Proc. Nat. Acad. Sci. U.S.A. 104, 16731-16738 (2007).

(11) "Are Water Simulation Models Consistent With Steady-State and Ultrafast Vibrational Spectroscopy Experiments?" J. R. Schmidt, A. Tokmakoff, M. D. Fayer, and J. L. Skinner Chem. Phys. 341, 143-157 (2007).

(12) "Water Inertial Reorientation: Hydrogen Bond Strength and the Angular Potential," David E. Moilanen, Emily E. Fenn, Yu-Shan Lin, J. L. Skinner, B. Bagchi, and M. D. Fayer Proc. Nat. Acad. U.S.A. 105, 5295-5300 (2008).

(13) "Ultrafast 2D-IR Vibrational Echo Spectroscopy: A Probe of Molecular Dynamics," Sungnam Park, Kyungwon Kwak, and M. D. Fayer Laser Phys. Lett. 4, 704-718 (2007).

(14) "Polarization Selective Spectroscopy Experiments: Methodology and Pitfalls," Howe-Siang Tan, Ivan R. Piletic and M. D. Fayer, J.O.S.A. B 22, 2009-2017 (2005).

**Proton Transfer and Photoacids in Solution and Nanoconfinement**

(15) "Identification and Properties of the $^1L_a$ and $^1L_b$ States of Pyranine (HPTS)," D. B. Spry, A. Goun, C. B. Bell III, and M. D. Fayer, J. Chem. Phys. 125, 144514-(12) (2006).

(16) "The Deprotonation Dynamics and Stokes Shift of Pyranine (HPTS)," D. B. Spry, A. Goun, and M. D. Fayer J. Phys. Chem. A 111 230-237 (2007).

(17) "Proton Transport and the Water Environment in Nafion Fuel Cell Membranes and AOT Reverse Micelles," D. B. Spry, A. Goun, K. Glusac, David E. Moilanen, W. Childs, and M. D. Fayer J. Am. Chem. Soc. 129 8122-8130 (2007).

(18) "Water Dynamics and Proton Transfer in Nafion Fuel Cell Membranes," David E. Moilanen, D.B. Spry, and M. D. Fayer Langmuir 24, 3690-3698 (2007).

(19) "Observation of Slow Charge Redistribution Preceding Excited State Proton Transfer," D. B. Spry and M. D. Fayer J. Chem. Phys. 127, 204501 (2007).

(20) "Charge Redistribution and Photoacidity: Neutral vs. Cationic Photoacids," D. B. Spry and M. D. Fayer J. Chem. Phys. 128, 084508 (2008).

(21) "Charge Transfer in Photoacids Observed by Stark Spectroscopy," Lisa N. Silverman, D. B. Spry, Steven G. Boxer and M. D. Fayer J. Phys. Chem. A accepted (2008).

**Electron Transfer in Solution and Nanoconfinement**

(22) "Photoinduced Electron Transfer and Geminate Recombination in Liquids on Short Time Scales: Experiments and Theory," Alexei Goun, Ksenija Glusac, and M. D. Fayer, J. Chem. Phys. 124, 084504(11) (2006).

(23) "Photoinduced Electron Transfer and Geminate Recombination in the Head Group Region of Micelles," Ksenija Glusac, Alexei Goun, and M. D. Fayer, J. Chem. Phys. 125, 054712(12 pages) (2006).

(24) "Photoinduced Electron Transfer in the Head Group Region of Sodium Dodecyl Sulfate Micelles," J. Nanda, P. K. Behera, H. L. Tavernier and M. D. Fayer, J. Lum. 115, 138-146 (2005).

**Chemical Kinetics and Dynamics at Interfaces**
*Fundamentals of Solvation under Extreme Conditions*

John L. Fulton
Chemical and Materials Sciences Division
Pacific Northwest National Laboratory
902 Battelle Blvd., Mail Stop K1-83
Richland, WA 99354
john.fulton@pnl.gov

## Program Scope

The primary objective of this project is to describe, on a molecular level, the solvent/solute structure and dynamics in fluids such as water under extremely non-ideal conditions. The scope of studies includes solute–solvent interactions, clustering, ion-pair formation, and hydrogen bonding occurring under extremes of temperature, concentration and pH. The effort entails the use of spectroscopic techniques such as x-ray absorption fine structure (XAFS) spectroscopy, coupled with theoretical methods such as molecular dynamics (MD-XAFS), and electronic structure calculations in order to test and refine structural models of these systems. In total, these methods allow for a comprehensive assessment of solvation and the chemical state of an ion or solute under any condition. The research is answering major scientific questions in areas related to energy-efficient separations, hydrogen storage (thermochemical water splitting) and sustainable nuclear energy (aqueous ion chemistry and corrosion). This program provides the structural information that is the scientific basis for the chemical thermodynamic data and models in these systems under non-ideal conditions.

## Recent Progress

Contact ion pairs underlie processes in a large number of aqueous systems. Direct experimental measurement of ion-ion interactions decoupled from those of ion-water are non-existent from neutron and x-ray diffraction studies and have only recently been reported for XAFS studies. X-ray absorption fine structure (XAFS) spectroscopy, coupled with molecular dynamics (MD-XAFS) are used to test and refine structural models of these systems. As an example[7], a clearer picture of hydration of common ions such as $Cl^-$, $K^+$, and $Ca^{2+}$ has emerged from XAFS that allows one to measure the structure in the first solvation shell about ions including precise measurements of the atomic distances, coordination numbers and oxidation states.

At moderate- to low concentrations and under ambient conditions, most cations and anions would normally be fully dissociated. However, in high temperature water, contact-ion pairs are the predominate species in an aqueous solvent where the hydrogen bonding network has been largely destroyed and electrostatic interactions between ions start to prevail. We have recently developed XAFS methods to probe light element ions in solution at high temperatures. In this approach, a focused, 50 μm diameter x-ray beam passes through the pressurized solution contained between two, 25 μm-thick diamond windows in the sample cell. This allows us to reach the low energies of the Ca K-edge (4038.5 eV) and Cl K-edge (2822 eV). Using this

method, the first detailed structure of the $Ca^{2+}/Cl^-$ interaction has emerged. Figure 1 shows the complete structure of $Ca^{2+}$ associating with two $Cl^-$ including the measured bond distances, bond disorder and the degree of hydration around the cation and the anion.

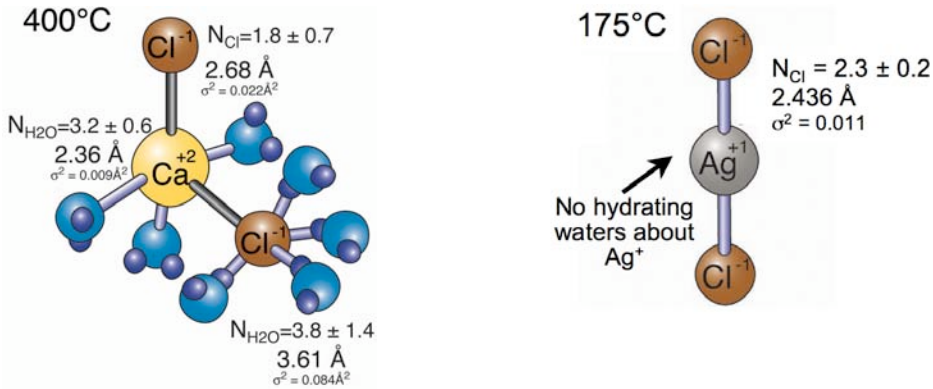


Figure 1. Schematics of the $Ca^{2+}/Cl^-$ and $Ag^+/Cl^-$ ion pairs at 400°C and 175°C, respectively.

We have also completed an investigation of another benchmark system, that of the hydrated $Ag^+$ and of the ion paired $Ag^+/Cl^-$ species. The importance of $Ag^+$ hydration and ion pairing lies in the fact that it is often used as an analog for understanding the solvation of $Na^+$. However when a transition metal ion forms a contact ion pair with a halide ion the resultant bond often involves a certain degree of covalency. This association profoundly changes the coordination structure about the hydrated ion. As shown in Figure 1, as the contact ion pairs form, the $Ag^+$ ion undergoes nearly complete dehydration to form an unusual collinear $AgCl_2^-$ species. Figure 2 shows the special spectral feature due to photoelectron multiple scattering that establishes the collinear nature of the Cl-Ag-Cl bond

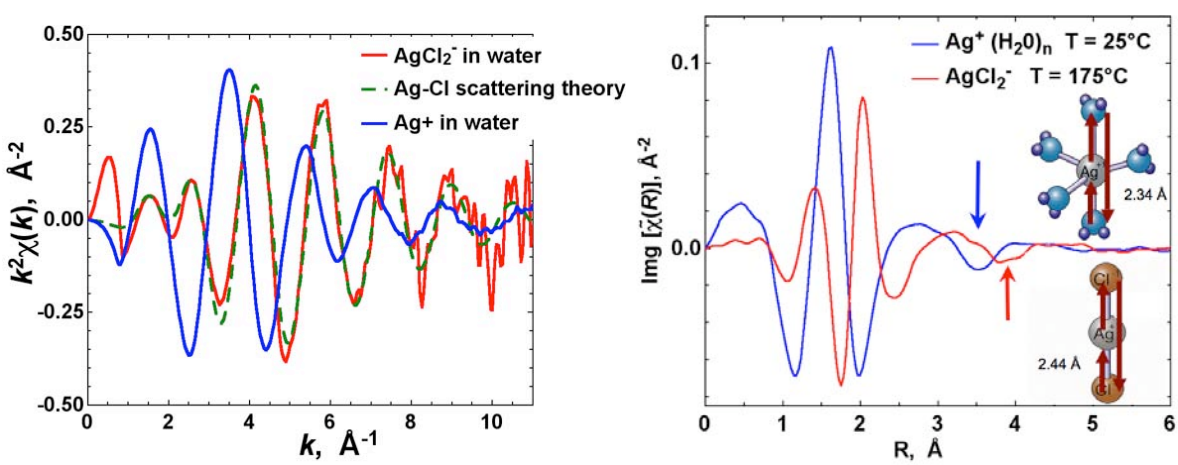


Figure 2. XAFS $k^2$-weighted $\chi(k)$ and $\mathrm{Im}[\tilde{\chi}(R)]$ plots for hydrated and ion-paired $Ag^+$ showing the significant photoelectron multiple scattering features used to establish the first-shell symmetry.

These structural transitions have been benchmarked to electronic structure calculations of a Cl-Ag-Cl cluster that shows a large amount of charge transfer between the Cu and the Cl, reducing the local electrostatic charge on Ag from +1 to about +0.26. (by S. Kathmann) Hence we have shown that $Ag^+$ loses waters-of-hydration upon formation of the $AgCl_2^-$ ion pair due to

reduced ionic charge on Ag via covalent bonding with Cl. We are also using ab initio molecular dynamics simulations to explore the structure of the contact ion pair and of the hydrated $Ag^+$ ion.

**Future Plans**

We are exploring the structure of hydronium ($H_3O^+$) contact-ion pair formation with halide ions ($Cl^-$, $Br^-$, and $I^-$) in concentrated acids using XAFS and high-energy x-ray diffraction. XAFS provides a measure of the Cl-O pair distribution function for both $H_2O$ and $H_3O^+$ in the first shell about the halide ion. High-energy x-ray diffraction (HXD) provides an overall measure of the halide, water and hydronium pair distribution functions. This experimental effort compliments ongoing theoretical efforts in the Molecular Interactions and Transformations group. Comparisons will be made to i) electronic structure calculations of small $H_3O^+/Cl^-/H_2O$ clusters, ii) newly-developed classical intermolecular potentials for $Cl^-/H_3O^+$ used in a classical molecular dynamics simulation and iii) efforts modeling the chemistry of hydronium using Car-Parrinello molecular dynamics methods. The interest in hydronium structure pertains to its role in a large number of biological, chemical, and geochemical systems. No previous experimental studies have directly measured the structure of the $Cl^-/H_3O^+$ contact ion pair.

We have recently developed methods for making XAFS transmission measurements of aqueous systems at these low x-ray energies. As shown in the schematic of Figure 3, preliminary data shows a shortening of the Cl-O distance (from $H_3O^+$) that is approximately equal to the theoretical value. Thus this study will provide the first direct measure of the $Cl^-/H_3O^+$ distance and provide an excellent comparison to ab initio molecular dynamics studies of the same system.

We are exploring the possibility (with G. Kimmel and B. Kay in experimental chemical physics) of using XAFS to study the structure of ionic species in amorphous solid water (ASW). We propose exploring mixtures of different ionic species such as HCl, NaCl, RbCl, KCl, $CaCl_2$, $SrCl_2$, or $NH_4Cl$ in amorphous solid water (ASW). We will generate the amorphous metastable mixture at low temperatures and then probe the structure using EXAFS or XANES. These studies would be conducted at or below 100K providing an unprecedented detailed picture of the structure about the ion. At these temperatures, the thermal disorder is eliminated providing excellent opportunity for XAFS to resolve the structure in the first solvation shell as well as possibly providing information about the second shell. These results will provide an interesting comparison to the structure in bulk water.

There is a great deal of interest in the chemistry of hydrogen chloride on ice. Hydrogen chloride is fully dissociated in water up to the saturation concentration. On the other hand, HCl on the surface of ice at about 100K is believed to exist in an equilibrium between dissociated and undissociated forms. Cl XANES is a highly sensitive probe of the bonding state of Cl. Undissociated HCl has an intense $1s \rightarrow 3p$ pre-edge peak, whereas as the hydrated $Cl^-$ has none. Hence Cl XANES is an extremely sensitive technique to explore the $HCl/H_3O^+/Cl^-$ equilibrium. Studies of the polarization dependence of the XANES pre-edge peak will allow us to determine the orientation of the HCl on the ice surface.

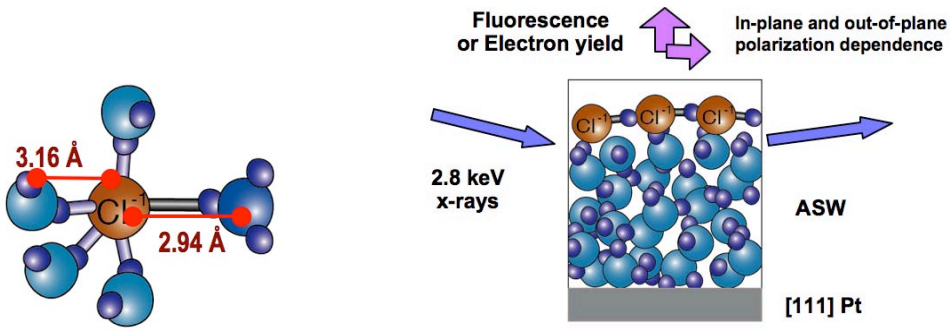


Figure 3. Preliminary XAFS result for hydronium ion pairing with $Cl^-$ in concentrated HCl solutions. Schematic of XAFS method for probing HCl structure on the surface of amorphous solid water.

Collaborators on this project include G.K Schenter, S. M. Kathmann, C. J. Mundy, L. X. Dang. Battelle operates Pacific Northwest National Laboratory for the U. S. Department of Energy.

**References to publications of DOE sponsored research (2005-present)**


1. Y. Chen, J. L. Fulton, W. Partenheimer. The structure of the homogeneous oxidation catalyst, Mn(II)- $(Br^{-1})_x$, in supercritical water: An x-ray absorption fine structure study. **J. Am. Chem. Soc**. 127, 14085-14093, (2005).
2. Y. Chen, J. L. Fulton, J. C. Linehan, T. Autrey, "In-situ XAFS and NMR Study of Rhodium Catalyst Structure during Dehydrocoupling of Dimethylamine Borane. "**J. Am. Chem. Soc.**, 127, 3254-3255, (2005)
3. Y. Chen, J. L. Fulton, W. Partenheimer. A XANES and XAFS Study of Hydration and Ion Pairing in Ambient Aqueous $MnBr_2$ Solutions. **J. Solution Chem.** 34(9) **2005**, 993-1007.
4. J. L. Fulton, D. W. Matson, K. H. Pecher, J. E. Ammonette, J. C. Linehan, "Iron-based and Iron Oxide Nanoparticle Synthesis from the Rapid Expansion of Carbon Dioxide Solutions" **Journal of Nanoscience and Nanotechnology**, 6, 562-567 (2006).
5. V. Glezakou, Y. Chen, J. L. Fulton, G. K. Schenter and L. X. Dang. Electronic structure, statistical mechanical simulations, and EXAFS spectroscopy of aqueous potassium. **Theor. Chem. Acc**. 115, 86-99, (2006)
6. "Calcium Ion Hydration and Ion Pairing in Supercritical Water", J. L. Fulton Y. Chen, S. M. Heald, and M. Balasubramanian, **J. Chem. Phys.**, 125(9), Art. No. 094507, (2006).
7. "Molecular simulation analysis and X-ray absorption measurement of $Ca^{2+}$, $K^+$ and $Cl^-$ ions in solution", Liem X. Dang, Gregory K. Schenter, Vassiliki-Alexandra Glezakou and John L. Fulton, **J. Phys. Chem. B**, 110(47), 23644, (2006)
8. J. L. Fulton, J. C. Linehan, T. Autrey, M. Balasubramanian, Y. Chen, and N. K. Szymczak. When is a Nanoparticle a Cluster? An Operando EXAFS Study of Amine Borane Dehydrocoupling by $Rh_{4-6}$ Clusters. **J. Am. Chem. Soc**., 129(39), 11936-11949, (2007).

**Reactions of Ions and Radicals in Aqueous Systems**

Bruce C. Garrett[1] and Marat Valiev[2]
[1]Chemical & Materials Sciences Division and
[2]Environmental Molecular Sciences Laboratory
Pacific Northwest National Laboratory
902 Battelle Blvd.
Mail Stop K9-90
Richland, WA 99352
bruce.garrett@pnl.gov

The long-term objective of this project is to understand the factors that control the chemical reactivity of atomic and molecular species in aqueous environments. Chemical reactions in condensed phase environments play crucial roles in a wide variety of problems important to the Department of Energy (DOE), (e.g., corrosion in nuclear reactors promoted by reactive radical species such as OH, release of hydrogen from hydrogen storage materials, catalysis for efficient energy use, and contaminant degradation in the environment by natural and remedial processes). The need in all of these areas is to control chemical reactions to eliminate unwanted reactions and/or to produce desired products. The control of reactivity in these complex systems demands knowledge of the factors that control the chemical reactions and requires understanding how these factors can be manipulated to affect the reaction rates. The goals of this research are the development of theoretical methods for describing reactions in condensed phases (primary aqueous liquids) and their application to prototypical systems to develop fundamental knowledge need to solve problems of interest to DOE.

The focus of our work is to gain a theoretical understanding of factors that control ground and excited-state properties of chemical systems in condensed phase and other complex environments. This is a challenging problem requiring simultaneous consideration of the electronic structure of reactive species, collective degrees of freedom associated with the environment, reaction dynamics, and thermal fluctuations. To address these issues, we are developing multi-scale, multi-physics approaches that recognize the advantages of using different theoretical models (multi-physics) to address the natural decomposition of the chemical system into distinct regions (multi-scale). These theoretical models can be associated with different parts of the overall chemical system and/or can coexist in a layered fashion. This flexibility in the system description significantly extends the scope, accuracy, and reliability of ab-initio modeling of ground and excited-state processes in complex systems. Based on this methodology, we are pursuing novel approaches for efficient utilization of high-level electronic structure methods such as coupled cluster (CC) theory in real condensed phase applications.

We recently presented a method for calculating free energy profiles for chemical reactions in solution utilizing high-level ab initio methods (reference 14). We begin with the standard separation of the condensed phase system into a reactive part (denoted the solute), which is treated quantum mechanically, and the rest of the system (denoted the solvent), which is treated by a classical molecular mechanics (MM) model. Three different descriptions of the solute are employed – CC, density functional theory (DFT) and electrostatic potential (ESP). In the ESP, the QM atoms are represented by effective ESP charges such that the electrostatic potential outside the solute region is the same as that produced from the full electron density $\rho(\mathbf{r})$. We use a thermodynamic cycle as depicted in the Figure 1 to take advantage of the state

function property of the potential of mean force (PMF), $W$. The PMF for going from a point in the configuration space of the solute, $\mathbf{r}_A$, to a second point, $\mathbf{r}_B$, is given by

$$\begin{aligned}\Delta W_{AB} &= \Delta W_{AA}^{cc\to dft} - \Delta W_{BB}^{cc\to dft} \\ &+ \Delta W_{AA}^{dft\to esp} - \Delta W_{BB}^{dft\to esp} \\ &+ \Delta W_{AB}^{esp}\end{aligned}$$

The first and second lines represent free energy differences for changing the description of the *fixed* solute region from the CC to DFT representations and from DFT to classical ESP representations, respectively. The last term represents the free energy difference for changing solute configuration from $\mathbf{r}_A$ to $\mathbf{r}_B$ within the classical ESP/MM description. The benefit of using an intermediate DFT description is that the ground state DFT electron density approximates well the nearly exact density generated by CC theory. The electron density is the sole coupling parameter between the solute electronic degrees of freedom and the solvent; therefore, the potential of mean force for the change from CC to DFT can be approximated by a simple total energy difference. The potential of mean force calculated with the electrostatic potential, $\Delta W_{AB}^{esp}$, involves only classical molecular mechanics terms, which allows sampling to be performed over ensembles that are sufficiently large to converge the averages. Evaluation of $\Delta W_{AA}^{dft\to esp}$ uses a resampling strategy in which a small number of solvent configurations from the ESP/MM simulation are used to evaluate the average. Figure 1 also illustrates an application of this approach to the $S_N2$ reaction of $CHCl_3$ and $OH^-$ in aqueous solution.

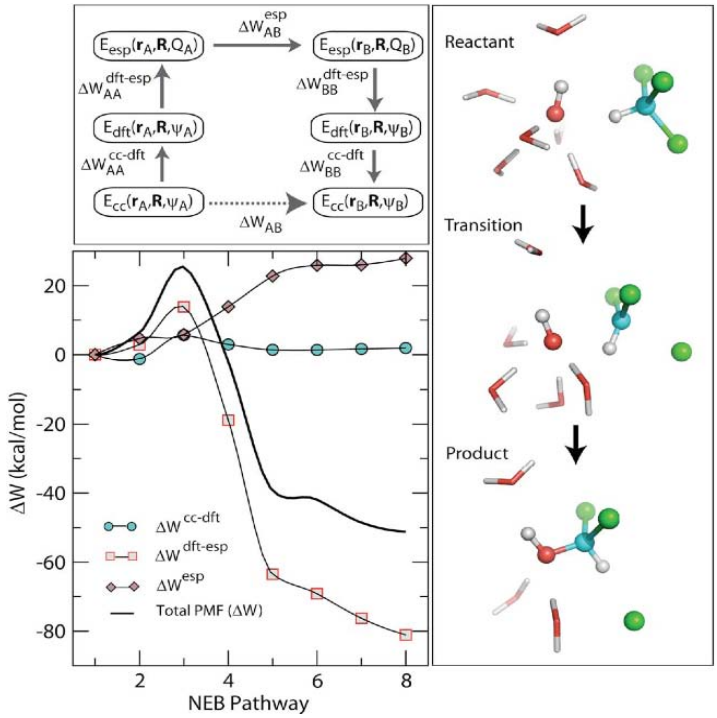


**Figure 1:** Thermodynamic cycle for free energy calculations (top left); free energy profile (bottom left) and reactants, transition state, and products (right) for the reaction $OH^- + CHCl_3 \rightarrow CHCl_2OH + Cl^-$.

Similar methodology can also greatly benefit the description of processes involving excited states where the accuracy of the electronic structure calculations becomes especially problematic. Our current work in this direction involves studies of electronic excitation of the hydrated $OH\text{-}Cl^-$ species. We combine plane wave DFT dynamical simulations with the hybrid coupled cluster/molecular mechanics (CC/MM) approach to provide an accurate description of excited states at finite temperatures. Dynamical simulations at the DFT level efficiently generate the representative ensemble of configurations corresponding to the system. These configurations are then processed using the CC/MM approach leading to an accurate description of the excitation energies. Our results (see Figure 2) clearly illustrate the inadequacy of time-dependent DFT (TD-DFT), further demonstrating the need for accurate quantum mechanical treatment of excited-state processes. Our calculations also highlight the importance of including dynamical fluctuations into the analysis of excited states in condensed phases, for example, we observe a blue shift in the excited-state spectrum when dynamical effects are included.

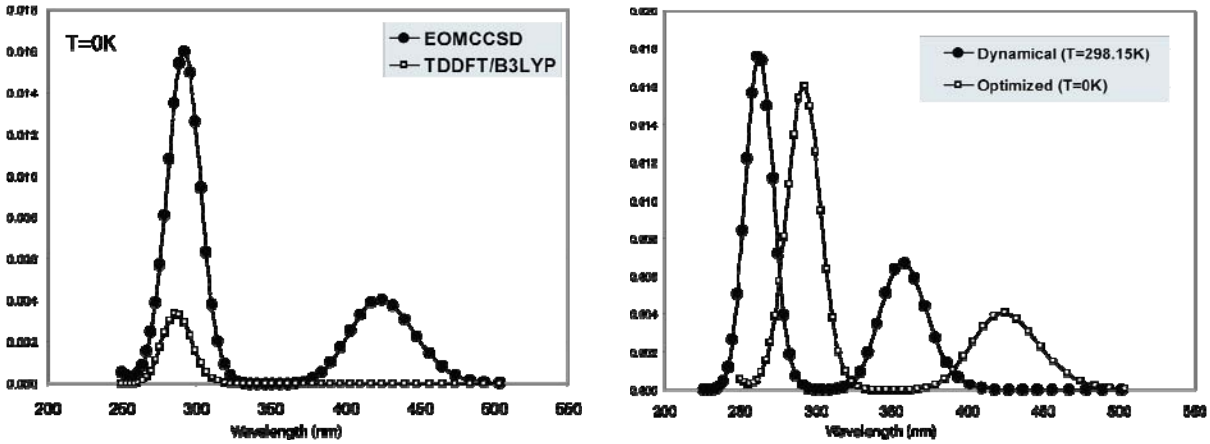


**Figure 2:** Excited-state spectra for hydrated OH-Cl$^-$. Simulations were performed with OH-Cl$^-$ in a cubic box containing 57 water molecules. (left) Simulated spectra for an optimized (T = 0K) geometry at the DFT/MM level of theory. The 13 waters closest to OH-Cl$^-$ were treated quantum mechanically with TDDFT or EOMCCSD levels of theory and the rest by molecular mechanics. (right) Comparison of a simulated spectrum for an optimized (T = 0K) geometry (same as in the left panel) with the spectrum averaged over an ensemble of 32 configurations at room temperature (T = 298K). Both spectra are computed treating OH-Cl$^-$ at the EOMCCSD level of theory and all water molecular using molecular mechanics. The configurations were sampled from a trajectory that was generated by treating the whole system using DFT (e.g., Car-Parrinello dynamics). All simulated spectra include a Gaussian broadening of the peaks.

Collaborators on this project include M.-K. Tsai, G. K. Schenter, M. Dupuis, T. Iordanov, S. S. Xantheas, J. Li, S. Du, J. Francisco, Doug Tobias, and Rafaella D'Auria. Some of the work was performed using the Molecular Science Computing Facility in the Environmental Molecular Sciences Laboratory, a national scientific user facility sponsored by the Department of Energy's Office of Biological and Environmental Research, located at Pacific Northwest National Laboratory (PNNL). Battelle operates PNNL for DOE.

References to publications of DOE sponsored research (2005-present)

1. B. C. Garrett, D. A. Dixon, D. M. Camaioni, D. M. Chipman, M. A. Johnson, C. D. Jonah, G. A. Kimmel, J. H. Miller, T. N. Rescigno, P. J. Rossky, S. S. Xantheas, S. D. Colson, A. H. Laufer, D. Ray, P. F. Barbara, D. M. Bartels, K. H. Becker, H. Bowen, S. E. Bradforth, I. Carmichael, J. V. Coe, L. R. Corrales, J. P. Cowin, M. Dupuis, K. B. Eisenthal, J. A. Franz, M. S. Gutowski, K. D. Jordan, B. D. Kay, J. A. LaVerne, S. V. Lymar, T. E. Madey, C. W. McCurdy, D. Meisel, S. Mukamel, A. R. Nilsson, T. M. Orlando, N. G. Petrik, S. M. Pimblott, J. R. Rustad, G. K. Schenter, S. J. Singer, A. Tokmakoff, L. S. Wang, C. Wittig, and T. S. Zwier, "Role of Water in Electron-Initiated Processes and Radical Chemistry: Issues and Scientific Advances," Chemical Reviews 105, 355-389 (2005).
2. S. M. Kathmann, G. K. Schenter, and B. C. Garrett, "Ion-Induced Nucleation: The Importance of Chemistry," Physical Review Letters 94, 116104 (2005).
3. J. Vieceli, M. Roeselova, N. Potter, L. X. Dang, B. C. Garrett, and D. J. Tobias, "Molecular Dynamics Simulations of Atmospheric Oxidants at the Air-Water Interface: Solvation and Accommodation of OH and O3," Journal of Physical Chemistry B 109, 15876-15892 (2005).
4. B. C. Garrett and D. G. Truhlar, "Variational Transition State Theory," in Theory and Applications of Computational Chemistry: The First 40 Years, edited by C. E. Dykstra, G. Frenking, K. S. Kim, and G. E. Scuseria (Elsevier, Amsterdam, 2005), p. 67-87.

5. T. D. Iordanov, G. K. Schenter, and B. C. Garrett, “Sensitivity analysis of thermodynamic properties of liquid water: A general approach to improve empirical potentials,” *Journal of Physical Chemistry A* **110**, 762-771 (2006).
6. L. X. Dang, T. M. Chang, M. Roeselova, B. C. Garrett, and D. J. Tobias, “On $NO_3$--$H_2O$ Interactions in Aqueous Solutions and at Interfaces,” *Journal of Chemical Physics* **124** 066101 (2006).
7. B. C. Garrett, G. K. Schenter, and A. Morita, “Molecular Simulations of the Transport of Molecules Across the Liquid/Vapor Interface of Water,” *Chemical Reviews* **106**, 1355-1374 (2006).
8. S. Du, J. S. Francisco, G. K. Schenter, T. D. Iordanov, B. C. Garrett, M. Dupuis, and J. Li, “The OH Radical - $H_2O$ Molecular Interaction Potential,” *Journal of Chemical Physics* **124**, 224318 (2006).
9. D. G. Truhlar and B. C. Garrett, “Variational Transition State Theory in the Treatment of Hydrogen Transfer Reactions,” in Handbook of Hydrogen Transfer, edited by H. H. Limbach, J. T. Hynes, J. Klinman, and R. L. Schowen (Wiley-VCH, New York, 2007), Vol. 2, pp. 833-875.
10. A. Fernandez-Ramos, B. A. Ellingson, B. C. Garrett, and D. G. Truhlar, “Variational Transition State Theory with Multidimensional Tunneling,” in Reviews in Computational Chemistry, edited by K. B. Lipkowitz, Cundari, T. R., and D. B. Boyd (John Wiley & Sons, Hoboken, 2007), Vol. 23, pp. 125-232.
11. S. Y. Du, J. S. Francisco, G. K. Schenter, and B. C. Garrett, “Ab initio and Analytical Intermolecular Potential for ClO-$H_2O$,” *Journal of Chemical Physics* **126**, 114304 (2007).
12. S. M. Kathmann, G. K. Schenter, and B. C. Garrett, “Comment on "Quantum Nature of the Sign Preference in Ion-Induced Nucleation",” *Physical Review Letters* **98**, 109603 (2007).
13. D. G. Truhlar and B. C. Garrett, “Variational transition state theory in the treatment of hydrogen transfer reactions,” in Hydrogen-Transfer Reactions, Vol. 2, edited by H. H. Limbach, J. T. Hynes, J. Klinman, and R. L. Schowen (Wiley-VCH, New York, 2007), p. 833-875.
14. M. Valiev, B. C. Garrett, M.-K. Tsai, K. Kowalski, S. M. Kathmann, G. K. Schenter, and M. Dupuis, “Hybrid Approach for Free Energy Calculations with High-Level Methods: Application to the $S_N2$ Reaction of $CHCl_3$ and $OH^-$ in Water,” *Journal of Chemical Physics* **127**, 051102 (2007).
15. S. M. Kathmann, B. J. Palmer, G. K. Schenter, and B. C. Garrett, “Activation Energies and Potentials of Mean Morce for Water Cluster Evaporation,” *Journal of Chemical Physics* **128**, 064306 (2008).
16. S. Y. Du, J. S. Francisco, G. K. Schenter, and B. C. Garrett, “Many-Body Decomposition of the Binding Energies for $OH(H_2O)_2$ and $OH(H_2O)_3$ complexes,” *Journal of Chemical Physics* **128**, 084307 (2008).
17. D. T. Chang, G. K. Schenter, and B. C. Garrett, “Self-Consistent Polarization Neglect of Diatomic Differential Overlap: Application to Water Clusters,” *Journal of Chemical Physics* **128**, 164111 (2008).
18. M. Valiev, E. J. Bylaska, M. Dupuis, and P. G. Tratnyek, “Combined Quantum Mechanical and Molecular Mechanics Studies of the Electron-Transfer Reactions Involving Carbon Tetrachloride in Solution,” *Journal of Physical Chemistry A* **112**, 2713-2720 (2008).
19. S. M. Kathmann, G. K. Schenter, and B. C. Garrett, “The Impact of Molecular Interactions in Atmospheric Radiative Forcing,” in Advances in Quantum Chemistry: Applications of Theoretical Methods to Atmospheric Science, Vol. 55, edited by M. E. Goodsite and M. S. Johnson (Elsevier, Oxford, 2008), p. 429-447.
20. A. Morita and B. C. Garrett, “Molecular Theory of Mass Transfer Kinetics and Dynamics at Gas-Water Interface,” *Fluid Dynamics Research* **40**, 459-473 (2008).

# Ion Solvation in Nonuniform Aqueous Environments

Principal Investigator
**Phillip L. Geissler**
Faculty Scientist, Chemical Sciences, Physical Biosciences, and Materials Sciences Divisions

Mailing address of PI:
Lawrence Berkeley National Laboratory
1 Cyclotron Road
Mailstop: HILDEBRAND
Berkeley, CA 94720

Email: geissler@cchem.berkeley.edu

Research in this program applies computational and theoretical tools to determine structural and dynamical features of aqueous salt solutions. It focuses specifically on heterogeneous environments, such as liquid-substrate interfaces and crystalline lattices, that figure prominently in the chemistry of energy conversion. In these situations conventional pictures of ion solvation, though quite accurate for predicting bulk behavior, appear to fail dramatically, e.g., for predicting the spatial distribution of ions near interfaces. We develop, simulate, and analyze reduced models to clarify the chemical physics underlying these anomalies. We also scrutinize the statistical mechanics of intramolecular vibrations in nonuniform aqueous systems, in order to draw concrete connections between spectroscopic observables and evolving intermolecular structure. Together with experimental collaborators we aim to make infrared and Raman spectroscopy a quantitative tool for probing molecular arrangements in these solutions.

During the past year we have made progress both toward understanding the spatial distributions of ions near water-vapor interfaces, and toward developing a physical interpretation of the nonlinear spectroscopies that report on them. Others have shown that detailed empirical models of liquid water predict accumulation of certain anions (e.g., iodide) at such an interface. By contrast, physical intuition developed for ion solvation in bulk polar solvents suggests that ions should be unambiguously repelled from the interface. Ion polarizability appears to play a key role in this surface phenomenon, but the physical mechanism underlying its influence remains unclear.

We have used thermodynamic perturbation theory to express the statistics of polarizable ion behavior in terms of averages within a reference system lacking polarizability. As a practical advantage, this result allows the restoring force for a solute's dipole to be varied over a wide range without need for additional computer simulations. More importantly, it provides a quantitative context for assessing how fluctuations in a solvent's electric field bias the location of polarizable ions. As a charged solute approaches the interface from the liquid side, the electrostatic force exerted by the solvent changes in two important ways. First, it develops a nonzero average value that would be prohibited in bulk solution by symmetry. Second, spontaneous fluctuations about this average decline in magnitude. It is a competition between these effects that determines in a simple molecular model whether an ion tends to "adsorb" at the interface. We are investigating systematically how they depend on solute size and charge, both in a detailed model of liquid water and in a schematic model of a polar liquid (the Stockmayer fluid).

Nonlinear spectroscopies that specifically probe interfacial structure and dynamics do not permit as straightforward an interpretation as their linear counterparts in bulk solution. Nonetheless, one expects the microscopic factors that determine their lineshapes to be similar in nature. Exploiting this notion, we have extended our physical perspective on bulk vibrational spectroscopy to treat sum frequency generation (SFG) in non-centrosymmetric environments. Our theory clarifies how the interplay between orientational bias of hydrogen bonds and the electric fields they experience conspire to generate complex spectroscopic lineshapes. In particular we have identified two orientational averages, conditioned on electric field, that control the frequency dependence of SFG susceptibilities. We have also shown that seemingly arbitrary choices involved in calculating SFG from computer simulations can influence spectroscopic predictions profoundly. This result highlights a need for detailed consideration of interactions between hydroxyl vibration and the electromagnetic field.

Articles supported by DOE funding, 2005-2008

1. Geissler, P. L. "Temperature Dependence of Inhomogeneous Broadening: On the Meaning of Isosbestic Points" *J. Am. Chem. Sci.* **2005**, *127*, 13019.

2. Eaves, J. D.; Tokmakoff, A.; Geissler, P. L. "Electric Field Flucuations Drive Vibrational Dephasing in Water" *J. Phys. Chem. B* **2005**, *109*, 9424.

3. Smith, J. D.; Cappa, C. D.; Wilson, K. R.; Cohen, R. C.; Geissler, P. L.; Saykally, R. J. "Unified Description of Temperature-Dependent Hydrogen Bond Rearrangements in Liquid Water" *Proc. Natl. Acad. Sci. U.S.A.* **2005**, *102*, 14171.

4. Smith, J.; Saykally, R.; Geissler, P. L. "The Effects of Dissolved Halide Anions on Hydrogen Bonding in Liquid Water" *J. Am. Chem. Soc.* **2007**, *129*, 13847.

Program Title: Theoretical Studies of Surface Science and Intermolecular Interactions

Principal Investigator: Mark S. Gordon, 201 Spedding Hall, Iowa Sate University and Ames Laboratory, Ames, IA 50011; mark@si.msg.chem.iastate.edu

Program Scope. Our research effort spans the study of a variety or problems in surface science using *ab initio* cluster and embedded cluster methods, the development and application of sophisticated model potentials for the investigation of intermolecular interactions, including solvent effects in ground and excited electronic states, the liquid-surface interface, the development and implementation of methods related to the study of molecules containing heavy elements, and general studies of mechanisms in organometallic chemistry. Many of the surface science studies are in collaboration with James Evans.

Recent Progress. Several studies of the Si(100) and related surfaces and processes that occur on these surfaces have been completed. Combined kinetic Monte Carlo (KMC)/electronic structure theory studies of the etching of the Si(100) surface and the diffusion of group III metals on the Si(100) surface are ongoing; however, several papers in this general area have already been published. SIMOMM studies have also been carried out on the diamond surface[4,11].

Because MCSCF calculations are limited with regard to the size of the active space that can be included, extensive studies have been initiated on methods that are designed to significantly increase the sizes of systems that can be realistically treated with this method. Studies have also been completed on the structures of $Si_mO_n$ clusters and on the prediction of novel silicon-based nanowires, and on the design of a new class of quantum dots.

As part of a NERI grant (PI: Francine Battaglia), an extensive series of calculations has been initiated to study the chemical vapor deposition processes of SiC, starting from $CH_3SiCl_3$ (MTS). The overall mechanism involves more than 100 reactions whose overall reaction energetics and barrier heights and activation energies have been predicted with many body perturbation theory and coupled cluster theory. As part of this effort, it has been demonstrated that the new CR-CCSD(T)$_L$ method is in almost perfect agreement with full configuration interaction (FCI) for breaking a wide variety of single bonds in both closed and open shell molecules.

Development of the effective fragment potential (EFP) method has continued with the derivation and implementation of a new approach to electrostatic damping and the application to the benzene dimmer and an extensive series of substituted benzene dimers, the derivation and implementation of analytic gradients for the most demanding terms in the potential, and the implementation of a scalable EFP algorithm. The EFP method has recently been extended to open shell species. EFP applications have included a study of the aqueous solvation of $F^-$ and $Cl^-$ and to a new definitive interpretation of the dipole moment of water in the bulk.

Several studies of non-adiabatic interactions, including spin-orbit coupling have been published, and several papers on advances in high quality electronic structure theory have been completed. Of particular note is a sequence of definitive papers (with K. Ruedenberg) on the $F_2$ molecule, in which the most accurate potential energy curves and vibrational spectrum for this molecule are presented, together with an interpretation of the long-range tails of the PE curve.

As part of the Ames Laboratory catalysis effort, a detailed study of the nitroaldol reaction, both in the gas phase and in solution, has been completed, and a paper on this work is in press. Because the central feature of the catalysis effort is the use of silica nanopores as the host and catalyst, an interface was derived and coded between our effective fragment potential (EFP) method and the universal force field molecular mechanics method. A paper on this EFP-MM interface is in press.

Future Plans. In order to significantly expand the sizes of clusters that can realistically been modeled with MCSCF wavefunctions, the ORMAS (Occupation restricted Multiple Active Spaces) method is being tested on clusters of increasing size and compared with the full CASSCF calculations. This initial study is nearing completion. An exhaustive study of the diffusion of one and two Al atoms on the Si(100) surface will be completed and then extended to heavier group III elements. The etching of the Si(100) surface by O was studied previously. This system is being revisited, partially to explore the importance of using larger basis sets and better levels of theory, and partially to study the diffusion of O along the surface. The energetics and structural information obtained for these processes will then be incorporated into the kinetic Monte Carlo analyses performed by the Evans group. The SIMOMM method is being extended to more complex species, such as silica. A primary motivation for this is to model the catalysis of various reactions in silica-based MSM pores.

The EFP method is currently being interfaced with both the CI singles and CI singles with perturbative doubles [CIS(D)], as well as time dependent density functional theory(TDDFT) methods, so that solvent-induced shifts in electronic spectra can be investigated. Improved methods for treating weak intermolecular interactions, such as dispersion, will be developed and implemented, and then applied to important problems. A preliminary molecular dynamics (MD) code for the EFP method and a combined *ab initio* EFP MD code has been implemented, and more robust algorithms are being developed. Several studies of the aqueous solvation of ions and electrolytes, including $NO_3^-$, $Na^+$, $OH^-$, and NaOH are underway. This includes a systematic study of the solvated structures (internal vs. external ions) and the convergence of ionization potentials and electron affinities to their gas phase values. The EFP method will also be used in extensive investigations of atmospheric aerosols, including the structures and reactions clusters of $H_2SO_4$, $HNO_3$, and their ions with water molecules. The latter study is in collaboration with Theresa Windus (Iowa State) and Shawn Kathmann (PNNL) and is supported by a generous computer grant from PNNL.

Ruedenberg and Bytautas have developed the very excited CEEIS (Correlation Energy Extrapolation with Intrinsic Scaling) that facilitates the prediction of the exact wavefunction (full CI at the complete basis set limit) for small molecules. This method has been shown to provide essentially exact energies for diatomic molecules (e.g., $F_2$) We will now move on to address more complex species, most notably the ground and excited state potential energy surfaces of $O_3$.

Analytic gradients and Hessians for the Klobukowski model core potentials (MCP) have been derived and implemented into GAMESS. Combined with the correlation consistent basis sets, this provides a powerful approach to study mechanisms of reactions in transition metal organometallic chemistry, in collaboration with the Ames Laboratory catalysis group, especially Andreja Bakac, and studies of uranium complexes with Theresa Windus (Ames) and Bert de Jong (PNNL).

In collaboration with Francine Battaglai and Rodney Fox, the NERI project will continue with the incorporation of the thermodynamic and rate constant data discussed above into bulk kinetic models, such as ChemKin. This will provide important insights to our experimentalist colleagues at ORNL.

**References to publications of DOE sponsored research, 2005-present**.

**[1]** *Multi-Reference Second-Order Perturbation Theory: How Size Consistent is Almost Size Consistent?* J. M. Rintelman, I. Adamovic, S. Varganov, and M. S. Gordon, J. Chem. Phys., **122**, 044105 (2005).

**[2]** *Advances in Electronic Structure Theory: GAMESS a Decade Later* M. S. Gordon and M. W. Schmidt *Theory and Applications of Computational Chemistry*, Ch. 41, C. E. Dykstra, G. Frenking, K. S. Kim, G. E. Scuseria, Eds., Elsevier, 2005.

**[3]** *Theoretical Study of the Solvation of Fluorine and Chlorine Anions by Water*, D. D. Kemp and M. S. Gordon, J. Phys. Chem. A, **109**, 7688 (2005) [13th most downloaded paper July-Sept. 2005].

**[4]** *Potential Energy Surfaces of $Si_mO_n$ Cluster Formation and Isomerization*, P. V. Avramov, I. Adamovic, K.-M. Ho, C. Z. Wang, W. C. Lu, and M. S. Gordon, J. Phys. Chem. A**, 109**, 6294 (2005).

**[5]** *Ab initio study of Nucleation on the Diamond(100) Surface during Chemical Vapor Deposition with Methyl and H Radicals*, H. Tamura and M. S. Gordon, Chem. Phys. Lett, **406**, 197 (2005).

**[6]** *Competitive Etching and Oxidation of Vicinal Si(100) Surfaces*, M. A. Albao, D.-J. Liu, C. H. Choi, M.S. Gordon, and J.W. Evans, MRS Proceedings, **859E**, JJ3.6.1-6 (MRS Pittsburgh, 2005), edited by J. W. Evans, C. Orme, M. Asta, and Z. Zhang.*

**[7]** *Monotonically Decreasing Size Distributions for One-dimensional Ga Rows on Si(100)*, M.A. Albao, M.M.R. Evans, J. Nogami, D. Zorn, M.S. Gordon, and J.W. Evans, Phys. Rev. B, **72**, 035426 (2005), 8pp. (Also listed in Virtual J. Nanoscale Science and Technology, 2005)

**[8]** *Simultaneous Etching and Oxidation of Vicinal Si(100) Surfaces: Atomistic Lattice-Gas Modeling of Morphological Evolution*, M. A. Albao, D.-J. Liu, M.S. Gordon, and J.W. Evans, Phys. Rev. B, **72**, 195420 (2005), 12pp.*

**[9]** *Theoretical Study of the Formation and Isomerization of $Al_2H_2$*, T. J. Dudley and M. S. Gordon, Mol. Phys., **104**, 751 (2006)

**[10]** *Dissociation Potential Curves of Low-Lying States in Transition Metal Hydrides. III. Hydrides of Groups 6 and 7*, S. Koseki, T. Matsushita, and M.S. Gordon, J. Phys. Chem, **A110**, 2560 (2006).
**[11]** *Parallel Coupled Perturbed CASSCF Equations and Analytic CASSCF Second Derivatives*, T. J. Dudley, R. M. Olson, M. W. Schmidt and M. S. Gordon, J. Comp. Chem. **27**, 353 (2006).*
**[12]** *Gradients of the Exchange-Repulsion Energy in the Effective Fragment Potential Method*, H. Li and M. S. Gordon, Theor. Chem. Accts., **115**, 385 (2006).*
**[13]** *Scalable Implementation Of Analytic Gradients For Second-Order Z-Averaged Perturbation Theory Using The Distributed Data Interface*, C.M. Aikens and M.S. Gordon, J. Chem. Phys., **124**, 014107 (2006).*
**[14]** *Gradients of the Polarization Energy in the Effective Fragment Potential Method*, H. Li, H.M Netzloff, and M.S. Gordon, J. Chem. Phys., **125**, 194103 (2006).*
**[15]** *Reinvestigation of $SiC_3$ with Multi-reference Perturbation Theory*, J. M. Rintelman, M. S. Gordon, G. D. Fletcher, and J. Ivanic, J. Chem. Phys., **124**, 034303 (2006).
**[16]** *Reply to Comment on monotonically decreasing size distributions for one-dimensional Ga rows on Si(100)*, M.A. Albao, M.M.R. Evans, J. Nogami, D. Zorn, M.S. Gordon, and J.W. Evans, Phys. Rev. B, 74, 037402 (2006).
**[17]** *Electrostatic Energy in the Effective Fragment Potential (EFP) Method. Theory and Application to Benzene Dimer*, L. Slipchenko and M.S. Gordon, J. Comp. Chem., 28, 276 (2007)
**[18]** *Theoretical Study of the Pyrolyisis of Methyltrichlorosilane in the Gas Phase. I. Thermodynamics*, Y. Ge, M.S. Gordon, F. Battaglia, and R.O. Fox, J. Phys. Chem., A111, 1462 (2007).
**[19]** *Theoretical Study of the Pyrolyisis of Methyltrichlorosilane in the Gas Phase. II. Reaction Paths and Transition States*, Y. Ge, M.S. Gordon, F. Battaglia, and R.O. Fox, J. Phys. Chem., A111, 1475 (2007).
**[20]** *Multiterminal Nanowire Junctions of Silicon: A Theoretical Prediction of Atomic Structure and Electronic Properties*, P.A. Avramov, L.A. Chernozatonskii, P.B. Sorokin, and M.S. Gordon, Nano Letters, 7, 2063 (2007).
**[21]** *Breaking Bonds with the Left Eigenstate Completely Renormalized Coupled Cluster Method*, Y. Ge, M.S. Gordon, and P. Piecuch, J. Chem. Phys., J. Chem. Phys., 127, 174106 (2007).
**[22]** *Polarization Energy Gradients in Combined Quantum Mechanics, Effective Fragment Potential and Polarizable Continuum Model Calculations*, H. Li and M.S. Gordon, J. Chem. Phys., 126, 124112 (2007).*
**[23]** *Accurate ab initio potential energy curve of $F_2$. I. Non-relativistic full valence CI energies by the CEEIS method*, L. Bytautas, T. Nagata, M. S. Gordon, and K. Ruedenberg, J. Chem. Phys., 127, 164317 (2007).
**[24]** *Accurate ab initio potential energy curve of $F_2$. II. Core-valence correlations, relativistic contributions and long-range interactions, Core-valence correlations, relativistic contributions and long-range interactions*, L. Bytautas, N. Matsunaga, T. Nagata, M. S. Gordon, and K. Ruedenberg, J. Chem. Phys., 127, 204301 (2007).
**[25]** *Accurate ab initio potential energy curve of $F_2$. III. The Vibration rotation spectrum*, L. Bytautas, N. Matsunaga, T. Nagata, M. S. Gordon, and K. Ruedenberg, J. Chem. Phys., 127, 204301 (2007).
**[26]** *Atomic and electronic structure of new hollow-based symmetric families of silicon nanoclusters*, P.V. Avramov, D.G, Fedorov, P.V. Sorokin, L.A. Chernozatonskii, and M.S. Gordon, J. Phys. Chem C, 111, 18824 (2007).
**[27]** *An Interpretation of the Enhancement of the Water Dipole Moment Due to the Presence of Other Water Molecules*, D. D. Kemp and M.S. Gordon, J. Phys. Chem., A112, 4885 (2008).
**[28]** *Modeling π-π interactions with the effective fragment potential method: The benzene dimer and substituents*, T. Smith, L.V. Slipchenko, and M.S. Gordon, J. Phys. Chem. A, 112, 5286 (2008).
**[29]** *Comparison of Nitroaldol Reaction Mechanisms Using Accurate Ab Initio Calculations*, D. Zorn, V. S.-Y. Lin, M. Pruski, and M.S. Gordon, J. Phys. Chem. A, in press.
**[30]** *An Interface Between the Universal Force Field and the Effective Fragment Potential Method*, D. Zorn, V.S.-Y. Lin, M. Pruski and M.S. Gordon, J. Phys. Chem. A, in press.
**[31]** *Breaking bonds of open-shell species with the restricted open-shell size extensive left eigenstate completely renormalized coupled-cluster method*, Y. Ge, M.S. Gordon, P. Piecuch, M. Wloch, and J.R. Gour, J. Chem. Phys., in press.
*Work includes partial support from USDOE Computational Chemistry SciDAC program.

# COMPUTATIONAL NANOPHOTONICS: MODELING OPTICAL INTERACTIONS AND TRANSPORT IN TAILORED NANOSYSTEM ARCHITECTURES

Stephen K. Gray (gray@tcg.anl.gov),[1] Julius Jellinek (jellinek@anl.gov),[1]
George C. Schatz (schatz@chem.northwestern.edu),[2] Mark A. Ratner (ratner@chem.northwestern.edu),[2] Mark I. Stockman (mstockman@gsu.edu),[3] Koblar A. Jackson (jackson@phy.cmich.edu),[4] Serdar Ogut (ogut@uic.edu)[5]

[1]*Chemistry Division, Argonne National Laboratory, Argonne, IL 60439;* [2]*Department of Chemistry, Northwestern University, Evanston, IL 60208;* [3]*Department of Physics and Astronomy, Georgia State University, Atlanta, GA 30303;* [4]*Department of Physics, Central Michigan University, Mt. Pleasant, MI 48859;* [5]*Department of Physics, University of Illinois at Chicago, Chicago, IL 60607*

## PROGRAM SCOPE

We use computational methods to study light interactions with nanosystems. Microscopic studies of electronic, structural and optical properties, and continuum-level electrodynamics studies are involved. A goal is to learn how to confine and manipulate electromagnetic energy on the nanoscale. A wide range of methods is needed, and another goal is to develop a suite of nanophotonics simulation tools. We also work with applied mathematicians and computer scientists in developing algorithms and software with high-performance capabilities.

At a microscopic level, we must understand the mechanisms underlying the assembly of atoms into clusters and clusters into larger systems. Understanding these mechanisms and the parameters they depend on is essential for designing cluster-based architectures with desired nanophotonics properties. Atomic-level mechanisms are ultimately defined by interatomic interactions. Accurate, efficient descriptions of these interactions are sought in order to uncover correct mechanisms. This work also provides optical information, e.g. static and dynamic polarizabilities, for the estimation of size-dependent dielectric properties relevant to our electrodynamics work.

The electromagnetic fields that result when light interacts with nanostructures are predicted with computational electrodynamics. We seek to develop and apply theory and computational methods that enable a quantitative description of metallic nanostructures and, from this, understanding of the physical phenomena that are taking place.

## RECENT PROGRESS

*Microscopic Electronic, Structural and Optical Properties*: We continued work on construction of more accurate, yet computationally efficient, many-body potentials for metals. Our emphasis is on making these potentials more adequate in the finite-size regime. This is central for performing reliable large-scale dynamical simulations of nanoassembly relevant to nanophotonics. In collaboration with M. J. Lopez (Univ. of Valladolid), we used the developed potentials for Ni, Ag, Au, Al, Cu, and Pt to explore structural and thermal properties of clusters over a broad range of sizes. Current analysis focuses on understanding element-specific trends in these properties as defined by the ranges of the attractive and repulsive parts of the potentials. Work is also in progress on the development of a new potential for Pd.

We continued DFT-based work on the development and application of a new methodology for atomic-level analysis of dipole moments and polarizabilities of finite systems. The central feature is a partitioning of the system volume into atomic volumes and analyzing charge densities within these volumes, as well as changes in these densities in response to a static external electric field [24]. Atomic volumes are defined as Voronoi cells for homogeneous (one-component) systems

and we apply the Hirschfeld (or "stockholder") recipe for heterogeneous (e.g., two-component) systems [41].

We first applied this methodology to Si clusters [8, 24]. Sodium clusters, $Na_n$, n=2-20 [25, 42] and, recently, $Na_n$, n=21-30, as well as heterogeneous $Si_nH_m$ clusters ranging in size and composition from $SiH_4$ to $Si_{35}H_{36}$ were studied [41]. We characterized the site-, size-, and shape-dependence of the resulting polarizabilities. An interesting finding for $Na_n$ is that whereas the dipole part of the total cluster polarizability (a measure of a dielectric type of response [24]), evaluated on a per atom basis, decreases smoothly with cluster size, the corresponding charge-transfer part (a measure of a metallic type of response [24]), shows only modest and nonmonotonic size-variations that are explained through the size-dependence of the cluster structure/shape. The charge transfer part is already close to the polarizability of bulk Na at the level of $Na_{20}$. Similar trends were found in K, Cu, and Ag clusters. In bulk metals the polarizability is entirely due to charge transfer. Our observation suggests that even in small metallic clusters the charge-transfer response to an external electric field is similar to that in bulk metals when evaluated on a per atom basis.

We studied $Si_nH_m$ systems representing hydrogen-terminated Si clusters [41]. We analyzed the separate roles of the surfaces and interiors of these quantum-dot-like systems in defining their overall polarizability and its partitioning into the dipole and charge-transfer components. We find that atoms in the surface and near-surface parts of the clusters are the ones that are primarily responsible for the charge-transfer component, whereas both surface and interior atoms contribute to the dipole component. Therefore, the main contribution to the total polarizability comes from the exterior parts of the clusters. Removal of the terminating H atoms results in an increase of the polarizability of the surface Si atoms and, consequently, of the overall polarizability. The polarizability of the pure Si clusters on a per atom basis is larger than the bulk Si polarizability, and the bulk value is slowly approached as the clusters grow in size.

We also investigated $Si_nH_m$ quantum dots that form Si shells with a cavity inside, and the H atoms terminating the Si atoms in the outer and inner surfaces of the shells. We examined the quasiparticle gap (the difference between electron affinity and ionization potential) and the unscreened exciton binding energy. An empirical model based on the single-band effective mass approximation for impenetrable nanoshells predicts that the quasiparticle gap should depend only on the thickness $t=R_2-R_1$ of the nanoshell and scale as $t^{-2}$. Based on our first-principles ΔSCF computations, we find that it, in fact, depends on both $R_1$ and $R_2$. Another interesting finding is that the unscreened exciton Coulomb energy (as evaluated both perturbatively from first principles and analytically in the effective mass approximation) decreases as the nanoshell becomes more confining (i.e., the radius of its inner shell increases while that of its outer shell is kept constant). We showed that this result is a consequence of the increase in the average electron-hole distance, which gives rise to reduced Coulomb interaction.

We continued to explore the optical properties of noble metal clusters [28, 43]. We performed an extensive TDLDA study of the optical absorption spectra of $Ag_n$, n=10-20[43]. For each cluster size, we considered its three lowest energy isomeric forms and computed spectra for all of them. We found that *d*-electrons play an important role in optical transitions (70-80%) even at low energies. We were able to explain all the computed spectra in terms of the classical Mie-Gans theory, using the dielectric function of bulk Ag and taking into account the isomer shapes. This is surprising because the clusters have dimensions in the sub-nanometer range and would at first glance be considered too small for Mie-Gans theory. Our computed spectra are in excellent agreement with measured data.

Methodological developments included clarification of the subtleties that define the comparative accuracy of two approaches used to compute electronic and optical excitations, namely the GW Bethe-Salpeter (GWBS) formalism and the TDLDA framework [44]. A comparative study was performed on $Ag_n$, n=1-8, clusters. We found that although the GWBS formalism, applied with a pseudopotential that incorporates the *d*-electrons in the core, gives accurate values of the ionization potentials and electron affinities where the relevant orbitals are largely *sp* in character, it does not give good results for optical transitions where the *d*-electrons play a role by screening the *s*-electrons. The TDLDA approach is more robust in this respect. For more accurate reproduction of the optical spectra, the GWBS formalism requires a pseudopotential derived with the semi-core 4*s* and 4*p* states taken into account explicitly.

*Electrodynamics*: We worked on developing a theory which combines electronic structure methods and electrodynamics methods [45] so that we can describe the spectroscopy of molecules that interact with metal particles. In addition, we continue to develop the algorithms and software associated with computational electrodynamics [46, 47], and we completed several projects with our discrete dipole approximation (DDA) and finite-difference time-domain (FDTD) codes. We highlight a few of these projects.

We continue to be interested in the interpretation of surface enhanced Raman scattering (SERS) experiments [48] and very recently we used our electrodynamics methods in a collaboration with Hupp to describe the encapsulation of Ag nanoparticles by $TiO_2$ for applications in dye-sensitized solar cells [49].This work demonstrated that relatively thin films provide a pin-hole free coating for which there are enhanced electromagnetic fields outside the $TiO_2$ surface.

We also examined the scattering spectra of pyramidal-shaped Au nanoparticles that are made using a soft-lithography method [50]. We showed that, in addition to the expected TE mode resonances, an unusual TM resonance occurs that can be used as a switch due to sensitivity of this resonance intensity to small changes in particle structure [50].

A major direction was to model experiments on light transmission through thin Au films that contain arrays of nanoholes [33, 34]. A variety of possible electromagnetic excitations can occur, including Bloch-wave surface plasmon polaritons (SPPs), Rayleigh anomalies (RAs) and localized surface plasmons, that leaded so structured transmission spectra. In collaboration with the Odom experimental group, we identified a particularly sensitive transmission resonance which is a combination of an SPP excitation on one side of a Au film and a RA excitation on the other side. We showed that the RA-SPP transmission resonance has very high sensitivity to the local refractive index on either side of the film, and because it is so narrow, it provides an excellent target for the development of chemical sensors that measure index of refraction changes. Although this special feature in the transmission spectra was initially discovered in the experiments, it was only as a result of the theoretical analysis that the origin of the effect was revealed, and subsequently FDTD calculations were used to optimize the effect for choices of index of refraction that are of relevance to chemical sensing.

In collaboration with experimentalists from Troyes, we explored a "non-invasive" procedure for imaging near-fields [51]. Polymers doped with certain azobenzene molecules can respond to the intense near-fields around nanoparticles. When a nanoparticle system is coated with a thin layer of such a polymer and exposed to light of appropriate wavelength, the polymer surface distorts where the near-fields are high. After exposure the surface topography can measured with atomic force microscopy. Our detailed FDTD and DDA calculations of the near-fields correlated very well with a picture of rapid trans-cis-trans isomerizations of the azobenzene molecules occurring that leads to molecular transport away from electromagnetic hot spots, i.e. our calculated field

intensities were high where the surface topography exhibited a dip. Thus, roughly speaking, the surface topography represents a negative image of the near-field intensity. Other applications of near-field imaging that we have done [35] involved the use of intense laser fields to induce etching of a silica surface that supports metal nanoparticles at the locations of electromagnetic hot spots associated with the particles. This provides complimentary information to the polymer experiments, but is restricted to etchable substrates, and only describes the "hottest" of the near-field components.

**FUTURE PLANS**

The work on more accurate metal potentials will expand to include new elements and bimetallic systems. Potentials for metal particle-support interactions will also be developed. These potentials will be used in large-scale dynamical simulations of cluster-based nanoassembly on supports. The aim is to understand and characterize the mechanisms governing the assembly processes as a function of the cluster material and size, as well as the material, morphology, and temperature of the support. Such an understanding is the prerequisite of rational design and eventual assembly of nanoarchitectures with desired characteristics.

We will continue our DFT studies of structural, electronic, and optical properties of homogeneous and heterogeneous nanosystems. Our recent exploration of structural and electronic features of Cu clusters [1] will be extended to their optical properties. The same is true for medium size Au clusters, for which we found hollow cage and compact conformations that are energetically competitive [5]. Explorations of optical properties will also include compact and nanoshell $Si_nH_m$ quantum dots. Additional systems that will be considered are alloy particles and metal particles deposited on supports (e.g., transition metal clusters on $TiO_2$ surfaces). The issues here are the effects of the composition and of the support on the structural, electronic and optical characteristics.

We will continue to develop and apply our new methodology for atomic-level analysis of finite system response properties. Applications will involve various homogeneous and inhomogeneous clusters and nanoparticles, including those of alloys. We will develop an understanding of the role of composition as another "knob" for tuning the dipole and polarizabilty features of different nanoscale systems to desired characteristics. Methodological developments will include further refinement of the scheme as a tool for quantitative characterization of finite-size metallicity and for establishing a correlation between the degree of metallicity of a finite system and its other characteristics. Another methodological development will target the issue of transferability. The task here is to define "site-specific" polarizabilities of small systems (individual atoms or groups of atoms) that are transferable between large systems containing the small system as a part, when the "site" of the small system as defined by its local bonding environment in these various larger systems is the same or similar. Such transferable polarizabilities will lead to efficient models of total polarizability for systems of large sizes and arbitrary shapes. The methodological work will also include formulation of a more robust GWBS theory capable of treating *s*-, *p*-, and *d*-electrons on equal footing without the explicit inclusion of semi-core states.

Regarding our electrodynamics simulations, we will expand our simulations capabilities by further developing and applying a frequency-domain finite element approach [47] that complements our existing DDA and FDTD capabilities and allows accurate predictions of near-field intensities. New applications to the excitation of clusters of nanoparticles via both ordinary light and point dipole excitation consistent with an emitting molecule, and to particle and hole arrays of relevance to chemical sensing and SERS are planned. This latter work will be in close collaboration with ongoing experimental work. Finally, building on our work concerning molecular interactions with plasmons [45, 51] we will couple our electrodynamics approaches

with molecular electronic structure theory in order to explore the potential of surface plasmon enhanced chemistry.

**PUBLICATIONS OF DOE SPONSORED RESEARCH (2006-2008)**


1. Structure and shape variations in intermediate size copper clusters, M. L. Yang, K. A. Jackson, C. Koehler, T. Frauenheim, and J. Jellinek, *J. Chem. Phys*. **124**, 024308 (2006) [6 pages].
2. First-principles study of intermediate size silver clusters: Shape evolution and its impact on cluster properties, M. Yang, K. A. Jackson, and J. Jellinek, J. *Chem. Phys*.**125**, 144308 (2006) [6 pages].
3. Structural evolution of anionic silicon clusters $Si_N$ ($20 \leq N \leq 45$), J. Bai, L.-F. Cui, J. Wang, S. Yoo, X. Li, J. Jellinek, C. Koehler, T. Frauenheim, L.-S. Wang, and X. C. Zeng, *J. Phys. Chem. A* **110**, 908-912 (2006).
4. Density-functional study of small and medium-sized $As_n$ clusters up to n = 28, J. Zhao, X. Zhou, X. Chen, J. Wang, and J. Jellinek, *Phys. Rev. B* **73**, 115418 (2006) [10 pages].
5. Dipole polarizabilities of medium-sized gold clusters, J. Wang, M. Yang, J. Jellinek, and G. Wang, *Phys. Rev. A* **74**, 023202 (2006) [5 pages].
6. Structural, electronic, and optical properties of noble metal clusters from first principles, S. Ogut, J. C. Idrobo, J. Jellinek, and J. Wang, *J. Clust. Sci.*, **17**, 609-626 (2006).
7. First principles absorption spectra of medium-sized Si clusters: Time-dependent local density approximation versus predictions from Mie theory, J. C. Idrobo, M. Yang, K. A. Jackson and S. Ogut, *Phys. Rev. B*, **74**, 153410 (2006) [4 pages].
8. Site-specific polarizabilities: Probing the atomic response of silicon clusters to an external electric field, K. Jackson, M. Yang, and J. Jellinek, in *Lecture Series in Computer and Computational Sciences*, Vol. 6, G. Maroulis and T. Simos, Eds., Brill, Leiden, 2006, pp. 165-176.
9. Multiple plasmon resonances in gold nanorods, E. K. Payne, K. L. Shuford, S. Park, G. C. Schatz and C. A. Mirkin, *J. Phys. Chem. B* **110**, 2150-2154 (2006).
10. Manipulating the optical properties of pyramidal nanoparticle arrays, J. Henzie, K. L. Shuford, E.-S. Kwask, G. C. Schatz and T. W. Odom, *J. Phys. Chem. B* **110**, 14028-14031 (2006).
11. Finite-difference time-domain studies of light transmission through nanohole structures, K. L. Shuford, Mark A. Ratner, S. K. Gray and G. C. Schatz, *Appl. Phys. B* **84**, 11-18 (2006).
12. Apertureless scanning near-field optical microscopy: a comparsion between homodyne and heterodyne approaches, L. Gomez, R. Bachelot, A. Bouhelier, G. P. Wiederrecht, S.-H. Chang, S. K. Gray, G. Lerondel, F. Hua, S. Jeon, J. A. Rogers, M. E. Castro, S. Blaize, I. Stephanon, and P. Royer, *J. Opt. Soc. Am. B* **23**, 823-833 (2006).
13. Error signal artifact in apertureless scanning near-field optical microscopy, L. Billot, M. Lamy de la Chapelle, D. Barchiesi, S.-H. Chang, S. K. Gray, J.A. Rogers, A. Bouhelier, P.-M. Adam, J.-L. Bijeon, G. P. Wiederrecht, R. Bachelot, and P. Royer, *Appl. Phys. Lett.* **89**, 023105 (2006) [3 pages].
14. A computational study of the interaction of light with silver nanowires of different eccentricity, J. M. Oliva and S. K. Gray, *Chem. Phys. Lett.* **427**, 383-389 (2006).
15. Fourier spectral simulations and Gegenbauer reconstructions for electromagnetic waves in the presence of a metal nanoparticle, M. S. Min, T.-W. Lee, P. F. Fischer, and S. K. Gray, *J. Comp. Phys*. **213**, 730-747 (2006).
16. Ultrafast pulse excitation of a metallic nanosystem containing a Kerr nonlinear material, X. Wang, G. C. Schatz, and S. K. Gray, *Phys. Rev. B*, **74**, 195439 (2006) [5 pages].
17. Quantitative multispectral biosensing and 1D imaging using quasi-3D plasmonic crystals, M. E. Stewart, N. H. Mack, V. Malyarchuk, J. A. N. T. Soares, T.-W. Lee, S. K. Gray, R. G. Nuzzo, and J. A. Rogers, *Proc. Nat. Acad. Sci. (USA)* **103**, 17143-17148 (2006).
18. Geometry dependent features of optically induced forces between silver nanoparticles, V. Wong and M. A. Ratner, *J. Phys. Chem. B* **110**, 19243-19253 (2006).
19. Generation of traveling surface plasmon waves by free-electron impact, M. V. Bashevoy, F. Jonsson, A. V. Krasavin, N. I. Zheludev, Y. Chen, and M. I. Stockman, *Nano Lett.* **6**, 1113-1115 (2006).
20. Slow Propagation, Anomalous Absorption, and Total External Reflection of Surface Plasmon Polaritons in nanolayer systems, M. I. Stockman, *Nano Lett.* **6**, 2604-2608 (2006).
21. M. Stockman, in Topics in Applied Physics, edited by K. Kneipp, M. Moskovits and H. Kneipp, *Electromagnetic Theory of SERS* (Springer Verlag, 2006), p. 47-66.

22. Reply to comment on self-similar chain of metal nanospheres as an efficient nanolens, K. Li, M. I. Stockman, and D. J. Bergman, *Phys. Rev. Lett.* **97**, 079702 (2006).
23. Octupolar metal nanoparticles as optically driven, coherently controlled nanorotors, M. I. Stockman, K. Li, S. Brasselet, and J. Zyss, *Chem. Phys. Lett.* **433**, 130–135 (2006).
24. Site-specific analysis of dielectric properties of finite systems, K. A. Jackson, M. Yang, and J. Jellinek, *J. Phys. Chem. C* **111**, 17952-17960 (2007) (R. E. Smalley Memorial Issue).
25. Site-specific analysis of response properties of Na clusters, K. A. Jackson, M. Yang and J. Jellinek, in *Latest Advances in Atomic Cluster Collisions: Structure and Dynamics from Nuclear to the Biological Scale*, Eds. J.-P. Connerade and A. V. Solov'yov, Imperial College Press, London, 2008, pp. 72-86.
26. First-principles isomer-specific absorption spectra of $Ag_{11}$, J. C. Idrobo, S. Ogut, K. Nemeth, J. Jellinek, and R. Ferrando, *Phys. Rev. B* **75**, 233411 (2007) [4 pages].
27. Gold-coated transition metal anion $[Mn_{13}@Au_{20}]^-$ with ultrahigh magnetic moment, J. Wang, J. Bai, J. Jellinek, and X. C. Zeng, *J. Am. Chem. Soc.* **129**, 4110-4111 (2007). (Communication).
28. Static Polarizabilities and Optical Absorption Spectra of Gold Clusters ($Au_n$, n=2-14 and 20) from First Principles, J. C. Idrobo, W. Walkosz, S. F. Yip, S. Ogut, J. Wang, and J. Jellinek *Phys. Rev. B* **76**, 205422 (2007) [12 pages].
29. Heterodyne apertureless near-field scanning optical microscopy on periodic gold nanowells, J. F. Hall, G. P. Wiederrecht, S. K. Gray, S.-H. Chang, S. Jeon, J. A. Rogers, R. Bachelot, and P. Royer, *Opt. Express* **15**, 4098-4105 (2007).
30. Computational study of fluorescence scattering by silver nanoparticles, M. H. Chowdhury, S. K. Gray, J. Pond, C. D. Geddes, K. Aslan, and J. R. Lakowicz, *J. Opt. Soc. Am. B* **24**, 2259-2267 (2007).
31. Multigrid FDTD with Chombo, Z. Meglicki, S. K. Gray, and B. Norris, *Comp. Phys. Comm.* **176**, 109-120 (2007).
32. Electric field enhancement and light transmission in cylindrical nanoholes, K. L. Shuford, M. A. Ratner, S. K. Gray, and G. C. Schatz, *J. Comp. Theor. Nanoscience* **4**, 1-8 (2007).
33. Tailoring the sensing capabilities of nanohole arrays in gold films with Rayleigh anomaly-surface plasmon polaritons. J. M. McMahon, J. Henzie, T. W. Odom, G. C. Schatz, and S. K. Gray, *Opt. Express* **15**, 18119-18129 (2007).
34. Tailoring the parameters of nanohole arrays in gold films for sensing applications, G. C. Schatz, J. M. McMahon, and S. K. Gray, *Proc. SPIE-Int. Soc. Opt. Eng.* **6641**, 664103(2007) [8 pages].
35. Optical near-fields of triangular nanostructures, J. Boneberg, J. Koenig-Birk, H. J. Muenzer, P. Leiderer, K. L. Shuford, and G. C. Schatz, *Appl. Phys. A* **89**, 299-303 (2007).
36. Surface plasmon enhanced spectroscopy and photochemistry, S. K. Gray, Plasmonics **2**, 143-146 (2007).
37. Optical properties of rod-like and bipyramidal gold nanoparticles, M. Liu, P. Guyot-Sionnest, T.-W. Lee, and S. K. Gray, *Phys. Rev. B* **76**, 235428 (2007) [10 pages].
38. Toward full spatio-temporal control on the nanoscale, M. Durach, A. Rusina, K. Nelson, and M. I. Stockman, *Nano Lett.* **7**, 3145-3149 (2007).
39. Criterion for negative refraction with low optical losses from a fundamental principle of causality M. I. Stockman, , *Phys. Rev. Lett.* **98**, 177404 (2007) [4 pages].
40. Attosecond Nanoplasmonic Field Microscope, M. I. Stockman, M. F. Kling, U. Kleineberg, and F. Krausz, *Nature Photonics* **1**, 539-544 (2007).
41. Atomistic Description of electric dipole polarizability in $Si_nH_m$. S. Srinivas, M. Yang, K. A. Jackson and J. Jellinek, in *Computational Methods in Science and Engineering*, AIP Press, *in press*, 2008.
42. Atomistic dipole moments and polarizabilities of $Na_N$ clusters, N= 2-20. K. Jackson, L. Ma, M. Yang and J. Jellinek, *J. Chem. Phys. in press*, 2008.
43. Optical absorption spectra of intermediate size silver clusters from first principles, K. Baishya, J. C. Idrobo, S. Ogut, M. Yang, K. Jackson and J. Jellinek, *Phys. Rev. B* **78**, 075439 (2008) [9 pages].
44. Comparison of time-dependent density functional theory and gw-bethe-salpeter equation methods for optical excitations in $Ag_n$ (n=1-8) Clusters, M. Tiago, J. C. Idrobo, S. Ogut, J. Jellinek and J. R. Chelikowsky *Phys. Rev. B* (*submitted*).
45. Many-body theory of surface-enhanced Raman scattering, D. J. Masiello and G. C. Schatz, *Phys. Rev. A, submitted*, 2008.
46. A discrete action principle for electrodynamics and the construction of explicit symplective integrators, J. M. McMahon, S. K. Gray, and G. C. Schatz, *J. Comp. Phys., submitted*, 2008.

47. Methods for describing the electromagnetic properties of anisotropic silver and gold nanoparticles, J. Zhao, A. O. Pinchuk, J. M. McMahon, S. Li, K. L. Ausman, A. L. Atkinson, and G. C. Schatz, *Accts. Chem. Res. in press*, 2008.
48. Surface plasmon-mediated energy transfer in hetero-gap Au-Ag nanowires, W. Wei, S. Li., L. Qin, C. Xue, J. E. Millstone, X. Xu, G. C. Schatz, and C. A. Mirkin, Millstone, J. E.; Xu, X.; Schatz, G. C.; Mirkin, *Nano Lett., in press*, 2008.
49. Protection of silver nanoparticles using atomic layer deposition of $TiO_2$, G. C. Standridge, G. C. Schatz, and J. T. Hupp, *Langmuir, submitted*, 2008.
50. Optical properties of gold pyramidal shape nanoshells, K. L. Shuford, J. Lee, T. W. Odom, and G. C. Schatz, *J. Phys. Chem. C* **112**, 6662-6666 (2008).
51. Near-field polarization effects in molecular-motion-induced photochemical imaging. C. Hubert, R. Bachelot, J. Plain, S. Kostechhv, G. Lerondel, M. Juan, P. Royer, S. Zou, G. C. Schatz, G. P. Wiederrecht, and S. K. Gray, *J. Phys. Chem. C* **112**, 4111-4116 (2008).
52. Nanostructured plasmonic sensors, M. E. Stewart, C. R. Anderton, L. B. Thompson, J. Maria, S. K. Gray, J. Rogers, and R. G. Nuzzo, *Chem. Rev.* **108**, 494-521 (2008).
53. Exciting surface plasmon polariton propagtion lengths via coupling to asymmetric waveguide structures, J. M. Montgomery and S. K. Gray, *Phys. Rev. B* **77**, 125407 (2008) [9 pages].
54. Systematic computational study of the effect of silver nanoparticle dimers on the coupled emission from nearby fluorophores, M. H. Chowdhury, J. Pond, S. K. Gray, and J. R. Lakowicz, *J. Phys. Chem. C* **112**, 11236-11249 (2008).
55. Theory and modeling of light interactions with metallic nanostructures, J. M. Montgomery, T. W. Lee, and S. K. Gray, *J. Phys. Cond. Matt.* **20**, 323201 (2008) [11 pages].
56. Seeing molecules by eye: Surface plasmon resonance imaging at visible wavelengths with high spatial resolution and submonolayer sensitivity, J. M. Yao, M. E. Stuart, J. Maria, T. W. Lee, S. K. Gray, J. A. Rogers, and R. G. Nuzzo, *Angew. Chem. Int. Ed.* **47**, 5013-5017 (2008).
57. Electrodynamic effects in plasmonic nanolenses, J. H. Dai, F. Cajko, I. Tsukerman, and M. I. Stockman, *Phys. Rev. B* **77**, 115419 (2008) [5 pages].
58. Highly efficient spatiotemporal control of nanoplasmonics on a nanometer-femtosecond scale by time reversal, X. T. Li and M. I. Stockman, *Phys. Rev. B* **77**, 195109 (2008) [10 pages].
59. Optimized nonadiabatic nanofocusing of plasmons by tapered metal rods, D. K. Gramotnev, M. W. Vogel, and M. I. Stockman, *J. App. Phys.* **104**, 034311 (2008) [8 pages].

**Acknowledgment:** Work at Argonne National Laboratory was supported by the U.S. Department of Energy, Office of Basic Energy Sciences, Division of Chemical Sciences, Geosciences, and Biosciences under DOE Contract No. DE-AC02-06CH11357.

# Dynamics of Electrons at Interfaces on Ultrafast Timescales

Charles B. Harris P.I.
Chemical Sciences Division
Lawrence Berkeley National Lab
1 Cyclotron Road, Mail Stop Latimer
Berkeley, CA 94720
CBHarris@berkeley.edu

## Program Scope

The research funded under this program is aimed at understanding the energetics and lifetimes of electrons at molecule/metal interfaces on the femtoseconds timescale. We are interested in electronic behavior in molecular adlayers of thicknesses ranging from sub nanometer to tens of nanometers. These length and time scales are the natural scales for a wide range of electronic behavior, including interfacial band structure, band bending, Fermi level pinning, charge localization, polaron formation, and morphologies imposed by a metal/molecule junction.

In order to study such complex systems, we employ time and angle resolved two photon photoemission (2PPE). Generally, we use either a visible or ultra violet femtosecond pulse to promote an electron at the interface into an excited state. For wide band gap systems, it is typically a UV pulse which excites an electron from the valence band of Ag(111) into an interfacial state. For many organic semiconductors, a visible pulse is used to promote either charge transfer from the metal to the molecule, or an on molecule excitation. After some time, $\Delta t$, a second laser pulse impinges upon the interface and photoemits the excited electron. We then measure the kinetic energy of these photoelectrons using a home built time of flight detector. By altering the wavelength of the laser pulses, we can determine the binding energy of the photoelectron, as well as whether the state was initially occupied or not.

Not only does 2PPE provide information about the energetic distribution of both unoccupied and occupied electronic states at interfaces, but it also reveals the kinetics of population decay and dynamical energy shifts. Our energetic resolution of 35 meV and temporal resolution of 50 fs allows us to follow two dimensional solvation in real time. Furthermore, by varying the sample angle with respect to our detector, we can pick out individual momentum slices parallel to the surface. Combining our angular resolution with our temporal resolution, we can follow the two dimensional band structure of excited electronic states, and directly observe events such as polaron formation and exciton relaxation.

We are using this technique to study two primary classes of electronic behavior. Firstly, we are studying the response of small molecules adsorbed at metal surfaces to excess charge. Image potential states are a class of metal derived states, which have been shown via their surface proximity to behave as good sensors of adsorbate electronic and nuclear motion. Secondly, we are studying the barriers to and lifetimes of electronic excitations organic semiconductor / metal interfaces.

## Recent Progress

*Morphology-dependent Photo-conductivity of Organic Semiconductors* : Photoconductivity in organic semiconductors has garnered considerable research attention in the search for sustainable energy sources. In particular, the factors for consideration in optimizing these devices, which include the efficiency of photogeneration and the carrier dynamics at an interface, merit a close investigation of the physical chemistry at the interface. Using 2PPE, we have probed the dynamics of charge carriers at the interface of Ag(111) and PTCDA, a widely-studied planar aromatic hydrocarbon. By varying the morphology of the surface, we have quantitatively examined the role of crystallinity versus structural disorder in affecting the carrier dynamics and

electronic structure at an interface. High substrate temperatures (> 400 K) cause the growth of a wetting layer with islands, and the exposed wetting layer inhibits the evolution of the vacuum level and valence band to bulk PTCDA values. In the layer-by-layer growth of low substrate temperatures, we observe the transition of molecular state energies from monolayer to bulk values. Effective masses of the conduction band and the $n = 1$ image potential state varied from 2.1 *me* and 1.4 *me*, resp., in disordered PTCDA layers to 0.5 *me* and 1.1 *me* in the most crystalline layers. Decay constants were obtained for electrons excited into the conduction band and into image potential states at different layer thicknesses and morphologies. Decay constants for the LUMO in crystalline systems were mediated by electron transfer back to the surface and were on the order of 100 fs, whereas layer-by-layer amorphous growth resulted in exponential decays with time constants of picoseconds present in films thicker than ~ 7 monolayers.

DMSO : In electrochemically relevant systems, interfacial capacitance affects electrochemical signal collection and heterogeneous charge transfer. At noble metal electrodes, dimethyl sulfoxide (DMSO), a common electrochemical solvent, exhibits an uncharacteristically low interfacial capacitance of 7–10 µF/cm2 over a 1.5 V range which includes the potential of zero charge. This stands in contrast to similar, polar, high-dielectric constant electrochemical solvents, e.g., 50 µF/cm2 for acetonitrile under identical experimental conditions. Si and Gewirth have proposed that hindered rotation of the DMSO dipole at the surface lowers its interfacial capacitance and reduces the response of interfacial DMSO to changes in potential [1]. We directly tested this hypothesis with 2PPE by modeling the injected electron as a planar charge outside a capacitive layer. We measured a much weaker solvation response in a monolayer than multilayer coverages, which we attribute to hindered dipole rotation in the monolayer. The solvation responses are then interpreted as a comparison of the dielectric response of the monolayer with those of various multilayer coverages.

Thiophene: Thiophene is the basic building block of a host of oligomers used in organic solar cells and light emitting diodes. We have investigated the bonding and electronic structure of this important monomer bonded to Ag(111). Using temperature programmed desorption, we have observed two physisorbed structures for the monolayer adsorbate in agreement with previous literature. The most strongly bound layer is a low density layer with its pi network parallel to the surface. Electrons in both the LUMO and IPS in this layer are strongly influenced by the underlying substrate, and have electron effective masses of 1. At colder temperatures, a higher density tilted layer exists. This slightly decouples the pi network from the valence electrons of the metal, resulting in a 40% increase in the effective mass of excited electrons. This sensitivity to orientation is being used help understand electronic couplings in larger thiophene oligamer systems.

**Continuing and Ongoing Work**

Phthalocyanines: Molecular semiconductor research has extensively utilized phthalocyanines due to their high mobility, tunable bandgap and Farmi level, and variable (p- or n- type majority charge carrier properties. Preliminary 2PPE studies focused on titanyl phtalocyanine (TiOPc), a common derivative with a strong dipole through the metal-oxide center. The strong dipole and poor ordering of this molecule are thought to limit its conductivity through charge trapping events. Initial 2PPE work was able to identify two sets of LUMO energy levels, which compare well to inverse photoemission studies[2]. These unoccupied levels were found to overlap very strongly with the s-p bands of silver and thus had ultrashort (<20fs) lifetimes past 5 monolayers; decay to the metal is thus kinetically favorable to either charge trapping events or small polaron formation. Molecular disorder prevented resolving peaks with thicker films. Further the low position of the LUMO with respect to the Fermi level prevented characterization of either the LUMO or the HOMO-LUMO exciton. This study is continuing while trying to characterize the

hole transporting copper phthalocyanine and electron transporting copper hexadecafluorophthalocyanine. These two molecules have some of the highest mobilities and are well utilized in device research. Their increased packing order and an energetically higher LUMO level should allow the LUMO band to be observed, and spectra may be resolvable at thicker coverage, where there will be weaker metal-molecule coupling. This investigation also aims to study changes in the HOMO-LUMO exciton electron near the metal surface.

Thiophene Oligamers: Current studies are extending our work studying the thiophene monomer to the tetramer, seximer, and octamer. The evolution of the bandgap in thiophene systems is known to approach that of polythiophene by between 6 and 8 thiophene units. Moreover, sexithiophene is the oligamer most commonly studied as a model for the polymer. We are currently mapping the evolution of the HOMO, LUMO and surface states that exist at the metal / oligamer interface. For both quaterthiophene and sexithiophene, the LUMO and LUMO +1 have been identified. Interestingly, for layers as thick as 4 monolayers, no interband coupling or polaron formation has been observed. Rather, intraband coupling to the metal has proven to be the fasted decay mechanism, indicating a strong intermixing of molecular orbitals with the metallic valence band. Further studies are aimed at elucidating the nature of this coupling, and determining the band structure beyond this highly coupled regime.

Room-temperature ionic liquids (RTIL's): RTIL's are a relatively new class of potentially useful compounds for synthesis and electrochemistry. An array of physical investigations has been stimulated by these highly unusual solutions composed completely of ions. The solvation behavior of RTIL's has been studied by multiple groups in bulk solution, and controversy remains over the nature of solvation at ultrafast timescales [3]. Energy relaxation of the image potential state in RTIL ultrathin films is currently being investigated to elucidate solvation behavior. Unlike most small molecules, ionic liquids remain in the liquid phase even at a metal surface in ultra high vacuum. This provides a unique opportunity to study the response of liquid/metal interfaces to excess charge. More specifically, there are questions about the specific nature of charge solvation in these ionic systems. Will charges be solvated by ion translation, or through some charged bi-layer flipping mechanism? We are attempting to answer these questions by studying the moleculue $[bmpyr]^{+}[NTFS]^{-}$. Preliminary work shows a strong temperature dependence to the solvation. We are also investigating the possibility of a 2D phase transition.

**References**

[1] S. K. Si and A. A. Gewirth. "Solvent organization above metal surfaces: Ordering of DMSO on Au." *Journal of Physical Chemistry B*, 104, 10775 (2000).
[2] Murdey, R.; Sato, N.; Bouvet, M. *Mol. Cryst. Liq Cryst.*, **2006**, *455*, 211-218.
[3] H. Cang, J. Li, and M. D. Fayer. "Orientational dynamics of the ionic organic liquid 1-ethyl-3-methylimidazolium nitrate." *Journal of Chemical Physics*, 119, 13017 (2003).

## Articles Supported by DOE funding 2004-2008

[1] K.R. Sawyer, R.P. Steele, E.A. Glascoe, J.F. Cahoon, J.P. Schlegel, M. Head-Gordon, C.B. Harris, "Direct observation of photoinduced bent nitrosyl excited-state complexes" *J. Phys. Chem. A*, ASAP article. Funded by *NSF* using *DOE* equipment.
[2] J.F. Cahoon, M.F. Kling, K.R. Sawyer, L.K. Andersen, C.B. Harris, "DFT and Time-resolved IR Investigation of Electron Transfer between Photogenerated 17- and 19-electron organometallic radicals" *J. Mol. Struct.* (honor issue for F. Albert Cotton), in press. Funded by *NSF* using *DOE* equipment.
[3] K.R. Sawyer, E.A. Glascoe, J.F. Cahoon, J.P. Schlegel, C.B. Harris, "The mechanism of iron-catalyzed alkene isomerization in solution" *Organometallics*, ASAP article. Funded by *NSF* using *DOE* equipment.

[4] J.F. Cahoon, K.R. Sawyer, J.P. Schlegel, C.B. Harris, "Determining Transition-state Geometries in Liquids Using 2D-IR" *Science* **319**, 1820-1823 (2008). Funded by *NSF* using *DOE* equipment.
[5] M.L. Strader, S. Garrett-Roe, P. Szymanski, S.T. Shipman, J.E. Johns, A. Yang, E. Muller, C.B. Harris. "The ultrafast dynamics of image potential state electrons at the dimethylsulfoxide/Ag(111) interface" *J. Phys. Chem. C*, **112**, 6880-6886, (2008).
[6] A. Yang, S.T. Shipman, S. Garrett-Roe, J. Johns, M. Strader, P. Szymanski, E. Muller, C. Harris. "Two-photon photoemission of ultrathin film PTCA morphologies on Ag(111)" *J. Phys. Chem. C*, **112**, 2506-2513, (2008).
[7] E. A. Glascoe, M. F. Kling, J. E. Shanoski, J. R. A. DiStasio, C. K. Payne, B. V. Mork, T. D. Tilley, and C. B. Harris. "Photoinduced beta-hydrogen elimination and radical formation with $CpW(CO)_3(CH_2CH_3)$: Ultrafast IR and DFT studies." *Organometallics*, **26**, 1424 (2007). Funded by *NSF* using *DOE* equipment.
[8] E. A. Glascoe, K. R. Sawyer, J. E. Shanoski, and C. B. Harris. "The influence of the metal spin state in the iron-catalyzed alkene isomerization reaction studied with ultrafast infrared spectroscopy." *J. Phys. Chem. C.*, **111**, 8789 (2007). Funded by *NSF* using *DOE* equipment.
[9] J. F. Cahoon, M. F. Kling, K. R. Sawyer, H. Frei, and C. B. Harris. "19-electron intermediates in the ligand substitution of $CpW(CO)_3$ with a Lewis base." *J. Am. Chem. Soc.*, **128**, 3152 (2006). Funded by *NSF* using *DOE* equipment.
[10] E. A. Glascoe, M. F. Kling, J. E. Shanoski, and C. Harris. "Nature and role of bridged carbonyl intermediates in the ultrafast photoinduced rearrangement of $Ru_3(CO)_{12}$." *Organometallics*, **25**(775) (2006). Funded by *NSF* using *DOE* equipment.
[11] J. E. Shanoski, E. A. Glascoe, and C. Harris. "Ligand rearrangement reactions of $Cr(CO)_6$ in alcohol solutions: Experiment and theory." *J. Phys. Chem. B.*, **110**(996) (2006). Funded by *NSF* using *DOE* equipment.
[12] S. Shipman, S. Garrett-Roe, P. Szymanski, A. Yang, M. Strader, and C. B. Harris. "Determination of band curvatures by angle-resolved two-photon photoemission in thin films of $C_{60}$ on Ag(111)." *J. Phys. Chem. B*, **110**, 10002 (2006).
[13] J. F. Cahoon, M. F. Kling, S. Schmatz, and C. B. Harris. "19-electron intermediates and cage-effects in the photochemical disproportionation of $[CpW—(CO)_3]_2$ with Lewis bases." *J. Am. Chem. Soc.*, **127**(12555) (2005). Funded by *NSF* using *DOE* equipment.
[14] S. Garrett-Roe, S. T. Shipman, P. Szymanski, M. L. Strader, A. Yang, and C. B. Harris. "Ultrafast electron dynamics at metal interfaces: Intraband relaxation of image state electrons as friction." *J. Phys. Chem. B*, **109**, 20370 (2005).
[15] J. E. Shanoski, C. K. Payne, M. F. Kling, E. A. Glascoe, and C. B. Harris. "Ultrafast infrared mechanistic studies of the interaction of 1-hexyne with group 6 hexacarbonyl complexes." *Organometallics*, **24**(1852) (2005). Funded by *NSF* using *DOE* equipment.
[16] P. T. Snee, J. E. Shanoski, , and C. B. Harris. "Mechanism of ligand exchange studied using transition path sampling." *J. Am. Chem. Soc.*, **127**(1286) (2005). Funded by *NSF* using *DOE* equipment.
[17] P. Szymanski, S. Garrett-Roe, and C. B. Harris. "Time- and angle-resolved two-photon photoemission studies of electron localization and solvation at interfaces." *Prog. Surf. Sci.*, **78**, 1 (2005).
[18] I. Bezel, K. J. Gaffney, S. Garrett-Roe, S. H. Liu, A. D. Miller, P. Szymanski, and C. B. Harris. "Measurement and dynamics of the spatial distribution of an electron localized at a metal–dielectric interface." *J. Chem. Phys.*, **120**, 845 (2004).
[19] M. F. Kling, J. F. Cahoon, E. A. Glascoe, J. E. Shanoski, and C. B. Harris. "The role of odd-electron intermediates and in-cage electron transfer in ultrafast photochemical disproportionation reactions in Lewis bases." *J. Am. Chem. Soc.***126** (11414) (2004). Funded by *NSF* using *DOE* equipment.

# Catalysis at Metal Surfaces Studied by Non-Equilibrium and STM Methods

Ian Harrison
Department of Chemistry, University of Virginia
Charlottesville, VA 22904-4319
harrison@virginia.edu

**Program Scope:**

This research program aims to employ non-equilibrium techniques to investigate the nature of the transition states for activated dissociative chemisorption of small molecules on catalytic metal surfaces. Two separate approaches/ideas are under investigation. In the first, we posit that dissociative chemisorption reactions on metal surfaces are primarily surface mediated electron transfer reactions for many hard-to-activate small molecules. Accordingly, the lowest lying affinity levels of these adsorbates, which are accessible by surface photochemistry and scanning tunneling microscopy (STM), will play a key electronic structure role in determining barrier heights for dissociative chemisorption. Electron transfer excitation into these adsorbate affinity levels followed by image potential acceleration towards the surface and rapid quenching may leave the adsorbate in the "transition state region" of the ground state potential relevant to thermal catalysis from where desorption and/or dissociation may ultimately occur. Using low temperature scanning tunneling microscopy (STM) and surface science techniques we have been investigating the thermal, electron, & photon induced chemistry of $CH_3Br$,[1] $CO_2$, and $CH_4$ on Pt(111). The photochemical dissociation and desorption dynamics of $CO_2$ on Pt(111) seem consistent with this kind of "Antoniewicz bounce"[2] chemical activation. In our second approach towards probing surface transition states, we dose hot gas-phase molecules on to a cold surface and measure dissociative sticking coefficients macroscopically[3,4] via Auger electron spectroscopy (AES) or microscopically by imaging chemisorbed fragments via low $T_s$ STM. A local hot spot, microcanonical unimolecular rate theory (MURT) model of gas-surface reactivity[5,6,7] can be used to extract transition state characteristics for dissociative chemisorption. The MURT model has proven useful for understanding, analyzing, and simulating the dynamics of activated dissociative chemisorptions for systems ranging in size from $H_2$ on Cu(111)[8] to $C_2H_6$ on Pt(111),[4] even though mode-specific chemistry is sometimes observed[9-12] and energy transfer with the surface will become increasingly important for larger molecules. An important long-range goal of our research is to microscopically characterize the different transition states for dissociative chemisorption occurring at metal terrace sites as compared to step sites – a goal of long-standing interest to the catalysis and electronic structure theory communities.[13]

**Recent Progress:**

Activated dissociative chemisorption of methane is believed to be rate limiting in the steam reforming of natural gas on Ni catalysts,[14] the process that yields the industrial supply of $H_2$ and synthesis gas. MURT simulations of thermal dissociative sticking coefficients, $S_T$, for $CH_4$ on low index single crystal metal surfaces, based on prior extraction of transition state parameters from analysis of supersonic molecular beam experiments, are several orders of magnitude higher than apparent $S_T$ values derived from turnover rates for $CH_4$ reforming on supported nanocatalysts.[15] It is likely that most of the surface atoms on the nanocatalysts become poisoned or tempered by a build-up of graphitic carbon under the high working temperatures and

pressures of catalysis such that their *macroscopically* averaged reactivity does not accurately characterize the microscopic reactivity at their most active sites. We are working towards using low $T_s$ STM in conjunction with heated effusive molecular beam measurements to *microscopically* characterize the transition states for $CH_4$ dissociation on terraces and at step edges on a Pt(111) surface. Experiments have also begun to employ a new low energy electron microscope (LEEM) at Virginia as a complementary, in situ, means to characterize the high $T_s$ dynamics and reactivity of adsorbed C derived from alkane and olefin dissociative chemisorption.

**Future Plans:**

The ability to surmount barriers for activated gas-surface reactions using energy derived from the incident molecules[16] rather than the surface affords opportunities to react molecules at surface temperatures low enough that (i) reaction products cannot diffuse away from their initial reaction sites and that (ii) nanoscale modifications to the surface are not annealed away. Furthermore, the pressures and dosing requirements to study gas-surface reactions of catalytic interest can be lowered using hot incident molecules. The MURT provides a simple means to analyze these kinds of non-equilibrium experiments and extract transition state characteristics. The technical realization of consistent low $T_s$ STM imaging coupled with heated effusive molecular beam dosing remains our top priority. A new STM head affording isothermal operation has been built and should help in this regard. Our ambition is to explore the site resolved activation of small alkanes, alcohols, and $CO_2$ on a range of catalytic metal surfaces.

**DOE Publications (2005-):**

T.C. Schwendemann, I. Samanta, T. Kunstmann, and I. Harrison, "$CH_3Br$ Structures on Pt(111): Kinetically Controlled Self-Assembly of Dipolar and Weakly Adsorbed Molecules," J. Phys. Chem. C, 1347-1354 (2007).

**References**:


1 T.C. Schwendemann, I. Samanta, T. Kunstmann, and I. Harrison, "$CH_3Br$ Structures on Pt(111): Kinetically Controlled Self-Assembly of Dipolar and Weakly Adsorbed Molecules," J. Phys. Chem. C, 1347-1354 (2007).

2 P.R. Antoniewicz, "Model for Electron- and Photon-stimulated Desorption," Phys. Rev. B **21**, 3811-3815 (1980).

3 K. M. DeWitt, L. Valadez, H. L. Abbott, K. W. Kolasinski, and I. Harrison, "Using effusive molecular beams and microcanonical unimolecular rate theory to characterize $CH_4$ dissociation on Pt(111)," J. Phys. Chem. B **110**, 6705-6713 (2006).

4 K. M. DeWitt, L. Valadez, H. L. Abbott, K. W. Kolasinski, and I. Harrison, "Effusive molecular beam study of $C_2H_6$ dissociation on Pt(111)," J. Phys. Chem. B **110**, 6714-6720 (2006).

5 A. Bukoski, D. Blumling, and I. Harrison, "Microcanonical unimolecular rate theory at surfaces. I. Dissociative chemisorption of methane on Pt(111)," J. Chem. Phys. **118**, 843-871 (2003).

6 H. L. Abbott, A. Bukoski, and I. Harrison, "Microcanonical unimolecular rate theory at surfaces. II. Vibrational state resolved dissociative chemisorption of methane on Ni(100)," J. Chem. Phys. **121**, 3792-3810 (2004).

[7] A. Bukoski, H. L. Abbott, and I. Harrison, "Microcanonical unimolecular rate theory at surfaces. III. Thermal dissociative chemisorption of methane on Pt(111) and detailed balance," J. Chem. Phys. **123**, 094707 (2005).

[8] H. L. Abbott and I. Harrison, "Microcanonical transition state theory for activated gas-surface reaction dynamics: Application to $H_2$/Cu(111) with rotation as a spectator," J. Phys. Chem. A **111**, 9871-9883 (2007).

[9] C. T. Rettner, H. A. Michelsen, and D. J. Auerbach, "Quantum-State-Specific Dynamics of the Dissociative Adsorption and Associative Desorption of $H_2$ at a Cu(111) Surface," J. Chem. Phys. **102**, 4625-4641 (1995).

[10] R. R. Smith, D. R. Killelea, D. F. DelSesto, and A. L. Utz, "Preference for vibrational over translational energy in a gas-surface reaction," Science **304**, 992-995 (2004).

[11] Daniel R. Killelea, Victoria L. Campbell, Nicholas S. Shuman, and Arthur L. Utz, "Bond-Selective Control of a Heterogeneously Catalyzed Reaction," Science **319**, 790-793 (2008).

[12] Regis Bisson, Tung T. Dang, Marco Sacchi, and Rainer D. Beck, "Vibrational activation in direct and precursor-mediated chemisorption of $SiH_4$ on Si(100)," J. Chem. Phys. **129**, 081103-081104 (2008).

[13] F. Abild-Pedersen, O. Lytken, J. Engbaek, G. Nielsen, I. Chorkendorff, and J. K. Norskov, "Methane activation on Ni(111): Effects of poisons and step defects," Surf. Sci. **590**, 127 (2005).

[14] J. M. Wei and E. Iglesia, "Isotopic and kinetic assessment of the mechanism of reactions of $CH_4$ with $CO_2$ or $H_2O$ to form synthesis gas and carbon on nickel catalysts," J. Catal. **224**, 370-383 (2004).

[15] H. L. Abbott and I. Harrison, "Methane dissociative chemisorption on Ru(0001) and comparison to metal nanocatalysts," J. Catal. **254**, 27-38 (2008).

[16] M. B. Lee, Q. Y. Yang, S. L. Tang, and S. T. Ceyer, "Activated Dissociative Chemisorption of CH4 on Ni(111) - Observation of a Methyl Radical and Implication for the Pressure Gap in Catalysis," J. Chem. Phys. **85**, 1693-1694 (1986).

# Fluctuations in Macromolecules Studied Using Time-Resolved, Multi-spectral Single Molecule Imaging

Carl Hayden
Sandia National Laboratories
P. O. Box 969, MS 9055
Livermore, CA 94551-0969
cchayde@sandia.gov

Haw Yang
Department of Chemistry
University of California at Berkeley
Berkeley, CA
hawyang@uclink.berkeley.edu

## Program Scope

The goal of this research program is to study local chemical environments and their fluctuations in macromolecules using single molecule methods. We focus on methods that provide simultaneous, correlated measurements of both the spectrum and temporal decay of fluorescence from probe fluorophores in single macromolecules. An important component of this work is the development of new data analysis methods to extract the maximum information about the macromolecule fluctuations from the experimental record of photons.

In bulk samples the averaging of many fluctuations makes the system essentially time independent and hence the fluorescence properties can usually be measured sequentially. In contrast, to determine the time-dependent behavior of a fluorophore within a single macromolecule the relevant fluorescence properties must be measured simultaneously, with the sensitivity to detect single fluorophores. In many cases multiple fluorescence properties will fluctuate at the same time, thus the ability to interpret the result will be enhanced by measurements that reveal correlations between multiple fluorescence properties.

## Recent Progress:

### Föster resonance energy transfer (FRET) in single quantum dot-dye hybrids.

Using results from experiments on quantum dot-dye hybrid assemblies we have developed statistical methods for analyzing correlated single particle time traces. Single particle data are typically noisy, which can make it difficult to convincingly determine the nature of observed events. However, if information is available in a multiple-parameter space, the correlation among different channels allows greater confidence in interpretations, particularly in time-dependent experiments. FRET from a quantum dot (QD) donor to multiple dye acceptors is a good system in which to develop analytical methods for such situations. These QD-dye hybrids are typically made by binding dyes to a central QD hub, which serves as the single FRET donor.

A number of processes can obscure changes in the desired FRET signal, including QD and dye blinking. The use of multiple dyes on one QD can also lead to acceptor fluorescence due to direct excitation rather than energy transfer. We focus on resolving the energy transfer process from the confounding signals. The experiment and analysis are carried out photon-by-photon so that the most information can be extracted. The collected photons are first separated into donor and acceptor channels based on their wavelengths. Because full spectra are recorded, the wavelength division into donor and acceptor channels can be determined particle-by-particle to

accommodate differing QD emission spectra, for example. A model-free change-point detection algorithm is then independently applied to the donor and acceptor intensity trajectories to extract the intensity change-point locations as well as their associated uncertainties. Using a tool from information theory, the affinity functional, we do a joint analysis of the change point information to determine the probability that change-points, close together in time, are truly synchronized. Finally, the difference in the correlated donor and acceptor behavior is used to identify the event. For example, donor blinking leads to intensity changes of the same polarity in both donor and acceptor traces, while acceptor photobleaching leads to changes of opposite polarity in the intensity traces of the donor and acceptor. Thus we have developed a general approach based on multi-parameter spectroscopy and statistical analysis to identify events in complex single particle systems and to quantify the degree of confidence in the identification.

**Rigidity of poly-L-proline peptides**

Poly-L-proline peptides have long been considered to be relatively rigid, with an all-*trans* configuration in water.[1-3] They have served as model systems for Förster resonance energy transfer (FRET) studies. However, poly-L-proline has recently been reexamined carefully by several groups using a variety of methods,[4-9] and found to have a mean end-to-end length in water shorter than that predicted by the standard all-*trans* poly-L-proline II structure. These new results lead to questions about the nature of poly-L-proline peptides. These questions cannot be answered by measurements of the mean end-to-end distances alone because, the mean distances from a series of poly-L-proline peptides can be fit equally well by different models of the flexibility of their structure. On the other hand, different models give very different distributions of distances even though they have the same averaged end-to-end distance. For example, a freely jointed chain (FJC) model gives a distance distribution that is broad and symmetric while a worm-like chain (WLC) model gives a distribution that is narrower and asymmetric.

Here, we address this question by directly measuring poly-L-proline conformational distributions using high-resolution single-molecule FRET.[10, 11] A series of polyprolines, $P_nCG_3K$ (n = 8, 15, 24), were investigated in which the donor dye (Alexa-555, Invitrogen) was attached to the N terminus and the acceptor dye (Alexa-647, Invitrogen) to the cysteine residue. The measured distance distributions were then compared with the FJC and WLC models. To account for possible effects on the fluorescence characteristics of the dyes due to immobilization in close proximity to a surface, we also measure single molecule FRET spectra and lifetimes. These measurements give the dye characteristics necessary to calibrate the FRET distance calculations.

The end-to-end distance distribution is found to become progressively broader as the poly-L-proline chain length increases. This observation is consistent with the idea that longer-chain peptides sample more conformational space within a given time window. More specifically, the end-to-end length distribution of $P_8CG_3K$ is determined to be a narrow peak centered at $R_8$ = 31.6 Å, in sharp contrast to the broader distributions predicted by both theoretical models. For longer-chain polyprolines, $P_{15}CG_3K$ and $P_{24}CG_3K$, the mean distances become longer (46.5 Å and 60.1 Å, respectively) with increasingly greater variances (25.31 $Å^2$ and 37.5 $Å^2$, respectively); however, the experimentally measured distributions remain consistently narrower than those predicted by the theoretical models. The results therefore provide clear and direct evidence that neither theoretical model is appropriate for describing the behavior of poly-L-proline peptides.

We are currently comparing the characteristics of the FRET pairs on immobilized single molecules to the dyes in bulk samples to confirm the absolute values of the calculated distances. A representative single molecule measurement is shown in Figure 1.

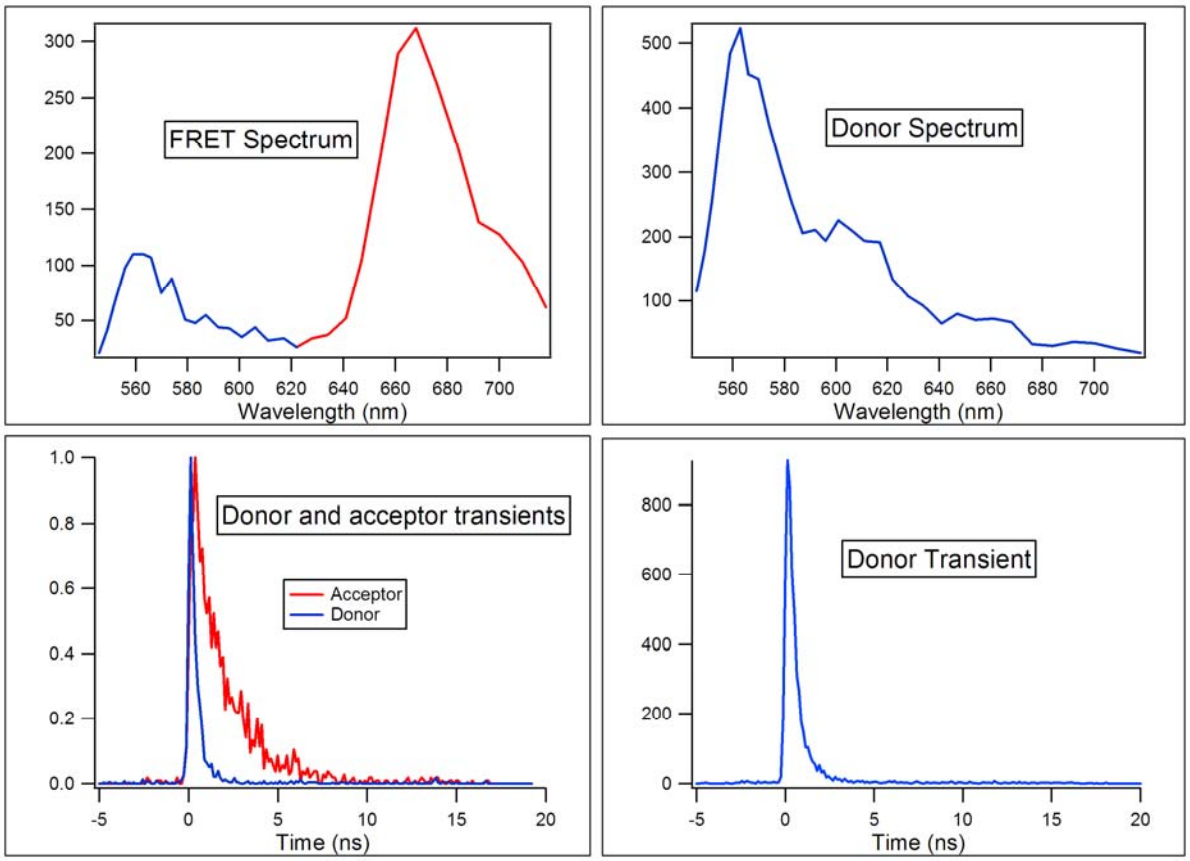


Figure 1. Fluorescence spectra and lifetimes from a single FRET labeled $P_{15}CG_3K$ molecule immobilized via streptavidin on a polyethylene glycol surface. The initial FRET spectrum (upper left) shows strong energy transfer from donor to acceptor. The donor transient (lower left) is quenched by this energy transfer. After about one second the acceptor photobleaches and the spectrum (upper right) is that of the donor. The donor decay is extended when the energy transfer to the acceptor ceases (lower right).

**Ongoing Work and Future Plans:**

**Conformational dynamics of maltose binding protein (MBP)**

We have an ongoing investigation of the conformational dynamics of MBP from *E.Coli* using single molecule FRET. The two lobes of this protein close around the maltose ligand upon binding. Our experiments are to determine the fraction of open versus closed states in the presence and absence of the ligand. To detect the open and closed states we have performed single molecule experiments using FRET to measure the time dependent distance changes between the two lobes of the protein. Recently, increases in the time resolution of these experiments have much more clearly distinguished the open and closed states. We are also using spectral and lifetime measurements in this system to calibrate the FRET distance determinations.

**Streptavidin with tetramethylrhodamine (TMR) interaction**

We also have ongoing studies of the interaction between the biotin binding protein streptavidin and the dye TMR linked to the protein through biotin. Depending on the linker between the biotin and dye this protein strongly quenches the dye fluorescence. Recently we

have found that addition of excess biotin to saturate the unfilled binding pockets on streptavidin eliminates the quenching. This suggests that quenching results from direct interact of the dye with an adjacent binding site. We are now working to test this effect on immobilized streptavidin. These studies provide an opportunity to study the details of how fluorophores interact with specific protein chemical environments.

**Protein immobilization with lipid systems**

We are exploring methods to directly immobilize $His_6$-tagged proteins to lipid bilayers using metal chelating lipids. This will provide an alternative surface to measure effects of surface interaction with protein function.

**Detector development**

We have recently done proof of principle measurements with a new detector system using an improved photocathode. This detector system will substantially enhance the sensitivity of our multi-parameter measurements.

**References:**


1. Cowan, P. M.; McGavin, S. *Nature*, **1955**, *176*, 501-503.
2. Schimmel, P. R.; Flory, P. J. *Proc. Natl. Acad. Sci. U.S.A.*, **1967**, *58*, 52-59.
3. Stryer, L.; Haugland, R. P. *Proc. Natl. Acad. Sci. U.S.A.*, **1967**, *58*, 719-726.
4. Schuler, B.; Lipman, E. A.; Steinbach, P. J.; Kumke, M.; Eaton, W. A. *Proc. Natl. Acad. Sci. U.S.A.*, **2005**, *102*, 2754-2759.
5. Watkins, L. P.; Chang, H.; Yang, H. *J. Phys. Chem. A* **2006**, *110*, 5191-5203.
6. Rüttinger, S.; Macdonald, R.; Krämer, B.; Koberling, F.; Roos, M.; Hildt, E. *Journal of Biomedical Optics* **2006**, *11*.
7. Best, R. B.; Merchant, K. A.; Gopich, I. V.; Schuler, B.; Bax, A.; Eaton, W. A. *Proc. Natl. Acad. Sci. U.S.A.* **2007**, *104*, 18964-18969.
8. Sahoo, H.; Roccatano, D.; Hennig, A.; Nau, W. M. *J. Am. Chem. Soc.*, **2007**, *129*, 9762-9772.
9. Doose, S.; Neuweiler, H.; Barsch, H.; Sauer, M. *Proc. Natl. Acad. Sci. U.S.A.*, **2007**, *104*, 17400-17405.
10. Watkins, L. P.; Yang, H. *Biophysical Journal* **2004**, *86*, 4015-4029.
11. Hanson, J. A.; Duderstadt, K.; Watkins, L. P.; Bhattacharyya, S.; Yang, H. *Proc. Natl. Acad. Sci. U.S.A.* **2007**, *104*, 18055-18060.


**DOE sponsored publications, 2007-2008**


1. C. S. Xu, H. Kim, H. Yang and C. C. Hayden, "Multiparameter Fluorescence Spectroscopy of Single Quantum Dot-Dye FRET Hybrids**,"** *J. Am. Chem. Soc.*, **129** (36), 11008 -11009, 2007.
2. C. S. Xu, H. Kim, C. C. Hayden and H. Yang, "Joint Statistical Analysis of Multi-Channel Time Series from Single Quantum Dot-$(Cy5)_n$ Constructs," *J. Phys. Chem. B*, 112 (19), 5917-5923, 2008.
3. H. Liu, G. D. Bachand, H. Kim, C. C. Hayden, E. A. Abate, and D. Y. Sasaki, "Lipid Nanotube Formation from Streptavidin-Membrane Binding," *Langmuir*, **24** (8), 3686 -3689, 2008

# ELECTRONIC STRUCTURE AND OPTICAL RESPONSE OF NANOSTRUCTURES

Martin Head-Gordon (mhg@cchem.berkeley.edu) [1],
Steven G. Louie (sglouie@berkeley.edu) [2],
Lin-Wang Wang (lwwang@lbl.gov) [3],
Emily A. Carter (eac@princeton.edu) [4],
James R. Chelikowsky (jrc@ices.utexas.edu) [5],

*[1]Department of Chemistry, University of California, and Chemical Sciences Division, Lawrence Berkeley National Laboratory, Berkeley, CA 94720; [2] Department of Physics, University of California, and Materials Sciences Division, Lawrence Berkeley National Laboratory, Berkeley, CA 94720; [3] Computational Research Division, Lawrence Berkeley National Laboratory, Berkeley, CA 94720; [4] Department of Mechanical & Aerospace Engineering, Princeton University, Princeton, NJ 08544; [5] Departments of Physics and Chemical Engineering, Institute for Computational Engineering and Sciences, University of Texas, Austin, TX 78712*

## 1. Scope of Project.

There has been much progress in the synthesis, characterization and theoretical studies of various nanostructures such as nanotubes, nanocrystals, atomic wires, organic and biological nanostructures, and molecular junctions. However, there remain immense challenges to obtain a basic understanding of the properties of these structures and their interactions with external probes to realize their potential for applications. Some exciting frontiers in nanoscience include molecular electronics, nanoscale opto-electronic devices, nanomechanics (nanomotors), light harvesting and emitting nanostructures. The ground and electronic excited properties of the nanostructures and how they are coupled to the external stimulations/probes are crucial issues.

Since nanostructures are neither at the molecular nor the bulk limits, the calculations of their electronic and optical properties are subject to severe computational bottlenecks. The present program therefore focuses on the electronic structure theory and modeling of nanostructures, including their electronic excited-state and optical properties, with applications to topics of current interest. We are attacking the rate-determining steps in these approaches in collaboration with a team of applied mathematicians, led by Juan Meza, Head of LBNL's High Performance Computing Research Department.

## 2. Summary of Recent Progress.

As this is a large multi-investigator program, space precludes us summarizing all projects that are underway. Below, we highlight a selection of recent accomplishments, with a focus on recent algorithmic developments that are helping to enable improved simulations (either larger numbers of atoms, or greater accuracy, or both) of nanoscale systems.

***High Performance algorithms for nano-scale systems containing more than 10,000 atoms*** One of the most significant goals in computational materials science is the development of new algorithms and physical concepts for describing matter at all length scales, especially at the nano-scale. Achieving an efficacious algorithm for predicting the role of quantum confinement and its role in determining the properties of nanocrystals is a difficult task owing to the complexity of nanocrystals. However, we have made notable progress by implementing new algorithms designed for highly parallel platforms. Our goal is to solve the electronic structure for large systems using pseudopotentials and density functional theory. The spatial and energetic distributions of electrons can be described by a solution of the Kohn-Sham

equation. A traditional procedure for solving this equation is to approximate an input potential and then iterate the equation until the charge density and potential are self-consistent. This method is often used with a full diagonalization step at each iteration. The diagonalization step is very costly and can be replaced with a "filtering operation." By eliminating the explicit diagonalization step from the self-consistency loop, one can speed up the solution process by *one to two orders* of magnitude *with no sacrifice in the accuracy of the method*. This allows us to examine much larger systems than what we could otherwise examine [41]. Our initial applications have been to nanocrystals containing large numbers of atoms, e.g., we have looked at systems as large $Si_{9041}H_{1860}$ and examined the role of doping in these materials [21].

***Linear scaling divide and conquer method for nanostructures.*** We developed a linear scaling divide-and-conquer method for large system total energy calculations based on density functional theory [19,20]. The main point of this method is a novel patching method that cancels out the boundary effects. During this year, an efficient code implementing this method has been developed which has reached 107 Tflop/s on 160,000 cores of the BlueGene/P (Intrepid) computer in ALCF at Argone National Laboratory. The code scales linearly up to 160,000 cores in terms of its parallelization, and it also scales linearly with the size of the system in terms of its total computational cost.

***Accurate density functionals for nanoscience.*** Due to efforts such as the algorithms above, DFT methods are now applicable to nanoscale systems. However existing density functionals have well-known deficiencies due to self-interaction errors such as underestimation of chemical reaction barriers, over-delocalization of odd electrons, and failure for charge-transfer excited states. An additional physical deficiency is the neglect of dispersion interactions. We have completed the systematic development of an exciting new class of density functionals which overcome some of these issues. The new feature is these functionals are fully optimized to include 100% long-range exact exchange – thereby eliminating long-range self-interaction error. On test sets the new functionals, ωB97X [30], and ωB97X-D [42] (the latter is optimized with inclusion of empirical damped dispersion terms) outperform the best GGA's and conventional hybrid functionals. While no approximate functional can claim to be without flaws, ωB97X, and ωB97X-D correct known physical deficiencies and yield improved overall performance, and are therefore promising candidates for broad chemical applications. They are available in our own codes and will soon be incorporated in other programs that can treat exact exchange efficiently. We have also explored a "double hybrid" which treats London forces without the need for empirical dispersion [33].

***Advances in orbital-free DFT (OFDFT) and application to Nanostructures*** The most efficient possible form of density functional theory involves no orbitals at all. Our second generation OFDFT code [36] has advanced in four ways this past year: implementation of the Wang-Govind-Carter (WGC) nonlocal kinetic energy density functional (KEDF) within Dirichlet boundary conditions so isolated nanostructures can be treated [14], all terms involving ions were rendered linear scaling [10], massive parallelization introduced via domain decomposition to enable study of realistic nanoscale systems ($10^5$ atoms!), and construction of new local pseudopotentials [38], which exhibited improved accuracy for various phases of Mg, Al, Si, and for a Mg-Al alloy. These advances allowed us to study Al nanowires of widths 0.3 nm to 6.0 nm with OFDFT [37]. Among the interesting predictions are that Al nanowires of bulk fcc morphology originally oriented in the [001] direction may undergo a transition to either a body-centered tetragonal [001] or a fcc [110] orientation under compression. The relative stability of the two states is tunable by varying the size of the nanowires. It may be possible to switch the state of the nanowire by uniaxial compression and expansion, leading to applications as a nanoscale actuator or switch.

***Embedding methods for metallic systems with application to the Kondo effect.*** We have been developing an embedded correlated wavefunction methodology for the study of localized features (e.g. point defects, adsorbates) in solids. For metals, the highly delocalized conduction electrons require us to

combine a high-level, ab initio wavefunction treatment for the localized region of interest, with a lower-level density functional theory (DFT) model for the periodic background [15]. One exciting application of the theory is the reproduction of striking differences for the lineshape of the experimentally observed Kondo resonance for Co on the (111) and (100) surfaces of Cu. Our embedded wavefunction approach finds that the Co d-electron configuration and symmetries differ when adsorbed on the (111) and (100) surfaces, which provides an explanation for the striking difference seen in the Kondo lineshapes [11]. Very recently, we have performed similar calculations for Co on Ag(111) and Ag(100), where we are again able to explain the lineshapes on the basis of the ECI Kondo wavefunctions. The correlated wavefunctions reveal that the low-lying excitations of the Kondo state are all spin-coupling fluctuations within 10 meV of the ground state; this finding is consistent with the very narrow (~10 meV) width of the Kondo resonance and the fact that the Kondo effect is only seen at low temperature (very weak coupling between the conduction and impurity electrons)

***Local coupled cluster theory with smooth potential energy surfaces.*** Over the past year, we have completed a production code that makes accurate many body coupled cluster calculations applicable to large systems by using so-called bump functions to smoothly (differentiably) combine perturbation theory treatment of weak (generally distant) correlations with infinite order coupled cluster treatment of strong correlations [29]. This is the first production level local correlation code that yields continuous potential energy surfaces, and we have reported tests that show it can correctly describe even electronically delocalized systems while yielding linear scaling of the coupled cluster calculation itself [29,35].

## 3. Partial list of publications from DOE Sponsored Work, 2007-present.


[1] J. Deslippe, C. D. Spataru, D. Prendergast, and S. G. Louie, “Bound excitons in metallic single-walled carbon nanotubes” Nano Letters 7, 1626 (2007).

[2] R.C. Lochan, Y. Shao, and M. Head-Gordon, “Quartic scaling analytical gradient of scaled opposite spin second order Møller-Plesset Perturbation theory”, J. Chem. Theory Comput. 3, 988-1003 (2007).

[3], Y. Jung, Y. Shao, and M. Head-Gordon, “Fast evaluation of scaled opposite spin second order Møller-Plesset correlation energies using auxiliary basis expansions and exploiting sparsity”, J. Comput. Chem. 28, 1953-1964 (2007).

[4] R. Lochan, M. Head-Gordon, “Orbital-optimized opposite-spin 2nd order correlation: an economical method to improve the description of open-shell molecules”, J. Chem. Phys. 126, 164101 (2007)

[5] Y.M. Rhee, M. Head-Gordon, “Scaled 2nd order perturbation corrections to configuration interaction singles: efficient and reliable excitation energy methods”, J. Phys. Chem. A 111, 5314-5326 (2007).

[7] B. Lee, L.W. Wang, C. D. Sparatus, S. G. Louie, "Nonlocal exchange-correlation in screened exchange density functional methods", Phys. Rev. B 76, 245114 (2007).

[8] T.-L. Chan, M.L. Tiago, and J.R. Chelikowsky: “Algorithms for Defects in Nanostructures,” Physica B 401-402, 531 (2007).

[9] S. Beckman and J.R. Chelikowsky: “The structure and properties of vacancies in Si nano-crystals calculated by real space pseudopotential methods,” Physica B 401-402, 537 (2007)

[10] J.E. Subotnik, A. Sodt and M. Head-Gordon, “Localized orbital theory and ammonia triborane”, Phys. Chem. Chem. Phys. 9, 5522-5530 (2007).

[11] P. Huang and E. A. Carter, “Ab initio explanation of tunneling lineshapes for the Kondo impurity state,” *Nano Lett.* 8, 1265 (2008).

[12] S. Sharifzadeh, P. Huang and E. A. Carter, “Embedded configuration interaction description of CO on Cu(111): Resolution of the site preference conundrum,” *J. Phys. Chem. C*, 112, 4649 (2008).

[13] G. Ho, C. Huang, and E. A. Carter, “Describing Metal Surfaces and Nanostuctures with Orbital-Free Density Functional Theory,” *Curr. Opin. Solid State Mater. Sci.*, 11, 57 (2008).

[14] G. Ho, V. L. Lignères, and E. A. Carter, “Analytic form for a non-local kinetic energy functional with a density-dependent kernel for orbital-free density functional theory under periodic and Dirichlet boundary conditions,” *Phys. Rev. B*, 78, 045105 (2008).

[15] P. Huang and E. A. Carter, “Advances in Correlated Electronic Structure Methods for Solids, Surfaces, and Nanostructures,” *Ann. Rev. Phys. Chem.*, 59, 261 (2008).

[16] E. A. Carter, "Challenges in Modeling Materials Properties without Experimental Input," *Science*, 321, 800 (2008).
[17] B. Lee, A. Canning, L.W. Wang, "Effects of d-electrons in pseudopotential screened-exchange density functional calculations", J. Appl. Phys. 103, 113713 (2008).
[18] J. Schrier, B. Lee, L.W. Wang, "Mechanical and electronic structure properties of compressed CdSe tetrapod nanocrystals", J. Nanosci. Nanotech. 8, 1994 (2008).
[19] L.W. Wang, Z. Zhao, J. Meza, "A linear scaling three dimensional fragment method for large scale electronic structure calculations", Phys. Rev. B 77, 165113 (2008).
[20] Z. Zhao, J. Meza, L.W. Wang, "A divide-and-conquer linear scaling three dimensional fragment method for large scale electronic structure calculations", J. Phys. Conds. Matt. 20, 294203 (2008).
[21] T.-L. Chan, M. L. Tiago, E. Kaxiras and J.R. Chelikowsky, "Size Limits on Doping Phosphorus into Silicon Nanocrystals," Nano Letters 8, 596 (2008).
[22] M. Lopez del Puerto, M.L. Tiago, and J.R. Chelikowsky: "Ab initio methods for the optical properties of CdSe clusters," Phys. Rev. B 77, 045404 (2008).
[23] L. Kong and J.R. Chelikowsky: "Transport properties of transition-metal-encapsulated Si cages," Phys. Rev. B 77, 073401 (2008).
[24] M.M.G. Alemany, X. Huang, M. L. Tiago , L.J. Gallego, and J.R. Chelikowsky: "Ab initio calculations for p-type doped bulk indium phosphide," Solid State Commun. 146, 245 (2008).
[25] N. Sai, M.L. Tiago, J.R. Chelikowsky, and F. A. Reboredo: "Optical spectra and exchange-correlation effects in molecular crystals," Phys. Rev. B 77, 161306 (2008).
[26] A.T. Zayak, P. Entel, and J.R. Chelikowsky: "Minority spin polarization and surface magnetic enhancement in Heusler clusters," Phys. Rev. B (in press).
[27] H. Kwak, M.L. Tiago, T.-L. Chan and J.R. Chelikowsky: "Hyperfine splitting of partially ionized Li donors in ZnO nanocrystals," Chem. Phys. Lett. 454, 337 (2008).
[28] A. Natan, A. Mor, D. Naveh, L. Kronik, M.L. Tiago, S.P. Beckman and J.R. Chelikowsky: "Real-space pseudopotential method for first principles calculations of general periodic and partially periodic systems," Phys. Rev. B 78, 075109 (2008).
[29] J.E. Subotnik, A. Sodt and M. Head-Gordon, "The limits of local correlation theory: electronic delocalization and chemically smooth potential energy surfaces", J. Chem. Phys. 128, 034103 (2008) (12 pages).
[30] Jeng-Da Chai and M. Head-Gordon, "Systematic optimization of long-range corrected hybrid density functionals", J. Chem. Phys. 128, 084106 (2008).
[31] A.D. Dutoi and M. Head-Gordon, "A two-parameter Coulomb attenuator with a cutoff radius for two-electron repulsion integrals: the effect of attenuation on correlation energies", J. Phys. Chem A 112, 2110-2119 (2008).
[32] A. Sodt and M. Head-Gordon. "Hartree-Fock exchange computed using the atomic resolution of the identity approximation", J. Chem. Phys. 128, 104106 (2008).
[33] T. Benighaus, R.A. Distasio Jr., R.C. Lochan, J.D. Chai and M. Head-Gordon, "Semiempirical double-hybrid density functional with improved description of long-range correlation", J. Phys. Chem. A, 112, 2702-2712 (2008).
[34] D. Casanova, Y.M. Rhee and M. Head-Gordon, "Quasidegenerate scaled opposite spin second order perturbation corrections to single excitation configuration interaction", J. Chem. Phys. 128, 164106 (2008)
[35] J.E. Subotnik and M. Head-Gordon, "Exploring the accuracy of relative molecular energies in local correlation theory", J. Phys.: Condens. Matter 20 (2008) 294211.
[36] G. Ho, V. L. Lignères, and E. A. Carter, "Introducing PROFESS: a new program for orbital-free density functional theory calculations," *Comput. Phys. Commun.*, in press (2008).
[37] G. Ho and E. A. Carter, "Mechanical Response of Aluminum Nanowires via Orbital-Free Density Functional Theory," *J. Comput. Theor. Nanos.*, in press (2008).
[38] C. Huang and E. A. Carter, "Transferable local pseudopotentials for magnesium, aluminum and silicon," *Phys. Chem. Chem. Phys.*, in press (2008).
[39] A.T. Zayak, S. Beckman, M. Tiago, P. Entel, and J.R. Chelikowsky: "Switchable Heusler Clusters," J. Appl. Phys. (in press).
[40] J. Han, M. L. Tiago, T.-L. Chan, and J. R. Chelikowsky: "Real-Space First-Principles Method for the Electronic Structure of One Dimensional Periodic Systems," J. Chem. Phys. (in press).
[41] J.R. Chelikowsky, A. T. Zayak, T.-L. Chan, M. L. Tiago, Y. Zhou and Y. Saad: "Algorithms for the Electronic and Vibrational Properties of Nanocrystals," J. Phys. Cond. Matter (in press).
[42] J.-D. Chai and M. Head-Gordon, "A hybrid density functional with dispersion corrections that is free of self-interaction at long distances", Phys. Chem. Chem. Phys. (in press, 2008).

# EXPERIMENTAL AND SIMULATION STUDIES OF BULK WATER AND HYDRATION WATER AT INTERFACES

TERESA HEAD-GORDON
PHYSICAL BIOSCIENCES DIVISION, LAWRENCE BERKELEY NATIONAL LAB
DEPARTMENT OF BIOENGINEERING, UC BERKELEY
TLHead-Gordon@lbl.gov

## PROGRAM SCOPE

Water and its anomalies continue to haunt us in our developing a unified understanding of the physical behavior of common, everyday materials. Water appears to be unique relative to other liquids in anomalous features of structure, dynamics, and thermodynamics exhibited in its metastable extension of the liquid part of the phase diagram. The observed anomalies in thermodynamic and transport properties can also be manifested or exaggerated when studying the pure liquid under physical confinement in nanometer-sized pores or as a solution when water participates as a solvent or co-solvent. While these systems can be very insightful, and practical given the ability to study them in extreme parts of the phase diagram while avoiding nucleation of ice, they need to be calibrated to understand whether the water component behavior under confinement or in solution is representative of the molecular features relevant for the bulk neat liquid. Similarly, hydration layers surrounding a biological molecule show transport (and structural) signatures that differ appreciably from those of bulk water, more closely resembling the supercooled liquid, whose larger implications for biological function and analogies to glass formers are an active area of exploration. My experimental and theory/simulation program involves study of water and solutes over the phase diagram, using models of varying complexity, and studied as bulk, solution, and under confinement. We use x-ray and quasi-elastic neutron scattering and atomistic and coarse-grained chemical model simulations, to address fundamental questions about the origin of waters thermodynamic and dynamical trends with temperature and density, and ways to modify interfacial chemical properties to exploit changes in water behavior for nanoscale function [references 9-21 accomplished with CPIMS support since 2005]. The proposed research is of fundamental importance that will ultimately aid in new biomaterials synthesis and function at the nanoscale. These results and our approach are relevant for our new interest involving ionic liquids for cracking biomass discussed in Future Plans.

## RECENT PROGRESS

***Assessing Thermodynamic Theories of Bulk Liquid Dynamics [1]***. We investigated a family of isotropic water-like glass-forming liquids [7], in which each thermodynamic state point corresponds to a different potential energy surface, each of which are structurally prescribed to reproduce the $g_{OO}(r;\ T,\rho)$ of the reference TIP4P-Ew water model potential. Although each isotropic potential is simulated separately, together the family of potentials displays anomalous dynamics with density and fragile diffusivity with temperature. By removing a common energy landscape, and therefore expected thermodynamic trends with temperature and density, we can more rigorously evaluate whether various entropic measures used in popular phenomenological thermodynamic theories can quantitatively predict the diffusivity or viscosity. We find that the Adam-Gibbs relation between diffusion (or viscosity) and the temperature scaled configurational entropy, $S_c$, is a poor predictor of fragility trends and density anomalies when necessary

anharmonic corrections are added. By contrast the Dzugutov relationship that uses the excess entropy $S_{excess}$ or the pair correlation approximation to $S_{excess}$~$S_2$ provides quantitative predictions of the temperature-dependent trends of the scaled diffusivity, but only $S_2$ also predicts the density-dependent dynamical trends. The success of $S_2$ approximation suggests that the available configurations are fully captured by the structural correlations rather than the underlying interaction potential, and that dynamics can be predicted without ever needing to consider the transitions between the available configurations over large regions of the phase diagram.

***Hydration water dynamics near biological interfaces [2].*** We perform classical molecular dynamics simulations using both fixed-charge and polarizable water and protein force fields to contrast the hydration dynamics near hydrophilic and amphiphilic peptides as a function of temperature. The high peptide concentrations we use should provide a reasonable model of the hydration dynamics for the folded state of a protein since the protein surface will also have hydration shells around surface amino acids that overlap, whereas the dilute concentrations of the same peptides explored by recent NMR experiments by Halle and co-workers are more representative of the hydration dynamics of the unfolded state. Through simulation we determine that there are notable differences in the water dynamics analyzed from the outer and inner hydration layer regions of the amphiphilic peptide solution that explains the experimentally observed presence of two translational relaxations, while the hydrophilic peptide solution shows only a single non-Arrhenius translational process with no distinction between hydration layers. Given that water dynamics for the amphiphilic peptide system reproduces all known rotational and translational hydration dynamical anomalies exhibited by hydration water near protein surfaces, our analysis provides strong evidence that dynamical signatures near biological interfaces arises because of frustration in the hydration dynamics induced by chemical heterogeneity, as opposed to just topological roughness, of the protein surface.

***Aqueous Peptides as Experimental Models for Hydration Water Dynamics Near Protein Surfaces [3].*** We report quasi-elastic neutron scattering experiments to contrast the water dynamics as a function of temperature for hydrophilic and amphiphilic peptides under the same level of confinement, as models for understanding hydration dynamics near chemically heterogeneous protein surfaces. We find that the hydrophilic peptide shows only a single non-Arrhenius translational process with no evidence of spatial heterogeneity unlike the amphiphilic peptide solution that exhibits two translational relaxations with an Arrhenius and non-Arrhenius dependence on temperature. Together these results provide experimental proof that heterogeneous dynamical signatures near protein surfaces arises in part from chemical heterogeneity (energy disorder) as opposed to mere topological roughness of the protein surface.

***The Influence of Co-solvents on Solution Structure Organization and Dynamics [work in progress].*** In order to probe the molecular origins of the water-protein and interactions with different chaotrope and kosmotrope co-solvents, we are presently studying the structure and dynamics of water near single amino acid peptide with and without the co-solvent included. Recent (elastic) neutron scattering work we have performed at ISIS, shows a clear difference in the water-amphiphilic peptide N-acetyl-leucine-methylamide (NALMA) interactions and water-water interaction when DMSO co-solvent is added compared to glycerol. The hydrogen bond between the carbonyl group of NALMA and water disappears when DMSO cosolvent is added but is still present when glycerol is present. This shows that neither the water-NALMA direct correlation nor the water-water distribution is affected by the presence of a kosmotrope but both are disrupted when a chaotrope is added.

These well-characterized water-amino acid systems are currently being used as a benchmark to study the effect of a kosmotrope and chaotrope co-solvents on the dynamics of water as a function of temperature. In order to clearly characterize the effect of a kosmotrope and chaotrope cosolvents on the water dynamics at the surface of the hydrophilic and amphiphilic model peptides we will use the combination of two experiments with different resolutions (using DCS and HBFS), supported by simulations and empirical polarizable force field models that show promise in quantitative descriptions of structure and dynamics for these systems. This work is being prepared for publication.

## Future Plans

Recently ionic liquid have been promoted for their ability for cracking biomass material[1] while ameliorating some of the negative environmental and economic consequences of more traditional solvent extractions, due to their low volatility and broad thermodynamically stable liquid range which allows them to be easily separated and recovered for reuse. The generic mode of action of the ionic liquid is to swell the biomass to increase surface exposure of the cellulose material for chemical conversion or for easier digestion by cellulase enzymes such as cellobiohydrolase. However the molecular interactions of the ionic liquids that promote the depolymerization of the cell wall material is currently unknown, as are the diffusion rates of the ionic liquid into the polymer matrix. Furthermore co-solvents of water and ionic liquids offer significant advantages over either neat solvent alone, by possibly permitting the dissolution and cracking and catalysis steps to occur simultaneously. While promising, ionic liquids (ILs) and their role as an aqueous co-solvent are poorly understood, especially in their relevant context of interactions with the bioorganic interface of the plant cell wall material.

We propose the use of x-ray and neutron diffraction and quasi-elastic neutron scattering, combined with molecular dynamics simulations, in characterizing the structure and dynamics of ionic liquids and the aqueous solvent interface for functional monomer units of crystalline cellulose, hemicellulose, and lignin as a function of temperature. The Head-Gordon lab has extensive experience in the use of these spectroscopic and theoretical techniques in the characterization of pure water, aqueous hydration structure, and dynamics near model amphiphilic and hydrophilic peptides, with chaotrope and kosmotrope co-solvents, investigated over a large temperature range, supported by the CPIMS program in DOE/BES since 2005. The tight coupling between experiment and simulation in the condensed phase has driven the development of robust simulation methods and the vetting of polarizable models that should be extensible to the difficult systems we pursue here, which involve chemical heterogeneous systems away from ambient conditions. The proposed research would enhance our understanding of how biological feedstocks are converted into portable fuel, with an emphasis on the associated physical, chemical processes, and their coupling with bio- and biomimetic approaches. The research highlighted here would be greatly enhanced by next generation light sources that utilize new x-ray absorption measurements and time-resolved data that would provide more fundamental information about the first-coordination shell or direct interaction dynamics of ionic liquid solvents and interactions of the biomass constituents. Finally, the advent of next generation light sources, future advances in time-resolved dynamics, and will provide training for the next generation of scientists in x-ray and neutron scattering research, expanding the user base of facilities in liquids characterization at the ALS, IPNS and SNS.

**PUBLISHED WORK UNDER DOE/CPIMS SUPPORT (2005-2008)**

1. M.E. Johnson and T. Head-Gordon (**2008**). Assessing thermodynamic theories of bulk liquid dynamics. *Submitted*

2. M.E. Johnson, C. Malardier-Jugroot, R.K. Murarka, and T. Head-Gordon (**2008**). Hydration water dynamics near biological interfaces. *J. Phys. Chem. B* accepted.

3. C. Malardier-Jugroot, M.E. Johnson, R.K. Murarka, and T. Head-Gordon (**2008**). Aqueous peptides as experimental models for hydration water dynamics near protein surfaces. *Phys. Chem. Chem. Phys.* 10, 4303-4308.

4. T. Head-Gordon and R. M. Lynden-Bell (**2008**). Hydrophobic solvation of Gay-Berne particles in modified water models. *J. Chem. Phys.* **128**, 104506-104512.

5. R. K. Murakra and T. Head-Gordon (**2008**). Dielectric relaxation of aqueous solutions of hydrophobic and hydrophilic peptides. *J. Phys. Chem. B 112*, 179-186.

6. R. K. Murakra and T. Head-Gordon (**2007**). Single particle and collective hydration dynamics of hydrophobic and hydrophilic peptides. *J. Chem. Phys.* 126, 215101-215109.

7. M. E. Johnson, T. Head-Gordon, A. A. Louis (**2007**). Representability problems for coarse-grained water models. *J. Chem. Phys.* 126, 144509-144519.

8. C. Malardier-Jugroot and T. Head-Gordon (**2007**). Separable cooperative and localized translational motions of confined water. *Phys. Chem. Chem. Phys.* 9, 1962-1971.

9. T. Head-Gordon and S. Rick (**2007**). Consequences of chain networks on thermodynamic, dielectric and structural properties for liquid water. *Phys. Chem. Chem. Phys*. 8, 83-91.

10. R. M. Lynden-Bell and T. Head-Gordon (**2006**). Solvation in modified water models: toward understanding hydrophobic solvation. *Mol. Phys.* 104, 3593-3605.

11. T. Head-Gordon & M. E. Johnson (**2006**). Tetrahedral structure or chains for liquid water? *Proc. Natl. Acad. Sci*. 103, 7973-7977.

12. D. Russo, R. K. Murakra, J. R.D. Copley, T. Head-Gordon (**2005**). Hydration dynamics near a model protein backbone. *J. Phys.Chem. B* 109; 12966-12975

# Chemical Kinetics and Dynamics at Interfaces

*Laser induced reactions in solids and at surfaces*

**Wayne P. Hess (PI), Kenneth M. Beck, and Alan G. Joly**

Chemical and Materials Sciences Division
Pacific Northwest National Laboratory
P.O. Box 999, Mail Stop K8-88,
Richland, WA 99352, USA
wayne.hess@pnl.gov

Additional collaborators include A L Shluger, P V Sushko, J T Dickinson, K Tanimura, G Xiong, J.M. White, M Henyk and O. Diwald

## Program Scope

The chemistry and physics of electronically excited solids and surfaces is relevant to the fields of photocatalysis, radiation chemistry, and solar energy conversion. Irradiation of solid surfaces by UV, or higher energy photons, produces energetic species such as core holes and free electrons, that relax to form electron-hole pairs, excitons, and other transient species capable of driving surface and bulk reactions. These less energetic secondary products induce the transformations commonly regarded as radiation damage. The interaction between light and nanoscale oxide materials is fundamentally important in catalysis, microelectronics, sensor technology, and materials processing. Photo-stimulated desorption, of atoms or molecules, provides a direct window into these important processes and is particularly indicative of electronic excited state dynamics. Excited state chemistry in solids is inherently complex and greater understanding is gained using a combined experiment/theory approach. We therefore collaborate with leading solid-state theorists who use *ab initio* calculations to model results from our laser desorption and photoemission experiments.

*Approach:*

We measure velocities and state distributions of desorbed atoms or molecules from ionic crystals using resonance enhanced multiphoton ionization and time-of-flight mass spectrometry. Photon energies are chosen to excite specific surface structural features that lead to particular desorption reactions. The photon energy selective approach takes advantage of energetic differences between surface and bulk exciton states and probes the surface exciton directly. Application of this approach to controlling the yield and state distributions of desorbed species requires detailed knowledge of the atomic structure, optical properties, and electronic structure. To date we have thoroughly demonstrated surface-selective excitation and reaction on alkali halides. However, the technological applications of alkali halides are limited compared to oxide materials. Oxides serve as dielectrics in microelectronics and form the basis for exotic semi- and super-conducting materials. Although the electronic structure of oxides differs considerably from alkali halides, it now appears possible to generalize the exciton model for laser surface reactions to these interesting new materials. Our recent studies have explored nanostructured samples grown by chemical vapor deposition or thin films grown by reactive ballistic deposition (RBD). We have demonstrated that desorbed atom product states can be selected by careful choice of laser wavelength, pulse duration, and delay between laser pulses. Recently, we have applied the technique of photoemission electron microscopy (PEEM) to these efforts. In particular, we are

developing a combined PEEM two-photon photoemission approach to probe spatially-resolved excited electronic state dynamics in nanostructured materials. Our experiments are designed specifically to test hypothetical models and theoretical predictions resulting from the calculations.

## Recent Progress

Calculations indicate that it is possible to excite preferentially either the surface or bulk of ionic materials (crystals) and induce surface or bulk specific reactions. We have excited low-coordinated surface sites (e.g. corners, steps and terraces) using sub-bandgap photons and induced hyperthermal neutral atom emission. In parallel experiments we excited bulk transitions using above bandgap photon energies and induce only thermal neutral atom emission. The kinetic energy distributions provide a signature for the surface or bulk origin of the desorption mechanism. In the particular case of rough CaO films, we irradiate nanostructured CaO samples using tunable UV laser pulses and observe hyperthermal O-atom emission indicative of a surface excited-state desorption mechanism. The O-atom yield increases dramatically with photon energy, between 3.75 and 5.4 eV, well below the bulk absorption threshold. The peak of the kinetic energy distribution does not increase with photon energy in this energy range. When the data are analyzed, in the context of a laser desorption model developed previously for nanostructured MgO samples, the results are consistent with desorption induced by exciton localization at corner-hole trapped surface sites following electronic energy transfer from higher coordinated surface sites. In a study of nanostructured MgO thin films, neutral magnesium atom emission is induced using two-color nanosecond laser excitation. We find that combined visible/UV excitation, for single-color pulse energies below the desorption threshold, induces neutral Mg-atom emission with hyperthermal kinetic energies in the range of 0.1 – 0.2 eV. The observed metal atom emission is consistent with a mechanism involving rapid electron transfer to 3-coordinated Mg surface sites. The two-color Mg-atom signal is significant only for parallel laser polarizations and temporally overlapped laser pulses indicating that intermediate excited states are short-lived and likely of sub-nanosecond duration.

### Future Directions

Since it is possible to selectively excite terrace, step, or corner surface sites, we have explored various sample preparation techniques that produce high concentrations of low-coordinated surface sites such as 4-coordinated steps and 3-coordinated corner or kink sites. In particular, we have employed reactive ballistic deposition (a technique developed in Bruce Kay's lab) to grow very high surface area MgO and CaO thin films. These films have been thoroughly characterized using XPS, SEM, TEM, and XRD techniques. Similarly, we have also studied laser desorption of MgO and CaO nano-powders grown by a chemical vapor deposition technique (in collaboration with Oliver Diwald of the Technical University of Vienna). The MgO nano-powders show cubic structure and edge lengths ranging between 3 and 10 nm (through TEM analysis).

If exciton-based desorption can be generalized from alkali halides to metal oxides then selective excitation of specific surface sites could lead to controllable surface modification, on an atomic scale, for a general class of technologically important materials. While exciton-based desorption is plausible for MgO and CaO, we note that the higher valence requires a more complex mechanism. With the aid of DFT calculations we have developed such a hyperthermal desorption mechanism that relies on the combination of a surface exciton with a three-coordinated surface-trapped hole, a so-called "hole plus exciton" mechanism. In every instance we have studied, a hyperthermal O-atom KE distribution can be linked to an electronic surface excited state desorption mechanism. In contrast, a thermal O-atom KE distribution clearly indicates a bulk derived origin for desorption. In analogy to alkali halide thermal desorption, we have considered

a bulk-based thermal desorption mechanism involving trapping of two holes at a three-coordinated site (a "two-hole localization" mechanism). Our calculations, however, do not indicate that two-hole localization is likely without invoking a dynamical trapping process. The details of these mechanisms need to be further delineated and confirmed by demonstrating control of the various desorption processes.

We have recently observed hyperthermal neutral Mg-atom desorption. This is quite a novel result as Mg-atom desorption requires that two electrons transfer to a corner site $Mg^{2+}$ ion in a very short time and then desorb prior to relaxation. The hyperthermal distribution indicates that the exciton model is extendable now to metal atom desorption processes – a previously unknown mechanism. We plan to grow and study several other oxide surfaces in the near term including BaO, ZnO, $ZrO_2$, and $TiO_2$. Future plans include femtosecond PEEM to study Plasmon resonant photoemission from noble metal nanostructures and pulse-pair PEEM to probe dynamics of oxide nanostructures on surfaces. We are also presently developing capabilities to perform energy-resolved TPPE using a hemispherical analyzer XPS instrument. In combination we expect these two techniques will provide the first *spatially-resolved* electronic state dynamics of nanostructured oxide materials.

**References to publications of DOE BES sponsored research (2005 to present)**

1. "A mechanism of photo-induced desorption of oxygen atoms from MgO nano-crystals." PE Trevisanutto, PV Sushko, AL Shluger, KM Beck, M Henyk, A.G. Joly, and W.P. Hess. Surf. Sci. **593**, 210 (2005).

2. "Laser control of desorption through selective surface excitation." WP Hess, AG Joly, KM Beck, M Henyk, PV Sushko, PE Trevisanutto, and AL Shluger, J. Phys. Chem. **109**, (2005).

3. "Surface electronic properties and site-specific laser desorption processes of highly structured nanoporous MgO thin films." M Henyk, KM Beck, MH Engelhard, AG Joly, WP Hess, and JT Dickinson, Surf. Sci. **593**, 242 (2005).

4. "Interaction of wide band gap single crystals with 248 nm excimer laser irradiation: laser induced near-surface absorption in single crystal NaCl." K H Nwe, SC Langford, WP Hess, and JT Dickinson, J. Appl. Phys. **97**, 043501 (2005).

5. "Interaction of wide band gap single crystals with 248 nm excimer laser irradiation: The effect of water vapor and temperature on laser desorption of neutral atoms from sodium chloride." KH Nwe, SC Langford, WP Hess, and JT Dickinson, J. Appl. Phys. **97**, 043502 (2005).

6. "Introduction to Photoelectron Emission Microscopy: Principles and Applications." G Xiong, AG Joly, WP Hess, M Cai, and JT Dickinson, J. Chin. Elec. Microsc. Soc. **25**, 16 (2006).

7. "Carrier Dynamics in $\alpha$-$Fe_2O_3$ Thin-films and Single Crystals Probed by Femtosecond Transient Absorption and Reflectivity." AG Joly, JR Williams, SA Chambers, G Xiong, WP Hess, and DM Laman, J. Appl. Phys. **99**, 1 (2006).

8. "In-situ photoemission electron microscopy study of thermally-induced martensitic transformation in CuZnAl shape memory alloy." G Xiong , AG Joly, KM Beck, WP Hess, M Cai, SC Langford, and JT Dickinson, Appl. Phys. Lett. **88**, 091910 (2006).

9. “Site-specific laser modification of MgO nano-clusters: Towards atomic scale surface structuring.” KM Beck, M Henyk, C Wang, PE Trevisanutto, PV Sushko, WP Hess, and AL Shluger, Phys. Rev. B **74**, 045404 (2006).

10. “Two-hole localization mechanism for electronic bond rupture of surface atoms by laser-induced valence excitation of semiconductors.” K Tanimura, E Inami, J Kanasaki, and WP Hess Phys. Rev. B **74**, 035337 (2006).

11. “Excited carrier dynamics of $\alpha$-$Cr_2O_3$/$\alpha$-$Fe_2O_3$ core-shell nanostructures.” G Xiong , AG Joly, WP Hess, G Holtom, CM Wang, DE McCready, and KM Beck, J. Phys Chem. B **110**, 16937 (2006).

12. “Probing electron transfer dynamics at MgO surfaces by Mg-atom desorption.” A.G. Joly, M Henyk, KM Beck, PE Trevisanutto, PV Sushko, WP Hess, and AL Shluger, J. Phys. Chem. B Lett. **110**, 18093 (2006).

13. “Laser-induced oxygen vacancy formation and diffusion on $TiO_2$ (110) surfaces probed by photoemission electron microscopy.” G Xiong, AG Joly, KM Beck, WP Hess, Phys. Stat. Sol. (c) **3**, 3598 (2006).

14. “Study of martensitic phase transformation in a NiTiCu thin film shape memory alloy using photoelectron emission microscopy.” M Cai, SC Langford, JT Dickinson, MJ Wu, WM Huang, G Xiong, TC Droubay, AG Joly, KM Beck, and WP Hess, Adv. Funct. Mater. **17**, 161 (2007).

15. “An *In-situ* Study of the Martensitic Transformation in Shape Memory Alloys using Photoemission Electron Microscopy,” M Cai, SC Langford, JT Dickinson, G Xiong, TC Droubay, AG Joly, KM Beck and WP Hess, J. Nuc. Mater. **361**, 306 (2007).

16. “Study of copper diffusion through a ruthenium thin film by photoemission electron microscopy.” W. Wei, S. L. Parker, Y.-M. Sun, and J. M. White, G Xiong, AG Joly, KM Beck, and WP Hess, Appl. Phys. Lett. **90**, 111906 (2007).

17. “Synthesis and photoexcited charge carrier dynamics of $\beta$-FeOOH nanorods.” AG Joly, G Xiong, C Wang, DE McCready, KM Beck, and WP Hess, Appl. Phys. Lett. **90**, 103504 (2007).

18. “Photoemission electron microscopy of $TiO_2$ anatase films embedded with rutile nanocrystals.” G Xiong, R Shao, TC Droubay, AG Joly, KM Beck, SA Chambers, and WP Hess, Adv. Funct. Mater. **17**, 2133 (2007).

19. “Proceedings of the Eighth International Conference on Laser Ablation (COLA 05).” WP Hess, PR Herman, D Bäuerle, and H Koinuma, Editors, Journal of Physics: Conference Series, Vol. **59**, pages 1 -729 (2007).

20. K.M. Beck, A.G. Joly, O. Diwald, S. Stankic, P.E. Trevisanutto, P.V. Sushko, A.L. Shluger, and W.P. Hess, “Energy and site selectivity in O-atom photodesorption from nanostructured MgO,” Surf. Sci. **602**, 1968 (2008).

21. A.G. Joly, K.M. Beck, and W.P. Hess, “Electronic energy transfer on CaO surfaces,” J. Chem. Phys. **129**, 13 (2008).

# Breakthrough Design and Implementation of Electronic and Vibrational Many-Body Theories

So Hirata (principal investigator: DE-FG02-04ER15621)
Quantum Theory Project and The Center for Macromolecular Science and Engineering, Departments of Chemistry and Physics, University of Florida, Gainesville, FL 32611
hirata@qtp.ufl.edu

## Program Scope

Predictive chemical computing requires hierarchical many-body methods of increasing accuracy for both electronic and vibrational problems. Such hierarchies are established, at least conceptually, as configuration-interaction (CI), many-body perturbation (PT), and coupled-cluster (CC) methods for electrons and for vibrations, which all converge at the exact limit with increasing rank of a hierarchical series. These methods can generate results of which the convergence with respect to various parameters of calculations can be demonstrated and which can be predictive in the absence of experimental information.

The progress in these methods and their wide use are, however, hindered by (1) the immense complexity and cost of designing and implementing some of the high-rank members of the hierarchical methods and by (2) the extremely slow convergence of electronic energies and wave functions with respect to one-electron basis set sizes, which is compounded with the high-rank polynomial or even factorial molecular size dependence of the computational cost of these methods.

The overarching goal of our research is to address both difficulties for electrons and vibrations. We will eradicate the first difficulty for electrons by developing a computerized symbolic algebra system that completely automates the mathematical derivations of electron-correlation methods and their implementation. For vibrations, the vibrational SCF (VSCF) and CI (VCI) codes will be developed in the general-order algorithm that is applicable to polyatomic molecules and allows us to include anharmonicity and vibrational mode-mode couplings to any desired extent. We address the second difficulty by radically departing from the conventional Gaussian basis set and introduce a new hierarchy of converging electron-correlation methods with completely flexible but rational (e.g., satisfying asymptotic decay and cusp conditions) basis functions such as numerical basis functions on interlocking multicenter quadrature grids and explicit $r_{12}$ (inter-electronic distance) dependent basis functions. They, when combined with high-rank electron-correlation methods, can possibly achieve the exact solutions of the Schrödinger equation.

## Recent Progress

Several breakthroughs have been made: First, a grid-based, numerical solver of the Hartree–Fock (HF) equation has been developed.[9] It provides essentially exact HF energies of polyatomic molecules. Second, the complete explicitly-correlated CC theory has been formulated up to a high rank for the first time by our newly-developed computerized symbolic algebra.[6] It is "complete" in the sense that every diagrammatic contribution is accounted for. The CCSD-R12 method based on the nontruncated diagrammatic equations has been implemented into an efficient program.[3] Third, a multi-reference or quasi-degenerate PT has been extended to anharmonic vibrations and has been demonstrated to be highly effective for strong anharmonic couplings such as Fermi resonances.[7] Chemical applications have been made to the vibrational and NMR spectra of the $FHF^-$ molecule.[5] Fourth, linear-scaling electron-correlation methods have been proposed for molecular crystals.[2] The energies, structures, and phonons and their dispersions can now be routinely computed by *ab initio* PT and CC theories with a basis-set superposition error correction.

Since the 2007 CPIMS Research Meeting, seven (7) papers[2–3,5–9] and one book chapter[4] have been published and one more[1] is under review for publication. In total, twenty-eight (28) publications[2–29] have resulted from this grant in 2005–08. In 2007–08, the PI has been an invited speaker at twenty (20) conferences and universities. The PI has also been selected to receive Hewlett–Packard Outstanding Junior Faculty Award (2008) and Medal of the International Academy of Quantum Molecular Science (2008).

**Predictive electronic and vibrational many-body methods for molecules and macromolecules**.[2] Chemical simulations with predictive accuracy are being realized by hierarchical many-body methods for treating electrons and vibrations. Ascending these hierarchies one can reach arbitrarily high accuracy and extract reliable chemical information without conducting an experiment. This 'Frontiers Article' of *Chemical Physics Letters* summarizes our methodological developments, supported by the DOE funding, which are intended to make such simulations possible or more widely applicable. They include (1) a computer-aided approach to developing converging many-body methods for electrons and its application to a novel class of complex electron-correlation methods, (2) an effort to reduce the errors arising from the expansion bases of electronic wave functions, (3) an extension of mathematical techniques established in electronic many-body methods to anharmonic molecular vibrations and vibrationally averaged quantities, and (4) two approaches to extending these systematic electronic and vibrational methods to large molecules and solids.

**Grid-based numerical Hartree–Fock solutions of polyatomic molecules**.[9] Numerical solutions of the Hartree–Fock (HF) equation of polyatomic molecules have been obtained by an extension of the numerical density-functional method of Becke and Dickson [J. Chem. Phys. **89**, 2993 (1988); **92**, 3610 (1990)]. A finite-difference method has been used to solve Poisson's equation for the Coulomb and exchange potentials and to evaluate the action of the Laplace operator on numerical orbitals expanded on an interlocking multicenter quadrature grid. Basis-set-limit HF results for an atom and diatomic and triatomic molecules are obtained with the total energies and the highest occupied orbital energies converged to within $10^{-5}$ Hartree without any extrapolation, which is more accurate than HF/aug-cc-pV5Z by three orders of magnitude. A combination of this and the explicitly-correlated CC methods up to a high rank (see below), which together offers the most rapid convergence of correlation energies, may realize the dream of every quantum chemist, namely, the exact numerical solutions of the (non-relativistic) Schrödinger equation of general polyatomic molecules.

**Explicitly-correlated CC methods based on complete diagrammatic equations**.[3,6] The tensor contraction expressions defining a variety of high-rank CC energies and wave functions that include the inter-electronic distances ($r_{12}$) explicitly (CC-R12) have been derived with the aid of a newly-developed computerized symbolic algebra SMITH. Efficient computational sequences to perform these tensor contractions have also been suggested, defining intermediate tensors as a sum of binary tensor contractions. SMITH can elucidate the index permutation symmetry of intermediate tensors that arise from an expectation value of any number of excitation, de-excitation and other general second-quantized operators. SMITH also automates additional algebraic transformation steps specific to R12 methods, i.e. the identification and isolation of the special intermediates that need to be evaluated analytically and the resolution-of-the-identity insertion to facilitate high-dimensional molecular integral computation.

The tensor contraction expressions defining the CC-R12 methods including through the connected quadruple excitation operator (CCSDTQ-R12) have been documented and efficient computational sequences have been suggested not just for the ground state but also for excited states via the equation-of-motion formalism (EOM-CC-R12) and for the so-called $\Lambda$ equation ($\Lambda$-CC-R12) of the CC analytical gradient theory. Additional equations (the geminal amplitude equation) arise in CC-R12 and need to be solved to determine the coefficients multiplying the $r_{12}$-dependent factors. The operation cost of solving the geminal amplitude equations of rank-$k$ CC-R12 and EOM-CC-R12 (right-hand side) is asymptotically not greater than that of solving the usual amplitude equations. This suggests that the unabridged equations should be solved in high-rank CC-R12 for benchmark accuracy.

As an initial application, the explicitly-correlated CC singles and doubles (CCSD-R12) and related methods—its linearized approximation, CCSD(R12), and explicitly correlated second-order Møller–Plesset perturbation method MP2-R12—have been implemented into efficient computer codes that take into account point-group symmetry and applicable to closed- and open-shell molecules. The implementation is based on the nontruncated formalisms and has been largely automated by SMITH, which can handle complex index permutation symmetry of intermediate tensors that occur in the explicitly correlated methods. The CCSD-R12 correlation energies are obtained for selected systems using the Slater-type correla-

tion function, which can serve as benchmarks for rigorous assessment of other approximate CC-R12 methods. It reproduces typically 97 and 99 % of complete-basis-set correlation energies with the aug-cc-pVDZ and TZ basis sets, respectively, in contrast to mere 65 and 85 % by the non-R12 counterparts.

**Anharmonic vibrational frequencies and vibrationally averaged structures and NMR parameters of bifluoride ion**.[5] The anharmonic vibrational frequencies of $FHF^-$ were computed by the vibrational self-consistent-field, CI, and second-order PT methods with a multiresolution composite potential energy surface generated by the electronic CC method with various basis sets. Anharmonic vibrational averaging was performed for the bond length and NMR indirect spin-spin coupling constants, the latter computed by the equation-of-motion CC method. The calculations placed the vibrational frequencies at 580 ($\nu_1$), 1292 ($\nu_2$), and 1313 ($\nu_3$), the zero-point H–F bond length ($r_0$) at 1.1539 Å, the zero-point one-bond spin-spin coupling constant [$^1J_0$(HF)] at 124 Hz, and the bond dissociation energy ($D_0$) at 43.3 kcal/mol. They agreed excellently with the corresponding experimental values: $\nu_1$ = 583 cm$^{-1}$, $\nu_2$ = 1286 cm$^{-1}$, $\nu_3$ = 1331 cm$^{-1}$, $r_0$ = 1.1522 Å, $^1J_0$(HF) = 124±3 Hz, and $D_0$ = 44.4±1.6 kcal/mol. The vibrationally averaged bond lengths matched closely the experimental values of five excited vibrational states, furnishing a highly dependable basis for correct band assignments. Our calculations predicted a value of 186 Hz for experimentally inaccessible $^2J_0$(FF).

**Fast electron-correlation methods for molecular crystals, with an application to solid formic acid**.[1] A method for the routine first-principles determination of energies, structures, and phonons of molecular crystals by high-accuracy electron-correlation theories has been proposed. It approximates the energy per unit cell of a crystal by a sum of monomer and dimer energies in an embedding field of self-consistent (and, therefore, polarizable) atomic charges and dipole moments. First and second energy derivatives with respect to atom positions and lattice constants (useful for characterizing structures and phonons) have also been computed efficiently with a long-range electrostatic correction. The method has been applied to solid formic acid, which is of significant contemporary interest in relation to the structure of hydrogen-bonded solid, liquid, and aerosols, phase transitions, polymorphism, concerted proton transfer, etc. Accurate energies (with corrections for basis-set superposition errors), structural parameters, and frequencies and reliable assignments of infrared, Raman, and inelastic neutron scattering spectral bands have been obtained for three polymorphic structures ($\beta_1$, $\beta_2$, and $\alpha$) with second-order perturbation theory or higher. They have suggested that observed diffraction and spectroscopic data are consistent with the pristine $\beta_1$ form (**Figure**) and the hitherto-inexplicable infrared band splitting can be assigned to the in-phase and out-of-phase vibrations of adjacent hydrogen-bonded molecules rather than speculated polymorphism. Spectral features expected from the $\beta_2$ and $\alpha$ forms have also been predicted and are shown to be incompatible with the observed Raman and inelastic neutron scattering spectra in the low-frequency region.

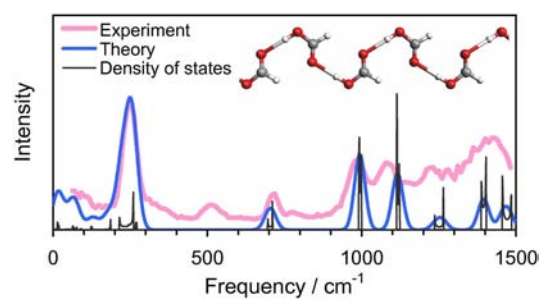


**Fig.** Inelastic neutron scattering from solid formic acid in the $\beta_1$ form.

## Future Plans

High-rank explicitly-correlated CC and EOM-CC methods up to the connected quadruple excitation operator are being developed and tested. Anharmonic vibrational frequencies and vibrationally averaged structures of several molecules of importance in combustion chemistry have been obtained with predictive accuracy. Anharmonic phonon frequencies of polyethylene, polyacetylene, and solid hydrogen fluoride have been obtained with *ab initio* electronic and vibrational many-body methods. The fast method for molecular crystals is being extended to two- and three-dimensional molecular crystals and an application is planned for two-dimensional hydrogen-bonded network of formamide and a proton-ordered ice. A promising approximation that accelerates the *ab initio* crystalline orbital calculations of polymers at correlated levels by downsampling of wave vectors has been implemented and is being tested.

# Submitted Publications of DOE Sponsored Research

1. S. Hirata, "Fast electron-correlation methods for molecular crystals: An application to the $\alpha$, $\beta_1$, and $\beta_2$ modifications of solid formic acid," (submitted, 2008).

# References to Publications of DOE Sponsored Research (2005–Present)

2. **Invited article:** S. Hirata and K. Yagi, *Chemical Physics Letters* (in press, 2008) [a Frontiers article], "Predictive electronic and vibrational many-body methods for molecules and macromolecules."
3. T. Shiozaki, M. Kamiya, S. Hirata and E. F. Valeev, *The Journal Chemical Physics* (*Communications*) **129**, 071101 (2008) (4 pages), "Explicitly correlated coupled-cluster singles and doubles method based on complete diagrammatic equations."
4. **Invited book chapter:** S. Hirata, P.-D. Fan, T. Shiozaki, and Y. Shigeta, *Radiation Induced Molecular Phenomena in Nucleic Acid: A Comprehensive Theoretical and Experimental Analysis*, in the book series *Challenges and Advances in Computational Chemistry and Physics, Vol. 5* edited by Jerzy Leszczynski and Manoj Shukla (Springer, 2008), "Single-reference methods for excited states in molecules and polymers."
5. S. Hirata, K. Yagi, S. A. Perera, S. Yamazaki, and K. Hirao, *The Journal of Chemical Physics* **128**, 214305 (2008) (9 pages), "Anharmonic vibrational frequencies and vibrationally averaged structures and nuclear magnetic resonance parameters of $FHF^-$."
6. **Invited article:** T. Shiozaki, M. Kamiya, S. Hirata, and E. F. Valeev, *Physical Chemistry Chemical Physics* **10**, 3358–3370 (2008) [in the themed issue on "Explicit-R12 correlation methods and local correlation methods"], "Equations of explicitly-correlated coupled-cluster methods."
7. K. Yagi, S. Hirata, and K. Hirao, *Physical Chemistry Chemical Physics* **10**, 1781–1788 (2008), "Vibrational quasi-degenerate perturbation theory: Application to Fermi resonances in $CO_2$, $H_2CO$, and $C_6H_6$."
8. M. Kamiya, S. Hirata, and M. Valiev, *The Journal of Chemical Physics* **128**, 074103 (2008) (11 pages), "Fast electron correlation methods for molecular clusters without basis set superposition errors."
9. T. Shiozaki and S. Hirata, *Physical Review A* (*Rapid Communications*) **76**, 040503(R) (2007) (4 pages), "Grid-based numerical Hartree–Fock solutions of polyatomic molecules."
10. K. Yagi, S. Hirata, and K. Hirao, *The Journal of Chemical Physics* **127**, 034111 (2007) (7 pages), "Efficient configuration selection scheme for vibrational second-order perturbation theory."
11. T. Shiozaki, K. Hirao, and S. Hirata, *The Journal of Chemical Physics* **126**, 244106 (2007) (11 pages), "Second- and third-order triples and quadruples corrections to coupled-cluster singles and doubles in the ground and excited states."
12. M. Kamiya and S. Hirata, *The Journal of Chemical Physics* **126**, 134112 (2007) (10 pages), "Higher-order equation-of-motion coupled-cluster methods for electron attachment."
13. P.-D. Fan, M. Kamiya, and S. Hirata, *The Journal of Chemical Theory and Computation* **3**, 1036–1046 (2007), "Active-space equation-of-motion coupled-cluster methods through quadruple excitations for excited, ionized, and electron-attached states."
14. V. Rodriguez-Garcia, S. Hirata, K. Yagi, K. Hirao, T. Taketsugu, I. Schweigert, and M. Tasumi, *The Journal of Chemical Physics* **126**, 124303 (2007) (6 pages), "Fermi resonance in $CO_2$: A combined electronic coupled-cluster and vibrational configuration-interaction prediction."
    K. Yagi, S. Hirata, and K. Hirao, *Theoretical Chemistry Accounts* **118**, 681–691 (2007) [Fraga special issue], "Multiresolution potential energy surfaces for vibrational state calculations."
15. S. Hirata, T. Yanai, R. J. Harrison, M. Kamiya, and P.-D. Fan, *The Journal of Chemical Physics* **126**, 024104 (2007), "High-order electron-correlation methods with scalar relativistic and spin-orbit corrections."
16. **Invited article:** S. Hirata, *Journal of Physics: Conference Series* **46**, 249-253 (2006), "Automated symbolic algebra for quantum chemistry."
17. M. Kamiya and S. Hirata, *The Journal of Chemical Physics* **125**, 074111 (2006), "Higher-order equation-of-motion coupled-cluster methods for ionization processes."
18. **Invited article:** S. Hirata, *Theoretical Chemistry Accounts* **116**, 2–17 (2006) [a part of the special issue "*New Perspective in Theoretical Chemistry*"], "Symbolic algebra in quantum chemistry."
19. V. Rodriguez-Garcia, K. Yagi, K. Hirao, S. Iwata, and S. Hirata, *The Journal of Chemical Physics* **125**, 014109 (2006) [selected as an article in *Virtual Journal of Biological Physics Research*, July 15 (2006)], "Franck–Condon factors based on anharmonic vibrational wave functions of polyatomic molecules."
20. **Invited article:** Y. Shao, *et al*. *Physical Chemistry Chemical Physics* **8**, 3172–3191 (2006), "Advances in methods and algorithms in a modern quantum chemistry package."
21. P.-D. Fan and S. Hirata, *The Journal of Chemical Physics* **124**, 104108 (2006), "Active-space coupled-cluster methods through connected quadruple excitations."
22. Y. Shigeta, K. Hirao, and S. Hirata, *Physical Review A* (*Rapid Communications*) **73**, 010502(R) (2006), "Exact-exchange time-dependent density-functional theory with the frequency-dependent kernel."
23. **Invited article:** P. Piecuch, S. Hirata, K. Kowalski, P.-D. Fan, and T. L. Windus, *International Journal of Quantum Chemistry* **106**, 79–97 (2006), "Automated derivation and parallel computer implementation of renormalized and active-space coupled-cluster methods."
24. H. Wang, J. Szczepanski, S. Hirata, and M. Vala, *The Journal of Physical Chemistry A* **109**, 9737–9746 (2005), "Vibrational and electronic absorption spectroscopy of dibenzo[b,def]chrysene and its ions."
25. S. Hirata, *The Journal of Chemical Physics* (*Note*) **123**, 026101 (2005), "Time-dependent density functional theory based on optimized effective potentials for van der Waals forces."
26. S. A. Perera, P. B. Rozyczko, R. J. Bartlett, and S. Hirata, *Molecular Physics* (Special Issue for Professor Rodney J. Bartlett) **103**, 2081 (2005), "Improving the performance of direct coupled cluster analytical gradients algorithms."
27. S. Hirata, M. Valiev, M. Dupuis, S. S. Xantheas, S. Sugiki, and H. Sekino, *Molecular Physics* (Special Issue for Professor Rodney J. Bartlett) **103**, 2255 (2005), "Fast electron correlation methods for molecular clusters in the ground and excited states."
28. S. Hirata, S. Ivanov, R. J. Bartlett, and I. Grabowski, *Physical Review A* **71**, 032507 (2005), "Exact-exchange time-dependent density functional theory for static and dynamic polarizabilities."
29. S. Hirata, *The Journal of Chemical Physics* **122**, 094105 (2005), "Third- and fourth-order perturbation corrections to excitation energies from configuration interaction singles."

# Optical Spectroscopy at the Spatial Limit

*Wilson Ho*

Department of Physics & Astronomy and Department of Chemistry
University of California, Irvine
Irvine, CA 92697-4575 USA

wilsonho@uci.edu

**Program Scope:**

The main goal of the DOE supported project is to beat the diffraction limit in the spatial resolution resolvable in optical phenomena. Optical microscopy has played an enabling role in experimental observation, particularly the biological sciences. The desire for observing increasingly finer details has pushed instrument development toward the limit of spatial resolution. By using a low temperature scanning tunneling microscope (STM) and coupling light to the nano-junction, it has become possible to probe optical phenomena with sub-atomic resolution. Such capability provides a new window for viewing molecular properties. In "molecular acupuncture", the way the molecule behaves can be controlled by pinpointing the specific part of the molecule that is initially perturbed. Specific examples of such control include the spatial dependence of single molecule fluorescence and the primary steps of electron transfer to a single molecule. In the conversion of sun light to energy and in optoelectronics, a promising scheme involves the use of nanoscale objects as the active media. The investigation of the fundamental mechanisms of how light can be efficiently coupled to nanostructures not only can lead to new scientific phenomena but also form the basis for new technology.

**Recent Progress:**

The STM allows us to inject one electron at a time into a specific physical location and at a particular energy of the molecule. The electron is in an excited state and subsequently decays via a number of different pathways. One of the pathways involves an optical transition between two electronic states and the emitted photons have a spectral distribution and spatial dependence that are determined by the initial electron injection location and energy. In all the other single molecule fluorescence experiments, emission appears as a speckle and no internal structure is resolved; the spectral distribution is thus an integrated spectrum. While laser induced single molecule spectroscopy eliminates averaging over an ensemble of molecules, the spectrum is an average over the internal structure of the molecule. Taking it one step further, light emission from single molecules induced by tunneling electrons in a STM not only eliminates ensemble averaging, the spatial variations in the spectral distribution and intensity are resolved inside a single molecule. The emission is obtained from single Mg-porphine molecules adsorbed at ~10 K on ~5 Å thick $Al_2O_3$ grown on NiAl(110) surface. Figure 1 shows the topographical image and simultaneously acquired light emission integrated over the entire spectral range (720 nm to 840 nm). The top image show that not all the molecules emit in the selected wavelength range, and the emission intensity and pattern vary from molecule to molecule. The middle and the

bottom images reveal increasingly finer details as the image zooms into a single molecule. Distinct pattern is seen in the emission; the molecular interior is far from being homogeneous.

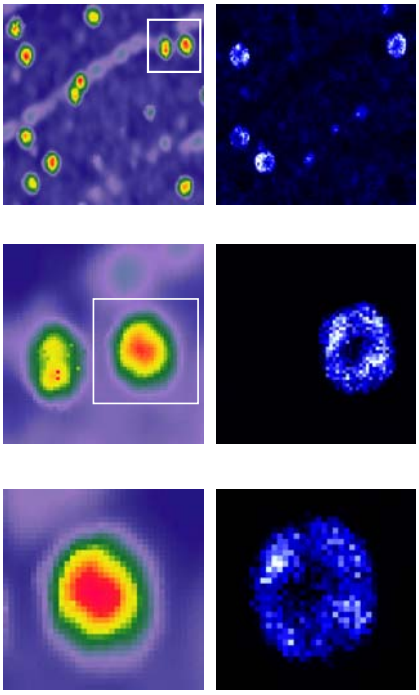

Fig. 1: (Left column) STM Topographic images of single Mg-porphine molecules adsorbed on ~5 Å thick $Al_2O_3$ grown on NiAl(110) surface. (Right column) Tunneling electron induced light emission images zooming onto a single molecule and revealing in increasing detail the spatial distribution of the emission intensity integrated over the spectral range 720 nm to 840 nm. The symmetry of the emission pattern reflects the spatial pattern of the final state molecular orbital involved in the optical transition. (C. Chen, C. Bobisch, and W. Ho, unpublished results, 2008).

The combination of spectroscopy and microscopy enables imaging of specific features in the spectral distribution. In the case of Mg-porphine, imaging of individual vibronic peaks in the fluorescence spectrum can be carried out. Additionally, spatially resolved spectroscopy is obtained by tunneling into a particular part of the molecule. Other variables that can be varied are the energy of the tunneling electrons (bias voltage) and the magnitude of the tunneling current. Thus the experiment is multi-dimensions: sample bias voltage, tunneling current, position of tunneling, emission wavelength, polarization, and spatial distribution. A detailed picture is obtained for the optical transition inside a single molecule. In Figure 2, imaging of the individual vibronic states in single molecule is demonstrated, revealing not only the spatial pattern but also the assignment of the different vibronic progressions in the spectra, the specific vibrations that are excited in the optical transition.

**Future Plans:**

The ability to probe changes in real time with sub-Ångström spatial resolution would open a new window for viewing the inner machinery of matter. A promising approach involves the combination of laser with the scanning tunneling microscope (STM). During the current grant period, diffraction limited spatial resolution and thermal effects due to laser irradiation have been defeated through the demonstration of sub-Ångström resolution in spectroscopic, optical imaging and photo-induced electron transfer. The plan for the future aims at reaching an additional goal in the time domain by pushing spectroscopic imaging toward the simultaneous limits of sub-Ångström and 10 femtoseconds. Four focused activities have been identified, and all are designed to probe and image the dynamic properties in the interior of single molecules

and artificially created nanostructures: 1. Spatially, spectroscopically, and temporally resolved photon imaging, 2. Direct measurement of photo-induced tunneling current, 3. Photo-induced electron tunneling in the time domain, and 4. Two-electron induced light emission. These experiments lead to a fundamental understanding of matter by revealing them in previously unattainable regimes of space and time. Furthermore, knowledge of the coupling of light to nanoscale objects bring us one step closer toward the realization of efficient conversion of sun light to energy, broad range of optoelectronics and plasmonics, and economically competitive photocatalysis.

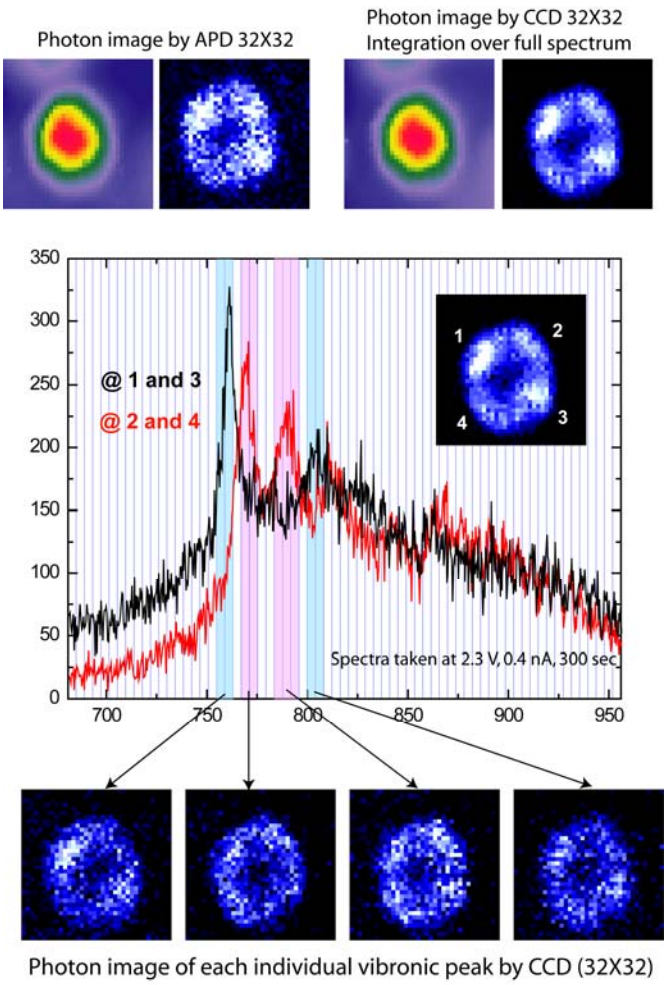


Fig. 2: Photon emission from a single Mg-porphine molecule. (Upper Left) Simultaneously acquired topographic and photon emission images recorded with an avalanche photodiode, integrated over the entire emission spectral range. (Upper Right) Corresponding images recorded with a monochromator and a liquid nitrogen cooled CCD, showing the same pattern with better signal. (Middle) Spectral distribution obtained by tunneling into the four parts of the molecule as indicated in the photon image. Two vibronic progressions are observed in the fluorescence spectra and the two progressions are spatially distinct, separated $90^{o}$ from each other, revealing the orthogonality of the two nearly degenerate molecular orbitals that the progressions originate. (Bottom) Imaging individual vibronic states by recording the spatial distribution of the emission intensity integrated over the narrow band of wavelengths as indicated by the vertical blue and pink color bands in the emission spectra. (C. Chen, C. Bobisch, and W. Ho, unpublished results, 2008).

**<u>References to Publications of DOE Sponsored Research (2005-present)</u>:**


[1] H..J. Lee, J.H. Lee, and W. Ho, *"Vibronic Transitions in Single Metalloporphyrins"*, ChemPhysChem **6**, 971-975 (2005).

[2] G.V. Nazin, X.H. Qiu, and W. Ho, *"Vibrational Spectroscopy of Individual Doping Centers in a Monolayer Organic Crystal"*, J. Chem. Phys. **122**, 181105-1-4 (2005).

[3] G.V. Naxin, S.W. Wu, and W. Ho, *"Tunneling Rates in Electron Transport Through Double-Barrier Molecular Junctions in a Scanning Tunneling Microscope"*, Proc. Nat. Acad. Sci. **102**, 8832-8837 (2005).

[4] J.R. Hahn and W. Ho, *"Orbital Specific Chemistry: Controlling the Pathway in Single-Molecular Dissociation"*, J. Chem. Phys. **122**, 244704-1-3 (2005).

[5] G.V. Nazin, X.H. Qiu, and W. Ho, *"Charging and Interaction of Individual Impurities in a Monolayer Organic Crystal"*, Phys. Rev. Lett. **95**, 166103-1-4 (2005).

[6] J.R. Hahn and W. Ho, *"Direct Observation of $C_2$ Hydrocarbon-Oxygen Complexes on Ag(110) With a Variable-Low-Temperature Scanning Tunneling Microscope"*, J. Phys. Chem. B **109**, 20350-20354 (2005).

[7] J.R. Hahn and W. Ho, *"Chemisorption and Dissociation of Single Oxygen Molecules on Ag(110)"*, J. Chem. Phys. **123**, 214702-1-6 (2005).

[8] J.R. Hahn and W. Ho, "Imaging and Vibrational Spectroscopy of Single Pyridine Molecules on Ag(110) Using a Low-Temperature Scanning Tunneling Microscope", J. Chem. Phys. **124**, 204708-1-4 (2006).

[9] S.W. Wu, N. Ogawa, and W. Ho, *"Atomic Scale Coupling of Photons to Single-Molecule Junction"*, Science **312**, 1362-1365 (2006).

[10] S.W. Wu, N. Ogawa, G.V. Nazin, and W. Ho, *"Conductance Hysteresis and Switching in Single-Molecule Junction"*, J. Phys. Chem. C 112, 5241-5244 (2008).
*** Figure from this paper appeared on the cover of this issue of the J. Phys. Chem. C.

[11] S.W. Wu, G.V. Nazin, and W. Ho, *"Intramolecular Photon Emission From a Single Molecule in a Scanning Tunneling Microscope"*, Phys. Rev. B 77, 205430-1-5 (2008).

# THEORY OF THE REACTION DYNAMICS OF SMALL MOLECULES ON METAL SURFACES

Bret E. Jackson

Department of Chemistry
701 LGRT
710 North Pleasant Street
University of Massachusetts
Amherst, MA 01003
jackson@chem.umass.edu

## Program Scope

Our objective is to develop realistic theoretical models for molecule-metal interactions important in catalysis and other surface processes. The dissociative adsorption of molecules on metals, Eley-Rideal and Langmuir-Hinshelwood reactions, recombinative desorption and sticking on surfaces are all of interest. To help elucidate the UHV-molecular beam experiments that study these processes, we examine how they depend upon the nature of the molecule-metal interaction, and experimental variables such as substrate temperature, beam energy, angle of impact, and the internal states of the molecules. Electronic structure methods based on Density Functional Theory (DFT) are used to compute the molecule-metal potential energy surfaces. Both time-dependent quantum scattering techniques and quasi-classical methods are used to examine the reaction dynamics. Effort is directed towards developing improved quantum scattering methods that can adequately describe reactions on surfaces, as well as include the effects of temperature (lattice vibration) in quantum dynamical studies.

## Recent Progress

In an earlier study of H atom recombination on Ni(100), we allowed the lattice atoms to move, which required that we construct a potential energy surface based upon the instantaneous positions of the lattice atoms and the adsorbates. We avoided the usual problems associated with pairwise potentials by using a potential based upon ideas from embedded atom and effective medium theory, but instead of using the isolated atom electron densities, we fit the one and two-body terms to reproduce the results of our DFT calculations. More recently we used the part of this potential describing the Ni-Ni interactions to study the sputtering of Ni surfaces by Ar beams, in order to further test the utility of these potentials [1]. We find that this form for the potential very accurately describes the energy required to severely distort the lattice or to remove one or more Ni atoms from the lattice. Agreement of sputtering yields and threshold energies with experiments is greatly improved over earlier models.

We completed our studies of H-graphite reactions, which play an important role in the formation of molecular Hydrogen on graphitic dust grains in interstellar space, as well as in the etching of the graphite walls of fusion reactors. In earlier work, using DFT-based electronic structure methods, we demonstrated that an H atom could chemisorb onto a graphite terrace carbon, with the bonding C atom puckering out of the surface plane by several tenths of an Å. We computed the potential energy surface for the Eley-Rideal (ER) reaction of an incident H atom with this chemisorbed H atom, and suggested that the reaction cross sections should be very large – on the order of 10 $Å^2$. Motivated by our studies, the group of Küppers (Bayreuth) showed experimentally that H could indeed chemisorb, that the lattice did pucker, and that the cross

section for the H(g) + D/graphite ER reaction to form HD(g) was about 8 $Å^2$. We demonstrated that the $H_2$ formed in these reactions should be very highly excited, vibrationally, and might be responsible for some of the unique chemistry that occurs in interstellar clouds. Hydrogenation of the edge carbons was also explored. We demonstrated that the vapor pressure of $H_2$ in equilibrium with these hydrogenated structures is too small to be useful for hydrogen storage.

More recently we have focused on the remaining unsolved question as to why the measured sticking probabilities of H on graphite are so large, roughly 0.4. Given the significant lattice distortion required for chemisorption, this is surprising. We used DFT to map out the H-graphite interaction as a function of the position of the bonding carbon, and found a barrier to chemisorption of about 0.2 eV, in excellent agreement with recent experiments. A potential energy surface for trapping and sticking was constructed, and a low-dimensional collinear quantum study of the trapping process was implemented [2]. We found that the bonding carbon reconstructs in about 50 fs. Our results suggested that sticking proceeds via a trapping resonance, which relaxes by dissipating energy into the substrate over a ps or so. More recently we computed the full three-dimensional potential, and used classical mechanics to compute the sticking cross sections [4], which are on the order of 0.1 $Å^2$ at energies not too far above the barrier. However, when averaged over the experimental incident energy distribution, the computed sticking probabilities were only around 0.08. The proposed mechanism involving a trapping resonance was confirmed. An improved model that included a large dynamical graphite lattice of over 100 Carbon atoms provided a more accurate (and converged) description of the relaxation and stabilization of the C-H bond, but did not give a significantly different sticking probability [7]. However, we have since come to understand the (apparent) discrepancy between experiment and theory. Using DFT, we computed the potential energy surfaces for the addition of H atoms to Carbon sites adjacent to chemisorbed H atoms. These show that after the addition of one H atom to the surface, there are surface sites where the barrier to H sticking is small, and the binding energy is large [7]. Thus, while the initial (true zero coverage) sticking may indeed be small, as we computed, the addition of subsequent H atoms in preferred locations relative to the initial adsorbates may happen with a large probability. This has now been confirmed by two sets of experiments. The Küppers group has now measured sticking down to (true) zero coverage, finding probabilities of around 0.1. They observe that sticking increases as coverage increases. This group and another have also observed pair formation, via STM, where H atoms are observed to cluster together on the surface, due to these preferred binding sites.

It is likely that in interstellar space much of the ER-reactive adsorbed H is physisorbed. In order to estimate the rates for $H_2$ formation via this pathway, it is necessary to know the sticking probability of H into the physisorption well. We have developed a powerful approach to these types of problems based on the reduced density matrix, which allows us to evolve a quantum system weakly coupled to a bath over a relatively long time. Thus, we can not only compute, quantum mechanically, the scattering into free and bound states, we can observe over long times the relaxation and/or desorption from these states; i.e., the evolution towards true sticking. We have tested this approach in a study of He scattering and trapping/desorption on corrugated metal surfaces over timescales of 100's of ps [8]! This method was applied to H physisorption on graphite, and we demonstrated that sticking can be enhanced at low energies due to diffraction mediated trapping states that relax into the substrate [8].

We concluded our studies of the H(g) + Cl/Au(111) reaction, motivated by two detailed experimental studies of this system. These experiments observe strong H atom trapping and a thermal Langmuir-Hinshelwood channel for HCl formation, as well as ER and hot atom (HA) channels. One of our findings is that the ER reaction cross section is much larger than for H(g) +

H/metal reactions, roughly 1 –2 $Å^2$. This is due to a steering mechanism, and arises from the relatively large distance of the adsorbed Cl above the metal. The incoming H atom is strongly attracted to both the Cl and the metal, but it encounters the layer of adsorbed Cl atoms first, and steers towards them. There are also some interesting variations of ER reactivity with the Cl vibrational state, and an exchange pathway is observed (for the first time), in which the H remains bound while the Cl desorbs. Quasi-classical trajectories were used to study this reaction for the case of large Cl coverages, and with dissipation of the trapped hot atoms' energy into the lattice [3]. The ER and HA reaction pathways for HCl formation are a bit more complicated than for molecular Hydrogen formation. We find that HA reactions dominate the formation of HCl. We also find that there must be significant energy loss into the substrate excitations, perhaps into electron hole pair excitations, from either the trapping hot H atoms, or the excited product HCl, in order to agree with experiment.

Most of the past two years have been spent exploring the dissociative adsorption of methane on metals. A problem that is not well understood is how methane reactivity varies with the temperature of the metal, and why the nature of this variation differs from metal to metal. To examine this we have used DFT to compute the barriers and explore the potential energy surfaces for methane dissociation on several metal surfaces. We have also examined how these barriers change due to lattice motion. Starting with the Ni(111) surface, we found that at the transition state for dissociation, the Ni atom over which the molecule dissociates would prefer to pucker out of the surface by 0.23 Å. Put another way, when this Ni atom vibrates in and out of the plane of the surface, the barrier to dissociation over this Ni atom increases and decreases, respectively. This should lead to a strong variation in the reactivity with temperature. In addition, it is not clear that a metal atom would have time to move or relax during a reactive collision. To explore these issues, high dimensional quantum scattering calculations were implemented, which allowed for the motion of several key methane degrees of freedom, as well as the metal lattice atom over which the reaction occurs. It was found that the lattice has time to at least partially relax (pucker) during the reaction, even at collision energies of an eV or so. The net result is that the reactivity was significantly larger than for the static lattice case. We compared our results with the surface oscillator model, used for many years to explain the effects of thermal lattice motion on dissociative adsorption. For this model, the lattice recoils into the surface during the collision, leading to a lower reactivity. We clearly demonstrated that when lattice relaxation in the presence of an adsorbate is possible, the physics is very different from what has long been assumed [5, 6].

This model was also used to elucidate recent experiments of the Utz group (Tufts), who examined $CD_3H$ dissociation on Ni(111). They were able to significantly enhance reactivity by laser exciting the C-H stretch of the molecule. Generally, the reactivity of the laser-excited molecules are compared with the "laser off" reactivity, and an open question has been to what extent vibrationally excited molecules contribute to this "laser off" reactivity. We were able to show that vibrationally excited molecules can make significant contributions, particularly at lower incident energies where the ground vibrational state is "below the barrier"[6].

We have since used DFT to explore the reaction pathways for methane dissociation on Ni(100), Pt(111) and Pt(100). We find that there are similar forces for lattice relaxation and puckering of the metal atom over which the molecule dissociates. In an attempt to understand recent experimental results on Ni(111) and Pt(111) from the Beck group, we have implemented a detailed comparison of methane dissociation on these two surfaces (submitted). First, DFT-based potential energy surfaces, much improved over our previous work, were constructed. The static surface barrier to reaction is about 0.13 eV lower on the Pt surface. Then, quantum scattering

studies were implemented as before. While the forces for lattice puckering are similar on the two metals, the heavier Pt is much less able to move during the reaction. We also find that under the experimental conditions, vibrationally excited molecules were more likely to contribute to the reactivity on Ni(111) than on Pt(111). When all of the initial states of the molecule and the lattice are properly averaged over, we are able to explain the Ni(111) reactivity well. However, we underestimate the reactivity on Pt(111), particularly at lower energies. This may be due to the way we treat the motion of the methyl group in our model, or errors in the DFT energies.

## Future Plans

The most significant shortcoming of our quantum scattering model is that it neglects motion parallel to the surface, including only the most reactive pathway (over the top site). On Ni(111) and (100) we have shown that during the reaction the methyl group moves towards a hollow site, while on Pt(111) and (100) the methyl remains at the top site. This may be the source of our inability to explain the relative reactivity on these two surfaces. We have formulated, and plan to implement, an approximate quantum way to include this type of motion, which also effectively averages over the surface impact sites, giving us probabilities more directly comparable with experiment. Another way to improve our model is to describe some of the degrees of freedom classically. We are writing and testing a code that treats the motion of the heavy lattice atom classically, and the other variables quantum mechanically. This has required us to change our coordinate system and develop a new way to energy-resolve our results, and we are (hopefully) close to solving these problems. Once completed, additional lattice atoms or molecular variables are easily added classically. We will then use these improved models to re-explore the Ni(111) and Pt(111) surfaces. Similarly, we will develop potential energy surfaces for methane reaction on Ni(100) and Pt(100), based on our DFT studies. There are numerous experimental studies on these surfaces, and as before, we want to understand the variation in reactivity with respect to surface, temperature, and the vibrational state of the molecule. We will continue to work with the Utz group, who can now measure methane reactivity over a wide range of surface temperatures. Eventually we hope to also examine methane dissociation on the step and defect sites of these and other metal surfaces. It is likely that the magnitudes of the thermal fluctuations and any relaxations are larger at these defect sites than on the terraces.

## References

[1]. Z. B. Guvenc, R. Hippler and B. Jackson, “Bombardment of Ni(100) surface with low-energy argons: molecular dynamics simulations, Thin Solid Films 474, 346-357 (2005).
[2]. X. Sha, B. Jackson, D. Lemoine and B. Lepetit,"Quantum studies of H Atom Trapping on a graphite surface," J. Chem. Phys. 122, 014709, 1-8 (2005).
[3]. J. Quattrucci and B. Jackson, "Quasi-classical study of Eley-Rideal and Hot Atom reactions of H atoms with Cl adsorbed on a Au(111) surface, J. Chem. Phys. 122, 074705, 1-13 (2005).
[4]. J. Kerwin, X. Sha and B. Jackson," Classical studies of H atom trapping on a graphite surface," J. Phys. Chem. B 110, 18811-18817 (2006).
[5]. S. Nave and B. Jackson," Methane dissociation on Ni(111): the role of lattice reconstruction," Phys. Rev. Lett. 98, 173003, 1-4 (2007).
[6]. S. Nave and B. Jackson," Methane dissociation on Ni(111): The effects of lattice motion and relaxation on reactivity," J. Chem. Phys. 127, 224702-1 - 11 (2007).
[7]. J. Kerwin and B. Jackson, "The sticking of H and D atoms on a graphite (0001) surface: the effects of coverage and energy dissipation”, J. Chem. Phys. 128, 084702-1 - 7 (2008).
[8]. Z. Medina and B. Jackson,"Quantum studies of light particle trapping, sticking and desorption on metal surfaces, J. Chem. Phys. 128, 114704-1 - 9 (2008).

# Probing catalytic activity in defect sites in transition metal oxides and sulfides using cluster models: A combined experimental and theoretical approach

Caroline Chick Jarrold and Krishnan Raghavachari
*Indiana University, Department of Chemistry, 800 East Kirkwood Ave.*
*Bloomington, IN 47405*
cjarrold@indiana.edu, kraghava@indiana.edu

## I. Program Scope

Applied heterogeneous catalysts are typically highly defective materials deposited on support materials. Varying the type of processing, the doping, and the type of support are known to influence catalytic activity. Yet, because of the complexity of these systems, experimental reproducibility is difficult, and theoretical modeling is challenging. Our project takes a bottom-up approach to determining the roles of the various components of applied systems by using cluster models, with the primary focus on transition metal (TM) oxides and sulfides. The strategy of this project is to determine the defect structures that exhibit the essential balance between structural stability and electronic activity necessary to be simultaneously robust and catalytically active, and to find trends and patterns in activity that can lead to improving applied catalytic systems. Since bonding in metal oxides and sulfides is largely ionic, it is also very localized, and extending what is learned from small cluster systems can be more rationally scaled to applied particulate and supported catalysts.

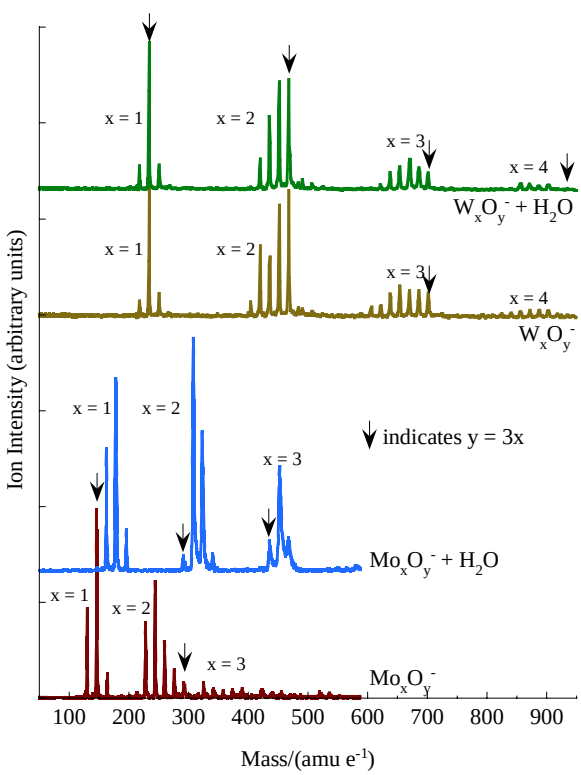


Figure 1. Comparison of water reactions with $Mo_xO_y^-$ and $W_xO_y^-$.

This project involves both experimental and computational approaches. Experimentally, the bare metal oxide and sulfide clusters are produced using a laser ablation/pulsed molecular beam cluster source, and the mass distribution of the negative ions is measured using mass spectrometry. Anions are of particular interest because of the propensity of metal oxide and sulfides to accumulate electrons in applied systems. Cluster structures are probed using a combination of mass-specific anion photoelectron (PE) spectroscopy and calculations. Clusters are then exposed to a variety of reagents relevant in a range of catalytic applications, including $H_2O$, $CH_4$, CO, and $CO_2$. Reaction products are probed mass spectrometrically and with PE spectroscopy, and detailed studies of the mechanisms and energetics of the reactions are done computationally.

## II. Recent Progress

### A. Reactions between $H_2O$ and $M_xO_y^-$ (M = Mo, W) clusters

The role of defects on the interaction between the group 6 metal oxides is relevant to understanding the mechanisms associated with the photocatalytic decomposition of water. We have undergone a series of reactivity studies involving both $Mo_xO_y^-$ clusters and $W_xO_y^-$ clusters with water, and have found remarkable differences in how the clusters interact with water. $Mo_xO_y^-$ suboxide clusters essentially undergo a combination of oxidation and hydroxide formation upon exposure to water, as seen by comparing the two bottom traces in Figure 1 (in order to guide the eye, ↓'s indicate the $M_xO_{3x}^-$ stoichiometric clusters). $W_xO_y^-$ clusters exposed to water, on the other hand, appear to slightly increase oxidation state on average, but very few hyperoxides are formed. Rather, very specific $W_xO_y^-$ appear to add a complete water, presumably dissociatively. Figure 2 shows a higher-resolution mass spectrum of the $W_2O_y^-$ manifold, in which $W_2O_6H_2^-$ is the only H-containing cluster. In the $W_3O_y^-$ manifold (not shown), $W_3O_7H_2^-$ is the only H-containing cluster. This evokes a picture of $W_xO_y^- + H_2O \rightarrow W_xO_{y+1}^- + H_2$ in general, but with deviations from this in very specific cases, such as $W_2O_5^- + H_2O \rightarrow W_2O_6H_2^-$. Anion PE spectra have been obtained for the relevant participants in these reactions.

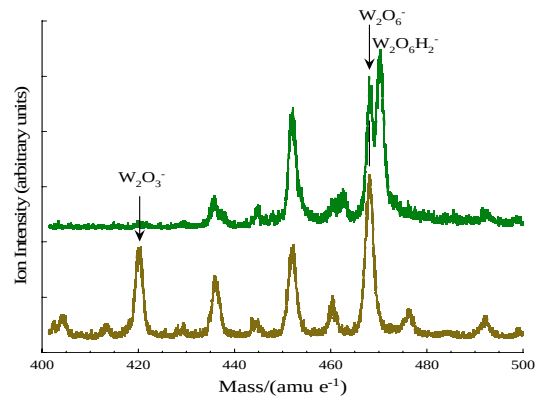


Figure 2. $W_2O_y^-$ manifold and $H_2O$ reaction products.

Computational approaches to quantifying and explaining chemical reactivity on metal oxides relies on the initial identification of experimentally relevant structural isomers. Much of this work has already been done by us and other researchers.[1,2] However, recently we have discovered new low energy isomers of the $W_2O_2^-$ and $W_2O_3^-$ clusters that have different electronic structures than previously reported. These isomers have either higher spin states, or antiferromagnetically coupled metal centers. These findings will be significant for water reactivity studies in that the release or uptake of molecular oxygen (two unpaired electrons) often requires a change in multiplicity, which is facilitated by systems with more unpaired electrons.

### B. Comparison of reactions between $CH_4$ and $M_xO_y^-$ (M = Mo, W) clusters

Our previous studies on reactions between $Mo_xO_y^-$ clusters and $CH_4$ (and $C_2H_6$) showed, in general, oxidative addition reaction products that resulted in the destruction of the Mo-O-Mo bridge bonds in the cluster, which is evocative of the Mars-van Krevelen mechanism for the partial oxidation of hydrocarbons. $W_xO_y^-$ clusters, in contrast, were non-reactive toward $CH_4$, except when $CH_4$ was present in the carrier gas at the site of the ablation. We have published work on the mechanistic explanation of methane activation on $Mo_2O_y^-$ clusters, which essentially shows that the oxidative addition reactions become energetically feasible with the addition of at least two $CH_4$ molecules.[3]

We have recently examined the role of the unreacting metal center(s) in two possible types of reactive interactions: An oxidative addition in which the metal center is inserted into the C-H bond, and a σ-bond metathesis reaction which involves the C-H and M-O bonds

reacting to form C-M and H-O bonds. Binary clusters were also considered for comparison. The adjacent table summarizes the results for $MM'O_5^-$ clusters.

| | Oxidative Addition | | σ-Bond Metathesis | |
|---|---|---|---|---|
| kcal/mol | Barrier | $\Delta E_{Reaction}$ | Barrier | $\Delta E_{Reaction}$ |
| $Mo_2O_5^-$ | 7.66 | -19.85 | 14.05 | -12.29 |
| $MoWO_5^-$ | 7.47 | -20.29 | 17.8 | -10.24 |
| $W_2O_5^-$ | 9.25 | -30.52 | 20.92 | -18.03 |

The oxidative addition reaction is both thermodynamically and kinetically more favorable than the σ-bond metathesis reaction for each sub-oxide cluster studied. Similar conclusions have been drawn by Goddard and coworkers through investigations into the single metal center $MO_x$ (M = Cr, Mo, W; x = 1,2,3) reactions with methane,[4] though the current results with the $M_2O_y^-$ clusters are likely to be more experimentally relevant as the saturated metal centers assume the tetrahedral geometries observed in bulk systems. The barrier for oxidative addition to $W_2O_5^-$ is somewhat higher than for Mo-containing analogs.

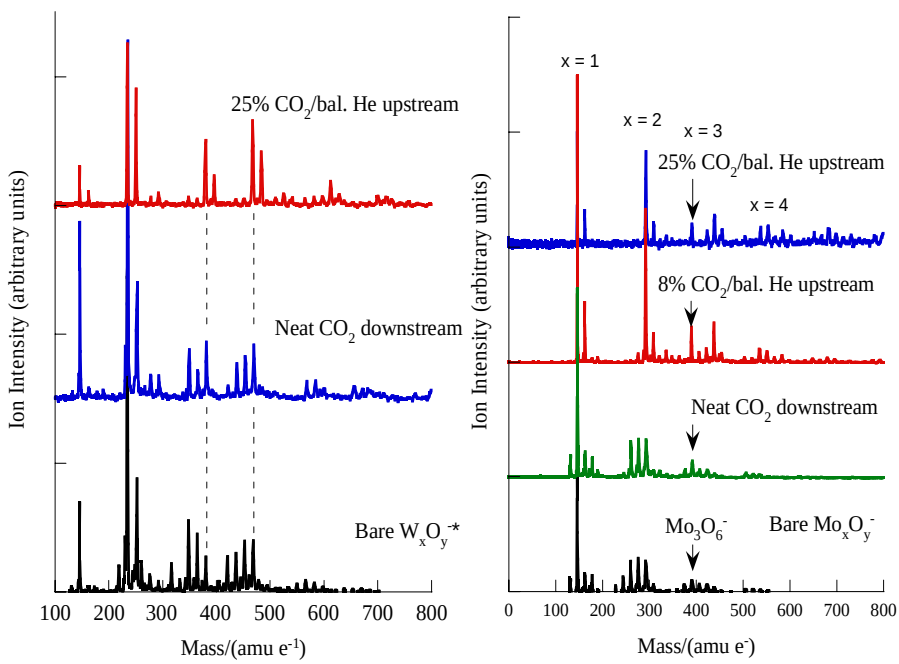


Figure 3. Reactions with $CO_2$ under various conditions

C. Exploring potential oxidation of CO and reduction of $CO_2$ by $Mo_xO_y^-$ and $W_xO_y^-$ clusters

We have previously run experiments on the reactivity of $Mo_xO_y^-$ toward CO, a notorious poison in a number of catalytic applications, including Pt electrocatalysts used in proton exchange membranes used in fuel cells. Addition of dispersed Mo/C particles in these systems has been found to improve the system's overall tolerance to CO.[5]

The reaction product distribution measured in the $Mo_xO_y^-$ + CO reactions, in addition to suggesting that the oxidation of CO was a primary reaction, revealed an interesting set of coordinatively unsaturated molybdenum and molybdenum oxide carbonyls [e.g, $Mo(CO)_5^-$, $MoO(CO)_3^-$, $MoO_2(CO)_{1,2}^-$]. We have just finished a series of calculations on the observed product anions and neutrals, in addition to intermediates that were not observed under the experimental conditions [e.g., $Mo(CO)_{1-3}^-$/ $Mo(CO)_{1-3}$, etc.]. The results of the calculations have allowed us to (1) correlate spin state with coordination, (2) correlate the nature of the Mo–CO bond while varying charge state and oxidation state, and (3) determine the nature of partially-occupied or low-lying un-occupied orbitals that may be relevant in catalytic processes. For instance, experimentally, we found that $MoO(CO)_3^-$ undergoes

photodissociation: $OMo(CO)_3^- + h\nu$ (3.49 eV) → $MoO^-$ ($^4\Pi$) + 3 CO. Computationally, we determined that the ground state of $OMo(CO)_3^-$ is a $^2A_1$ state, so this is a spin-forbidden process that appears to happen readily. The facility of spin-forbidden reactions is a hallmark of the second- and third-row TM-based catalysts. All of the explored effects are all relevant in supported systems, in which a CO-coordinated Mo-center may interact strongly with negatively charged oxygen atoms of the support.

The oxidation of CO by $Mo_2O_y^-$ occurs only for y = 2; $Mo_2O_2^-$ merely adds CO. The question of whether $CO_2$ could be reduced by extremely oxygen-deficient clusters was therefore raised. Also, $W_xO_y^-$ clusters have been found to be *completely non-reactive* toward CO, which is expected considering the relative bond dissociation energies of Mo–O (5.2 eV), W–O (7.5 eV) and OC–O (5.43 eV). Figure 3 shows some new results on reactions between $CO_2$ and the Mo– and W-based clusters. Very interesting size and oxygen content-specific reactivities have emerged from these studies, which will further be explored spectroscopically and computationally.

## III. Future Plans

A wide range of new reaction products have been observed with both $H_2O$ and $CO_2$ that suggest very interesting reaction mechanisms. Mass-specific reactivity studies will be carried out, once the mass filter has been optimized, along with spectroscopic investigation of the resulting complexes to characterize the bonding in these systems. We will also explore the energetics associated with catalyst activity and regeneration: The impact of electronic excitation of the complexes will be studied using resonant two-color experiments in which the effect of electronic excitation on structural rearrangement or photodissociation of the complex will be determined. DFT and TD-DFT studies are ongoing in parallel with all the experimental studies to facilitate the data interpretation as well as to predict full-cycle catalytic processes on the clusters. Full experimental and computational studies on Mo and W sulfide clusters, relevant to hydrodesulfurization, will be initiated in the next 12 months.

## IV. References to publications of DOE sponsored research that have appeared in 2004–present or that have been accepted for publication

(Four manuscripts currently in preparation.)

## References

[1]"Electronic and structural evolution and chemical bonding in ditungsten oxide clusters: $W_2O_n^-$ and $W_2O_n$ (n=1-6)," H.J. Zhai, X. Huang, L.F. Cui, X. Li, J. Li, and L.S. Wang, J. Phys. Chem. A **109**, 6019 (2005).
[2] "Structures of $Mo_2O_y^-$ and $Mo_2O_y$ (y = 2, 3, and 4) studied by anion photoelectron spectroscopy and density functional theory calculations," B. L. Yoder, J. T. Maze, K Raghavachari, and C.C. Jarrold, J. Chem. Phys. **122**, 094313 (2005); "Appearance of bulk properties in small tungsten oxide clusters," Q. Sun, B. K. Rao, and P. Jena, D. Stolcic, Y. D. Kim, G Gantefor, and A. W. Castleman, Jr. J. Chem. Phys. **121**, 9417 (2004).
[3] "Two methanes are better than one: A density functional theory study of the reactions of $Mo_2O_y^-$ (y=2-5) with methane," N.J. Mayhall and K. Raghavachari, J. Phys. Chem. A. **111**, 8211(2007).
[4] Methane activation by transition-metal oxides, MOx (M = Cr, Mo, W; x = 1, 2, 3)," X. Xu, F. Faglioni, and W.A. Goddard, J. Phys. Chem. A **106**, 7171 (2002).
[5] "Mechanism of CO tolerance on molybdenum-based electrocatalysts for PEMFC," E.I. Santiago, M.S. TBatista, E.M. Assaf, and E.A. Ticianelli, J. Electrochem. Soc. **151**, A944 (2004).

**Understanding the Electron-Water Interaction at the Molecular Level: Integrating Theory and Experiment in the Cluster Regime: DE-FG02-06ER15800**

**Program Manager: Dr. Gregory Fiechtner**

**K. D. Jordan (jordan@pitt.edu), Dept. of Chemistry, University of Pittsburgh, Pittsburgh, PA 15260**
**and M. A. Johnson (mark.johnson@yale.edu), Dept. of Chemistry, Yale University, New Haven, CT 06520**

The focus of our work is to understand the cooperative mechanics governing the interaction of an excess electron with well-defined networks of water molecules using the unique properties of size-selected ionic clusters. In the smallest size regime, clusters containing fewer than 10 or so water molecules, the advantage of this approach is that the entire cluster can be treated both experimentally and theoretically as a "supermolecule" in the sense that spectra can be effectively assigned to vibrational modes associated with particular minimum energy structures. Perfecting this exercise has been a central theme of our joint work over the past decade, which has been considerably assisted through DOE support since 2003. Challenges for the field are now to increase the scope of the cluster-based studies to capture more of the complexity at play in the condensed phase. This involves working with larger systems with finite (and controlled) internal energy content.

From the theoretical perspective, this extension requires the use of a model potential approach calibrated in the small cluster regime where the spectral signatures of structure are definitive and accurate calculations are feasible. In this regard, the so-called "Drude" model, developed in the Jordan group and which enables calculation of the properties of large clusters at finite temperature, plays a central role in our joint work. On the experimental side, working with larger systems inevitably introduces the complication of multiple isomers contributing to size-selective measurements. The isomer issue has two aspects: first, we need to understand the spectral patterns of the isomers present, and second, we must establish the free-energy barriers to interconversion between these isomers in the microcanonical ensemble. We have made great progress on both of these challenges in the past year, primarily due to the technical advances and focus we now enjoy as a result of our new apparatus commissioned in the spring of 2007 and dedicated to this DOE supported project. This multi-faceted instrument incorporates a highly efficient velocity map imaging photoelectron spectrometer for size-selected negative ions and implements a novel, three-stage mass-analysis approach that enables us to obtain the structures of isomers and follow the pathways for their interconversion. The water cluster anions occur in four distinct structural classes (denoted I', I, II and III in decreasing order of electron binding energy). In the past year, we have established how these isomers evolve upon growth by condensation[11] and obtained the first results on the barriers for their interconversion.[10] The latter measurements were the first results from our newly implemented, Ar-mediated pump-probe scheme in which two tunable infrared lasers manipulate isomer populations.

## I. *Exploring isomerization pathways upon aggregation: Ar-mediated incorporation of a single $D_2O$ molecule into $(H_2O)_6^- \cdot Ar_m$ clusters*

In this component of the program, we follow the Ar-mediated condensation of an isotopically labeled water molecule onto a high binding (type I) cluster:

$$(H_2O)_6^-\ (I)\cdot Ar_m + D_2O \rightarrow D_2O\cdot(H_2O)_6^-\ (I,I',II)\ \cdot Ar_n + (n-m)\ Ar$$

and then establish the isomeric composition (I, I' or II) of the adduct by acquiring its photoelectron and vibrational predissociation spectra. This procedure allowed us to deduce not only the types of isomers that can be formed, but also trace where the $D_2O$ molecule resides in the resulting network! The vibrational predissociation spectrum of the product in the bending region is indicated in Fig. 1, which reveals bands of both the newly incorporated $D_2O$ as well as the water molecules in the original hexamer reactant. Interestingly, three isomers are formed upon condensation, and the $D_2O$ molecule is observed to displace the special water molecule in the AA binding site that traps the excess electron in the high binding forms (I and I'). This work is reported in ref. (11).

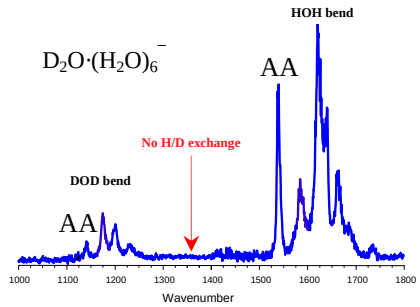


**Figure 1**. Ar predissociation spectrum of $D_2O\cdot(H_2O)_6^-\cdot Ar_6$ product ions from condensation of $D_2O$ molecules onto the $(H_2O)_6^-\cdot Ar_{12}$ parent cluster, in the region of the bending fundamentals of the $H_2O$, $D_2O$ and HOD molecules. These data indicate that the $D_2O$ molecule can displace the $H_2O$ molecule at the AA binding site for the excess electron.

## II. *Vibrationally mediated isomerization using a pump-probe approach with multiple stages of mass selection.*

We have engaged a major new effort to establish the barriers for isomer interconversion and thus illuminate the significant features of the potential landscape underlying the cluster dynamics. One aspect of the method is shown schematically in Fig. 2, where we selectively inject energy into a particular isomer by exciting one of its characteristic vibrational transitions, and then interrogate the distribution of isomers in the photofragments after mass-selection using velocity map photoelectron imaging. The instrument also has the capability of acquiring the vibrational predissociation spectra of the photofragments to further characterize the isomer distribution in the photoproducts. The important aspect of this approach is that the isomerization event

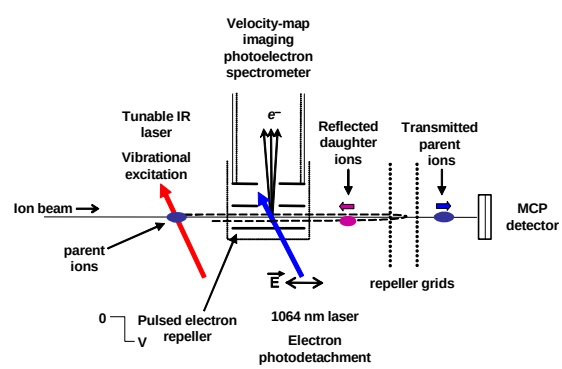


**Figure 2**. Schematic of experimental arrangement in which the product isomer distribution generated by vibrational excitation of a particular isomer of $(H_2O)_6^-\cdot Ar_8$ is established using imaging photoelectron spectroscopy of the photofragment ions.

occurs within moderately large Ar clusters, and evaporation of Ar atoms effectively quenches the system back into minimum energy configurations.

Using the Ar cluster–mediated pump-probe approach, we have established that conversion is very inefficient starting from isomer I when excited at relatively high energy in the OH stretching region (~3400 $cm^{-1}$), but isomer I' readily converts to types I and II upon photoexcitation in this range. The most labile isomer is type II, which yields type I upon excitation in the lower energy intramolecular HOH bending region around 1500 $cm^{-1}$. These results suggest that isomer II occurs as a rather high energy form, which can be converted to lower energy type I iomers over a barrier which is less than 1500 $cm^{-1}$. The Ar-cluster quenching approach also affords the capability of monitoring the relative energies of isomers by counting the number of Ar atoms that are ejected when intracluster isomerization occurs. To carry out this measurement, we have measured the predissociation spectra of several photofragments corresponding to different Ar loss channels. Preliminary results indicate that the type II form of the octamer anion lies about 1200 $cm^{-1}$ above the type I species, as isomerization yields fragments with about three fewer Ar atoms attached than the excited clusters that relax back into the isomer II minimum.

## III. *Theoretical studies*

One of the major challenges in interpreting the experimental data on the $(H_2O)_n^-$ clusters is identifying stationary points (both minima and transition states) accessed experimentally. We have recently used the quantum Drude model developed in the Pittsburgh group to carry out parallel tempering Monte Carlo (PTMC) method in simulations of the $(H_2O)_7^-$ cluster[12], which has been characterized experimentally by the Yale group.[9]. More recently we have interfaced the polarization model code for describing excess electrons[13] with transition state searching diagrams to map out the reaction pathways for the $(H_2O)_6^-$ cluster. (A partial disconnectivity diagram from this analysis is shown in Fig 3.) This capability will be especially valuable for analyzing the rearrangement pathways being explored by the Yale group.

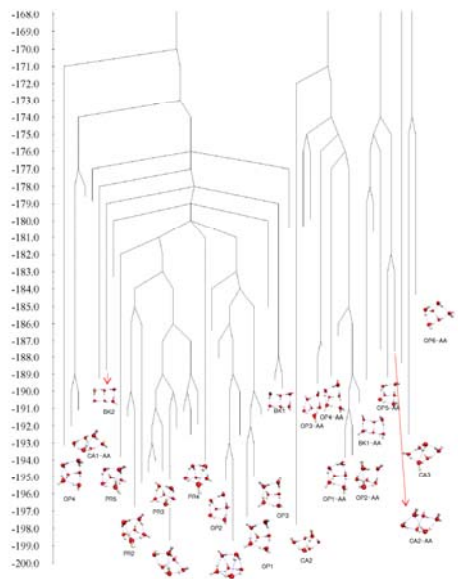


**Figure 3**. Partial disconnectivity diagram of $(H_2O)_6^-$. (Energies in kJ/mol.)

## VI. *Publications acknowledging DOE support under this grant*

1. **"Vibrational predissociation spectroscopy of the $(H_2O)_{6\text{-}21}^-$ clusters in the OH stretching region: Evolution of the excess electron-binding signature into the intermediate cluster size regime,"** N. I. Hammer, J. R. Roscioli, J. C. Bopp, J. M. Headrick and M. A. Johnson, *J. Chem. Phys.*, **123**, 244311, 2005.

2. **"Infrared spectrum and structural assignment of the water trimer anion,"** N. I. Hammer, J. R. Roscioli, M. A. Johnson, E. M. Myshakin and K. D. Jordan, *J. Phys. Chem. A*, **109**, 11526-11530, 2005.

3. **"An infrared investigation of the $(CO_2)_n^-$ clusters: Core ion switching from both the ion and solvent perspectives,"** J.-W. Shin, N. I. Hammer, M. A. Johnson, H. Schneider, A. Glob and J. M. Weber, *J. Phys. Chem. A*, **109**, 3146-3152, 2005.

4. **"Identification of two distinct electron binding motifs in the anionic water clusters: A vibrational spectroscopic study of the $(H_2O)_6^-$ isomers,"** N. I. Hammer, J. R. Roscioli and M. A. Johnson, *J. Phys. Chem. A*, **109**, 7896-7901, 2005.

5. **"Infrared spectroscopy of water cluster anions, $(H_2O)_{n=3\text{-}24}^-$ in the HOH bending region: Persistence of the double H-bond acceptor (AA) water molecule in the excess electron binding site of the class I isomers,"** J. R. Roscioli, N. I. Hammer and M. A. Johnson, *J. Phys. Chem. A*, **110**, 517-7520, 2006.

6. **"Low-lying isomers and finite temperature behavior of $(H_2O)_6^-$,"** T. Sommerfeld, S. D. Gardner, A. DeFusco, and K. D. Jordan, *J. Chem. Phys.*, **125**, 174309 (2006).

7. "**Infrared multiple photon dissociation of the hydrated electron clusters $(H_2O)_{15\text{-}50}^-$,"** K. R. Asmis, G. Santambrogio, J. Zhou, E. Garand, J. Headrick, D. Goebbert, M. A. Johnson, D. M. Neumark, *J. Chem. Phys.*, **126**, 191105 (2007).

8. **"Isomer-specific spectroscopy of the $(H_2O)_8^-$ cluster anion in the intramolecular bending region by selective photodepletion of the more weakly electron binding species (isomer II),"** J. R. Roscioli and M. A. Johnson, *J. Chem. Phys.*, **126**, 024307, 2007.

9. **"Exploring the correlation between network structure and electron binding energy in the $(H_2O)_7^-$ cluster through isomer photoselected vibrational predissociation spectroscopy and ab initio calculations: Addressing complexity beyond types I-III",** J. R. Roscioli, N. I. Hammer, M. A. Johnson, K. Diri and K. D. Jordan, *J. Chem. Phys.*, **128**, 104314, 2008.

10. **"Probing isomer interconversion in anionic water clusters using an Ar-mediated pump-probe approach: Combining vibrational predissociation and velocity-map photoelectron imaging spectroscopies**," Laura R. McCunn, George H. Gardenier, Timothy L. Guasco, Ben M. Elliott, Joseph C. Bopp, Rachael A. Relph, and Mark A. Johnson *J. Chem. Phys.*, **128**, 234311, 2008.

11. "**Site-specific addition of $D_2O$ to the $(H_2O)_6^-$ "hydrated electron" cluster: Isomer interconversion and substitution at the double H-bond acceptor (AA) electron-binding site**," Laura R. McCunn, Jeffrey M. Headrick and Mark A. Johnson, *Phys. Chem. Chem. Phys.*, **10**, 3118, 2008.

12. **"Parallel tempering Monte Carlo simulations of the water heptamer anion,"** A. DeFusco, T. Sommerfeld, K. D. Jordan, *Chem. Phys. Lett.*, **455**, 135-138 (2008).

13. **"Model potential approaches for describing the interactions of excess electrons with water clusters: incorporation of long-range correlation effects**, T. Sommerfeld, A. DeFusco, and K. D. Jordan, feature article for *J. Phys. Chem.*, in press. (cover art).

# *Nucleation: From Vapor Phase Clusters to Crystals in Solution*

Shawn M. Kathmann
Chemical and Material Sciences Division
Pacific Northwest National Laboratory
902 Battelle Blvd.
Mail Stop K1-83
Richland, WA 99352
shawn.kathmann@pnl.gov

## Program Scope

The objective of this work is to develop a understanding of the chemical physics governing nucleation in both the vapor and in solution. The thermodynamics and kinetics of the embryos of the nucleating phase are important because they have a strong dependence on size, shape and composition and differ significantly from bulk or isolated molecules. The technological need in these areas is to control chemical transformations to produce specific atomic or molecular products without generating undesired byproducts, or nanoparticles with specific properties.

Compared to gas-phase chemical transformation, which in most cases can be viewed as isolated encounters of two reactant species, the proximity of condensing solvent atoms or molecules can profoundly alter reaction kinetics and thermodynamics. Computing reaction barriers and understanding condensed phase mechanisms is much more complicated than those in the gas phase because the reactants are surrounded by solvent molecules and the configurations, energy flow, and electronic structure of the entire statistical assembly must be considered.

## Recent Progress

*Electronic Effects on the Surface Potential of Water*

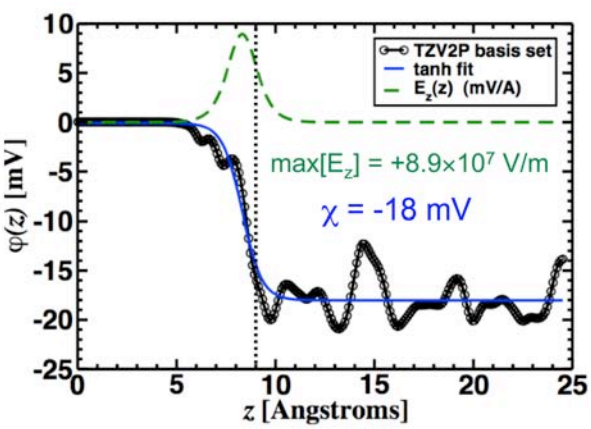


**Figure 1.** The TZV2P electrostatic potential $\varphi(z)$ data (black circles) along with a tanh fit (smooth solid blue curve) to the $\varphi(z)$ data and the corresponding interfacial electric field $E_z(z)$ (dashed green curve). The Gibbs dividing surface is located at $z$ = 9 Å (vertical dotted line).

The surface potential of the vapor-liquid interface of pure water is relevant to electrochemistry, solvation thermodynamics of ions, and interfacial reactivity. The chemistry of an ion near the vapor-liquid interface is influenced by the surface potential. Indirect determinations of the surface potential have been experimentally attempted many times, yet there has been little agreement as to its magnitude and sign (–1.1 to +0.5 V). We performed the first computation of the surface potential of water using *ab initio* molecular dynamics and find a surface potential $\chi$ = -18 mV with a maximum interfacial electric field = + 8.9 × $10^7$ V/m consistent with structural data from SHG and SFS measurements. We find that explicit treatment of the electronic density makes a dramatic contribution to the electric properties of the vapor-liquid interface of water. For example, our calculation of the surface

potential is ~30 times smaller than all previous molecular simulations. The associated *E*-field can alter interfacial reactivity and transport while the surface potential can be used to determine the "chemical" contribution to the real and electrochemical potentials for ionic transport through the vapor-liquid interface.

*Relaxation Effects in Small Water Cluster Dissociation in Photoionization Experiments*

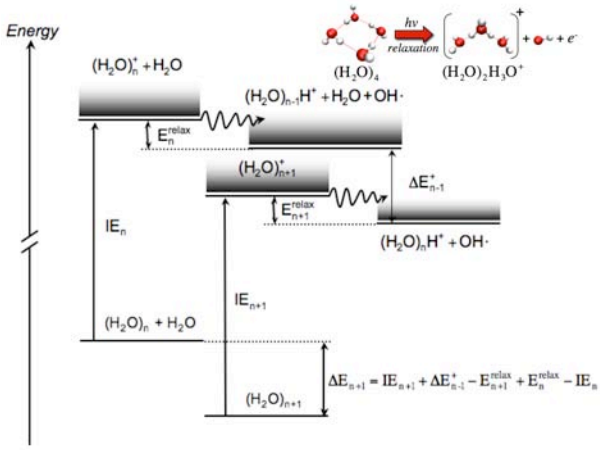


**Figure 2.** Illustration of the thermodynamic cycle, including relaxation, used to obtain monomer dissociation energies for small neutral water clusters from their measured vertical ionization energies.

Recently, monomer dissociation energies of neutral water clusters were estimated via a thermodynamic cycle that utilized the measured appearance energies of vacuum ultraviolet (VUV) photoionized water clusters and the previously reported dissociation energies of protonated water clusters. We investigated the role of relaxation and found it to be significant. Thus, the neutral water cluster monomer dissociation energies cannot be directly determined from the measured ionization potentials because they are themselves involved in the thermodynamic cycle.

*Understanding $(Ag^+)_{aq}$ from EXAFS and ab initio Molecular Dynamics*

Crystallization is one of the most challenging problems in chemical physics. Salts having large solubilities require higher salt concentrations to crystallize than salts with lower solubilities. Charge transfer effects are important in dictating the difference between salts of AgCl versus NaCl. To this end, we calculate EXAFS signals using electronic structure and *ab initio* dynamics of an $Ag^+$ ion in water to test the validity of the interactions and statistical mechanical sampling.

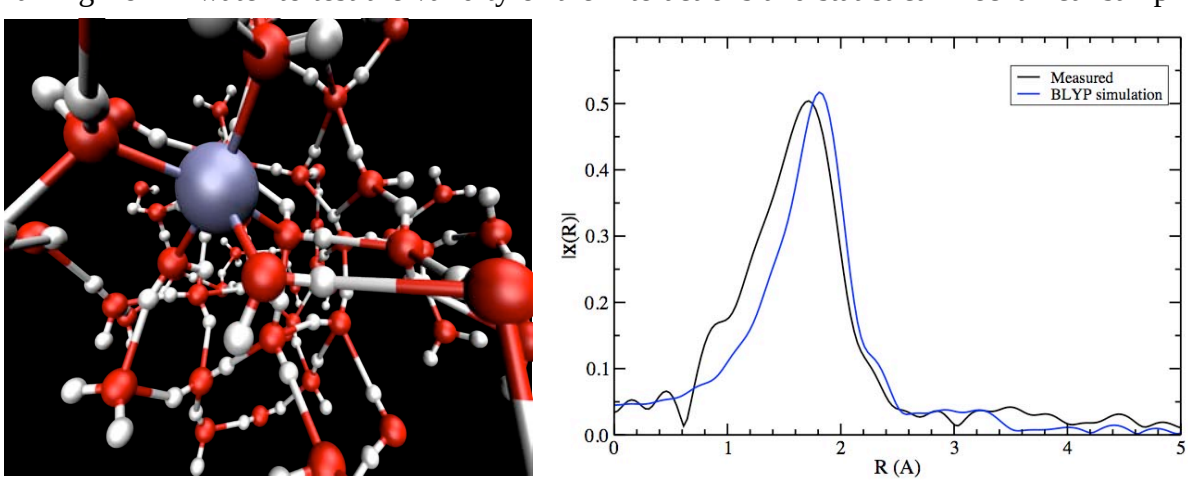


**Figure 3.** (Left) Aqueous solvation of Silver cation (Ag+). Comparison between the measured EXAFS and the Fourier transform of the absorption fine structure from *ab initio* molecular dynamics.

We are also interested in the relative populations between tetrahedral, octahedral, or trigonal by-pyramidal coordination, which has been a controversial issue in inorganic chemistry.

## Future Plans

*Thermodynamics and Electrodynamics of Solvation and Crystallization*

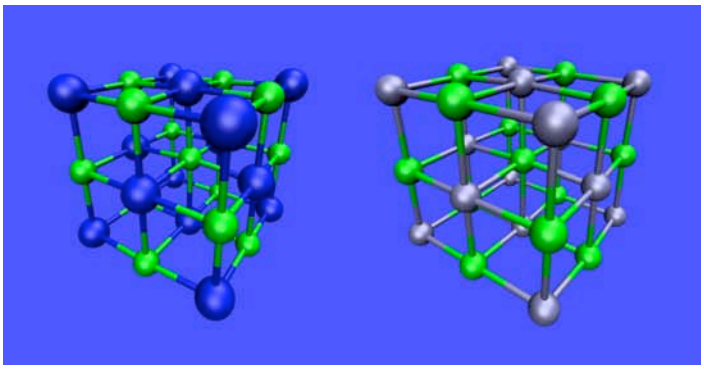

**Figure 4.** Calculations are being performed to understand the influence of the electric potential and field differences between freshly forming crystal phase and the bulk aqueous phase.

The surface potential and electric field at the interface between a salt crystal and liquid water influence the formation and growth of crystals from aqueous solution. Accurate inclusion of electronic effects, charge transfer, polarization, etc. are essential to understand the extreme differences found in crystallization thermodynamics and kinetics between NaCl and AgCl. To this end, we are computing the interfacial potential and electric field experienced by ions as they move from aqueous solvation to the crystal phase.

*Crystalloluminescence*

It has been known since the 1700's that the crystallization of certain substances from solution is accompanied by the emission of light - *crystalloluminescence*. It is found that at the early stage of crystal nucleation a burst of some $10^5$ photons in the range of 390 to 570 nm is emitted. Figure 3 shows the TDDFT excited state frequencies and oscillator strengths of NaCl crystal fragments with and without $Ag^+$ trace impurities – observation shows the presence of $Ag^+$ enhances crystalloluminescence. Larger clusters and the inclusion of solvent effects are currently in progress.

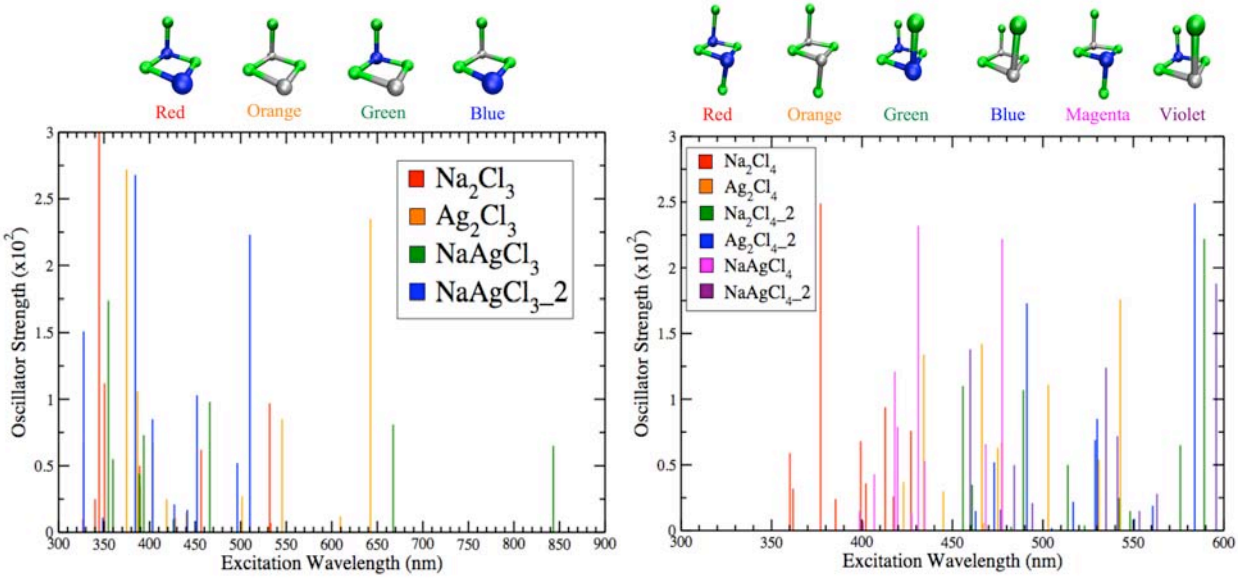


**Figure 5.** Excited state energies and oscillator strengths of NaCl including substitution with $Ag^+$ are consistent with observation.

Direct collaborators on this project include G.K. Schenter, C.J. Mundy, S.S. Xantheas, L.X. Dang, and B.C. Garrett. I would also like to thank collaborators Will Kuo, Theresa Windus, Lonnie Crosby, Marat Valiev, Michel Dupuis, and Karol Kowalski.

*Acknowledgement:* This research was performed in part using the Molecular Science Computing Facility in the Environmental Molecular Sciences Laboratory located at PNNL. Battelle operates PNNL for DOE.

**Publications of DOE Sponsored Research (2005-present)**

1. Ion-Induced Nucleation: The Importance of Chemistry, S.M. Kathmann, G.K. Schenter, and B.C. Garrett, *Physical Review Letters*, **94**, 116104 (2005).
2. **Invited Article:** Understanding the Chemical Physics of Nucleation, S.M. Kathmann, A New Perspectives Issue: *Theoretical Chemistry Accounts*, **116**, 169-182, (2006).
3. The Use of Processor Groups in Molecular Dynamics Simulations to Sample Free Energy States, B.J. Palmer, S.M. Kathmann, M. Krishnan, V. Tipparaju, and J. Nieplocha, *Journal of Chemical Theory and Computation*, **3**, 583 (2006).
4. The Critical Role of Anharmonicity in the Aqueous Ionic Clusters Relevant to Nucleation, S.M. Kathmann, G.K. Schenter, and B.C. Garrett, *Journal of Physical Chemistry B*, **111**, 4977 (2007).
5. Comment on "Quantum Nature of the Sign Preference in Ion-Induced Nucleation", S.M. Kathmann, G.K. Schenter, and B.C. Garrett, *Physical Review Letters*, **98**, 109603 (2007).
6. Activation Energies and Potentials of Mean Force for Water Cluster Evaporation, S.M. Kathmann, B.J. Palmer, G.K. Schenter, and B.C. Garrett, *Journal of Chemical Physics*, **128**, 064306 (2007).
7. **Invited Article:** "Water, The Wellspring of Life", C.J. Mundy, S.M. Kathmann, G.K. Schenter, *Natural History*, November, **116**(9) (2007).
8. Hybrid Coupled Cluster Approach for Free Energy Calculations: Application to the reaction of $CHCl_3$ and $OH^-$ in Water, M. Valiev, B.C. Garrett, M-K. Tsai, K. Kowalski, S.M. Kathmann, G.K. Schenter, M. Dupuis, *Journal of Chemical Physics*, **127**, 051102 (2007).
9. **Invited Article:** The Impact of Molecular Interactions on Atmospheric Aerosol Radiative Forcing, S.M. Kathmann, G.K. Schenter, and B.C. Garrett, *Advances in Quantum Chemistry: Applications of Theoretical Methods to Atmospheric Sciences*, **55**, Chapter 20, 429 (2008).
10. **Letter** - On the Determination of Monomer Dissociation Energies of Small Water Clusters from Photoionization Experiments, S.M. Kathmann, G.K. Schenter, and S.S. Xantheas, *Journal of Physical Chemistry A - Letter*, **112**, 1851 (2008).
11. **Invited Article** - T.L. Windus, S.M. Kathmann, and L.D. Crosby, "High Performance Computations using Dynamical Nucleation Theory," *Journal of Physics: Conference Series*, **125**, 012017 (2008).
12. **Invited Article** - C.J. Mundy, R. Rousseau, A. Curioni, S.M. Kathmann, and G.K. Schenter,"A Molecular Approach to Understanding Complex Systems: Computational Statistical Mechanics Using State-of-the-Art Algorithms on Tera-Scale Computational Platforms," *Journal of Physics: Conference Series*, **125**, 012014 (2008).
13. Implementation of Dynamical Nucleation Theory with Quantum Potentials, L.D. Crosby, S.M. Kathmann, and T.L. Windus, *Journal of Computational Chemistry*, **in press**, (2008).
14. Electronic Effects on the Surface Potential at the Vapor-Liquid Interface of Water, S. M. Kathmann, I.F. Kuo, and C.J. Mundy, *Journal of the American Chemical Society*, **accepted**, (2008).

# Chemical Kinetics and Dynamics at Interfaces

*Structure and Reactivity of Ices, Oxides, and Amorphous Materials*

**Bruce D. Kay (PI), R. Scott Smith, and Zdenek Dohnálek**

Chemical and Materials Sciences Division
Pacific Northwest National Laboratory
P.O. Box 999, Mail Stop K8-88
Richland, Washington 99352
bruce.kay@pnl.gov

Additional collaborators include P. Ayotte, C. T. Campbell, J. L. Daschbach, H. Jonsson, J. Kim, G. A. Kimmel, C. B. Mullins, N. G. Petrik, G. K. Schenter, J. M. White, and T. Zubkov

## Program Scope

The objective of this program is to examine physiochemical phenomena occurring at the surface and within the bulk of ices, oxides, and amorphous materials. The microscopic details of physisorption, chemisorption, and reactivity of these materials are important to unravel the kinetics and dynamic mechanisms involved in heterogeneous (i.e., gas/liquid) processes. This fundamental research is relevant to solvation and liquid solutions, glasses and deeply supercooled liquids, heterogeneous catalysis, environmental chemistry, and astrochemistry. Our research provides a quantitative understanding of elementary kinetic processes in these complex systems. For example, the reactivity and solvation of polar molecules on ice surfaces play an important role in complicated reaction processes that occur in the environment. These same molecular processes are germane to understanding dissolution, precipitation, and crystallization kinetics in multiphase, multicomponent, complex systems. Amorphous solid water (ASW) is of special importance for many reasons, including the open question over its applicability as a model for liquid water, and fundamental interest in the properties of glassy materials. In addition to the properties of ASW itself, understanding the intermolecular interactions between ASW and an adsorbate is important in such diverse areas as solvation in aqueous solutions, cryobiology, and desorption phenomena in cometary and interstellar ices. Metal oxides are often used as catalysts or as supports for catalysts, making the interaction of adsorbates with their surfaces of much interest. Additionally, oxide interfaces are important in the subsurface environment; specifically, molecular-level interactions at mineral surfaces are responsible for the transport and reactivity of subsurface contaminants. Thus, detailed molecular-level studies are germane to DOE programs in environmental restoration, waste processing, and contaminant fate and transport.

Our approach is to use molecular beams to synthesize “chemically tailored” nanoscale films as model systems to study ices, amorphous materials, supercooled liquids, and metal oxides. In addition to their utility as a synthetic tool, molecular beams are ideally suited for investigating the heterogeneous chemical properties of these novel films. Modulated molecular beam techniques enable us to determine the adsorption, diffusion, sequestration, reaction, and desorption kinetics in real-time. In support of the experimental studies, kinetic modeling and Monte Carlo simulation techniques are used to analyze and interpret the experimental data.

## Recent Progress and Future Directions

***Deeply Supercooled Binary Liquid Solutions from Nanoscale Amorphous Films*** Supercooled liquids and amorphous materials (glasses) are thermodynamically metastable and typically have extremely low diffusivities. These properties make studies of these fundamentally important regimes difficult. One challenge in the study of supercooled liquids is the difficulty in preventing crystallization. We have previously demonstrated an alternate approach to create and study these elusive liquids which we call “beakers without walls.” Through the use of molecular beams and nanoscale amorphous solid films, we are able to produce deeply supercooled liquid solutions and study their transport properties in these nanoscale films not possible in macroscopic samples. Our approach is to heat an amorphous solid above

its glass transition temperature, $T_g$, where upon it transforms into a supercooled liquid prior to crystallization. Using this approach we were able to create and study the properties of a metastable deeply supercooled liquid solution of methanol and ethanol.

The lifetime of the supercooled liquid is limited by the kinetics associated with the thermodynamic drive to form the lower free energy crystalline phase. By making the films thicker, we can extend the time the system spends in the metastable region. This enables us to "watch" the metastable liquid phase separate into the equilibrium components dictated by the binary liquid-solid phase diagram. For example, on the ethanol-rich side of the phase diagram, the methanol desorption rates and the simulation predictions are in agreement for all films but eventually deviate above the simulation prediction for thicker films. Concurrent FTIR measurements reveal the departures from ideal solution behavior occur in concert with the onset of precipitation of crystalline ethanol. Analogus experiments with methanol-rich film compositions show that the deviation from ideal solution desorption behavior is correlated with the onset of the precipitation of crystalline methanol. In principle, it may be possible to quantify the crystallization kinetics in metastable regions of the phase diagram. However in some thicker films, even at temperatures and compositions where a stable liquid should exist, we unexpectedly observe deviations from ideal solution behavior. Visual inspection of the sample indicates that these apparent departures from ideality arise from dewetting of the liquid film from the substrate. Film dewetting will make quantification of the equilibration kinetics of the metastable supercooled liquids a challenge.

In the supercooled liquid experiments, the intermixing of the methanol and ethanol has suppressed crystallization and allowed for the quantitative determination of the desorption rates for pure supercooled methanol and ethanol which are otherwise unattainable from the pure films due to rapid crystallization. The supercooled liquid and crystalline desorption rate curves cross at their respective melting temperatures. Below the melting temperature the crystalline rates are lower whereas above the melting temperature the liquid rates are lower. The pure liquid and crystalline desorption rates can be used to calculate the melting lines in the binary phase diagram. These results are in excellent agreement with, and extend well beyond the available melting data. The crossing of the curves yields a eutectic temperature of 123.3 K at $x_M = 0.5$. Determination of the supercooled liquid desorption rates has allowed for the accurate determination of all the phase boundaries previously not measurable. Future work will include bianry mixtures with water as one of the components.

***Effect of Incident Energy on the Properties of Amorphous Solid Water*** The interaction of water with a substrate is of considerable interest in numerous scientific disciplines including surface science, electrochemistry, environmental science, atmospheric science, and biology. Thus, understanding the water/substrate interaction at a fundamental level will have a wide range of applications. The adsorption of molecules on the surfaces of solids is an important step in many processes, in particular, crystal growth, catalysis, and atmospheric chemistry. In order for a molecule not to be reflected after colliding with a solid surface, it needs to lose the energy associated with the component of momentum normal to the surface. It is, therefore, commonly assumed that the sticking coefficient, $S_0$, scales with the energy that is normal (perpendicular) to the surface. In collaboration with Hannes Jonsson (Univ. of Washington and Univ. of Iceland), we conducted both experimental and theoretical studies of the sticking of water molecules on ice over a wide range in energy (0.5 eV–1.5 eV) and incident angle (0-75º). Surprisingly, we find that the sticking coefficient for a water molecule on ice is found to scale well with only the incident momentum component along the surface. That is, molecules with the same velocity along the surface but quite different velocity normal to the surface have roughly the same probability of sticking. Molecular dynamics simulations show that the explanation for this unusual behavior appears to be a strong variation of the molecule-surface interaction energy as the molecule rotates. At normal incidence, the incoming molecule has time to orient itself as it approaches the surface into the optimal attractive orientation. At glancing incidence and high incident energy, the molecule moves so fast it does not have sufficient time to reorient and has a repulsive interaction leading to scattering into the vapor phase.

Also related to water/substrate interactions is the question of whether the incident kinetic energy can affect the phase of vapor deposited water. In general, whether a vapor deposited material grows as an amorphous or crystalline solid depends on the ability of an incident molecule to explore the energetically

available configurational landscape to find the crystalline minimum. The energy and time needed to find the thermodynamically favored crystalline configuration will depend on the incident flux, incident energy, incident angle, substrate temperature, and other factors related to the dynamics of energy transfer between the incoming molecule and the substrate. In these experiments, molecular beams were used to vary the incident collision energy of water and TPD and FTIR were employed to probe the phase of the deposited film and the subsequent crystallization kinetics. We find that for films deposited at 20 K, the collision energy (up to 205 kJ/mole) has no effect on either the initial phase of the deposited film or its crystallization kinetics. These results suggest that the crystallization of amorphous solid water requires cooperative motion of the water molecules for crystallization to occur.

***Synthesis, Characterization, and Reactivity of Nanoporous Thin Films*** Highly nanoporous materials can have useful applications in a variety of areas including catalysis and chemical sensors. A convenient method of growing model porous materials in ultra-high vacuum (UHV) is using collimated molecular beams at high incident deposition angles under ballistic deposition conditions. A simple physical mechanism, ballistic deposition, can be used to understand the dependence of morphology on the growth angle. At glancing angles, random height differences that arise during the initial film growth can block incoming flux essentially creating shadows that result in void regions in the shadowed region. If surface and/or bulk diffusion are slow compared to the incident flux, i.e., the molecules "hit and stick", then the voids remain unfilled. Continued deposition results in porous films with filamentous columnar morphologies. The approach has been used to grow porous metals, Si, and oxides. These thin films can have extremely large porosities and surface areas. Varying degrees of film porosity can be achieved by varying the deposition angle.

Adsorbate transport and desorption within and from porous ASW is important for understanding the desorption of gases and evolution of cometary and interstellar ices largely composed of ASW. In recent work, adsorption and desorption kinetics of $N_2$ on porous ASW films were studied. The experimental results show that the $N_2$ condensation coefficient is essentially unity until near saturation, independent of the ASW film thickness indicating that $N_2$ transport within the porous films is rapid. The TPD results show that the desorption of a fixed dose of $N_2$ shifts to higher temperature with ASW film thickness. A kinetic analysis based on our previously developed TPD inversion method yields coverage dependent activation energy curves that when rescaled by the film thickness results in a single master curve. Simulation of the TPD spectra using this single curve results in a quantitative fit to the experiments over a wide range of ASW thicknesses and nitrogen doses.

The success of the rescaling model means that transport within the porous film is rapid enough to maintain a uniform distribution throughout the film on a time scale faster than desorption. Clearly, the ability to maintain a uniform distribution throughout the film will depend on length scale of the film, and in very thick films, one can envision the onset of transport limitations. We do find that in thicker films (>1 μm) and at low temperature (<30 K) $N_2$ mobility is limited on the length-scale of the thicker films and this results in a non-uniform distribution in the ASW film during adsorption. Specifically, there is a greater concentration of $N_2$ in regions of the film near the vacuum interface (near the pore opening). Further, the desorption spectra indicate that $N_2$ mobility is not able to equilibrate the $N_2$ concentration across the thicker films prior to desorption. The transport limitations arise from the trapping of $N_2$ on the high energy binding sites of the porous ASW film. Nonetheless, the simple $1/N$ scaling model should be quantitatively applicable to a variety porous materials as long as the adsorbate distribution is uniform throughout the material and that this distribution rapidly adjusts during desorption. Future studies will focus on examining the transport kinetics in other nanoporous materials.

**References to Publications of DOE sponsored Research (CY 2005- present)**


1. "Role of water in electron-initiated processes and radical chemistry: Issues and scientific advances", B. C. Garrett, et al. *Chemical Reviews*, **105**, 355, (2005).
2. "Influence of surface morphology on $D_2$ desorption kinetics from amorphous solid water", L. Hornekaer, A. Baurichter, V. V. Petrunin, A. C. Luntz, B. D. Kay and A. Al-Halabi, *Journal of Chemical Physics*, **122**, 124701, (2005).

3. “n-Alkanes on MgO(100). I. Coverage-dependent desorption kinetics of n-butane”, S. L. Tait, Z. Dohnalek, C. T. Campbell and B. D. Kay, *Journal of Chemical Physics*, **122**, 164707, (2005).
4. “n-Alkanes on MgO(100). II. Chain length dependence of kinetic desorption parameters for small n-alkanes”, S. L. Tait, Z. Dohnalek, C. T. Campbell and B. D. Kay, *Journal of Chemical Physics*, **122**, 164708, (2005).
5. “Structural characterization of nanoporous Pd films grown via ballistic deposition”, J. Kim, Z. Dohnalek and B. D. Kay, *Surface Science*, **586**, 137, (2005).
6. “Adsorption and Desoprtion of HCl on Pt(111)”, JL Daschbach, J Kim, P Ayotte, RS Smith and BD Kay, *Journal of Physical Chemistry B*, **109**, 15506, (2005).
7. “Water Adsorption, Desorption and Clustering on FeO(111)”, J. L. Daschbach, Z. Dohnálek, S-R. Liu, R. S. Smith, and B. D. Kay, *Journal of Physical Chemistry B* **109**, 10362, (2005).
8. “Methane Adsorption and Dissociation and Oxygen Adsorption and Reaction with CO on Pd Nanoparticles on MgO(100) and on Pd(111)”, S. L. Tait, Z. Dohnálek, C. T. Campbell, B. D. Kay,” *Surface Science* **591,** 90, (2005).
9. “Crystalline Ice Growth on Pt(111): Observation of a Hydrophobic Water Monolayer”, G. A. Kimmel, N. G. Petrik, Z. Dohnálek, and B. D. Kay, *Physical Review Letters* **95**, 166102, (2005).
10. “What Determines the Sticking Probability of Water Molecules on Ice?”, E.R. Batista, P. Ayotte, A. Bilic, B.D. Kay, and H. Jonsson, *Physical Review Letters* **95**, 223201, (2005).
11. “Cryogenic $CO_2$ Formation on Oxidized Gold Clusters Synthesized via Reactive Layer Assisted Deposition”, J. Kim, Z. Dohnálek, and B. D. Kay, *Journal of The American Chemical Society Communication*, **127**, 14592, (2005).
12. “The Effect of Incident Collision Energy on the Phase and Crystallization Kinetics of Vapor Deposited Water Films”, R. S. Smith, T. Zubkov, and B. D. Kay, *Journal of Chemical Physics*, **124**, 114710, (2006)
13. “Layer-by-layer Growth of Thin Amorphous Solid Water Films on Pt(111) and Pd(111)”, G. A. Kimmel, N. G. Petrik, Z. Dohnálek, and B. D. Kay, *Journal of Chemical Physics*, **125**, 044713, (2006)
14. “Growth of Epitaxial Thin Pd(111) Films on Pt(111) and Oxygen Terminated FeO(111) Surfaces”, Z. Dohnálek, J. Kim, and B. D. Kay, , *Surface Science* **600**, 3461 (2006).
15. “Physisorption of $N_2$, $O_2$, and CO on Fully-oxidized $TiO_2$(110)”, Z. Dohnálek, J. Kim, O. A. Bondarchuk, J. M. White and B. D. Kay, *Journal of Physical Chemistry B*, **110**, 6229, (2006)
16. “Crystalline ice growth on Pt(111) and Pd(111): Non-wetting growth on a hydrophobic water monolayer”, A. Kimmel, N. G. Petrik, Z. Dohnálek, and B. D. Kay, *Journal of Chemical Physics*, **126**, 114702, (2007).
17. “Reactive Ballistic Deposition of Porous $TiO_2$ Films: Growth and Characterization”, D. W. Flaherty, Z. Dohnálek, A. Dohnálková, B. W. Arey, D. E. McCready, N. Ponnusamy, C. B. Mullins, and B. D. Kay, *Journal of Physical Chemistry C* **111**, 4765, (2007).
18. “Adsorption, Desorption and Diffusion of Nitrogen in a Model Nanoporous Material: I.: Surface Limited Desorption Kinetics in Amorphous Solid Water”, T. Zubkov, R. S. Smith, T.R. Engstrom, and B. D. Kay, *Journal of Chemical Physics*, **127**, 184707 (2007).
19. “Adsorption, Desorption and Diffusion of Nitrogen in a Model Nanoporous Material: II.: Diffusion Limited Kinetics in Amorphous Solid Water”, T. Zubkov, R. S. Smith, T.R. Engstrom, and B. D. Kay, *Journal of Chemical Physics*, **127**, 184708 (2007).
20. “Formation of Supercooled Liquid Solutions from Nanoscale Amorphous Solid Films of Methanol and Ethanol”, R. S. Smith, P. Ayotte, and B. D. Kay, *Journal of Chemical Physics* **127**, 244705 (2007).
21. “Understanding How Surface Morphology and Hydrogen Dissolution Influence Ethylene Hydrogenation on Palladium”, Z. Dohnalek, J. Kim and B.D. Kay, *Journal of Physical Chemistry C* (Accepted for publication August 2008).
22. “The Effect of the Incident Collision Energy on the Porosity of Vapor Deposited Amorphous Solid Water Films” R. S. Smith, T. Zubkov, Z. Dohnalek, and BD Kay, *Journal of Physical Chemistry B* (Accepted for publication August 2008).

# Chemical Kinetics and Dynamics at Interfaces

*Non-Thermal Reactions at Surfaces and Interfaces*

**Greg A. Kimmel (PI) and Nikolay G. Petrik**
Chemical and Materials Sciences Division
Pacific Northwest National Laboratory
P.O. Box 999, Mail Stop K8-88
Richland, WA 99352
gregory.kimmel@pnl.gov

## Program Scope

The objectives of this program are to investigate 1) the thermal and non-thermal reactions at surfaces and interfaces, and 2) the structure of thin adsorbate films and how this influences the thermal and non-thermal chemistry. The fundamental mechanisms of radiation damage to molecules in the condensed phase are of considerable interest to a number of scientific fields ranging from radiation biology to astrophysics. In nuclear reactor design, waste processing, radiation therapy, and many other situations, the non-thermal reactions in aqueous systems are of particular interest. Since the interaction of high-energy radiation (gamma-rays, alpha particles, etc.) with water produces copious amounts of low-energy secondary electrons, the subsequent reactions of these low-energy electrons are particularly important. The general mechanisms of electron-driven processes in homogeneous, dilute aqueous systems have been characterized in research over the last several decades. More recently, the structure of condensed water and its interactions with electrons, photons, and ions have been extensively studied and a variety of non-thermal reaction mechanisms identified. However, the complexity of the electron-driven processes, which occur over multiple length and time scales, has made it difficult to develop a detailed molecular-level understanding of the relevant physical and chemical processes.

We are focusing on low-energy, electron-stimulated reactions in thin water films. Our approach is to use a molecular beam dosing system to create precisely controlled thin films of amorphous solid water (ASW) and crystalline ice (CI). Using isotopically layered films of $D_2O$, $H_2{}^{16}O$ and $H_2{}^{18}O$ allows us to explore the spatial relationship between where the incident electrons deposit energy and where the electron-stimulated reactions subsequently occur within the films. Furthermore, working with thin films allows us to explore the role of the substrate in the various electron-stimulated reactions.

## Recent Progress:

### *Tetraoxygen on reduced $TiO_2$(110): Oxygen adsorption and reactions with oxygen vacancies*

The interaction of oxygen with $TiO_2$ is critical for a variety of applications including the photooxidation of organic materials, purification of water and air, and (potentially) photocatalytic water splitting. In photocatalysis, $O_2$ is frequently used as an electron scavenger, but its exact role is unclear. The interactions of 'simple' molecules, such as $O_2$ and $H_2O$, with $TiO_2$(110) are also scientific benchmarks for testing our understanding of the fundamental physical and chemical processes relevant to a broad class of oxide surfaces.

We have investigated the interaction of oxygen with reduced, rutile $TiO_2$(110) using temperature programmed desorption (TPD) and electron-stimulated desorption (ESD) [11]. Surprisingly for $O_2$ coverages of 2 $O_2$ per oxygen vacancy ($O_v$) or less, essentially no $O_2$ desorbs as the sample is heated up to 700 K. The amount of this chemisorbed oxygen, $\theta_{Chem}$, increases proportionally with increasing vacancy concentration. For $\theta_{Chem}$ = 2 $O_2/O_v$, the $O_2$ ESD yield versus annealing temperature indicates that a precursor state with 2 $O_2$ converts to a new species with 4 oxygen atoms – "tetraoxygen" – as the film is heated above ~200 K, and that this species decomposes upon annealing above ~400 K. In contrast for $\theta_{Chem}$ < 1 $O_2/O_v$, annealing above 280 K heals the vacancies and prevents further $O_2$ chemisorption. These experimental results, which provide a new model for the interaction of oxygen with $TiO_2$(110), are

consistent with the recent prediction that $O_4^{2-}$ is the most stable form of oxygen in bridging oxygen vacancies.

Figure 1 shows the integrated $O_2$ TPD and ESD signals versus the amount of $O_2$ adsorbed on $TiO_2(110)$. When $O_2$ is adsorbed at 25 K, all the $O_2$ is chemisorbed for oxygen coverages, $\theta_{O2}$, less than 2 $O_2/O_v$ and the integrated TPD signal corresponding to physisorbed $O_2$ is zero (Fig. 1, circles). For higher coverages, the amount of physisorbed $O_2$ increases linearly, and a small amount of $O_2$ also desorbs at ~440 K (Fig. 2, triangles). We used $O_2$ ESD to investigate changes in the chemisorbed $O_2$ (i.e. the $O_2$ which does not desorb thermally). The squares in Figure 2 show the $O_2$ ESD signal versus the amount of absorbed $O_2$ for films where the $O_2$ was adsorbed at 25 K and then annealed at 400 K prior to measuring the $O_2$ ESD with 100 eV electrons at 100 K. For $\theta_{O2} < 1$ $O_2/O_v$, the chemisorbed $O_2$ dissociates upon annealing to heal the oxygen vacancy and, as a result, the $O_2$ ESD signal is small. For $\theta_{O2} > 2$ $O_2/O_v$, the chemisorbed oxygen molecules are converted to a new species – tetraoxygen – upon annealing to 400 K. The $O_2$ ESD signal from this species is kinetically distinct from molecularly adsorbed $O_2$ (data not shown). For 1 $O_2/O_v < \theta_{O2} < 2$ $O_2/O_v$, the amount of tetraoxygen formed upon annealing increases linearly and the $O_2$ ESD signal increases correspondingly (Fig. 1, squares).

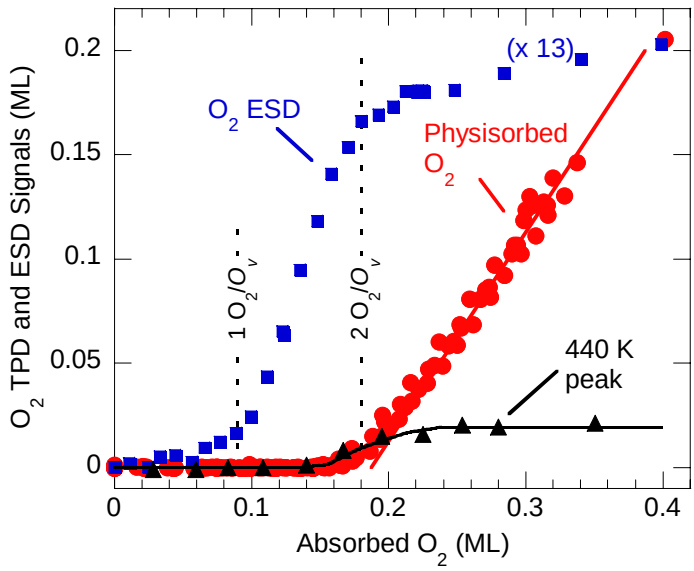


Fig. 1. $O_2$ TPD and ESD signals versus $O_2$ coverage.

***Hydrogen bonding, H/D exchange and molecular mobility in thin water films on $TiO_2(110)$***

The interaction of water with $TiO_2$ has technological implications for a variety of areas ranging from photocatalysis to self-cleaning surfaces. Scientifically, water on rutile $TiO_2(110)$ is widely considered to be an important "benchmark" system for metal oxides. Thus, the interactions of water with $TiO_2(110)$ for coverages, $\theta$, of 1 monolayer (ML) and less have been extensively studied. However, understanding the water structure for $\theta > 1$ ML is important since the corrugated structure of $TiO_2(110)$ and the strong binding of the first water ML are both likely to influence the structural transition to bulk water further from the surface, and thus the chemistry of aqueous/$TiO_2(110)$ interfaces.

We have used the electron-stimulated desorption (ESD) of water from films of $D_2O$, $H_2{}^{16}O$ and $H_2{}^{18}O$ to investigate hydrogen bonding, H/D exchange and molecular mixing between water adsorbed in the first monolayer ($H_2O_{Ti}$) and water in the second monolayer ($H_2O_{BBO}$) on $TiO_2(110)$ for $\theta \leq 2$ ML [9]. By depositing $H_2O_{Ti}$ at 190 K using one water isotope and $H_2O_{BBO}$ at ≤ 70 K using a different isotope, films with no appreciable mixing isotopes between layers can be prepared. When $H_2O_{BBO}$ is deposited at T > 70 K, partial or complete mixing with $H_2O_{Ti}$ occurs depending on the temperature and time. H/D exchange between $H_2O_{Ti}$ and $H_2O_{BBO}$ occurs at ~15 K lower temperatures than $H_2{}^{16}O/H_2{}^{18}O$ exchange. Isothermal experiments demonstrate that the mixing occurs with a distribution of activation energies centered on 0.29 ± 0.07 eV (0.26 ± 0.07 eV) for $H_2{}^{16}O/H_2{}^{18}O$ (H/D) exchange. Thus in contrast to MD simulations, the results show that $H_2O_{Ti}$ rapidly exchanges with $H_2O_{BBO}$ at temperatures well below 300 K. The results also demonstrate that $H_2O_{BBO}$ is hydrogen bonded to $H_2O_{Ti}$. Since the lateral distance (0.325 nm) for atop adsorption at these sites is too large for hydrogen bonding, one (or both) of the adsorbates must be displaced laterally toward the other in agreement with theoretical predictions.

***Photoionization of Sodium Salt Solutions in a Liquid Jet***

Heterogeneous gas/liquid interfaces are important in a wide variety of fields such as atmospheric, environmental, materials and planetary sciences. Atmospheric ice particles and droplets provide crucial platforms for reactions. Several of these reactions involving ice particles and liquid aerosol droplets in polar stratospheric cloud (PSCs) have implications for ozone destruction. Despite their importance, these interfaces are not well understood due to experimental limitations. Some studies have used low temperature amorphous ice as a surrogate for liquid water in atmospherically relevant interactions. While these studies utilize surface sensitive methods to examine reactions, the necessity for ultra-high vacuum conditions limit the temperature to < 160 K, and equilibrating interactions with vapor phase water are absent. The ability to use liquid surfaces under ultrahigh vacuum allows the application of the same highly surface-sensitive techniques on a more realistic interface.

In collaboration with Prof. Thomas Orlando and co-workers at the Georgia Institute of Technology, we have studied aqueous interfaces using multiphoton ionization and time-of-flight (TOF) mass spectrometry on micron-size liquid jets of $Na^+X^-$ (X=Cl, Br, and I) solutions [12]. Since we examined ions that escape directly from the liquid interface, this approach allowed us to address the nature of the salt solution/vacuum interface and the mechanisms of condensed phase cluster ion formation and ejection. A liquid microjet was employed to examine the gas/liquid interface of aqueous sodium halide salt solutions. Laser excitation at 193 nm produced and ejected cations of the form $H^+(H_2O)_n$ and $Na^+(H_2O)_m$ from liquid jet surfaces containing either NaCl, NaBr or NaI. The protonated water cluster yield varied inversely with increasing salt concentration, while the solvated sodium ion cluster yield varied by anion type. The distribution of $H^+(H_2O)_n$ at low salt concentration was identical to that observed from low-energy electron irradiated amorphous ice and the production of these clusters can be accounted for using a localized ionization/Coulomb expulsion model. Production of $Na^+(H_2O)_m$ was not accounted for by this model but requires ionization of solvation shell waters and a contact ion/Coulomb expulsion mechanism. The reduced yields of $Na^+(H_2O)_m$ from high concentration ($10^{-2}$ and $10^{-1}$ M) NaBr and NaI solutions indicate a propensity for $Br^-$ and $I^-$ at the solution surfaces and interfaces. This hypothesis is supported by the observation of multiphoton-induced production and desorption of $Br^+$ and $I^+$ from the $10^{-2}$ and $10^{-1}$ M solution surfaces.

**Future Directions:**

Important questions remain concerning the factors that determine the structure of thin water films on various substrates. We plan to investigate the structure of thin water films on non-metal surfaces, such as oxides, and on metals where the first layer of water does not wet the substrate. For the non-thermal reactions in water films, we will use FTIR spectroscopy to characterize the electron-stimulated reaction products and precursors. The mechanisms of the non-thermal precursor migration through ASW films need to be further explored. We will also investigate the non-thermal reactions at lower electron energies (i.e. closer to the ionization threshold for water). Finally, we plan to investigate the lifetimes of excited states in ASW and CI using pump-probe fluorescence measurements.

**References to publications of DOE sponsored research (FY 2005 – present)**


[1] Nikolay G. Petrik and Greg A. Kimmel, "Electron-stimulated sputtering of thin amorphous solid water films on Pt(111)," *J. Chem. Phys.* **123**, 054702 (2005).

[2] Bruce C. Garrett, et al., "Role of Water in Electron-Initiated Processes and Radical Chemistry: Issues and Scientific Advances," *Chem. Rev.* **105**, 355 (2005).

[3] Greg A. Kimmel, Nikolay G. Petrik, Zdenek Dohnálek and Bruce D. Kay, "Crystalline ice growth on Pt(111): Observation of a hydrophobic water monolayer," *Phys. Rev. Lett.* **95** (2005) 166102.

[4] Nikolay G. Petrik, Alexander Kavetsky and Greg A. Kimmel, "Electron-Stimulated Production of Molecular Oxygen in Amorphous Solid Water," *J. Phys. Chem. B.* **110**, 2723 (2006).

[5] Greg A. Kimmel, Nikolay G. Petrik, Zdenek Dohnálek and Bruce D. Kay, "Layer-by-layer growth of thin amorphous solid water films on Pt(111) and Pd(111)," *J. Chem. Phys.* **125**, 044713 (2006).

[6] Nikolay G. Petrik, Alexander Kavetsky and Greg A. Kimmel, "Electron-stimulated production of molecular oxygen in amorphous solid water on Pt(111): Precursor transport through the hydrogen bonding network," *J. Chem. Phys.* **125**, 124702 (2006).
[7] Greg A. Kimmel, Nikolay G. Petrik, Zdenek Dohnálek and Bruce D. Kay, "Crystalline ice growth on Pt(111) and Pd(111): Non-wetting growth on a hydrophobic water monolayer," *J. Chem. Phys.* **126**, 114702 (2007).
[8] Christopher D. Lane, Nikolay G. Petrik, Thomas M. Orlando, and Greg A. Kimmel, "Electron-stimulated oxidation of thin water films adsorbed on $TiO_2$(110)," *J. Phys. Chem. C* **111**, 16319 (2007).
[9] Nikolay G. Petrik and Greg A. Kimmel, "Hydrogen bonding, H/D exchange and molecular mobility in thin water films on $TiO_2$(110)," *Phys. Rev. Lett.* **99**, 196103 (2007).
[10] Christopher D. Lane, Nikolay G. Petrik, Thomas M. Orlando, and Greg A. Kimmel, "Site-dependent electron-stimulated reactions in water films on $TiO_2$(110)," *J. Chem. Phys.* **127**, 224706 (2007).
[11] Greg A. Kimmel and Nikolay G. Petrik, "Tetraoxygen on reduced $TiO_2$(110): Oxygen adsorption and reactions with oxygen vacancies," *Phys. Rev. Lett.* **100**, 196102 (2008).
[12] G. A. Grieves, N. Petrik, J. Herring-Captain, B. Olanrewaju, A. Aleksandrov, R. G. Tonkyn, S. A. Barlow, G. A. Kimmel, and T. M. Orlando, "Photoionization of Sodium Salt Solutions in a Liquid Jet," *J. Phys. Chem. C* **112**, 8359 (2008)**.**

# Radiation Effects in Heterogeneous Systems and at Interfaces

Jay A. LaVerne, Dan Meisel, Ian Carmichael, Daniel M. Chipman

Radiation Laboratory, University of Notre Dame, Notre Dame, IN 46556

laverne.1@nd.edu; dani@nd.edu; carmichael.1@nd.edu; chipman.1@nd.edu

## Program Scope

Fundamental chemical processes induced by the passage of ionizing radiation are being examined in heterogeneous systems and at interfaces using a combination of experimental and theoretical methods. Experimental studies of systems ranging from aqueous dispersions of nanoparticles to hydroxide monolayers are focusing on the transport of charge carriers through interfaces and the identity and reactivity of species bound to interfaces. These studies are coupled with model calculations on the stability of transient and interfacial species to give a complete description of the radiolytic processes. Interfaces provide the opportunity for the transfer of energy and charge between two phases and are relevant to many practical technological problems of importance to the Department of Energy. Heterogeneous systems are frequently encountered in the management of nuclear materials and nuclear waste, and in nuclear power plant infrastructure.

## Recent Progress

The construction of a chamber for the *in situ* examination of irradiated ceramic oxides and ices during heavy ion irradiation is underway. The chamber will also allow the heating and cooling of a sample with the capability of *in situ* observation of the changes in the IR spectrum. Isolation and manipulation of the sample has been achieved and coupling with the IR is in progress. This chamber will be used for examination of the formation or destruction of selected molecules such as $H_2O_2$ on the surface of ceramic oxides under controlled atmospheric conditions.

Processes that occur at the interface between aqueous solutions and metallic-particle surfaces are believed to be an essential component in many solar conversion schemes as catalysts for water splitting processes in both the oxidation and reduction cycles. They are also explored as sensing elements in radio-sensitization and radiotherapy. In these studies, the ionizing radiation may be absorbed by either phase but our effort focuses on the reactions of the fraction of ionization events that arrive at the interface. Consequently, a surface specific technique is required that will be able to detect the minority surviving species at the interface from the majority of the processes that occur in the bulk liquid and solid phases. Surface enhanced Raman spectroscopy (SERS) is ideal for this purpose because of its extreme sensitivity, specificity to the metallic surface and the wealth of information that it can provide on the target molecule (or radical) and its orientation relative to the surface. In combination with radiation-chemical techniques, photo physical tools, materials-characterization microscopies, and conventional wet-chemistry colloidal approaches, the chemical systems are built, characterized, and finally the interfacial processes induced by the radiation are examined. Computational efforts on model systems that preserve the essential characteristics of the species of interest facilitate our interpretation of the experimental observations and offer predictive directions for these complex interfacial processes.

SERS has been used in this period to identify processes that occur at the surface of metallic, silver or gold, particles in response to the absorption of ionizing radiation in the aqueous phase. To demonstrate the approach, clean silver nanoparticles of various sizes from 30-200 nm were synthesized utilizing the reaction between the metal oxide and $H_2$ to generate the particles in the absence of any foreign stabilizers. The particles were then characterized as described in our earlier reports. Their surface potential and its size dependence, as well as the associated species in solution and at the surface, were all determined. Recently we demonstrated that sub-micro molar concentrations of probe molecules, e.g. *p*-amino-thiophenol (*p*-ATP), could easily be detected on the nanoparticles. Furthermore, even under heavy irradiation doses (>Mrad) there is essentially no destruction of the probe. While the particles continuously catalyze hydrogen evolution, the probe molecule reports on the processes that occur at the metallic surface. Adsorption isotherms of the probe molecule were constructed using SERS and competitive adsorption measurements allow estimates of relative adsorption enthalpies. Electron transfer to the particles occurs from strongly-reducing radiolytically-generated radicals. In parallel, the overpotential that is building on the particles could be estimated using the correlation between the SERS intensity of the probe and electrochemically determined bias on silver electrodes. The potential is found to decrease to values below – 0.4 V *vs.* NHE before the particles start to reduce water to hydrogen. This overpotential could be chemically controlled by injection of electrons or holes ($Ag^+$) to the particles. The dependence of SERS intensity on potential is attributed to the effect of the Fermi-level position on coupling of the particle's plasmon band to vibrational levels of the electronic ground state. The vibrational coupling in turn leads to borrowed signal intensity due to the existence of a particle-molecule charge-transfer state for the adsorbed molecule. Electronic structure calculations on representative model *p*-ATP@Ag species suggest that redistribution of charge between the molecule and the particle already exists in the ground state. The redistribution of charge then implies the existence of an adsorbed radical-charged metallic particle in addition to the original molecule/metal-particle pair. Changes in the SERS spectra during the injection of $e^-/h^+$ cycles and relative line intensities then could be attributed either to the charge redistribution or to reorientation of the probe on the particle surface.

A complete computational description has been obtained of the structures and energetics involved in the hydroxylation, wetting, and eventual dissolution of alumina surfaces by water. First-principles total energy calculations were performed within the Density Functional Theory (DFT) framework with the VASP code. Periodic boundary conditions were used in three perpendicular directions. The exchange and correlation energies were calculated within the Generalized Gradient Approximation (GGA). The cut-off kinetic energy of the plane wave basis set was set to 400 eV, and a set of 5 Γ-point-centered *k*-points was used to ensure convergence. Water completely wets the clean, defect-free $Al_2O_3$ (0001) surface at 2 monolayers (ML) of coverage.

Dissociative adsorption, to produce surface hydroxides, is exothermic with respect to gas phase molecular water and the clean surface, and it is thermochemically favored over molecular absorption at all coverages less that 1.5ML. However, coverage regimes are possible in which molecular and dissociated species coexist. A simple model has been developed for dissociation of aluminum ions from the surface of the bulk.

Hydrogen peroxide is a major product formed in the radiolysis of water and its decomposition at solid surfaces is thought to be a major initiator of corrosion in nuclear reactor components. Diffuse reflectance infrared Fourier transform, DRIFT, studies of hydrogen

peroxide on the surface of zirconia and titania have identified distinctive bound species. These species decay concurrently with production of molecular oxygen and EPR studies have identified surface oxide radical species. Details of the decomposition and identity of the surface species are currently being explored.

## Future Plans

Two different approaches will be used for *in situ* examination of the processes occurring in the radiolysis of water – ceramic oxide interfaces under near ambient conditions. Probing for species at a solid surface is hindered by the presence of the overlayer of physisorbed water. One technique for the future examination of powder surfaces will combine a radioactive source with a controlled atmosphere chamber in a spectrometer for DRIFT measurements. The powders will be cleaned, irradiated and examined within the spectrometer housing. The second technique will make use of a device based on material science studies for irradiation of powders or solids in vacuum conditions using accelerators. This device will allow for preparation of samples with controlled amounts of adsorbed water followed by radiolysis with helium ions to mimic alpha particle radiolysis. Optical variations of the ceramic oxide surfaces will be coupled with stable product formation and theoretical predictions of interfacial species in order to elucidate the radiation induced reactions at interfaces.

In the studies on metallic particles in aqueous suspensions, efforts to expand the metallic surfaces to include other metals have started and gold is now being explored. To verify the effect of surface potential on reorientation of the probe, the effects of pH and of excitation wavelength on the SERS spectra during irradiation will be determined. Electronic structure calculations on more realistic, select cluster-molecule or cluster-radical structures will be performed in order to predict the vibrational transitions of the molecule (radical) on the surface. To further demonstrate the utility of the approach other redox reactions (specifically, reduction of nitro-aromatics to their amine analogues), will be examined. Any efforts beyond this level will require time domain capabilities with SERS as the analytical tool.

Minimum energy paths linking the various locally-stable structures for water absorption onto the $\alpha$-$Al_2O_3$ (0001) surface will be elucidated and kinetically accessible transformations characterized. Calculations will be extended to encompass more relevant ceramic oxides such as zirconia.

## Publications Sponsored by this DOE Program, 2005-2008


Enomoto K.; LaVerne J.A.; Tandon L.; Enriquez A.E.; Matonic J.H. **2008**, "The radiolysis of poly(4-vinylpyridine) quaternary salt ion exchange resins," **J. Nucl. Mater.** *373*, 103-111.

Hull K.L.; Carmichael I.; Noll B.C.; Henderson K.W. **2008**, "Homo- and heterodimetallic geminal dianions derived from the bisphosphinimine $\{Ph_2P(Me_3Si)N\}_2CH_2$ and the alkali metals Li, Na and K," **J. Am. Chem. Soc.** *14*, 3939-3953.

LaVerne J.A.; Carrasco-Flores E.A.; Araos M.S.; Pimblott S.M. **2008**, "Gas production in the radiolysis of poly(vinyl chloride)," **J. Phys. Chem. A** *112*, 3345-3351.

Merga G.; Cass L.C.; Chipman D.M.; Meisel D. **2008**, "Probing silver nanoparticles during catalytic $H_2$ evolution," **J. Amer. Chem. Soc.** *130*, 7067-7076.

Ranea V.A.; Schneider W.F.; Carmichael I. **2008**, "DFT characterization of coverage dependent molecular water absorption on α−$Al_2O_3$(0001)," **Surf. Sci.** *602*, 268-275.

Zhang Z.; Meisel D.; Kamat P.V.; Kuno M. **2008**, "Layer-by-layer self-assembly of colloidal gold-silica multilayers," **Chem. Educator** *13*, 153-157.

Benoit R.; Saboungi M.-L.; Tréguer-Delapierre M.; Milosavljevic B.H.; Meisel D. **2007**, "Reactions of radicals with hydrolyzed bismuth(III) ions. A pulse radiolysis study," **J. Phys. Chem. A** *111*, 10640-10645.

Carrasco-Flores E.A.; LaVerne J.A. **2007**, "Surface species produced in the radiolysis of zirconia nanoparticles," **J. Chem. Phys.** *127*, 234703.

Merga, G.; Wilson, R.; Lynn, G.; Milosavljevic, B. H.; Meisel, D. **2007,** "Redox Catalysis on "Naked" Silver Nanoparticles," **J. Phys. Chem. C** *111*, 12220-12226.

Pimblott S.M.; LaVerne J.A. **2007**, "Production of low energy electrons by ionizing radiation," **Radiat. Phys. Chem.** *76*, 1244-1247.

Rajesh P.; LaVerne J.A.; Pimblott S.M. **2007**, "High dose radiolysis of aqueous solutions of chloromethanes: Importance in the storage of radioactive organic wastes," **J. Nucl. Mater.** *361*, 10-17.

Zidki, T.; Cohen, H.; Meyerstein, D.; Meisel, D. **2007**, "Effect of silica-supported silver nanoparticles on dihydrogen yields from irradiated aqueous solutions," **J. Phys. Chem. C** *111*, 10461-10466.

Dai, Q.; Menzies, D.; Wang, Q.; Ostafin, A. E.; Brown, S. N.; Meisel, D.; Maginn, E. J. **2006, "**Synthesis and composition analysis of microsilica encapsulated acetyl-acetonato-carbonyl-triphenylphosphine-rhodium," **Catalyst Nanotech.** *5*, 677-682.

Merga, G.; Milosavljevic, B. H.; Meisel, D. **2006,** "Radiolytic yields in aqueous suspensions of gold particles," **J. Phys. Chem. B** *110*, 5403-5408.

Stevens, F.; Carmichael, I.; Callens, F.; Waroquier, M. **2006,** "Density functional investigation of high-spin XY (X = Cr, Mo, W and Y = C,N,O) molecules," **J. Phys. Chem. A** *110*, 4846-4853.

Stevens, F.; Van Speybroeck, V.; Carmichael, I.; Callens, F.; Waroquier, M. **2006,** "The Rh-ligand bond: RhX (X = C, N, O, F, P and C) molecules," **Chem. Phys. Lett.** *421*, 281-286.

Hiroki, A.; LaVerne, J. A. **2005,** "Decomposition of hydrogen peroxide at water-ceramic oxide interfaces," **J. Phys. Chem. B** *109*, 3364-3370.

Garrett, B. C. et al. **2005,** "The role of water in electron-initiated processes and radical chemistry: issues and scientific advances," **Chem. Rev.** *105*, 355-390.

Lahiri, D.; Bunker, B. A.; Mishra, B.; Zhang, Z.; Meisel, D.; Doudna, C. M.; Bertino, M. F.; Blum, F. D.; Tokuhiro, A. T.; Chattopadhyay, S.; Shibata, T.; Terry, J. **2005,** "Bimetallic Pt-Ag and Pd-Ag nanoparticles," **J. App. Phys.** *97*, 094304-12.

LaVerne, J. A. **2005,** "$H_2$ formation from the radiolysis of liquid water with zirconia," **J. Phys. Chem. B** *109*, 5395-5397.

Meisel, D. **2005,** "Radiation effects on nanoparticles", Proceedings of the International Atomic Energy Agency Panel on "Emerging Applications of Radiation in Nanotechnology, "IAEA Press, Vienna, ISSN 1011-4289, ISBN 92-0-100605-5, pp. 130-141.

# Intermolecular Interactions of Hydroxyl Radicals on Reactive Potential Energy Surfaces

Marsha I. Lester
Department of Chemistry, University of Pennsylvania
Philadelphia, PA 19103-6323
milester@sas.upenn.edu

## I. Program Scope

The hydroxyl radical plays a major role in combustion and atmospheric environments as well as in the condensed phase. It is typically detected using the $A\,^2\Sigma^+$ - $X\,^2\Pi$ band system by direct absorption or laser-induced fluorescence. Collision partners that efficiently quench electronically excited OH $A\,^2\Sigma^+$ radicals are ubiquitous in these environments. As a result, great effort has been made to quantify the rates for collisional quenching. Yet, the mechanism by which OH $A\,^2\Sigma^+$ is quenched by molecular partners has remained elusive. The experimental work carried out under DOE funding in this laboratory is aimed at understanding the fundamental chemical dynamics governing quenching of OH $A\,^2\Sigma^+$ by molecular partners of significance in these environments. In addition, recent work is focused on the solvation of hydroxyl radicals, starting with the binary interaction of an open-shell OH $X\,^2\Pi$ radical with a water molecule, as a prototype for interactions of radicals in aqueous environments.

## II. Recent Progress

The OH $A\,^2\Sigma^+$ + $H_2$ system has emerged as a benchmark system for examining the nonadiabatic processes that lead to quenching,[1-6] in part because of its theoretical tractability. Collisions with $H_2$ can remove population from the electronically excited OH $A\,^2\Sigma^+$ state by two competing channels. The first is nonreactive quenching, which returns OH to its ground electronic state

$$\text{OH } A\,^2\Sigma^+ + H_2 \rightarrow \text{OH } X\,^2\Pi + H_2$$

while the second is reactive, and leads to the formation of water and hydrogen atoms[4-6]

$$\text{OH } A\,^2\Sigma^+ + H_2 \rightarrow H_2O + H$$

Quenching of OH $A\,^2\Sigma^+$ by $H_2$ is rapid at room temperature (10 Å$^2$),[7-9] and displays the typical negative temperature and initial rotational dependencies. *Ab initio* calculations of the interaction energy between $H_2$ and OH in its ground $X\,^2\Pi$ and excited $A\,^2\Sigma^+$ electronic states have identified specific orientations that lead to seams of *conical intersection* between the ground and excited state surfaces.[1-3]

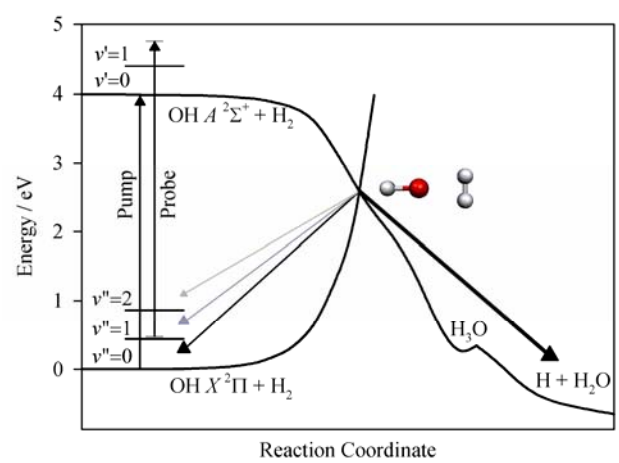


Fig. 1 Schematic potentials for quenching of OH in its excited $A\,^2\Sigma^+$ electronic state by $H_2$, illustrating a conical intersection (CI) that couples the potentials in the T-shaped HO–$H_2$ configuration. Two pathways emerge from the CI, leading to nonreactive and reactive quenching products; arrows indicate qualitative distribution of products. The pump-probe laser scheme for characterizing the OH $X\,^2\Pi$ product state distribution is also shown.

In this grant period, we examined the outcome of OH $A\,^2\Sigma^+$ ($v'$=0, N′=0) + $H_2$ quenching events that lead to OH $X\,^2\Pi$ + $H_2$ products (nonreactive quenching) as well as the branching between reactive and nonreactive quenching.[10-13] The OH $X\,^2\Pi$ products were detected in $v''$=0, 1 and 2; the distribution peaks in $v''$=0 and decreases monotonically with increasing vibrational excitation as shown in Fig. 2. In all vibrational

levels probed, the OH $X\,^2\Pi$ products are found to be highly rotationally excited, with the distribution peaking at $N''$=15. A marked propensity for production of $\Pi(A')$ Λ-doublet levels was also observed. By contrast, both OH $X\,^2\Pi$ spin-orbit manifolds were equally populated. We attribute these dynamical signatures to the forces at play as the OH–$H_2$ system passes through the conical intersection region that couple the ground and excited state potential energy surfaces.

The OH $X\,^2\Pi$ rotational distribution peaks at even higher rotational levels, $N''$=17 for $D_2$ (shown in Fig. 2) and $N''$=27 for $N_2$, with heavier collision partners. The modest increase for quenching by $D_2$ and much greater rotational excitation resulting from quenching by $N_2$ can be rationalized by kinematic arguments based on conservation of angular momentum.

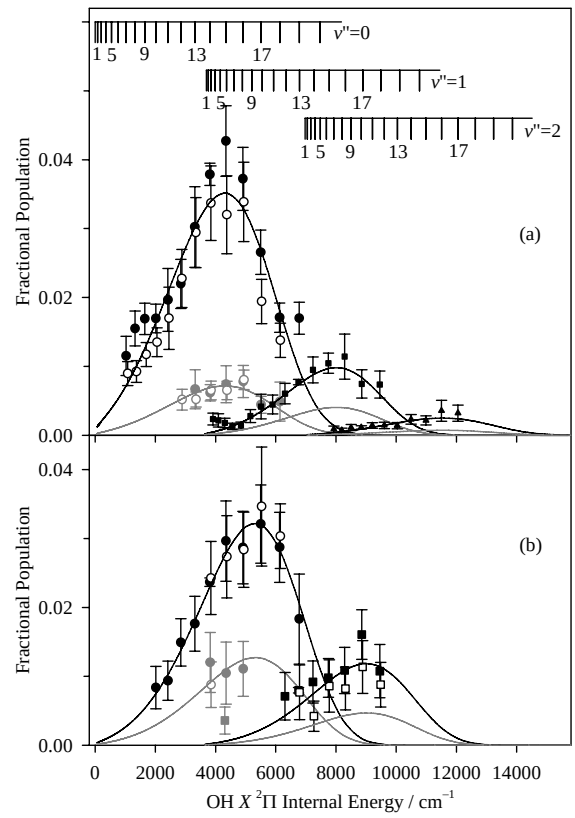


Fig. 2 Nascent OH $X\,^2\Pi$ (v″, N″) state distribution following collisional quenching of OH $A\,^2\Sigma^+$ by (a) $H_2$ and (b) $D_2$. Symbols indicate the populations in $v''$=0 (circles), $v''$=1 (squares) and $v''$=2 (triangles); filled and open symbols show the $F_1$ and $F_2$ spin-orbit manifolds; the $\Pi(A')$ Λ-doublets are indicated in black and $\Pi(A'')$ levels in gray. The lines are best-fit functions.

To better understand these results, the measurements have been complemented by an extensive theoretical study of the OH-$H_2$ interaction potential in the conical intersection region by Kłos and Alexander.[12] Calculations exploring the potential energy surface (PES) show a steep angular gradient into and away from the conical intersection whenever the O-end of the OH radical approaches the $H_2$ molecule. This causes a substantial torque to be placed on the OH radical as it passes through the conical intersection, resulting in the pronounced rotational excitation observed experimentally. The recent calculations did not examine the OH vibrational dependence. The earlier theoretical work of Hoffman and Yarkony[3] indicated little change in OH bond length as the system evolves through the conical intersection region, suggesting minimal vibrational excitation of OH products as now observed experimentally.

The observed propensity for production of the $\Pi(A')$ Λ-doublet is a consequence of the symmetries of the electronic states that form the conical intersection, and which correlate with A′ surfaces in planar geometries. For low rotational levels, the approximation of $H_2$ or $D_2$ as a spherical partner is fairly reasonable and the system can be considered as pseudo-triatomic. The OH $X\,^2\Pi$ products emerge on the lower 1 $^2$A′ surface, with the unpaired electron primarily in the plane of the collision, which is also the plane of OH rotation. These theoretical studies indicate that state-resolved measurements of the product quantum state distribution as well as the branching between the reactive and nonreactive pathways should provide sensitive probes of the dynamics of passage through a conical intersection region.

We have also made the first experimental determination of the branching between the nonreactive and reactive quenching pathways.[11] The branching fraction is measured by comparing the total population in OH $X\,^2\Pi$ product states arising from nonreactive quenching with the initial population excited to the OH $A\,^2\Sigma^+$ ($v'$=0, $N'$=0) state. Our detailed measurements indicate that collisional quenching

of OH $A\,^2\Sigma^+$ by $H_2$ yields only ~12(5)% of the products through the nonreactive pathway with the majority of products generated via the reactive pathway (~88%). Analogous measurements have been performed for the collisional quenching of OH $A\,^2\Sigma^+$ by $D_2$, yielding a branching fraction of 0.15(8), which is consistent with the value determined for $H_2$. It is, however, *counter to theoretical predictions*, which suggest that the steeper paths leading to OH $X\,^2\Pi + H_2$ should be dynamically more facile than the much shallower paths leading to $H_2O + H$.[3] Note that no collision-induced OD $X\,^2\Pi$ products were detected from an exchange reaction. By comparison, quenching OH $A\,^2\Sigma^+$ by $N_2$ proceeds almost exclusively by the nonreactive pathway.

These results for the prototypical OH $+H_2/D_2$ systems are an important step towards understanding nonadiabatic passage via conical intersections. However, there is still a need for more work on this and other systems of significance in these environments to fully understand the dynamical processes by which quenching occurs.

## III. Ongoing Work

Hydroxyl radicals are predicted to form strong hydrogen bonds with water, making complexes of OH with water important in a variety of environments from the atmosphere to heterogeneous interfaces of water. This system also provides a framework for understanding solvation of radicals in water. Spectroscopic studies of binary OH-water complexes using microwave[14-16] and infrared methods are expected to shed new light on the intermolecular interaction between the OH radical and water molecule.[17] We have predicted,[18] and recently observed, the rotational band structure associated with infrared transitions of the OH-water complex as an initial step to our infrared spectroscopic studies of this complex and OH embedded in small water clusters. In our initial experimental study, the binary OH-$H_2O$ complex is produced by association of photolytically generated OH radicals with $H_2O$ from dilute nitric acid. Infrared action spectroscopy is used to identify the fundamental OH radical stretch of the complex, which displays a frequency shift of nearly 80 $cm^{-1}$, consistent with theoretical predictions. Following infrared excitation of OH-$H_2O$, the OH products of vibrational predissociation are detected by laser-induced fluorescence. By utilizing information from the OH product state distribution, we estimate a binding energy for the complex of $D_0 \leq 5.1$ kcal $mol^{-1}$. Work is continuing in other spectral regions using an improved dual nozzle design for introducing water vapor into the carrier gas.

## IV. References


1. M. I. Lester, R. A. Loomis, R. L. Schwartz, and S. P. Walch, J. Phys. Chem. A **101**, 9195 (1997).
2. D. R. Yarkony, J. Chem. Phys. **111**, 6661 (1999).
3. B. C. Hoffman and D. R. Yarkony, J. Chem. Phys. **113**, 10091 (2000).
4. D. T. Anderson, M. W. Todd, and M. I. Lester, J. Chem. Phys. **110**, 11117 (1999).
5. M. W. Todd, D. T. Anderson, and M. I. Lester, J. Phys. Chem. A **105**, 10031 (2001).
6. M. Ortiz-Suárez, M. F. Witinski, and H. F. Davis, J. Chem. Phys. **124**, 201106 (2006).
7. D. E. Heard and D. A. Henderson, Phys. Chem. Chem. Phys. **2**, 67 (2000).
8. B. L. Hemming, D. R. Crosley, J. E. Harrington, and V. Sick, J. Chem. Phys. **115**, 3099 (2001).
9. B. L. Hemming and D. R. Crosley, J. Phys. Chem. A **106**, 8992 (2002).
10. L. P. Dempsey, C. Murray, P. A. Cleary, and M. I. Lester, Phys. Chem. Chem. Phys. **10**, 1424 (2008).
11. L. P. Dempsey, C. Murray, and M. I. Lester, J. Chem. Phys. **127**, 151101 (2007).
12. P. A. Cleary, L. P. Dempsey, C. Murray, M. I. Lester, J. Kłos, and M. H. Alexander, J. Chem. Phys. **126**, 204316 (2007).
13. I. B. Pollack, Y. X. Lei, T. A. Stephenson, and M. I. Lester, Chem. Phys. Lett. **421**, 324 (2006).
14. Y. Ohshima, K. Sato, Y. Sumiyoshi, and Y. Endo, J. Am. Chem. Soc. **127**, 1108 (2005).
15. C. S. Brauer, G. Sedo, E. M. Grumstrup, K. R. Leopold, M. D. Marshall, and H. O. Leung, Chem. Phys. Lett. **401**, 420 (2005).

[16] C. S. Brauer, G. Sedo, E. Dahlke, S. Wu, E. M. Grumstrup, K. R. Leopold, M. D. Marshall, H. O. Leung, and D. G. Truhlar, J. Chem. Phys. **129**, 104304 (2008).
[17] S. Du, J. S. Francisco, G. K. Schenter, T. D. Iordanov, B. C. Garrett, M. Dupuis, and J. Li, J. Chem. Phys. **124**, 224318 (2006).
[18] M. D. Marshall and M. I. Lester, J. Phys. Chem. B **109**, 8400 (2005).

## V. Publications supported by this project 2006-2008

1. I. B. Pollack, Y. Lei, T. A. Stephenson, and M. I. Lester, "Electronic Quenching of OH $A\ ^2\Sigma^+$ Radicals in Collisions with Molecular Hydrogen", *Chem. Phys. Lett.* **421**, 324-328 (2006).
2. P. A. Cleary, L. P. Dempsey, C. Murray, M. I. Lester, J. Kłos and M. H. Alexander, "Electronic Quenching of OH $A\ ^2\Sigma^+$ Radicals in Single Collision Events with Molecular Hydrogen: Quantum State Distribution of the OH $X\ ^2\Pi$ Products", *J. Chem. Phys.* **126**, 204316 (2007).
3. L. P. Dempsey, C. Murray, and M. I. Lester, "Product Branching between Reactive and Nonreactive Pathways in the Collisional Quenching of OH $A\ ^2\Sigma^+$ Radicals by $H_2$", *J. Chem. Phys.* [Communication] **127**, 151101 (2007).
4. L. P. Dempsey, C. Murray, P. A. Cleary, and M. I. Lester, "Electronic Quenching of OH $A\ ^2\Sigma^+$ Radicals in Single Collision Events with $H_2$ and $D_2$: A Comprehensive Quantum State Distribution of the OH $X\ ^2\Pi$ Products", *Phys. Chem. Chem. Phys.* **10**, 1424-1432 (2008).

# *Single-Molecule Chemical Imaging Studies of Interfacial Electron Transfer*

**H. Peter Lu**
Bowling Green State University
Department of Chemistry and Center for Photochemical Sciences
Bowling Green, OH 43403
hplu@bgsu.edu

## Program Scope

Our research is focused on the use of single-molecule high spatial and temporal resolved techniques to understand molecular dynamics in condensed phase and at interfaces, especially, the complex reaction dynamics associated with electron and energy transfer rate processes. Single-molecule approaches are unique for heterogeneous and complex systems because the static and dynamic inhomogeneities can be identified, characterized, and/or removed by studying one molecule at a time. Single-molecule spectroscopy reveals statistical distributions correlated with microscopic parameters and their fluctuations, which are often hidden in ensemble-averaged measurements. Single molecules are observed in real time as they traverse a range of energy states, and the effect of this ever-changing "system configuration" on chemical reactions and other dynamical processes can be mapped. In our research, we have been integrating two complementary methodologies; single-molecule spectroscopy (fluorescence and Raman) and scanning probe microscopy (STM and AFM) to study interfacial electron transfer dynamics in solar energy conversion, environmental redox reactions, and photocatalysis. We have been primarily focusing on studying electron transfer under ambient condition and electrolyte solution involving both single crystal and colloidal $TiO_2$ and related substrates. An understanding of the fundamental interfacial ET processes will be important for developing efficient light harvesting systems for solar energy transformation and be broadly applicable to problems in interface chemistry, catalysis, and nanoscience.

## Recent Progress

**Probing intermittent single-molecule interfacial electron transfer dynamics.** In this project, we have studied single-molecule interfacial electron transfer (ET) dynamics by using single-molecule fluorescence spectroscopy and photon-stamping technique. The interfacial electron transfer in zinc-tetra (4-carboxyphenyl) porphyrin (ZnTCPP)/$TiO_2$ nanoparticle system has been studied at ensemble-averaged level extensively, being demonstrated as an efficient photosensitization system. We have observed that the single-molecule fluorescence trajectories from (ZnTCPP)/$TiO_2$ show strong fluctuation and blinking between bright and dark states. We have identified that the single-molecule fluorescence intensity fluctuation is not due to triplet state or single-molecule rotational or translational motions during the measurements. The intermittency and fluctuation of the single-molecule fluorescence are attributed to the variation of the reactivity of interfacial electron transfer (Figure 1). The dark state in the fluorescence trajectory is due to ET process with a high activity quenching the fluorescence, and the bright state is due to fluorescence emission without ET quenching, i.e., a low activity in ET process (Figure 1 and 2). When the non-radiative FET process is much faster than the nanosecond radiative decay, the single molecule is dark; when the non-radiative FET process is much slower than the nanosecond radiative decay, the single-molecule is bright; when the non-radiative FET time is comparable to the nanosecond radiative decay, the single-molecule fluorescence state is in between bright and dark states. The comparative and rate-fluctuating non-radiative and radiative decay processes determined the fate of the excited states, and in turn determined the brightness of the single molecules (Figure 1).

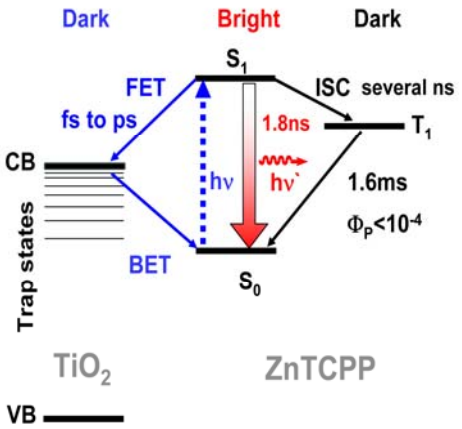


**Figure 1.** Schematic presentation of energy levels and basic photo-induced process in ZnTCPP/$TiO_2$ system. CB: conduction band; VB: valence band; FET: forward electron transfer; BET: Backward electron transfer; ISC: intersystem crossing. Ensemble-averaged experiments have demonstrated the interfacial ET in this dye-sensitization system. The time scale of the FET is reported to be fs to ps, and the time scale of BET is stretched from ns to ms.

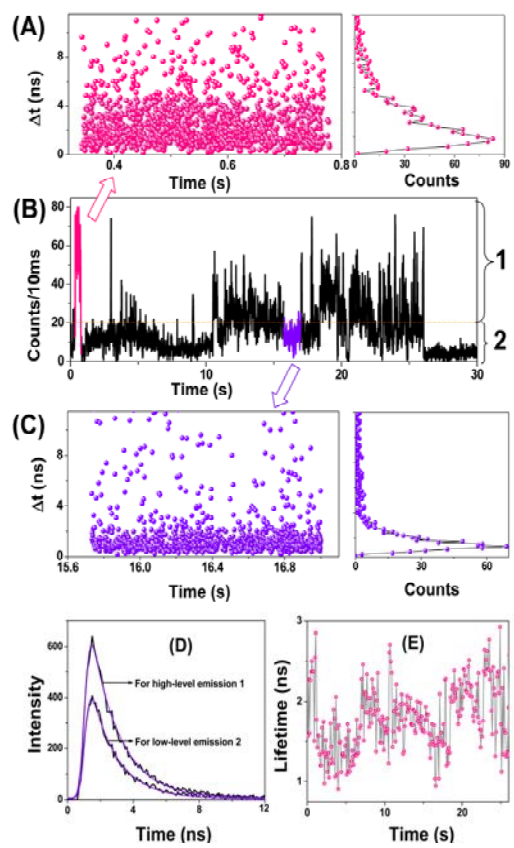


**Figure 2**. Single-molecule fluorescence decay profile of ZnTCPP on $TiO_2$ NP surface. In a single-molecule photon-stamping measurement, the chronic arrival time and the delay time from the laser pulse excitation are recorded for each detected photon. Each data point in A and C represents a detected photon with recorded delay time (y-axes) and chronic arrival time (x-axes). A distribution along the y-axes gives a typical single-molecule fluorescence decay curve, and a binning along the x-axes gives a typical single-molecule fluorescence intensity trajectory. Photon-stamping data (including arriving time and delay time for each photon) for typical high emission intensity state (in pink) and low emission intensity state (in purple) are displayed in (A) and (C), respectively. (B) Using 20 photocounts/10ms as threshold, the emission trajectory is separated to higher level (1) and lower level (2) periods. In (D), fluorescence decay profile for duration 1 and 2 are shown, and the decay times are 1.75 and 1.6 ns, respectively. (E) Single-molecule lifetime fluctuating trajectory of the same molecule from 0 to 26s.

The fluctuation of the single-molecule emission intensity is a reflection of the rate fluctuation of the non-radiative FET process; and the fluctuation of the FET dynamics is practically probed by the nanosecond radiative decay process in determining the fluorescence quantum efficiency. The non-

exponential autocorrelation function and the power-law distribution of the probability density of dark times imply the dynamic and static inhomogeneities of the interfacial ET dynamics. On the basis of the power-law analysis, the variation of single-molecule interfacial ET reactivity is analyzed as a fluctuation according to the Lévy statistics for the ZnTCPP/$TiO_2$ system. The intermittent interfacial electron transfer dynamics has been reported lately for other interfacial ET systems, and it is most likely that the intermittency of interfacial ET dynamics is a general behavior of chemical reactions that regulated by the vibronic coupling between the adsorbed molecules and the solid substrate surfaces related to solar energy transformation and catalysis.

**Revealing memory effect in single-molecule interfacial electron-cation recombination dynamics by photon-to-photon pair time analysis.** Interfacial electron-cation recombination in ZnTCPP)/$TiO_2$ nanoparticle system has been probed by recording and analyzing photon-to-photon pair times of the single-molecule ZnTCPP fluorescence. Memory effect of photon pair times, which reflects the real-time characteristics of interfacial electron-cation recombination dynamics, have been revealed by analyzing autocorrelation function and two-dimension joint probability distributions of the pair times. We have identified characteristic diagonal features in the two-dimension joint probability distributions. The diangnal distribution features indicate that a long pair time tends to be followed by a long pair time, and a short pair time tends to be followed by a short pair time (Figure 3). For ZnTCPP/$TiO_2$, the pair time trajectories associated with higher ET activity give well-defined correlation functions at decay time of 70±7 ms. Figure 3A and 3B show that the two-dimensional joint probability distributions for the pair times separated by 1 and 250 index numbers, i.e., g ($\tau_i$, $\tau_{i+1}$) and f($\tau_i$, $\tau_{i+250}$). Figure 3D shows the difference of two-dimensional joint probability distribution of pair times: $\delta(\tau_i,\tau_{i+1}) = g(\tau_i, \tau_{i+1}) - f(\tau_i, \tau_{i+250})$. Distribution $\delta(\tau_i, \tau_{i+1})$, i.e., the non-Markovian part, can be viewed as an analogue of the memory function. $f(\tau_i,\tau_{i+250}) = f(\tau_i)(\tau_{i+250})$ represents the Markovian part that gives no memory effect (Figure 3C). The 2D distribution (Figure 3D) calculated from an experimental single-molecule pair-time trajectory shows a characteristic diagonal feature reflecting that a long pair time tends to be followed by a long one and a short pair time tends to be followed by a short one. This non-Markovian behavior is interpreted by a proposed single-molecule interfacial electron-cation geminate recombination model. The convoluted multiple Poisson rate processes give rise to a memory effect in interfacial electron-cation recombination dynamics. On the basis of this model, the recombination time of ZnTCPP/$TiO_2$ system is deduced to be around 10-$10^2$ μs time scale.

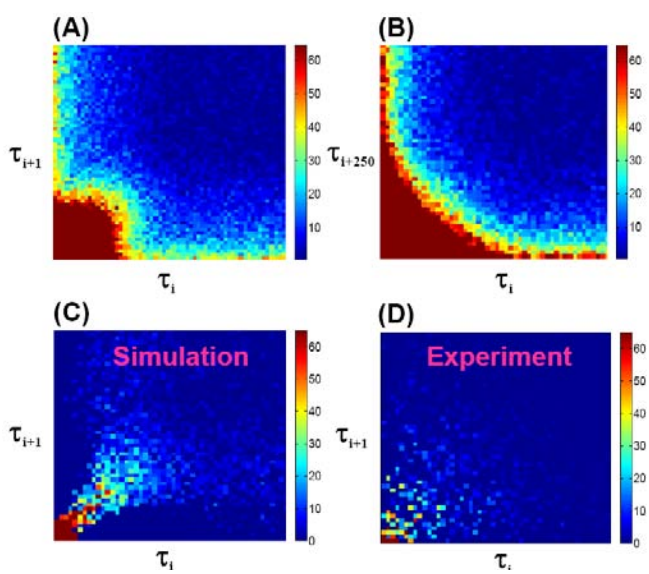


**Figure 3.** Simulated and experimental **t**wo-dimensional joint probability distributions of pair times: (**A**) simulated $g(\tau_i,\tau_{i+1})$; (**B**) simulated $f(\tau_i,\tau_{i+250})$; (**C**) simulated $\delta(\tau_i,\tau_{i+1}) = g(\tau_i,\tau_{i+1})-f(\tau_I, \tau_{i+250})$; (**D**) experimental $\delta(\tau_i,\tau_{i+1}) = g(\tau_i,\tau_{i+1}) - f(\tau_i, \tau_{i+250})$. $g(\tau_i,\tau_{i+1})$ and $f(\tau_I,\tau_{i+250})$ are the 2D distributions for adjacent pair times and pair times separated by 250 indexes, respectively. All the pair times vary from 0 to 5 ms.

**Future Plans**

We will further develop our new approach that combines complementary techniques: single-molecule time-resolved spectroscopy and scanning tunneling microscopy imaging to analyze the spatially and temporally complex interfacial ET dynamics. Our experimental measurements will focus on electron transfer involving individual molecules, dimers, and small clusters of adsorbed molecules, on $TiO_2$ surfaces, under ambient conditions. The substrates will consist of single-crystal and colloidal rutile and anatase. AFM metal-tip and STM imaging will be performed on identical sites to extract dynamical data at a molecular spatial resolution. Correlated information on the adsorption-site structure, molecular orientation, vibronic interaction, and single-molecule interfacial electron transfer dynamics will be obtained for the forward and backward electron transfer reactions. We will also conduct femtosecond single-molecule spectroscopy study on electron transfer dynamics in order to resolve the ultrafast single-molecule FET dynamics.

**Publications of DOE sponsored research (FY2005-2008)**


1. Yuanmin Wang, Xuefei Wang, H. Peter Lu, "Single-Molecule Electron-Cation Recombination Dynamics," *J. Phys. Chem.* Submitted (2008).
2. Yuanmin Wang, Xuefei Wang, Sujit Kumar Ghosh, H. Peter Lu, "Probing Intermittent Single-Molecule Interfacial Electron Transfer Dynamics of Porphyrin on $TiO_2$ Nanoparticles," *J. Am. Chem. Soc.* Submitted (2008).
3. Xuefei Wang, H. Peter Lu, "2D Regional Correlation Analysis of Single-Molecule Time Trajectories," *J. Phys. Chem.* In press (2008).
4. Duohai Pan, Dehong Hu, Ruchuan Liu, Xiaohua Zeng, Samuel Kaplan, H. Peter Lu, "Fluctuating Two-State Light Harvesting in a Photosynthetic Membrane," *J. Phys. Chem. C*, **111**, 8948-8956 (2007).
5. V. Biju, D. Pan, Yuri A. Gorby, Jim Fredrickson, J. Mclean, D. Saffarini and H. Peter Lu, "Correlated Spectroscopic and Topographic Characterization of Nanoscale Domains and Their Distributions of a Redox Protein on Bacterial Cell Surfaces," *Langmuir* **23**, 1333-1338 (2007).
6. Dehong Hu and H. Peter Lu, "Single molecule electron transfer process of ruthenium complexes," *Proc. SPIE* Vol. **6092**, 609207 (2006).
7. Duohai Pan, Nick Klymyshyn, Dehong Hu, and H. Peter Lu, "Tip-enhanced near-field Raman spectroscopy probing single dye-sensitized $TiO_2$ nanoparticles," *Appl. Phys. Lett.*, **88**, 093121(2006).
8. Duohai Pan, Dehong Hu, and H. Peter Lu, "Probing Inhomogeneous Vibrational Reorganization Energy Barriers of Interfacial Electron Transfer," *J. Phys. Chem.* B, **109**, 16390-16395 (2005).
9. Dehong Hu and H. Peter Lu, "Single-Molecule Triplet-State Photon Antibunching at Room Temperature," *J. Phys. Chem. B*, **109**, 9861-9864 (2005).
10. H. Peter Lu, invited review article, "Site-Specific Raman Spectroscopy and Chemical Dynamics of Nanoscale Interstitial Systems," *J. Physics: Condensed Matter*, **17**, R333-R355 (2005).

**Spectroscopy of Organometallic Radicals**

Michael D. Morse
Department of Chemistry
University of Utah
315 S. 1400 East, Room 2020
Salt Lake City, UT 84112-0850
morse@chem.utah.edu

## I. Program Scope:

In this project, we seek to obtain fundamental physical information about unsaturated, highly reactive organometallic radicals containing open *d* subshell transition metal atoms. Gas phase electronic spectroscopy of jet-cooled transition metal (TM) molecules is used to obtain fundamental information about ground and excited electronic states of such species as the transition metal carbides and organometallic radicals such as $CrC_2H$, $CrCH_3$, and $NiCH_3$. Ionic species will become available for investigation when the construction of a new ion trap spectrometer is complete.

## II. Recent Progress:

### A. Optical spectroscopy of OsC, OsN, and YF

During 2005-2008, we have used resonant two-photon ionization (R2PI) and dispersed fluorescence (DF) spectroscopic methods to investigate the TM carbide, OsC,[1] the TM nitride, OsN, and have also analyzed a spin-forbidden band system in YF.[2] Our work on the previously unknown molecule, OsC, has established that the ground state derives from a $1\delta^3\ 3\sigma^1$ configuration, making the ground term a $^3\Delta_3$ term, as was found for FeC. This contrasts with the $1\delta^4$, $^1\Sigma^+$ ground term of RuC. In the case of OsC, it is the relativistic stabilization of the 6*s* orbital that results in the $1\delta^3\ 3\sigma^1$, $^3\Delta_3$ ground term. In addition to determining the ground state, our work on OsC shows that the first excited state of this molecule is the $1\delta^2\ 3\sigma^2$, $^3\Sigma^-$ ($\Omega = 0^+$) term,[1] which lies very high in energy in RuC. The observation of a low-energy $1\delta^2\ 3\sigma^2$, $^3\Sigma^-$ state in OsC demonstrates the relativistic stabilization of the $3\sigma$ orbital, which is shown by our hyperfine measurements to be primarily Os 6*s* in character.

In subsequent work on osmium containing compounds, we have begun an investigation of the osmium nitride molecule, OsN. Although the molecule has been spectroscopically investigated in the near infrared region, and has been determined to have a $1\delta^3\ 3\sigma^2$, $^2\Delta_{5/2}$ ground state, the location of the $1\delta^4\ 3\sigma^1$, $^2\Sigma^+$ and $1\delta^3\ 3\sigma^1\ 2\pi^1$, $^2\Pi(2)$ and $^2\Phi(2)$ states are experimentally unknown. So far, our investigation has identified $^2\Pi_{3/2} \leftarrow X\ ^2\Delta_{5/2}$ and $^2\Phi_{7/2} \leftarrow X\ ^2\Delta_{5/2}$ band systems in the blue portion of the spectrum. By investigating the dispersed fluorescence, we hope to locate the $1\delta^3\ 3\sigma^1\ 2\pi^1$, $^2\Pi_{3/2} \rightarrow 1\delta^3\ 3\sigma^1$, $^2\Sigma^+$ fluorescence system. If both $^2\Pi$ and both $^2\Phi$ terms originating from the $1\delta^3\ 3\sigma^1\ 2\pi^1$ configuration are located, and the $1\delta^4\ 3\sigma^1$, $^2\Sigma^+$ term is likewise identified, all of the expected low-lying electronic states will have been found. Shown in Figure 1 below is a rotationally resolved spectrum of the 0-0 band of the [21.2] $^2\Phi_{7/2} \leftarrow X\ ^2\Delta_{5/2}$ system of OsN

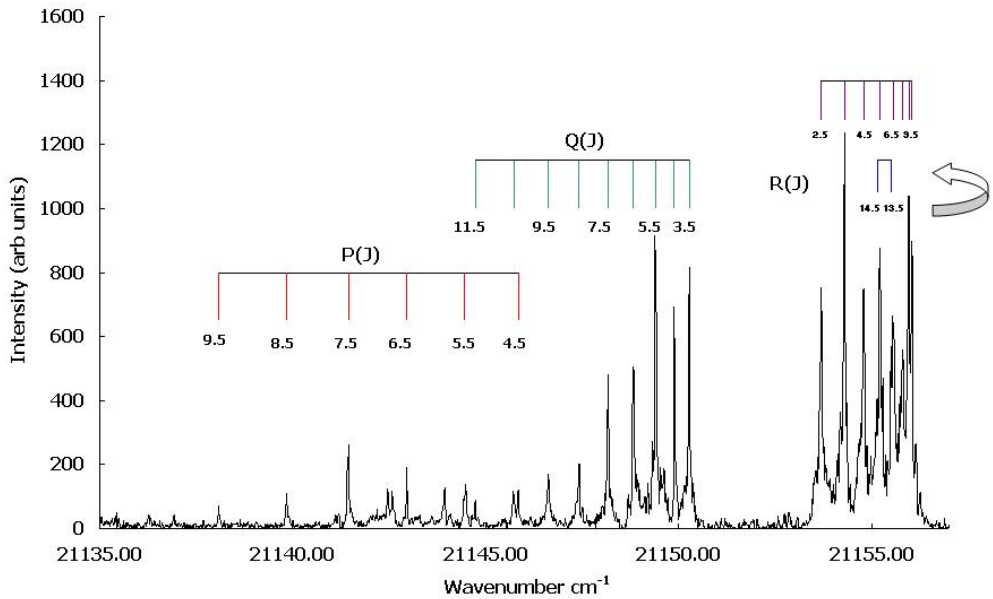


Figure 1. Rotationally resolved spectrum of the 0-0 band of the [21.2] $^2\Phi_{7/2} \leftarrow X\,^2\Delta_{5/2}$ system of OsN.

During a study of the YCo diatomic metal molecule (funded by the NSF), we noticed transitions occurring at the mass of YF.[2] The YF molecules are formed by accident by the reaction of atomic yttrium with Teflon tape residue that remains in the instrument after it was used many years ago. A quick scan of the published spectroscopy of YF showed that some of the bands that were observed in this extremely well-studied molecule had not been previously observed. Accordingly, we expanded our investigation to include a study of these features, which fall within the framework of the DOE project. The new bands were found to belong to the spin-forbidden $c\,^3\Sigma_1^+ \leftarrow X\,^1\Sigma^+$ band system. Our investigation provided a linkage between the singlet and triplet manifolds of YF, along with a detailed analysis of the spin-orbit interactions within the states arising from the $Y^+$ ($^{1,3}D$) + $F^-$ ($^1S$) states of the separated ions. The analysis showed that the $c\,^3\Sigma_1^+$ state is contaminated with approximately 2% $B^1\Pi$ character, and this spin-orbit mixing causes the $c\,^3\Sigma_1^+ \leftarrow X\,^1\Sigma^+$ band system to gain sufficient intensity to be observed.

## III. Future Plans

### A. R2PI and DF spectroscopy of transition metal carbides and radicals

Projects for the upcoming year include: (1) Measurement of dispersed fluorescence from the osmium molecules OsC and OsN, to locate some of the expected low-lying electronic states and flesh out the electronic structure of these species. (2) Assignment of the rotational lines in the $^6\Sigma^+ \leftarrow X^6\Sigma^+$ band system of CrCCH and fitting of the spectrum to extract the spectroscopic constants; (3) Analysis of the rotationally resolved spectrum of TiC, using dispersed fluorescence from single rovibronic levels to identify the lines; (4) Attempts to record and analyze the spectra of several transition metal cyanides (or isocyanides) will be made. Species to be investigated will include CuCN, AgCN, AuCN, ScNC, and YNC (these latter two molecules are thought to be isocyanides, while the former are expected to be cyanides). When the spectrum of CrCCH has been successfully analyzed, we will attempt to record the spectrum of the isovalent molecule, CrCN.

**B. Photodissociation spectroscopy of cold, trapped ions**

During my 2005 sabbatical leave working with John Maier at the University of Basel, I was very impressed with the capabilities of his newly-constructed mass-selected ion trap photodissociation spectrometer, which produces spectra of cryo-cooled gas phase ions with unprecedented signal-to-noise ratios. In my 2007 DOE renewal proposal, I proposed to build a similar device here at the University of Utah, for the study of unsaturated transition metal cation species. With the funds that have been awarded for this project from the DOE (and some supplementary funds from the NSF for a Nd:YAG-pumped dye laser), I will be able to construct the spectrometer. To this end, I have now hired an undergraduate mechanical engineering student to help design the instrument, and am searching for a postdoctoral researcher with mass spectrometry expertise. The proposed design is shown in Figure 2 below.

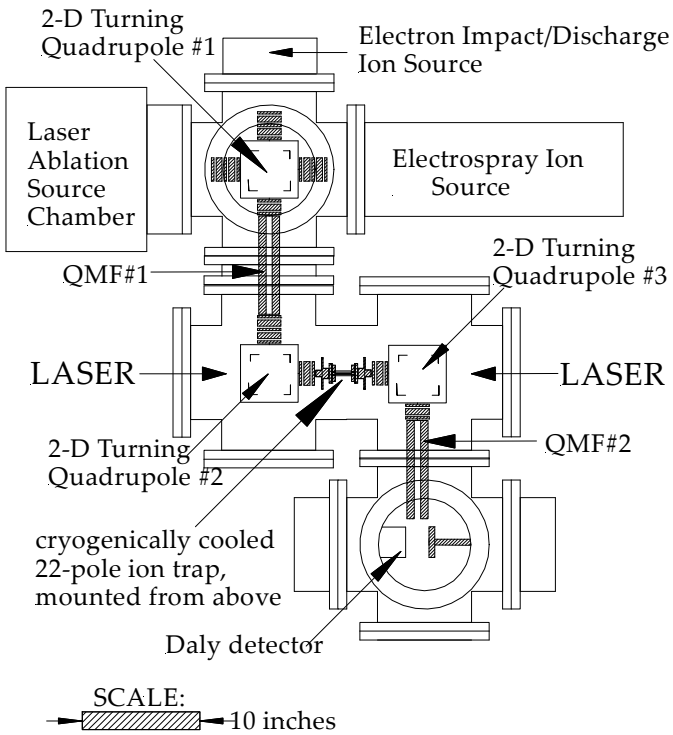


Figure 2. Design plan for the Utah ion trap photodissociation spectrometer.

The instrument will make use of a variety of ion sources, with initial experiments concentrating on an electron impact ionization source or a discharge source. For some experiments, a laser ablation ion source will be more useful. Ultimately, I would also like to implement an electrospray ion source as well, to allow the investigation of transition metal ion species that occur commonly in solution. These three ion sources will be attached to a chamber housing a two-dimensional turning quadrupole that will be used to direct the ion beam into a quadrupole mass filter for initial mass selection. A second two-dimensional turning quadrupole will then direct the mass-selected ions into a 22-pole radio frequency ion trap that is cooled by a

closed-cycle helium cryostat operating at 10 K. Helium (~ 1 mTorr) in the trap will transfer the low temperature of the walls to the trapped ions. Experience in Basel shows that ions can be routinely cooled to 20-25 K. After allowing a period of perhaps 70 ms for the trapped ions to be cooled, the ions will be subjected to the tunable output of one or two pulsed lasers. Absorption of the laser radiation will be detected by photofragmentation of the mass-selected parent ion. After allowing a short period for the fragmentation to occur, the ions will be released from the trap and a second quadrupole mass filter will be used to transmit the fragment ions to a Daly detector, where they can be counted. The ion signal at the mass of the fragment will then be measured as a function of laser wavenumber to obtain an optical spectrum of the trapped ion.

The beauty of this technique is that it can be used for any ion that can be trapped and induced to photodissociate. Thus, we anticipate quite general applicability of the method to a wide variety of species. Our first target for study will be $FeCO^+$, to be produced by electron impact ionization of $Fe(CO)_5$ vapor. We will follow this up by studies of $Fe(CO)_2^+$ and $NiCO^+$, also produced by electron impact on the stable metal carbonyls. Further down the line, we plan to investigate more chemically interesting species, such as the transition metal-acetylene complexes, $M^+ \cdot H\text{-}C{\equiv}C\text{-}H$.

At this point in time, the turning quadrupoles and mass-selective quadrupoles are in hand, along with the required vacuum pumps. We are currently in the process of designing the mechanical system, purchasing the quadrupole mass filter controllers, Daly detector electronics, *etc*. There is a lot of work to be done to put the system together, but we hope to have successfully trapped ions within about a year.

**IV. Publications from DOE Sponsored Research 2005-present:**


1. Olha Krechkivska and Michael D. Morse, "Resonant two-photon ionization spectroscopy of jet-cooled OsC," J. Chem. Phys. **128**, 084314 (2008).

2. Ramya Nagarajan and Michael D. Morse, "Spin-forbidden $c\,^3\Sigma_1^+ \leftarrow X\,^1\Sigma^+$ band system of YF," J. Chem. Phys. **126**, 144309/1-6 (2007).

# *Ab initio* approach to interfacial processes in hydrogen bonded fluids

Christopher J. Mundy
Chemical and Materials Sciences Division
Pacific Northwest National Laboratory
902 Battelle Blvd, Mail Stop K1-83
Richland, WA 99352
chris.mundy@pnl.gov

## Program Scope

The long-term objective of this research is to develop a fundamental understanding of processes, such as transport mechanisms and chemical transformations, at interfaces of hydrogen-bonded liquids. Liquid surfaces and interfaces play a central role in many chemical, physical, and biological processes. Many important processes occur at the interface between water and a hydrophobic liquid. Separation techniques are possible because of the hydrophobic/hydrophilic properties of liquid/liquid interfaces. Reactions that proceed at interfaces are also highly dependent on the interactions between the interfacial solvent and solute molecules. The interfacial structure and properties of molecules at interfaces are generally very different from those in the bulk liquid. Therefore, an understanding of the chemical and physical properties of these systems is dependent on an understanding of the interfacial molecular structure. The adsorption and distribution of ions at aqueous liquid interfaces are fundamental processes encountered in a wide range of physical systems. In particular, the manner in which solvent molecules solvate ions at the interface is relevant to problems in a variety of areas. Another major focus lies in the development of models of molecular interaction of water and ions that can be parameterized from high-level first principles electronic structure calculations and benchmarked by experimental measurements. *All of the aforementioned studies are performed using novel algorithms based in density functional theory (DFT) in conjunction with high performance computing through a* ***2008 INCITE award***. These models will be used with appropriate simulation techniques for sampling statistical mechanical ensembles to obtain the desired properties.

## Progress Report

Calculation of the surface potential for the aqueous liquid-vapor interface (with Shawn M. Kathmann). The electrostatic potential at the coexisting liquid-vapor phases is another sensitive probe of the structure of the fluid interface. Moreover, it is a quantity that cannot easily be measured and there is even some controversy as to the over-all sign of the surface potential from both theory and experiment.[1] The importance of understanding the origins and the sign of the surface potential has far reaching implications of understanding the free-energies of ion solvation and the hydrophobic interactions.[2,3] In light of the new conventional wisdom emerging on the structure of ions at aqueous interfaces and interfacial structure of neat water and neat methanol interfaces, knowledge of the surface potential provides a piece of the fundamental chemical physics of hydrogen-bonded fluids. Although there have been many attempts to compute the surface potential using both fixed charge and polarizable models yielding qualitative agreement between studies,[4-8] it has been suggested that without the explicit treatment of electrons, the computed surface potential could yield a different relative sign.[3,5-7] We have performed the first calculation of the surface potential of water using DFT interaction potentials. These calculations have yielded a surface potential of -18 mV that is roughly thirty times smaller than a calculation

based on empirical interaction potentials (both fixed charge and polarizable). The salient feature of the electrodynamic approach (used in this study) versus the thermodynamic approach is that the electrodynamic approach is not plagued with difficulties of obtaining accurate free energetics of the thermodynamic cycles. Moreover, our approach examined the surface potential without assumptions on the form of the electronic multipoles used to describe the electrostatic interactions. Besides giving a reliable estimate of the real chemical potential crucial to understanding solvation free energies, these calculations will be used to further judge the accuracy and transferability of DFT applied to heterogeneous environments.

Development of a intermolecular interactions based on a self-consistent treatment of polarization and dispersion within a minimal basis set density functional theory (DFT) (with Gregory K. Schenter and Garold Murdachaew): One of the major deficiencies of DFT is the lack of dispersion interactions. This active area of research has spawned several solutions to this problem ranging from simple empirical parameterizations to more rigorous approaches based in perturbation theory. Although successful, these methods suffer from their lack of rigor and computational expense. Our novel formulation is based in perturbation theory and is an extension of self-consistent polarization theory in conjunction with neglect of diatomic differential overlap (SCP-NDDO)[9] to DFT and the condensed phase. In order to routinely perform large calculations on interfaces using DFT interaction potentials, we will take full advantage of the existing framework for parallelization and fast electronic structure that is currently present in CP2K (www.cp2k.berliose.de). To this end, our formulation is now available in the CP2K package (SCP-DFT) and contains auxiliary polarization functions whose coefficients are simultaneously and self-consistently determined along with standard orbital coefficients for the basis set. Furthermore, within this theoretical framework, a consistent expression for the dispersion energy that is based on second-order perturbation theory can be formulated. This is an extension of an approach that has already been applied to DFT and forms that basis of empirical generalizations of London dispersion [10,11]. Thus, we have a self-consistent theory that is easy to parameterize and allows for efficient condensed phase calculations (including both charge transfer and chemistry) with the inclusion of dispersion. Remarkably, with a single parameter, we are able to reproduce benchmark calculations on the energetics of clusters (to n=10), the cohesion energy of the solid, the second virial coefficient, and the liquid structure for argon. This comprehensive theoretical study thus validates our novel approach, and to our knowledge is the first successful application of DFT based methods to quantitatively capture *both* thermodynamic and structural properties of a weakly interacting system in all three phases of matter. Our results have been extended to water where again, we are able to reproduce cluster energetics obtained at the MP2 complete basis set level. Moreover, our approach gives a softer liquid structure for water, and nearly quantitatively captures the frequency shifts obtained by MP2 due to subtle hydrogen bonding arrangements (see Abstract of G.K. Schenter).

Large-scale density functional theory studies of the free-energies of transfer of $OH^-$ from bulk to interface (with L.X. Dang): Although there appears to be a consensus between various theoretical calculations and experiments on the distributions of several inorganic ions in the interfacial region, there is considerable disagreement of the water ions, specifically, the hydroxide anion and the excess proton, at the air-water interface. [12] This is problematic, because an accurate knowledge of the propensities of the water ions for the air-water interface is central to our understanding of chemistry at aqueous interfaces. The relative populations of these ions at

the interface vs. in bulk neat water determine whether the interfacial region is neutral, as in the bulk, or acidic or basic. Corresponding data for hydroxide could be interpreted in terms of a range of behavior, from slight enhancement to strong repulsion.[13] It is clear from the collection of experimental and theoretical data summarized here that more research is needed to resolve the important issue of the acidity/basicity of the water surface. We have weighed in on this critical debate by performing the largest and most extensive DFT studies of the hydroxide anion in water in an interfacial geometry. These calculations were made possible by the 2008 INCITE award and 2008 NERSC large-scale reimbursement program. Our results, presented in **Figure 1** indicate that hydroxide ion is free-energetically stable and resembles the "$H_3O_2^-$" moiety in the vicinity of the aqueous liquid-vapor interface.

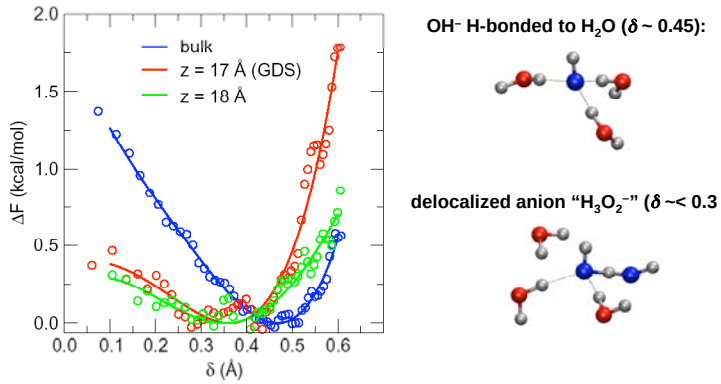


**Figure 1:** Free-energy surfaces and representative clusters as a function of the sampled reaction coordinate ("δ" being a measure of the distance from the proton transfer transition state). One can see a distinct difference in the free-energy as compared to the bulk (blue). The red and green curves represent free-energy profile at the onset of (the so-called Gibbs dividing surface (GDS)) and slightly above the interface. To the right of the graph are representative clusters of $OH^-$ in the interfacial region as a function of "δ." The salient feature is the clear delocalization of charge at δ<0.3 that is stabilized near the interface (see minima of red and green curves vs. blue).

## Future directions

1. We plan to extend SCP-DFT to interfacial systems and chemical reactions in aqueous and heterogeneous environments. We also are thinking of ways to provide effective parameterizations for the first two rows of the periodic table and important halide ions to be used within the SCF-DFT formulation.
2. We plan to continue large-scale DFT calculations to determine novel heterogeneous reaction mechanisms in hydrogen bonding fluids. In particular, we will validate the conventional wisdom on the propensity for hydronium at the liquid vapor interface by utilizing DFT interaction potentials that contain *both* polarization and chemistry.

**Acknowledgements**. This research was performed using computational resources through the large-scale reimbursement program at NERSC and the 2008 INCITE award (JAGUAR at ORNL and BG/P at ANL). This work benefited greatly from active collaborations with D.J. Tobias (UC-I), M.E. Tuckerman (NYU), and I.-F.W. Kuo (LLNL).

### Publications from BES support (2006- present)

1. "Time-dependent properties of liquid water: A comparison of Car-Parrinello and Born-Oppenheimer molecular dynamics simulations," I.-F.W. Kuo, C.J. Mundy, M.J. McGrath, J.I. Siepmann, *Journal of Chemical Theory and Computation* **2**, 1274 (2006).
2. "First-principles approaches to the structure and reactivity of atmospherically relevant aqueous interfaces," C.J. Mundy, I.-F.W. Kuo, *Chemical Reviews* **106**, 1282 (2006).

3. "Molecular dynamics simulations of liquid water: Hybrid density functionals," T. Todorova, A. Sietsonen, J. Hutter, I.-F.W. Kuo, C.J. Mundy, *Journal of Physical Chemistry B* **110**, 3685 (2006).
4. "Structure and dynamics of the aqueous liquid-vapor interface: A comprehensive particle based study," I.-F.W. Kuo, C.J. Mundy, E.L. Eggimann, M.J. McGrath, J.I. Siepmann, B. Chen, J. Vieceli, D.J. Tobias, *Journal of Physical Chemistry B*, **110**, 3738 (2006).
5. "Simulating fluid phase equilibria from first principles," M.J. McGrath, J.I. Siepmann, I.-F.W. Kuo, C.J. Mundy, J. VandeVondele, J. Hutter, F. Mohamed, M. Krack, *Journal of Physical Chemistry A* **110**, 640 (2006).
6. "Time-dependent properties of liquid water: A comparison of Car-Parrinello and Born-Oppenheimer molecular dynamics," I.-F.W. Kuo, C.J. Mundy, M.J. McGrath, and J.I. Siepmann, *Journal of Chemical Theory and Computation*, **2**, 1274 (2006).
7. "Spatial correlation of dipole fluctuations in liquid water," M.J. McGrath, J.I. Siepmann, I.-F.W. Kuo, C.J. Mundy, *Molecular Physics* **105**, 1411 (2007).
8. "A special brew," C.J. Mundy, S.M. Kathmann, and G.K. Schenter, *Natural History* **116**, 32 (2007).
9. "Acid/base equilibria in clusters an their role in proton exchange membranes: computational insight," V.A. Glezakou, M. Dupuis, and C.J. Mundy, *Physical Chemistry Chemical Physics* **9**, 5753 (2007)
10. "The effect of polarizability for understanding the molecular structure of aqueous interfaces," C.D. Wick, I.-F.W. Kuo, C.J. Mundy, and L.X. Dang, *Journal of Chemical Theory and Computation* **3**, 2002 (2007)
11. "A microscopic approach to understanding complex systems: computational statistical mechanics using state-of-the-art computational platforms," C.J. Mundy, R. Rousseau, A. Curioni, S.M. Kathmann, G.K. Schenter, *Journal of Physics* **125**, 0120414 (2008).
12. "Structure of the methanol liquid-vapor interface: A comprehensive particle based simulation study," I.-F.W. Kuo, C.J. Mundy, M.J. McGrath, and J.I. Siepmann, *Journal of Physical Chemistry B* **in press** (2008).

## References:


(1) Parfenyuk, V. I. *Colloid Journal* **2002**, *64*, 588-595.

(2) Pegram, L. M.; Record, M. T. *Proceedings of the National Academy of Sciences of the United States of America* **2006**, *103*, 14278-14281.

(3) Beattie, J. K. *The Intrinsic Charge at the Hydrophobe/Water Interface*; Wiley-VCH Verlag GmbH & Co. KGaA: Weinheim, 2006.

(4) Sokhan, V. P.; Tildesley, D. J. *Molecular Physics* **1997**, *92*, 625-640.

(5) Pratt, L. R. *Journal of Physical Chemistry* **1992**, *96*, 25-33.

(6) Wilson, M. A.; Pohorille, A.; Pratt, L. R. *Journal of Chemical Physics* **1988**, *88*, 3281-3285.

(7) Wilson, M. A.; Pohorille, A.; Pratt, L. R. *Journal of Physical Chemistry* **1987**, *91*, 4873-4878.

(8) Wick, C. D.; Dang, L. X.; Jungwirth, P. *Journal Of Chemical Physics* **2006**, *125*, 024706.

(9) Chang, D. T.; Schenter, G. K.; Garrett, B. C. *Journal of Chemical Physics* **2008**, *128*.

(10) Misquitta, A. J.; Jeziorski, B.; Szalewicz, K. *Physical Review Letters* **2003**, *91*, 033201.

(11) Misquitta, A. J.; Podeszwa, R.; Jeziorski, B.; Szalewicz, K. *Journal of Chemical Physics* **2005**, *123*, 214103.

(12) Petersen, P. B.; Saykally, R. J. *Chemical Physics Letters* **2008**, *458*, 255-261.

(13) Petersen, M. K.; Iyengar, S. S.; Day, T. J. F.; Voth, G. A. *Journal of Physical Chemistry B* **2004**, *108*, 14804-14806.

# LASER DYNAMIC STUDIES OF PHOTOREACTIONS ON SINGLE-CRYSTAL & NANOSTRUCTURED SURFACES (DE-FG02-90ER14104)

**Richard Osgood,**
Center for Integrated Science and Engineering, Columbia University, New York, NY 10027, Osgood@columbia.edu

## Program Scope or Definition:

This talk will discuss progress in our research toward understanding photoreaction dynamics on nanostructured surfaces and, in particular, the surfaces of nanoobjects. Our overall program plan is to first emphasize developing an STM-based method for study of uncapped nanocrystals *with specific reconstructions and orientation*; the particles will be formed via several unconventional methods of UHV growth. We will then use our separate time-of-flight quadrupole mass spectrometer instrumentation to explore photoreaction dynamics on these particles through measurement of fragment energetics and angular distributions from UV-irradiated adsorbates on metal-oxide nanocrystal surfaces. A second thrust of the research will be to explore fragmentation dynamics on *in situ*-formed metal nanoparticles, which have plasmon-enhanced-reaction rates. The research tools are time-of-flight detection XPS, STM, standard UHV probes, and theoretical *E&M* (metal nanoparticles) and molecular computational tools. Collaboration with the Surface Dynamics Group and Catalysis Group at Brookhaven National Laboratory is on-going. The work is complementary to other programs in $TiO_2$ nanoparticle synthesis, reactions, and photoreactions at the Fritz-Haber Institute, PNNL, and Harvard.

From the perspective of energy needs, photoexcitation has been of continuing interest for its importance in photocatalytic destruction of environmental pollutants, in several methods of solar-energy conversion, and for a variety of applications in nanotechnology. Our recent work in this program has yielded several new research findings regarding the preparation of nanoparticles, the basic chemical dynamics of surface photofragmentation, and plasmonic surface enhancement and scattering.

*This talk will emphasize our recent progress on the growth and characterization of fully crystalline nanoparticles of $TiO_2$ on single-crystal Au. We show that high-quality low-size-dispersion particles of ~2-10nm in size can be grown by two very different approaches. The crystal type and orientation and their dependence on growth chemistry are also discussed.*

## Recent Progress:

*STM Study of In Situ Formed $TiO_2$ Nanocrystals on Au(111):* In this portion of our research, we have investigated a chemically based approach to *in situ* $TiO_2$ oxide formation; this approach, which uses Ti reacting with a monolayer water layer or an $NO_2$ layer and is termed Reactive Layer-Assisted Deposition (RLAD), was initially examined by Dr. Song in our group and published in Nanoletters. These results showed the formation of ~5nm-scale $TiO_2$ nanocrystallites. Now we have completed a detailed study of the structure and areal distribution of these nanocrystallites formed by RLAD on Au(111). Our results show that the distribution and size of these crystallites depend on the thickness of the $H_2O$ layer and on their thermal treatment after formation. The large-scale sur-

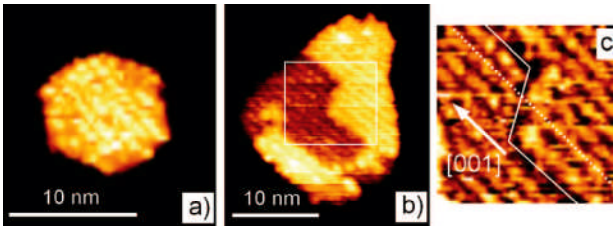


**Fig. 1:** STM images of hexagonal $TiO_2$ nanocrystallites: (a) A fully formed hexagonal crystallite; (b) an irregular hexagonal crystallite with two-layer structure; (c) "zoom in" of the marked area in b). The solid line marks the position of the step edge. The dotted line demonstrates the registry between the two layers and marks the position of a ridge in the top terrace (right side). Crystallographic directions in c) are rutile(100) structure.

face distribution of our titania nanocrystals suggests formation of liquid-water droplets in the RLAD process. Thus, the thickness of the reactive water layer must be minimized if one desires an even distribution of nanocrystals on the surface. Three types of crystallites are seen after a surface with $TiO_2$ nanoparticles is annealed to 900 K: hexagonal crystallites are in the majority and 3D "ridges" and octagonal crystallites are found in low concentration. In the case of the first two types, their structure is that of rutile $TiO_2$; see Fig.1 for examples of the structure of the hexagonal crystals. In addition, despite relatively weak oxide/metal-surface interactions, most of the structures seen here are partially oriented by the Au(111) substrate. More generally, our results show that STM observations can be used to probe the formation of nanocrystals of metal oxides, to determine their crystallography, and to understand the characteristics of the process leading to their formation.

In addition, we have just completed an investigation of a second approach, which is based on diffusive transport of one constituent from a surface alloy. In this approach a shallow-depth surface alloy is formed from Ti in Au(111). Oxidation of the alloy is then used to form nanoparticles of $TiO_2$ on Au(111). *In situ* STM studies show that the approach yields arrays of particles with good size dispersion and controllable shape. Scanning tunneling spectroscopy indicates that the particles have a well developed bandgap, comparable to that in bulk $TiO_2$. The particle crystallographic form is rutile, being triangular or hexagonal in shape.

This process of surface-alloy oxidation was examined in order to provide a controlled metal source for crystallite formation. Thus, exposure of the surface-Ti-alloy Au(111) samples to a flux of molecular oxygen, ~500L, at elevated temperatures of ~900K was found to cause uniform growth of flat crystallites across the surface. As we have shown earlier, the crystalline nature of such small-scale particles can be determined via STM imaging of the nanoscale $TiO_2$ crystals. The STM images of such surfaces revealed that all crystallites had either a triangular or hexagonal shape, with flat-top faces parallel to the surface. Statistical analysis of the sizes of the crystallites yields a relatively narrow particle-area distribution: the average area is 45 ± 16 $nm^2$. About 95% of the crystallites are hexagonal shaped. We have identified this type of surface structure as rutile $TiO_2$ crystallites with a top-face (100) plane. The remaining 5 % of the crystallites were ridge-like structures, identified also as rutile

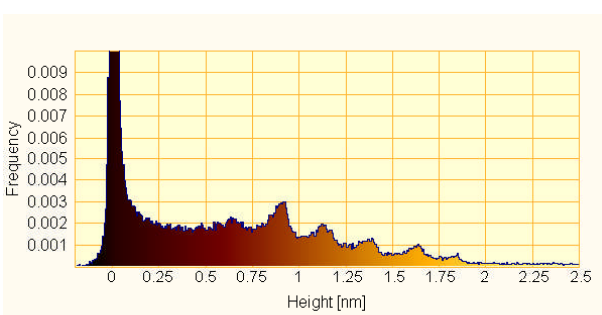


**Fig.2:** Histogram of crystal heights in 100 ×100nm STM image.

$TiO_2$ but with two (110)-like faces on the two ridge slopes. At relatively low initial Ti coverage, each crystallite is largely unaffected by the growth of neighboring crystallites, while at higher coverage oxidation produces crystallites of mostly irregular shapes arising from lateral growth restriction due to the presence of surrounding crystallites.

The plot in Fig. 2 presents the height distribution histogram of an area of Au(111) surface with $TiO_2$ crystallites grown from a typical surface alloy; it shows a large peak at 0nm due to the substrate, followed by a series of peaks on the right at intervals of 0.23nm. These peaks originate from the flat top faces of the crystallites in the STM image. The lowest apparent height of these $TiO_2$ crystallites is 0.6 nm, while the height of a single structural layer is 0.23 nm. From the histogram it follows that the crystallites in the image have up to 5 additional $TiO_2$ layers on a 0.6nm base.

*STS Measurements of Crystallites:*

STS imaging of the surface prepared with 0.7 ML of Ti (Fig. 3) shows that all crystallites have similar electronic structures irrespectively of their heights or shapes. In particular, the shades of green in the STS image in Fig. 3a correspond to the values of dI/dV (V = +2.5 V). Thus, the image shows that all the crystallites yield nearly the same values of dI/dV, in spite of different geometrical parameters. The STS spectra of each of the crystallites show a band gap in the electronic states, which is consistently ~ 3 eV(excluding bandgap tailing); this value corresponds to the known value for bulk rutile. The center of the band gap is shifted towards a negative sample bias, which signifies an n-type semiconductor. Reduced bulk $TiO_2$ is known to be an n-type semiconductor due to the presence of reduced titanium ions that act as electron donors.

A closer scrutiny of the dI/dV spectra of the titania crystallites makes it apparent that both conduction and valence bands have long tails within the band gap. In general

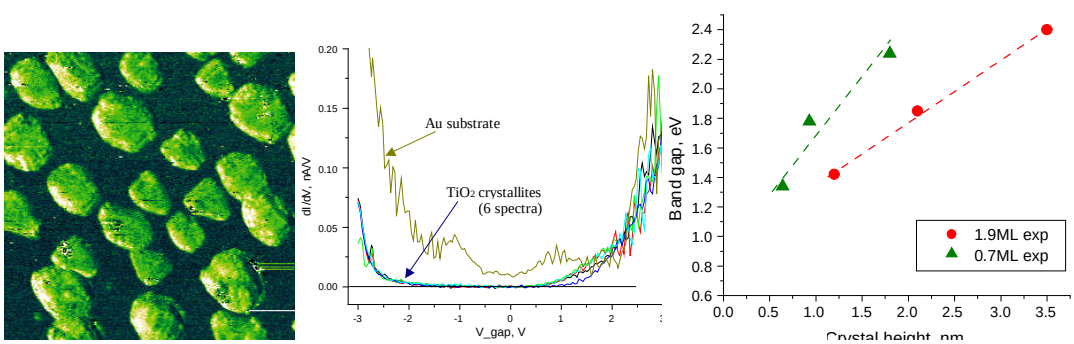


**Fig. 3**: 50 × 50nm (a) STS images of a sample with 900k annealing. (b) STS spectra taken from different areas of the same surface. (c) measured band gap widths as a function of the height of the crystallites.

these values of the "tail-reduced" apparent band gaps were 1.34 - 2.40 eV (see Fig. 3c), significantly lower than the bulk band gap of ~ 3.0 eV. Previously, similar observations were made for STS-derived values of the band gap of $TiO_2$ and $SnO_2$, including comparison to nearly perfect crystals and nanoparticles. The lowered values of the band gap were attributed to defect-induced electronic surface states of the nanoparticles. Figure 3c also indicates that thinner $TiO_2$ crystallites show narrower "effective" band gaps than thicker crystallites. There are several possible explanations for this coupling of effective bandgap to thickness; we are currently analyzing our data to determine which is appropriate for our materials systems.

*Plasmonic Photochemistry and Surface Probing:* In nanophoto-chemistry, surface plasmon polaritons (SPP) have recently attracted much interest, including work in the DOE surface-reaction-dynamics community. Thus the scattering of SPPs on surfaces has been an area of several talks at prior CPIMS meetings. Because of their spatial localization, SPPs are ideal excitations both to study and probe metallic nanostructures and to initiate enhanced photochemical reactions. To this end, we have examined the interaction of plasmon waves with two-dimensional (2D), radially symmetric surface nanodefects. Our analysis presents an additional complexity in the two dimensional case that stems from the more intricate polarization properties of the electromagnetic field that is generated near our earlier studies with 1D metallic nanodefects. Our results clearly show that the properties of the emitted fundamental and second harmonic light are highly sensitive to the material and geometrical characteristics of the metallic surface or interface, through the surface susceptibility $\chi^{(2)}$and surface profile function.

## Future Plans

Our future research efforts are, first, focused on the formation of $TiO_2$ nanoparticles on single-crystal Au(111) surfaces using the very controllable new method of surface alloy oxidation in UHV. Second, we will then investigate thermal reactions and photoreaction dynamics of methyl bromide adsorbed on these $TiO_2$/Au nanoparticle surfaces using TPD and time-of-flight and quadrupole mass spectrometry.

### Recent DOE-Sponsored Publications


1. G. G. Totir, Y. Le and R. M. Osgood, Jr., "Photoinduced-Reaction Dynamics of Halogenated Alkanes on Iron-Oxide Surfaces: $CH_3I$ on $Fe_3O_4$(111)-(2×2)," J. Phys. Chem. B 109, 8452 (2005).
2. Z. Zhu, T. Andelman, M. Yin, T-L. Chen, S.N. Ehrlich, S.P. O'Brien, R.M. Osgood, Jr., "Synchrotron X-ray Scattering of ZnO Nanorods: Periodic Ordering and Lattice Size," J. Mater. Res. 21, 1033 (2005).
3. Z. M. Zhu, T. Chen, Y. Gu, J. Warren and R. M. Osgood, Jr., "Zinc-oxide Nanowires Grown by Vapor-Phase Transport Using Selected Metal Catalysts: A Comparative Study," Chem. Mats. 17, 4227 (2005).
4. Z. Song, J. Hrbek, R.M. Osgood, Jr., "Formation of $TiO_2$ Nanoparticles by Reactive-Layer-Assisted Deposition and Characterization By XPS and STM," Nano. Letts. 5, 1357(2005).
5. G.Y. Le, G.G. Totir, G.W. Flynn, and R.M. Osgood, Jr., "Chloromethane Surface Chemistry on $Fe_3O_4$(111)-(2×2): A Thermal Desorption Spectroscopy Comparison of $CCl_4$, $CBr_2Cl_2$, and $CH_2Cl_2$." Surf. Sci. 600, 665 (2006).
6. N. Camillone III, T.R. Pak, K. Adib, R.M. Osgood, Jr., "Tuning Molecule-Surface Interactions with Sub-Nanometer-Thick Covalently-Bound Organic Monolayers." J. Phys. Chem B 110, 11334 (2006).
7. R.M. Osgood, Jr., "Photoreaction Dynamics of Molecular Adsorbates on Semiconductor and Oxide Surfaces." Chem. Rev. 106, 4379 (2006).
8. L. Cao, N.-C. Panoiu, and R.M. Osgood, Jr., "Surface Second-Harmonic Generation from Surface Plasmon Waves Scattered by Metallic Nanostructures." Phys. Rev. B 75, 205401 (2007)

9. D. Potapenko, J. Hrbek, and R.M. Osgood, Jr., "Scanning Tunneling Microscopy Study of Titanium Oxide Nanocrystals Prepared on Au(111) by Reactive-Layer-Assisted Deposition." ACS Nano 2, 7, 1353 (2008)
10. D. Potapenko, J. Hrbek, and R. M. Osgood, Jr., "Growth of $TiO_2$ Nanoparticles Through Au-Ti surface Alloy Oxidation" (in preparation)
11. T.-L. Chen, M.B. Yilmaz, D. Potapenko, A. Kou, N. Stojilovic, R.M. Osgood, Jr., "Chemisorption of Tert-Butanol on Si(100)." Surf. Sci. (Accepted)

**X-ray Spectroscopy of Volatile Liquids and their Surfaces**

Richard J. Saykally
Department of Chemistry
University of California
Berkeley, CA 94720-1460
saykally@berkeley.edu
and
Chemical Sciences Division
Lawrence Berkeley National Laboratory

## Program Scope or Definition

**The goal of this project is to explore and develop novel methodologies for probing the nature of volatile liquids and solutions and their surfaces, employing combinations of liquid microjet technology with synchrotron X-ray and Raman spectroscopies.**

## Recent Progress

Utilizing the intense monochromatic soft X-Rays available at the LBNL Advanced Light Source (ALS), and employing liquid microjets for convenient temperature and composition control, we have extended our systematic investigation of the local hydration environments of simple inorganic cations and anions to tri- and tetravalent species. Earlier studies have established that monovalent cations have a very small effect on the local water electronic structure, whereas simple anions are strongly perturbative[2]. Moreover, these anions exhibit markedly ion-specific perturbations, while the monovalent cations all produce nearly identical effects, which we attribute to electric field perturbations of the empty water orbitals. Divalent cations[9] exhibit ion-specific perturbations, however, and we attribute these (as well as the ion-specific anion perturbations) to a combination of electric field effects on and charge transfer with the first solvent shell water molecules, as deduced via comparisons with density functional theory calculations. While the analysis of new XAS data for the highly charged ions is still ongoing, these same trends of increasing charge transfer with ion charge are evidenced. We have carried out a similar study of the hydration of the hydroxide ion, finding support for recent predictions of a hyper-coordinated first solvation shell, wherein the ion accepts four H-bonds but donates none[13]. Also, we previously identified a strong blue-shift in the K-edge spectrum of the hydronium ion, relative to that of water, probably due to the tighter electron binding[8].

We have found that Raman spectroscopy of liquid microjets provides a useful complement to our XAS studies. Building on our recent investigation of the temperature-dependent Raman spectrum of water, wherein we (with Phil Geissler) found that a histogram of the electric field projections along the OH bonds computed from a Monte Carlo simulation accurately represents the observed spectra[5], we have proceeded to study ionic solutions by this combined experimental/theoretical approach as a means of characterizing the local environments around aqueous ions. We again find that Geissler's E-field histograms faithfully reproduce the T-dependent Raman spectra, and make it possible to deduce a detailed new molecular picture of how simple ions are solvated in water[15].

Liquid microjet technology affords the opportunity to study the details of water evaporation, free from the obfuscating effects of condensation that have plagued previous studies. Studying small (diameter < 5 μm) jets with Raman thermometry, we find compelling evidence for the existence of a small but significant energetic barrier to evaporation, in contrast to most current models[7,11]. Studies of heavy water indicate a similar evaporation coefficient, and thus an energetic barrier similar to that of normal water[18]. A transition state model developed for this process provides a plausible mechanism for evaporation in which variations in libration and translational frequencies account for the small observed isotope effects[12]. The most important practical result of this work is the quantification of the water evaporation coefficient (0.6), which has been highly controversial, and is a critical parameter in models of climate and cloud dynamics.

Using liquid microjets to avoid the often incapacitating problem of radiation damage to fragile solutes, we have measured the pH-dependent NEXAFS spectra of several amino acids, including glycine, proline, lysine, and the dipeptide diglycine[1,6]. We find evidence that the nitrogen terminus of primary amino acids is sterically shielded at high pH, and exists in an "acceptor-only" state, wherein neither amine proton is involved in hydrogen bonding to the surrounding solvent. The diglycine study characterized a similar behavior in this first investigation of the peptide bond hydration. This work has been extended to examine the hydration of several nucleotide bases and related molecules. We have also exploited the sensitivity of XAS to ionic perturbations of the empty orbitals of carboxylates to support the theoretical prediction that sodium interacts more strongly than potassium with protein carboxylate groups[16], offered as an explanation for the much higher intracellular concentration of sodium existing in cells.

We have recently addressed the long-standing controversy over whether continuum or a multi-component ("intact" or "broken bond," etc.) models best describe the hydrogen bond interactions in liquid water. The temperature dependence of water's Raman spectrum has long been considered to be among the strongest evidence for a multi-component distribution. However, we (with Phil Geissler) have shown, using a combined experimental and theoretical approach, that many of the features of the Raman spectrum considered to be hallmarks of a multi-state system, including the asymmetric band profile, the isosbestic (temperature invariant) point, and van't Hoff behavior, actually result from a continuous distribution[2]. This work complements our study of the structure of pure liquids by X-ray absorption spectroscopy that has been ongoing. We have published a joint theory/experiment study of liquid methanol that characterized the nature of H-bonded domains[3,4].

We have examined the high electrical charging of liquid water microjets that can be effected by metal nozzles, proposing a mechanism based on selective adsorption of hydroxide to the metal surface and subsequent electrokinetic charge separation, and we have demonstrated the use of this "protonic charging" for a novel method of hydrogen generation[14]. Subsequently, we have examined the electrical power generation capabilities of metal nozzle microjets, finding an order of magnitude improvement in efficiency (~10%) over published results[19].

**Future Plans**

1. Complete the XAS study of ionic perturbation of local water structure, such that the entire

Hofmeister series is ultimately addressed. We seek a comprehensive picture of the effects of both cations and anions on the local structure of water. Raman spectroscopy measurements will also be performed on these systems, the data from which provide complementary insights and aid in the theoretical modeling. We will further develop the use of E-field distributions from simulations to interpret the spectra.

2. With LBNL staff scientist David Prendergast, we are testing a new theoretical methodology for predicting core-level spectra of complex molecules (e.g. biomolecules), for which standard approaches often fail dramatically.

3. Extend our XAS studies of local hydration to important free radical species, generated in liquid water microjets by excimer laser photolysis. A new student (Alice England) spent the summer working with the Notre Dame Radiation Lab group to learn techniques for studying free radical chemistry.

4. Extend our studies of amino acid hydration vs. pH to include all natural amino acids. Use the same approach to study hydration of the peptide bonds in small polypeptides, nucleotide bases, nucleosides, and nucleotides, as well as the novel "peptoid" molecules.

5. Measure NEXAFS spectra for pure liquid water, alcohols, and hydrocarbons, seeking to achieve deep supercooling via controlled evaporation. In conjunction with theoretical modeling, we will seek a coherent description of the liquid structure and bonding in these systems.

6. We will continue to explore and compare ion and electron detection of NEXAFS spectra, seeking to obtain a reliable means for characterizing liquid surfaces. Thus far, we have not been able to reproduce the original measurements of the water surface with our newly-designed X-ray spectrometer, and we have shown that the original calculations on which the interpretation of those spectra in terms of "acceptor only" molecules was based were flawed[16].

7. We plan to continue our exploration of the evaporation of liquid water by Raman thermometry and mass spectrometry, seeking to ascertain the effects of salts and surfactants on the evaporation process.

**References (DOE supported papers 2005-present) – 19 total**

[available at http://www.cchem.berkeley.edu/rjsgrp/opening/pubs.htm]

1. B.M. Messer, C.D. Cappa, J.D. Smith, K.R. Wilson, M.K. Gilles, R.C. Cohen, and R.J. Saykally, "pH Dependence of the Electronic Structure of Glycine," *J. Phys. Chem. B* **109**, 5375-5382 (2005). LBNL-56348 **Cover Article.*

2. C.D. Cappa, J.D. Smith, K.R. Wilson, B.M. Messer, M.K. Gilles, R.C. Cohen, and R.J. Saykally, "Effects of Alkali Metal Halide Salts on the Hydrogen Bond Network of Liquid Water,"*J. Phys. Chem. B* **109**, 7046-7052 (2005). LBNL-56812 **Cover Article.*

3. J.D. Smith, C.D. Cappa, B.M. Messer, R.C. Cohen and R.J. Saykally, Response to Comment on "Energetics of Hydrogen Bond Network Rearrangements in Liquid Water,"*Science* **308**, 793b (2005). LBNL-57117

4. K.R. Wilson, M. Cavalleri, B.S. Rude, R.D. Schaller, T. Catalano, A. Nilsson, L.G.M.

Pettersson, and R.J. Saykally, "X-ray Absorption Spectroscopy of Liquid Methanol Microjets: Bulk Electronic Structure and Hydrogen Bonding Network," *J. Phys. Chem. B* **109**, 10194-10203 (2005). LBNL-56350 **Cover Article.*
5. J.D. Smith, C.D. Cappa, K.R. Wilson, R.C. Cohen, P.L. Geissler, and R.J. Saykally, "Unified description of temperature-dependent hydrogen-bond rearrangements in liquid water," *PNAS* **102**, 14171-14174 (2005). LBNL-58789
6. B.M. Messer, C.D. Cappa, J.D. Smith, W.S. Drisdell, C.P. Schwartz, R.C. Cohen, R.J. Saykally, "Local Hydration Environments of Amino Acids and Dipeptides Studied by X-ray Spectroscopy of Liquid Microjets," *J. Phys. Chem. B* **109**, 21640-21646 (2005). LBNL-59184
7. C.D. Cappa, W. Drisdell, J.D. Smith, R.J. Saykally, and R.C. Cohen, "Isotope Fractionation of Water During Evaporation Without Condensation," *J. Phys. Chem. B* **109**, 24391-24400 (2005). LBNL-59505
8. C.D. Cappa, J.D. Smith, B.M. Messer, R.C. Cohen, and R.J. Saykally, "The Electronic Structure of the Hydrated Proton: A Comparative X-ray Absorption Study of Aqueous HCl and NaCl Solutions," *J. Phys. Chem. B* **110**, 1166-1171 (2006). LBNL-59504
9. C.D. Cappa, J.D. Smith, B.M. Messer, R.C. Cohen, and R.J. Saykally, "Effects of Cations on the Hydrogen Bond Network of Liquid Water: New Results from X-ray Absorption Spectroscopy of Liquid Microjets," *J. Phys. Chem. B* **110**, 5301-5309 (2006). LBNL-59955
10. J.D. Smith, C.D. Cappa, B.M. Messer, W.S. Drisdell, R.C. Cohen, and R.J. Saykally, "Probing the Local Structure of Liquid Water by X-ray Absorption Spectroscopy," *J. Phys. Chem. B* **110**, 20038-20045 (2006). LBNL-61736
11. J.D. Smith, C.D. Cappa, W.S. Drisdell, R.C. Cohen, and R.J. Saykally, "Raman Thermometry Measurements of Free Evaporation from Liquid Water Droplets," *JACS* **128**, 12892-12898 (2006). LBNL-61735
12. C.D. Cappa, J.D. Smith, W.S. Drisdell, R.J. Saykally, and R.C. Cohen, "Interpreting the H/D Isotope Fractionation of Liquid Water During Evaporation Without Condensation," *J. Phys. Chem. C* **111**, 7011-7020 (2007). LBNL-62751
13. C.D. Cappa, J.D. Smith, B.M. Messer, R.C. Cohen, and R.J. Saykally, "Nature of the Aqueous Hydroxide Ion Probed by X-ray Absorption Spectroscopy," *J. Phys. Chem. A* **111**, 4776-4785 (2007). LBNL-62752 **Cover Article.*
14. A.M. Duffin and R.J. Saykally, "Electrokinetic Hydrogen Generation from Liquid Water Microjets," *J. Phys. Chem. C* **111**, 12031-12037 (2007). LBNL-63475
15. J.D. Smith, R.J. Saykally, and P.L. Geissler, "The Effects of Dissolved Halide Anions on Hydrogen Bonding in Liquid Water," *J. Am. Chem. Soc.* **129**, 13847-13856 (2007). LBNL-63579
16. C.D. Cappa, J.D. Smith, K.R. Wilson, and R.J. Saykally, "Revisiting the total ion yield x-ray absorption spectra of liquid water microjets," *J. Phys.: Condens. Matter* **20**, 205105 (2008). LBNL-189E
17. J.S. Uejio, C.P. Schwartz, A.M. Duffin, W.S. Drisdell, R.C. Cohen, and R.J. Saykally, "Characterization of selective binding of alkali cations with carboxylate by x-ray absorption spectroscopy of liquid microjets," *PNAS* **105**, 6809-6812 (2008). LBNL-894E
18. W.S. Drisdell, C.D. Cappa, J.D. Smith, R.J. Saykally, and R.C. Cohen, "Determination of the Evaporation Coefficient of $D_2O$," *Atmos. Chem. Phys. Discuss.* **8**, 8565-8583 (2008). LBNL-TBA
19. A.M. Duffin and R.J. Saykally, "Electrokinetic Power Generation from Liquid Water Microjets," *J. Phys. Chem. C* (accepted 8/28/2008). LBNL-TBA

**Molecular Theory & Modeling**

*Development of Statistical Mechanical Techniques for Complex Condensed-Phase Systems*

Gregory K. Schenter
Chemical & Materials Sciences Division
Pacific Northwest National Laboratory
902 Battelle Blvd.
Mail Stop K1-83
Richland, WA 99352
greg.schenter@pnl.gov

The long-term objective of this project is to advance the understanding of the relation between detailed descriptions of molecular interactions and the prediction and characterization of macroscopic collective properties. To do this, we seek to better understand the relation between the form and representation of intermolecular interaction potentials and simulation techniques required for statistical mechanical determination of properties of interest. Molecular simulation has the promise to provide insight and predictive capability of complex physical and chemical processes in condensed phases and interfaces. For example, the transport and reactivity of species in aqueous solutions, at designed surfaces, in clusters and in nanostructured materials play significant roles in a wide variety of problems important to the Department of Energy.

We start from the premise that a detailed understanding of the intermolecular interactions of a small collection of molecules, through appropriate modeling and statistical analysis, will enable us to understand the collective behavior and response of a macroscopic system, thus allowing us to predict and characterize thermodynamic, kinetic, material, and electrical properties. Our goal is to improve understanding at the molecular level in order to address increasingly more complex systems ranging from homogeneous bulk systems to multiple phase or inhomogeneous ones, to systems with external constraints or forces. Accomplishing this goal requires understanding and characterization of the limitations and uncertainties in the results, thereby improving confidence in the ability to predict behavior as systems become more complex.

In developing representations of molecular interaction it is necessary to understand the balance between efficiency and accuracy. The evaluation of intermolecular potential energy needs to be efficient enough to allow for effective statistical mechanical and dynamical sampling. At the same time, enough of the underlying physical chemistry and sufficient parameterization needs to be contained in the models of molecular interaction so that the resulting simulation of collective molecular properties are reliable. Towards these ends, we have been exploring techniques that are based on efficient electronic structure methods such as NDDO semiempirical theory and density functional theory (DFT). These methods have the advantage that they are atom based, allowing for bond breaking and chemically reactive processes. Furthermore, the electronic structure response of atomic sites can adapt to a variety of chemical environments, leading to a more robust parameterization and transferability to different systems. A disadvantage of such electronic structure methods is their limited polarization response and their ability to describe hydrogen bonding and dispersion interactions. Recently we have successfully developed a Self Consistent Polarization (SCP) method [Ref. 21] that enhances the polarization response of an efficient electronic structure method while providing a consistent representation of the dispersive interaction that is based on second-order perturbation theory. The

first application of this method resulted in the effective parameterization of the interaction of water clusters, based on NDDO semiempirical electronic structure theory. We are able to reproduce the accurate MP2/CBS estimates of small water cluster binding energies of Xantheas *et al*, as well as the intramolecular frequency shifts as a function of cluster size. (See Figure 1.)

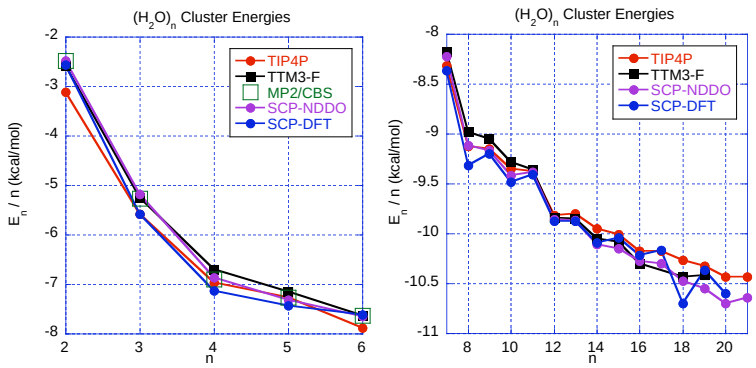


**Figure 1:** Water cluster energies, $E_n$, as a function of size, n.

One limitation of the NDDO based approach was the degree of parameterization that was required in developing an accurate model. Future work will be dedicated to better understand the process of parameterization and the transferability of parameters. Initial studies that are based on DFT electronic structure (SCP-DFT) have revealed a theory that requires significantly less parameterization. A new feature of the theory is the importance of properly accounting for basis set superposition (BSSE) and incompleteness error. To account for this we have explored two approaches. First we developed an effective two-body correction term that accounts for basis set effects. Second, we have employed Molecularly Optimized (MOLOPT) basis sets developed by VandeVondele and Hutter, that give small BSSE, are well conditioned, and recover results that are close to the complete basis set limit.[a] We have preliminary results for water clusters and bulk water properties that are encouraging. Binding energies as a function of cluster size is shown in Figure 1. These are consistent with MP2 electronic structure, TIP4P, and TTM3-F empirical potential results. In Figure 2 we demonstrate how the SCP-DFT theory recovers the vibrational red shift as a function of cluster size, the hydrogen bonding "vibrational fingerprint". Harmonic frequency density of states (convoluted with a 10 $cm^{-1}$ Gaussian width) computed using SCP-DFT theory is compared to MP2 /aug-cc-pVDZ calculations as function of cluster size. In Figure 3 we display the O-O radial distribution function corresponding to the simulation of the liquid state. DFT calculations were performed using a BLYP functional and a TZV2P-MOLPT basis set.

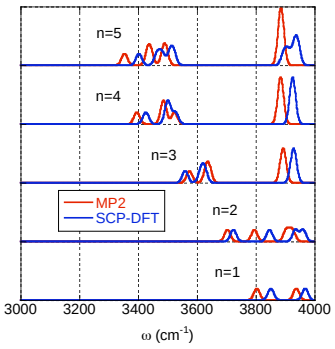


**Figure 2:** Harmonic frequency distribution as a function of cluster size.

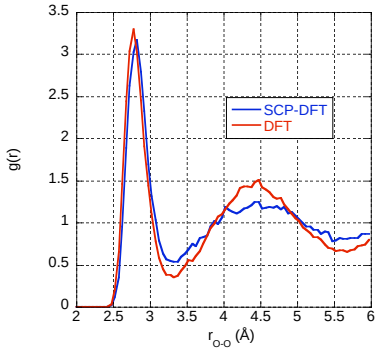


**Figure 3:** Simulated O-O radial distribution function.

We have also tested our SCP-DFT approach on the dispersion-dominated system of the gas, liquid and solid phases of Argon. The SCP-DFT approach has been implemented in the

molecular simulation package, CP2K.[b] Future plans will include expanding the numerical efficiency of the approach by improving preconditioning of the combined SCP and orbital optimization procedure. We will also explore the implementation of screening functions that partition the SCP component from the conventional electronic structure, leading to a more flexible and robust method. Current implementations of the SCP-NDDO method are limited to a cluster based code and an inefficient periodic code. Future work will concentrate on implementation of the SCP-NDDO method within the CP2K code.

With efficient implementations of our SCP approach, we plan to explore complex solvation in more complex environments. Initial steps have been made to parameterize protonated and hydroxide water clusters. Future efforts will extend the parameterization to aqueous solvation of more complex ions. In conjunction with these efforts we will continue our analysis of EXAFS measurements as a probe of solvation structure. [See Refs. 3, 9, and 19] From our representation of molecular interaction we will generate ensembles of configurations. From this ensemble, a series of electron multiple scattering calculations are performed using the FEFF8 code[c] to generate a configuration averaged EXAFS spectra. In future studies we will consider the influence of molecular interaction between ion-pairs. Our challenge is to be able to account for changes in features in EXAFS measurement as a function of solute concentration. In an additional extension of our bulk EXAFS analysis, we will attempt to understand the influence of an interface on the observed ion solvation structure and how it manifests itself in an EXAFS measurement.

*Acknowledgements*: Direct collaborators on this project include C.J. Mundy and G. Murdachaew. Interactions with B. C. Garrett, S. S. Xantheas, L. X. Dang and S. M. Kathmann have significantly influenced the course of this work. This research was performed in part using the computational resources in the National Energy Research Supercomputing Center (NERSC) at Lawrence Livermore National Laboratory. Battelle operates Pacific Northwest National Laboratory for the US Department of Energy.

**References**

a. J. VandeVondele and J. Hutter, J. Chem. Phys. **127**, 114105 (2007).
b. The CP2K developers group, http://cp2k.berlios.de/ (2008) J. VandeVondele, M. Krack, F. Mohamed, M. Parrinello, T. Chassaing and J. Hutter, Comp. Phys. Comm. **167**, 103 (2005).
c. J.J. Rehr, R. C.Albers, S.I. Zabinsky, Phys. Rev. Lett. **69**, 3397 (1992); M. Newville, B. Ravel, D. Haskel, J. J. Rehr, E. A. Stern, and Y. Yacoby, Physica B, **208-209**, 154 (1995); A. L. Ankudinov, C. Bouldin, J. J. Rehr, H. Sims, and H. Hung, Phys Rev. B **65**, 104107 (2002).

**References to publications of DOE sponsored research (2005-present)**

1. S. M. Kathmann, G. K. Schenter, and B. C. Garrett, "Ion-Induced Nucleation: The Importance of Chemistry," Phys. Rev. Lett. **94**, 116104 (2005).
2. B. C. Garrett, D. A. Dixon, et al "The Role of Water on Electron-Initiated Processes and Radical Chemistry: Issues and Scientific Advances," Chem. Rev. **105**, 355 (2005).
3. V. -A. Glezakou, Y. C. Chen, J. L. Fulton, G. K. Schenter and L. X. Dang "Electronic Structure, Statistical Mechanical Simulations, and EXAFS Spectroscopy of Aqueous Potassium" Theoret. Chem. Acc. **115**, 86 (2006).
4. T. D. Iordanov, G. K. Schenter, and B. C. Garrett, "Sensitivity Analysis of Thermodynamics Properties of Liquid Water: A General Approach to Improve Empirical Potentials," J. Phys. Chem. A **110**, 762 (2006).

5. C. D. Wick and G. K. Schenter, “Critical Comparison of Classical and Quantum Mechanical Treatments of the Phase Equilibria of Water,” J. Chem. Phys. **124**, 114505 (2006).
6. B. C. Garrett, G. K. Schenter, and A. Morita, “Molecular Simulations of the Transport of Molecules across the Liquid/Vapor Interface of Water,” Chem. Rev. **106**, 1355 (2006).
7. S. Du, J. S. Francisco, G. K. Schenter, T. D. Iordanov, B. C. Garrett, M. Dupuis, and J. Li, “The OH radical – $H_2O$ molecular interaction potential,” J. Chem. Phys. **124**, 224318 (2006).
8. G. S. Fanourgakis, G. K. Schenter, and S. S. Xantheas, “A Quantitative Account of Quantum Effects in Liquid Water,” J. Chem. Phys. **125**, 141102 (2006).
9. L. X. Dang, G. K. Schenter, V. A. Glezakou and J. L. Fulton, "Molecular simulation analysis and X-ray absorption measurement of $Ca^{2+}$, $K^+$ and $Cl^-$ ions in solution," J. Phys. Chem. B **110**, 23644 (2006).
10. S. M. Kathmann, G. K. Schenter and B. C. Garrett, "Comment on "Quantum nature of the sign preference in ion-induced nucleation"," Phys. Rev. Lett. **98**, 109603 (2007).
11. S. Kathmann, G. Schenter and B. Garrett, "The critical role of anharmonicity in aqueous ionic clusters relevant to nucleation," J. Phys. Chem. C **111**, 4977 (2007).
12. S. Y. Du, J. S. Francisco, G. K. Schenter and B. C. Garrett, "Ab initio and analytical intermolecular potential for ClO-$H_2O$," J. Chem. Phys. **126**, 114304 (2007).
13. M. Valiev, B. C. Garrett, M.-K. Tsai, K. Kowalski, S. M. Kathmann, G. K. Schenter, and M. Dupuis, “Hybrid approach for free energy calculations with high-level methods: Application to the $S_N2$ reaction of $CHCl_3$ and $OH^-$ in water,” J. Chem. Phys. **127**, 051102 (2007).
14. C. J. Mundy, S. M. Kathmann, G. K. Schenter, “Strange Brew,” Natural History **116**, 32 (2007).
15. S. Du, J. S. Francisco, G. K. Schenter, and B. C. Garrett, "Many-Body Decomposition of the Binding Energies for OH $(H_2O)_2$ and OH $(H_2O)_3$ Complexes," J. Chem. Phys. **128**, 084307 (2008).
16. S. M. Kathmann, B. J. Palmer, G. K. Schenter, and B. C. Garrett, "Activation Energies and Potentials of Mean Force for Water Cluster Evaporation," J. Chem. Phys. **128**, 064306 (2008).
17. S. Eustis, D. Radisic, K. Bowen, R. A. Bachorz, M. Haranczyk, G. K. Schenter and M. Gutowski “Electron-Driven Acid-Base Chemistry: Proton Transfer from Hydrochloric Acid to Ammonia Studied by Anion Photoelectron Spectroscopy and Ab Initio Theory,” Science **319**, 936 (2008).
18. S. M. Kathmann, G. K. Schenter and S. S. Xantheas, “On the Determination of Monomer Dissociation Energies of Small Water Clusters from Photoionization Experiments,” J. Phys. Chem. A **112**, 1851 (2008).
19. P. Nichols, E. J. Bylaska, G. K. Schenter, and W. de Jong, "Equatorial and Apical Solvent Shells of the $UO_2^{2+}$ Ion," J. Chem. Phys. **128**, 124507 (2008).
20. S. M. Kathmann, G. K. Schenter, and B. C. Garrett, "The Impact of Molecular Interactions on Atmospheric Aerosol Radiative Forcing," Advances in Quantum Chemistry: Applications of Theoretical Methods to Atmospheric Sciences, **55**, 429 (2008).
21. D. T. Chang, G. K. Schenter, and B. C. Garrett, “Self-consistent polarization-neglect of diatomic differential overlap: Application to water clusters,” J. Chem. Phys. **128**, 164111 (2008).
22. H. Wang, R. C. Bell, J. P. Cowin, G. K. Schenter, and M. J. Iedema, "The Pyroelectricity of Water Ice," J. Phys. Chem. B **112**, 6379 (2008).
23. C. J. Mundy, R. Rousseau, A. Curioni, S. M. Kathmann, and G. K. Schenter, “A molecular approach to understanding complex systems: computational statistical mechanics using state-of-the-art algorithms on tera-scale computational platforms,” Journal of Physics Conference Series **125**, 012014 (2008).

# Generation, Detection and Characterization of Gas-Phase Transition Metal Containing Molecules

Timothy C. Steimle
Department of Chemistry and Biochemistry
Arizona State University
Tempe, Arizona 85287-1604
E-mail: tsteimle@asu.edu

## I. Program Scope

The objective of this experimental project is to produce simple transient, metal containing, molecules and extract from the analysis of their spectra geometric structure, force constants, permanent electric dipole moments, $\mu_{el}$, and magnetic dipole moments, $\mu_m$. This highly quantitative data is used to construct qualitative, molecular-orbital based, bonding models and to evaluate the quantitative predictability of electronic structure calculations performed by others. The synergism between experiments and theory that is established for these simple molecular systems will guide computational predictions, particularly those based on density functional theory methodologies, for more extended systems (e.g. clusters, nanoparticles and surfaces). The contributions to bonding from electron correlation, relativistic effects and structure are de-convoluted by selecting a variety of related molecules. Studies of 3*d* metal dioxides, such as $TiO_2$, are being performed to provide benchmark data and elucidate the catalytic activity of supported metal dioxide clusters. Simple PtX, RhX and IrX (X=OH, NH, CH, H, S, O, F and N) molecules are used to investigate trends in later 4*d* and 5*d* bonding. Lanthanide and actinide oxides are used for investigations of the role of *f*-orbitals, relativistic effects and methodologies for treating such effects.

Two classes of gas-phase spectroscopic studies are implemented: a) visible and near infrared electronic spectroscopy using laser induced fluorescence (LIF) detection, b) mid-infrared vibrational spectroscopy in the fundamental OH, CH and NH stretching region (2.8μm-3.6μm). Small magnetic (Zeeman) and electric (Stark) field induced shifts in the spectra are analyzed to produce experimental values for $\mu_m$ and $\mu_{el}$, respectively. Molecular beams of the transition metal containing radical molecules are produced using either a pulsed laser ablated/reagent supersonic expanding gas or a pulsed d.c. discharge. The molecules are produced with an internal temperature of typically 10 K to minimize spectral congestion and recorded at near the natural line width limit (typically 30 MHz) to maximize the information content.

## II. Recent Progress

### A. Generation and Characterization of Gas-Phase $TiO_2$

Among the more important of the numerous technological applications of titanium dioxide is its use as a photocatalyst to degrade organic pollutants or to perform other useful chemical transformations. Nanomeric and subnanomeric clusters of $TiO_2$ prepared on, or incorporated in, zeolites are particularly promising photocatalysts. Studies of gas-phase clusters of $TiO_2$ provide a practical experimental and theoretical means of gaining a molecular level understanding of the properties that influence the photocatalytic activity of zeolite supported $TiO_2$ clusters. This data may also be applicable to even large systems. Indeed, there is experimental evidence that the properties of small gas-phase clusters of $TiO_2$ emulate those of the bulk. For example, the observed band gap of molecular $(TiO_2)_n$ clusters approach that of bulk $TiO_2$ at $n$ = 6 and remains relatively constant up to $n$=10, the largest clusters studied [Zhai, H. J.; Wang, L.S.; *J. Am. Chem. Soc.* **2007**, 129, 3022]. Furthermore, clusters of mixtures of $(TiO_2)_n$ and $(Ti_2O_3)_m$ are observed to have an intense vibrational transition at 13.5 μm, which coincides with an intense rutile spectral feature, independently of their size and stoichiometry [Demyk, K. et al *A& A.* **2004**, 420, 547].

The most quantitative information can be derived for the isolated $TiO_2$ monomer. A comparison of theoretically predicted and experimentally derived properties for the monomer is the primary means of assessing methodologies being implemented for predicting the properties of clusters of $TiO_2$. Theoretical predictions for this prototypical metal dioxide should be highly quantitative because of the limited number of valence electrons (eight) and the small relativistic

effects owing to the low atomic number. A goal of the present study is to experimentally determine the permanent electric dipole moments, vibrational frequencies, and geometric structure for the ground and low-lying states of molecular $TiO_2$ using optical spectroscopy.

Gas phase spectroscopic studies of $TiO_2$ are very few in number. Forty years ago the Harvard group performed an electrostatic deflection measurement on a molecular beam sample of $TiO_2$ demonstrating that the ground state had a permanent electric dipole, thus ruling out a linear O=Ti=O structure. The electronic structure of $TiO_2$, and small clusters thereof, was investigated by photoelectron spectroscopy [Wu, H.; Wang, L.S.; *J. Chem. Phys.* **1997**, 107, 8221.]. Recently, the pure rotational transition in the (0,0,0) $\tilde{X}^1A_1$ vibronic state were recorded and analyzed to produce the first experimental structure with the determined effective bond length of $R_{Ti\text{-}O}$ = 1.651 Å, angle $\theta$ =111.57° [Brünken, et al; *Ap. J.* **2008**, 676, 1367].

A laser ablation/supersonic expansion scheme was used for the generation of molecular $TiO_2$. A portion of the near natural line width limit laser induced fluorescence spectrum in the region of the origin of the $\tilde{A}^1B_2 \leftarrow \tilde{X}^1A_1$(0,0,0) transition is presented in Figure 1. The spectrum is complicated because $TiO_2$ assumes a bent oxo (O=Ti=O) form in both the $\tilde{A}^1B_2$ and $\tilde{X}^1A_1$ states and has a rotational structure of a near prolate asymmetric top. The spectrum was analyzed to produce rotational parameters for the $\tilde{A}^1B_2$ state from which the bond angle and length were determined to be $\theta$=100.14° and 1.704 Å, respectively.

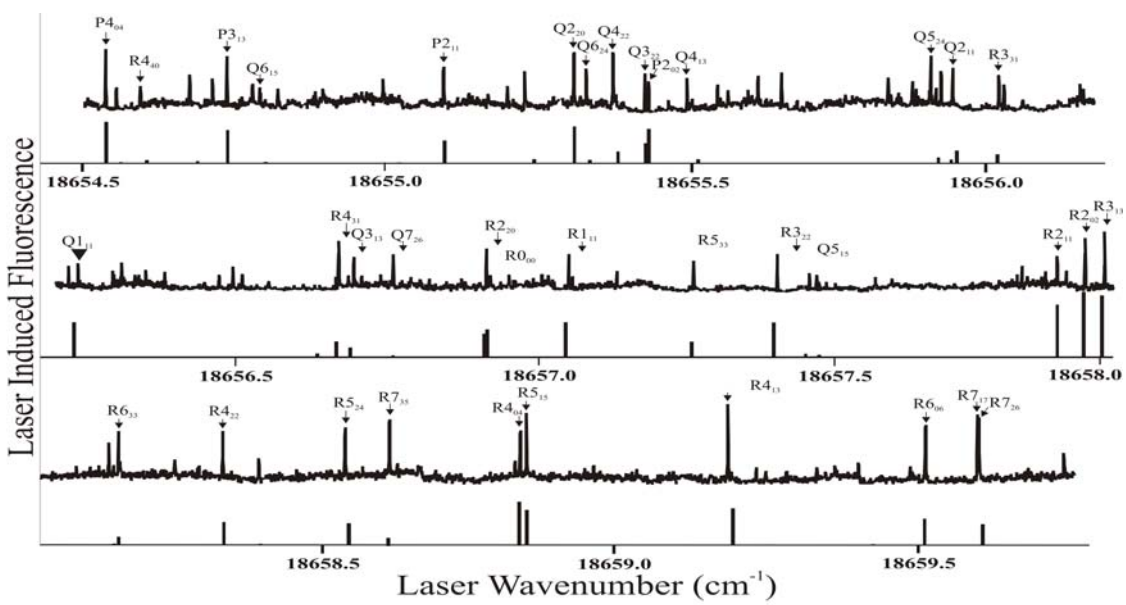


**Figure 1**. The observed and calculated laser induced fluorescence spectrum in the region of the origin of the $\tilde{A}^1B_2$ (0,0,0)$\leftarrow \tilde{X}^1A_1$(0,0,0) band of $TiO_2$. "#" → dispersed fluorescence "*"→ optical Stark.

The dispersed fluorescence (Figure 2) revealed a progression in the $\nu_2$ ($a_1$) symmetric stretch. Analysis resulted in the first determination of $\omega_2$ (= 322±7 $cm^{-1}$) for the $\tilde{X}^1A_1$(0,0,0) state.. Theoretical predictions for $\omega_2$ vary from 393 $cm^{-1}$[Chertihin, G.V.; Andrews, L. *J. Phys. Chem.* **1995**, 97, 6356] to 318 $cm^{-1}$ [Kim; K. H. et al Moon, *J. Chem. Phys.* **2002**, 117, 8385] with most high level DFT calculations giving approximately 340 $cm^{-1}$. There is no evidence of other low-lying electronic states.

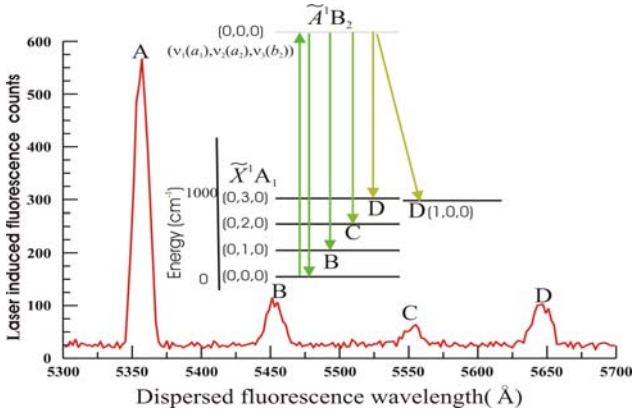


**Figure 2**. The dispersed fluorescence of $TiO_2$ resulting from exciting the $\tilde{A}^1B_2(0,0,0)5_{14} \leftarrow \tilde{X}^1A_1(0,0,0)\ 4_{13}$ line at 18659.2311cm$^{-1}$. The progression in the $\nu_2$ ($a_1$) symmetric stretch produced a harmonic vibrational frequency, $\omega_2$ ,=322±7 cm$^{-1}$.

The optical Stark spectra (Figure 3) were recorded and analyzed to produce the permanent electric dipole moment, $\mu_{el}$, of 6.28 ± 0.06 D and 2.58± 0.07D for the $\tilde{X}^1A_1(0,0,0)$ and $\tilde{A}^1B_2$ (0,0,0) states, respectively. The large value of $\mu_{el}$ for the $\tilde{X}^1A_1$ state

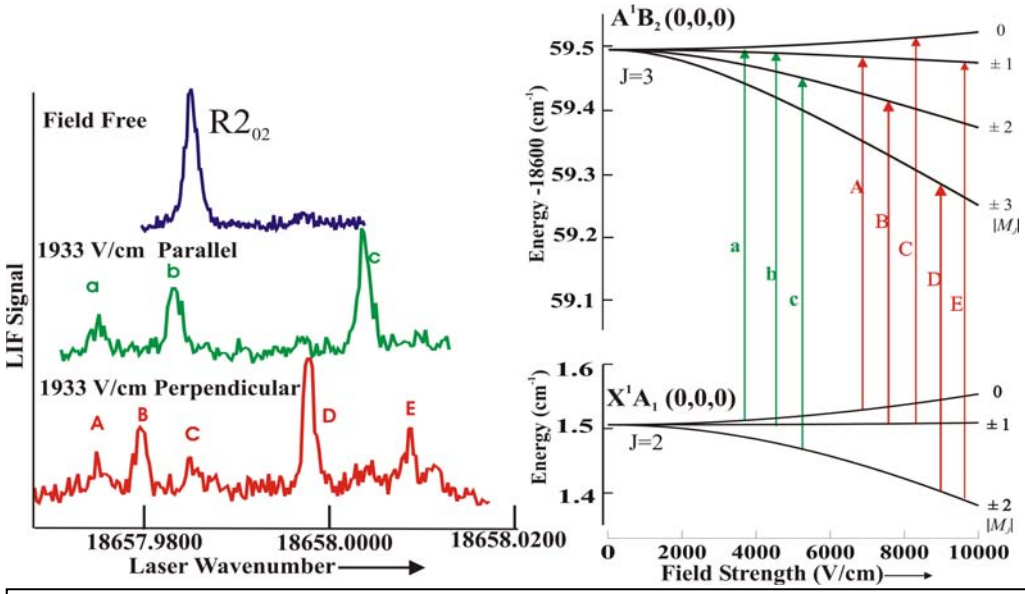


**Figure 3**. The optical Stark $TiO_2$ spectra and energy levels for the $\tilde{A}^1B_2 \leftarrow \tilde{X}^1A_1$ ($3_{03}$-$2_{02}$) line.

is the first experimental evidence that this state results from coupling between $Ti^{2+}(4s^0 3d^2)$ and $O_2^{2-}(\pi^{*4})$ having a dominant $1a_2^2 3b_1^2 9a_1^2 6b_2^2$ configuration. A simple molecular orbital correlation diagram predicts that the $6b_2$ orbital is a O-O $\pi$-antibonding orbital. The large reduction in $\mu_{el}$ upon excitation is evidence that the excited state has a dominant $1a_2^2 3b_1^2 9a_1^2 6b_2^1 10a_1^1$ configuration where the $10a_1$ orbital is essentially a $Ti^+$ centered 4*s*.

**B. Lanthanide Monoxides: CeO, PrO and NdO(Publ. # 8)**

We reported, in collaboration with the Emory group, on the Stark and Zeeman effects of uranium monoxide (UO) [M. C. Heaven, et al, *J. Chem Phys*. **125** 204314 (2006)]. Experiments involving the actinides are particularly challenging and significant insight into their chemistry may be derived from the study of the isovalent lanthanides. For example, the $\mu_{el}$ value for the ground state of UO was measured as 3.363(26) D and it was argued in our publication that this should be nearly identical to that of isovalent NdO. The electric dipole moment of NdO had not been measured at that time, but was estimated to be 3.31 D based on an empirical plot of previously

measured dipole moments of other lanthanide monoxides The agreement between this estimated value for NdO and the measured value for UO supported the premise that studies of the lanthanides provide quantitative insight into the actinides. In order to substantiate this premise, we have recently measured $\mu_{el}$ for the [16.7]3(=3.742 (16)D) and $X4$ (=3.369(13)D) states of NdO (Publ. #8). The experimental result for the ground state is in very close to our empirical estimate. We also have preliminary results for the [18.07]5.5 (=2.813±0.3 D) and [0.2]4.5(=2.813±0.3 D) states of PrO and CeO (not yet analyzed). Magnetic dipole moments for these molecules were also determined from the analysis of the optical Zeeman effect. Interestingly, all theoretical predicted $\mu_{el}(X4)$ values for NdO are significantly larger than our experimentally determined value indicating that the current computational methodologies do not adequately account for the polarization of the metal centered non-bonding electrons. A plot of the experimentally derived ground state values $\mu_{el}$ for the lanthanide monoxides reveals a smooth trend across the series. Interestingly, the plot of $\mu_{el}$ does not exhibit discontinuities at LaO EuO and YbO where the $M^{2+}$ $6s^2$ and the $f^7$ and $f^{14}$ should have more of an influence than the $M^{2+} f^n s$ configuration.

**III. Future Plans**

**A. Near uv ultrahigh resolution LIF of metal systems**

Many of the late transition metal (Rh, Pt, and Ir) containing radicals of interest have intense electronic transitions in the near uv (370-460 nm) spectral region where we previously did not have tunable monochromatic radiation sources. We recently purchased an external cavity doubler to be used with our cw-dye and Ti:Sapphire lasers that will extend our wavelength coverage down to 420 nm. Attempts to detect near uv electronic transitions associated with the bent-to-linear conformer in $TiO_2$ will be made.

**B. Improving the sensitivity of the Mid-IR spectrometer**

Although we have successfully detected OH and CH radicals generated in supersonic pulsed d.c. discharge, we have not been able to detect metal monohydroxides (e.g. CaOH) or methlyadines (e.g. WCH) generated using our supersonic pulsed laser ablation source. Evidentially, the total amount of metal containing radicals produced in the ablation pulse is too small. We are currently replacing the ablation source with a pulsed d.c. discharge capable of using metal-organic precursors. Initial studies will use optical transient frequency modulation spectroscopy.

**Publications of DOE sponsored research - 2005-present:**


1. "The permanent electric dipole moment and hyperfine interaction in Ruthenium Monoflouride, RuF." T. C. Steimle, W. L. Virgo and T. Ma, J. Chem. Phys. **124**, 024309-7 (2006).
2. "High Resolution Laser Induced Fluorescence Spectroscopy of the [18.8] $^3\Phi_i - X\ ^3\Phi_i$ (0,0) Band of Cobalt Monofluoride" T.C. Steimle, T.Ma, A.G. Adam, W. D. Hamilton and A. J. Merer, J. Chem. Phys. **125,** 6 064302-1-064302-9 (2006).
3. "The permanent electric dipole moment and magnetic *g*-factors of uranium monoxide, UO" Michael. C. Heaven, Vasiliy Goncharon, Timothy C. Steimle, Tongmei Ma, Colan Linton J. Chem Phys. **125** 204314/1-20431/11 (2006).
4. "A Molecular Beam Optical Stark Study of the [15.8] and [16.0] $^2\Pi_{1/2} - X^2\Sigma^+$ (0,0) Band Systems of Rhodium Monoxide, RhO." Jamie Gengler, Tongmei M, Allan G. Adam, and Timothy C. Steimle, J. Chem. Phys.**126** 134304-11 (2007).
5. "A Molecular Beam Optical Stark Study of Rhodium Mononitride, RhN" Tongmei Ma, Jamie Gengler, Zhong Wang, Hailing Wang and T.C. Steimle, J. Chem. Phys. J.Chem. Phys. J. Chem. Phys. **126** 244312-8 (2007).
6. "A Molecular Beam Optical Stark Study of the [18.1]$^2\Pi_{1/2}$-$X^4\Sigma^-_{1/2}$, RhS" Tongmei Ma, Hailing Wang and T.C. Steimle, J. Chem. Phys. **127**, 124311-1/6 (2007).
7. "Optical Stark spectroscopy of molybdenum carbide, MoC" Wilton L. Virgo and Timothy C. Steimle, J. Chem. Phys. J. Chem. Phys. **127** 124302-1/6 (2007).
8. "The permanent electric dipole moment and magnetic $g_e$-factors of neodymium monoxide (NdO)" Colin Linton, Tonmei Ma, Hailing Wang and Timothy C. Steimle J.Chem. Phys. (accepted August 2008).

# Understanding Nanoscale Confinement Effects in Solvent-Driven Chemical Reactions

Ward H. Thompson
*Department of Chemistry, University of Kansas, Lawrence, KS 66045*
Email: *wthompson@ku.edu*

## Program Scope

It is now possible to synthesize nanostructured porous materials with a tremendous variety of properties including sol-gels, zeolites, organic and inorganic supramolecular assemblies, reverse micelles, vesicles, and even proteins. The interest in these materials derives from their potential for carrying out useful chemistry (*e.g.*, as microporous and mesoporous catalysts with critical specificity, fuel cell electrodes and membranes, molecular sieves, and chemical sensors) and for understanding the chemistry in similar systems found in nature. Despite the advances in synthetic techniques, our understanding of chemistry in solvents confined in nanoscale cavities and pores is still relatively limited. Ultimately, one would like to design nanostructured materials adapted for specific chemical purposes, *e.g.*, catalysis or sensing, by controlling the cavity/pore size, geometry, and surface chemistry. To develop guidelines for this design, we must first understand how the characteristics of the confining framework affect the chemistry. Thus, the overarching question addressed by our work is *How does a chemical reaction occur differently in a nano-confined solvent than in a bulk solvent?*

Solvent-driven reactions, typically those involving charge transfer, should be most affected by confinement of the solvent. The limited number of solvent molecules, geometric constraints of the nanoscale confinement, and solvent-wall interactions can have dramatic effects on both the reaction energetics and dynamics. Our primary focus is thus on proton transfer, time-dependent fluorescence, and other processes strongly influenced by the solvent. A fundamental understanding of such solvent-driven processes in nano-confined solvents will impact many areas of chemistry and biology. The diversity among nanoscale cavities and pores (*e.g.*, in their size, shape, flexibility, and interactions with the solvent and/or reactants) makes it difficult to translate studies of one system into predictions for another. Thus, we are focusing on developing a unified understanding of chemical dynamics in the diverse set of confinement frameworks, including nanoscale silica pores of varying surface chemistry.[1,2]

## Recent Progress

In our recent work we have continued to explore the equilibrium and dynamical properties of nanoconfined liquids. In particular, we have examined a number of processes that are strongly affected by nanoscale confinement either directly or through interactions with a confined solvent. These include proton transfer,[4–6] time-dependent fluorescence,[7–12] and conformational equilibria.[2,13] Moreover, we have tested, at the molecular level, the validity of a number of common

models and approximations for nanoconfined systems such as the ubiquitous two-state models, linear response approximations, and Smoluchowski equation descriptions. The interesting behavior of nanoconfined liquids is evident from our studies that illustrate, for example, how new mechanisms which are not relevant in bulk liquids appear, how models that appear to agree with experiments are not microscopically accurate, and how the success of a given approximation can depend strongly on the specific phenomenon of interest.

**Proton Transfer.** We have investigated a number of properties of a model intramolecular phenol-amine proton transfer system in a $CH_3Cl$ solvent confined in a smooth, hydrophobic spherical cavity. We have developed a valence bond description for the reaction complex based loosely on a widely applied model.[3] Monte Carlo and mixed quantum-classical molecular dynamics simulations have previously been used to investigate complex position distributions,[4] free energy curves,[4] and proton transfer reaction dynamics including identification of multiple reaction mechanisms.[5]

Recently we have calculated the infrared spectrum of this model proton transfer reaction complex in a nanoconfined solvent using mixed quantum-classical molecular dynamics for different reaction free energies.[6] We found that, not surprisingly, the vibrational transition frequency is strongly related to a collective solvent coordinate, *i.e.*, the reaction coordinate for the proton transfer reaction. The proton transfer is sufficiently slow that it does not cause significant spectral broadening for this system; rather, the calculated spectra are motionally narrowed in the nanoconfined $CH_3Cl$ solvent. We determined that the spectra can be modelled using information only from equilibrium simulations of the reactants and products and knowledge of the equilibrium constant – an important result for PT reactions with larger barriers where direct simulation of the spectrum is not feasible. We found that the frequency autocorrelation function has a long-time decay that contains information about the *ground state* proton transfer reaction rate constant. This preliminary result on a simple model system suggests that nonlinear infrared photon echo experiments, which can access this autocorrelation function, might be used to measure these rate constants (in contrast to the current focus of measurements on *excited state* proton transfer rate constants). These results provide an impetus for additional work to understand how sensitive the results are to vibrational relaxation, more realistic modeling of the reaction complex, and the nature of the confining framework.

*Smoluchowski Equation Description of Dynamics in Nanoconfined Solvents.* A number of models have been proposed to describe the multi-exponential, long-time decay observed in time-dependent fluorescence studies of nanoconfined solvents. While molecular dynamics simulation provides a particularly appealing avenue for exploring these models, full nonequilibrium simulations can be quite time consuming. In nanoconfined solvents the effort is compounded by the heterogeneity of the system and the long-time dynamics, which together mean that many lengthy nonequilibrium trajectories are required. This provides an impetus for developing other ways of rapidly simulating the TDF dynamics, and ultimately reaction dynamics, for a large number of nanoconfined solvent systems. To that end, we have developed a Smoluchowski equation approach for the description of time-dependent fluorescence in solvents confined in spherical cavities and

cylindrical pores.[9] In addition to providing a rapid approach to simulating the time-dependent Stokes shift and solute diffusive motion, the Smoluchowski equation has a number of other advantages. Specifically, the entire time-dependent fluorescence spectrum is obtained as a function of time; this is typically not feasible in nonequilibrium MD simulations. The full time-dependent solute position distribution function is also calculated in the approach, allowing insight into the mechanism(s) of diffusion. We have validated the Smoluchowski equation approach by comparison to MD simulation results[9] for which at least part of the free energy surfaces are known accurately.[8]

Recently we have applied this Smoluchowski equation approach to probe different physical models.[10] Model one-dimensional free energy curves with a single barrier in the solute coordinate – appropriate for relatively small, *e.g.*, $\sim 2$ nm diameter, cavities or pores – were used to construct full two-dimensional free energy surfaces. The effect of position-dependence of diffusion coefficients and solvent coordinate force constants were also considered. The results indicate that the inclusion of radial diffusion leads to rich phenomena in the TDF. The position dependence of the diffusion coefficients was also found to have significant effects on the solute diffusion and solvation dynamics relevant to TDF. The results allow the comparison of the characteristics of the TDF signal predicted by different physical models that have been proposed to account for the long-time decays found for measurements in nanoconfined solvents.

**Future Plans**

We are currently pursuing work in three main areas: **1)** Simulations of time-dependent fluorescence of a coumarin 153 dye molecule in confined ethanol to provide direct comparisons with previous experimental measurements and establish the mechanism for the observed multi-exponential, long-time decays; **2)** Exploration of the connection between confining framework properties and proton transfer reaction dynamics of Mannich bases dissolved in confined aprotic, polar solvents studied with a Smoluchowski equation approach; and **3)** Simulation of linear and nonlinear infrared spectra of Mannich base proton transfer reaction complexes by mixed quantum-classical molecular dynamics to understand what the spectra can tell us about reaction dynamics in experimentally accessible systems. All three areas of study will focus on amorphous silica pore models, that we have previously developed,[1,2] as the nanoconfining framework; these models allow control over the pore size ($\sim 2-5$ nm in diameter) and surface chemistry (-OH and -$OC(CH_3)_3$ surface densities). This work will provide both results that can be directly compared to existing experimental data, as in the case of the time-dependent fluorescence study, and predictions that can be tested by future experiments, as in the case of the Mannich base intramolecular proton transfer systems.

## References


[1] †T.S. Gulmen and W.H. Thompson, "Model Silica Pores with Controllable Surface Chemistry for Molecular Dynamics Simulations" in *Dynamics in Small Confining Systems VIII*, edited by J.T. Fourkas, P. Levitz, R. Overney, M. Urbakh (Mater. Res. Soc. Symp. Proc. **899E**, Warrendale, PA, 2005), 0899-N06-05.

[2] †T.S. Gulmen and W.H. Thompson, "Testing the Two-State Model of Nanoconfined Liquids: The Conformational Equilibrium of Ethylene Glycol in Amorphous Silica Pores," *Langmuir*

**22**, 10919-10923 (2006).

[3] H. Azzouz and D. Borgis, *J. Chem. Phys.* **98**, 7361-7375 (1993).

[4] †S. Li and W.H. Thompson, *J. Phys. Chem. B* **109**, 4941-4946 (2005). "Proton Transfer in Nano-confined Polar Solvents. I. Free Energies and Solute Position "

[5] †W.H. Thompson, *J. Phys. Chem. B* **109**, 18201-18208 (2005). "Proton Transfer in Nano-confined Polar Solvents. II. Adiabatic Proton Transfer Dynamics"

[6] †K.R. Mitchell-Koch and W.H. Thompson, *J. Phys. Chem. B* **112**, 7448-7459 (2008). "Infrared Spectroscopy of a Model Phenol-Amine Proton Transfer Complex in Nanoconfined $CH_3Cl$"

[7] †W.H. Thompson, *J. Chem. Phys.* **120**, 8125-8133 (2004). "Simulations of Time-Dependent Fluorescence in Nano-Confined Solvents"

[8] †K.R. Mitchell-Koch and W.H. Thompson, *J. Phys. Chem. C* **111**, 11991-12001 (2007). "How Important is Entropy in Determining the Position-Dependent Free Energy of a Solute in a Nanoconfined Solvent?"

[9] †X. Feng and W.H. Thompson, *Journal of Physical Chemistry C* **111**, 18060-18072 (2007). "Smoluchowski Equation Description of Solute Diffusion Dynamics and Time-dependent Fluorescence in Nanoconfined Solvents"

[10] †X. Feng and W.H. Thompson, (in preparation). "Time-dependent Fluorescence in Nanoconfined Solvents. A Smoluchowski Equation Model Study"

[11] †B.B. Laird and W.H. Thompson, (in preparation). "Time-Dependent Fluorescence in Nanoconfined Solvents: Linear Response Approximations and Gaussian Statistics"

[12] †B.B. Laird and W.H. Thompson, *J. Chem. Phys.*, **126**, 211104 (2007). "On the Connection between Gaussian Statistics and Excited-State Linear Response for Time-Dependent Fluorescence,"

[13] †J.A. Gomez, A.K. Tucker, T.D. Shepherd, and W.H. Thompson, *J. Phys. Chem. B* **109**, 17479-17487 (2005). "Conformational Free Energies of 1,2-Dichloroethane in Nanoconfined Methanol"

†DOE-sponsored publication.

# Structural Dynamics in Complex Liquids Studied with Multidimensional Vibrational Spectroscopy

Andrei Tokmakoff

*Department of Chemistry, Massachusetts Institute of Technology, Cambridge, MA 02139*
*E-mail: tokmakof@MIT.edu*

Water is an unique solvent due to the fact that it can form up to four hydrogen bonds, creating a structured tetrahedral network of molecules that evolves with time as hydrogen bonds break and form. It is the fluctuations of this network that allow water to rapidly solvate nascent charge and to participate in chemical reactions. Moreover, it is predicted that the breakage and rearrangement of hydrogen bonds plays a major role in the autoionization of water molecules and in the transport of the products of that reaction, the hydronium and hydroxide ions. The goal of our research is to develop ultrafast spectroscopic probes that are sensitive to the fluctuations of water's hydrogen bonding network and to use these probes to obtain a mechanistic understanding of how the rearrangements of water molecules influence aqueous charge transport and reactivity.

As a probe of water's structure, we make use of ultrafast two dimensional infrared spectroscopy (2D IR) of the OH stretch of a solution of dilute HOD in $D_2O$. This particular isotopic combination of water is well suited for studies investigating the fluctuations of water's hydrogen bonding network since the OH absorption lineshape is broadened due to distribution of hydrogen bonding environments present in the liquid. Molecules that participate in strong hydrogen bonds absorb at lower frequencies than molecules in strained or broken hydrogen bonds. Thus, if we can excite a water molecule at a initial frequency and then watching how that frequency changes as a function of time we can gain direct information on how water's time dependent structure. 2D IR spectroscopy provides us with this ability to track how different hydrogen bonding environments interconvert over time. A 2D spectrum correlates how a molecule excited at an initial frequency evolves to a final frequency after a given waiting time. By varying the waiting time, we can follow how molecules initially in strong or weak hydrogen bonds exchange environments.

As a function of waiting time, many changes occur to the 2D IR lineshape that indicate the loss of frequency memory and give a timescale for the rearrangements of water's hydrogen bonding network. Our group has developed a number of metrics that can be used to quantify the loss of correlation in 2D lineshapes. More interesting however, are the frequency dependent changes of the lineshape that indicate molecules in strained or broken hydrogen bonds experience different fluctuations than molecules in strong hydrogen bonds. On the high frequency side of the lineshape which describes molecules in strained or broken hydrogen bonds, a rapid relaxation of intensity towards center frequency is observed on a ~60 fs timescale. Due to the rapidity of this decay, this argues that broken hydrogen bonding configurations do not correspond to stable minima on water's free energy landscape. Moreover, this timescale corresponds well with that for libratations, which implies that these hindered rotational motions that act to drive hydrogen bond rearrangements in water. MD simulations of hydrogen bond switching events indicate that the free energy surface describing switching projects well onto a bifurcation coordinate that describes distance and/or angular changes in configuration between the hydrogen bond donor and the initial and final acceptor molecules.

We are currently working to better understand the role that librations play in hydrogen bond rearrangements by measuring 2D IR spectra with different polarizations of the exciting fields and using that to calculate a two dimensional anisotropy. This measurement is analogous to the anisotropy decay which can be calculated from 1D pump-probe techniques which report on the reorientation of molecules as a function of time. The advantage of measuring a 2D anisotropy

decay over a 1D decay is the ability to correlate both the initial and final frequencies with the degree of rotation of the HOD molecule. Thus, we can determine if a molecule initially at high frequency (weak hydrogen bonding) that moves to lower frequency (strong hydrogen bonding) undergoes a different degree of reorientation than a molecule that remains on either side of the lineshape. Preliminary results of this measurement suggest that molecules initially in strained or broken hydrogen bonds undergo a significant degree of reorientation within 100 fs whereas molecules that remain in strong hydrogen bonds retain memory of their initial orientation but lose this memory if they move toward high frequency. These results are qualitatively similar to those obtained from molecular dynamics simulations and support the conclusion that the exchange of molecules from one side of the OH lineshape to the other involves molecular reorientation.

While we are able to infer a great deal about how hydrogen bond rearrangements proceed in water from HOD in $D_2O$, the OH stretch is primarily sensitive to the location of the nearest neighboring oxygen atom which limits the distance over which we can gain information on water's structure. We are currently in the process of extending our viewing window into the liquid by making use of tritium labeled water which will allow us to gain information on the relative orientation of two water molecules by measuring the cross peak between the OD and OT stretches of a solution of HOT and HOD in $H_2O$. We have characterized the OT stretch of HOT in $H_2O$ by measuring the first infrared spectrum of this isotopic solution. We have also performed preliminary pump-probe measurements on the OT stretch and found that it relaxes on a ~850 fs timescale. This agrees with existing proposals that the OT stretch relaxes via the intramolecular HOT bend.

Over the course of the last year, we have worked to understand how the water dynamics observed in the above experiments play a role in the transport of products of the autoionization of water, the hydronium and hydroxide ions. Both of these ions undergo anomalously fast diffusion due to their ability to undergo proton transfer with neighboring water molecules leading to the translocation of the ion. Simulations have suggested that hydrogen bond rearrangements play a strong role in guiding proton transfer processes involving these ions. However, experimental work that is able to directly capture proton motion is lacking due in large part to the difficulty of finding probes that can measure the timescales predicted for the transfer, which range from 10s of femtoseconds to picoseconds.

We have made 2D IR measurements of solutions of dilute HOD in concentrated NaOD: D2O solution. Upon the addition of NaOD to HOD:$D_2O$ solution, two new spectral features appear, a new peak at high frequency due to the $OH^-$ stretch and a broad shoulder that extends down to very low frequency due to HOD molecules hydrogen bonded to $OD^-$ ions. Pump probe and transient grating measurements find that as the NaOD concentration increases, a second vibrational relaxation component appears with an extremely fast timescale of 115 fs. Three pulse photon echo peak shift (3PEPS) experiments show a large offset with increasing NaOD concentration indicating that long lived static inhomogeneity is present in these solutions. This agrees with the increase in solution viscosity upon addition of NaOD.

Most interestingly though, is the presence of large offdiagonal intensity on the low frequency side of the 2D IR lineshape that disappears on a ~100 fs timescale, which roughly matches the fast decay timescale observed in the pump probe measurements. At longer waiting times a new peak in the 2D spectra which may indicate chemical exchange between $OH^-$ and HOD molecules grows in on a ~2ps timescale. In order to better understand these features, we have modeled our experiments using an EVB (empirical valence bond) molecular dynamics simulation model of aqueous sodium hydroxide developed by Todd Martinez's group at the University of Illinois Urbana-Champaign. In order to calculate spectra, we have developed a DFT based electrostatic frequency map which we can use to determine the "instantaneous" OH frequency of a given OH bond for a static configuration of the simulation. We find that in configurations where a proton is significantly shared between two water molecules, all of the transitions within the proton stretching potential undergo significant red shifts, and in particular

the OH stretch overtone ($\nu = 2 \leftarrow \nu = 0$) tunes into our experimentally accessible bandwidth. Thus, the rapid loss of intensity in the 2D and pump probe measurements is due to direct excitation of the overtone transition for configurations corresponding to nearly shared protons. As the proton moves to one side of the complex, stabilizing a water molecule, the overtone will blue shift out of our bandwidth, leading to the relaxation we see in the 2D and pump probe spectra.

Although water's structure is largely shaped by its ability to form hydrogen bonds, the strength of the hydrogen bonds formed by water are rather weak. Significantly stronger hydrogen bonds are formed by asymmetric doubly hydrogen bonded interfaces between amidine and carboxylic acid functionalities. Such interfaces are important structural motifs for biological systems exhibiting proton-coupled-electron-transfer. A limiting case of PCET is excited state proton transfer (ESPT) and we have investigated two symmetric and two asymmetric cyclic doubly hydrogen-bonded dimmers that display ESPT. The four dimers are the two homo-dimers of 7-azaindole (7-AI) and 1*H*-pyrrolo[3,2-*h*]quinoline (PQ) and their hetero-dimer counterparts with acetic acid. We have performed a complete set of third order spectroscopies: transient grating, echo peak shift, pump probe and full 2D-IR surface of all four dimers in the NH region. This has lead to a complete understanding of the NH vibrational dynamics in the electronic ground state. Whereas the linear spectra might be dominated by Fermi-resonances, the transient grating and echo peak-shift measurements have shown that the vibrational dynamics are dominated by the low-frequency inter-monomer stretching and twisting vibrations. These are the low-frequency modes that directly modulate the hydrogen-bond strength of the NH bond.

In addition to using 2D spectroscopy to better understand chemical dynamics, we have also worked to develop new, easier methods for the acquisition of 2D IR surfaces. We have implemented a method of quickly acquiring 2D data by scanning the stage that sets one of the experimental time delays at constant velocity and finding the stage position by measuring the phase of a HeNe alignment beam that copropagates with the infrared excitation pulses. We have also demonstrated a new method that greatly simplifies the acquisition of 2D data by using a pump probe geometry wherein the pump is a collinear pulse pair. Simultaneous collection of the third order response and the interferometric autocorrelation of the pulse pair allows for automated phasing of the data as well as rapid acquisition since only a single delay stage needs to be scanned.

**DOE Supported Publications (2005-2008)**


1. "Local hydrogen bonding dynamics and collective reorganization in water: Ultrafast IR spectroscopy of HOD/$D_2O$," C. J. Fecko, J. J. Loparo, S. T. Roberts and A. Tokmakoff, *Journal of Chemical Physics*, **122** (2005) 054506.
2. "Amide I vibrational dynamics of N-methylacetamide in polar solvents: The role of electrostatic interactions," M. F. DeCamp, L. P. DeFlores, J. M. McCracken, A. Tokmakoff, K. Kwac, and M. Cho, *Journal of Physical Chemistry B*, **109** (2005) 11016.
3. "Upconversion multichannel infrared spectrometer," M. F. DeCamp and A. Tokmakoff, *Optics Letters*, **30** (2005) 1818.
4. "Electric field fluctuations drive vibrational dephasing in water," J. D. Eaves, A. Tokmakoff, and P. L. Geissler, *Journal of Physical Chemistry A*, **109** (2005) 9424.
5. "Hydrogen bonds in liquid water are broken only fleetingly," J. D. Eaves, J. J. Loparo, C. J. Fecko, S. T. Roberts, A. Tokmakoff and P. L. Geissler, *Proceedings of the National Academy of Sciences, USA*, **102** (2005) 13019.

6. "Polarizable molecules in the vibrational spectroscopy of water," E. Harder, J. D. Eaves, A. Tokmakoff and B. J. Berne, *Proceedings of the National Academy of Sciences, USA*, **102** (2005) 11611.
7. "A study of phonon-assisted exciton relaxation dynamics for a (6,5) enriched DNA-wrapped single walled carbon nanotubes sample," S. G. Chou, M. F. DeCamp, J. Jiang, Ge. G. Samsonidze, E. B. Barros, F. Plentz, A. Jorio, M. Zheng, G. B. Onoa, E. D. Semke, A. Tokmakoff, R. Saito, G. Dresselhaus, M. S. Dresselhaus, *Physical Review B*, **72** (2005) 195415.
8. "Single-shot two-dimensional spectrometer," M. F. DeCamp and A. Tokmakoff, *Optics Letters*, **31** (2006) 113.
9. "Spectral signatures of heterogeneous protein ensembles revealed by MD simulations of 2DIR spectra," Z. Ganim and A. Tokmakoff, *Biophysical Journal*, **91** (2006) 2636.
10. "Multidimensional infrared spectroscopy of water. I. Vibrational dynamics in 2D IR lineshapes," J. J. Loparo, S. T. Roberts, and A. Tokmakoff, *Journal of Chemical Physics*, **125** (2006) 194521.
11. "Multidimensional infrared spectroscopy of water. II. Hydrogen bond switching dynamics," J. J. Loparo, S. T. Roberts, and A. Tokmakoff, *Journal of Chemical Physics*, **125** (2006) 194522.
12. "Characterization of spectral diffusion from two-dimensional lineshapes," S. T. Roberts, J. J. Loparo, and A. Tokmakoff, *Journal of Chemical Physics*, **125** (2006) 084502.
13. "2D IR spectroscopy of hydrogen bond switching in liquid water," J. J. Loparo, S. T. Roberts, and A. Tokmakoff, in *Ultrafast Phenomena XV*, ed. by P. Corkum, D. Jonas, R. J. D. Miller, and A.M. Weiner (Springer, Berlin, 2007), p. 341.
14. "Single-shot two-dimensional infrared spectroscopy," M. F. DeCamp, L. P. DeFlores, K. C. Jones, and A. Tokmakoff, *Optics Express*, **15** (2007) 233.
15. "Are water simulation models consistent with steady-state and ultrafast vibrational spectroscopy experiments?" J. R. Schmidt, S. T. Roberts, J. J. Loparo, A. Tokmakoff, M. D. Fayer, and J. L. Skinner, *Chemical Physics*, **341** (2007) 143.
16. "Variation of the transition dipole moment across the OH stretching band of water," J. J. Loparo, S. T. Roberts, R. A. Nicodemus and A. Tokmakoff, *Chemical Physics*, **341** (2007) 218.
17. "Infrared spectroscopy of tritiated water," R. A. Nicodemus and A. Tokmakoff, *Chemical Physics Letters*, **449** (2007) 130.
18. "Shining light onto water's rapidly evolving structure," A. Tokmakoff, *Science*, **317** (2007) 54.
19. "Two-dimensional Fourier transform spectroscopy in the pump-probe geometry," L. P. DeFlores, R. A. Nicodemus, and A. Tokmakoff, *Optics Letters*, **32** (2007) 2966.
20. "Transient 2D IR spectroscopy of ubiquitin unfolding dynamics," H. S. Chung, Z. Ganim, K. C. Jones, and A. Tokmakoff, *Proceedings of the National Academy of Sciences, USA*, **104** (2007) 14237.
21. "Amide I two-dimensional infrared spectroscopy of proteins," Z. Ganim, H. S. Chung, A. W. Smith, L. P. DeFlores, K. C. Jones, and A. Tokmakoff, *Accounts of Chemical Research*, **41** (2008) 432.
22. "Ultrafast N-H vibrational dynamics of cyclic doubly hydrogen-bonded homo- and heterodimers" P. B. Petersen, S. T. Roberts, K. Ramasesha, D. G. Nocera, and A. Tokmakoff, *Journal of Physical Chemistry B*, accepted.
23. "The dynamics of aqueous hydroxide ion transport probed via ultrafast vibrational echo experiments," S.T. Roberts, P. B. Petersen, K. Ramasesha, and A. Tokmakoff in *Ultrafast Phenomena XVI*, Springer, Berlin (in press).

# The Role of Electronic Excitations on Chemical Reaction Dynamics at Metal, Semiconductor and Nanoparticle Surfaces

John C. Tully
*Department of Chemistry, Yale University, 225 Prospect Street,*
*P. O. Box 208107, New Haven, CT, 06520-8107 USA*
john.tully@yale.edu

## Program Scope

Achieving enhanced control of the rates and molecular pathways of chemical reactions at the surfaces of metals, semiconductors and nanoparticles will have impact in many fields of science and engineering, including heterogeneous catalysis, photocatalysis, materials processing, corrosion, solar energy conversion and nanoscience. However, our current atomic-level understanding of chemical reactions at surfaces is incomplete and flawed. Conventional theories of chemical dynamics are based on the Born-Oppenheimer separation of electronic and nuclear motion. Even when describing dynamics at metal surfaces where it has long been recognized that the Born-Oppenheimer approximation is not valid, the conventional approach is still used, perhaps patched up by introducing friction to account for electron-hole pair excitations or curve crossings to account for electron transfer. There is growing experimental evidence that this is not adequate. We are examining the influence of electronic transitions on chemical reaction dynamics at metal and semiconductor surfaces. Our program includes the development of new theoretical and computational methods for nonadiabatic dynamics at surfaces, as well as the application of these methods to specific chemical systems of experimental attention. Our objective is not only to advance our ability to simulate experiments quantitatively, but also to construct the theoretical framework for understanding the underlying factors that govern molecular motion at surfaces and to aid in the conception of new experiments that most directly probe the critical issues.

## Recent Progress

### *Nonadiabatic dynamics at metal surfaces beyond the friction theory*

Recent experiments by the Wodtke, McFarland, Hasselbrink and Somorjai groups demonstrate that individual electrons in a metal can receive as much as 1.5 eV or more of excitation upon molecular scattering, adsorption or chemical reaction at the surface. This cannot be described by an electronic friction theory or any theory based on a weak coupling assumption. In the first two years of this grant we developed a theoretical framework that applies in both the sudden electron jump and multiple low-energy excitation (friction) limits[2,4]. The approach takes advantage of the presence of the continuum of *parallel* potential energy surfaces to greatly simplify the electronic equations of motion. In addition, it correctly generates distributions of observables, rather than simply the averages yielded by Ehrenfest mean-field dynamics. Initial tests of both quantum mechanical and semiclassical implementations against numerically exact one-dimensional benchmarks were very promising. However, extension of these quantum mechanical and semiclassical procedures to simulate gas-surface dynamics with all adsorbate and surface atom motions included is prohibitive. We have now turned our attention to developing a mixed quantum-classical theory in which the nuclear motion evolves by classical mechanics subject to forces exerted by the time-dependent evolution

of the electronic wave function. The two widely-used methods for doing this in other contexts are Ehrenfest (mean field) and surface hopping. The former is the formalism on which the electronic friction theory is built. However, for the strong-coupling, multi-state processes we are now addressing, the friction theory is inadequate. Therefore we choose to extend surface hopping to situations involving a continuum of electronic states.

Our first step towards this goal was to develop an efficient method for representing the continuous spectrum by discrete states (as few as possible). Simply choosing equally-spaced levels requires far too many states. For example, for the specific problem at hand, it is critical that there be a high density of states near the Fermi level, whereas in other regions the states can be more sparse. We have developed a systematic method that we believe provides higher accuracy, for a given number of discrete states, than any other existing method[7]. This may have widespread use in other contexts, as well.

Our next step was to develop an adequate approximation to the electronic wave function. A many-electron description is required in order to incorporate the multiple electron-hole pair transitions that are responsible for electronic friction, while at the same time retaining the character of individual local ionic and neutral states that are critical for the multiquantum, Franck-Condon transitions that produce energetic electrons and holes. Following the Anderson-Newns model, we represent the total wave function by a single determinant in which each one-electron orbital is a time-varying linear combination of the diabatic (local adsorbate plus discretized conduction band) electronic states. For the NO-Au system described below, approximately 100 one-electron states and 20 electrons were found to satisfactorily represent the electronic space. We have developed efficient numerical procedures for propagating the wave function along a trajectory.

The final step is to incorporate this into a mixed quantum-classical dynamics simulation. Our first attempt at this failed. Whereas in gas phase applications surface hopping is far more reliable when the adiabatic rather than the diabatic representation is employed, because of the huge numbers of states involved in metallic systems we expected that the simpler diabatic representation would be adequate. This turned out to be untrue. For low-energy (thermal) motions where the forces are nearly adiabatic, assigning motion to one or another of the diabatic potential surfaces is inaccurate. In the case of NO on gold, e.g., even on the lowest energy diabatic surface the adsorbate rarely reached the strong coupling region, whereas it did so easily on the adiabatic surface. We have now implemented surface hopping in the adiabatic representation. Note that the evolution of the electronic wave function along the classical path is invariant to representation, and this is more conveniently carried out diabatically. The “fewest-switches” surface hopping algorithm, however, does depend on representation. This requires obtaining the forces on the occupied adiabatic state at each time step, a significant computational chore, but certainly not prohibitive. In contrast to the few (0-4) hops typically encountered in gas-phase applications of surface hopping, for NO on gold more than 100 per trajectory frequently occus. The resulting stochastic method is manageable, it accounts for both electronic friction and localized excitations, and it properly resolves the outcomes into final state probabilities. In its current implementation, however, it does not allow for excited electrons or holes to leave the local region via ballistic transport into the bulk. Incorporating this feature via properly introducing decoherence is an important goal of our future research.

***Dynamics of scattering of NO from Au(111)***

Because of the detailed experimental results by Wodtke and coworkers on nonadiabatic vibrational energy transfer upon scattering of nitric oxide molecules from the 111 face of gold, we have chosen this as our first target application. Previously, we constructed accurate neutral and ionic potential energy surfaces and their off-diagonal coupling terms, i.e., a "diabatic" 2x2 Hamiltonian matrix, required in order for us to examine dynamics beyond the adiabatic (ground state) approximation. In order to uniquely define a 2x2 symmetric matrix, we need three independent pieces of information at each nuclear configuration. The *ab initio* (plane wave density functional theory) ground state energy and local charge on the NO molecule provide two of the needed pieces. We obtained the third piece of information from the shift in the *ab initio* ground state energy upon application of a small electric field. We have now completed constructing a global model Hamiltonian that is convenient and, we believe, quite accurate, and which can now be used as a benchmark for testing theories of nonadiabatic dynamics. The Hamiltonian properly incorporates all major aspects of the interaction, including the image force and the electron transfer at extended N-O bond separations. Developing robust, accurate and practical methods for providing the required diabatic potential energy surfaces for more general applications is one of our research goals for the next funding period.

We have now carried out adiabatic dynamics on the scattering of vibrationally excited NO from the Au(111) surface to compare with the experiments of the Wodtke group. Diagonalization of the 2x2 Hamiltonian matrix described above provides the required ground state energies and forces. Our main interests are the importance and nature of nonadiabatic effects, of course, but we first need to understand adiabatic behavior. Our computed sticking probabilities are now in reasonably good accord with experiments of the Wodtke group, in contrast with our earlier attempts. However, vibrational energy transfer is greatly underestimated by the adiabatic simulations, confirming the expectation that nonadiabatic electron-hole pair excitations dominate.

Next, we have expanded the 2x2 diabatic Hamiltonian for NO-Au(111) into a very large order matrix of nested and coupled continua, consistent with the Anderson-Newns model, using our efficient discretization procedure described above. We then implemented the surface hopping code and have now carried out preliminary simulations. Our preliminary results indeed confirm that nonadiabatic transitions promoted by electron transfer, rather than direct excitation of electron-hole pairs (friction), dominate energy transfer in the scattering of vibrationally excited NO from Au(111). Vibrational energy distributions of scattered NO molecules are in qualitative accord with experiment, and a significant fraction of excited electrons have energy greater than 1.5 eV, consistent with the observation of electron emission from cesium covered gold surfaces.

**Future Plans**

The goals of our research program include completing our studies of the NO-Au system and more general investigations of nonadiabatic behavior at metal and semiconductor surfaces. Our plans for the next funding period include the following:

1. Complete the surface hopping dynamics simulations of NO scattering from gold to introduce electronic excitations and electron transfer beyond the friction model.

2 Carry out “molecular dynamics with electronic friction” (Head-Gordon and Tully) simulations to assess the ability of the more elaborate surface hopping method to both reproduce frictional effects and introduce localized, multiquantum transitions.
3. Derive and implement a practical procedure for introducing decoherence in the surface hopping approach, in order to account for the loss of excitation energy via transport of carriers into the bulk metal.
4. Through analysis of the results of application of this hierarchy of theoretical methods, draw conclusions about the importance and nature of nonadiabatic electronic transitions both in the NO-Au system and more generally.
5. Develop improved *ab initio* methods for computing energies and widths of lifetime-broadened electronic states near metal and semiconductor surfaces, through extension of “constrained density functional theory”. These are the properties that determine the rate and extent of electron transfer as a molecule approaches the surface; i.e., that are required to construct a diabatic Hamiltonian.
6. Carry out *ab initio* calculations of energies, charge distributions and level widths as input to constructing valence-bond type Hamiltonians for a number of chemical systems, including the CO oxidation reaction on platinum. Somorjai and coworkers have recently demonstrated that hot-electrons are produced as this reaction unfolds.
7. Explore the dynamics of open shell species with metal and semiconductor surfaces, and small metallic clusters. An example is the oxygen molecule where transitions between the ground state triplet and low-lying singlet states may occur without spin-orbit interactions via a two-electron exchange with the conduction band, with major implications to chemical reactivity.

**References to Publications of DOE-Sponsored Research: 2006-2008**

1. N. Shenvi, H. Z. Cheng and J. C. Tully, “Nonadiabatic dynamics near metal surfaces: Decoupling quantum equations of motion in the wide-band limit”, *Phys. Rev.* **A74**, 062902 (2006).
2. N. Shenvi, S. Roy, P. Parandekar and J. Tully, “Vibrational relaxation of NO on Au(111) via electron-hole pair generation”, *J. Chem. Phys.* **125**, 154703 (2006).
3. J. C. Tully, “Mode-selective control of surface reactions”, *Science* **312**, 1004 (2006). (This paper is an invited “Perspective” commenting on the results of others.)
4. H. Z. Cheng, N. Shenvi and J. C. Tully, “Semiclassical dynamics of electron transfer at metal surfaces”, *Phys. Rev. Lett.* **99**, 053201 (2007).
5. X. S. Li and J. C. Tully, “Ab initio time-resolved density functional theory for lifetimes of excited adsorbate states at metal surfaces”, *Chem. Phys. Lett*. **439**, 199-203 (2007). (primary support from NSF)
6. C. M. Isborn, X. S. Li and J. C. Tully, “Time-dependent density functional theory Ehrenfest dynamics: Collisions between atomic oxygen and graphite clusters” *J. Chem. Phys.* **126**, 134307 (2007). (primary support from NSF)
7. N. Shenvi, J. R. Schmidt, S. Edwards and J. C. Tully, “Efficient discretization of the continuum through complex contour deformation”, *Phys. Rev. A*, 2008, in press.
8. J. Zwickl, N. Shenvi, J.R. Schmidt and J. C. Tully, “Transition state barriers in multidimensional Marcus theory”, *J. Phys. Chem B*., 2008, in press.
9. J. R. Schmidt, N. Shenvi and J. C. Tully, “Controlling spin-contamination using constrained density functional theory”, *J. Chem. Phys*., 2008, in press.

# Chemical Kinetics and Dynamics at Interfaces

*Gas Phase Investigation of Condensed Phase Phenomena* [1]

**Lai-Sheng Wang (PI)**
Department of Physics, Washington State University, 2710 University Drive, Richland, WA, 99354 and the Chemical & Materials Sciences Division, Pacific Northwest National Laboratory, P.O. Box 999, MS K8-88, Richland, WA 99352. E-mail: ls.wang@pnl.gov

## Program Scope

The broad scope of this program is aimed at microscopic understanding of condensed phase phenomena using clusters as model systems. Our current focus is on the microsolvation of complex anions that are important in solution chemistry. The primary experimental technique is photoelectron spectroscopy of size-selected anions. Unique experimental techniques have been developed by coupling electrospray ionization with photoelectron spectroscopy, that allows complex anions, including multiply charged anions and solvated clusters, from solution samples to be investigated in the gas phase. Experimental studies are combined with *ab initio* calculations to:

- obtain a molecular-level understanding of the solvation of complex anions (both singly and multiply charged) important in condensed phases
- understand the molecular processes and initial steps of dissolution of salt molecules by polar solvents
- probe the structure and dynamics of solutions and air/solution interfaces

Complexes anions, in particular multiply charged anions, are ubiquitous in nature and often found in solutions and solids. However, few complex anions have been studied in the gas phase due to the difficulty in generating them and their intrinsic instability as a result of strong intramolecular Coulomb repulsion in the case of multiply charged anions. Microscopic information on the solvation and stabilization of these anions is important for the understanding of solution chemistry and properties of inorganic materials or atmospheric aerosols involving these species. Gas phase studies with controlled solvent numbers and molecular specificity are ideal to provide such microscopic information. We have developed a new experimental technique to investigate multiply charged anions and solvated species directly from solution samples and probe their electronic structures, intramolecular Coulomb repulsion, stability, and energetics using electrospray and PES. A central theme of this research program lies at obtaining a fundamental understanding of environmental materials and solution chemistry. These are important to waste storage, subsurface and atmospheric contaminant transport, and other primary DOE missions.

## Recent Progress (2005-2008)

***Development of a low-temperature photoelectron spectroscopy instrument using an electrospray ion source and a cryogenically controlled ion trap.*** The ability to control ion temperatures is critical for gas phase spectroscopy and has been a challenge in chemical physics. We have developed a low-temperature photoelectron spectroscopy instrument for the investigation of complex anions in the gas phase, including multiply charged anions, solvated species, and biological molecules. As shown schematically in Figure 1, the new apparatus consists of an electrospray ionization source, a 3D Paul trap for ion accumulation and cooling, a time-of-flight mass spectrometer, and a magnetic-bottle photoelectron analyzer. A key feature of the new instrument is the capability to cool and tune ion temperatures from 10

[1] Collaborators on these projects include X. B. Wang.

to 350 K in the 3D Paul trap, which is attached to the cold head of a closed-cycle helium refrigerator. Ion cooling is accomplished in the Paul trap via collisions with a background gas and has been demonstrated by observation of complete elimination of vibrational hot bands in photoelectron spectra of various anions ranging from small molecules to complex species. Further evidence of ion cooling is shown by the observation of $H_2$ physisorbed anions at low temperatures. Cold anions result in better resolved photoelectron spectra due to the elimination of vibrational hot bands and yield more accurate energetic and spectroscopic information. Temperature-dependent studies are made possible for weakly-bonded molecular and solvated clusters, allowing thermodynamic information to be obtained.

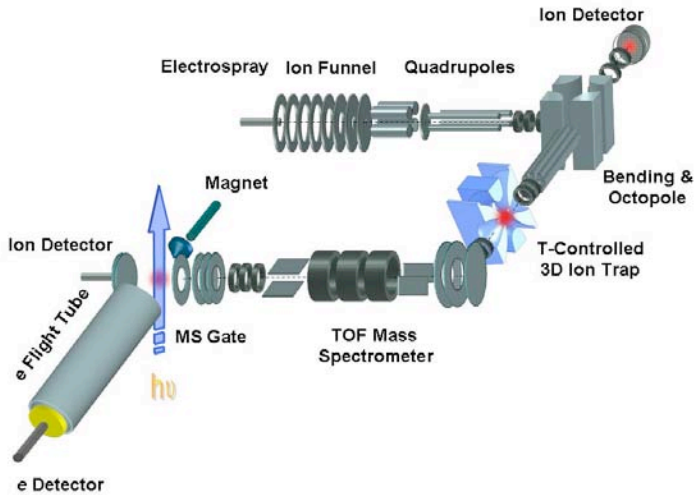


**Fig. 1.** Schematic view of the second generation low temperature electrospray photoelectron spectroscopy apparatus.

***Observation of entropic effect on conformation changes of complex systems under well-controlled temperature condition.*** We reported a direct observation of entropic effect in determining the folding of a linear dicarboxylate dianion with a flexible aliphatic chain [$^-O_2C$-$(CH_2)_6$-$CO_2^-$] by photoelectron spectroscopy as a function of temperature (18 – 300 K) and degree of solvation from 1 to 18 water molecules. A folding transition was observed to occur at 16 solvent water molecules at room temperature, but at 14 solvent molecules below 120 K due to the entropic effect. The $^-O_2C$-$(CH_2)_6$-$CO_2^-$ $(H_2O)_{14}$ hydrated cluster exhibits interesting temperature-dependent behaviors and its ratio of folded over linear conformations can be precisely controlled as a function of temperature, yielding the enthalpy and entropy differences between the two conformations. A folding barrier was observed at very low temperatures, resulting in kinetic trapping of the linear conformation. This work provides a simple model system to study the dynamics and entropic effect in complex systems and may be important for understanding the hydration and conformation changes of biological molecules.

## Future Plans

The main thrust of our BES program will continue to focus on cluster model studies of condensed phase phenomena in the gas phase. The experimental capabilities that we have developed give us the opportunities to attack a broad range of fundamental chemical physics problems pertinent to ionic solvation and solution chemistries. In particular, the temperature control will allow us to study different isomer populations and conformation changes as a function of temperature. We will also be able to study physisorption of various gas molecules onto negatively charged anions. The physisorption of $H_2$ is of particular interest because of its relevance to identifying potentially $H_2$ storage materials by providing fundamental energetic and structural information between $H_2$ and different types of molecules.

***Microsolvation of complex multiply-charged anions: temperature-dependent isomer populations.*** Many important inorganic multiply-charged anions, such as, $SO_4^{2-}$, $CO_3^{2-}$, and $PO_4^{3-}$, are not stable in the gas phase due to the strong intramolecular Coulomb repulsion leading to electron autodetachment. These anions exist in solution as a result of solvation stabilization and they participate in

important chemical reactions on environmental surfaces under conditions of low humidity. There are two important questions for gaseous studies: 1) Can these anions be stabilized in the gas phase by solvents and what is the minimum number of solvent molecules needed? 2) What are the solvation structures and how are the anions stabilized? Answers to these questions are important to understanding the stability of the anions themselves, as well as to providing molecular level information about their solvation in bulk solutions. We have already investigated the solvation and solvent-stabilization of $SO_4^{2-}$ and $C_2O_4^{2-}$ at room temperature previously. We plan to re-examine solvated clusters of these anions under low-temperature conditions. For each solvated clusters, there are many possible structural isomers. Two important questions arise: 1) can we observe the true global minimum isomer? and 2) can we vary the isomer populations as a function of temperature?

For example, in our first study on the $SO_4^{2-}(H_2O)_n$ clusters we concluded that three water molecules are needed to stabilize the $SO_4^{2-}$ dianion in the gas phase. Using density functional calculations, we also showed how this dianion is solvated by water from $n$ = 1 to 6. We found that the $SO_4^{2-}(H_2O)_6$ hydrated cluster has a $C_3$ global minimum structure. However, in two recent infrared studies, different conclusions have been reached, which are likely due to the different temperatures under which each experiment was conducted. We have carried out a preliminary low-temperature experiment and observed that the photoelectron spectrum of $SO_4^{2-}(H_2O)_6$ exhibited a shift of at least 0.1 eV to higher electron binding energies at 12 K relative to the room temperature spectrum. Our calculated vertical electron binding energy (VDE), done in collaboration with Prof. A. I. Boldyrev from Utah State University, showed that the global minimum $C_3$ structure (VDE = 2.26 eV) is in good agreement with the measured VDE (2.23 eV) in the low temperature experiment. The room temperature spectrum is broader with a VDE near 2.13 eV, in agreement with that of a slightly higher energy $C_1$ isomer (VDE = 2.13 eV). Clearly, different isomers are observed at low temperatures relative to room temperature. We plan to study hydrated $SO_4^{2-}$(H2O)n and $C_2O_4^{2-}$(H2O)n at low temperatures for a range of cluster sizes and see how the hydrated structures evolve with temperature. Such studies may be relevant to understanding temperature-dependent behaviors of bulk solutions, as well as providing fundamental information about the nature of these hydrated clusters, i.e., liquid-like vs. solid-like structures, as a function of temperature.

***Probing $H_2$ physisorption onto negative ions.*** Because of the light weight and low density of gaseous hydrogen, discovering viable hydrogen storage materials has become a critical step for the application of $H_2$ as a clean fuel. Understanding the intermolecular interaction between $H_2$ and different molecular species can provide fundamental information about the $H_2$ binding affinities of potential hydrogen storage materials. $H_2$-adsorbed molecular complexes provide simple model systems for investigating $H_2$ binding. Our low-temperature ion trap provides an ideal device to produce $H_2$ complexes with a variety of ionic species. In particular, for negatively charged anions we can use photoelectron spectroscopy to probe the energetics of $H_2$-anion interactions. It has been theoretically shown that $H_2$ binding can be significantly enhanced on charged species. Thus, we can also probe the dependence of $H_2$ binding on charge states. Figure 2 shows a set of mass spectra of a triply-charged anion (8-hydroypyrene-1, 3, 6-trisulfonate or $[3sPyOH]^{3-}$), when the helium background gas contains 20% $H_2$ in the ion trap at a total background pressure of about 0.1 to 1 mTorr. At a trapping temperature of 17 K, more than

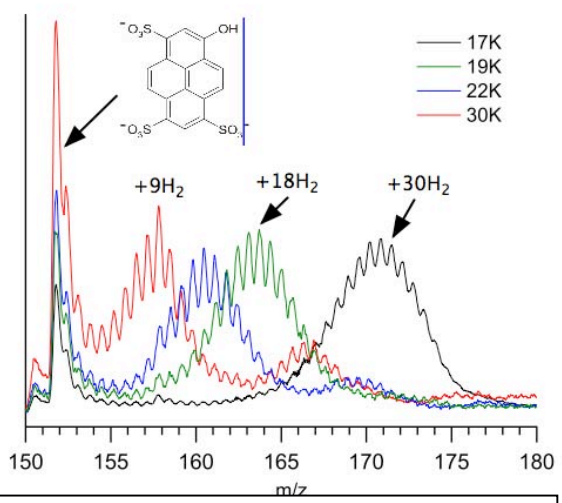


**Fig. 2.** Mass spectra of $[3sPyOH]^{3-}/H_2$ physisorbed complexes.

30 $H_2$ molecules can be adsorbed onto $[3sPyOH]^{3-}$ and the maximum adsorbed $H_2$ decreases with increasing temperature. Preliminary photoelectron spectra show that each $H_2$ molecule can provide an electron stabilization energy of about 0.03 eV for the first 10 $H_2$. We have also shown that the $H_2$ adsorption for the doubly-charged $Na^+[3sPyOH]^{3-}$ ion pair is significantly reduced under the same conditions, verifying the dependence of $H_2$ binding strengths on charge states. Potentially, our technique allows any negatively charged anions to be investigated. We plan to exploit this capability to probe the interaction of $H_2$ with different anions.

## References to Publications of DOE Sponsored Research (FY 2005-2008)


1. "The Role of Water on Electron-Initiated Processes and Radical Chemistry: Issues and Scientific Advances" (B. C. Garrett, *et al*.), *Chem. Rev*. **105**, 355-389 (2005).
2. "Interior and Interfacial Aqueous Solvation of Benzene Dicarboxylate Dianions and Their Methylated Analogues: A Combined Molecular Dynamics and Photoelectron Spectroscopy Study" (B. Minofar, L. Vrbka, M. Mucha, P. Jungwirth, X. Yang, X. B. Wang, F. J. Fu, and L. S. Wang), *J. Phys. Chem. A* **109**, 5042-5049 (2005).
3. "Observation of Weak C-H···O Hydrogen-Bonding by Unactivated Alkanes" (X. B. Wang, H. K. Woo, B. Kiran, and L. S. Wang), *Angew. Chem. Int. Ed*. **44**, 4968-4972 (2005).
4. "Vibrational Cooling in A Cold Ion Trap: Vibrationally Resolved Photoelectron Spectroscopy of Cold $C_{60}^-$ Anions" (X. B. Wang, H. K. Woo, and L. S. Wang), *J. Chem. Phys*. **123**, 051106 (2005).
5. "Probing the Low-Barrier Hydrogen Bond in Hydrogen Maleate in the Gas Phase: A Photoelectron Spectroscopy and *Ab initio* Study" (H. K. Woo, X. B. Wang, L. S. Wang, and K. C. Lau), *J. Phys. Chem. A* **109**, 10633-10637 (2005).
6. "Temperatures Dependent Photoelectron Spectroscopy of Methyl-Benzoate Anions: Observation of Steric Effect in *Ortho*-Methyl-Benzoate" (H. K. Woo, X. B. Wang, B. Kiran, and L. S. Wang), *J. Phys. Chem. A* **109**, 11395-11400 (2005).
7. "Determination of the Electron Affinity of the Acetyloxyl Radical ($CH_3COO$) by Low Temperature Anion Photoelectron Spectroscopy and *ab initio* Calculations" (X. B. Wang, H. K. Woo, L. S. Wang, B. Minofar, and P. Jungwirth), *J. Phys. Chem. A* **110**, 5047-5050 (2006).
8. "Low-Temperature Photoelectron Spectroscopy of Aliphatic Dicarboxylate Monoanions, $HO_2C(CH_2)_nCO_2^-$ ($n$ = 1 – 10): Hydrogen Bond Induced Cyclization and Strain Energies" (H. K. Woo, X. B. Wang, K. C. Lau, and L. S. Wang), *J. Phys. Chem. A* **110**, 7801-7805 (2006).
9. "First Steps Towards Dissolution of $NaSO_4^-$ by Water" (X. B. Wang, H. K. Woo, B. Jagoda-Cwiklik, P. Jungwirth, and L. S. Wang), *Phys. Chem. Chem. Phys*. **8**, 4294-4296 (2006).
10. "Microsolvation of the Dicyanamide Anion: $[N(CN)_2^-](H_2O)_n$ ($n$ = 0–12)" (B. Jagoda-Cwiklik, X. B. Wang, H. K. Woo, J. Yang, G. J. Wang, M. F. Zhou, P. Jungwirth, and L. S. Wang), *J. Phys. Chem. A* **111**, 7719-7725 (2007).
11. "Observation of Entropic Effect on Conformation Changes of Complex Systems under Well-Controlled Temperature Condition" (X. B. Wang, J. Yang, and L. S. Wang), *J. Phys. Chem. A* **112**, 172-175 (2008).
12. "Development of a Low-Temperature Photoelectron Spectroscopy Instrument Using an Electrospray Ion Source and a Cryogenically Controlled Ion Trap" (X. B. Wang and L. S. Wang), *Rev. Sci. Instrum.* **79**, 073108-1-8 (2008).
13. "Imaging Intramolecular Coulomb Repulsions in Multiply Charged Anions" (X. P. Xing, X. B. Wang, and L. S. Wang), *Phys. Rev. Lett*. **101**, 083003-1-4 (2008).
14. "Photoelectron Spectroscopy of Multiply Charged Anions" (X. B. Wang and L. S. Wang), *Ann. Rev. Phys. Chem.*, in press.

# Surface Chemical Dynamics

M.G. White [a], N. Camillone III [a], and A.L. Harris [b]
*Brookhaven National Laboratory, Chemistry Department, Building 555, Upton, NY 11973*
( mgwhite@bnl.gov, nicholas@bnl.gov, alexh@bnl.gov )

## 1. Program Scope

This program focuses on fundamental investigations of the dynamics, energetics and morphology-dependence of thermal and photoinduced reactions on planar and nanostructured surfaces that play key roles in energy-related catalysis and photocatalysis. Laser pump-probe methods are used to investigate the dynamics of interfacial charge and energy transfer that leads to adsorbate reaction and/or desorption on metal and metal oxide surfaces. State- and energy-resolved measurements of the gas-phase products resulting from thermal and photoinitiated reactions are used to infer the dynamics of product formation and desorption. Time-resolved correlation techniques are used to follow surface reactions in real time and infer the dynamics of adsorbate–substrate energy transfer and desorption. Planned extensions of this work include investigations of the size-dependence of photoinduced desorption and vibrational dynamics of small molecules on surfaces of supported metal nanoparticles. Complementary efforts use cluster ion beams for studying the structure, dynamics and reactivity of size-selected metal and metal compound nanoclusters in the gas-phase and deposited onto solid supports.

## 2. Recent Progress

***Ultrafast Investigations of Surface Chemical Dynamics.*** Motivated by a desire to follow in real time the evolution of surface chemical processes, we employ subpicosecond near-IR laser pulses to inject energy into adsorbate–substrate complexes, initiating reactions by fast substrate-mediated processes such as DIMET (desorption induced by multiple electronic transitions) and heating via electronic friction. Time-resolved monitoring of the excited complex is achieved by a two pulse correlation (2PC) method wherein the excitation pulse is split into two pulses separated by a delay. The two pulses act effectively as pump and probe, and a measurement of the desorbed product yield as a function of the delay is a measure of the relaxation timescale of energy deposited into the reaction coordinate.

An overarching theme of our work has been to connect and contrast ultrafast laser-initiated processes with conventional thermal chemical processes. We have examined in detail the dynamics of ultrafast photoinduced desorption of $O_2$ and CO from Pd(111), and the photoinduced oxidation of CO on Pd(111). We have found that thermal desorption activation energies can be used effectively within a three-temperature model of the energy flow to describe the photodesorption. This lends validity to the "pseudo-thermal" understanding of the photodesorption, wherein the substrate–adsorbate coupling is diabatic but the system subsequently evolves on a potential energy surface approximating that which governs thermal reactions.

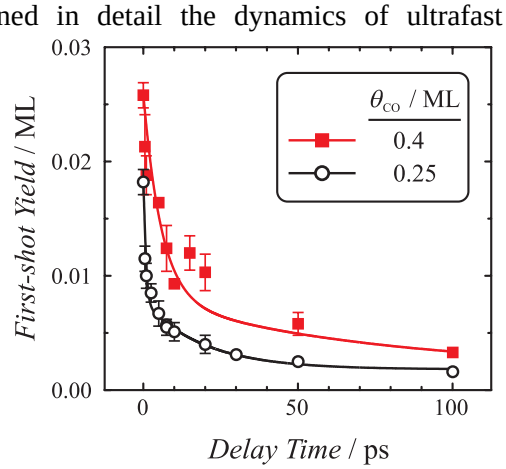


**FIG. 1.** Two-pulse correlation measurements of the ejected $CO_2$ photoproduct from CO+O/Pd(111) at initial CO coverages of 0.25 ML (circles) and 0.4 ML (squares) deposited on the O-(2×2)/Pd(111) (0.25 ML O) surface.

Our studies of the ultrafast photooxidation of CO in mixed monolayers of O and CO represent a major step forward in developing our capabilities to time-resolve surface reactions. Ultrafast photoexcitation of mixed CO + O adlayers results in the efficient photooxidation of CO. Fig. 1 shows 2PC measurements of the desorbing $CO_2$ photoproduct from

initial CO coverages corresponding to ~1:1 and ~2:1 CO:O mixtures, where the initial surface concentration of O is held fixed at 0.25 ML. There are three remarkable features in this data. First, the 2PC relaxation times are quite short, particularly at the lower coverage, where the response time is subpicosecond, clearly indicating that the oxidation is the result of electron-mediated surface–adsorbate energy transfer. Furthermore, these ultrafast relaxation times are consistent with the reaction taking place in the mixed phase, in contradistinction to conditions that prevail during slow thermal excitation where the reactants are known to phase segregate. This suggests that our approach provides the means to take "snapshots" of the reaction by measuring the dynamics from well-defined initial surface structures.

Second, the photooxidation percentage yield is high: the first-shot yield at zero delay represents desorption of ~0.02 ML-equivalents of $CO_2$, compared to a total yield (of desorbed plus reacted CO) of ~0.09 ML. Thus the oxidized percentage of the total desorption yield is ~20%, roughly an order of magnitude greater than prior ultrafast reaction measurements for Ru(001) under similar conditions, and approximately one-third to one-half that observed in TPR/D for the very efficient thermally-activated oxidation on Pd(111) (Fig. 2). The high efficiency of the $CO_2$ channel opens the possibility of time-domain measurements of surface dynamics by time-resolved pump-probe surface spectroscopy.

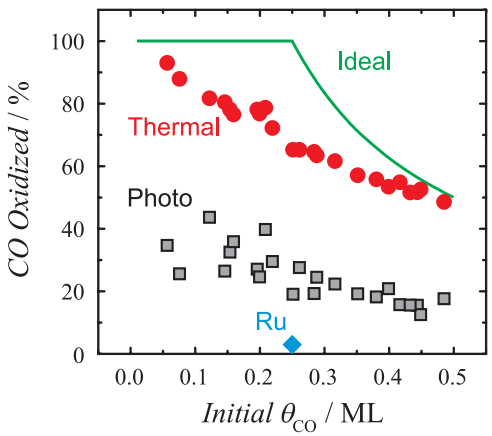


**FIG. 2.** The oxidation of CO on Pd(111): percent theoretical yield (solid line); thermal reaction percent yield in TPD/R experiments (circles); and the percent of desorbed flux that results from surface photooxidation following initiation by a single subpicosecond NIR pulse at ~20 mJ cm$^{-2}$. On Ru(001), subpicosecond photo-oxidation is markedly less efficient (diamond, as measured by M. Bonn *et al.*). The initial O atom coverage is 0.25 ML for Pd(111) and 0.5 ML for Ru(001).

Finally, the 2PC decay time is strongly coverage dependent (Fig. 1), an effect which, to the best of our knowledge, has not been observed previously. We attribute this dependence to a decrease in the CO–Pd coupling strength with increasing CO coverage, and a decrease in the reaction activation energy due to the occupation of top sites in the 2:1 mixture whereas in the 1:1 mixture only hcp sites are occupied.

***Pump-Probe Studies of Photodesorption and Photooxidation on $TiO_2$(110) Surfaces.*** We are currently investigating photoinduced reactions on single crystal $TiO_2$(110) surfaces with the goal of understanding the excitation and energy transfer processes important in photooxidation reactions. Adsorbed molecular oxygen is linked to the photooxidation activity of $TiO_2$ surfaces, however, fundamental questions remain as to the nature of the $O_2$ adsorption sites and the mechanism for desorption and/or reaction. Our initial studies focused on the photodynamics of adsorbed $O_2$ on reduced surfaces of $TiO_2$(110) using laser pump-probe techniques to measure the kinetic energy distributions of desorbed $O_2$ molecules as a function of UV photoexcitation energy and surface temperature. The experiments make use of a one-photon ionization scheme for $O_2$ detection with very high sensitivity recently developed in our laboratory. Pump-delayed probe experiments show that the velocity distributions of the photodesorbed $O_2$ molecules are trimodal, with most probable kinetic energies of 0.35 eV, 0.1 eV and near zero energy, independent of UV photoexcitation energy. The latter result is consistent with a substrate-mediated mechanism in which $O_2$ desorption results from capture of a hole ($h^+$) by an adsorbed $O_2^-/O_2^{2-}$ species, and not with direct photoexcitation of an $O_2$–$TiO_2$ surface complex as suggested in recent theoretical studies. The velocity distributions of the two "fast" channels are tentatively assigned to two distinct $O_2^-$ binding sites associated with surface defects (bridging oxygen vacancies and near surface $Ti^{3+}$ interstitials) whereas the slow channel is attributed to trapping of photoexcited $O_2$ prior to desorption.

More recently, we have used pump-probe techniques to examine the final state distributions of the gas-phase products resulting from the photooxidation of small organic molecules on $TiO_2(110)$. This work is motivated by the growing number of applications of $TiO_2$ in UV-induced photodegradation of air and water borne pollutants. In addition, recent experiments by Henderson (PNNL) using a UV lamp source showed that the photooxidation of small ketones on the $TiO_2(110)$ surface results in the direct ejection of radical species into the gas phase. Initial studies of acetone ($CH_3COCH_3$) and butanone ($CH_3CH_2COCH_3$) co-adsorbed with $O_2$ on $TiO_2(110)$ show that the primary gas-phase products of photooxidation ($h\upsilon$ = 3.70 eV) are methyl radical ($CH_3^{\bullet}$) and ethyl radical ($C_2H_5^{\bullet}$) with average translational energies of 0.15 eV and 0.05 eV, respectively. In the case of butanone, we used a variety of VUV ionization wavelengths to show that other $C_2$ hydrocarbon products (ethane or ethylene) proposed in previous studies are not formed to any significant extent. The methyl radical translational energy distribution is markedly different than that observed in gas-phase photolysis of acetone, and can be empirically fit to a "fast" and a "slow" component (see Fig. 3). The "fast" component is attributed to a prompt intramolecular fragmentation process of the molecular precursor (surface diolate species) and the "slow" component may be associated with methyl internal energy or a second fragmentation channel.

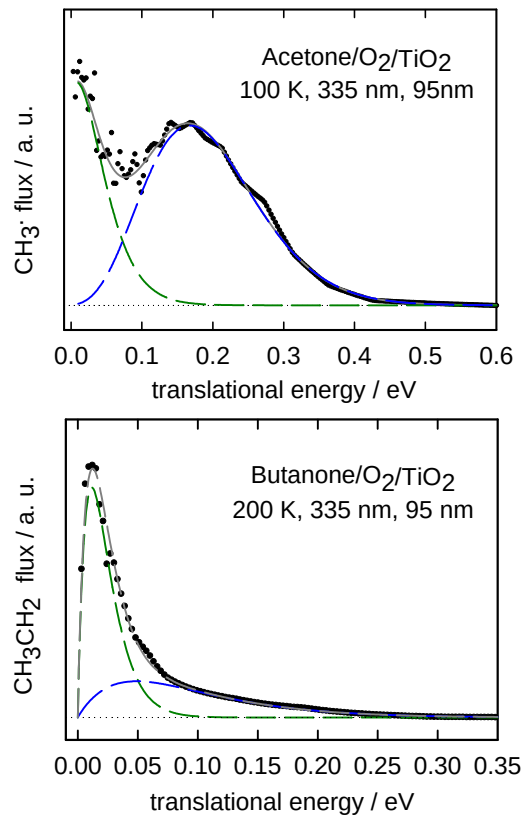


**Fig. 3:** Translational energy distributions of methyl radical (top) and ethyl radical (below) from photooxidation of acetone and butanone, respectively, on $TiO_2(110)$. Excitation wavelength: 335 nm; VUV detection wavelength: 95 nm.

***Structure and Reactivity of Transition Metal Compounds Clusters.*** We are using mass-selected cluster ion beams and surface science techniques to investigate the physical and chemical properties of transition metal compound clusters (*e.g.*, metal carbides, oxides and sulfides) deposited onto solid surfaces which are models for supported catalysts. In addition to providing precise knowledge of the cluster size (mass), stoichiometry and coverage, cluster beam deposition is particularly useful for investigations of small nanoclusters, 1–2 nm (< 200 atoms), where the geometric and electronic structure is evolving from molecular clusters to that of the extended solid. Work this year focused on the development of an ultrafast Ti:Sappire laser system for performing two photon photoemission (2PPE) measurements of size-selected nanoclusters supported on metal oxide substrates. The large band gap and work function of oxides provides an effective energy "window" within which the electronic structure of the supported nanoparticles may be observed by 2PPE with little interference from states associated with the underlying support. In particular, we are interested in probing the electronic structure and time-resolved dynamics of small $M_xS_y$ (M = Mo, W; x/y = 3/7, 4/6, 5/7, 6/8, 7/10, 8/12) nanoclusters which are expected to exhibit size dependent HOMO-LUMO gaps that correlate with reactivity.

### 3. Future Plans

Our planned work develops three interlinked themes: (i) the chemistry of supported nanoparticles and nanoclusters, (ii) the exploration of chemical dynamics on ultrafast timescales, and (iii) the photoinduced

chemistry of molecular adsorbates. The investigations are motivated by the fundamental need to connect chemical reactivity to chemical dynamics in systems of relevance to catalytic processes—in particular metal and metal-compound nanoparticles and nanoclusters supported on oxide substrates. They are also motivated by fundamental questions of physical changes in the electronic and phonon structure of nanoparticles and their coupling to adsorbates and to the nonmetallic support that may alter dynamics associated with energy flow and reactive processes.

Ultrafast experiments investigating the dynamics of photoinduced desorption from nanoparticles will address development of a fundamental understanding of the changes in this simplest surface reaction (desorption) as the size of the metal substrate material is reduced from macroscopic (planar bulk surfaces) to the nanoscale. Size-dependent chemical dynamics will also be the focus of experiments using our new cluster beam source to prepare a range of supported, size-selected nanoclusters for structure and reactivity studies. The latter will be complemented by ultrafast two-photon photoemission experiments to investigate the electronic structure and dynamics of the nanoclusters and molecular resonances involved in chemistry at their surfaces. Future studies of photoinduced processes on titania surfaces will work to resolve open questions regarding the photodesorption dynamics of molecular oxygen and explore the use of pump-probe techniques for elucidating molecular photooxidation mechanisms on titania and other oxide photocatalysts.

**DOE-Sponsored Research Publications (2005–2008)**


1. J.M. Lightstone, M.J. Patterson and M.G. White, "Reactivity of the $M_4S_6^+$ (M-Mo, W) cluster with CO and $NH_3$ in the gas-phase," *Chem. Phys. Lett.*, **413**, 429 (2005).
2. P. Liu, J.M. Lightstone, M.J. Patterson, J.A. Rodriguez, J.T. Muckerman and M.G. White, "Gas-phase interaction of thiophene with the $Ti_8C_{12}^+$ and $Ti_8C_{12}$ met-car clusters," *J. Phys. Chem. B*, **110**, 7449 (2006).
3. J. M. Lightstone, M. J. Patterson, P. Liu, and M. G. White, "Gas-phase reactivity of the $Ti_8C_{12}^+$ Met-car with triatomic sulfur-containing molecules: $CS_2$, SCO, and $SO_2$," *J. Phys. Chem. A*, **110**, 3505 (2006).
4. N. Camillone III, T. Pak, K. Adib, K.A. Khan, and R.M. Osgood, Jr., "Tuning molecule-surface interactions with nanometer-thick covalently-bound organic overlayers," *J. Phys. Chem. B*, **110**, 11334 (2006).
5. P. Szymanski, A.L. Harris, N. Camillone III, "Adsorption-state-dependent subpicosecond photoinduced desorption dynamics," *J. Chem. Phys.*, **126**, 214709 (2007). (Note: Selected for the July 2007 issue of the *Virtual Journal of Ultrafast Science*.)
6. P. Szymanski, A.L. Harris, N. Camillone III, "Temperature-dependent electron-mediated coupling in subpicosecond photoinduced desorption," *Surf. Sci.*, **601**, 3335 (2007).
7. P. Szymanski, A.L. Harris, N. Camillone III, "Temperature-dependent femtosecond photoinduced desorption in CO/Pd(111)," *J. Phys. Chem. A*, **111**, 12524 (2007).
8. W. Wen, J. Liu, M. G. White, N. Marinkovic, J. C. Hanson, J. A. Rodriguez, "*In situ* time-resolved characterization of novel Cu-$MoO_2$ catalysts during the water-gas shift reaction," *Catal. Lett.* **113**, 1 (2007).
9. M. Lightstone, M. Patterson, J. Lofaro, P. Liu and M. G. White, "Characterization and reactivity of the $Mo_4S_6^+$ cluster deposited on Au(111)," *J. Phys. Chem. C*, **112** , 11495 (2008).
10. P. Szymanski, A.L. Harris, N. Camillone III, "Efficient subpicosecond photoinduced surface chemistry: The ultrafast photooxidation of CO on palladium," *J. Phys. Chem. C*, **accepted** (2008).


---

[a] Principal Investigator; [b] Contributing Investigator

# Ionic Liquids: Radiation Chemistry, Solvation Dynamics and Reactivity Patterns

James F. Wishart
Chemistry Department, Brookhaven National Laboratory, Upton, NY 11973-5000
wishart@bnl.gov

**Program Definition**

Ionic liquids (ILs) are a rapidly expanding family of condensed-phase media with important applications in energy production, nuclear fuel and waste processing, improving the efficiency and safety of industrial chemical processes, and pollution prevention. ILs are generally nonvolatile, noncombustible, highly conductive, recyclable and capable of dissolving a wide variety of materials. They are finding new uses in chemical synthesis, catalysis, separations chemistry, electrochemistry and other areas. Ionic liquids have dramatically different properties compared to conventional molecular solvents, and they provide a new and unusual environment to test our theoretical understanding of charge transfer and other reactions. We are interested in how IL properties influence physical and dynamical processes that determine the stability and lifetimes of reactive intermediates and thereby affect the courses of chemical reactions and product distributions.

Successful use of ionic liquids in radiation-filled environments, where their safety advantages could be significant, requires an understanding of ionic liquid radiation chemistry. For example, characterizing the primary steps of IL radiolysis will reveal radiolytic degradation pathways and suggest ways to prevent them or mitigate their effects on the properties of the material. An understanding of ionic liquid radiation chemistry will also facilitate pulse radiolysis studies of general chemical reactivity in ILs, which will aid in the development of applications listed above. Very early in our radiolysis studies it became evident that slow solvation dynamics of the excess electron in ILs (which vary over a wide viscosity range) increases the importance of pre-solvated electron reactivity and consequently alters product distributions. Parallel studies of IL solvation phenomena using coumarin-153 dynamic Stokes shifts and polarization anisotropy decay rates are done to compare with electron solvation studies and to evaluate the influence of ILs on charge transport processes.

***Methods***. Picosecond pulse radiolysis studies at BNL's Laser-Electron Accelerator Facility (LEAF) are used to identify reactive species in ionic liquids and measure their solvation and reaction rates. We and our collaborators (R. Engel (Queens College, CUNY) and S. Lall-Ramnarine, (Queensborough CC, CUNY)) develop and characterize new ionic liquids specifically designed for our radiolysis and solvation dynamics studies. IL solvation and rotational dynamics are measured by TCSPC and fluorescence upconversion measurements in the laboratory of E. W. Castner at Rutgers Univ. Investigations of radical species in irradiated ILs are carried out at ANL by I. Shkrob and S. Chemerisov using EPR spectroscopy. Diffusion rates are obtained by PGSE NMR in S. Greenbaum's lab at Hunter College, CUNY and S. Chung's lab at William Patterson U. Professor Mark Kobrak of CUNY Brooklyn College performs molecular dynamics simulations of solvation processes. A collaboration with M. Dietz at U. Wisc. Milwaukee is centered around the properties and radiolytic behavior of ionic liquids for nuclear separations. Collaborations with C. Reed (UC Riverside), D. Gabel (U. Bremen) and J. Davis (U. South Alabama) are aimed at characterizing the radiolytic and other properties of borated ionic liquids, which could be used to make fissile material separations processes inherently safe from criticality accidents.

**Recent Progress**

***EPR studies of radical species in ILs.*** Since our standard technique of transient optical detection cannot detect many important intermediates that lack strong absorption features, particularly hole-derived species, we have begun to use EPR to identify ionization products in ILs [11]. Radical intermediates were generated by radiolysis or photoionization of low-temperature ionic liquid glasses composed of ammonium, phosphonium, pyrrolidinium, and imidazolium cations and bis(triflyl)amide, dicyanamide, and bis(oxalato)borate anions. Large yields of terminal and penultimate C-centered radicals are observed in the aliphatic chains of the phosphonium, ammonium and pyrrolidinium cations, but not for imidazolium cation (where the ring is the predominant site of oxidation). This pattern is indicative of efficient deprotonation of a hole trapped on the parent cation (the radical dication) that competes with rapid electron transfer from a nearby anion. This charge transfer leads to the formation of stable N- or

O-centered radicals; the dissociation of parent anions is a minor pathway. Production of $\bullet CF_3$ from $(CF_3SO_2)_2N^-$ evidently proceeds primarily through an excited state of the anion rather than via ionization.

***Radiolysis of simulated IL-based nuclear extraction systems.*** Addition of 10-40 wt% of trialkylphosphate (a common agent for nuclear separations) has relatively little effect on the fragmentation of the ILs. The yield of the alkyl radical fragment generated by dissociative electron attachment to the trialkylphosphate is < 4% of the yield of the radical fragments derived from the IL solvent. The currently used hydrocarbon/tributylphosphate extraction systems involve a highly resistant, structurally simple solvent (like kerosene) that efficiently transfers charge and energy to the functional solute (tributylphosphate), resulting in the fragmentation of the latter and degradation of extraction efficiency. The results suggest a different paradigm for radiation protection: a solvent in which the damage transfer is reversed. Such a solvent actively protects the functional solute in a sacrificial way, but overall radiolytic damage is still kept to a low level by the radiolytic properties of the solvent [11] (in collaboration with I. Shkrob and S. Chemerisov, ANL).

***Charge transfer in ionic liquids - effects on driving force/thermodynamics, reorganization energy and reorganizational dynamics.*** Charge transfer processes in ionic liquid (IL) media are important to understand because of their applications in solar photoelectrochemical cells, electrochromic displays, fuel cells, batteries and other advanced devices where the properties of ILs provide advantages. Our program to investigate the effects of ionic liquids on intramolecular charge transfer reactions continued with the development of a new peptide-bridged donor acceptor complex incorporating coumarin 343 and the excited-state electron acceptor and dimethylphenylenediamine as the donor (C343-$(pro)_n$-DMPD). This complex was chosen over the previously studied system using a tetramethylrhodamine acceptor because of the latter chromophore's conformational lability and resultant complicated photodynamics. The C343 chromophore has several advantages, the first being that it is conformationally rigid. The photophysics of the structurally similar coumarin 153 have been well characterized, and it has been used previously to measure solvation dynamics in many ionic liquids, as well as molecular solvents, by means of the emission Stokes shift. Solvation dynamics in ionic liquids are known to be slower than in molecular solvents and to have components that are spread across picosecond to nanosecond time scales. To the extent that the solvation process extends into the time scale for electron transfer (ET), it affects the thermodynamics and reorganization energy of the ET process, resulting in complicated kinetics that need to be understood in order to exploit the advantages of ILs in the above-mentioned applications. The emission Stokes shift of the C343 chromophore provides an internal gauge of the solvation process while at the same time participating in the electron transfer reaction. In preliminary work, the subject compounds have been prepared and studies in methanol (where solvation is much faster than ET) have indicated an electron transfer process with straightforward kinetics ($\tau$ ~ 470 ps at 21 °C for C343-$(pro)_1$-DMPD). (in collaboration with H. Y. Lee, E. W. Castner, S. S. Isied, and Y. Issa, Rutgers Univ.)

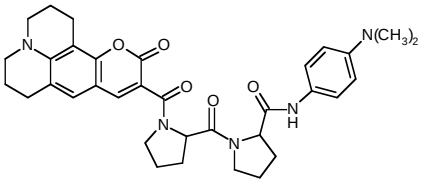

C343-$(pro)_2$-DMPD

***Ultrafast Single-Shot radiolysis of ionic liquids.*** UFSS experiments were done on the ionic liquids $C_4$mpyr $NTf_2$ and $MeBu_3N$ $NTf_2$ in neat form and with various concentrations of several electron scavengers. Data collected at 900 nm with increasing benzophenone concentrations shows the disappearance of the spectral shift associated with the electron solvation process, indicating highly effective scavenging of pre-solvated electrons. Additional results will be presented.

**Future Plans**

***Electron solvation and reactivity.*** The competition between the electron solvation and electron capture processes in ionic liquids will be explored to test the validity of pre-solvated electron scavenging mechanisms advanced in the literature. Electron solvation dynamics in several families of ILs will be measured by pulse-probe radiolysis and ultrafast single-slot spectroscopy (UFSS) developed at BNL by Andrew Cook.. Solvation phenomena in ionic liquids will also be measured by observing the time-resolved absorption spectral shift of highly solvatochromic benzophenone anion and time-resolved fluorescence Stokes shifts of solvatochromic dyes such as coumarin 153. Our experimental work will be supported by molecular dynamics simulations performed by Prof.

Mark Kobrak of Brooklyn College, CUNY. Subsequently, scavengers will be added to measure the kinetics of pre-solvated electron capture. It is well known from work in molecular solvents that many scavengers, for example $SeO_4^{2-}$, have widely different reactivity profiles towards pre-solvated and solvated electrons. We have begun quantitative measurement of the scavenging profiles of benzophenone, $SeO_4^{2-}$, $NO_3^-$, and $Cd^{2+}$ using the UFSS detection system. By quantitative measurement of the scavenging profiles of many reactants, we seek to provide a mechanistic basis for understanding scavenging profiles that can be applied to real-world applications such as predicting radiolytic product distributions during the processing of radioactive materials.

***The influence of ionic liquid on charge transfer reactions.*** Pulse radiolysis and flash photolysis will be used to study how ionic liquids affect electron-transport reactions related to solar energy photoconversion systems, where their characteristics may prove valuable. IL-based photoelectrochemical cells have already been reported. Focus areas will be the combined effects of ionic solvation and slow solvent relaxation on the energy landscape of charge transport, including specific counterion effects depending on the ionic liquid, and the influence of the lattice-like structure of ionic liquids on the distance dependence of electron transport reactions.

The studies of ionic liquid environment effects on photoinduced electron transfer in the C343-$(pro)_n$-DMPD system will be continued with extensive measurements on the n = 1, 2, 3 systems in several ionic liquids and representative molecular solvents (methanol, water, acetonitrile, dichloromethane). Electrochemistry will be used to estimate the reaction driving forces and kinetic measurements will be used to obtain activation parameters (including pressure dependence) for the ET systems in the various ionic and molecular liquids. The ionic liquids will be selected so as to vary the solvation time scales across the electron transfer regime, but the early work will focus on low-viscosity, quick-relaxing ionic liquids that most resemble molecular solvents. Conformational and electronic structure calculations will be performed on the donor-acceptor systems to aid interpretation of the experimental results. This detailed information will allow elucidation of ionic liquid effects and quantitative comparison of the differences between ionic and molecular liquids. In the second year, electron transfer studies on the C343-$(pro)_n$-DMPD system will be carried forward into ionic liquids that are more viscous and have solvation dynamics on longer timescales than electron transfer in order to examine the influence of dynamics on the electron transfer process, a long-sought but difficult to achieve goal when working with molecular solvents. The results with the C343 chromophore will be supplemented by studies using the system we studied previously in molecular solvents (*J. Phys. Chem. B.* **2007**, *111*, 6878) with pyrenesulfonate in place of C343. The dipole change in the pyrene excited state is much smaller than for C343, making the Stokes shift negligible and providing another vantage point from which to examine the ET process. (in collaboration with H. Y. Lee and E. W. Castner, Rutgers Univ.)

***EXAFS studies of structure and reaction dynamics in ionic liquids.*** In collaboration with R. Crowell and D. Polyanskiy, we are using Br EXAFS to study IL structure and $Br^-$ ion solvation environment in neat and diluted bromide ionic liquids and the effect of solutes. We will use photoionization coupled with time-resolved EXAFS to probe the solvation dynamics of $Br^0$ atoms in ILs and the effect of the ionic liquid environment on the $Br^- + Br^0 \rightarrow Br_2^-$ reaction. The results can be applied to understanding related iodide systems of interest in solar photoconversion.

**Publications on ionic liquids**


1. *Effects of Functional Group Substitution on Electron Spectra and Solvation Dynamics in a Family of Ionic Liquids* J. F. Wishart, S. I. Lall-Ramnarine, R. Raju, A. Scumpia, S. Bellevue, R. Ragbir, and R. Engel *Radiat. Phys. Chem.* **72**, 99-104 (2005).
2. *Dynamics of Fast Reactions in Ionic Liquids* A. M. Funston and J. F. Wishart in "Ionic Liquids IIIA: Fundamentals, Progress, Challenges and Opportunities" Rogers, R. D. and Seddon, K. R., Eds.; *ACS Symp. Ser.* **901**, Ch. 8, American Chemical Society, Washington, DC, 2005. (ISBN 0-84123-893-6).
3. *Ultrafast Dynamics of Pyrrolidinium Cation Ionic Liquids* H. Shirota, A. M. Funston, J. F. Wishart, E. W. Castner, Jr. *J. Chem. Phys.* **122**, 184512 (2005), selected for the *Virtual Journal of Ultrafast Science* (6/05).
4. *Radiation Chemistry of Ionic Liquids* J. F. Wishart, A. M. Funston, and T. Szreder in "Molten Salts XIV, Proceedings of the 2004 Joint International Meeting of the Electrochemical Society, Honolulu, HI, 2004", R. A. Mantz, et al., Eds.; The Electrochemical Society, Pennington, NJ, 2006, pp. 802-813. (ISBN 1-56677-514-0)
5. *Tetraalkylphosphonium polyoxometalates: electroactive, "task-specific" ionic liquids* P. G. Rickert, M. R. Antonio, M. A. Firestone, K.-A. Kubatko, T. Szreder, J. F. Wishart, and M. L. Dietz *Dalton Trans.* **2006**, 529-531 (2006).

6. *The Physical Chemistry of Ionic Liquids (Editorial for Special Issue)* J. F. Wishart, and E. W. Castner, *J. Phys. Chem. B*, **111**, 4639-4640 (2007). *Second Most-Accessed Article, *J. Phys. Chem. B*, April-June, 2007, 14th for the entire year.
7. *Tetraalkylphosphonium Polyoxometalate Ionic Liquids: Novel, Organic-Inorganic Hybrid Materials*, P. G. Rickert, M. P. Antonio, M. A. Firestone, K.-A. Kubatko, T. Szreder, J. F. Wishart, and M. L. Dietz, *J. Phys. Chem. B*, **111**, 4685-4692 (2007) DOI:10.1021/jp0671751.
8. *Intermolecular Interactions and Dynamics of Room Temperature Ionic Liquids that have Silyl- and Siloxy-Substituted Imidazolium Cations* H. Shirota, J. F. Wishart, and E. W. Castner, Jr., *J. Phys. Chem. B*, **111**, 4819-4829 (2007) DOI: 10.1021/jp067126o. *17th Most-Cited Article for 2007, *J. Phys. Chem. B*.
9. *Nuclear Magnetic Resonance Study of the Dynamics of Imidazolium Ionic Liquids with -$CH_2Si(CH_3)_3$ vs -$CH_2C(CH_3)_3$ Substituents* S. H. Chung, R. Lopato, S. G. Greenbaum, H. Shirota, E. W. Castner, Jr. and J. F. Wishart, *J. Phys. Chem. B*, **111**, 4885-4893 (2007) DOI:10.1021/jp071755w.
10. *Fluorescence Probing of Temperature-Dependent Dynamics and Friction in Ionic Liquid Local Environments* A. M. Funston, T. A. Fadeeva, J. F. Wishart, and E. W. Castner, *J. Phys. Chem. B*, **111**, 4963-4977 (2007) DOI:10.1021/jp068298o. *Fifth Most-Cited Article for 2007, *J. Phys. Chem. B*.
11. *The Initial Stages of Radiation Damage in Ionic Liquids and Ionic Liquid-Based Extraction Systems* I. A. Shkrob, S. D. Chemerisov, and J. F. Wishart, *J. Phys. Chem. B*, **111**, 11786-11793 (2007). DOI: 10.1021/jp073619x.
12. *Intermolecular Dynamics, Interactions and Solvation in Ionic Liquids* E. W. Castner, Jr., J. F. Wishart, and H. Shirota, *Acc. Chem. Res.* **40**, 1217-1227 (2007).
13. *Physical Properties of Ionic Liquids Consisting of the 1-Butyl-3-Methylimidazolium Cation with Various Anions and the Bis(trifluoromethylsulfonyl)imide Anion with Various Cations* H. Jin, B. O'Hare, J. Dong, S. Arzhantsev, G. A. Baker, J. F. Wishart, A. J. Benesi, and M. Maroncelli *J. Phys. Chem. B* **112**, 81-92 (2008).
14. *Trialkylammonio-Dodecaborates: Anions for Ionic Liquids with Potassium, Lithium and Proton as Cations* E. Justus, K. Rischka, J. F. Wishart, K. Werner and D. Gabel, *Chem. Eur. J.*, **14**, 1918-1923 (2008).
15. *Photo-detrapping of solvated electrons in an ionic liquid* K. Takahashi, K. Suda, T. Seto, Y. Katsumura, R. Katoh, R. A. Crowell, J. F. Wishart, *Radiat. Phys. Chem.*, accepted.

**Publications on other subjects**

16. *Convergence of Spectroscopic and Kinetic Electron Transfer Parameters for Mixed-Valence Binuclear Dipyridylamide Ruthenium Ammine Complexes* A. J. Distefano, J. F. Wishart, and S. S. Isied *Coord. Chem. Rev.*, **249**, 507-516 (2005).
17. *Radiolysis with RF Photoinjectors: Supercritical Xenon Chemistry* J. F. Wishart in "Femtosecond Beam Science" Uesaka, M., Ed.; Imperial College Press, London, 2005, pp. 351-356. (ISBN 1-86094-343-8).
18. *Reactivity of Acid Generators for Chemically Amplified Resists with Low-Energy Electrons* A. Nakano, T. Kozawa, S. Tagawa, T. Szreder, J. F. Wishart, T. Kai and T. Shimokawa *Jpn. J. Appl. Phys.*, **45**, L197-L200 (2006).
19. *Pulse radiolysis and steady-state analyses of the reaction between hydroethidine and superoxide and other oxidants* J. Zielonka, T. Sarna, J. E. Roberts, J. F. Wishart, B. Kalyanaraman, *Arch. Biochem. Biophys.*, **456**, 39-47 (2006).
20. *Conformational Analysis of the Electron Transfer Kinetics across Oligoproline Peptides Using* N,N-*dimethyl-1,4-benzenediamine Donors and Pyrene-1-sulfonyl Acceptors* J. B. Issa, A. S. Salameh, E. W. Castner, Jr., J. F. Wishart and S. S. Isied, *J. Phys. Chem. B*, **111**, 6878-6886 (2007).
21. *Tools for radiolysis studies*, J. F. Wishart in "Radiation chemistry: from basics to applications in material and life sciences" Spotheim-Maurizot, M., Douki, T., Mostafavi, M., and Belloni, J., Eds.; L'Actualité Chimique Livres, Paris, (2008) Ch. 2, pp. 17-33.

# Electronically Non-Adiabatic Interactions in Molecule-Metal Surface Scattering: Can We Trust the Born-Oppenheimer Approximation in Surface Chemistry, DE-FG02-03ER15441

*Alec M. Wodtke: Dept. of Chemistry and Biochemistry, University of California, Santa Barbara, CA 93106 USA; wodtke@chem.ucsb.edu*
*Daniel J. Auerbach: Gas Reaction Technologies, 861 Ward Dr., Santa Barbara, CA 93111, USA: auerbach@grt-inc.com*

## PROGRAM SCOPE

There are a number of experimental observations, some with coordinated theoretical study, that strongly suggest that the breakdown of the Born-Oppenheimer Approximation (BOA) can be an important aspect of the dynamics of molecules interacting with metal and semiconductor surfaces, the essential atomistic foundation of heterogeneous catalysis. Unfortunately, the best evidence we have and those observations that can best be compared to theory arise from a relatively small number of experiments on a relatively small number of molecules on small number of metal surfaces. It is quite difficult to extrapolate from these observations to a generalized knowledge and understanding of what chemical trends might persist for electronically non-adiabatic interactions. The purpose of this research project is to perform a series of well controlled experiments, by which a wider range of observations can be obtained that will provide a chemically diverse benchmark for theories of electronically non-adiabatic behavior. In this way, we hope to contribute to the development of a predictive understanding of when and when not electronically adiabatic potential energy surfaces is suitable for the simulation of reactions at metal interfaces.

## RECENT PROGRESS

We scattered vibrationally excited HCl(v=2,J=1) from Au(111) at incidence energies between 0.28 and 1.27 eV. Narrow (FWHM < 30$^o$) angular distributions as well as a strong dependence of final translational energy on initial translational energy show that energy transfer takes place through a direct scattering mechanism. High resolution TOF measurements revealed the translational inelasticity (translation to surface degrees of freedom) for vibrationally elastic (v=2→2) and inelastic (v=2→1) channels. For both channels ~56% of the incidence energy of translation is transferred to the surface. This reaches – or even slightly surpasses – a single-atom hard cube impulive collision limit also known in the literature as the Baule limit for mechanical energy transfer. One possible explanation of this observation is that the excitation of electron-hole pairs contributes significantly to the loss of HCl translational energy in collisions with Au(111). This suggests accurate theoretical trapping probabilities for HCl on Au(111) require inclusion of electron hole-pair excitation.

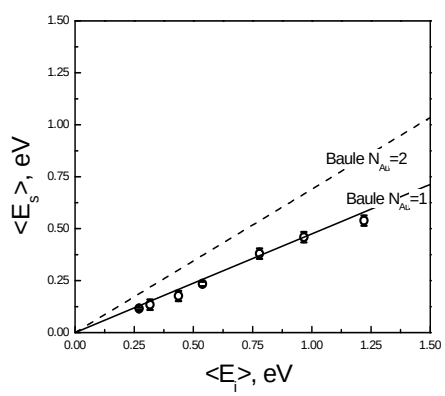


*Figure 1. Comparison to the binary-collision limit. Final translational energy for scattered HCl: vibrationally elastic (v=2→2) (open circles). All results shown here are for final J=5 and $T_S$ = 300K. The solid line shows the translational recoil expected from an zero impact-parameter elastic collision of an HCl molecule with an isolated Au atom. The dashed line shows results expected by doubling the effective mass of the Au atom.*

For vibrational relaxation channels, only 26% of the released vibrational energy appears as outgoing translation, while 74% couples to the surface. By comparison to previous work

where HCl(v=2) was scattered from an insulator (MgO), we conclude that vibrational relaxation of HCl(v=2) on Au occurs through an electronically nonadiabatic mechanism. Our observations show that the *translational spectator view* used to describe electronically nonadiabatic vibrational energy transfer at metal surfaces is only approximately correct. Possible mechanisms by which vibrational energy may be channeled into translation in electronically nonadiabatic vibrational relaxation were described in terms of transient charge transfer.

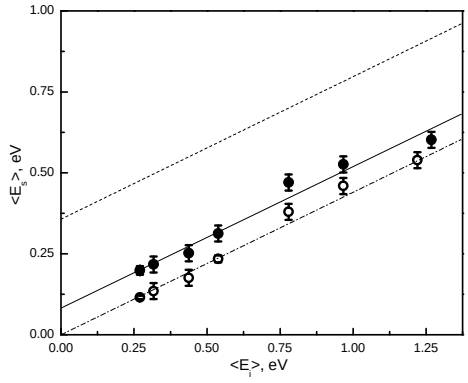


*Figure 2. Final translational energy for scattered HCl. Vibrationally elastic (v=2→2) (open circles) and inelastic (v=2→1) (closed circles) are shown. The dash-dotted line is a linear fit for vibrationally elastic (v=2→2) channel - $\langle E_S \rangle = 0.44 \langle E_I \rangle$; the solid line is a linear fit for vibrationally inelastic (v=2→1) scattering - $\langle E_S \rangle = 0.44 \langle E_I \rangle + 0.0821$ eV. The dashed line represents the simplistic "complete V-T" expectation. All results shown here are for final J=5 and surface temperature of 300 K.*

The experiments just described provide the translational inelasticity for vibrationally excited states of HCl. The implication is that trapping of the ground vibrational state of HCl to Au(111) would behave similarly. The behavior of the ground vibrational state is particularly important as comparison to theoretical work are most straightforward for the ground vibrational state and it is the ground state that is present in most real-world situations. Recently we have succeeded in obtaining similar results to that of Fig. 2 for the ground vibrational state of HCl. We find that the behavior is identical for ground vibrational state HCl.

Taken together, the results obtained in this work provide an important benchmark for future theoretical calculations that attempt to include electronically nonadiabatic influences on energy transfer at surfaces.

## FUTURE WORK

State-to-state TOF measurements provide a favorable means of observing translational (and vibrational) inelasticity and the combination of IR overtone pumping with REMPI detection can be applied to a wide variety of molecules. We already have preliminary results on the translational inelasticity of NO in collisions with Au(111). Here NO(v=0→3) overtone excitation is used in combination with 1+1 REMPI through the $A(^2\Sigma^+)$ state. The outcome of the HCl study described above also makes clear that the measurement of the incidence energy dependence of the trapping probability for HCl is an important benchmark for future theoretical work. This poses the question: "Can we accurately describe the molecular adsorption of a simple polar molecule to a metal with our present level of theoretical expertise?"

## PUBLICATIONS RESULTING FROM THIS WORK


1. *Direct translation-to-vibrational energy transfer of HCl on Gold: Measurement of absolute vibrational excitation probabilities, Qin Ran, Daniel Matsiev, Daniel J. Auerbach, Alec M. Wodtke, Proceedings of the 16th International Workshop on Inelastic Ion-Surface Collisions; Nuclear Instruments and Methods in Physics Research, Section B: Beam Interactions with Materials and Atoms (NIMB)* ***258****(1) 1-6 (2007)*

2. *Change of vibrational excitation mechanism in HCl/Au collisions with surface temperature: transition from electronically adiabatic to non-adiabatic behavior, Q. Ran, D. Matsiev, D. J. Auerbach, A. M. Wodtke, Physical Review Letters* ***98****(23), 237601 (2007)*

3. *An advanced molecule-surface scattering instrument for study of vibrational energy transfer in gas-solid collisions, Qin Ran, Daniel Matsiev, Daniel J. Auerbach, Alec M. Wodtke Rev. Sci.*

*Instr.* ***78****, 104104 (2007)*

4. *Energy Transfer and Chemical Dynamics at Solid Surfaces: The Special Role of Charge Transfer, Alec M. Wodtke, Daniel Matsiev, Daniel J. Auerbach, invited review for Progress in Surface Science,* ***83****(3), 167-214 (2008).*

5. *Dynamics of molecule-induced electron emission from surfaces, N. Hendrik Nahler and Alec M. Wodtke invited review article for special 50$^{th}$ Anniversary issue of Molecular Physics (accepted)*

6. *Efficient vibrational and translational excitation of a solid metal surface: State-to-state time-of-flight measurements of HCl (v=2,J=1) scattering from Au (111), Igor Rahinov, Russell Cooper, Cheng Yuan, Xueming Yang, Daniel J. Auerbach, Alec M. Wodtke, J. Chem. Phys. (submitted)*

7. *Translational Energy Transfer for Vibrational Ground State HCl Scattering from Gold, Russell Cooper, Igor Rahinov, Cheng Yuan, Daniel J. Auerbach, Xueming Yang, Alec M. Wodtke, J. Vac. Sci. Tech. A (manuscript in preparation)*

**Development of interaction potentials for the modeling of the vibrational spectra of aqueous environments**

Sotiris S. Xantheas
Chemical & Materials Sciences Division, Pacific Northwest National Laboratory
902 Battelle Blvd., Mail Stop K1-83, Richland, WA 99352
sotiris.xantheas@pnl.gov

The objective of this research effort is to develop a comprehensive understanding of the collective phenomena associated with aqueous solvation. The molecular level details of aqueous environments are central in the understanding of important processes such as reaction and solvation in a variety of homogeneous and heterogeneous systems. The fundamental understanding of the structural, thermodynamic and spectral properties of these systems is relevant to the solvation in aqueous solutions, the structure, reactivity and transport properties of clathrate hydrates, in homogeneous catalysis and in atmospheric processes.

The motivation of the present work stems from the desire to establish the key elements that a classical interaction potential should take into account for a more realistic description of the vibrational spectra of water in different environments. Analysis of the IR bulk water spectra can provide detailed information concerning the underlying structure and dynamics of water in its gas (clusters), liquid and solid phases as well as at interfaces and confined geometries. To this end, a novel scheme used to account for the change of the monomer dipole moment surface (DMS) in condensed environments was implemented to extend the previously developed flexible, polarizable Thole-type model for water [*J. Chem. Phys.* **116**, 5115 (2002); *J. Phys. Chem. A* **110**, 4100 (2006)] in order to account for the accurate description of the vibrational spectra of water in different environments.

The scheme used to account for the altering of the DMS upon solvation is based on the realization that, in the gas phase, the lowest dissociation asymptote of a water molecule corresponds to the homolytic dissociation, viz.

$$H_2O \rightarrow OH^{\bullet} + H^{\bullet}$$

whereas, in the condensed phase, it correlates with the heterolytic products

$$H_2O \rightarrow OH^{-} + H^{+}.$$

The condensed phase behavior is modeled by an "effective," non-linear Dipole Moment Surface (DMS) that is a function of the intramolecular degrees of freedom ($r_{OH_1}, r_{OH_2}, \theta$).

The variation of the "*effective*" charge $\tilde{q}^{H_1}$ with $r_{OH_1}$ and $\theta$ is shown in Fig. 1(a)-(b), for the gas phase, linear (const. charges) and "effective" DMSs, respectively. The "effective"

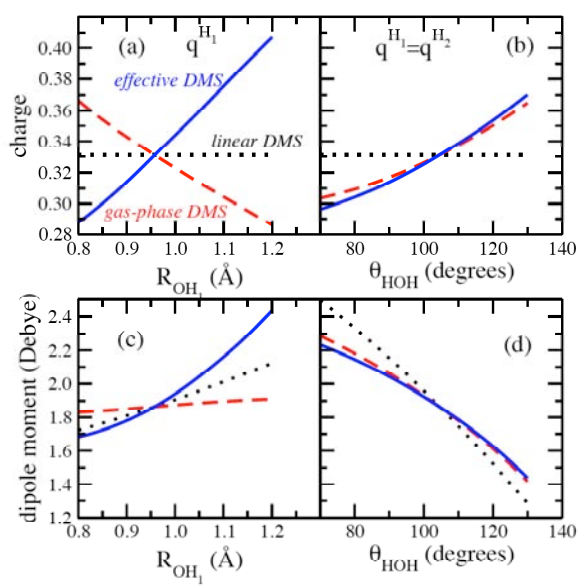


**Figure 1**. Atomic charges and total dipole moment for water monomer. Dotted lines: linear DMS (constant charges). Dashed lines: non-linear DMS (geometry dependent charges). Solid lines: non-linear "effective" DMS.

DMS has the correct behavior of increasing charge on the hydrogen atom upon elongation of $r_{OH_1}$. As in the previous versions of the potential, Thole's method was employed for the treatment of the electrostatic interactions. In contrast to the previous versions of the model that employed three polarizable sites, the current version employs only one polarizable site located on the M-site.

The O-O, O-H and H-H Radial Distribution Functions (RDFs) for liquid water from classical and quantum ($\mathcal{P}$=32 beads) simulations at T=300 K are similar with the ones obtained with version 2.1 of the potential and are within the error bars of the experimentally measured ones. The new potential results to a heat of vaporization of $\Delta H_v (= -\Delta E + k_\beta T)$ =11.4±0.1 kcal/mol and predicts a value of P=-271 atm ($\mathcal{P}$=32 beads) at the experimental density ($\rho$=0.997 gr/cm$^3$) for the pressure, a significant improvement over the previous value of -1800±385 atm obtained with version 2.1. The classical and quantum (NPT) simulations predict that the liquid density at T=298.15 K and P=1 atm is 0.994 gr/cm$^3$ and 1.008 gr/cm$^3$ ($\mathcal{P}$=32 beads). It however yields a different value for the magnitude of quantum effects, which is now just 0.1 kcal/mol as a result of the differences in the description of the intramolecular potential and dipole moment surfaces.

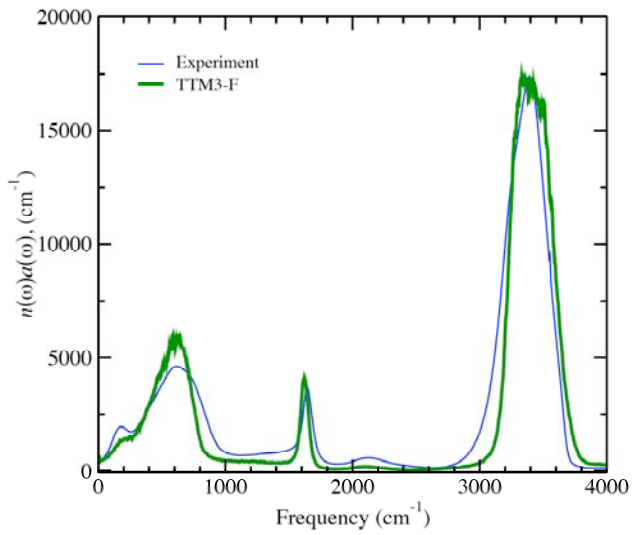


**Figure 2**. The IR spectra of liquid water obtained from classical simulations with the TTM3-F potential. The experimental results are also indicated.

The IR spectra of liquid water computed with the TTM3-F potential during a classical simulation at ρ=0.997 gr/cm$^3$ with the inclusion of harmonic quantum corrections is compared to the experimental results in Figure 2. The shape of the two spectra is similar especially in the 3,000-4,000 cm$^{-1}$ region that corresponds to the OH stretching vibrations and is used to identify the underlying hydrogen bonding network. Results of similar accuracy (with respect to the spectra obtained from electronic structure theory) are also obtained for water clusters up to *n*=20. To the best of our knowledge this is the first time that a classical interaction potential for water yields accurate red-shifts for *both* water clusters and liquid water.

The previous results demonstrate that the inclusion of a phenomenological monomer DMS is capable in capturing the main features of the vibrational spectra of water both in the gas and the liquid phases. We plan to extend the development of the potential to describe interactions between water and metal ($Li^+$, $Na^+$, $K^+$, $Rb^+$, $Cs^+$) as well as halide ($F^-$, $Cl^-$, $Br^-$, $I^-$) ions. Following our previous path in parametrizing to high level electronic structure results, we will perform accurate CCSD(T) calculations for the ion-water interaction using large basis sets in order to obtain results at the complete basis set (CBS) limit for the structure and interaction energy. These data will be supplemented with harmonic and fully anharmonic vibrational calculations (i.e VSCF, CC-VSCF, VCI and approaches based on higher energy derivatives) based on first principles potential energy surfaces to guide our development using the experimentally available spectra for the ion-water clusters. The resulting interaction potentials

will be suitable for use to perform quantum statistical mechanical simulations of aqueous ionic clusters and ions solvated at the bulk and at aqueous interfaces.

We will further use the developed potential to scan and optimize networks that correspond to cluster and 3-dimensional gas hydrate networks which are formed with the pentagonal dodecahedron in the center, such as the cubic structure I (sI) or the hexagonal sH structure. The low-energy cluster networks will be further refined at the DFT and MP2 levels of theory and their periodic clathrate hydrate structures will be subsequently optimized using the TTM3-F interaction potential. These optimal networks will be used as model for the accommodation of host molecules (such as $H_2$, $CH_4$, $CH_3OH$ and $H_2S$) either via empirical potentials or by plane wave, density functional based electronic structure calculations.

*Acknowledgements*: Several valuable discussions with Drs. G. K. Schenter, L. X. Dang, S. M. Kathmann, C. J. Mundy and B. C. Garrett are acknowledged. This research was performed in part using the computational resources of the National Energy Research Supercomputing Center (NERSC) at Lawrence Livermore National Laboratory and the Molecular Sciences Computing Facility (MSCF) at the Environmental Molecular Sciences Laboratory, a national scientific user facility sponsored by the Department of Energy's Office of Biological and Environmental Research located at Pacific Northwest National Laboratory. Battelle operates PNNL for the US Department of Energy.

References to publications of DOE sponsored research (2005-present)

1. B. C. Garrett, D. A. Dixon, *et al* "The Role of Water on Electron-Initiated Processes and Radical Chemistry: Issues and Scientific Advances", *Chemical Reviews* **106**, 355 (2005)
2. G. S. Fanourgakis, E. Aprà, W. A. de Jong, and S. S. Xantheas, "High-level *ab-initio* calculations for the four low-lying families of minima of $(H_2O)_{20}$: II. Spectroscopic signatures of the dodecahedron, fused cubes, face-sharing and edge-sharing pentagonal prisms hydrogen bonding networks", *Journal of Chemical Physics* **122**, 134304 (2005)
3. A. Lagutschenkov, G. S. Fanourgakis, G. Niedner-Schatteburg and S. S. Xantheas, "The spectroscopic signature of the "all-surface" to "internally solvated" structural transition in water clusters in the *n*=17-21 size regime", *Journal of Chemical Physics* **122**, 194310 (2005). Featured in the *Virtual Journal of Biological Physics Research*.
4. S. Hirata, M. Valiev, M. Dupuis and S. S. Xantheas, S. Sugiki and H. Sekino, "Fast electron correlation methods for molecular clusters in the ground and excited states", *Molecular Physics* (R. J. Bartlett special issue) **103**, 2255 (2005)
5. S. S. Xantheas, "Interaction potentials for water from accurate cluster calculations" in *Structure and Bonding: Intermolecular Forces and Clusters II*, Springer-Verlag Berlin Heidelberg, D. J. Wales (Editor), vol. **116**, pp. 119-148 (2005)
6. S. S. Xantheas, W. Roth, I. Fischer, "Competition between van der Waals and Hydrogen Bonding Interactions: The structure of the trans-1-Napthol/$N_2$ cluster", *Journal of Physical Chemistry A* **109**, 9584 (2005)
7. G. S. Fanourgakis and S. S. Xantheas, "The flexible, polarizable, Thole-type interaction potential for water (TTM2-F) revisited" *Journal of Physical Chemistry A* **110**, 4100 (2006)
8. G. S. Fanourgakis and S. S. Xantheas, "The bend angle of water in ice Ih and liquid water: The significance of implementing the non-linear monomer dipole moment surface in classical interaction potentials" *Journal of Chemical Physics* **124**, 174504 (2006). Featured in the *Virtual Journal of Biological Physics Research*.

9. K. A. Ramazan, L. M. Wingen, Y. Miller, G. M. Chaban, R. B. Gerber, S. S. Xantheas and B. J. Finlayson-Pitts, "New Experimental and Theoretical Approach to the Heterogeneous Hydrolysis of $NO_2$: Key Role of Molecular Nitric Acid and Its Complexes", *Journal of Physical Chemistry A* **110**, 6886 (2006)
10. T. A. Blake, S. S. Xantheas, "The Structure, Anharmonic Spectra and Puckering Barrier of Cyclobutane: A Theoretical Study", *Journal of Physical Chemistry A* **110**, 10487 (2006)
11. S .S. Xantheas, "Anharmonic vibrational spectra of hydrogen bonded clusters: Comparison between higher energy derivative and mean-field grid based methods", Roger E. Miller memorial issue (invited), *International Reviews in Physical Chemistry*" **25**, 719 (2006)
12. G. S. Fanourgakis, G. K. Schenter and S. S. Xantheas, "A quantitative account of quantum effects in liquid water", *Journal of Chemical Physics* **125**, 141102 (2006). Featured in the *Virtual Journal of Ultrafast Science*, November 2006
13. S. Bulusu, S. Yoo, E. Aprà, S. S. Xantheas, X. C. Zeng, "The lowest energy structures of water clusters $(H_2O)_{11}$ and $(H_2O)_{13}$", *Journal of Physical Chemistry A* **110**, 11781 (2006)
14. G. S. Fanourgakis, V. Tipparaju, J. Nieplocha and S. S. Xantheas, "An efficient parallelization scheme for molecular dynamics simulations with many-body, flexible, polarizable empirical potentials: Application to water", *Theoretical Chemistry Accounts* **117**, 73 (2007)
15. T. Pankewitz, A. Lagutschenkov, G. Niedner-Schatteburg, S. S. Xantheas, Y.-T. Lee, " The Infrared Spectrum of $NH_4^+(H_2O)$: Evidence for mode specific fragmentation", *Journal of Chemical Physics* **126**, 074307 (2007)
16. M. N. Slipchenko, B. G. Sartakov and A. F. Vilesov, S. S. Xantheas, "A study of NH stretching vibrations in small ammonia clusters by infrared spectroscopy in He droplets and *ab-initio* calculations", Roger E. Miller memorial issue (invited), *Journal of Physical Chemistry A* **111**, 7460 (2007)
17. L. Rubio-Lago, D. Zaouris, Y. Sakellariou, D. Sofikits and T. N. Kitsopoulos, F. Wang and X. Yang, B. Cronin and M. N. R. Ashfold, S. S. Xantheas, "Photofragment slice imaging studies of pyrrole and the Xe···pyrrole cluster", *Journal of Chemical Physics* **127**, 064306 (2007)
18. T. A. Blake, E. D. Glendening, R. L. Sams, S. W. Sharpe and S. S. Xantheas, "High Resolution Infrared Spectroscopy in the 1200 to 1300 $cm^{-1}$ Region and Accurate Theoretical Estimates for the Structure and Ring Puckering Barrier of Perfluorocyclobutane", Thom H. Dunning Jr. Festschrift (invited), *Journal Physical Chemistry A* **111**, 11328 (2007)
19. G. S. Fanourgakis and S. S. Xantheas, "Development of Transferable Interaction Potentials for Water: V. Extension of the flexible, polarizable, Thole-type Model potential (TTM3-F, v. 3.0) to describe the vibrational spectra of water clusters and liquid water", *Journal of Chemical Physics* **128**, 074506 (2008)
20. S. M. Kathmann, G. K. Schenter and S. S. Xantheas, "On the Determination of Monomer Dissociation Energies of Small Water Clusters from Photoionization Experiments", *Journal of Physical Chemistry A*, **112**, 1851 (2008)
21. M. V. Kirov, G. S. Fanourgakis and S. S. Xantheas, "Identifying the Most Stable Networks in Polyhedral Water Clusters", Frontiers article (invited), *Chemical Physics Letters* **461**, 180 (2008). Journal cover
22. M. L. Lipciuc, F. Wang, X. Yang and T. N. Kitsopoulos, G. S. Fanourgakis and S. S. Xantheas, "Cluster-Controlled Photofragmentation: The Case of the Xe-Pyrrole Cluster", Communication, *ChemPhysChem* **9** (in press, 2008), DOI: 10.1002/cphc.200800288

# *Author Index and List of Participants*

## Author Index


Ahmed, M. 7
Anderson, S. 11
Armentrout, P. 15
Auerbach, D. 225
Balasubramanian, K . 19
Bartels, D. 23,27
Beck, K . 127
Bentley, J 23
Bright, F. 3
Camillone, N. 217
Carmichael, I 27,163
Carter, E. 119
Castleman, Jr., A 31
Ceyer, S. . 35
Chandler, D. 39
Chelikowsky, J. 119
Chipman, D. 23,27,163
Cook, A.R. 43
Cowin, J. 47
Dang, L. 51
Dohnalek, Z. 155
Duncan, M. 55
Dupuis, M. 59
Eisenthal, K. 63
Ellison, G. 67
El-Sayed, M. 73
Evans, J. 77
Fayer, M. 81
Fulton, J. 85
Gaffney, K. 5
Garrett, B. 89
Geissler, P. 93
Gordon, M. 95
Gray, S. 99
Harris, C. 107
Harris, A.L. 217
Harrison, I. 111
Hayden, C. 115
Head-Gordon, M. 119
Head-Gordon, T. 123
Hess, W. 127
Hirata, S 131
Ho, W. 135
Jackson, B. 139
Jackson, K. 99
Jarrold, C. 143
Jellinek, J. 99
Johnson, M. 147
Joly, A. 127
Jordan, K. 147
Kathmann, S. 151
Kay, B. 155
Kimmel, G 159
LaVerne, J. 27,163
Leone, S. 7
Lester, M. 167
Liu, D.-J. 77
Louie, S. 119
Lu, H.P. 171
Meisel, D. 163
Miller, J.R. 43
Miller, Jan. 1
Morse, M. 175
Mundy, C 179
Ogut, S. 99
Osgood, R. 183
Petrik, N. 159
Ratner, M. 99
Raghavachari, K 143
Saykally, R. 189
Schatz, G. 99
Schenter, G. 193
Smith, R. S. 155
Steimle, T. 197
Stockman, M. 99
Thompson, W. 201
Tokmakoff, A. 205
Tully, J. 209
Valiev, M.. 89
Wang, L-S. 213
Wang, L.-W. 119
White, M.G. 217
Wilson, K. 7
Wishart, J. 221
Wodtke, A. 225
Xantheas, S. 229
Yang, H. 115

Musahid Ahmed
Lawrence Berkeley National Laboratory
MS 6R-2100
1 Cyclotron Road
Berkeley, CA 94720
E-Mail: mahmed@lbl.gov
Phone: (510) 486-6355

Peter Armentrout
University of Utah
Department of Chemistry
315 S 1400 E Rm 2020
Salt Lake City, UT 84112
E-Mail: armentrout@chem.utah.edu
Phone: (801) 581-7885

David Bartels
Notre Dame Radiation Laboratory
Notre Dame University
Notre Dame, Indiana 46556
E-Mail: bartels.5@nd.edu
Phone: (574) 631 5561

Nicholas Camillone
Brookhaven National Laboratory
Chemistry Department, Building 555
Upton, NY 11973
E-Mail: nicholas@bnl.gov
Phone: (631) 344-4412

Emily Carter
Princeton University
Olden Street, Equad, Suite D404A
Princeton, NJ 08544
E-Mail: eac@princeton.edu
Phone: (609) 258-5391

A. Welford Castleman, Jr.
Penn State University
104 Chemistry Building
University Park, PA 16802
E-Mail: awc@psu.edu
Phone: (814) 865-7242

Scott Anderson
University of Utah
Department of Chemistry
315 S. 1400 E.
Salt Lake City, UT 84112
E-Mail: anderson@chem.utah.edu
Phone: (801) 585 7289

Krishnan Balasubramanian
California State University East Bay
College of Science
25800 Carlos Bee Blvd
Hayward, CA 94542
E-Mail: kris.bala@csueastbay.edu
Phone: (925) 422-4984

Frank V. Bright
University at Buffalo
The State University of New York
511 Natural Sciences Complex
Buffalo, NY 14260-3000
E-Mail: chefvb@buffalo.edu
Phone: (716) 645-6800 ext. 2162

Ian Carmichael
Notre Dame Radiaton Laboratory
University of Notre Dame
Notre Dame, IN 46556
E-Mail: carmichael.1@nd.edu
Phone: (574) 631-4502

Michael Casassa
US DOE/Basic Energy Sciences
SC-22.11, 19901 Germantown Road
Germantown, MD 20874-1290
E-Mail: michael.casassa@science.doe.gov
Phone: (301) 903-0448

Daniel Chipman
Notre Dame Radiation Laboratory
303B Radiation Laboratory
Notre Dame, IN 46556
E-Mail: chipman.1@nd.edu
Phone: (574) 631-5562

Andrew Cook
Brookhaven National Laboratory
Bldg. 555 Chemistry
Upton, NY 11973
E-Mail: acook@bnl.gov
Phone: (631) 344-4782

James Cowin
Pacific Northwest National Laboratory
3335 Q Ave., M/S K8-88
Richland, WA 99337
E-Mail: jp.cowin@pnl.gov
Phone: (509) 371-6167

Robert Crowell
Brookhaven National Laboratory
Chemistry Department, Box 5000
Upton, NY 11973
E-Mail: crowell@bnl.gov
Phone: (631) 344-4515

Liem Dang
Pacific Northwest National Laboratory
PO Box 999, K1-83
Richland, WA 99352
E-Mail: liem.dang@pnl.gov
Phone: (509) 375-2557

Michael Duncan
University of Georgia
Department of Chemistry
Athens, Georgia 30602
E-Mail: maduncan@uga.edu
Phone: (706) 542-1998

Michel Dupuis
Pacific Northwest National Laboratory
PO Box 999, K1-82
Richland, WA 99352
E-Mail: Michel.Dupuis@pnl.gov
Phone: (509) 375-2617

Kenneth Eisenthal
Columbia University
3000 Broadway MC 3107
New York, New York 10027
E-Mail: kbe1@columbia.edu
Phone: (212) 854-3175

Barney Ellison
University of Colorado
Department of Chemistry
Boulder, CO 80309-0215
E-Mail: barney@jila.colorado.edu
Phone: (303) 492-8603

James Evans
Ames Laboratory
Iowa State University
Ames, Iowa 50011
E-Mail: evans@ameslab.gov
Phone: (515) 294-1638

Michael Fayer
Stanford University
Department of Chemistry
Stanford, CA 94305-5080
E-Mail: fayer@stanford.edu
Phone: (650) 723-4446

Gregory J. Fiechtner
US DOE/Basic Energy Sciences
SC-22.11, 19901 Germantown Road
Germantown, MD 20874-1920
E-Mail: gregory.fiechtner@science.doe.gov
Phone: (301) 903-5809

John Fulton
Pacific Northwest National Laboratory
P.O. Box 999 M.S. P8-19
Richland, WA 99354
E-Mail: john.fulton@pnl.gov
Phone: (509) 376-7011

Kelly Gaffney
PULSE Institute at SLAC and Stanford University
2575 Sand Hill Road
Menlo Park, CA 94025
E-Mail: kgaffney@slac.stanford.edu
Phone: (650) 926-2382

Bruce Garrett
Pacific Northwest National Laboratory
PO Box 999 (K9-90)
Richland, WA 99354
E-Mail: bruce.garrett@pnl.gov
Phone: (509) 372-6344

Phillip Geissler
Lawrence Berkeley National Laboratory
207 Gilman Hall, 1 Cyclotron Rd
Berkeley, CA 94720
E-Mail: geissler@berkeley.edu
Phone: (510) 642-8716

Mark Gordon
Ames National Laboratory
201 Spedding Hall - Iowa State University
Ames, IA 50011
E-Mail: mark@si.msg.chem.iastate.edu
Phone: (515) 294-0452

Stephen Gray
Argonne National Laboratory
Chemical Sciences and Engineering Division
Argonne, IL 60439
E-Mail: gray@tcg.anl.gov
Phone: (630) 252-3594

Charles Harris
Lawrence Berkeley National Laboratory,
Chemical Sciences Division
Department of Chemistry
University of California Berkeley
Berkeley, CA 94720
E-Mail: cbharris@berkeley.edu
Phone: (510) 642-2814

Alex Harris
Brookhaven National Laboratory
Chemistry Department, Building 555
PO Box 5000
Upton, NY 11973
E-Mail: alexh@bnl.gov
Phone: 6313444301

Ian Harrison
University of Virginia
Deptartment of Chemistry
Charlottesville, VA 22904-4319
E-Mail: harrison@virginia.edu
Phone: (434) 924-3639

Carl Hayden
Sandia National Laboratories
P.O. Box 969, MS 9055
Livermore, CA 94551
E-Mail: cchayde@sandia.gov
Phone: (925) 294-2298

Wayne Hess
Pacific Northwest National Laboratory
902 Battelle Blvd
Richland, WA 99352
E-Mail: wayne.hess@pnl.gov
Phone: (509) 371-6140

So Hirata
University of Florida
Quantum Theory Project, University of Florida
Gainesville, FL 32611-8435
E-Mail: hirata@qtp.ufl.edu
Phone: (352) 392-6876

Wilson Ho
University of California, Irvine
Department of Physics and Chemistry
Irvine, CA 92697-4575
E-Mail: wilsonho@uci.edu
Phone: (949) 824-5234

Koblar Jackson
Central Michigan University
Physics Department, Central Michigan University
Mount Pleasant, MI 48859
E-Mail: jacks1ka@cmich.edu
Phone: (989) 774-3310

Bret Jackson
University of Massachusetts Amherst
Department of Chemistry
701 LGRT, 710 N. Pleasant St.
Amherst, MA 01003
E-Mail: jackson@chem.umass.edu
Phone: (413) 545-2583

Caroline Jarrold
Indiana University
Department of Chemistry
800 East Kirkwood Avenue
Bloomington, IN 47405
E-Mail: cjarrold@indiana.edu
Phone: (812) 856-1190

Julius Jellinek
Argonne National Laboratory
9700 S. Cass Ave.
Argonne, IL 60439
E-Mail: jellinek@anl.gov
Phone: (630) 252-3463

Mark Johnson
Yale University
PO Box 208107
New Haven, CT 06520-8107
E-Mail: mark.johnson@yale.edu
Phone: (203) 436-4930

Kenneth Jordan
Department of Chemistry
University of Pittsburgh
Pittsburgh, PA 15260
E-Mail: jordan@pitt.edu
Phone: (412) 243-1455

Shawn Kathmann
Pacific Northwest National Laboratory
902 Battelle Boulevard
Richland, WA 99352
E-Mail: shawn.kathmann@pnl.gov
Phone: (509) 375-2870

Bruce Kay
Pacific Northwest National Laboratory
K8-88 PO Box 999
Richland, WA 99353
E-Mail: bruce.kay@pnl.gov
Phone: (509) 371-6143

Greg Kimmel
Pacific Northwest National Laboratory
MS K8-88, P.O. Box 999
Richland, WA 99352
E-Mail: gregory.kimmel@pnl.gov
Phone: (509) 371-6134

William Kirchhoff
DOE Retired
14511 Woodcrest Dr.
Rockville, MD 20853
E-Mail: william.kirchhoff@post.harvard.edu
Phone: (301) 460-5580

Allan Laufer
Retired (Guest Researcher at NIST)
100 Bureau Drive, Stop 8380
Gaithersburg, MD 20899-8380
E-Mail: allan.laufer@nist.gov
Phone: (301) 975-2062

Jay LaVerne
Notre Dame Radiation Laboratory
314 Radiation Laboratory
Notre Dame, IN 46556
E-Mail: laverne.1@nd.edu
Phone: (574) 631-5563

Marsha Lester
University of Pennsylvania
231 S. 34th Street
Philadelphia, PA 19104-6323
E-Mail: milester@sas.upenn.edu
Phone: (215) 898-4640

Diane Marceau
US DOE/Basic Energy Sciences
SC-22.1, 19901 Germantown Road
Germantown, MD 20874
E-Mail: diane.marceau@science.doe.gov
Phone: (301) 903-0235

Dan Meisel
University of Notre Dame
Radiation Laboratory & Department of Chemistry
Notre Dame, IN 46556
E-Mail: dani@nd.edu
Phone: (574) 631-5457

Raul Miranda
US DOE/Basic Energy Sciences
SC22.1, 19901 Germantown Road
Germantown, MD 20874
E-Mail: raul.miranda@science.doe.gov
Phone: (301) 903-8014

Christopher Mundy
Pacific Northwest National Laboratory
PO Box 999, K1-83
Richland, WA 99352
E-Mail: chris.mundy@pnl.gov
Phone: (509) 375-2404

Richard Osgood
Columbia University
345 Quaker St.
Chappaqua, NY 10514
E-Mail: osgood@columbia.edu
Phone: (914) 806-3696

H. Peter Lu
Bowling Green State University
021 Overman Hall
Bowling Green, OH 43402
E-Mail: hplu@bgsu.edu
Phone: (419) 372-1840

Andrew McIlroy
Sandia National Laboratories
PO Box 969, MS 9054
Livermore, CA 94551-0969
E-Mail: amcilr@sandia.gov
Phone: (925) 294-3054

Jan Miller
Department of Metallurgical Engineering
College of Mines and Earth Sciences
University of Utah
135 South 1460 East, Room 412
Salt Lake City, UT 84112-0114
E-Mail: Jan.Miller@utah.edu
Phone: (801) 581-5160

Michael Morse
University of Utah
Department of Chemistry
315 S. 1400 East
Salt Lake City, UT 84112-0850
E-Mail: morse@chem.utah.edu
Phone: (801) 581-8319

Serdar Ogut
University of Illinois at Chicago
845 West Taylor Street (M/C 273)
Chicago, IL 60607
E-Mail: ogut@uic.edu
Phone: (312) 413-2786

Mark Pederson
US DOE/Basic Energy Sciences
SC-22.11, 19901 Germantown Road
Germantown, MD 20874-1920
E-Mail: mark.pederson@science.doe.gov
Phone: (301) 903-9956

Hrvoje Petek
University of Pittsburgh
Department of Physics and Astronomy
Pittsburgh, PA 15260
E-Mail: petek@pitt.edu
Phone: (412) 624-3599

Krishnan Raghavachari
Indiana University
Department of Chemistry, 800 E. Kirkwood Avenue
Bloomington, IN 47405
E-Mail: kraghava@indiana.edu
Phone: (812) 856-1766

Larry Rahn
US DOE/Basic Energy Sciences
19901 Germantown Rd
Germantown, MD 20874-1920
E-Mail: Larry.Rahn@science.doe.gov
Phone: (301) 903-2508

Richard Saykally
University of California Berkeley
Department of Chemistry
D31 Hildebrand Hall
Berkeley, CA 94720-1460
E-Mail: saykally@berkeley.edu
Phone: (510) 642-8269

George Schatz
Northwestern University
Department of Chemistry
Evanston, IL 60201
E-Mail: schatz@chem.northwestern.edu
Phone: (847) 491-5657

Gregory Schenter
Pacific Northwest National Laboratory
902 Battelle Boulevard
Richland, WA 99352
E-Mail: greg.schenter@pnl.gov
Phone: (509) 375-4334

Wade Sisk
US DOE/Basic Energy Sciences
SC-22.11, 19901 Germantown Road
Germantown, MD 20874-1920
E-Mail: wade.sisk@science.doe.gov
Phone: (301) 903-5692

Timothy Steimle
Arizona State University
P.O. Box 871604
Tempe, AZ 85287
E-Mail: tsteimle@asu.edu
Phone: (480) 965-3265

Ward Thompson
University of Kansas
Department of Chemistry
Lawrence, KS 66045
E-Mail: wthompson@ku.edu
Phone: (785) 864-3980

Andrei Tokmakoff
Massachusetts Institute of Technology
Department of Chemistry
77 Massachusetts Ave. Rm 6-213
Cambridge, MA 02139
E-Mail: tokmakof@mit.edu
Phone: (617) 253-4503

John Tully
Yale University
225 Prospect Street
New Haven, CT 06520-8107
E-Mail: john.tully@yale.edu
Phone: (203) 432-3934

Marat Valiev
Pacific Northwest National Laboratory
902 Battelle Blvd, PO Box 999
Richland, WA 99352
E-Mail: marat.valiev@pnl.gov
Phone: (509)371-6459

Lai-Sheng Wang
Washington State University
2710 University Drive
Richland, WA 99354
E-Mail: ls.wang@pnl.gov
Phone: (509) 371-6138

Theresa Windus
Ames Laboratory
125 Spedding Hall
Ames, IA 50011
E-Mail: mduncalf@scl.ameslab.gov
Phone: (515) 294-2327

Sotiris Xantheas
Pacific Northwest National Laboratory
PO Box 999, K1-83
Richland, WA 99352
E-Mail: donna.sturdevant@pnl.gov
Phone: (509) 375-3684

Michael White
Brookhaven National Laboratory
Chemistry Department
Upton, NY 11973
E-Mail: mgwhite@bnl.gov
Phone: (631) 903-1117

James Wishart
Brookhaven National Laboratory
Chemistry Department
Upton, NY 11973
E-Mail: wishart@bnl.gov
Phone: (631) 344-4327

Hua-Gen Yu
Brookhaven National Laboratory
Chemistry Department
Upton, NY 11973
E-Mail: hgy@bnl.gov
Phone: (631) 344-4367